NOAA Atlas NESDIS 71

WORLD OCEAN ATLAS 2009
Volume 4: Nutrients (phosphate, nitrate, silicate)

Silver Spring, MD
March 2010

U.S. DEPARTMENT OF COMMERCE
National Oceanic and Atmospheric Administration
National Environmental Satellite, Data, and Information Service

National Oceanographic Data Center

Additional copies of this publication, as well as information about NODC data holdings and services, are available upon request directly from NODC.

National Oceanographic Data Center
User Services Team
NOAA/NESDIS E/OC1
SSMC III, 4th floor
1315 East-West Highway
Silver Spring, MD 20910-3282

Telephone: (301) 713-3277

Fax: (301) 713-3302

E-mail: NODC.Services@noaa.gov

NODC URL: http://www.nodc.noaa.gov/

For updates on the data, documentation, and additional information about the WOA09 please refer to:

http://www.nodc.noaa.gov/OC5/indprod.html

This document should be cited as:

Garcia, H. E., R. A. Locarnini, T. P. Boyer, J. I. Antonov, M. M. Zweng, O. K. Baranova, and D. R. Johnson, 2010. *World Ocean Atlas 2009, Volume 4: Nutrients (phosphate, nitrate, and silicate)*. S. Levitus, Ed., NOAA Atlas NESDIS 71, U.S. Government Printing Office, Washington, D.C., 398 pp.

This document is available on line at http://www.nodc.noaa.gov/OC5/indprod.html

NOAA Atlas NESDIS 71

WORLD OCEAN ATLAS 2009
Volume 4: Nutrients
(phosphate, nitrate, silicate)

Hernan E. Garcia, Ricardo A. Locarnini, Timothy P. Boyer,
John I. Antonov, Melissa M. Zweng, Olga K. Baranova, and Daphne R. Johnson

Editor: Sydney Levitus

Ocean Climate Laboratory
National Oceanographic Data Center

Silver Spring, Maryland
March, 2010

U.S. DEPARTMENT OF COMMERCE
Gary Locke, Secretary

National Oceanic and Atmospheric Administration
Jane Lubchenco,
Under Secretary of Commerce for Oceans and Atmosphere

National Environmental Satellite, Data and Information Service
Mary E. Kicza, Assistant Administrator

Table of Contents

Table of Contents i

List of Figures ii

List of Tables ii

List of Maps in the Appendices iii

Preface xiv

Acknowledgments xv

ABSTRACT 1

1. INTRODUCTION 1

2. DATA AND DATA DISTRIBUTION 2

2.1. DATA SOURCES 3
2.2. DATA QUALITY CONTROL 3
2.2.1. Duplicate elimination 4
2.2.2. Range and gradient checks 4
2.2.3. Statistical checks 4
2.2.4. Subjective flagging of data 5
2.2.5. Representativeness of the data 5

3. DATA PROCESSING PROCEDURES 6

3.1. VERTICAL INTERPOLATION TO STANDARD LEVELS 6
3.2. METHODS OF ANALYSIS 6
3.3. CHOICE OF OBJECTIVE ANALYSIS PROCEDURES 11
3.4. CHOICE OF SPATIAL GRID 12

4. RESULTS 12

4.1. COMPUTATION OF ANNUAL AND SEASONAL FIELDS 13
4.2. AVAILABLE STATISTICAL FIELDS 13
4.3. OBTAINING WOA09 FIELDS ONLINE 13

5. SUMMARY 14

6. FUTURE WORK 14

7. REFERENCES 14

8. APPENDICES 25

8.1 APPENDIX A: MAPS OF THE ANNUAL NUMBER OF OBSERVATIONS AND DISTRIBUTION OF PHOSPHATE AT SELECTED DEPTH LEVELS (PAGES 27 TO 50). 25
8.2 APPENDIX B: MAPS OF THE SEASONAL (WINTER, SUMMER, FALL, SPRING) NUMBER OF OBSERVATIONS, SEASONAL DISTRIBUTION, AND SEASONAL MINUS ANNUAL DISTRIBUTION OF PHOSPHATE AT SELECTED DEPTH LEVELS (PAGES 51 TO 90). 25
8.3 APPENDIX C: MAPS OF THE MONTHLY NUMBER OF OBSERVATIONS, MONTHLY DISTRIBUTION, AND MONTHLY MINUS ANNUAL DISTRIBUTION OF PHOSPHATE AT SELECTED DEPTH LEVELS (PAGES 91 TO 150). 25
8.4 APPENDIX D: MAPS OF THE ANNUAL NUMBER OF OBSERVATIONS OF NITRATE AT SELECTED DEPTH LEVELS (PAGES 151 TO 174). 25
8.5 APPENDIX E: MAPS OF THE SEASONAL (WINTER, SUMMER, FALL, SPRING) NUMBER OF OBSERVATIONS, SEASONAL DISTRIBUTION, AND SEASONAL MINUS ANNUAL DISTRIBUTION OF NITRATE AT SELECTED DEPTH LEVELS (PAGES 175 TO 214). 25
8.6 APPENDIX F: MAPS OF THE MONTHLY NUMBER OF OBSERVATIONS, MONTHLY DISTRIBUTION, AND MONTHLY

MINUS ANNUAL DISTRIBUTION OF NITRATE AT SELECTED DEPTH LEVELS (PAGES 215 TO 274). 25
8.7 APPENDIX G: MAPS OF THE ANNUAL NUMBER OF OBSERVATIONS OF SILICATE AT SELECTED DEPTH LEVELS (PAGES 275 TO 298). 25
8.8 APPENDIX H: MAPS OF THE SEASONAL (WINTER, SUMMER, FALL, SPRING) NUMBER OF OBSERVATIONS, SEASONAL DISTRIBUTION, AND SEASONAL MINUS ANNUAL DISTRIBUTION OF SILICATE AT SELECTED DEPTH LEVELS (PAGES 299 TO 338). 25
8.9 APPENDIX I: MAPS OF THE MONTHLY NUMBER OF OBSERVATIONS, MONTHLY DISTRIBUTION, AND MONTHLY MINUS ANNUAL DISTRIBUTION OF SILICATE AT SELECTED DEPTH LEVELS (PAGES 339 TO 398).....25

List of Figures

Figure 1. Response function of the WOA09, WOA05, WOA01, WOA98, WOA94, and Levitus (1982) objective analysis schemes. 23
Figure 2. Scheme used in computing annual, seasonal, and monthly objectively analyzed means for phosphate, silicate, and nitrate. 24

List of Tables

Table 1. Descriptions of climatologies for each nutrient variable in WOA09. The climatologies have been calculated based on bottle data (OSD) from WOD09. 19
Table 2. Acceptable distances (m) for defining interior and exterior values used in the Reiniger-Ross scheme for interpolating observed level data to standard levels. 19
Table 3. Response function of the objective analysis scheme as a function of wavelength for WOA09 and earlier analyses. 20
Table 4. Basins defined for objective analysis and the shallowest standard depth level for which each basin is defined. 21
Table 5. Objective and statistical data fields calculated as part of WOA09. 22

List of Maps in the Appendices

Appendix A: Maps of the annual number of observations and distribution of phosphate at selected depth levels (Pages 27 to 50).

Fig. A1. Annual phosphate observations at the surface. 27
Fig. A2. Annual phosphate observations at 50 m. depth. 27
Fig. A3. Annual phosphate observations at 75 m. depth. 28
Fig. A4. Annual phosphate observations at 100 m. depth. 28
Fig. A5. Annual phosphate observations at 150 m. depth. 29
Fig. A6. Annual phosphate observations at 200 m. depth. 29
Fig. A7. Annual phosphate observations at 250 m. depth. 30
Fig. A8. Annual phosphate observations at 400 m. depth. 30
Fig. A9. Annual phosphate observations at 500 m. depth. 31
Fig. A10. Annual phosphate observations at 700 m. depth. 31
Fig. A11. Annual phosphate observations at 1000 m. depth. 32
Fig. A12. Annual phosphate observations at 1500 m. depth. 32
Fig. A13. Annual phosphate observations at 2000 m. depth. 33
Fig. A14. Annual phosphate observations at 2500 m. depth. 33
Fig. A15. Annual phosphate observations at 3000 m. depth. 34
Fig. A16. Annual phosphate observations at 4000 m. depth. 34
Fig. A17. Annual phosphate [μmol l^{-1}] at the surface. 35
Fig. A18. Annual phosphate [μmol l^{-1}] at 50 m. depth. 36
Fig. A19. Annual phosphate [μmol l^{-1}] at 75 m. depth. 37
Fig. A20. Annual phosphate [μmol l^{-1}] at 100 m. depth. 38
Fig. A21. Annual phosphate [μmol l^{-1}] at 150 m. depth. 39
Fig. A22. Annual phosphate [μmol l^{-1}] at 200 m. depth. 40
Fig. A23. Annual phosphate [μmol l^{-1}] at 250 m. depth. 41
Fig. A24. Annual phosphate [μmol l^{-1}] at 400 m. depth. 42
Fig. A25. Annual phosphate [μmol l^{-1}] at 500 m. depth. 43
Fig. A26. Annual phosphate [μmol l^{-1}] at 700 m. depth. 44
Fig. A27. Annual phosphate [μmol l^{-1}] at 1000 m. depth. 45
Fig. A28. Annual phosphate [μmol l^{-1}] at 1500 m. depth. 46
Fig. A29. Annual phosphate [μmol l^{-1}] at 2000 m. depth. 47
Fig. A30. Annual phosphate [μmol l^{-1}] at 2500 m. depth. 48
Fig. A31. Annual phosphate [μmol l^{-1}] at 3000 m. depth. 49
Fig. A32. Annual phosphate [μmol l^{-1}] at 4000 m. depth. 50

Appendix B: Maps of the seasonal (winter, summer, fall, spring) number of observations, seasonal distribution, and seasonal minus annual distribution of phosphate at selected depth levels (Pages 51 to 90).

Fig. B1. Winter (Jan.-Mar.) phosphate observations at the surface. 51
Fig. B2. Winter (Jan.-Mar.) phosphate observations at 75 m. depth. 51
Fig. B3. Winter (Jan.-Mar.) phosphate observations at 150 m. depth. 52
Fig. B4. Winter (Jan.-Mar.) phosphate observations at 250 m. depth. 52

Fig. B5. Spring (Apr.-Jun.) phosphate observations at the surface. 53
Fig. B6. Spring (Apr.-Jun.) phosphate observations at 75 m. depth. 53
Fig. B7. Spring (Apr.-Jun.) phosphate observations at 150 m. depth. 54
Fig. B8. Spring (Apr.-Jun.) phosphate observations at 250 m. depth. 54
Fig. B9. Summer (Jul.-Sep.) phosphate observations at the surface. 55
Fig. B10. Summer (Jul.-Sep.) phosphate observations at 75 m. depth. 55
Fig. B11. Summer (Jul.-Sep.) phosphate observations at 150 m. depth. 56
Fig. B12. Summer (Jul.-Sep.) phosphate observations at 250 m. depth. 56
Fig. B13. Fall (Oct.-Dec.) phosphate observations at the surface. 57
Fig. B14. Fall (Oct.-Dec.) phosphate observations at 75 m. depth. 57
Fig. B15. Fall (Oct.-Dec.) phosphate observations at 150 m. depth. 58
Fig. B16. Fall (Oct.-Dec.) phosphate observations at 250 m. depth. 58
Fig. B17. Winter (Jan.-Mar.) phosphate [μmol l^{-1}] at the surface. 59
Fig. B18. Winter (Jan.-Mar.) minus annual phosphate [μmol l^{-1}] at the surface. 59
Fig. B19. Winter (Jan.-Mar.) phosphate [μmol l^{-1}] at 75 m. depth. 61
Fig. B20. Winter (Jan.-Mar.) minus annual phosphate [μmol l^{-1}] at 75 m. depth. 62
Fig. B21. Winter (Jan.-Mar.) phosphate [μmol l^{-1}] at 150 m. depth. 63
Fig. B22. Winter (Jan.-Mar.) minus annual phosphate [μmol l^{-1}]] at 150 m. depth. 64
Fig. B23. Winter (Jan.-Mar.) phosphate [μmol l^{-1}] at 250 m. depth. 65
Fig. B24. Winter (Jan.-Mar.) minus annual phosphate [μmol l^{-1}] at 250 m. depth. 66
Fig. B25. Spring (Apr.-Jun.) phosphate [μmol l^{-1}] at the surface. 67
Fig. B26. Spring (Apr.-Jun.) minus annual phosphate [μmol l^{-1}] at the surface. 68
Fig. B27. Spring (Apr.-Jun.) phosphate [[μmol l^{-1}] at 75 m. depth. 69
Fig. B28. Spring (Apr.-Jun.) minus annual phosphate [μmol l^{-1}] at 75 m. depth. 70
Fig. B29. Spring (Apr.-Jun.) phosphate [μmol l^{-1}] at 150 m. depth. 71
Fig. B30. Spring (Apr.-Jun.) minus annual phosphate [[μmol l^{-1}] at 150 m. depth. 72
Fig. B31. Spring (Apr.-Jun.) phosphate [μmol l^{-1}] at 250 m. depth. 73
Fig. B32. Spring (Apr.-Jun.) minus annual phosphate [μmol l^{-1}] at 250 m. depth. 74
Fig. B33. Summer (Jul.-Sep.) phosphate [μmol l^{-1}] at the surface. 75
Fig. B34. Summer (Jul.-Sep.) minus annual phosphate [μmol l^{-1}] at the surface. 76
Fig. B35. Summer (Jul.-Sep.) phosphate [μmol l^{-1}] at 75 m. depth. 77
Fig. B36. Summer (Jul.-Sep.) minus annual phosphate [μmol l^{-1}]at 75 m. depth. 78
Fig. B37. Summer (Jul.-Sep.) phosphate [μmol l^{-1}] at 150 m. depth. 79
Fig. B38. Summer (Jul.-Sep.) minus annual phosphate [μmol l^{-1}] at 150 m. depth. 80
Fig. B39. Summer (Jul.-Sep.) phosphate [μmol l^{-1}] at 250 m. depth. 81
Fig. B40. Summer (Jul.-Sep.) minus annual phosphate [μmol l^{-1}] at 250 m. depth. 82
Fig. B41. Fall (Oct.-Dec.) phosphate [μmol l^{-1}] at the surface. 83
Fig. B42. Fall (Oct.-Dec.) minus annual phosphate [μmol l^{-1}] at the surface. 84
Fig. B43. Fall (Oct.-Dec.) phosphate [μmol l^{-1}] at 75 m. depth. 85
Fig. B44. Fall (Oct.-Dec.) minus annual phosphate [μmol l^{-1}] at 75 m. depth. 86
Fig. B45. Fall (Oct.-Dec.) phosphate [μmol l^{-1}] at 150 m. depth. 87
Fig. B46. Fall (Oct.-Dec.) minus annual phosphate [μmol l^{-1}] at 150 m. depth. 88
Fig. B47. Fall (Oct.-Dec.) phosphate [μmol l^{-1}] at 250 m. depth. 89
Fig. B48. Fall (Oct.-Dec.) minus annual phosphate [μmol l^{-1}] at 250 m. depth. 90

Appendix C: Maps of the monthly number of observations, monthly distribution, and monthly minus annual distribution of phosphate at selected depth levels (Pages 91 to 150).

Fig. C1. January phosphate observations at the surface. 91
Fig. C2. January phosphate observations at 75 m. depth. 90
Fig. C3. February phosphate observations at the surface. 92
Fig. C4. February phosphate observations at 75 m. depth. 92
Fig. C5. March phosphate observations at the surface. 93
Fig. C6. March phosphate observations at 75 m. depth. 93
Fig. C7. April phosphate observations at the surface. 94
Fig. C8. April phosphate observations at 75 m. depth. 94
Fig. C9. May phosphate observations at the surface. 95
Fig. C10. May phosphate observations at 75 m. depth. 95
Fig. C11. June phosphate observations at the surface. 96
Fig. C12. June phosphate observations at 75 m. depth. 96
Fig. C13. July phosphate observations at the surface. 97
Fig. C14. July phosphate observations at 75 m. depth. 97
Fig. C15. August phosphate observations at the surface. 98
Fig. C16. August phosphate observations at 75 m. depth. 98
Fig. C17. September phosphate observations at the surface. 99
Fig. C18. September phosphate observations at 75 m. depth. 99
Fig. C19. October phosphate observations at the surface. 100
Fig. C20. October phosphate observations at 75 m. depth. 100
Fig. C21. November phosphate observations at the surface. 101
Fig. C22. November phosphate observations at 75 m. depth. 101
Fig. C23. December phosphate observations at the surface. 102
Fig. C24. December phosphate observations at 75 m. depth. 102
Fig. C25. January mean phosphate [μmol l^{-1}] at the surface. 103
Fig. C26. January minus annual phosphate [μmol l^{-1}] at the surface. 104
Fig. C27. January mean phosphate [μmol l^{-1}] at 75 m. depth. 105
Fig. C28. January minus annual phosphate [μmol l^{-1}] at 75 m. depth. 106
Fig. C29. February mean phosphate [μmol l^{-1}] at the surface. 107
Fig. C30. February minus annual phosphate [μmol l^{-1}] at the surface. 108
Fig. C31. February mean phosphate [μmol l^{-1}] at 75 m. depth. 109
Fig. C32. February minus annual phosphate [μmol l^{-1}] at 75 m. depth. 111
Fig. C33. March mean phosphate [μmol l^{-1}] at the surface. 111
Fig. C34. March minus annual phosphate [μmol l^{-1}] at the surface. 113
Fig. C35. March mean phosphate [μmol l^{-1}] at 75 m. depth. 113
Fig. C36. March minus annual phosphate [μmol l^{-1}] at 75 m. depth. 115
Fig. C37. April mean phosphate [μmol l^{-1}] at the surface. 115
Fig. C38. April minus annual phosphate [μmol l^{-1}] at the surface. 116
Fig. C39. April mean phosphate [μmol l^{-1}] at 75 m. depth. 117
Fig. C40. April minus annual phosphate [μmol l^{-1}] at 75 m. depth. 118
Fig. C41. May mean phosphate [μmol l^{-1}] at the surface. 119
Fig. C42. May minus annual phosphate [μmol l^{-1}] at the surface. 120

Fig. C43. May mean phosphate [μmol l^{-1}] at 75 m. depth. 121
Fig. C44. May minus annual phosphate [μmol l^{-1}] at 75 m. depth. 122
Fig. C45. June mean phosphate [μmol l^{-1}]] at the surface. 123
Fig. C46. June minus annual phosphate [μmol l^{-1}] at the surface. 124
Fig. C47. June mean phosphate [μmol l^{-1}] at 75 m. depth. 125
Fig. C48. June minus annual phosphate [μmol l^{-1}] at 75 m. depth. 126
Fig. C49. July mean phosphate [μmol l^{-1}] at the surface. 127
Fig. C50. July minus annual phosphate [μmol l^{-1}] at the surface. 128
Fig. C51. July mean phosphate [μmol l^{-1}] at 75 m. depth. 129
Fig. C52. July minus annual phosphate [μmol l^{-1}] at 75 m. depth. 130
Fig. C53. August mean phosphate [μmol l^{-1}] at the surface. 131
Fig. C54. August minus annual phosphate [μmol l^{-1}] at the surface. 132
Fig. C55. August mean phosphate [μmol l^{-1}]] at 75 m. depth. 133
Fig. C56. August minus annual phosphate [μmol l^{-1}] at 75 m. depth. 134
Fig. C57. September mean phosphate[μmol l^{-1}] at the surface. 135
Fig. C58. September minus annual phosphate [μmol l^{-1}] at the surface. 136
Fig. C59. September mean phosphate [μmol l^{-1}] at 75 m. depth. 137
Fig. C60. September minus annual phosphate [μmol l^{-1}] at 75 m. depth. 138
Fig. C61. October mean phosphate [μmol l^{-1}] at the surface. 139
Fig. C62. October minus annual phosphate [μmol l^{-1}] at the surface. 140
Fig. C63. October mean phosphate [μmol l^{-1}] at 75 m. depth. 141
Fig. C64. October minus annual phosphate [μmol l^{-1}] at 75 m. depth. 142
Fig. C65. November mean phosphate [μmol l^{-1}] at the surface. 143
Fig. C66. November minus annual phosphate [μmol l^{-1}] at the surface. 144
Fig. C67. November mean phosphate [μmol l^{-1}] at 75 m. depth. 145
Fig. C68. November minus annual phosphate [μmol l^{-1}] at 75 m. depth. 146
Fig. C69. December mean phosphate [μmol l^{-1}] at the surface. 147
Fig. C70. December minus annual phosphate [μmol l^{-1}] at the surface. 148
Fig. C71. December mean phosphate [μmol l^{-1}] at 75 m. depth. 149
Fig. C72. December minus annual phosphate [μmol l^{-1}] at 75 m. depth. 150

Appendix D: Maps of the annual number of observations of nitrate at selected depth levels (Pages 151 to 174).

Fig. D1. Annual nitrate observations at the surface. 151
Fig. D2. Annual nitrate observations at 50 m. depth. 151
Fig. D3. Annual nitrate observations at 75 m. depth. 152
Fig. D4. Annual nitrate observations at 100 m. depth. 152
Fig. D5. Annual nitrate observations at 150 m. depth. 153
Fig. D6. Annual nitrate observations at 200 m. depth. 153
Fig. D7. Annual nitrate observations at 250 m. depth. 154
Fig. D8. Annual nitrate observations at 400 m. depth. 154
Fig. D9. Annual nitrate observations at 500 m. depth. 155
Fig. D10. Annual nitrate observations at 700 m. depth. 155
Fig. D11. Annual nitrate observations at 1000 m. depth. 156

Fig. D12. Annual nitrate observations at 1500 m. depth. 156
Fig. D13. Annual nitrate observations at 2000 m. depth. 157
Fig. D14. Annual nitrate observations at 2500 m. depth. 157
Fig. D15. Annual nitrate observations at 3000 m. depth. 158
Fig. D16. Annual nitrate observations at 4000 m. depth. 158
Fig. D17. Annual nitrate [μmol l^{-1}] at the surface. 159
Fig. D18. Annual nitrate [μmol l^{-1}] at 50 m. depth. 160
Fig. D19. Annual nitrate [μmol l^{-1}] at 75 m. depth. 161
Fig. D20. Annual nitrate [μmol l^{-1}] at 100 m. depth. 162
Fig. D21. Annual nitrate [μmol l^{-1}] at 150 m. depth. 163
Fig. D22. Annual nitrate [μmol l^{-1}] at 200 m. depth. 164
Fig. D23. Annual nitrate [μmol l^{-1}] at 250 m. depth. 165
Fig. D24. Annual nitrate [μmol l^{-1}] at 400 m. depth. 166
Fig. D25. Annual nitrate [μmol l^{-1}] at 500 m. depth. 167
Fig. D26. Annual nitrate [μmol l^{-1}] at 700 m. depth. 168
Fig. D27. Annual nitrate [μmol l^{-1}] at 1000 m. depth. 169
Fig. D28. Annual nitrate [μmol l^{-1}] at 1500 m. depth. 170
Fig. D29. Annual nitrate [μmol l^{-1}] at 2000 m. depth. 171
Fig. D30. Annual nitrate [μmol l^{-1}] at 2500 m. depth. 172
Fig. D31. Annual nitrate [μmol l^{-1}] at 3000 m. depth. 173
Fig. D32. Annual nitrate [μmol l^{-1}] at 4000 m. depth. 174

Appendix E: Maps of the seasonal (winter, summer, fall, spring) number of observations, seasonal distribution, and seasonal minus annual distribution of nitrate at selected depth levels (Pages 175 to 214).

Fig. E1. Winter (Jan.-Mar.) nitrate observations at the surface. 175
Fig. E2. Winter (Jan.-Mar.) nitrate observations at 75 m. depth. 175
Fig. E3. Winter (Jan.-Mar.) nitrate observations at 150 m. depth. 176
Fig. E4. Winter (Jan.-Mar.) nitrate observations at 250 m. depth. 176
Fig. E5. Spring (Apr.-Jun.) nitrate observations at the surface. 177
Fig. E6. Spring (Apr.-Jun.) nitrate observations at 75 m. depth. 177
Fig. E7. Spring (Apr.-Jun.) nitrate observations at 150 m. depth. 178
Fig. E8. Spring (Apr.-Jun.) nitrate observations at 250 m. depth. 178
Fig. E9. Summer (Jul.-Sep.) nitrate observations at the surface. 179
Fig. E10. Summer (Jul.-Sep.) nitrate observations at 75 m. depth. 179
Fig. E11. Summer (Jul.-Sep.) nitrate observations at 150 m. depth. 180
Fig. E12. Summer (Jul.-Sep.) nitrate observations at 250 m. depth. 180
Fig. E13. Fall (Oct.-Dec.) nitrate observations at the surface. 181
Fig. E14. Fall (Oct.-Dec.) nitrate observations at 75 m. depth. 181
Fig. E15. Fall (Oct.-Dec.) nitrate observations at 150 m. depth. 182
Fig. E16. Fall (Oct.-Dec.) nitrate observations at 250 m. depth. 182
Fig. E17. Winter (Jan.-Mar.) nitrate [μmol l^{-1}] at the surface. 183
Fig. E18. Winter (Jan.-Mar.) minus annual nitrate [μmol l^{-1}] at the surface. 184
Fig. E19. Winter (Jan.-Mar.) nitrate [μmol l^{-1}] at 75 m. depth. 185
Fig. E20. Winter (Jan.-Mar.) minus annual nitrate [μmol l^{-1}] at 75 m. depth. 186

Fig. E21. Winter (Jan.-Mar.) nitrate [μmol l^{-1}] at 150 m. depth. 187
Fig. E22. Winter (Jan.-Mar.) minus annual nitrate [μmol l^{-1}] at 150 m. depth..... 188
Fig. E23. Winter (Jan.-Mar.) nitrate [μmol l^{-1}] at 250 m. depth. 189
Fig. E24. Winter (Jan.-Mar.) minus annual nitrate [μmol l^{-1}] at 250 m. depth..... 190
Fig. E25. Spring (Apr.-Jun.) nitrate [μmol l^{-1}] at the surface. 191
Fig. E26. Spring (Apr.-Jun.) minus annual nitrate [μmol l^{-1}] at the surface. 192
Fig. E27. Spring (Apr.-Jun.) nitrate [μmol l^{-1}]] at 75 m. depth. 193
Fig. E28. Spring (Apr.-Jun.) minus annual nitrate [μmol l^{-1}] at 75 m. depth. 194
Fig. E29. Spring (Apr.-Jun.) nitrate [μmol l^{-1}] at 150 m. depth. 195
Fig. E30. Spring (Apr.-Jun.) minus annual nitrate [μmol l^{-1}] at 150 m. depth. 196
Fig. E31. Spring (Apr.-Jun.) nitrate [μmol l^{-1}] at 250 m. depth. 197
Fig. E32. Spring (Apr.-Jun.) minus annual nitrate [μmol l^{-1}] at 250 m. depth. 198
Fig. E33. Summer (Jul.-Sep.) nitrate [μmol l^{-1}] at the surface. 199
Fig. E34. Summer (Jul.-Sep.) minus annual nitrate [μmol l^{-1}] at the surface. 200
Fig. E35. Summer (Jul.-Sep.) nitrate [μmol l^{-1}] at 75 m. depth. 201
Fig. E36. Summer (Jul.-Sep.) minus annual nitrate [μmol l^{-1}] at 75 m. depth. 202
Fig. E37. Summer (Jul.-Sep.) nitrate [μmol l^{-1}] at 150 m. depth. 203
Fig. E38. Summer (Jul.-Sep.) minus annual nitrate [μmol l^{-1}] at 150 m. depth. 204
Fig. E39. Summer (Jul.-Sep.) nitrate [μmol l^{-1}] at 250 m. depth. 205
Fig. E40. Summer (Jul.-Sep.) minus annual nitrate [μmol l^{-1}] at 250 m. depth. 206
Fig. E41. Fall (Oct.-Dec.) nitrate [μmol l^{-1}] at the surface. 207
Fig. E42. Fall (Oct.-Dec.) minus annual nitrate [μmol l^{-1}]] at the surface. 208
Fig. E43. Fall (Oct.-Dec.) nitrate [μmol l^{-1}]] at 75 m. depth. 209
Fig. E44. Fall (Oct.-Dec.) minus annual nitrate [μmol l^{-1}] at 75 m. depth. 210
Fig. E45. Fall (Oct.-Dec.) nitrate [μmol l^{-1}] at 150 m. depth. 211
Fig. E46. Fall (Oct.-Dec.) minus annual nitrate [μmol l^{-1}] at 150 m. depth. 212
Fig. E47. Fall (Oct.-Dec.) nitrate [μmol l^{-1}] at 250 m. depth. 213
Fig. E48. Fall (Oct.-Dec.) minus annual nitrate [μmol l^{-1}] at 250 m. depth. 214

Appendix F: Maps of the monthly number of observations, monthly distribution, and monthly minus annual distribution of nitrate at selected depth levels (Pages 215 to 274).

Fig. F1. January nitrate observations at the surface. 215
Fig. F2. January nitrate observations at 75 m. depth. 215
Fig. F3. February nitrate observations at the surface. 216
Fig. F4. February nitrate observations at 75 m. depth. 216
Fig. F5. March nitrate observations at the surface. 217
Fig. F6. March nitrate observations at 75 m. depth. 217
Fig. F7. April nitrate observations at the surface. 218
Fig. F8. April nitrate observations at 75 m. depth. 218
Fig. F9. May nitrate observations at the surface. 219
Fig. F10. May nitrate observations at 75 m. depth. 219
Fig. F11. June nitrate observations at the surface. 220
Fig. F12. June nitrate observations at 75 m. depth. 220
Fig. F13. July nitrate observations at the surface 221
Fig. F14. July nitrate observations at 75 m. depth. 221

Fig. F15. August nitrate observations at the surface. 222
Fig. F16. August nitrate observations at 75 m. depth. 222
Fig. F17. September nitrate observations at the surface. 223
Fig. F18. September nitrate observations at 75 m. depth. 223
Fig. F19. October nitrate observations at the surface. 224
Fig. F20. October nitrate observations at 75 m. depth. 224
Fig. F21. November nitrate observations at the surface. 225
Fig. F22. November nitrate observations at 75 m. depth. 225
Fig. F23. December nitrate observations at the surface. 226
Fig. F24. December nitrate observations at 75 m. depth. 226
Fig. F25. January mean nitrate [μmol l^{-1}] at the surface. 227
Fig. F26. January minus annual nitrate [μmol l^{-1}] at the surface. 228
Fig. F27. January mean nitrate [μmol l^{-1}] at 75 m. depth. 229
Fig. F28. January minus annual nitrate [μmol l^{-1}] at 75 m. depth. 230
Fig. F29. February mean nitrate [μmol l^{-1}] at the surface. 231
Fig. F30. February minus annual nitrate [μmol l^{-1}] at the surface. 232
Fig. F31. February mean nitrate [μmol l^{-1}] at 75 m. depth. 233
Fig. F32. February minus annual nitrate [μmol l^{-1}] at 75 m. depth. 234
Fig. F33. March mean nitrate [μmol l^{-1}] at the surface. 235
Fig. F34. March minus annual nitrate [μmol l^{-1}] at the surface. 236
Fig. F35. March mean nitrate [μmol l^{-1}] at 75 m. depth. 237
Fig. F36. March minus annual nitrate [μmol l^{-1}] at 75 m. depth. 238
Fig. F37. April mean nitrate [μmol l^{-1}] at the surface. 239
Fig. F38. April minus annual nitrate [μmol l^{-1}] at the surface. 240
Fig. F39. April mean nitrate [μmol l^{-1}] at 75 m. depth. 241
Fig. F40. April minus annual nitrate [μmol l^{-1}] at 75 m. depth. 242
Fig. F41. May mean nitrate [μmol l^{-1}] at the surface. 243
Fig. F42. May minus annual nitrate [μmol l^{-1}] at the surface. 244
Fig. F43. May mean nitrate [μmol l^{-1}] at 75 m. depth. 245
Fig. F44. May minus annual nitrate [μmol l^{-1}] at 75 m. depth. 246
Fig. F45. June mean nitrate [μmol l^{-1}] at the surface. 247
Fig. F46. June minus annual nitrate [μmol l^{-1}] at the surface. 248
Fig. F47. June mean nitrate [μmol l^{-1}] at 75 m. depth. 249
Fig. F48. June minus annual nitrate [μmol l^{-1}] at 75 m. depth. 250
Fig. F49. July mean nitrate [μmol l^{-1}] at the surface. 252
Fig. F50. July minus annual nitrate [μmol l^{-1}] at the surface. 252
Fig. F51. July mean nitrate [μmol l^{-1}] at 75 m. depth. 253
Fig. F52. July minus annual nitrate [μmol l^{-1}] at 75 m. depth. 254
Fig. F53. August mean nitrate [μmol l^{-1}] at the surface. 255
Fig. F54. August minus annual nitrate [μmol l^{-1}] at the surface. 256
Fig. F55. August mean nitrate [μmol l^{-1}] at 75 m. depth. 257
Fig. F56. August minus annual nitrate [μmol l^{-1}] at 75 m. depth. 258
Fig. F57. September mean nitrate [μmol l^{-1}] at the surface. 259
Fig. F58. September minus annual nitrate [μmol l^{-1}] at the surface. 260

Fig. F59. September mean nitrate [μmol l^{-1}] at 75 m. depth. 261
Fig. F60. September minus annual nitrate [μmol l^{-1}] at 75 m. depth. 262
Fig. F61. October mean nitrate [μmol l^{-1}] at the surface. 263
Fig. F62. October minus annual nitrate [μmol l^{-1}] at the surface. 264
Fig. F63. October mean nitrate [μmol l^{-1}] at 75 m. depth. 266
Fig. F64. October minus annual nitrate [μmol l^{-1}] at 75 m. depth. 266
Fig. F65. November mean nitrate [μmol l^{-1}] at the surface. 267
Fig. F66. November minus annual nitrate [μmol l^{-1}] at the surface. 267
Fig. F67. November mean nitrate [μmol l^{-1}] at 75 m. depth. 268
Fig. F68. November minus annual nitrate [μmol l^{-1}] at 75 m. depth. 270
Fig. F69. December mean nitrate [μmol l^{-1}] at the surface. 271
Fig. F70. December minus annual nitrate [μmol l^{-1}] at the surface. 272
Fig. F71. December mean nitrate [μmol l^{-1}] at 75 m. depth. 273
Fig. F72. December minus annual nitrate [μmol l^{-1}] at 75 m. depth. 274

Appendix G: Maps of the annual number of observations of silicate at selected depth levels (Pages 275 to 298).

Fig. G1. Annual silicate observations at the surface. 275
Fig. G2. Annual silicate observations at 50 m. depth. 275
Fig. G3. Annual silicate observations at 75 m. depth. 276
Fig. G4. Annual silicate observations at 100 m. depth. 276
Fig. G5. Annual silicate observations at 150 m. depth. 277
Fig. G6. Annual silicate observations at 200 m. depth. 277
Fig. G7. Annual silicate observations at 250 m. depth. 278
Fig. G8. Annual silicate observations at 400 m. depth. 278
Fig. G9. Annual silicate observations at 500 m. depth. 279
Fig. G10. Annual silicate observations at 700 m. depth. 279
Fig. G11. Annual silicate observations at 1000 m. depth. 280
Fig. G12. Annual silicate observations at 1500 m. depth. 280
Fig. G13. Annual silicate observations at 2000 m. depth. 281
Fig. G14. Annual silicate observations at 2500 m. depth. 281
Fig. G15. Annual silicate observations at 3000 m. depth. 282
Fig. G16. Annual silicate observations at 4000 m. depth. 282
Fig. G17. Annual silicate [μmol l^{-1}] at the surface. 283
Fig. G18. Annual silicate [μmol l^{-1}] at 50 m. depth. 284
Fig. G19. Annual silicate [μmol l^{-1}] at 75 m. depth. 285
Fig. G20. Annual silicate [μmol l^{-1}] at 100 m. depth. 286
Fig. G21. Annual silicate [μmol l^{-1}] at 150 m. depth. 287
Fig. G22. Annual silicate [μmol l^{-1}] at 200 m. depth. 288
Fig. G23. Annual silicate [μmol l^{-1}] at 250 m. depth. 289
Fig. G24. Annual silicate [μmol l^{-1}] at 400 m. depth. 290
Fig. G25. Annual silicate [μmol l^{-1}] at 500 m. depth. 291
Fig. G26. Annual silicate [μmol l^{-1}] at 700 m. depth. 292
Fig. G27. Annual silicate [μmol l^{-1}] at 1000 m. depth. 293
Fig. G28. Annual silicate [μmol l^{-1}] at 1500 m. depth. 294

Fig. G29. Annual silicate [μmol l^{-1}] at 2000 m. depth. 295
Fig. G30. Annual silicate [μmol l^{-1}] at 2500 m. depth. 296
Fig. G31. Annual silicate [μmol l^{-1}] at 3000 m. depth. 297
Fig. G32. Annual silicate [μmol l^{-1}] at 4000 m. depth. 298

Appendix H: Maps of the seasonal (winter, summer, fall, spring) number of observations, seasonal distribution, and seasonal minus annual distribution of silicate at selected depth levels (Pages 299 to 338).

Fig. H1. Winter (Jan.-Mar.) silicate observations at the surface. 299
Fig. H2. Winter (Jan.-Mar.) silicate observations at 75 m. depth. 299
Fig. H3. Winter (Jan.-Mar.) silicate observations at 150 m. depth. 300
Fig. H4. Winter (Jan.-Mar.) silicate observations at 250 m. depth. 300
Fig. H5. Spring (Apr.-Jun.) silicate observations at the surface. 301
Fig. H6. Spring (Apr.-Jun.) silicate observations at 75 m. depth. 301
Fig. H7. Spring (Apr.-Jun.) silicate observations at 150 m. depth. 302
Fig. H8. Spring (Apr.-Jun.) silicate observations at 250 m. depth. 302
Fig. H9. Summer (Jul.-Sep.) silicate observations at the surface. 303
Fig. H10. Summer (Jul.-Sep.) silicate observations at 75 m. depth. 303
Fig. H11. Summer (Jul.-Sep.) silicate observations at 150 m. depth. 304
Fig. H12. Summer (Jul.-Sep.) silicate observations at 250 m. depth. 304
Fig. H13. Fall (Oct.-Dec.) silicate observations at the surface. 305
Fig. H14. Fall (Oct.-Dec.) silicate observations at 75 m. depth. 305
Fig. H15. Fall (Oct.-Dec.) silicate observations at 150 m. depth. 306
Fig. H16. Fall (Oct.-Dec.) silicate observations at 250 m. depth. 306
Fig. H17. Winter (Jan.-Mar.) silicate [μmol l^{-1}] at the surface. 307
Fig. H18. Winter (Jan.-Mar.) minus annual silicate [μmol l^{-1}] at the surface. 308
Fig. H19. Winter (Jan.-Mar.) silicate [μmol l^{-1}] at 75 m. depth. 309
Fig. H20. Winter (Jan.-Mar.) minus annual silicate [μmol l^{-1}] at 75 m. depth. 310
Fig. H21. Winter (Jan.-Mar.) silicate [μmol l^{-1}] at 150 m. depth. 311
Fig. H22. Winter (Jan.-Mar.) minus annual silicate [μmol l^{-1}] at 150 m. depth. 312
Fig. H23. Winter (Jan.-Mar.) silicate [μmol l^{-1}] at 250 m. depth. 313
Fig. H24. Winter (Jan.-Mar.) minus annual silicate [μmol l^{-1}] at 250 m. depth. 314
Fig. H25. Spring (Apr.-Jun.) silicate [μmol l^{-1}] at the surface. 315
Fig. H26. Spring (Apr.-Jun.) minus annual silicate [μmol l^{-1}] at the surface. 316
Fig. H27. Spring (Apr.-Jun.) silicate [μmol l^{-1}] at 75 m. depth. 317
Fig. H28. Spring (Apr.-Jun.) minus annual silicate [μmol l^{-1}] at 75 m. depth. 318
Fig. H29. Spring (Apr.-Jun.) silicate [μmol l^{-1}] at 150 m. depth. 319
Fig. H30. Spring (Apr.-Jun.) minus annual silicate [μmol l^{-1}] at 150 m. depth. 320
Fig. H31. Spring (Apr.-Jun.) silicate [μmol l^{-1}] at 250 m. depth. 321
Fig. H32. Spring (Apr.-Jun.) minus annual silicate [μmol l^{-1}] at 250 m. depth. 322
Fig. H33. Summer (Jul.-Sep.) silicate [μmol l^{-1}] at the surface. 323
Fig. H34. Summer (Jul.-Sep.) minus annual silicate [μmol l^{-1}] at the surface. 324
Fig. H35. Summer (Jul.-Sep.) silicate [μmol l^{-1}] at 75 m. depth. 325
Fig. H36. Summer (Jul.-Sep.) minus annual silicate [μmol l^{-1}] at 75 m. depth. 326
Fig. H37. Summer (Jul.-Sep.) silicate [μmol l^{-1}] at 150 m. depth. 327

Fig. H38. Summer (Jul.-Sep.) minus annual silicate [μmol l^{-1}] at 150 m. depth. 328
Fig. H39. Summer (Jul.-Sep.) silicate[μmol l^{-1}] at 250 m. depth. 329
Fig. H40. Summer (Jul.-Sep.) minus annual silicate [μmol l^{-1}] at 250 m. depth. 330
Fig. H41. Fall (Oct.-Dec.) silicate [μmol l^{-1}] at the surface. 331
Fig. H42. Fall (Oct.-Dec.) minus annual silicate [μmol l^{-1}] at the surface. 332
Fig. H43. Fall (Oct.-Dec.) silicate [μmol l^{-1}] at 75 m. depth. 333
Fig. H44. Fall (Oct.-Dec.) minus annual silicate [μmol l^{-1}] at 75 m. depth. 334
Fig. H45. Fall (Oct.-Dec.) silicate [μmol l^{-1}] at 150 m. depth. 335
Fig. H46. Fall (Oct.-Dec.) minus annual silicate [μmol l^{-1}] at 150 m. depth. 336
Fig. H47. Fall (Oct.-Dec.) silicate [μmol l^{-1}] at 250 m. depth. 337
Fig. H48. Fall (Oct.-Dec.) minus annual silicate [μmol l^{-1}] at 250 m. depth. 338

Appendix I: Maps of the monthly number of observations, monthly distribution, and monthly minus annual distribution of silicate at selected depth levels (Pages 339 to 398).

Fig. I1. January silicate observations at the surface 339
Fig. I2. January silicate observations at 75 m. depth. 339
Fig. I3. February silicate observations at the surface 340
Fig. I4. February silicate observations at 75 m. depth. 340
Fig. I5. March silicate observations at the surface 341
Fig. I6. March silicate observations at 75 m. depth. 341
Fig. I7. April silicate observations at the surface 342
Fig. I8. April silicate observations at 75 m. depth. 342
Fig. I9. May silicate observations at the surface. 343
Fig. I10. May silicate observations at 75 m. depth. 343
Fig. I11. June silicate observations at the surface. 344
Fig. I12. June silicate observations at 75 m. depth. 344
Fig. I13. July silicate observations at the surface. 345
Fig. I14. July silicate observations at 75 m. depth. 345
Fig. I15. August silicate observations at the surface. 346
Fig. I16. August silicate observations at 75 m. depth. 346
Fig. I17. September silicate observations at the surface. 347
Fig. I18. September silicate observations at 75 m. depth. 347
Fig. I19. October silicate observations at the surface. 348
Fig. I20. October silicate observations at 75 m. depth 348
Fig. I21. November silicate observations at the surface. 349
Fig. I22. November silicate observations at 75 m. depth 349
Fig. I23. December silicate observations at the surface 350
Fig. I24. December silicate observations at 75 m. depth. 350
Fig. I25. January mean silicate [μmol l^{-1}]] at the surface. 351
Fig. I26. January minus annual silicate [μmol l^{-1}] at the surface. 352
Fig. I27. January mean silicate [μmol l^{-1}] at 75 m. depth. 353
Fig. I28. January minus annual silicate [μmol l^{-1}] at 75 m. depth. 354
Fig. I29. February mean silicate [μmol l^{-1}] at the surface 355
Fig. I30. February minus annual silicate [μmol l^{-1}] at the surface. 356
Fig. I31. February mean silicate [μmol l^{-1}] at 75 m. depth. 357

Fig. I32. February minus annual silicate [μmol l^{-1}] at 75 m. depth. 358
Fig. I33. March mean silicate [μmol l^{-1}] at the surface..... 359
Fig. I34. March minus annual silicate [μmol l^{-1}] at the surface..... 360
Fig. I35. March mean silicate [μmol l^{-1}] at 75 m. depth. 361
Fig. I36. March minus annual silicate [μmol l^{-1}]at 75 m. depth. 362
Fig. I37. April mean silicate [μmol l^{-1}] at the surface..... 363
Fig. I38. April minus annual silicate [μmol l^{-1}] at the surface..... 364
Fig. I39. April mean silicate [μmol l^{-1}] at 75 m. depth. 365
Fig. I40. April minus annual silicate [μmol l^{-1}]] at 75 m. depth. 366
Fig. I41. May mean silicate [μmol l^{-1}] at the surface..... 367
Fig. I42. May minus annual silicate [μmol l^{-1}] at the surface..... 368
Fig. I43. May mean silicate [μmol l^{-1}] at 75 m. depth. 369
Fig. I44. May minus annual silicate [μmol l^{-1}] at 75 m. depth. 370
Fig. I45. June mean silicate [μmol l^{-1}] at the surface..... 371
Fig. I46. June minus annual silicate [μmol l^{-1}] at the surface..... 372
Fig. I47. June mean silicate [μmol l^{-1}] at 75 m. depth. 373
Fig. I48. June minus annual silicate [μmol l^{-1}] at 75 m. depth. 374
Fig. I49. July mean silicate [μmol l^{-1}] at the surface. 375
Fig. I50. July minus annual silicate [μmol l^{-1}] at the surface..... 376
Fig. I51. July mean silicate [μmol l^{-1}] at 75 m. depth..... 377
Fig. I52. July minus annual silicate [μmol l^{-1}] at 75 m. depth. 378
Fig. I53. August mean silicate [μmol l^{-1}] at the surface. 379
Fig. I54. August minus annual silicate [μmol l^{-1}] at the surface..... 380
Fig. I55. August mean silicate [μmol l^{-1}]at 75 m. depth..... 381
Fig. I56. August minus annual silicate [μmol l^{-1}] at 75 m. depth. 382
Fig. I57. September mean silicate [μmol l^{-1}] at the surface..... 383
Fig. I58. September minus annual silicate [μmol l^{-1}] at the surface. 384
Fig. I59. September mean silicate [μmol l^{-1}] at 75 m. depth. 385
Fig. I60. September minus annual silicate [μmol l^{-1}] at 75 m. depth..... 386
Fig. I61. October mean silicate [μmol l^{-1}] at the surface. 387
Fig. I62. October minus annual silicate [μmol l^{-1}] at the surface. 388
Fig. I63. October mean silicate [μmol l^{-1}] at 75 m. depth..... 389
Fig. I64. October minus annual silicate [μmol l^{-1}] at 75 m. depth..... 390
Fig. I65. November mean silicate [μmol l^{-1}] at the surface. 391
Fig. I66. November minus annual silicate [μmol l^{-1}] at the surface. 392
Fig. I67. November mean silicate [μmol l^{-1}] at 75 m. depth..... 393
Fig. I68. November minus annual silicate [μmol l^{-1}] at 75 m. depth..... 394
Fig. I69. December mean silicate [μmol l^{-1}] at the surface..... 395
Fig. I70. December minus annual silicate [μmol l^{-1}] at the surface..... 396
Fig. I71. December mean silicate [μmol l^{-1}] at 75 m. depth..... 397
Fig. I72. December minus annual silicate [μmol l^{-1}] at 75 m. depth. 398

Preface

The oceanographic analyses described by this atlas series expand on earlier works, *e.g.,* the *World Ocean Atlas 2005* (WOA05), *World Ocean Atlas 2001* (WOA01)*, World Ocean Atlas 1998* (WOA98)*, World Ocean Atlas 1994* (WOA94) and *Climatological Atlas of the World Ocean* (Levitus, 1982). Previously published oceanographic objective analyses have proven to be of great utility to the oceanographic, climate research, and operational environmental forecasting communities. Such analyses are used as boundary and/or initial conditions in numerical ocean circulation models and atmosphere-ocean models, for verification of numerical simulations of the ocean, as a form of "sea truth" for satellite measurements such as altimetric observations of sea surface height, for computation of nutrient fluxes by Ekman transport, and for planning oceanographic expeditions.

We continue preparing climatological analyses on a one-degree grid. This is because higher resolution analyses are not justified for all the variables we are working with and we wish to produce a set of analyses for which all variables have been analyzed in the same manner. High-resolution analyses as typified by the work of Boyer *et al.* (2004) will be published separately.

In the acknowledgment section of this publication we have expressed our view that creation of global ocean profile and plankton databases and analyses are only possible through the cooperation of scientists, data managers, and scientific administrators throughout the international scientific community. I would also like to thank my colleagues and the staff of the Ocean Climate Laboratory of NODC for their dedication to the project leading to publication of this atlas series. Their integrity and thoroughness have made this database possible. It is my belief that the development and management of national and international oceanographic data archives is best performed by scientists who are actively working with the historical data.

Sydney Levitus
National Oceanographic Data Center
Silver Spring, MD
March 2010

Acknowledgments

This work was made possible by a grant from the NOAA Climate and Global Change Program which enabled the establishment of a research group at the National Oceanographic Data Center. The purpose of this group is to prepare research quality oceanographic databases, as well as to compute objective analyses of, and diagnostic studies based on, these databases. Support is now from base funds and from the NOAA Climate Program Office.

The data on which this atlas is based are in *World Ocean Database 2009* and are distributed on-line and on DVD by NODC/WDC. Many data were acquired as a result of the IOC/IODE *Global Oceanographic Data Archaeology and Rescue* (GODAR) project, and the IOC/IODE *World Ocean Database* project (WOD). At NODC/WDC, data archaeology and rescue projects were supported with funding from the NOAA Environmental Science Data and Information Management (ESDIM) Program and the NOAA Climate and Global Change Program which has included support from NASA and DOE. Support for some of the regional IOC/GODAR meetings was provided by the Marine Science and Technology (MAST) program of the European Union. The European Community has also provided support for the Mediterranean Data Archeology and Rescue (MEDAR/MEDATLAS) project which has resulted in the inclusion of substantial amounts of ocean profile data from the Mediterranean Sea. Additional Black Sea data have been acquired as a result of a NATO sponsored project.

We acknowledge the scientists, technicians, and programmers who have collected and processed data, those individuals who have submitted data to national and regional data centers as well as the managers and staff at the various data centers. We thank our colleagues at the NODC. Their efforts have made this and similar works possible.

WORLD OCEAN ATLAS 2009
Volume 4: Nutrients
(phosphate, nitrate, silicate)

ABSTRACT

This atlas consists of a description of data analysis procedures and horizontal maps of annual, seasonal, and monthly climatological distribution fields of dissolved inorganic nutrients (phosphate, nitrate, and silicate) at selected standard depth levels of the world ocean on a one-degree latitude-longitude grid. The aim of the maps is to illustrate large-scale characteristics of the distribution of these nutrients as a function of depth. The oceanographic data used to generate these climatological maps were computed by objective analysis of all scientifically quality-controlled historical nutrient data in the *World Ocean Database 2009*. Maps are presented for climatological composite periods (annual, seasonal, monthly, seasonal and monthly difference fields from the annual mean field, and the number of observations) at selected standard depths.

1. INTRODUCTION

The distribution of dissolved inorganic nutrients (DIN) in the world ocean is affected by biochemical (*e.g.,* marine production, respiration, and oxidation of labile organic matter) and physical processes (*e.g.,* water mass renewal and mixing). This atlas includes objective analyses of all scientifically quality-controlled historical dissolved inorganic nutrients (phosphate, nitrate, and silicate; $\mu mol\ l^{-1}$) available in the *World Ocean Database 2009* (WOD09; Boyer *et al.,* 2009). By DIN in this atlas, we mean chemically reactive dissolved inorganic nitrate or nitrate and nitrite (N+N), ortho-phosphate, and ortho-silicic acid or silicate. We present data analysis procedures and horizontal maps showing annual, seasonal, and monthly climatologies and related statistical fields at selected standard depth levels between the surface and the ocean bottom to a maximum depth of 5500 m. This atlas includes a subset of all available maps. The complete set of maps, statistical and objectively analyzed data fields, programs, and documentation are available on Digital Video Disk (DVD) by request to NODC.Services@noaa.gov and on-line at www.nodc.noaa.gov/OC5/indprod.html.

This work is part of the *World Ocean Atlas 2009* (WOA09) series. The WOA09 series include analysis for temperature (Locarnini *et al.,* 2010), salinity (Antonov *et al.,* 2010), dissolved oxygen, Apparent Oxygen Utilization, and oxygen saturation (Garcia *et al.,* 2010a), and nutrients (this work). Climatologies are here defined as climatological data mean oceanographic fields at selected standard depth levels based on the objective analysis of historical oceanographic profiles and selected surface-only data. A profile is defined as a set of measurements for a single variable (nitrate+nitrite, phosphate, *etc*.) at discrete depths taken as an instrument drops or rises vertically in the water column. All climatologies use all available data regardless of year of observation. The annual climatology was calculated using all data regardless of the month in which the observation was made. Seasonal climatologies were calculated using only

data from the defined season (regardless of year). Winter is defined as the months of January, February, and March. Spring is defined as April, May, and June. Summer is defined as July, August, and September. Fall is defined as October, November, and December. Monthly climatologies were calculated using data only from the given month regardless of the day of the month in which the observation was made.

The data used are available from the National Oceanographic Data Center (NODC) and World Data Center (WDC) for Oceanography, Silver Spring, Maryland (Boyer *et al.,* 2009). Large volumes of data have been acquired as a result of the fulfillment of several data management projects including:

a) the Intergovernmental Oceanographic Commission (IOC) Global Oceanographic Data Archaeology and Rescue (GODAR) project (Levitus *et al.,* 2005);

b) the IOC World Ocean Database project (WOD);

c) the IOC Global Temperature Salinity Profile project (GTSPP) (IOC, 1998).

The data used in the WOA09 series have been analyzed in a consistent, objective manner on a one-degree latitude-longitude grid at standard depth levels from the surface to a maximum depth of 5500m. The procedures are identical to those used in the World Ocean Atlas 2005 (WOA05) series (Locarnini *et al.,* 2006; Antonov *et al.,* 2006); Garcia *et al.,* 2006a,b), *World Ocean Atlas 2001* (WOA01) series (Stephens *et al.,* 2002; Boyer *et al.,* 2002; Locarnini *et al.,* 2002; Conkright *et al.,* 2002) and *World Ocean Atlas 1998* (WOA98) series (Antonov *et al.,* 1998 a, b, c; Boyer *et al.,* 1998 a, b, c; Conkright *et al.,* 1998, a, b, c; O'Brien *et al.,* 1998, a, b, c). Slightly different procedures were followed in earlier analyses (Levitus, 1982; *World Ocean Atlas 1994* series [WOA04, Levitus *et al.,* 1994; Levitus and Boyer 1994a, b; Conkright *et al.,* 1994]).

Objective analyses shown in this atlas are limited by the nature of the availability and data quality of the nutrient data base (data are non-uniform in both space and time), characteristics of the objective analysis techniques, and the grid used. These limitations and characteristics are briefly discussed below.

Since the publication of WOA05, substantial amounts of additional historical data have become available. However, even with these additional data, we are still hampered in a number of ways by a lack of DIN data. Because of the lack of data, we are forced to examine the annual cycle by compositing all data regardless of the year of observation. In some areas, quality control is made difficult by the limited number of data collected in these areas. Data may exist in an area for only one season, thus precluding any representative annual analysis. In some areas there may be a reasonable spatial distribution of data points on which to base an analysis, but there may be only a few (perhaps only one) data values in each one-degree latitude-longitude square.

We begin by describing the data sources and data distribution (Section 2). Then we describe the general data processing procedures (Section 3), the results (Section 4), summary (Section 5), and future work (Section 6). The appendices of this atlas include the maps for each nutrient at selected standard depth levels.

2. DATA AND DATA DISTRIBUTION

Data sources and quality control procedures are briefly described below. For further information on the data sources used in WOA09 refer to the *World Ocean Database*

2009 (WOD09, Boyer *et al.,* 2009). The quality control procedures used in preparation of these analyses are described by Johnson *et al.* (2009).

2.1. Data sources

Historical oceanographic nutrient data used in this atlas were obtained from the NODC/WDC archives and include all data gathered as a result of the GODAR and WOD projects (Boyer *et al.,* 2009). The nutrient data used in this atlas were typically obtained by means of analysis of serial (discrete) samples (Garcia *et al.,* 2010b). We refer to the discrete water sample dataset in WOD09 as Ocean Station Data (OSD). Typically, each profile in the OSD dataset consists of 1 to 36 water samples collected at various depths between the surface and the ocean bottom using Nansen or Niskin samplers. Johnson *et al.* (2009) describes the quality control procedures used in preparation of these analyses.

To understand the procedures for taking individual oceanographic observations and constructing climatological fields, definition of the terms "standard level data" and "observed level data" are necessary. We refer to the actual measured value of an oceanographic variable *in situ* (Latin for in place) as an "observation", and to the depth at which such a measurement was made as the "observed level depth". We refer to such data as "observed level data". Before the development of oceanographic instrumentation that measure at high frequencies along the vertical profile, oceanographers often attempted to make measurements at selected "standard levels" in the water column. Sverdrup *et al.* (1942) presented the suggestions of the International Association of Physical Oceanography (IAPSO) as to which depths oceanographic measurements should be made or interpolated to for analysis. Different nations or institutions have a slightly different set of standard depth levels defined. For many purposes, including preparation of the present climatologies, observed level data are interpolated to standard depth levels, if observations did not occur at the desired standard depths. The levels at which the nutrient climatologies were calculated are given in Table 1. Table 2 shows the depths of each standard depth level. Section 3.1 discusses the vertical interpolation procedures used in our work.

2.2. Data quality control

Quality control of the nutrient data is a major task, the difficulty of which is directly related to lack of data and metadata (for some areas) upon which to base statistical checks. Consequently certain empirical criteria were applied (see sections 2.2.1 through 2.2.4), and as part of the last processing step, subjective judgment was used (see sections 2.2.5 and 2.2.6). Individual data, and in some cases entire profiles or all profiles for individual cruises, have been flagged and not used because these data produced features that were subjectively judged to be non-representative or questionable. As part of our work, we have made available WOD09 which contains both observed levels profile data and standard depth level profile data with various quality control flags applied. The flags mark individual nutrient measurements or entire profiles which were not used in the next step of the procedure, either interpolation to standard depth levels for observed level data or calculation of statistical means in the case of standard depth level data.

Our knowledge of the variability of the world ocean based on the instrumental record now includes a greater appreciation and understanding of the ubiquity of eddies, rings, and lenses in some parts of the world ocean as well as inter-annual and inter-decadal variability of water mass properties

associated with modal variability of the atmosphere such as the North Atlantic Oscillation, Pacific Decadal Oscillation, and El Niño Southern Ocean Oscillation. Therefore, we have simply added quality control flags to the nutrient data, not eliminating them from the WOD09. In addition, some data values include the originator's quality flags (*e.g.*, World Ocean Circulation Experiment, CLIVAR repeat hydrography). Thus, individual investigators can make their own decision regarding the representativeness of the data. Investigators studying the distribution of features such as eddies will be interested in those data that we may regard as unrepresentative for the preparation of the analyses shown in this atlas.

2.2.1. Duplicate elimination

Because data are received from many sources, sometimes the same data set is received at NODC/WDC more than once but with slightly different time and/or position and/or data values, and hence are not easily identified as duplicate stations. Therefore, to eliminate the repetitive data values our databases were checked for the presence of exact and near exact replicates using eight different criteria. The first checks involve identifying stations with exact position/date/time and data values; the next checks involve offsets in position/date/time. Profiles identified as duplicates in the checks with a large offset were individually verified to ensure they were indeed duplicate profiles. In summary, we eliminated all but one profile from each set of replicate profiles at the first step of our data processing.

2.2.2. Range and gradient checks

Range checking (*i.e.,*checking whether individual nutrient concentration values are within preset minimum and maximum values as a function of depth and ocean region) was performed on all data values as a first quality control check to flag and withhold from further use the relatively few values that were grossly outside expected oceanic concentration ranges. Range checks were prepared for individual oceanic regions. A check as to whether excessive vertical gradients occur in the data has been performed for each nutrient variable in WOD09 both in terms of positive and negative gradients. Johnson *et al.* (2009) detail the quality control procedures.

2.2.3. Statistical checks

Statistical checks were performed as follows. All data for each nutrient variable (irrespective of year), at each standard depth level, were averaged within five-degree latitude-longitude squares to produce a record of the number of observations, mean, and standard deviation in each square. Statistics were computed for the annual, seasonal, and monthly compositing periods. Below 50 m depth, if data were more than three standard deviations from the mean, the data were flagged and withheld from further use in objective analyses. Above 50 m depth, a five-standard-deviation criterion was used in five-degree squares that contained any land area. In selected five-degree squares that are close to land areas, a four-standard-deviation check was used. In all other squares a three-standard-deviation criterion was used for the 0-50 m depth layer. For standard depth levels situated directly above the ocean bottom, a four-standard-deviation criterion was used.

The reason for the relatively weaker standard deviation criterion in coastal and near-coastal regions is the exceptionally large variability in the coastal five-degree square statistics for some variables. Frequency distributions of some variables in some coastal regions are observed to be skewed or bimodal. Thus to avoid flagging possibly good data in highly variable

environments, the standard deviation criteria were broadened.

For each nutrient variable, the total number of measurements in each profile, as well as the total number of nutrient observations exceeding the standard deviation criterion, were recorded. If more than two nutrient observations in a profile were found to exceed the standard deviation criterion, then the entire profile was flagged. This check was imposed after tests indicated that surface data from particular casts (which upon inspection appeared to be erroneous) were being flagged but deeper data were not. Other situations were found where erroneous nutrient data from the deeper portion of a cast were flagged, while near-surface data from the same cast were not flagged because of larger natural variability in surface layers. One reason for this was the decrease of the number of nutrient observations with depth and the resulting change in sample statistics. The standard-deviation check was applied twice to the data set for each compositing period.

In summary, first the five-degree square statistics were computed, and the data flagging procedure described above was used to provide a preliminary data set. Next, new five-degree-square statistics were computed from this preliminary data set and used with the same statistical check to produce a new, "clean" data set. The reason for applying the statistical check twice was to flag (and withhold from further use), in the first round, any grossly erroneous or non-representative data from the data set that would artificially increase the variances. The second check is then more effective in identifying smaller, but non-representative, observations.

2.2.4. Subjective flagging of data

The nutrient data were averaged by one-degree squares for input to the objective analysis program. After initial objective analyses were computed, the input set of one-degree means still contained questionable data contributing to unrealistic distributions, yielding intense bull's-eyes or spatial gradients. Examination of these features indicated that some of them were due to profiles from particular oceanographic cruises. In such cases, data from an entire cruise were flagged and withheld from further use by setting a flag on each profile from the cruise. In other cases, individual profiles or measurements were found to cause these features and were flagged.

2.2.5. Representativeness of the data

Another quality control issue is nutrient data representativeness. The general paucity of data forces the compositing of all historical nutrient data to produce "climatological" fields. In a given one-degree square, there may be data from a month or season of one particular year, while in the same or a nearby square there may be data from an entirely different year. If there is large interannual variability in a region where scattered sampling in time has occurred, then one can expect the analysis to reflect this. Because the observations are scattered randomly with respect to time, except for a few limited areas (*i.e.*, time series stations such as Hawaii Ocean Time Series, Bermuda Atlantic Time Series, CARIACO), the results cannot, in a strict sense, be considered a true long-term climatological average.

We present smoothed analyses of historical means, based (in certain areas) on relatively few observations. We believe, however, that useful information about the oceans can be gained through our procedures and that the large-scale features are representative of the real ocean. We believe that, if a hypothetical global synoptic set of ocean data (temperature, salinity, dissolved oxygen, nutrients, *etc*) existed and one were to

smooth these data to the same degree as we have smoothed the historical means overall, the large-scale features would be similar to our results. Some differences would certainly occur because of interannual-to-decadal-scale variability.

The nutrient observations diminish in number with increasing depth. In the upper ocean, the all-data annual mean distributions are reasonable for defining large-scale features, but for the seasonal and monthly periods, the data base is inadequate in some regions. With respect to the deep ocean, in some areas the distribution of observations may be adequate for some diagnostic computations but inadequate for other purposes. If an isolated deep basin or some region of the deep ocean has only one observation, then no horizontal gradient computations are meaningful. However, useful information is provided by the observation in the computation of other quantities (*e.g.*, a volumetric mean over a major ocean basin).

3. DATA PROCESSING PROCEDURES

3.1. Vertical interpolation to standard levels

Vertical interpolation of observed depth level data to standard depth levels followed procedures in JPOTS Editorial Panel (1991). These procedures are in part based on the work of Reiniger and Ross (1968). Four observed depth level values surrounding the standard depth level value were used, two values from above the standard level and two values from below the standard level. The pair of values furthest from the standard level are termed "exterior" points and the pair of values closest to the standard level are termed "interior" points. Paired parabolas were generated via Lagrangian interpolation. A reference curve was fitted to the four data points and used to define unacceptable interpolations caused by "overshooting" in the interpolation. When there were too few data points above or below the standard level to apply the Reiniger and Ross technique, we used a three-point Lagrangian interpolation. If three points were not available (either two above and one below or vice-versa), we used linear interpolation. In the event that an observation occurred exactly at the depth of a standard level, then a direct substitution was made. Table 2 provides the range of acceptable distances for which observed level data could be used for interpolation to a standard level.

3.2. Methods of analysis

3.2.1. Overview

An objective analysis scheme of the type described by Barnes (1964) was used to produce the fields shown in this atlas. This scheme had its origins in the work of Cressman (1959). In *World Ocean Atlas 1994* (WOA94), the Barnes (1973) scheme was used. This required only one "correction" to the first-guess field at each grid point in comparison to the successive correction method of Cressman (1959) and Barnes (1964). This was to minimize computing time used in the processing. Barnes (1994) recommends a return to a multi-pass analysis when computing time is not an issue. Based on our own experience we agree with this assessment. The single pass analysis, used in WOA94, caused an artificial front in the Southeastern Pacific Ocean in a data sparse area (Anne Marie Treguier, personal communication). The analysis scheme used in generating WOA98, WOA01, WOA05, and WOA09 analyses uses a three-pass "correction" which does not result in the creation of this artificial front.

Inputs to the analysis scheme were one-degree square means of data values at

standard levels (for time period and variable being analyzed), and a first-guess value for each square. For instance, one-degree square means for our annual analysis were computed using all available data regardless of date of observation. For July, we used all historical July data regardless of year of observation.

Analysis was the same for all standard depth levels. Each one-degree latitude-longitude square value was defined as being representative of its square. The 360x180 gridpoints are located at the intersection of half-degree lines of latitude and longitude. An influence radius was then specified. At those grid points where there was an observed mean value, the difference between the mean and the first-guess field was computed. Next, a correction to the first-guess value at all gridpoints was computed as a distance-weighted mean of all gridpoint difference values that lie within the area around the gridpoint defined by the influence radius. Mathematically, the correction factor derived by Barnes (1964) is given by the expression:

$$C_{i,j} = \frac{\sum_{s=1}^{n} W_s Q_s}{\sum_{s=1}^{n} W_s} \qquad (1)$$

in which:

(i,j) - coordinates of a gridpoint in the east-west and north-south directions respectively;

$C_{i,j}$ - the correction factor at gridpoint coordinates (i,j);

n - the number of observations that fall within the area around the point i,j defined by the influence radius;

Q_s - the difference between the observed mean and the first-guess at the S^{th} point in the influence area;

$W_s = e^{-\frac{Er^2}{R^2}}$ (for $r \le R$; W_s =0 for $r > R$);

r - distance of the observation from the gridpoint;

R - influence radius;

$E = 4$.

The derivation of the weight function, W_s, will be presented in the following section. At each gridpoint we computed an analyzed value $G_{i,j}$ as the sum of the first-guess, $F_{i,j}$, and the correction $C_{i,j}$. The expression for this is

$$G_{i,j} = F_{i,j} + C_{i,j} \qquad (2)$$

If there were no data points within the area defined by the influence radius, then the correction was zero, the first-guess field was left unchanged, and the analyzed value was simply the first-guess value. This correction procedure was applied at all gridpoints to produce an analyzed field. The resulting field was first smoothed with a median filter (Tukey, 1974; Rabiner *et al.,* 1975) and then smoothed with a five-point smoother of the type described by Shuman (1957) (hereafter referred as five-point Shuman smoother). The choice of first-guess fields is important and we discuss our procedures in section 3.2.5.

The analysis scheme is set up so that the influence radius, and the number of five-point smoothing passes can be varied with each iteration. The strategy used is to begin the analysis with a large influence radius and decrease it with each iteration. This technique allows us to analyze progressively smaller scale phenomena with each iteration.

The analysis scheme is based on the work of several researchers analyzing meteorological data. Bergthorsson and Doos (1955) computed corrections to a first-guess field using various techniques: one assumed that the difference between a first-guess value

and an analyzed value at a gridpoint was the same as the difference between an observation and a first-guess value at a nearby observing station. All the observed differences in an area surrounding the gridpoint were then averaged and added to the gridpoint first-guess value to produce an analyzed value. Cressman (1959) applied a distance-related weight function to each observation used in the correction in order to give more weight to observations that occur closest to the gridpoint. In addition, Cressman introduced the method of performing several iterations of the analysis scheme using the analysis produced in each iteration as the first-guess field for the next iteration. He also suggested starting the analysis with a relatively large influence radius and decreasing it with successive iterations so as to analyze smaller scale phenomena with each pass.

Sasaki (1960) introduced a weight function that was specifically related to the density of observations, and Barnes (1964, 1973) extended the work of Sasaki. The weight function of Barnes (1964) has been used here. The objective analysis scheme we used is in common use by the mesoscale meteorological community. Several studies of objective analysis techniques have been made. Achtemeier (1987) examined the "concept of varying influence radii for a successive corrections objective analysis scheme." Seaman (1983) compared the "objective analysis accuracies of statistical interpolation and successive correction schemes." Smith and Leslie (1984) performed an "error determination of a successive correction type objective analysis scheme." Smith *et al*. (1986) made "a comparison of errors in objectively analyzed fields for uniform and non-uniform station distribution."

3.2.2. Derivation of Barnes (1964) weight function

The principle upon which the Barnes (1964) weight function is derived is that "the two-dimensional distribution of an atmospheric variable can be represented by the summation of an infinite number of independent harmonic waves, that is, by a Fourier integral representation". If *f(x,y)* is the variable, then in polar coordinates *(r,θ)*, a smoothed or filtered function *g(x,y)* can be defined:

$$g(x,y)=\frac{1}{2\pi}\int_0^{2\pi}\int_0^{\infty}\eta f(x+r\cos\theta, y+r\sin\theta)\, d\left(\frac{r^2}{4K}\right)d\theta \qquad (3)$$

in which r is the radial distance from a gridpoint whose coordinates are *(x,y)*. The weight function is defined as

$$\eta = e^{-\frac{r^2}{4K}} \qquad (4)$$

which resembles the Gaussian distribution. The shape of the weight function is determined by the value of K, which relates to the distribution of data. The determination of K follows. The weight function has the property that

$$\frac{1}{2\pi}\int_0^{2\pi}\int_0^{\infty}\eta\, d\left(\frac{r^2}{4K}\right)d\theta = 1 \qquad (5)$$

This property is desirable because in the continuous case (3) the application of the weight function to the distribution *f(x,y)* will not change the mean of the distribution. However, in the discrete case (1), we only sum the contributions to within the distance R. This introduces an error in the evaluation of the filtered function, because the condition given by (5) does not apply. The error can be pre-determined and set to a reasonably small value in the following

manner. If one carries out the integration in (5) with respect to θ, the remaining integral can be rewritten as

$$\int_0^R \eta d\left(\frac{r^2}{4K}\right) + \int_R^\infty \eta d\left(\frac{r^2}{4K}\right) = 1 \qquad (6)$$

Defining the second integral as ε yields

$$\int_0^R e^{-\frac{r^2}{4K}} d\left(\frac{r^2}{4K}\right) = 1 - \varepsilon \qquad (7)$$

Integrating (7), we obtain

$$\varepsilon = e^{-\frac{R^2}{4K}} \qquad (7a)$$

Taking the natural logarithm of both sides of (7a) leads to an expression for K,

$$K = R^2 / 4E \qquad (7b)$$

where $E \equiv -\ln \varepsilon$

Rewriting (4) using (7b) leads to the form of weight function used in the evaluation of (1). Thus, choice of E and the specification of R determine the shape of the weight function. Levitus (1982) chose E=4 which corresponds to a value of ε of approximately 0.02. This choice implies with respect to (7) the representation of more than 98 percent of the influence of any data around the gridpoint in the area defined by the influence radius R. This analysis (WOA09) and previous analyses (WOA94, WOA98, WOA01, WOA05, WOA09) used E=4.

Barnes (1964) proposed using this scheme in an iterative fashion similar to Cressman (1959). Levitus (1982) used a four-iteration scheme with a variable influence radius for each pass. WOA94 used a one-iteration scheme. WOA98, WOA01, WOA05, and WOA09 employed a three-iteration scheme with a variable influence radius.

3.2.3. Derivation of Barnes (1964) response function

It is desirable to know the response of a data set to the interpolation procedure applied to it. Following Barnes (1964) and reducing to one-dimensional case we let

$$f(x) = A \sin(\alpha x) \qquad (8)$$

in which $\alpha = 2\pi/\lambda$ with λ being the wavelength of a particular Fourier component, and substitute this function into equation (3) along with the expression for η in equation (4). Then

$$g(x) = D\left[A \sin(\alpha x)\right] = Df(x) \qquad (9)$$

in which D is the response function for one application of the analysis and defined as

$$D = e^{-\left(\frac{\alpha R}{4}\right)^2} = e^{-\left(\frac{\pi R}{2\lambda}\right)^2}$$

The phase of each Fourier component is not changed by the interpolation procedure. The results of an analysis pass are used as the first-guess for the next analysis pass in an iterative fashion. The relationship between the filtered function $g(x)$ and the response function after N iterations as derived by Barnes (1964) is

$$g_N(x) = f(x) D \sum_{n=1}^{N} (1 - D)^{n-1} \qquad (10)$$

Equation (10) differs trivially from that given by Barnes. The difference is due to our first-guess field being defined as a zonal average, annual mean, seasonal mean, or monthly mean, whereas Barnes used the first application of the analysis as a first-guess. Barnes (1964) also showed that applying the analysis scheme in an iterative fashion will result in convergence of the analyzed field to the observed data field. However, it is not desirable to approach the observed data too closely, because at least seven or eight gridpoints are needed to represent a Fourier component.

The response function given in (10) is useful in two ways: it is informative to know what Fourier components make up the analyses, and the computer programs used in generating the analyses can be checked for correctness by comparison with (10).

3.2.4. Choice of response function

The distribution of nutrient observations (see appendices) at different depths and for the different averaging periods, are not regular in space or time. At one extreme, regions exist in which every one-degree square contains data and no interpolation needs to be performed. At the other extreme are regions in which few if any data exist. Thus, with variable data spacing the average separation distance between gridpoints containing data is a function of geographical position and averaging period. However, if we computed and used a different average separation distance for each variable at each depth and each averaging period, we would be generating analyses in which the wavelengths of observed phenomena might differ from one depth level to another and from one season to another. In WOA94, a fixed influence radius of 555 kilometers was used to allow uniformity in the analysis of all variables. For the present analyses (as well as for WOA98 and WOA01), a three-pass analysis, based on Barnes (1964), with influence radii of 888, 666 and 444 km was used.

Inspection of (1) shows that the difference between the analyzed field and the first-guess field values at any gridpoint is proportional to the sum of the weighted-differences between the observed mean and first-guess at all gridpoints containing data within the influence area.

The reason for using the five-point Shuman smoother and the median smoother is that our data are not evenly distributed in space. As the analysis moves from regions containing data to regions devoid of data, small-scale discontinuities may develop. The five-point Shuman and median smoothers are used to eliminate these discontinuities. The five-point Shuman smoother does not affect the phase of the Fourier components that comprise an analyzed field.

The response function for the analyses presented in the WOA10 series is given in Table 4 and in Figure 1. For comparison purposes, the response function used by Levitus (1982), WOA94, and others are also presented. The response function represents the smoothing inherent in the objective analysis described above plus the effects of one application of the five-point Shuman smoother and one application of a five-point median smoother. The effect of varying the amount of smoothing in North Atlantic sea surface temperature (SST) fields has been quantified by Levitus (1982) for a particular case. In a region of strong SST gradient such as the Gulf Stream, the effect of smoothing can easily be responsible for differences between analyses exceeding 1.0°C.

To avoid the problem of the influence region extending across land or sills to adjacent basins, the objective analysis routine employs basin "identifiers" to preclude the use of data from adjacent basins. Table 5 lists these basins and the depth at which no exchange of information between basins is allowed during the objective analysis of data, *i.e.,*"depths of mutual exclusion." Some regions are nearly, but not completely, isolated topographically. Because some of these nearly isolated basins have water mass properties that are different from surrounding basins, we have chosen to treat these as isolated basins as well. Not all such basins have been identified because of the complicated structure of the sea floor. In Table 5, a region marked with an "*" can interact with adjacent basins except for special areas such as the Isthmus of Panama.

3.2.5. First-guess field determination

There are gaps in the data coverage and, in some parts of the world ocean, there exist adjacent basins whose water mass properties are individually nearly homogeneous but have distinct basin-to basin differences. Spurious features can be created when an influence area extends over two basins of this nature (basins are listed in Table 5). Our choice of first-guess field attempts to minimize the creation of such features. To provide a first-guess field for the annual analysis at any standard level, we first zonally averaged the observed nutrient data variables in each one-degree latitude belt by individual ocean basins. The annual analysis was then used as the first-guess for each seasonal analysis and each seasonal analysis was used as a first-guess for the appropriate monthly analysis if computed.

We then reanalyzed the data for each nutrient variable using the newly produced analyses as first-guess fields described as follows and as shown in Figure 2. The new annual mean for each nutrient was computed as the mean of the twelve months at all depths, from the surface to 500 m depth (the maximum depth for seasonal and monthly climatologies for these variables). This new annual mean was used as the first-guess field for new seasonal analyses. These new seasonal analyses in turn were used to produce new monthly analyses. This procedure produces slightly smoother means. More importantly we recognize that fairly large data-void regions exist, in some cases to such an extent that a seasonal or monthly analysis in these regions is not meaningful. Geographic distribution of observations for the all-data annual periods (see appendices) is good for the upper layers of the ocean. By using an all-data annual mean, first-guess field regions where data exists for only one season or month will show no contribution to the annual cycle. By contrast, if we used a zonal average for each season or month, then, in those latitudes where gaps exist, the first-guess field would be heavily biased by the few data points that exist. If these were anomalous data in some way, an entire basin-wide belt might be affected.

One advantage of producing "global" fields for a particular compositing period (even though some regions are data void) is that such analyses can be modified by investigators for use in modeling studies. For example, England (1992) noted that the temperature distribution produced by Levitus (1982) for the Antarctic is too high (due to a lack of winter data for the Southern Hemisphere) to allow for the formation of Antarctic Intermediate Water in an ocean general circulation model. By increasing the temperature of the "observed" field the model was able to produce this water mass.

3.3. Choice of objective analysis procedures

Optimum interpolation (Gandin, 1963) has been used by some investigators to objectively analyze oceanographic data. We recognize the power of this technique but have not used it to produce analyzed fields. As described by Gandin (1963), optimum interpolation is used to analyze synoptic data using statistics based on historical data. In particular, second-order statistics such as correlation functions are used to estimate the distribution of first order parameters such as means. We attempt to map most fields in this atlas based on relatively sparse data sets. By necessity we must composite all nutrient data regardless of year of observation, to have enough data to produce a global, hemispheric, or regional analysis for a particular month, season, or even yearly. Because of the paucity of nutrient data, we prefer not to use an analysis scheme that is based on second order statistics. In addition, as Gandin has noted, there are two limiting cases associated with optimum interpolation.

The first is when a data distribution is dense. In this case, the choice of interpolation scheme makes little difference. The second case is when data are sparse. In this case, an analysis scheme based on second order statistics is of questionable value. For additional information on objective analysis procedures see Thiebaux and Pedder (1987) and Daley (1991).

3.4. Choice of spatial grid

The analyses that comprise WOA10 have been computed using the ETOPO5 land-sea topography to define ocean depths at each gridpoint (ETOPO5, 1988). From the ETOPO5 land mask, a quarter-degree land mask was created based on ocean bottom depth and land criteria. If four or more 5-minute square values out of a possible nine in a one-quarter-degree box were defined as land, then the quarter-degree gridbox was defined to be land. If no more than two of the 5-minute squares had the same depth value in a quarter-degree box, then the average value of the 5-minute ocean depths in that box was defined to be the depth of the quarter-degree gridbox. If three or more 5-minute squares out of the nine had a common bottom depth, then the depth of the quarter-degree box was set to the most common depth value. The same method was used to go from a quarter-degree to a one-degree resolution. In the one-degree resolution case, at least four points out of a possible sixteen (in a one-degree square) had to be land in order for the one-degree square to remain land and three out of sixteen had to have the same depth for the ocean depth to be set. These criteria yielded a mask that was then modified by:

a) Connecting the Isthmus of Panama,

b) Maintaining an opening in the Straits of Gibraltar and in the English Channel,

c) Connecting the Kamchatka Peninsula and the Baja Peninsula to their respective continents.

4. RESULTS

The appendices in this atlas include three types of black and white horizontal maps as a function of selected standard depth levels for phosphate, nitrate, and silicate, respectively:

a) Number of observations in each one-degree latitude-longitude grid used in the objective analysis binned into 1 to 5 and greater than 5 numbers of observations. Each map includes the total number of observations.

b) Objectively analyzed distribution fields. One-degree grids for which there were less than three values available in the objective analysis defined by the influence radius are denoted by a "+" symbol.

c) Seasonal and monthly difference fields from the annual mean field. One-degree grids for which there were less than three values available in the objective analysis defined by the influence radius are denoted by a "+" symbol.

The maps are arranged by composite time periods (annual, seasonal, month). Table 5 describes all available nutrient maps and data fields. The table of contents includes a list of maps included in the appendices. We note that the complete set of all maps (in color), objectively analyzed fields, associated statistical fields at all standard depth levels shown in Table 1 on DVD by sending an e-mail request to NODC.Services@noaa.gov and on-line at www.nodc.noaa.gov/OC5/indprod.html.

The maps use consistent symbols and notations for displaying information. Continents are displayed as solid black areas. Coastal and open ocean areas shallower than the standard depth level

being displayed are shown as solid light gray areas. The objectively analyzed fields include the minimum and maximum values and the contour interval used. The maps may include additional contour lines displayed as dashed black lines. All of the maps were computer drafted using Generic Mapping Tools (Wessel and Smith, 1998).

We describe next the computation of annual and seasonal fields (section 4.1) and available objective and statistical fields (section 4.2).

4.1. Computation of annual and seasonal fields

After completion of all of our analyses we define a final annual analysis as the average of our twelve monthly mean nutrient fields in the upper 500 m of the ocean (Figure 2). Our final seasonal analysis is defined as the average of monthly analyses in the upper 500 m of the ocean.

4.2. Available statistical fields

Table 5 lists all statistical fields calculated as part of this atlas. Climatologies of oceanographic variables and associated statistics described in this document, as well as global figures can be obtained on DVD by sending an e-mail request to NODC.Services@noaa.gov and on-line at http://www.nodc.noaa.gov/OC5/WOD09/pr_wod09.html.

The sample standard deviation in a gridbox was computed using:

$$s = \sqrt{\frac{\sum_{n=1}^{N}(x_n - \bar{x})^2}{N-1}} \qquad (11)$$

in which x_n= the n^{th} data value in the gridbox, $\bar{x}$=mean of all data values in the gridbox, and N= total number of data values in the gridbox. The standard error of the mean was computed by dividing the standard deviation by the square root of the number of observations in each gridbox.

In addition to statistical fields, the land/ocean bottom mask and basin definition mask are available on-line at http://www.nodc.noaa.gov/OC5/WOD09/pr_wod09.html. A user could take the standard depth level data from WOD09 with flags and these masks, and recreate the data fields following the procedures outlined in this document. Explanations and data file formats are found on-line under documentation on the WOA09 webpage.

4.3. Obtaining WOA09 fields online

The objective and statistical data fields can be obtained online in different digital formats at the WOA09 webpage (http://www.nodc.noaa.gov/OC5/WOA09/pr_woa09.html) and on DVD by sending a request to NODC.Services@noaa.gov. The WOA09 fields can be obtained in ASCII format (WOA native and comma separated value [CSV]) and netCDF through our WOA09 web page. For users interested in specific geographic areas, the World Ocean Atlas Select (WOAselect) selection tool can be used to designate a subset geographic area, depth, and oceanographic variable to view and optionally download climatological means or related statistics in shapefile format which is compatible with GIS software such as ArcMap. WOA09 includes a digital collection of "JPEG" and high resolution graphic (PDF) images of the objective and statistical fields. In addition, WOA09 can be obtained in Ocean Data View (ODV) format (http://odv.awi.de/). WOA09 will be available through other online locations as well. WOA98, WOA01, and WOA05 are presently served through the IRI/LDEO Climate Data Library with access to statistical and objectively analyzed fields in a variety of digital formats (http://iridl.ldeo.columbia.edu/).

5. SUMMARY

In the preceding sections we have described the results of a project to objectively analyze all historical nutrient data in WOD09. We desire to build a set of climatological analyses that are identical in all respects for all variables in WOA09 including relatively data sparse variables such as nutrients. This provides investigators with a consistent set of analyses to work with.

One advantage of the analysis techniques used in this atlas is that we know the amount of smoothing by objective analyses as given by the response function in Table 3 and Figure 1. We believe this to be an important function for constructing and describing a climatology of any parameter. Particularly when computing anomalies from a standard climatology, it is important that the field be smoothed to the same extent as the climatology, to prevent generation of spurious anomalies simply through differences in smoothing. A second reason is that purely diagnostic computations require a minimum of seven or eight gridpoints to represent any Fourier component. Higher order derivatives might require more data smoothing.

We have attempted to create objectively analyzed fields and data sets that can be used as a "black box." We emphasize that some quality control procedures used are subjective. For those users who wish to make their own choices, all the data used in our analyses are available both at standard depth levels as well as observed depth levels (http://www.nodc.noaa.gov/OC5/WOD09/pr_wod09.html). The results presented in this nutrient atlas show some features that are suspect and may be due to non-representative data that were not flagged by the quality control techniques used. Although we have attempted to eliminate as many of these "features" as possible by flagging the data which generate these features, some obviously could remain. Some may eventually turn out not to be artifacts but rather to represent real features, not yet capable of being described in a meaningful way due to lack of data. If any errors are found in this atlas, or for providing comments or suggestions please contact the Ocean Climate Laboratory (OCL) at OCL.help@noaa.gov. The views, findings, and any errors in this report are those of the authors.

6. FUTURE WORK

Our analyses will be updated when justified by additional water column nutrient observations. As more oceanographic nutrient data are received at NODC/WDC, we will also be able to extend the seasonal and monthly nutrient analysis to deeper levels and also to increase the number of vertical depth levels.

7. REFERENCES

Achtemeier, G. L., 1987. On the concept of varying influence radii for a successive corrections objective analysis. *Mon. Wea. Rev.,* 11, 1761-1771.

Antonov, J. I., R. A. Locarnini, T. P. Boyer, A. V. Mishonov, and H. E. Garcia, 2010. World Ocean Atlas 2009, Volume 2: Salinity. S. Levitus, Ed., NOAA Atlas NESDIS 69, U.S. Gov. Printing Office, Washington, D.C., 184 pp.

Antonov, J. I., R. A. Locarnini, T. P. Boyer, A. V. Mishonov, and H. E. Garcia, 2006. World Ocean Atlas 2005, Volume 2: Salinity. S. Levitus, Ed. NOAA Atlas NESDIS 62, U.S. Gov. Printing Office, Washington, D.C., 182 pp.

Antonov, J. I., S. Levitus, T. P. Boyer, M. E. Conkright, T. D. O' Brien, and C. Stephens, 1998a: *World Ocean Atlas*

1998. Vol. 1: Temperature of the Atlantic Ocean. NOAA Atlas NESDIS 27, U.S. Gov. Printing Office, Washington, D.C., 166 pp.

Antonov, J. I., S. Levitus, T. P. Boyer, M. E. Conkright, T.D. O' Brien, and C. Stephens, 1998b: *World Ocean Atlas 1998. Vol. 2: Temperature of the Pacific Ocean.* NOAA Atlas NESDIS 28, U.S. Gov. Printing Office, Washington, D.C., 166 pp.

Antonov, J. I., S. Levitus, T. P. Boyer, M. E. Conkright, T. D. O' Brien, C. Stephens, and B. Trotsenko, 1998c: *World Ocean Atlas 1998. Vol. 3: Temperature of the Indian Ocean.* NOAA Atlas NESDIS 29, U.S. Gov. Printing Office, Washington, D.C., 166 pp.

Antonov, J. I., R. A. Locarnini, T. P. Boyer, H.E. Garcia, and A.V.Mishonov, 2006: *World Ocean Atlas 2005, Vol. 2: Salinity*. S. Levitus, Ed., NOAA Atlas NESDIS 62, U.S. Gov. Printing Office, Washington, D.C. 182 pp.

Barnes, S. L., 1964. A technique for maximizing details in numerical weather map analysis. *J. App. Meteor.*, 3, 396-409.

Barnes, S. L., 1973. Mesoscale objective map analysis using weighted time series observations. NOAA Technical Memorandum ERL NSSL-62, 60 pp.

Barnes, S. L., 1994. Applications of the Barnes Objective Analysis Scheme, Part III: Tuning for Minimum Error. *J. Atmosph. and Oceanic Tech*. 11:1459-1479.

Bergthorsson, P. and B. Doos, 1955. Numerical Weather map analysis. *Tellus*, 7, 329-340.

Boyer, T. P., J. I. Antonov , O. K. Baranova, H. E. Garcia, D. R. Johnson, R. A. Locarnini, A. V. Mishonov, T. D. O'Brien, D. Seidov, I. V. Smolyar, M. M. Zweng, 2009. World Ocean Database 2009. S. Levitus, Ed., NOAA Atlas NESDIS 66, U.S. Gov. Printing Office, Wash., D.C., 219 pp., DVDs.

Boyer, T. P., S. Levitus, J. I. Antonov, M. E. Conkright, T. D. O' Brien, and C. Stephens, 1998a: *World Ocean Atlas 1998 Vol. 4: Salinity of the Atlantic Ocean*. NOAA Atlas NESDIS 30, U.S. Gov. Printing Office, Washington, D.C., 166 pp.

Boyer, T. P., S. Levitus, J. I. Antonov, M. E. Conkright, T. D. O' Brien, and C. Stephens, 1998b: *World Ocean Atlas 1998 Vol. 5: Salinity of the Pacific Ocean.* NOAA Atlas NESDIS 31, U.S. Gov. Printing Office, Washington, D.C., 166 pp.

Boyer, T. P., S. Levitus, J. I. Antonov, M. E. Conkright, T. D. O' Brien, C. Stephens, and B. Trotsenko, 1998c: *World Ocean Atlas 1998 Vol. 6: Salinity of the Indian Ocean*. NOAA Atlas NESDIS 32, U.S. Gov. Printing Office, Washington, D.C., 166 pp.

Boyer, T. P., C. Stephens, J. I. Antonov, M. E. Conkright, R. A. Locarnini, T. D. O'Brien, H. E. Garcia, 2002: *World Ocean Atlas 2001, Vol. 2: Salinity*. S. Levitus, Ed., NOAA Atlas NESDIS 50, U.S. Gov. Printing Office, Washington D.C., 165 pp.

Boyer, T. P, S. Levitus, H. E. Garcia, R. A. Locarnini, C. Stephens, and J. I. Antonov, 2004. Objective Analyses of Annual, Seasonal, and Monthly Temperature and Salinity for the World Ocean on a ¼ degree Grid, *International J. of Climatology*, 25, 931-945.

Boyer, T. P., J. I. Antonov, H. E. Garcia, D. R. Johnson, R.A. Locarnini, A.V. Mishonov, M. T. Pitcher, O. K. Baranova, and I.V. Smolyar, 2006. *World Ocean Database 2005*. S. Levitus, Ed., NOAA Atlas NESDIS 60, U.S. Gov. Printing Office, Washington, D.C., 190 pp

Conkright, M. E., S. Levitus, and T. Boyer, 1994: *World Ocean Atlas 1994, Vol. 1:*

Nutrients. NOAA Atlas NESDIS 1, U.S. Gov. Printing Office, Washington, D.C., 150 pp.

Conkright, M. E., T. D. O' Brien, S. Levitus, T. P. Boyer, J. I. Antonov, and C. Stephens, 1998a: *World Ocean Atlas 1998 Vol. 10: Nutrients and Chlorophyll of the Atlantic Ocean.* NOAA Atlas NESDIS 36, U.S. Gov. Printing Office, Washington, D.C., 245 pp.

Conkright, M. E., T. D. O' Brien, S. Levitus, T.P. Boyer, J.I. Antonov, and C. Stephens, 1998b: *World Ocean Atlas 1998 Vol. 11: Nutrients and Chlorophyll of the Pacific Ocean.* NOAA Atlas NESDIS 37, U.S. Gov. Printing Office, Washington, D.C., 245 pp.

Conkright, M. E., T. D. O' Brien, S. Levitus, T. P. Boyer, J. I. Antonov, and C. Stephens, 1998c: *World Ocean Atlas 1998 Vol. 12: Nutrients and Chlorophyll of the Indian Ocean.* NOAA Atlas NESDIS 38, U.S. Gov. Printing Office, Washington, D.C., 245 pp.

Conkright, M. E., H. E. Garcia, T. D. O'Brien, R. A. Locarnini, T. P. Boyer, C. Stephens, and J .I. Antonov, 2002: *World Ocean Atlas 2001, Vol. 4: Nutrients*. S. Levitus, Ed., NOAA Atlas NESDIS 52, U.S. Gov. Printing Office, Washington, D.C., 392 pp.

Cressman, G. P., 1959. An operational objective analysis scheme. *Mon. Wea. Rev.*, 87, 329-340.

Daley, R., 1991. *Atmospheric Data Analysis.* Cambridge University Press, Cambridge, 457 pp.

England, M. H., 1992. On the formation of Antarctic Intermediate and Bottom Water in Ocean general circulation models. *J. Phys. Oceanogr., 22, 918- 926.*

ETOPO5, 1988. Data Announcements 88-MGG-02, Digital relief of the Surface of the Earth. NOAA, National Geophysical Data Center, Boulder, CO.

Gandin, L. S., 1963. *Objective Analysis of Meteorological fields*. Gidrometeorol Izdat, Leningrad (translation by Israel program for Scientific Translations, Jerusalem, 1966, 242 pp.

Garcia, H. E., R. A. Locarnini, T. P. Boyer, and J. I. Antonov, 2010a. World Ocean Atlas 2009, Volume 3: Dissolved Oxygen, Apparent Oxygen Utilization, and Oxygen Saturation. S. Levitus, Ed. NOAA Atlas NESDIS 70, U.S. Gov. Printing Office, Washington, D.C., 344 pp.

Garcia, H. E., J. I. Antonov, O. K. Baranova, T. P. Boyer, D. R. Johnson, R. A. Locarnini, A. V. Mishonov, D.; Seidov, M. Zweng, and I.V. Smolyar, 2010b. *Chapter 2*: OSD-Ocean Station Data, Low-resolution CTD, Low resolution XCTD, and Plankton Tows, *In*: Boyer *et al.* (2009).

Garcia, H. E., R. A. Locarnini, T. P. Boyer, and J. I. Antonov, 2006a. World Ocean Atlas 2005, Volume 3: Dissolved Oxygen, Apparent Oxygen Utilization, and Oxygen Saturation. S. Levitus, Ed., NOAA Atlas NESDIS 63, U.S. Gov. Printing Office, Washington, D.C., 342 pp.

Garcia, H. E., R. A. Locarnini, T. P. Boyer, and J. I. Antonov, 2006b World Ocean Atlas 2005, Volume 4: Nutrients (phosphate, nitrate, silicate). S. Levitus, Ed., NOAA Atlas NESDIS 64, U.S. Gov. Printing Office, Washington, D.C., 396 pp.

IOC, 1998. *Global Temperature-Salinity Profile Programme (GTSPP) – Overview and Future*. IOC Technical Series, 49, Intergovernmental Oceanographic Commission, Paris, 12 pp.

JPOTS (Joint Panel on Oceanographic Tables and Standards) Editorial Panel, 1991. Processing of Oceanographic Station Data. UNESCO, Paris, 138 pp.

Johnson, D. R., T. P. Boyer, H. E. Garcia, R. A. Locarnini, O. K. Baranova, and M. M.

Zweng, 2009. World Ocean Database 2009 Documentation. Edited by Sydney Levitus. NODC Internal Report 20, NOAA Printing Office, Silver Spring, MD, 175 pp.

Levitus, S., 1982. *Climatological Atlas of the World Ocean,* NOAA Professional Paper No. 13, U.S. Gov. Printing Office, 173 pp.

Levitus, S. and T. P. Boyer, 1994a: *World Ocean Atlas 1994, Vol. 2: Oxygen*. NOAA Atlas NESDIS 2, U.S. Gov. Printing Office, Washington, D.C., 186 pp.

Levitus, S. and T. P. Boyer, 1994b: *World Ocean Atlas 1994, Vol. 4: Temperature*. NOAA Atlas NESDIS 4, U.S. Gov. Printing Office, Washington, D.C., 117 pp.

Levitus, S., R. Burgett, and T. P. Boyer, 1994: *World Ocean Atlas 1994, Vol. 3: Salinity*. NOAA Atlas NESDIS 3, U.S. Gov. Printing Office, Washington, D.C., 99 pp.

Levitus, S., S. Sato, C. Maillard, N. Mikhailov, P. Caldwell, and H. Dooley, 2005, *Building Ocean Profile-Plankton Databases for Climate and Ecosystem Research*, NOAA Technical Report NESDIS 117, U.S. Gov. Printing Office, Washington, D.C., 29 pp.

Locarnini, R. A., A. V. Mishonov, J. I. Antonov, T. P. Boyer, and H. E. Garcia, 2010. World Ocean Atlas 2009, Volume 1: Temperature. S. Levitus, Ed., NOAA Atlas NESDIS 68, U.S. Gov. Printing Office, Washington, D.C., 184 pp.

Locarnini, R. A., A. V. Mishonov, J. I. Antonov, T. P. Boyer, and H. E. Garcia, 2006. World Ocean Atlas 2005, Volume 1: Temperature. S. Levitus, Ed., NOAA Atlas NESDIS 61, U.S. Gov. Printing Office, Washington, D.C., 182 pp.

Locarnini, R. A., T. D. O'Brien, H. E. Garcia, J. I. Antonov, T. P. Boyer, M. E. Conkright, and C. Stephens, 2002: *World Ocean Atlas 2001, Vol. 3: Oxygen*. S. Levitus, Ed., NOAA Atlas NESDIS 51, U.S. Gov. Printing Office, Washington, D.C., 286 pp.

Locarnini, R. A., A. V. Mishonov, J. I. Antonov, T. P. Boyer, and H. E. Garcia, 2006: *World Ocean Atlas 2005, Vol. 1: Temperature*. S. Levitus, Ed., NOAA Atlas NESDIS 61, U.S. Gov. Printing Office, Washington, D.C., 182 pp.

O' Brien, T. D., S. Levitus, T. P. Boyer, M. E. Conkright, J. I. Antonov, and C. Stephens, 1998a: *World Ocean Atlas 1998 Vol. 7: Oxygen of the Atlantic Ocean*. NOAA Atlas NESDIS 33, U.S. Gov. Printing Office, Washington, D.C., 234 pp.

O' Brien, T. D., S. Levitus, T. P. Boyer, M. E. Conkright, J. I. Antonov, and C. Stephens, 1998b: *World Ocean Atlas 1998 Vol. 8: Oxygen of the Pacific Ocean.* NOAA Atlas NESDIS 34, U.S. Gov. Printing Office, Washington, D.C., 234 pp.

O' Brien, T. D., S. Levitus, T. P. Boyer, M. E. Conkright, J.I. Antonov, and C. Stephens, 1998c: *World Ocean Atlas 1998 Vol. 9: Oxygen of the Indian Ocean.* NOAA Atlas NESDIS 35, U.S. Gov. Printing Office, Washington, D.C., 234 pp.

Rabiner, L. R., M. R. Sambur, and C. E. Schmidt, 1975. *Applications of a nonlinear smoothing algorithm to speech processing, IEEE Trans. on Acoustics, Speech and Signal Processing*, 23, 552-557.

Reiniger, R .F. and C. F. Ross, 1968. A method of interpolation with application to oceanographic data. *Deep-Sea Res.*, 9, 185-193.

Sasaki, Y., 1960. An objective analysis for determining initial conditions for the primitive equations. Ref. 60-1 6T, Atmospheric Research Lab., Univ. of

Oklahoma Research Institute, Norman, 23 pp.

Seaman, R. S., 1983. Objective Analysis accuracies of statistical interpolation and successive correction schemes. *Australian Meteor. Mag.*, 31, 225-240.

Shuman, F. G., 1957. Numerical methods in weather prediction: II. Smoothing and filtering. *Mon. Wea. Rev.*, 85, 357-361.

Smith, D. R., and F. Leslie, 1984. Error determination of a successive correction type objective analysis scheme. *J Atm. and Oceanic Tech.*, 1, 121-130.

Smith, D. R., M. E. Pumphry, and J. T. Snow, 1986. A comparison of errors in objectively analyzed fields for uniform and nonuniform station distribution, *J. Atm. Oceanic Tech.*, 3, 84-97.

Stephens, C., J. I. Antonov, T. P. Boyer, M. E. Conkright, R. A. Locarnini, T.D. O'Brien, and H.E. Garcia, 2002: *World Ocean Atlas 2001, Vol. 1: Temperature*. S. Levitus, Ed., NOAA Atlas NESDIS 49, U.S. Gov. Printing Office, Washington**,** D.C**.,** 167 pp.

Sverdrup, H. U., M. W. Johnson, and R. H. Fleming, 1942. *The Oceans: Their physics, chemistry, and general biology.* Prentice Hall, 1060 pp.

Thiebaux, H .J. and M. A. Pedder, 1987. *Spatial Objective Analysis: with applications in atmospheric science*. Academic Press, 299 pp.

Tukey, J. W., 1974. Nonlinear (nonsuperposable) methods for smoothing data, in *"Cong. Rec."*, 1974 EASCON, 673 pp.

Wessel, P., and W. H. F. Smith., 1998, New, improved version of Generic Mapping Tools released, *EOS Trans. Amer. Geophys. U.*, 79, 579.

Table 1. Descriptions of climatologies for each nutrient variable in WOA09. The climatologies have been calculated based on bottle data (OSD) from WOD09. The standard depth levels are shown in Table 2.

Oceanographic Variable	Depths For Annual Climatology	Depths For Seasonal Climatology	Depths For Monthly Climatology
Nitrate (N+N), Phosphate, and Silicate	0-5500 m (33 levels)	0-500 m (14 levels)	0-500 m (14 levels)

Table 2. Acceptable distances (m) for defining interior and exterior values used in the Reiniger-Ross scheme for interpolating observed level data to standard levels.

Standard Level number	Standard depths (m)	Acceptable distances (m) for interior values	Acceptable distances (m) for exterior values
1	0	5	200
2	10	50	200
3	20	50	200
4	30	50	200
5	50	50	200
6	75	50	200
7	100	50	200
8	125	50	200
9	150	50	200
10	200	50	200
11	250	100	200
12	300	100	200
13	400	100	200
14	500	100	400
15	600	100	400
16	700	100	400
17	800	100	400
18	900	200	400
19	1000	200	400
20	1100	200	400
21	1200	200	400
22	1300	200	1000
23	1400	200	1000
24	1500	200	1000
25	1750	200	1000
26	2000	1000	1000
27	2500	1000	1000
28	3000	1000	1000
29	3500	1000	1000
30	4000	1000	1000
31	4500	1000	1000
32	5000	1000	1000
33	5500	1000	1000

Table 3. Response function of the objective analysis scheme as a function of wavelength for WOA09 and earlier analyses. Response function is normalized to 1.0.

Wavelength*	Levitus (1982)	WOA94	WOA98, 01, 05, 09
360ΔX	1.000	0.999	1.000
180ΔX	1.000	0.997	0.999
120ΔX	1.000	0.994	0.999
90ΔX	1.000	0.989	0.998
72ΔX	1.000	0.983	0.997
60ΔX	1.000	0.976	0.995
45ΔX	1.000	0.957	0.992
40ΔX	0.999	0.946	0.990
36ΔX	0.999	0.934	0.987
30ΔX	0.996	0.907	0.981
24ΔX	0.983	0.857	0.969
20ΔX	0.955	0.801	0.952
18ΔX	0.923	0.759	0.937
15ΔX	0.828	0.671	0.898
12ΔX	0.626	0.532	0.813
10ΔX	0.417	0.397	0.698
9ΔX	0.299	0.315	0.611
8ΔX	0.186	0.226	0.500
6ΔX	3.75×10^{-2}	0.059	0.229
5ΔX	1.34×10^{-2}	0.019	0.105
4ΔX	1.32×10^{-3}	2.23×10^{-3}	2.75×10^{-2}
3ΔX	2.51×10^{-3}	1.90×10^{-4}	5.41×10^{-3}
2ΔX	5.61×10^{-7}	5.30×10^{-7}	1.36×10^{-6}

For ΔX = 111 km, the meridional separation at the Equator.

Table 4. Basins defined for objective analysis and the shallowest standard depth level for which each basin is defined.

#	Basin	Standard Depth Level	#	Basin	Standard Depth Level
1	Atlantic Ocean	1*	30	North American Basin	29
2	Pacific Ocean	1*	31	West European Basin	29
3	Indian Ocean	1*	32	Southeast Indian Basin	29
4	Mediterranean Sea	1*	33	Coral Sea	29
5	Baltic Sea	1	34	East Indian Basin	29
6	Black Sea	1	35	Central Indian Basin	29
7	Red Sea	1	36	Southwest Atlantic Basin	29
8	Persian Gulf	1	37	Southeast Atlantic Basin	29
9	Hudson Bay	1	38	Southeast Pacific Basin	29
10	Southern Ocean	1*	39	Guatemala Basin	29
11	Arctic Ocean	1	40	East Caroline Basin	30
12	Sea of Japan	1	41	Marianas Basin	30
13	Kara Sea	8	42	Philippine Sea	30
14	Sulu Sea	10	43	Arabian Sea	30
15	Baffin Bay	14	44	Chile Basin	30
16	East Mediterranean	16	45	Somali Basin	30
17	West Mediterranean	19	46	Mascarene Basin	30
18	Sea of Okhotsk	19	47	Crozet Basin	30
19	Banda Sea	23	48	Guinea Basin	30
20	Caribbean Sea	23	49	Brazil Basin	31
21	Andaman Basin	25	50	Argentine Basin	31
22	North Caribbean	26	51	Tasman Sea	30
23	Gulf of Mexico	26	52	Atlantic Indian Basin	31
24	Beaufort Sea	28	53	Caspian Sea	1
25	South China Sea	28	54	Sulu Sea II	14
26	Barents Sea	28	55	Venezuela Basin	14
27	Celebes Sea	25	56	Bay of Bengal	1*
28	Aleutian Basin	28	57	Java Sea	6
29	Fiji Basin	29	58	East Indian Atlantic Basin	32

Basins marked with a "" can interact with adjacent basins in the objective analysis.

Table 5. Objective and statistical data fields calculated as part of WOA09 ("√"denotes field was calculated and is publicly available).

Statistical Field	One-Degree Field Calculated	Five-Degree Field Calculated
Objectively analyzed climatology	√	
Statistical mean	√	√
Number of observations	√	√
Seasonal (monthly) climatology minus annual climatology	√	
Standard deviation from statistical mean	√	√
Standard error of the statistical mean	√	√
Statistical mean minus objectively analyzed climatology	√	
Number of mean values within radius of influence	√	

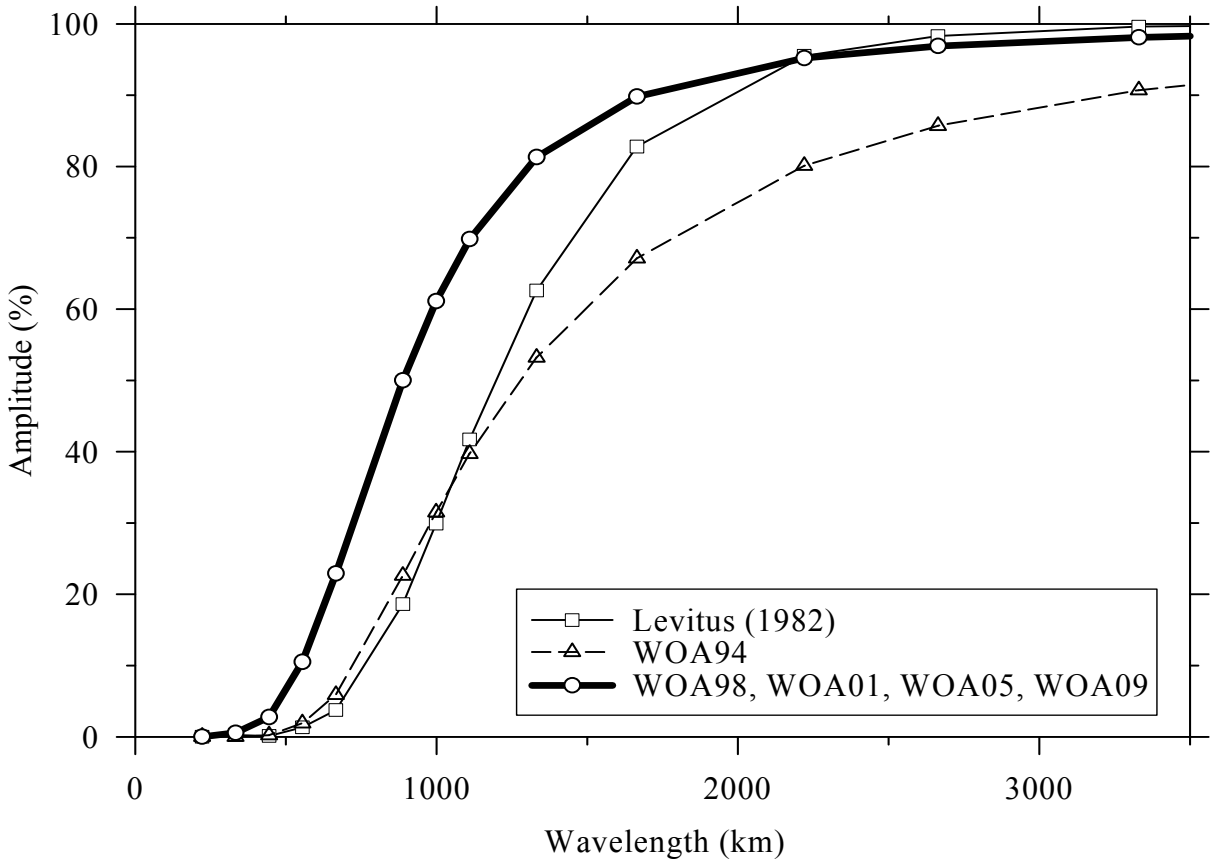

Figure 1. Response function of the WOA09, WOA05, WOA01, WOA98, WOA94, and Levitus (1982) objective analysis schemes.

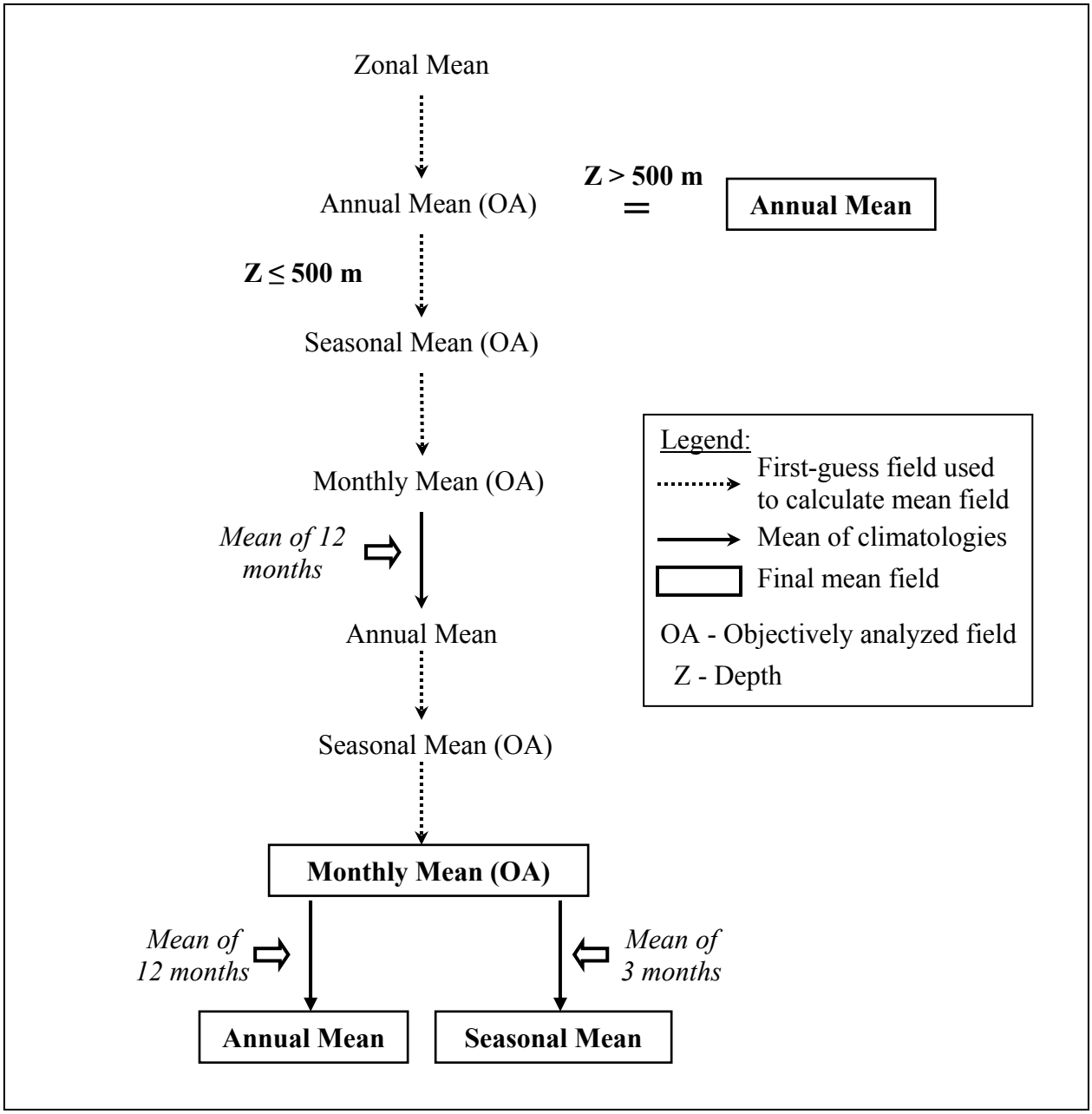

Figure 2. Scheme used in computing annual, seasonal, and monthly objectively analyzed means for phosphate, silicate, and nitrate.

8. APPENDICES

8.1 Appendix A: Maps of the annual number of observations and distribution of phosphate at selected depth levels (pages 25 to 48).

8.2 Appendix B: Maps of the seasonal (winter, summer, fall, spring) number of observations, seasonal distribution, and seasonal minus annual distribution of phosphate at selected depth levels (pages 49 to 88).

8.3 Appendix C: Maps of the monthly number of observations, monthly distribution, and monthly minus annual distribution of phosphate at selected depth levels (pages 88 to 147).

8.4 Appendix D: Maps of the annual number of observations of nitrate at selected depth levels (pages 149 to 172).

8.5 Appendix E: Maps of the seasonal (winter, summer, fall, spring) number of observations, seasonal distribution, and seasonal minus annual distribution of nitrate at selected depth levels (pages 173 to 212).

8.6 Appendix F: Maps of the monthly number of observations, monthly distribution, and monthly minus annual distribution of nitrate at selected depth levels (pages 213 to 272).

8.7 Appendix G: Maps of the annual number of observations of silicate at selected depth levels (pages 273 to 296).

8.8 Appendix H: Maps of the seasonal (winter, summer, fall, spring) number of observations, seasonal distribution, and seasonal minus annual distribution of silicate at selected depth levels (pages 297 to 336).

8.9 Appendix I: Maps of the monthly number of observations, monthly distribution, and monthly minus annual distribution of silicate at selected depth levels (pages 337 to 396).

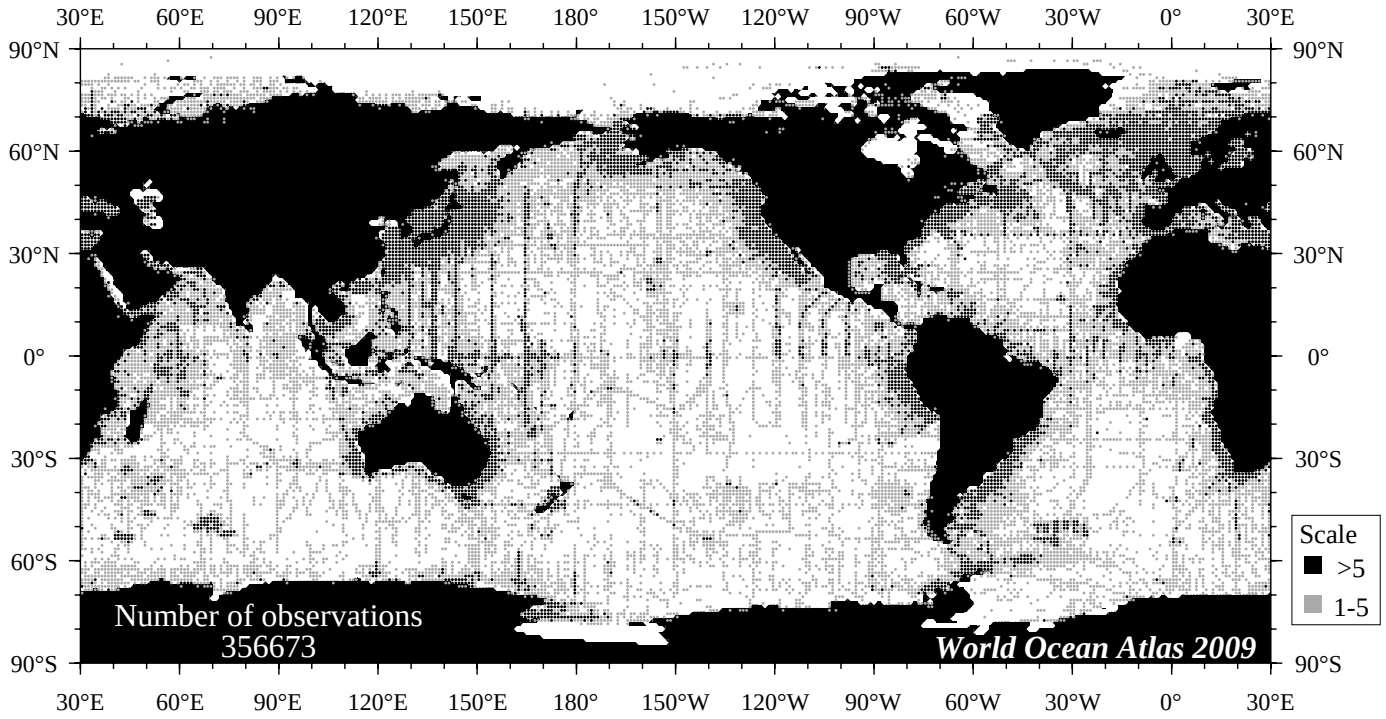

Fig A1 Annual phosphate observations at the surface.

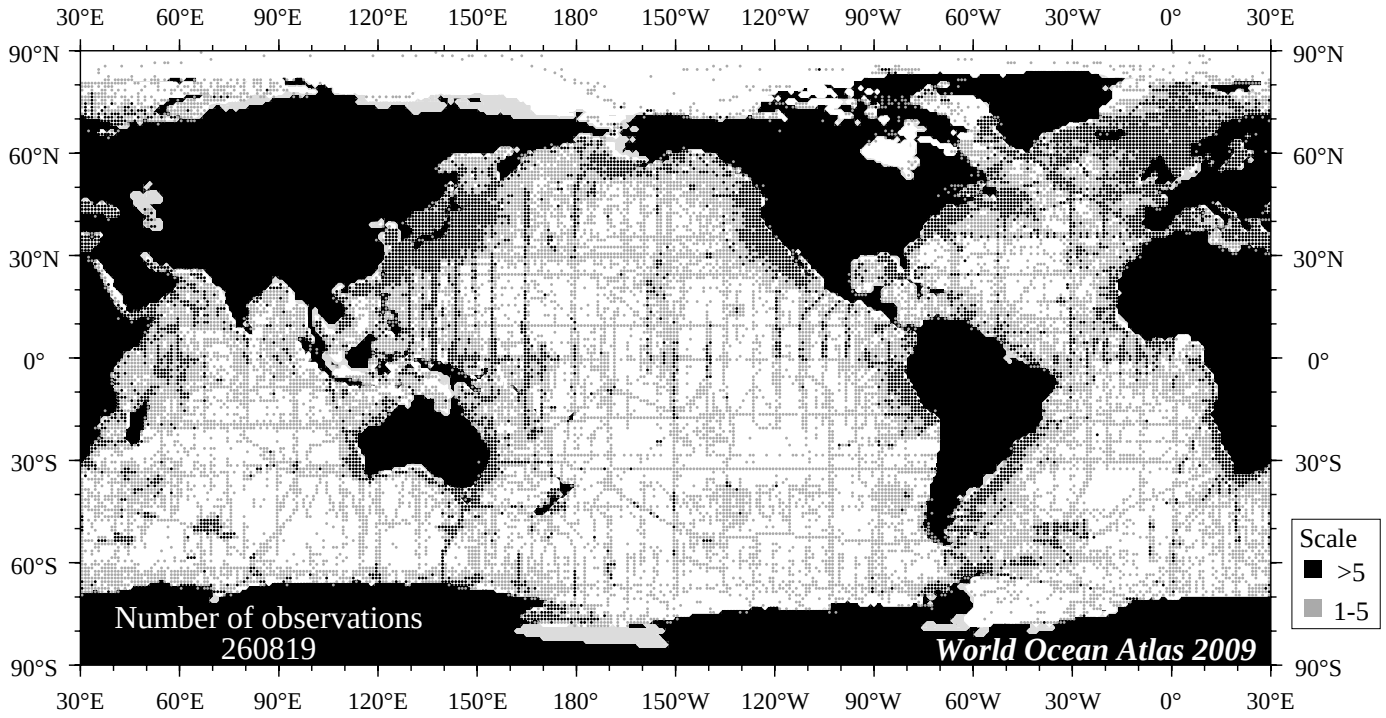

Fig A2 Annual phosphate observations at 50 m. depth.

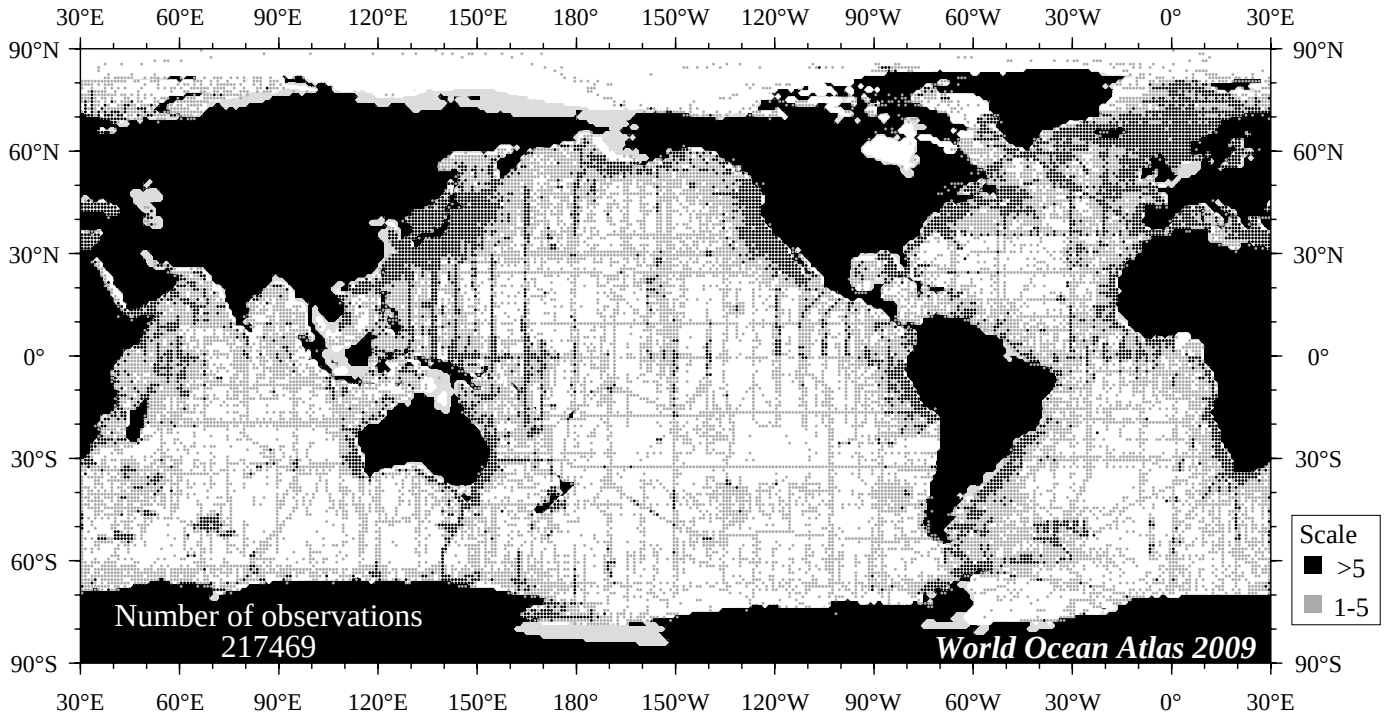

Fig A3 Annual phosphate observations at 75 m. depth.

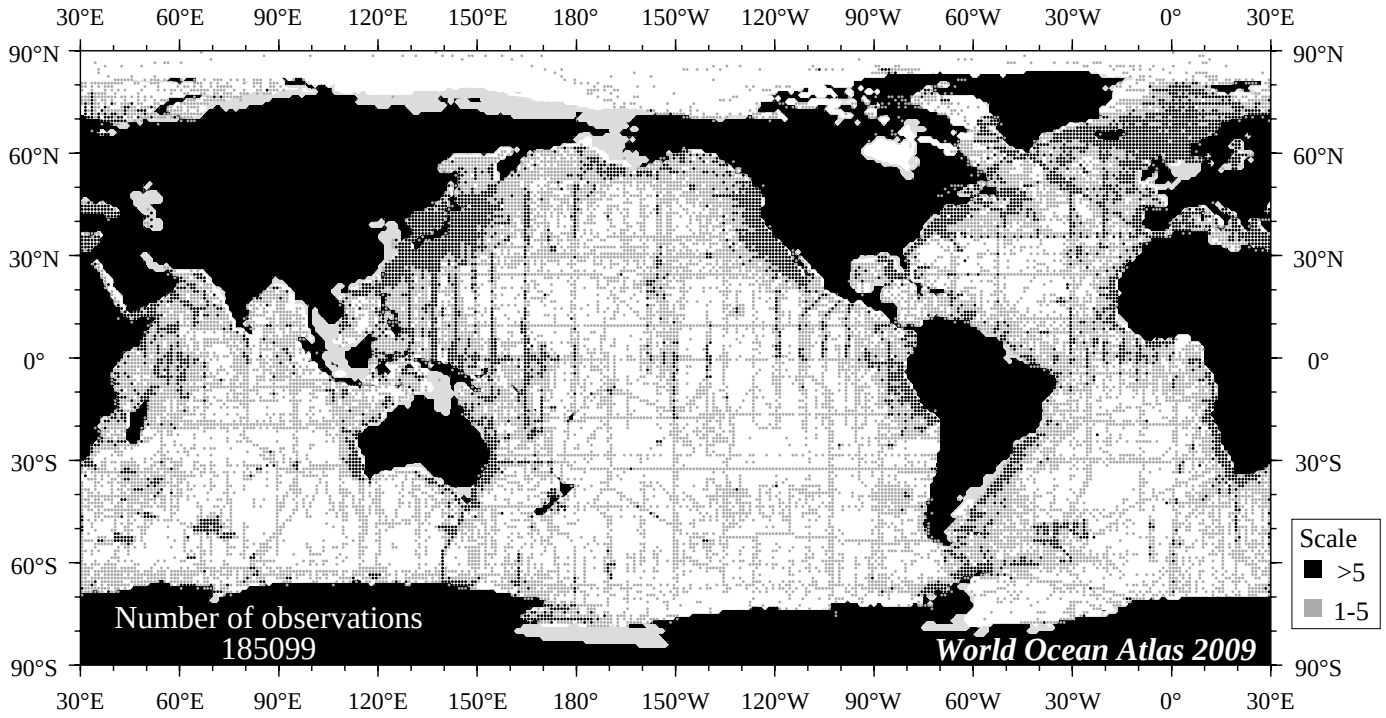

Fig A4 Annual phosphate observations at 100 m. depth.

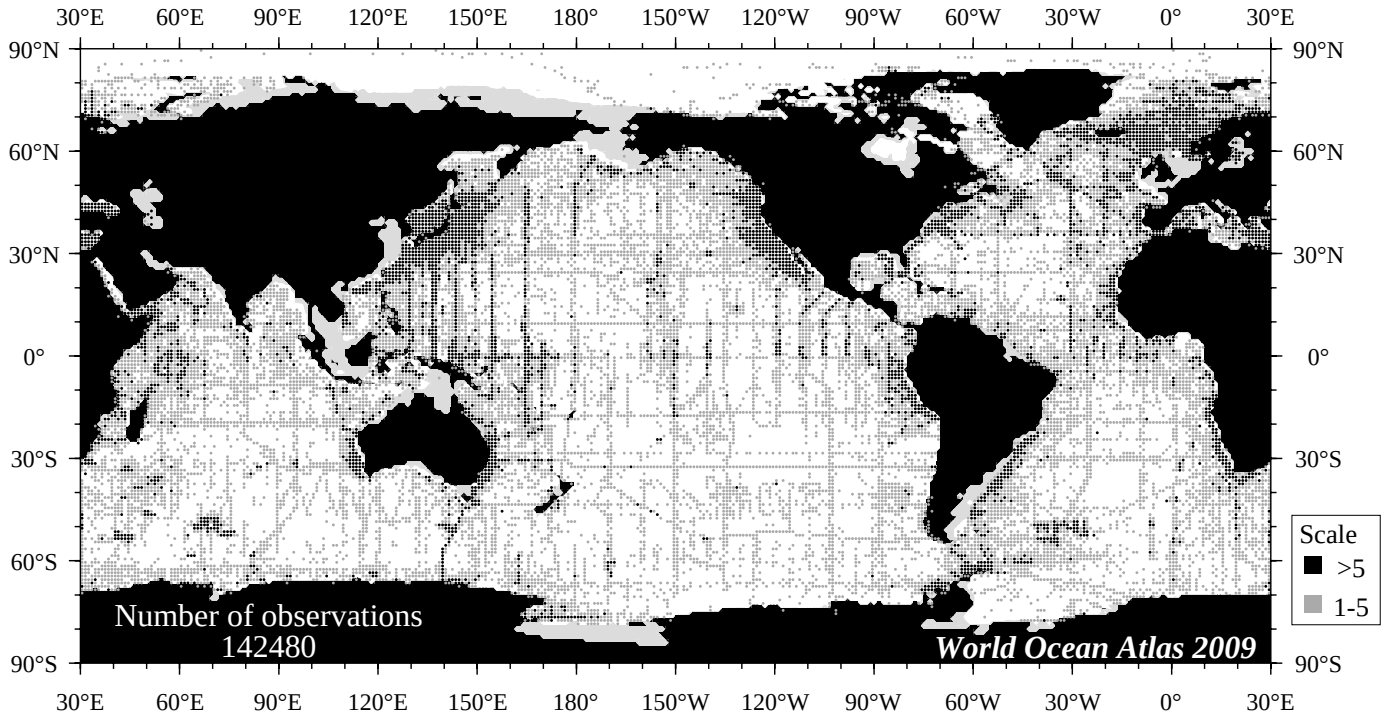

Fig A5 Annual phosphate observations at 150 m. depth.

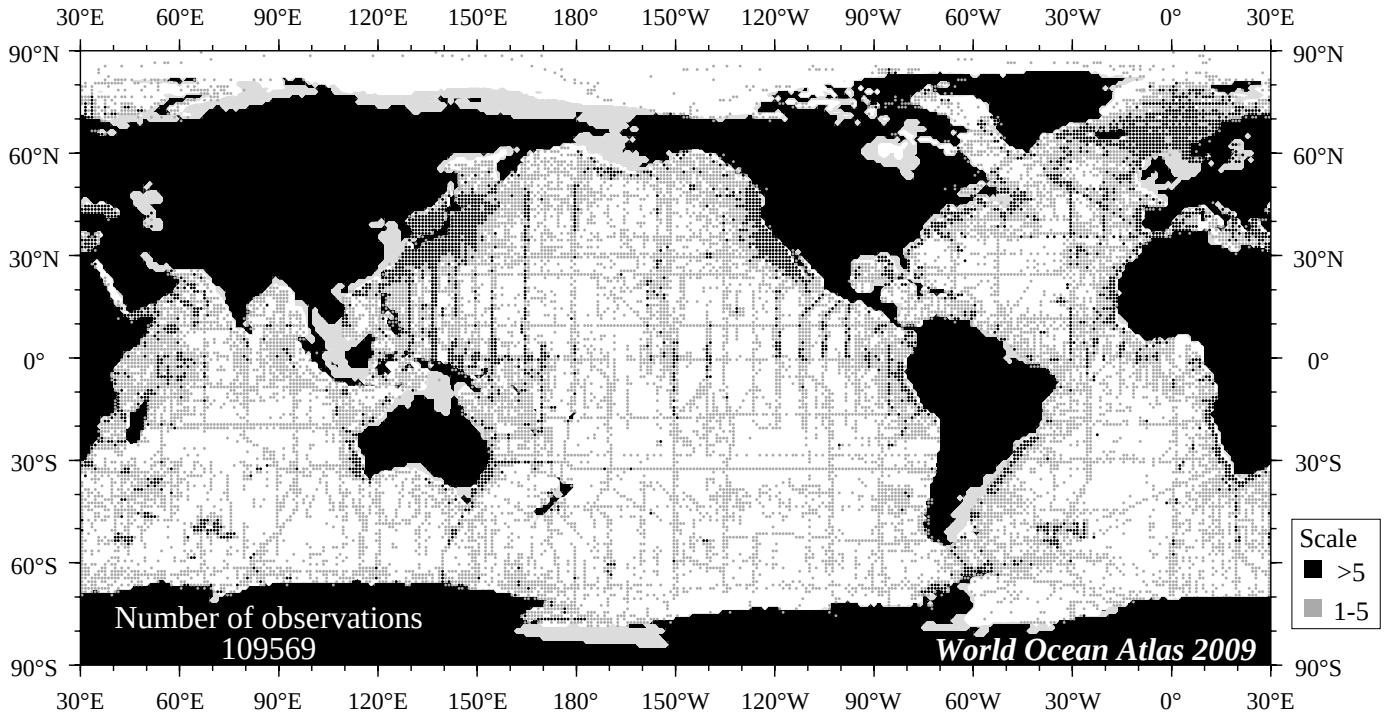

Fig A6 Annual phosphate observations at 200 m. depth.

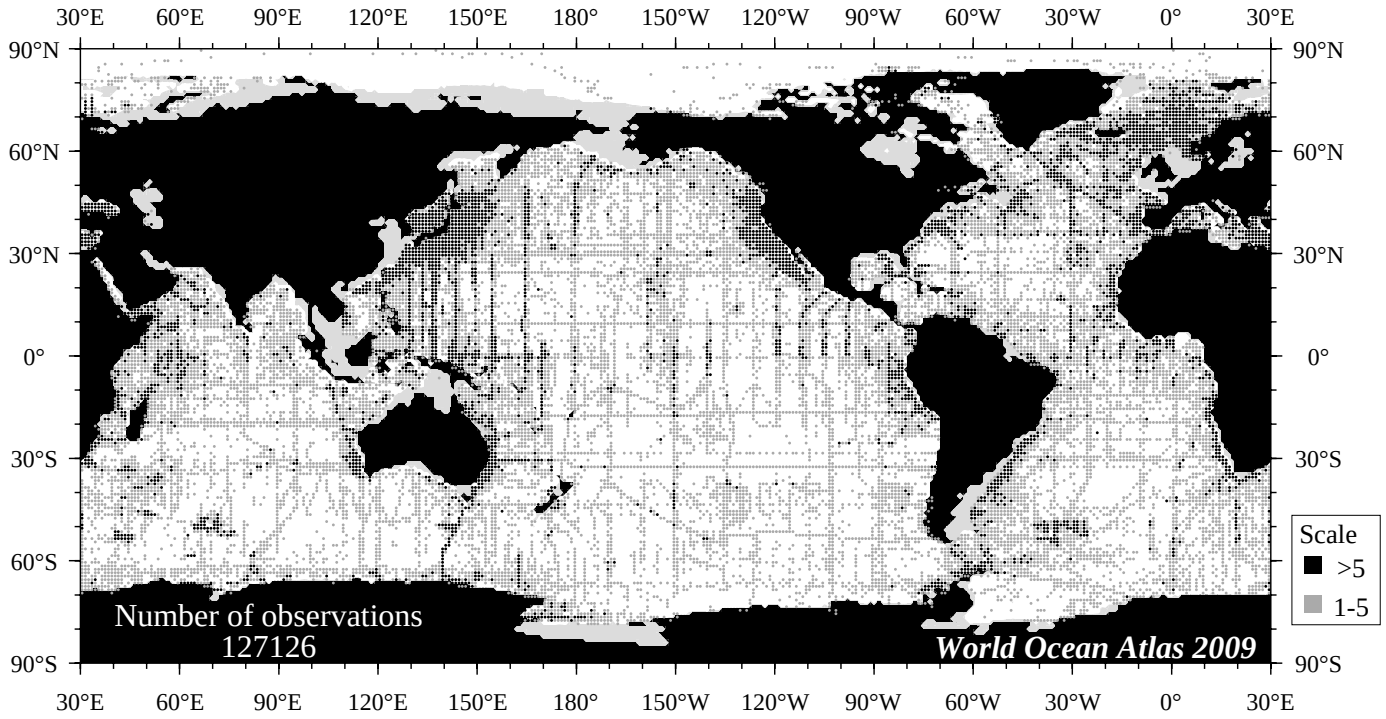

Fig A7 Annual phosphate observations at 250 m. depth.

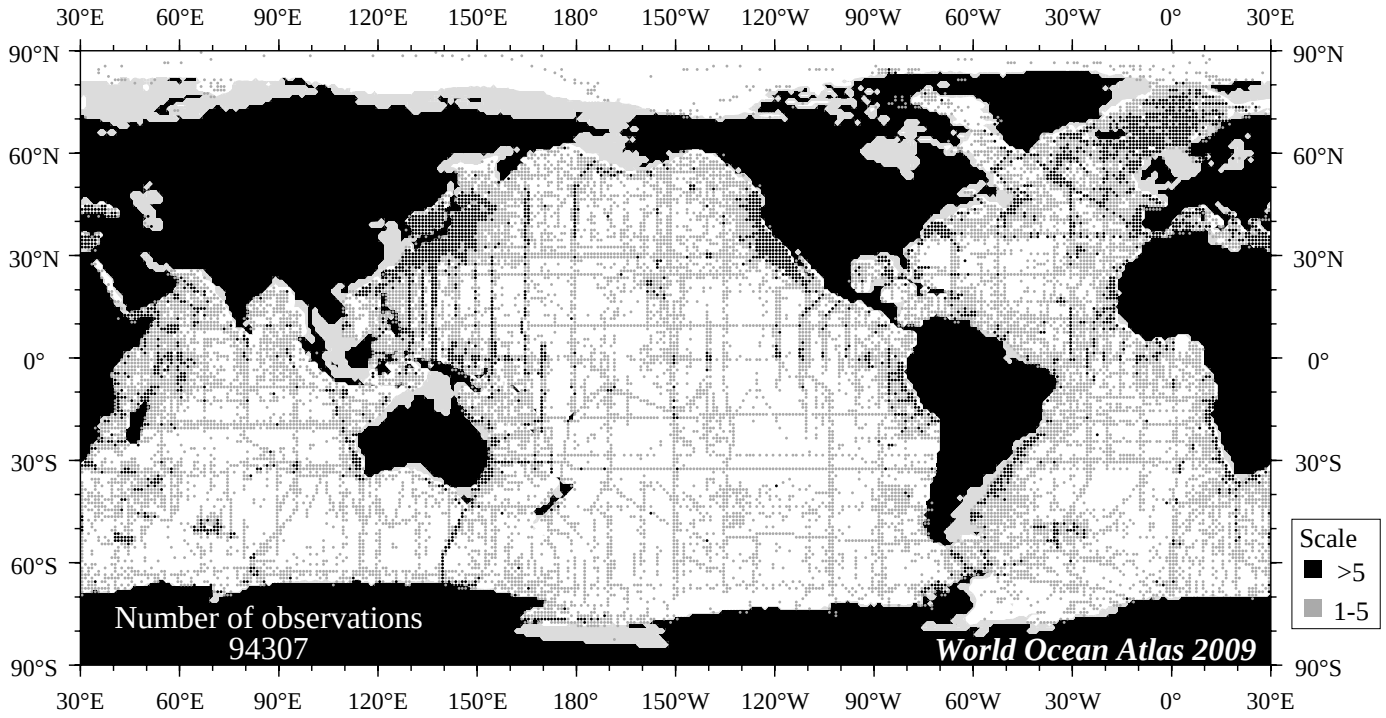

Fig A8 Annual phosphate observations at 400 m. depth.

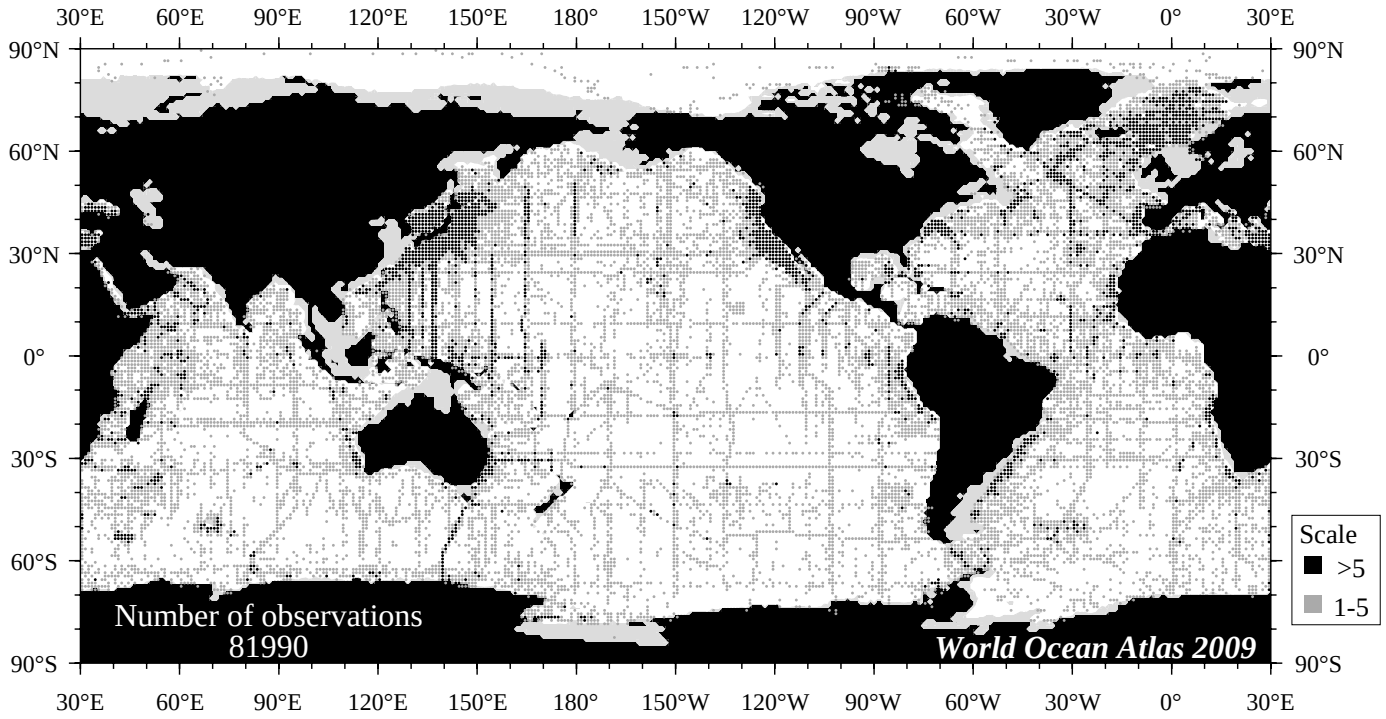

Fig A9 Annual phosphate observations at 500 m. depth.

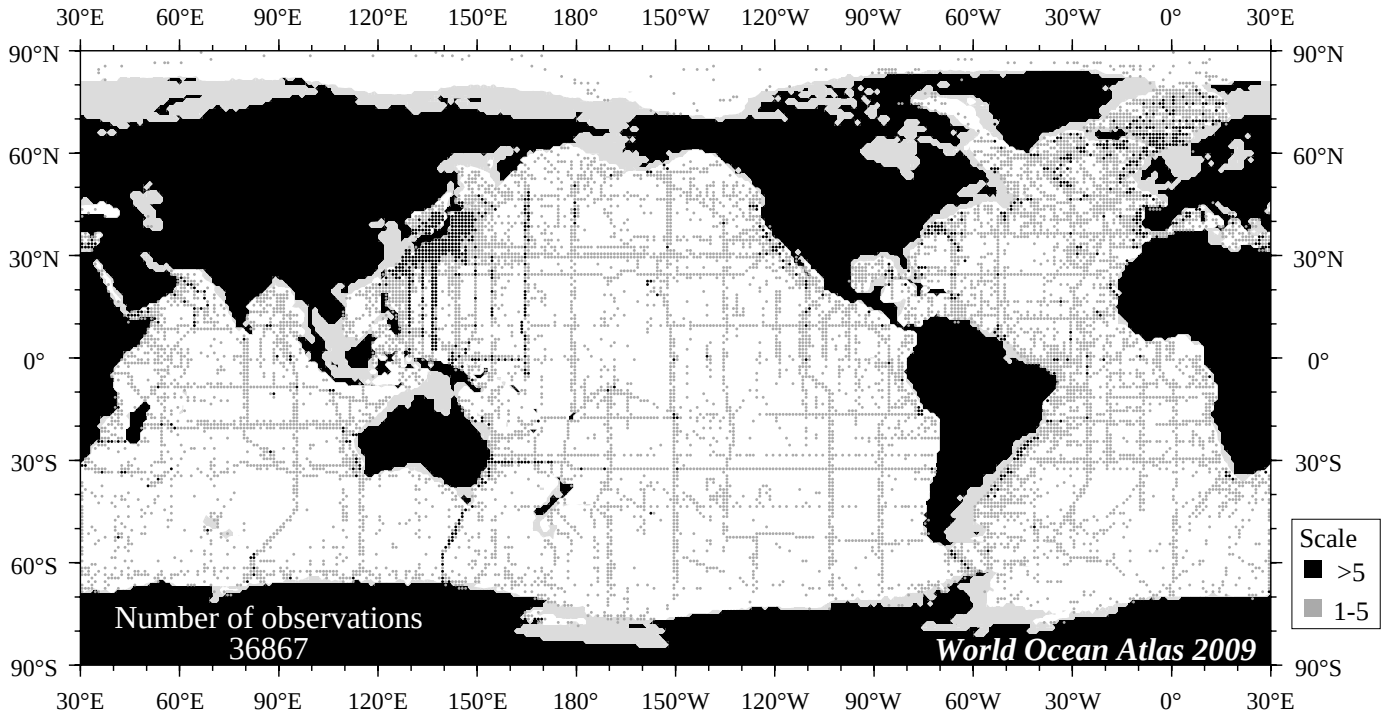

Fig A10 Annual phosphate observations at 700 m. depth.

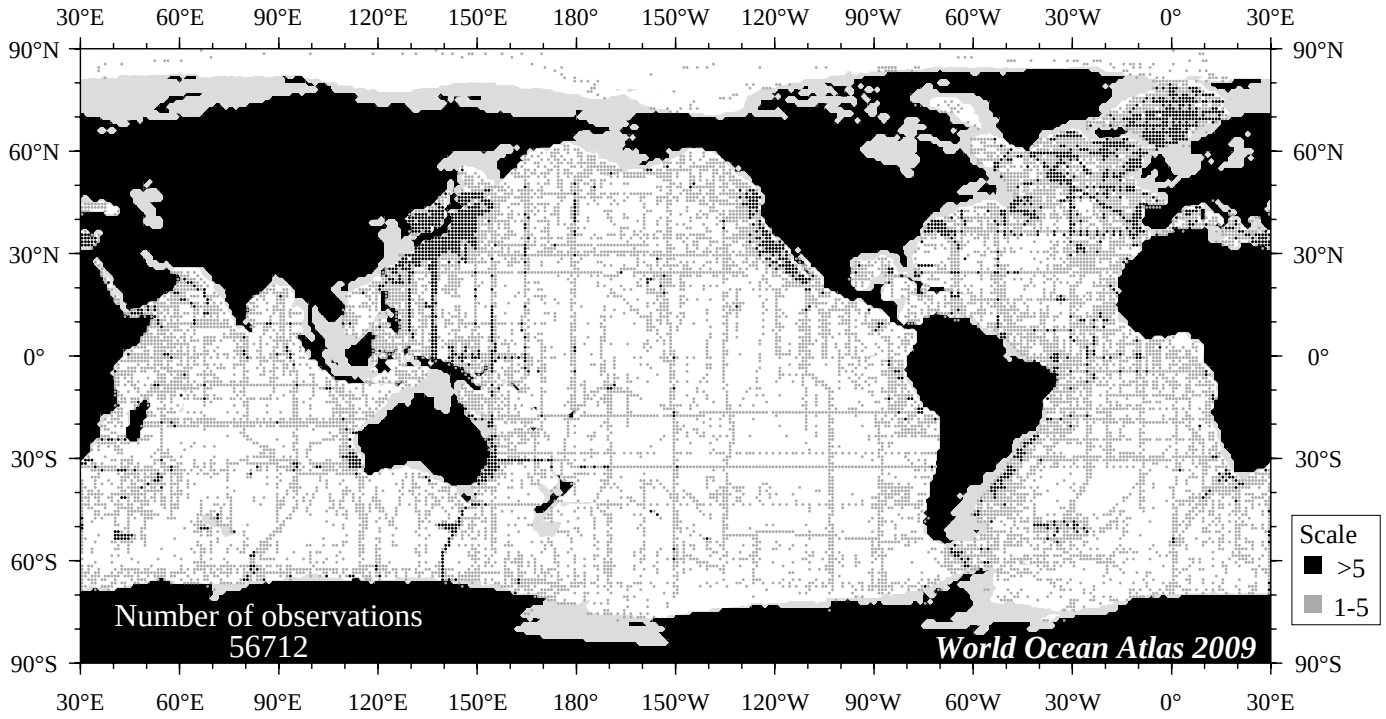

Fig A11 Annual phosphate observations at 1000 m. depth.

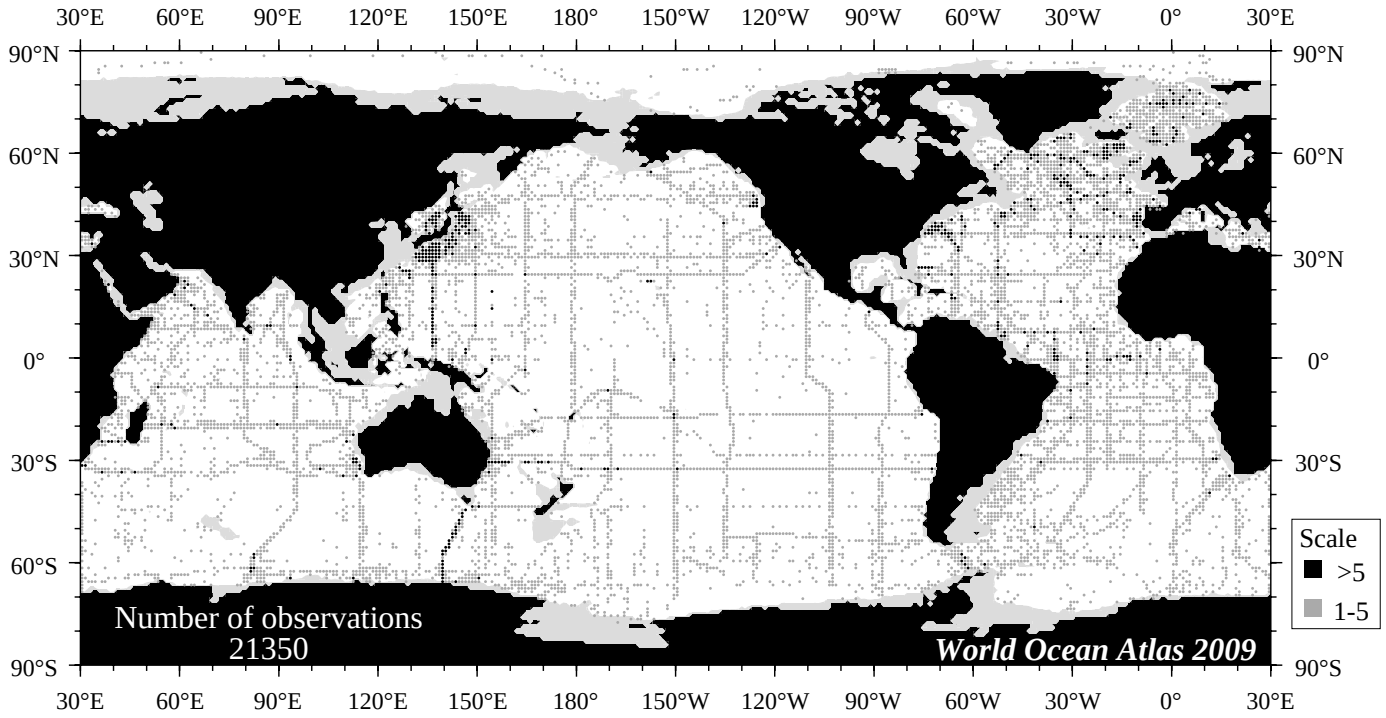

Fig A12 Annual phosphate observations at 1500 m. depth.

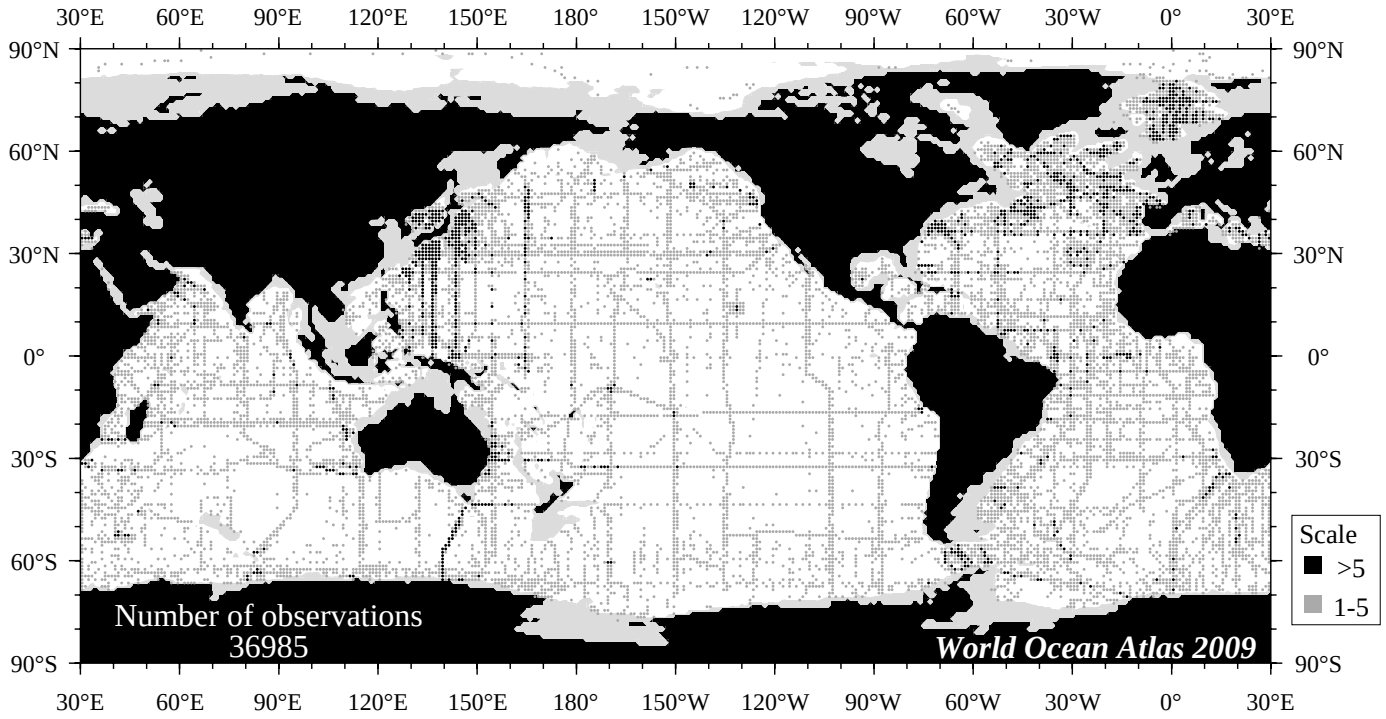

Fig A13 Annual phosphate observations at 2000 m. depth.

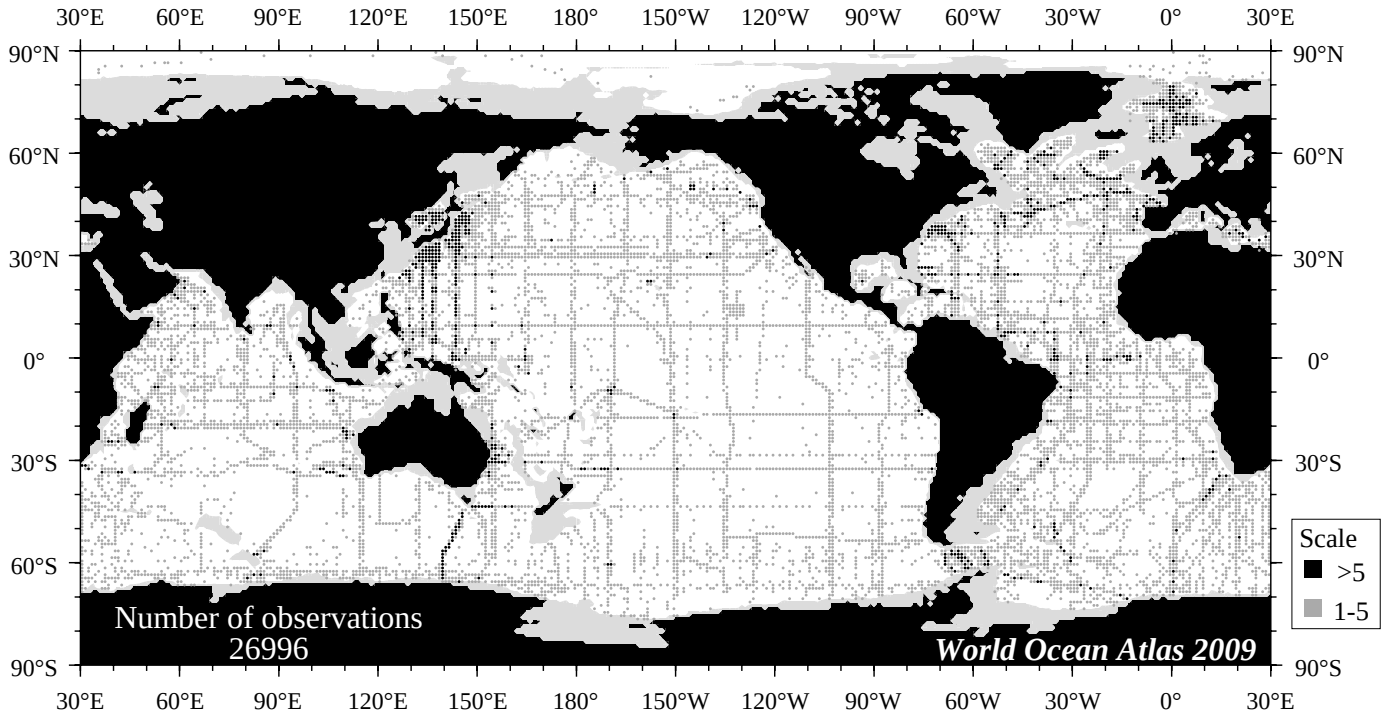

Fig A14 Annual phosphate observations at 2500 m. depth.

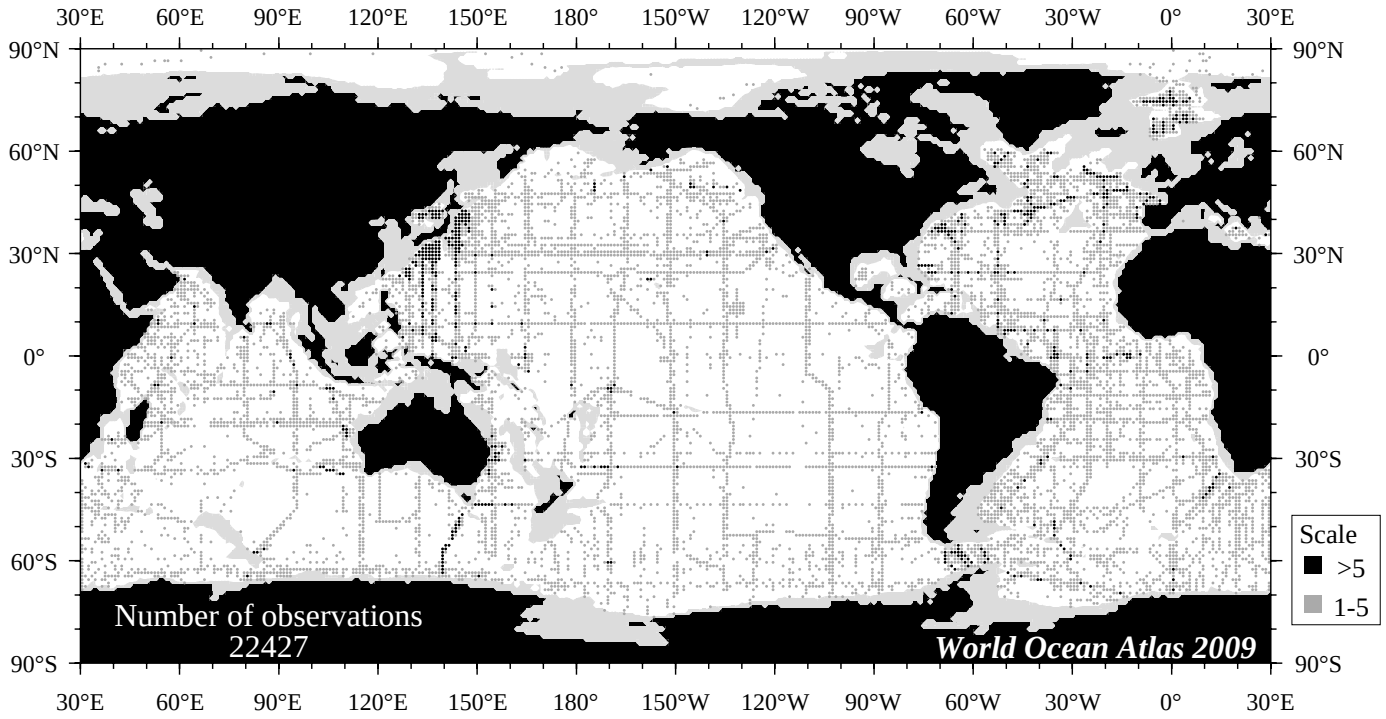

Fig A15 Annual phosphate observations at 3000 m. depth.

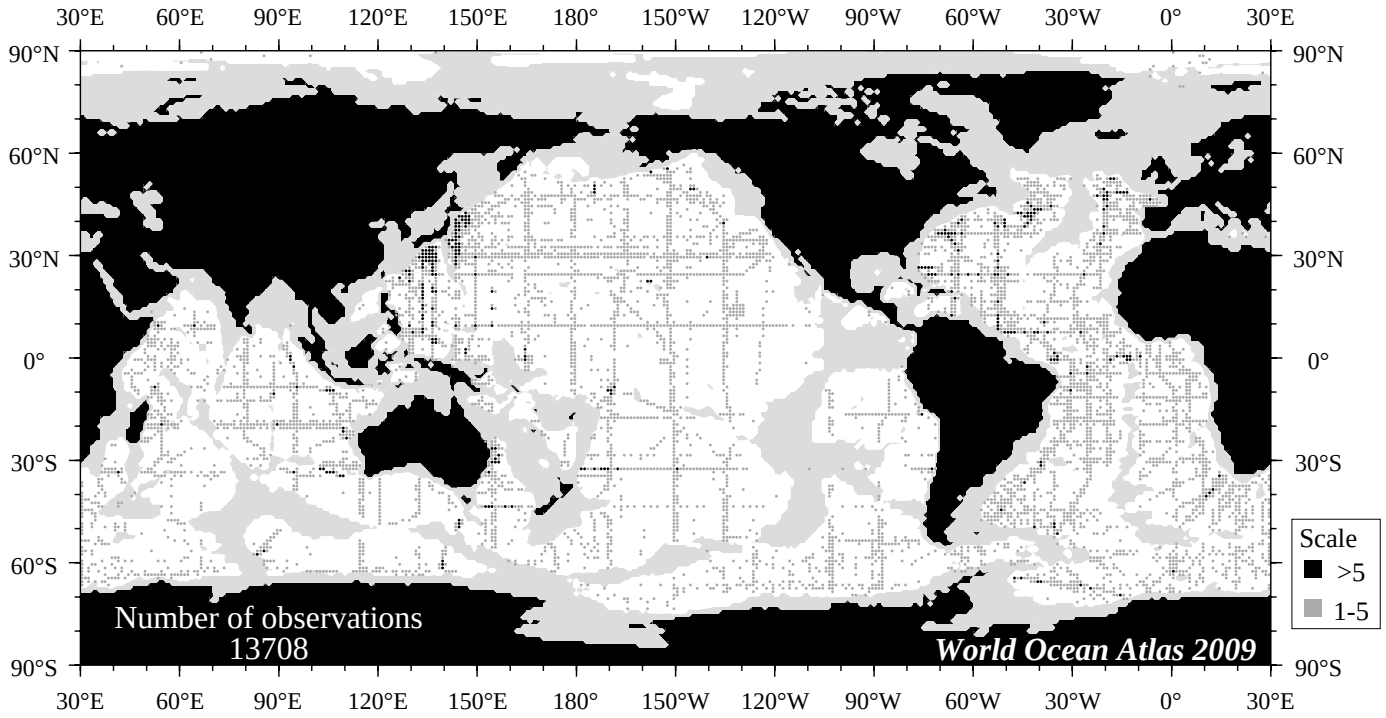

Fig A16 Annual phosphate observations at 4000 m. depth.

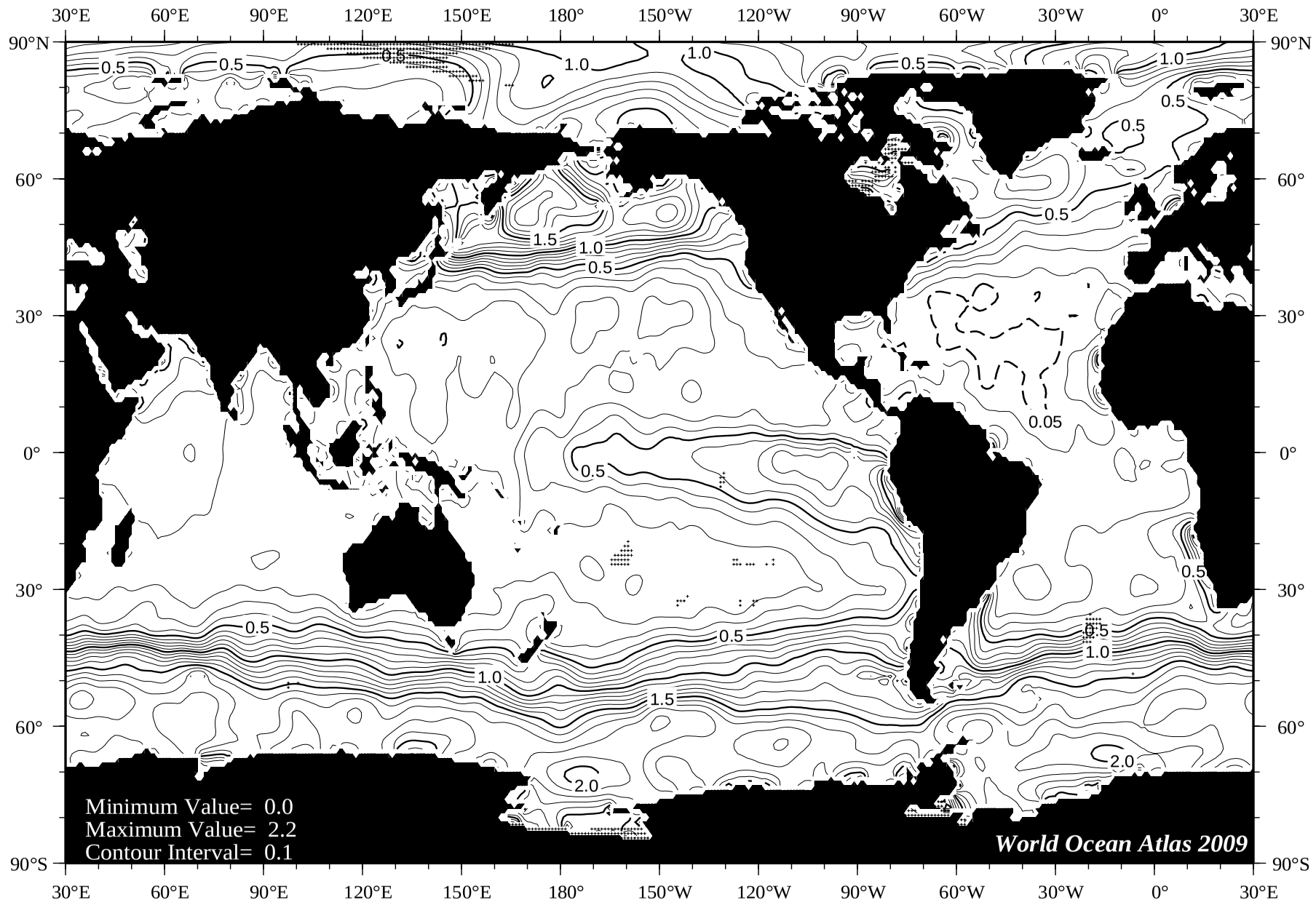

Fig A17 Annual phosphate [umol/l] at the surface.

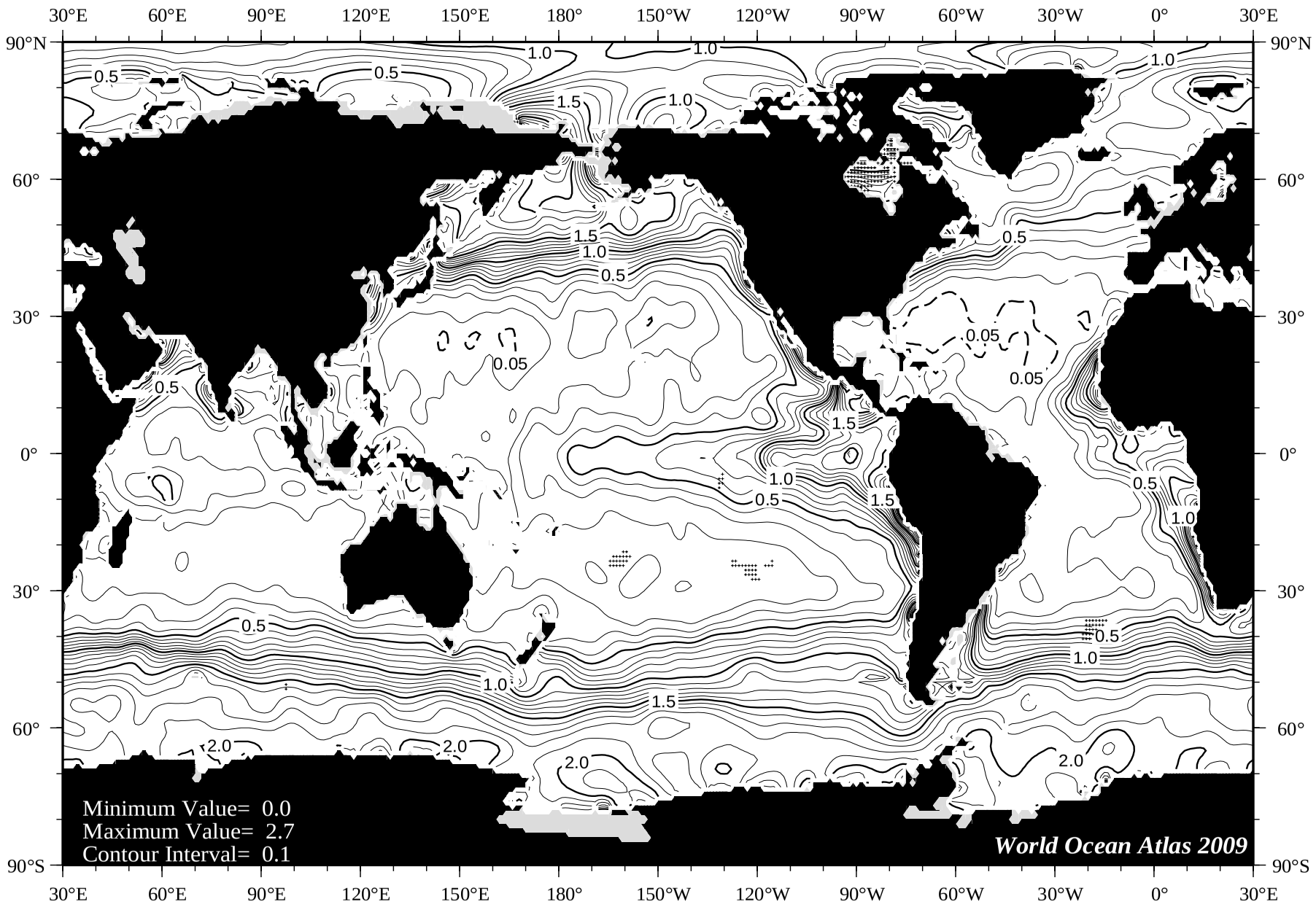

Fig A18 Annual phosphate [umol/l] at 50 m. depth.

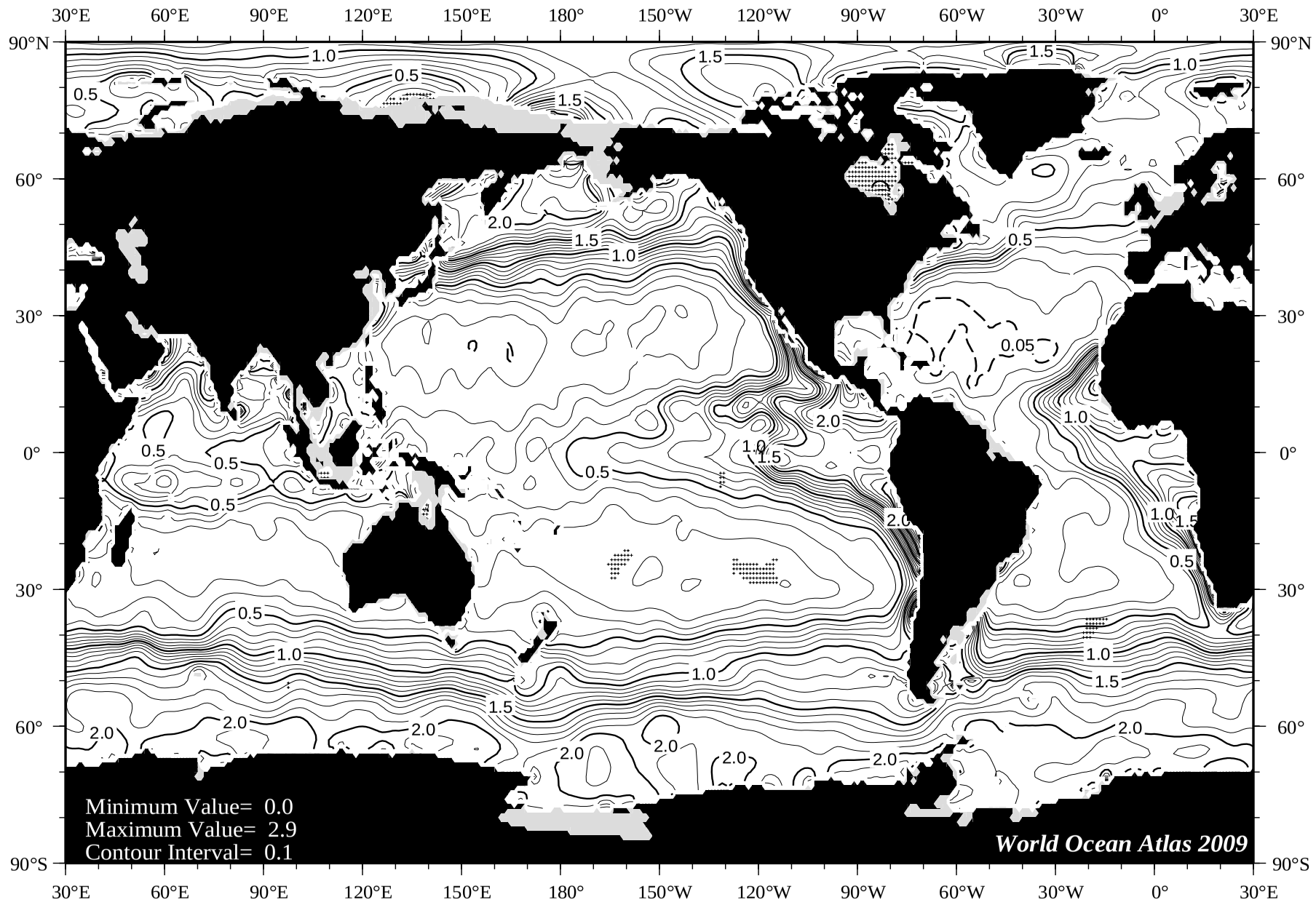

Fig A19 Annual phosphate [umol/l] at 75 m. depth.

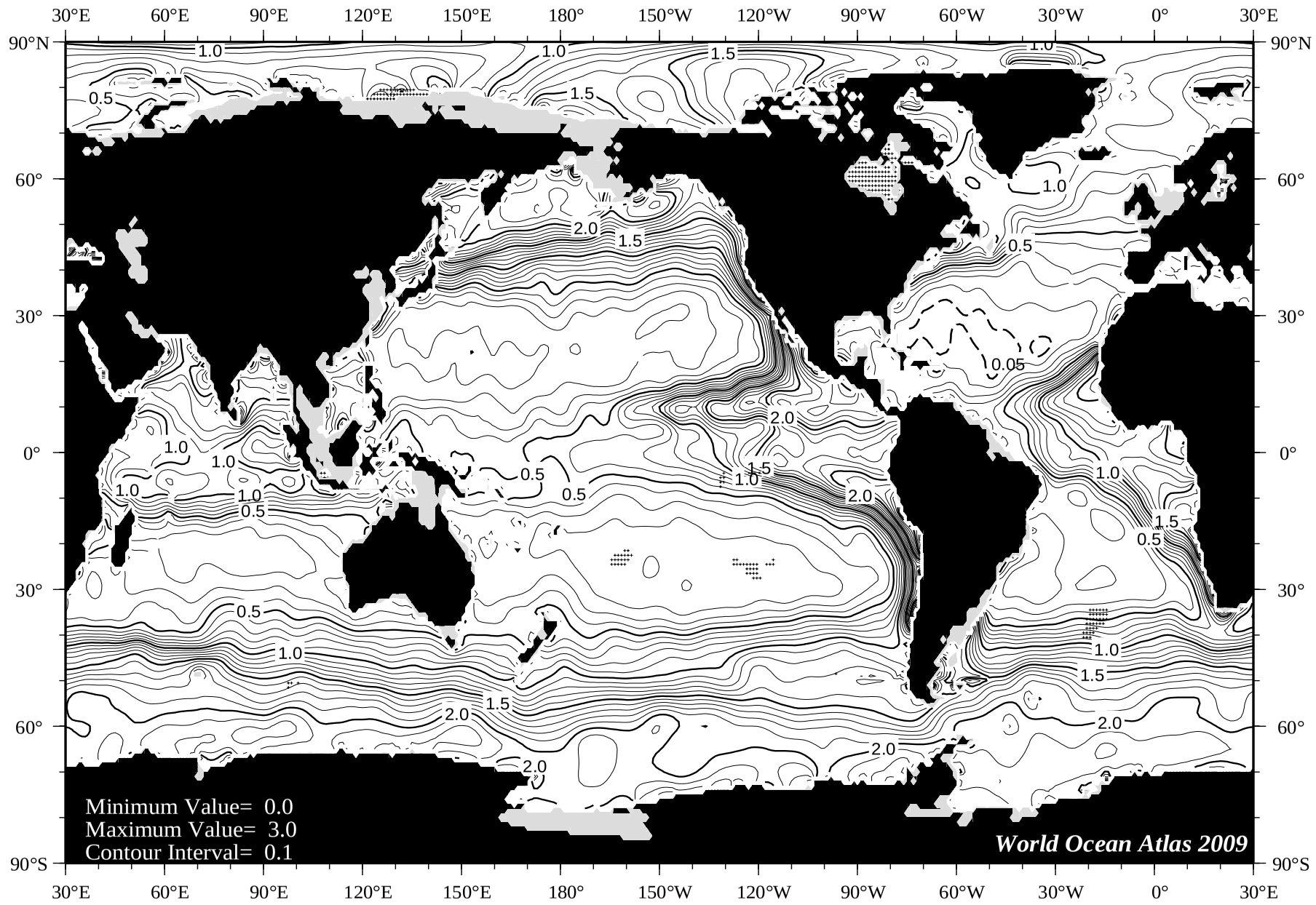

Fig A20 Annual phosphate [umol/l] at 100 m. depth.

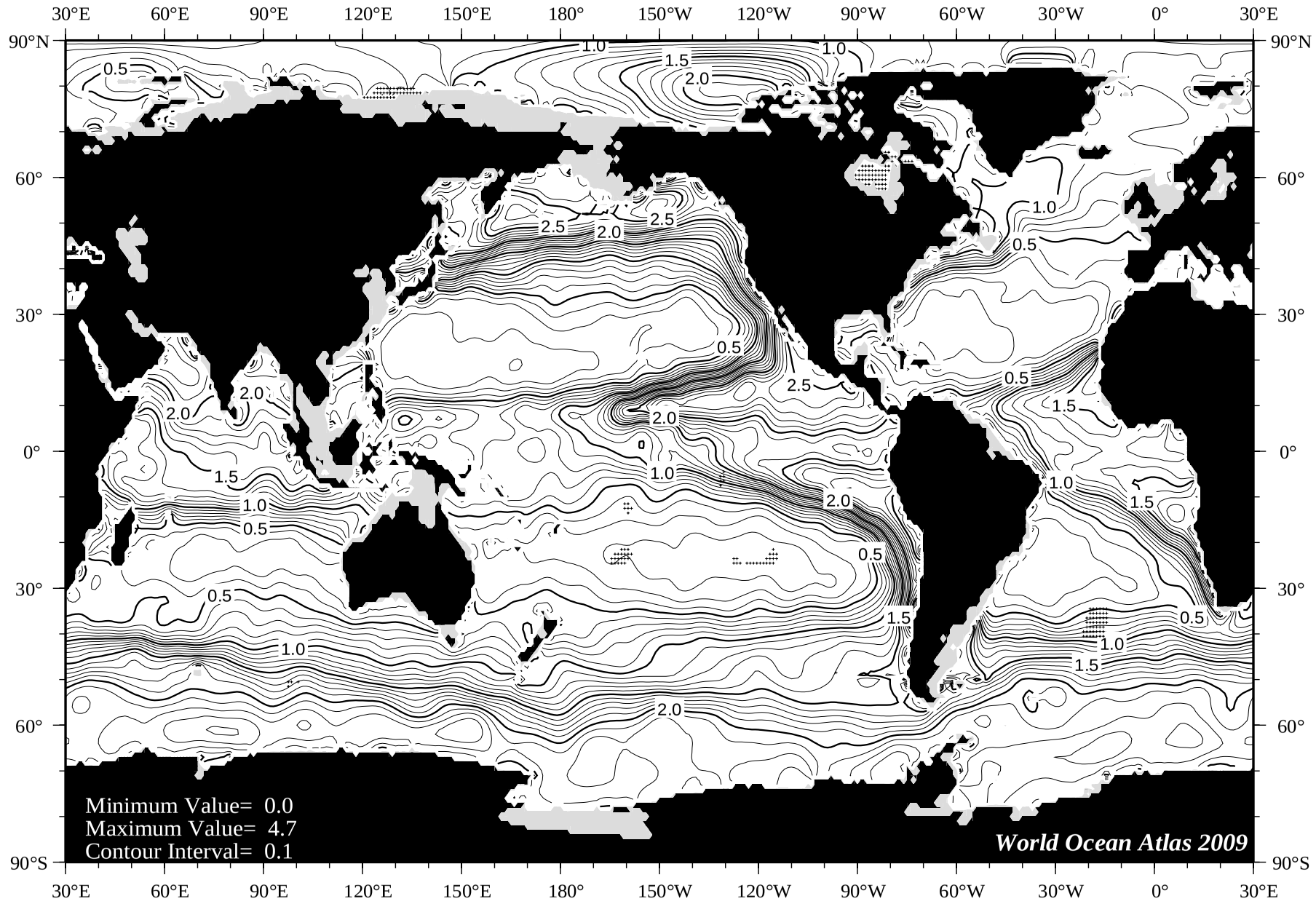

Fig A21 Annual phosphate [umol/l] at 150 m. depth.

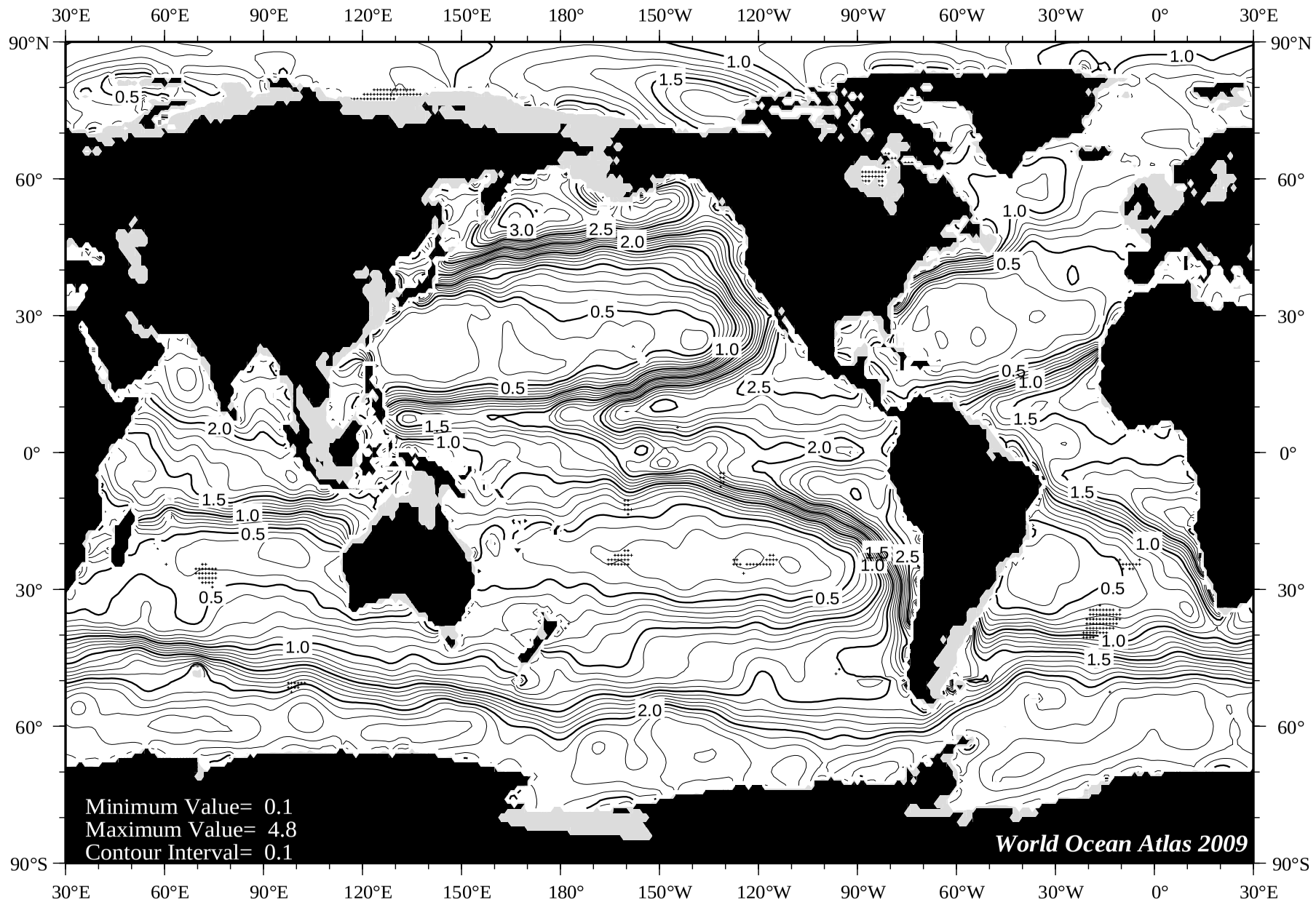

Fig A22 Annual phosphate [umol/l] at 200 m. depth.

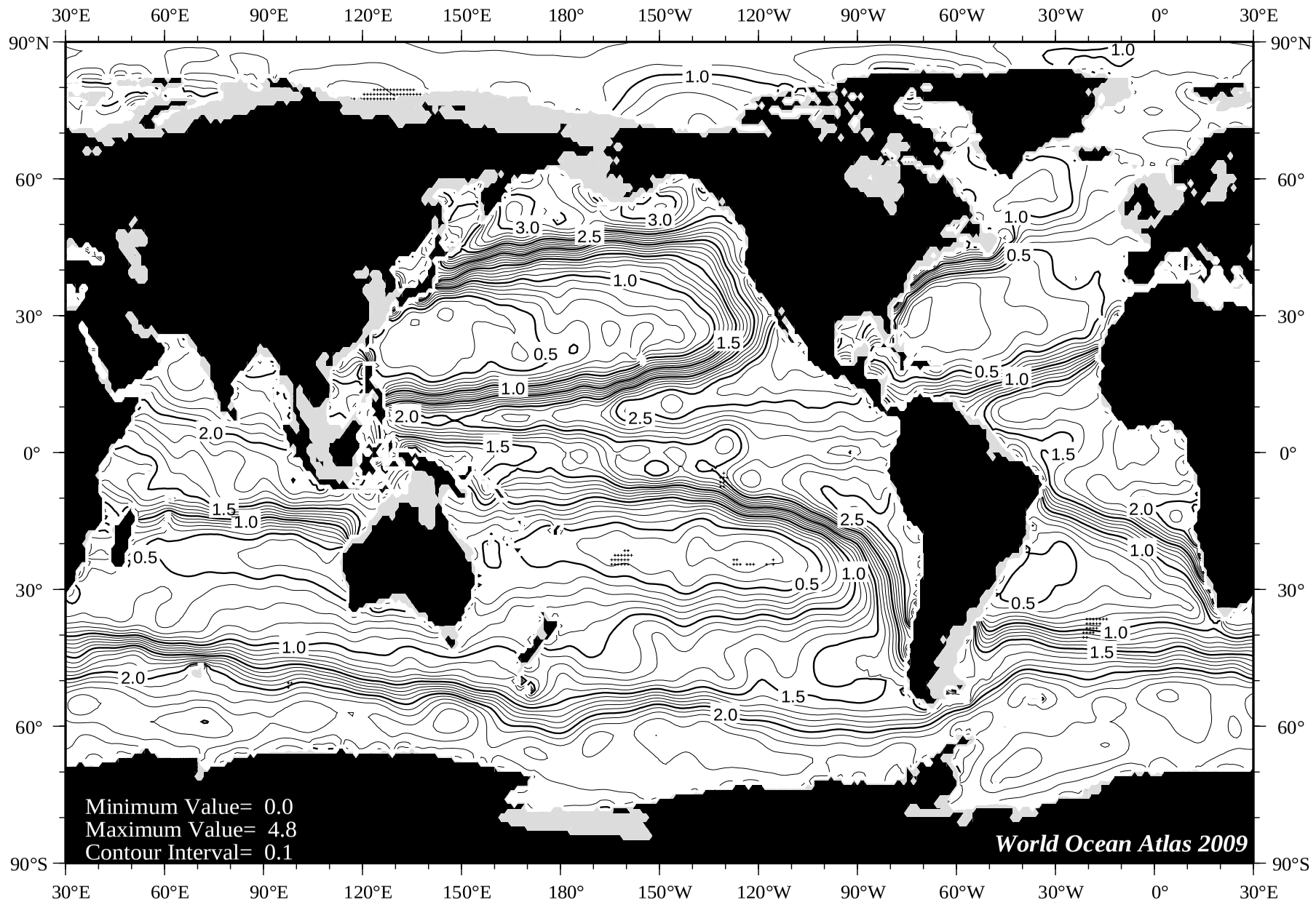

Fig A23 Annual phosphate [umol/l] at 250 m. depth.

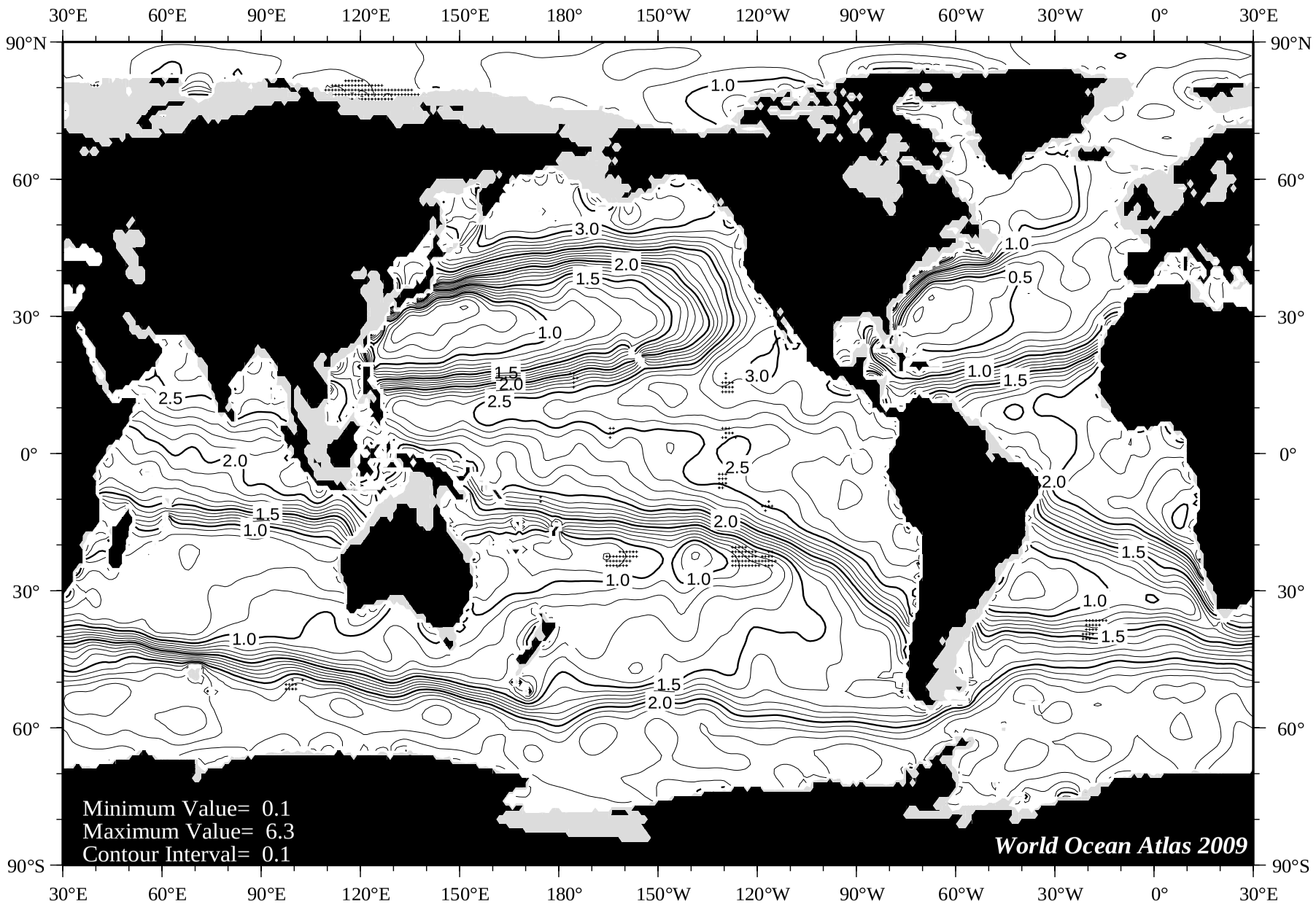

Fig A24 Annual phosphate [umol/l] at 400 m. depth.

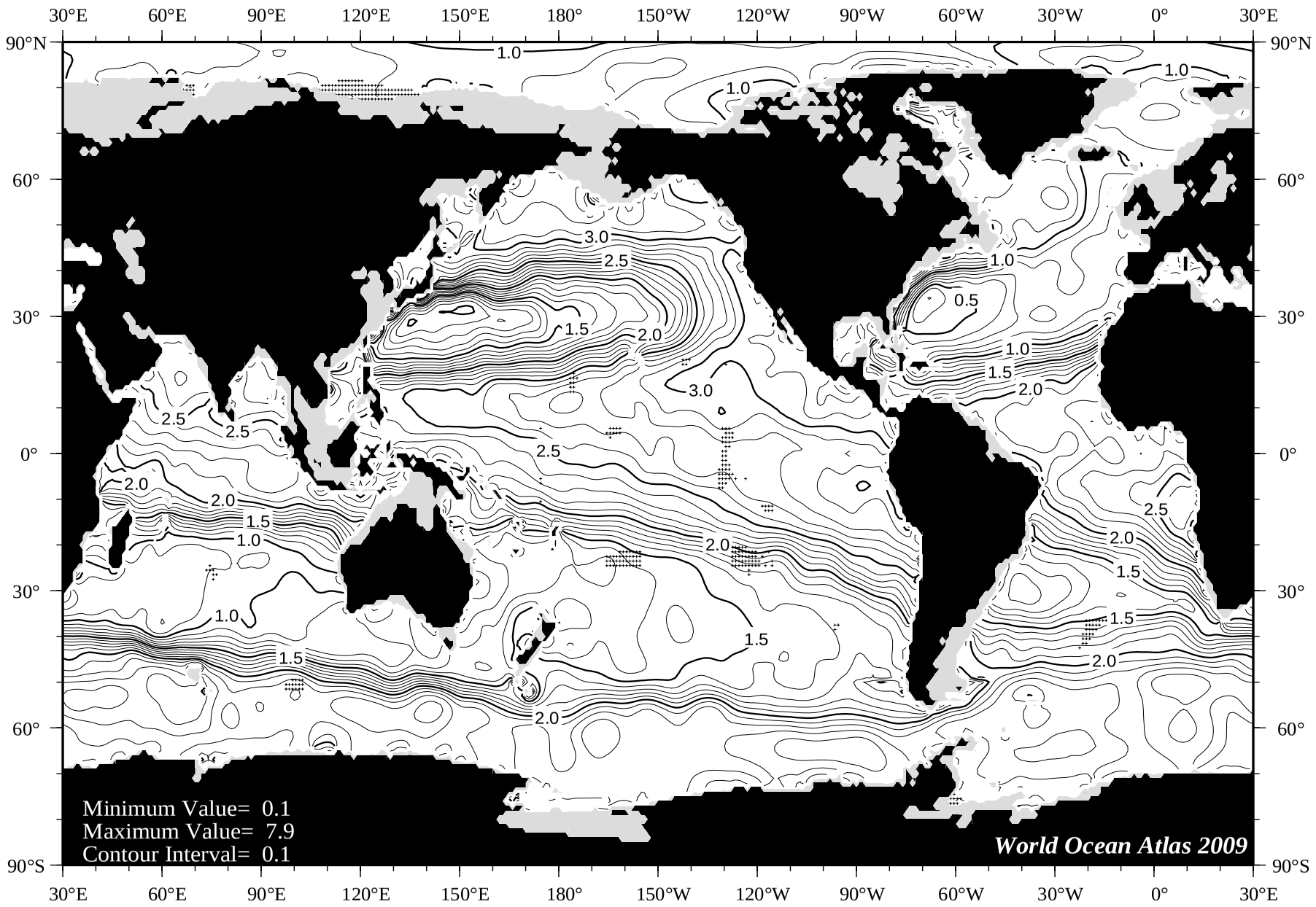

Fig A25 Annual phosphate [umol/l] at 500 m. depth.

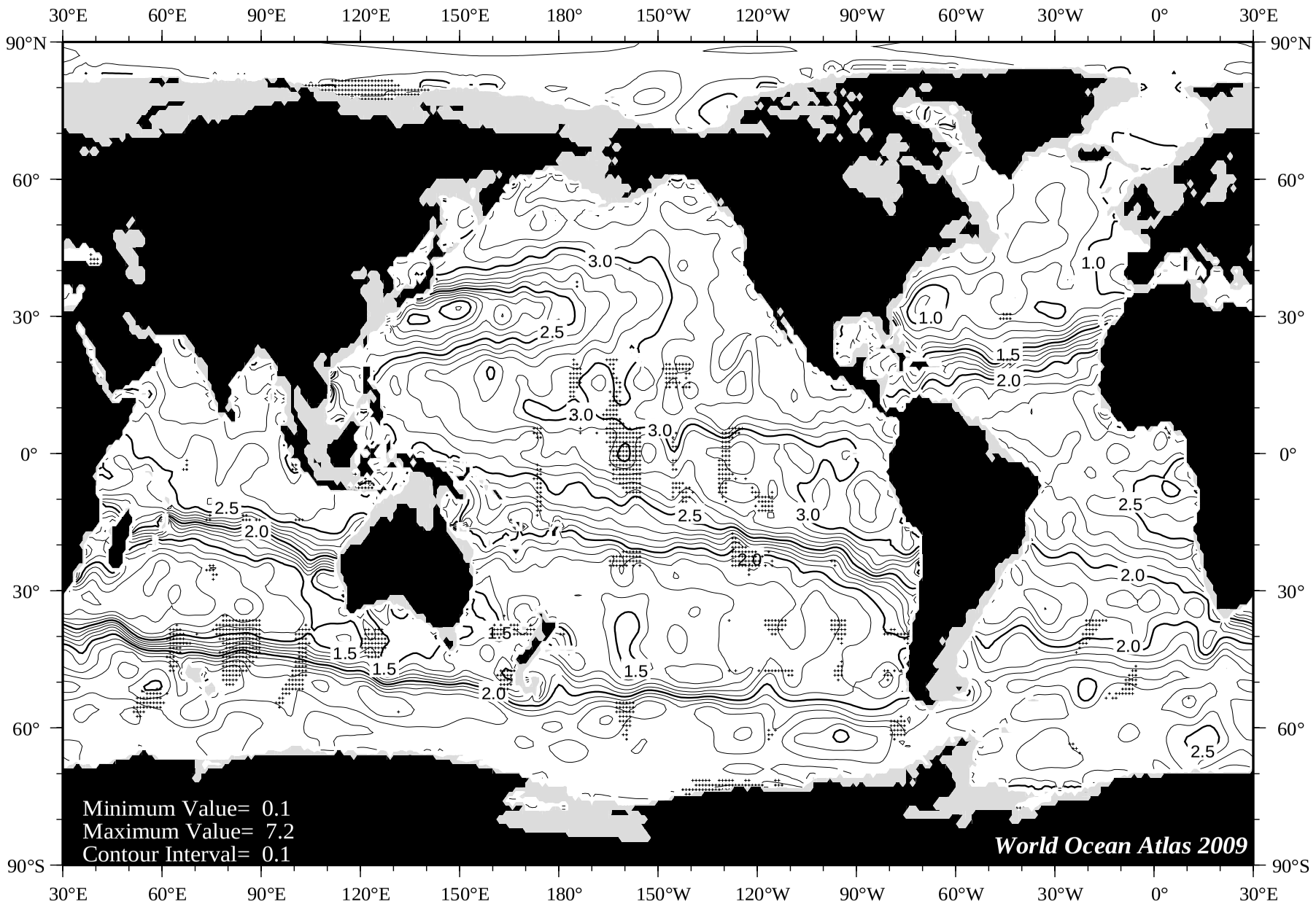

Fig A26 Annual phosphate [umol/l] at 700 m. depth.

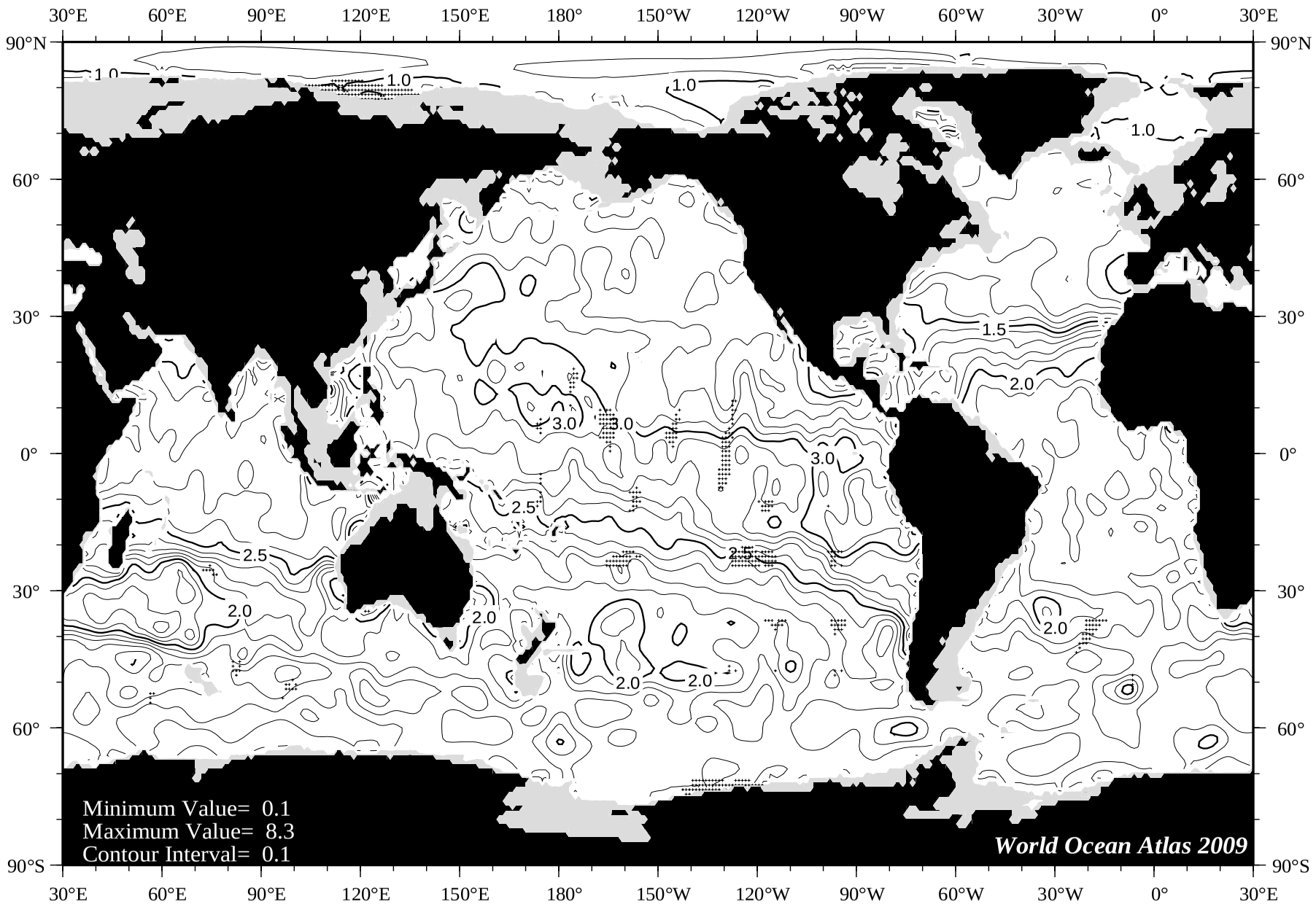

Fig A27 Annual phosphate [umol/l] at 1000 m. depth.

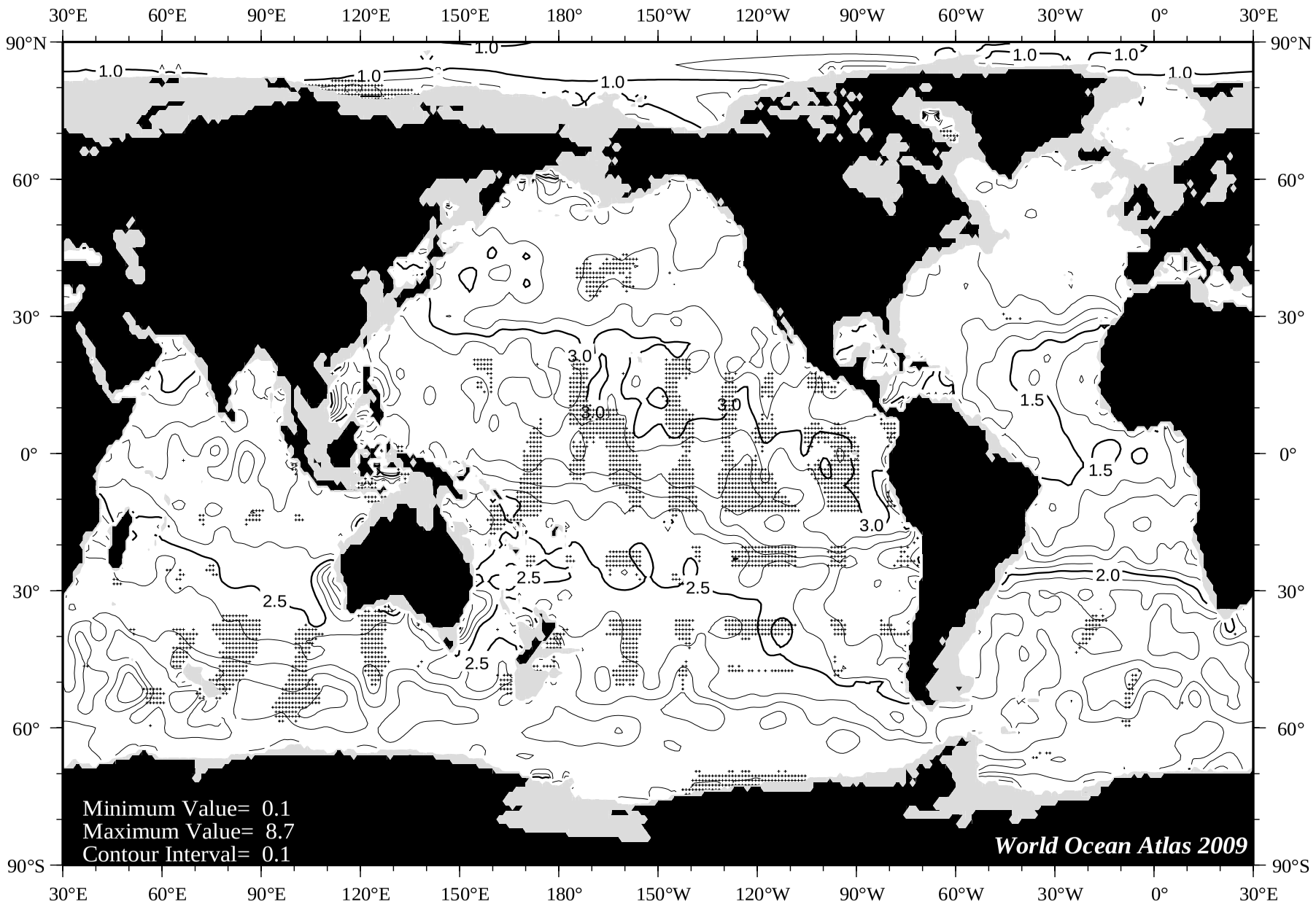

Fig A28 Annual phosphate [umol/l] at 1500 m. depth.

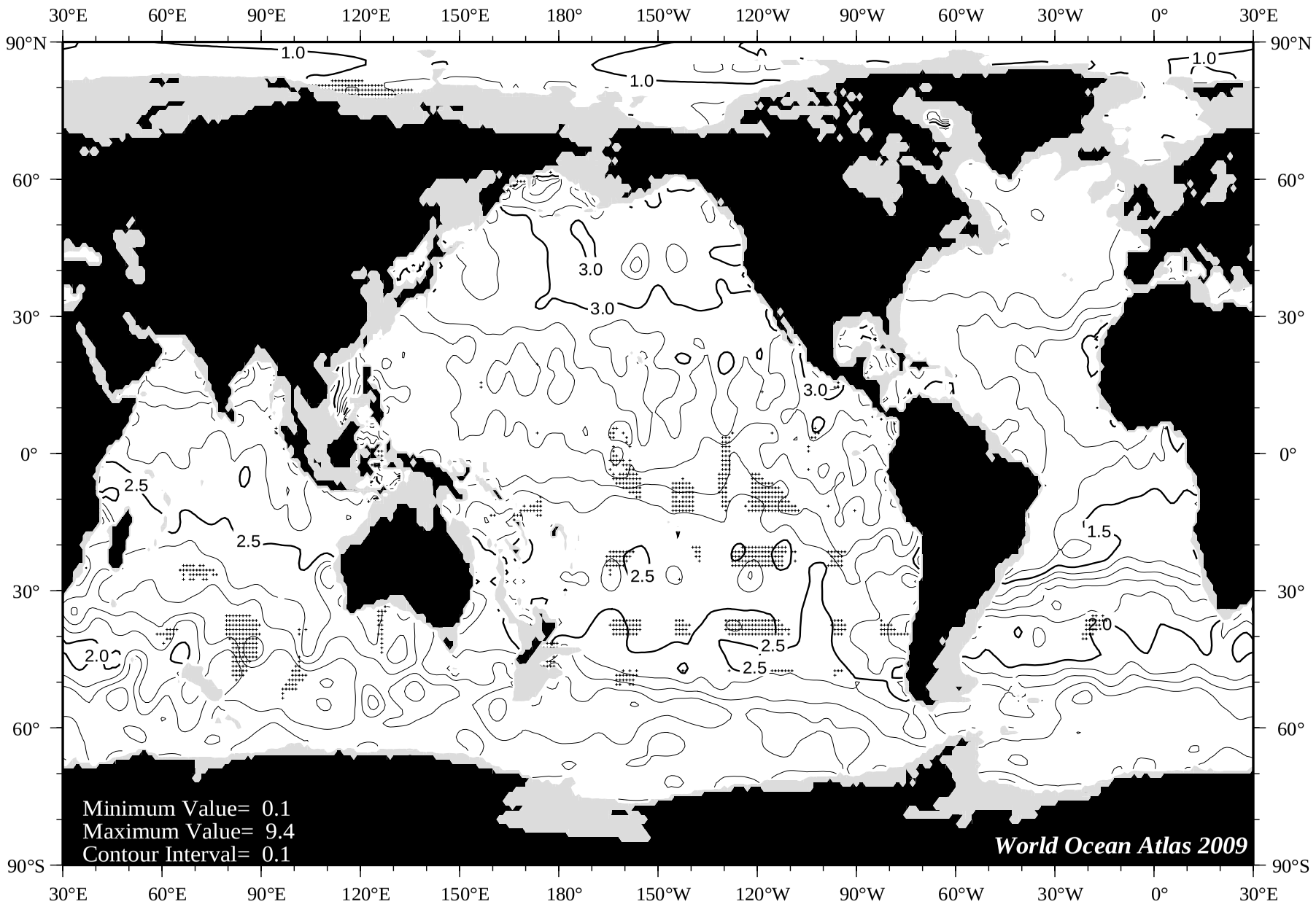

Fig A29 Annual phosphate [umol/l] at 2000 m. depth.

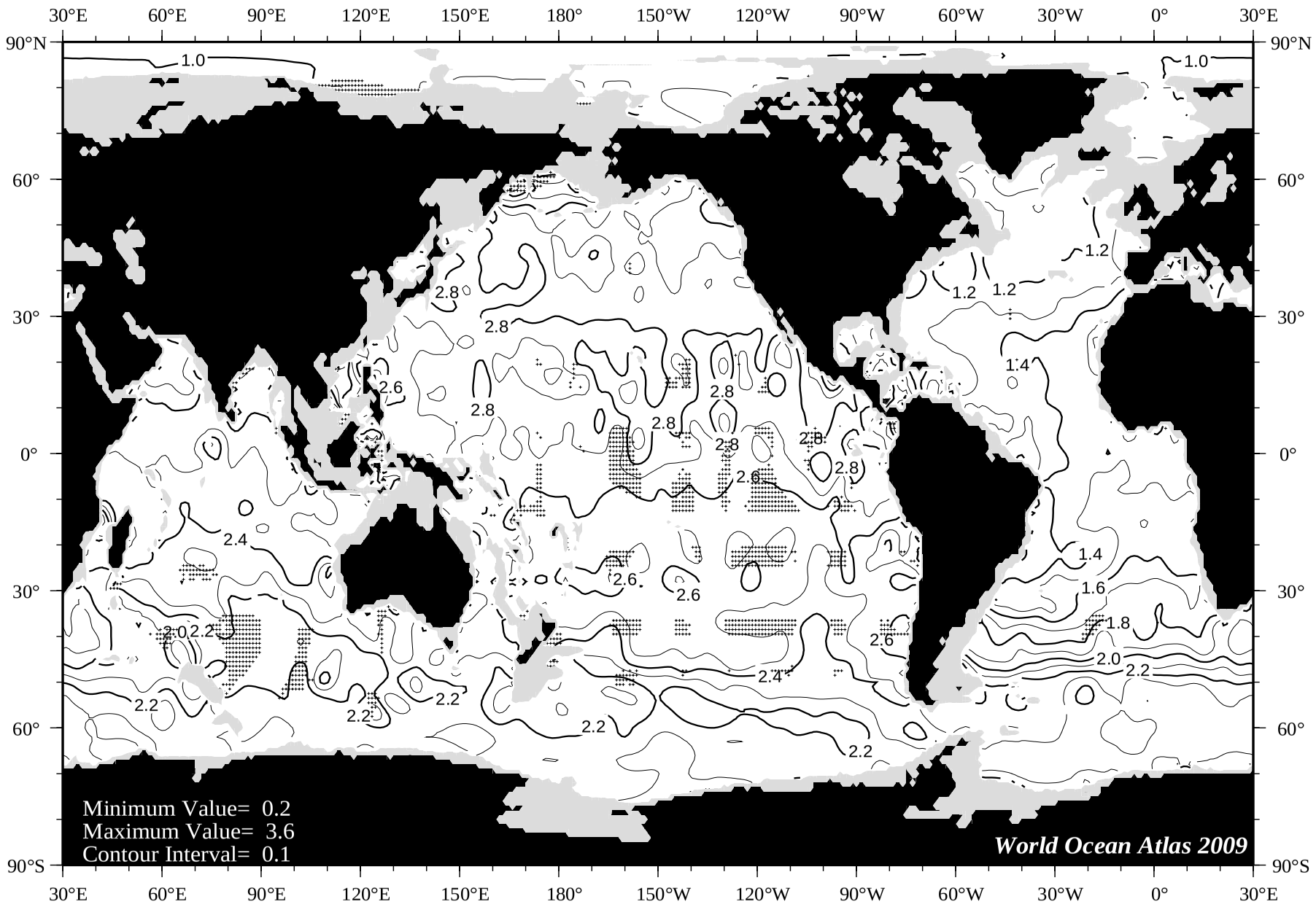

Fig A30 Annual phosphate [umol/l] at 2500 m. depth.

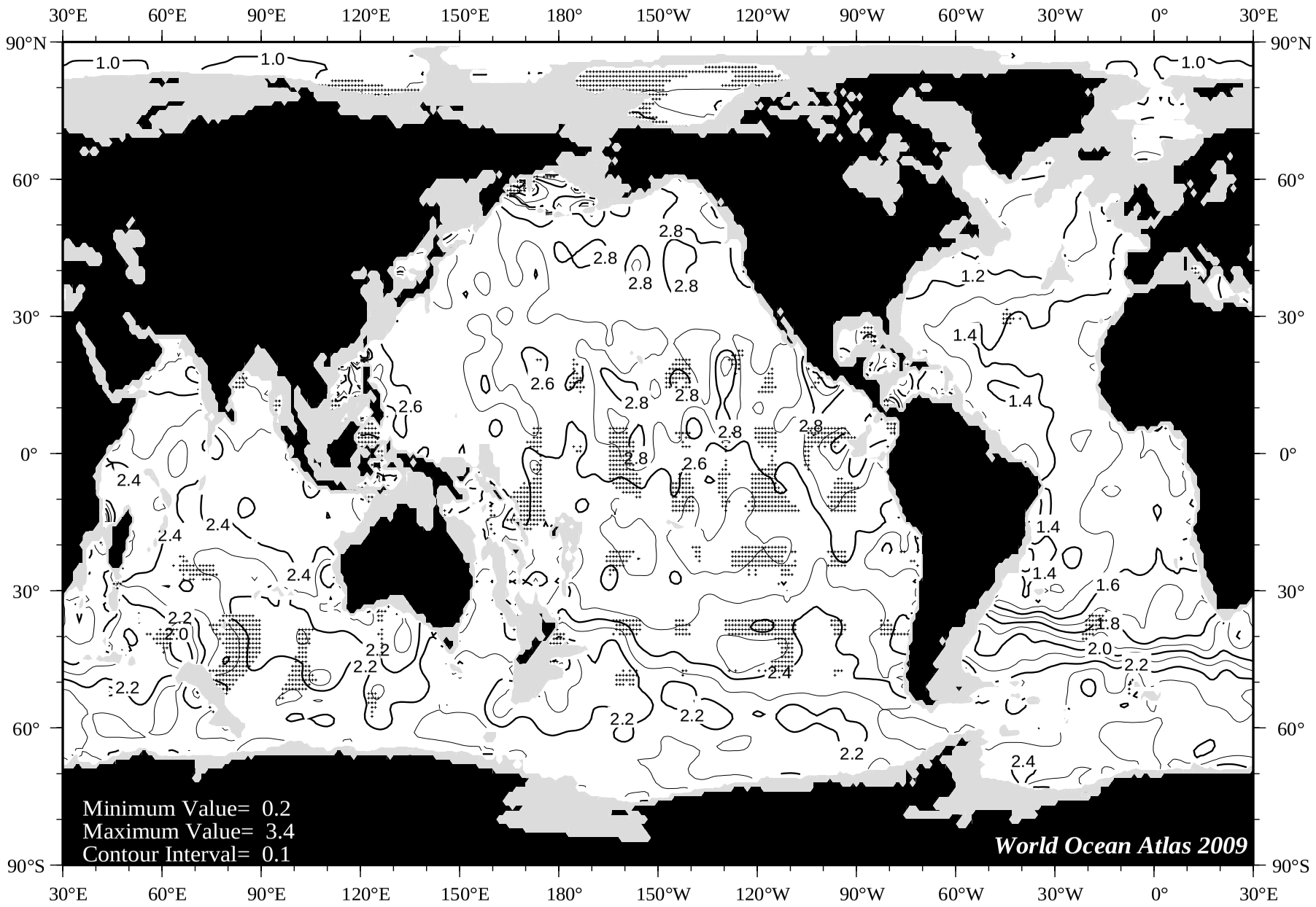

Fig A31 Annual phosphate [umol/l] at 3000 m. depth.

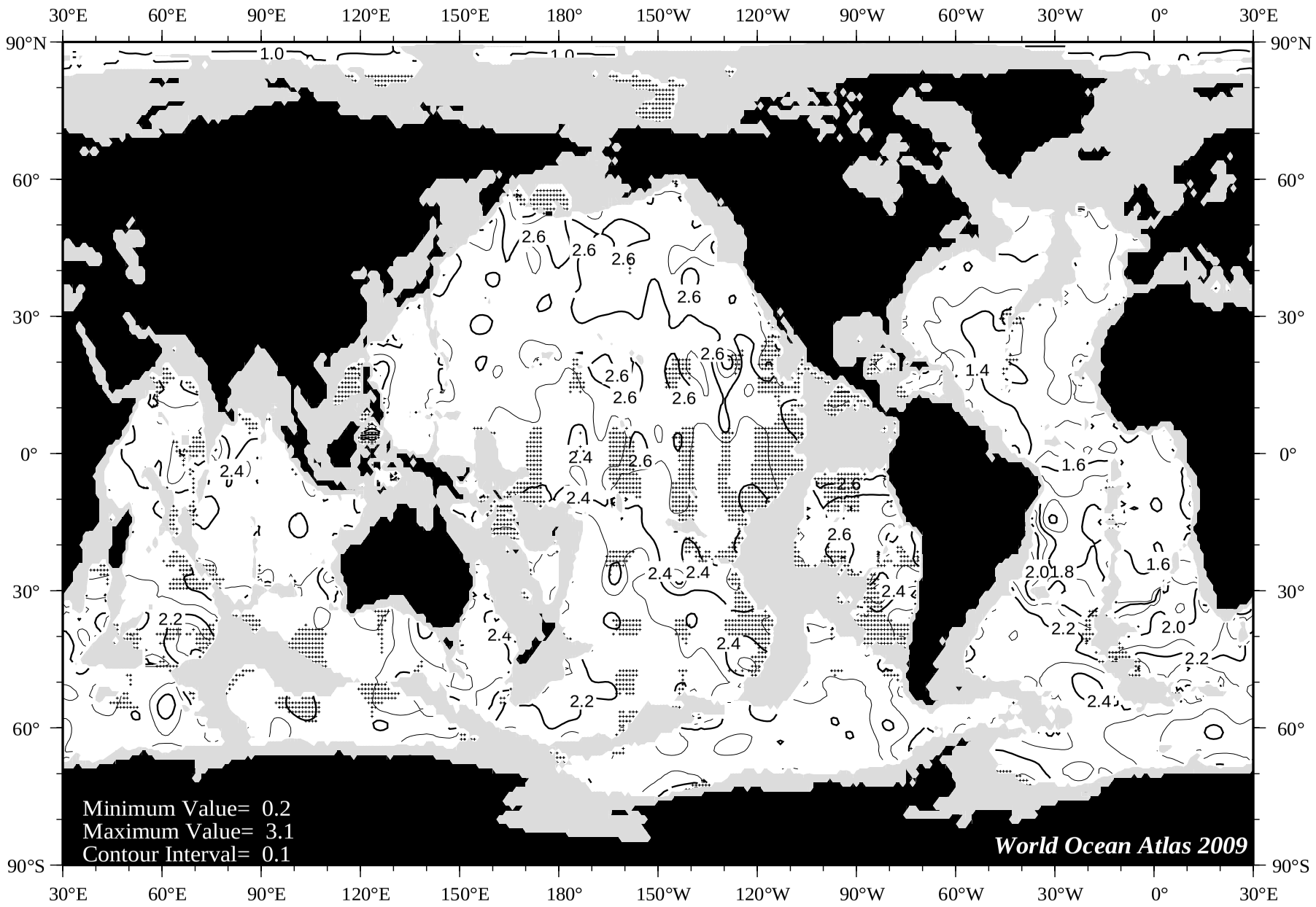

Fig A32 Annual phosphate [umol/l] at 4000 m. depth.

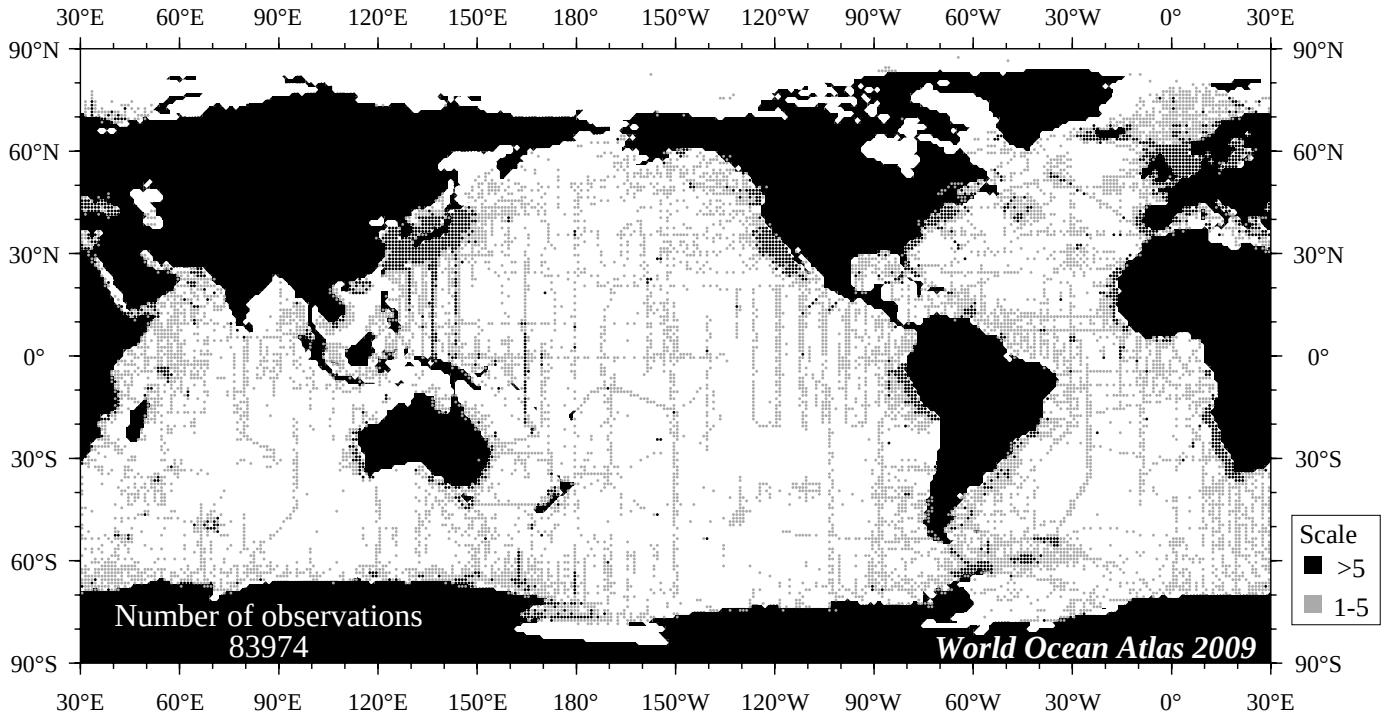

Fig B1 Winter (Jan.-Mar.) phosphate observations at the surface.

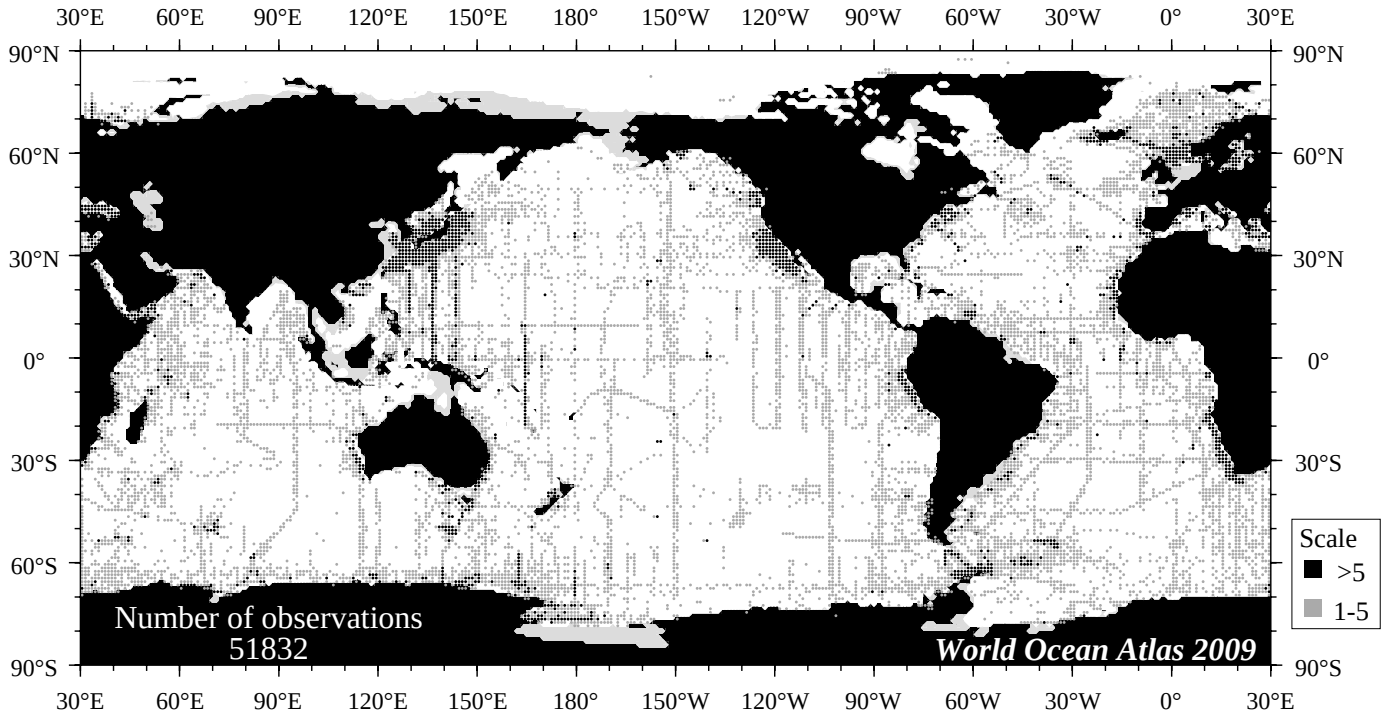

Fig B2 Winter (Jan.-Mar.) phosphate observations at 75 m. depth.

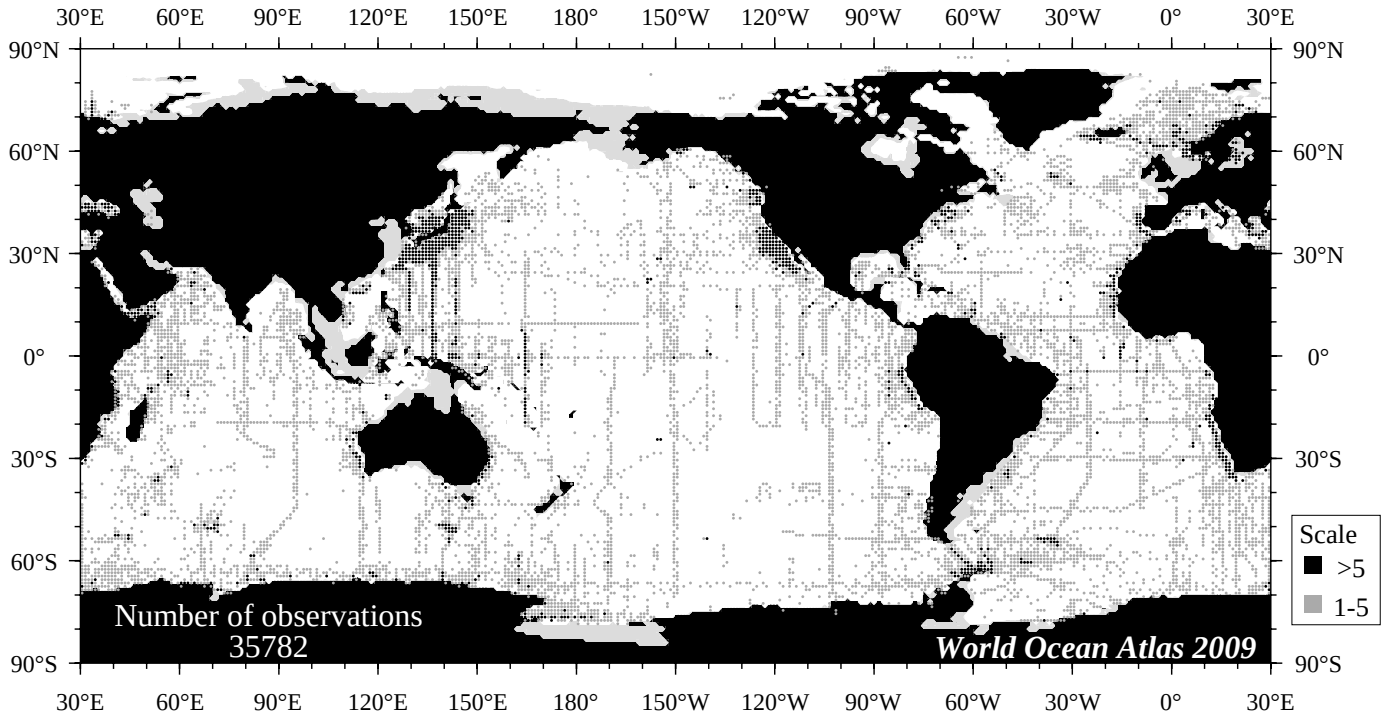

Fig B3 Winter (Jan.-Mar.) phosphate observations at 150 m. depth.

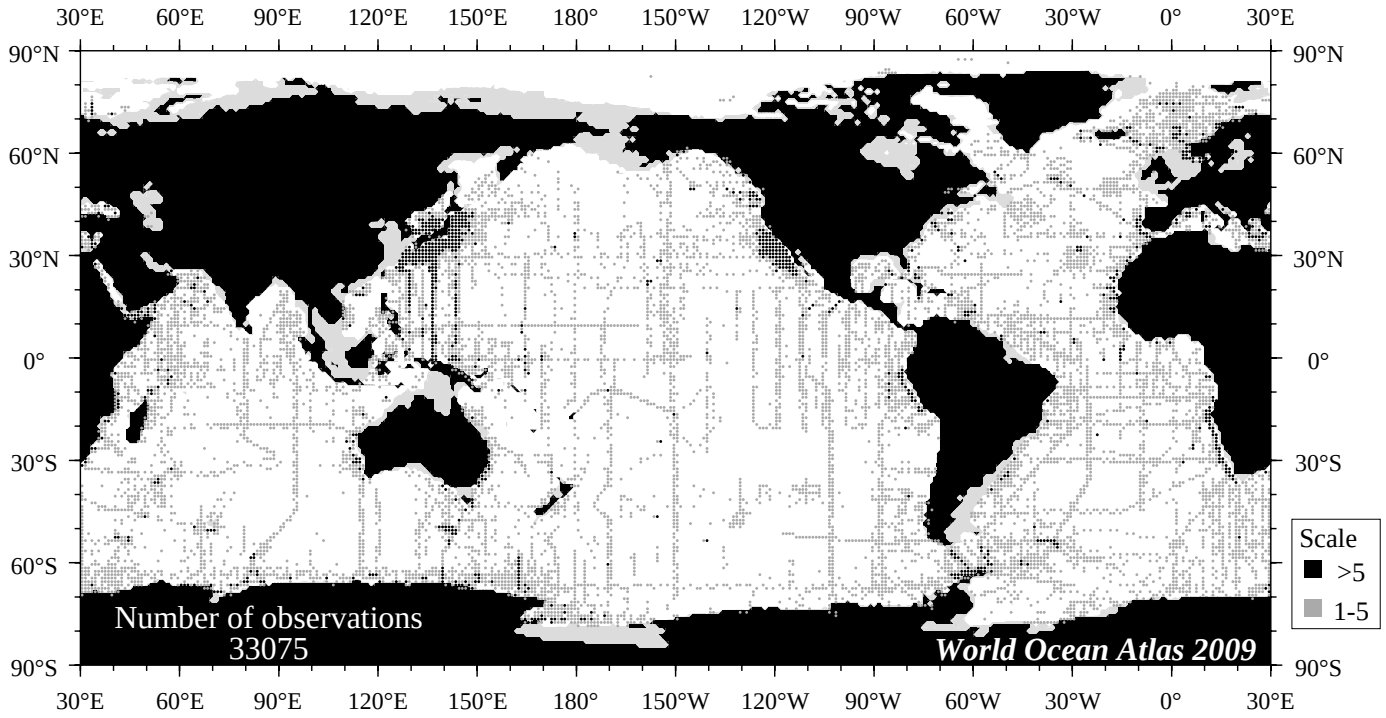

Fig B4 Winter (Jan.-Mar.) phosphate observations at 250 m. depth.

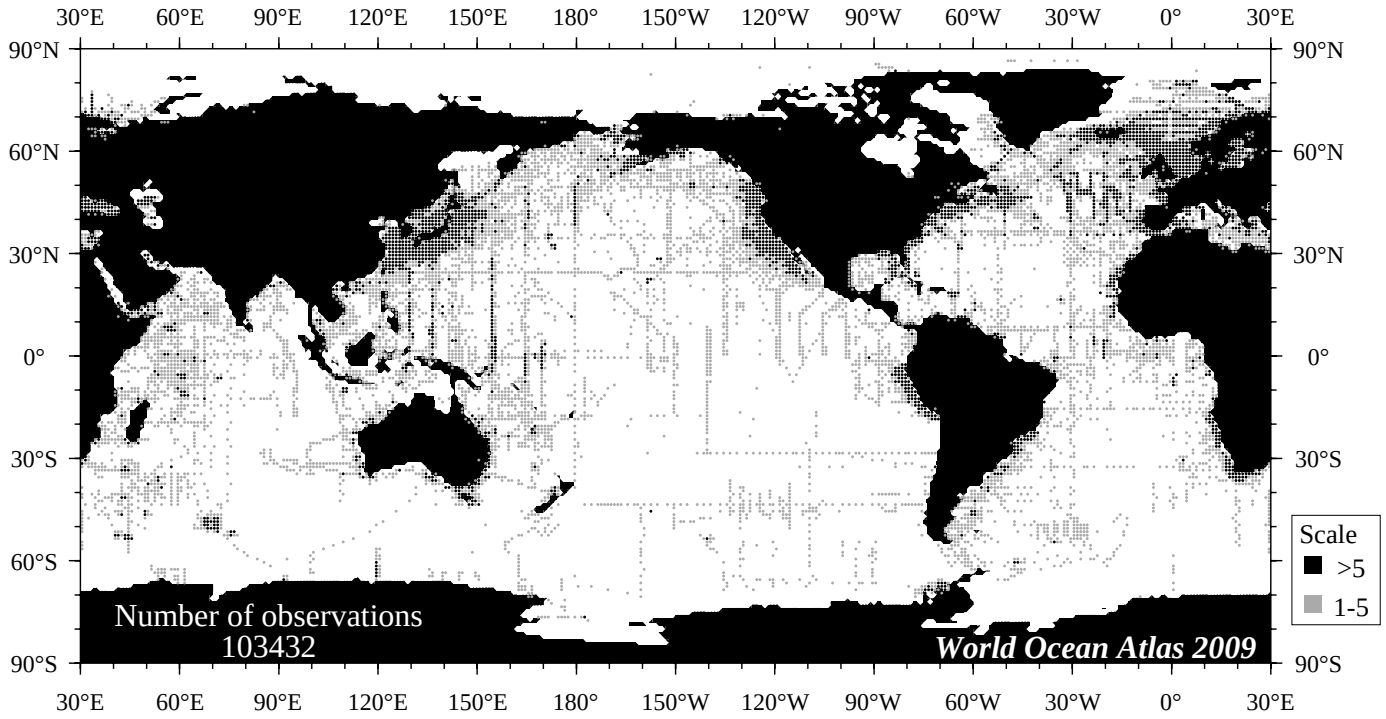

Fig B5 Spring (Apr.-Jun.) phosphate observations at the surface.

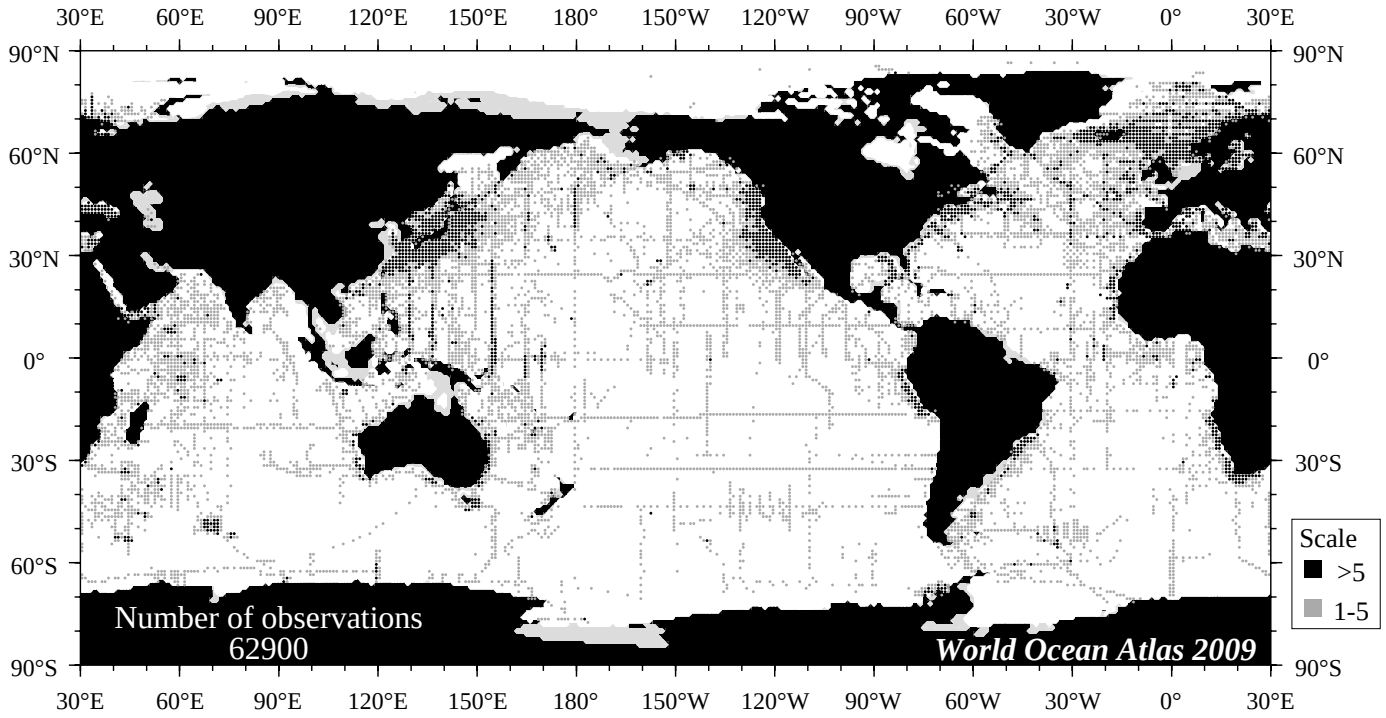

Fig B6 Spring (Apr.-Jun.) phosphate observations at 75 m. depth.

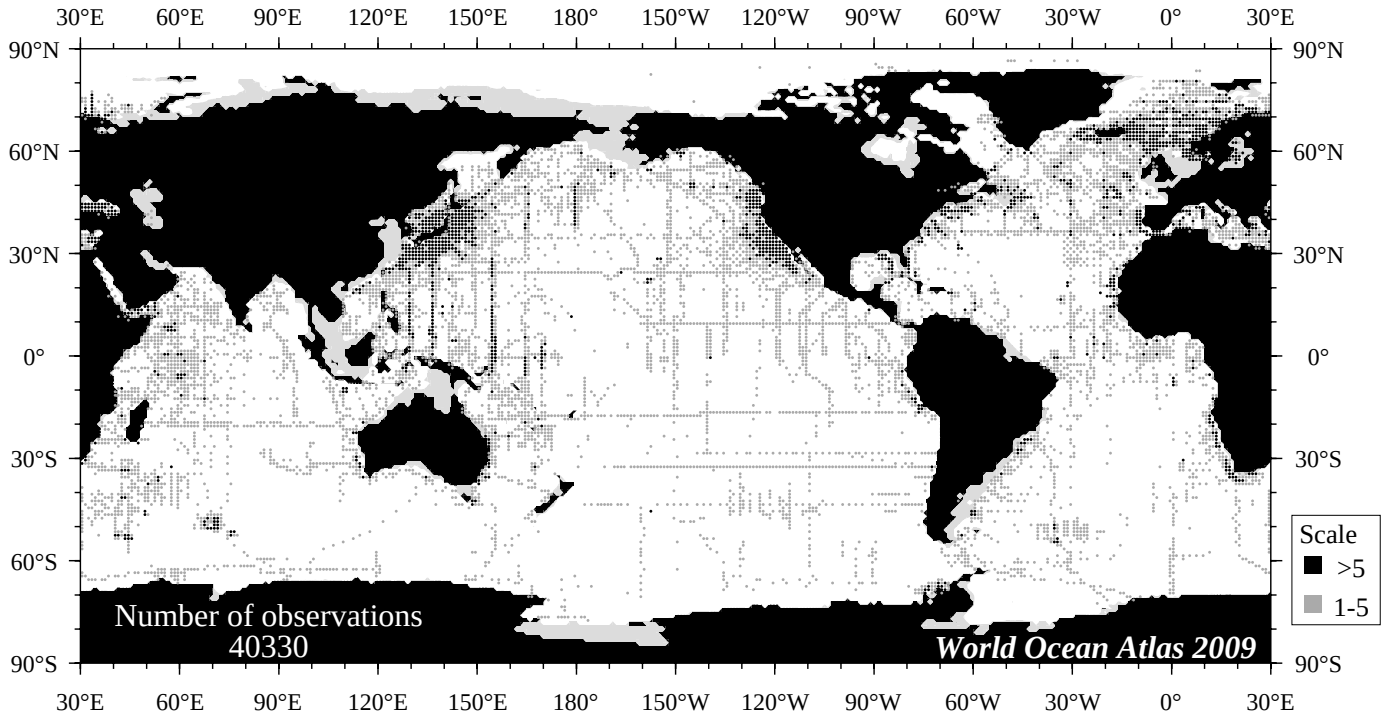

Fig B7 Spring (Apr.-Jun.) phosphate observations at 150 m. depth.

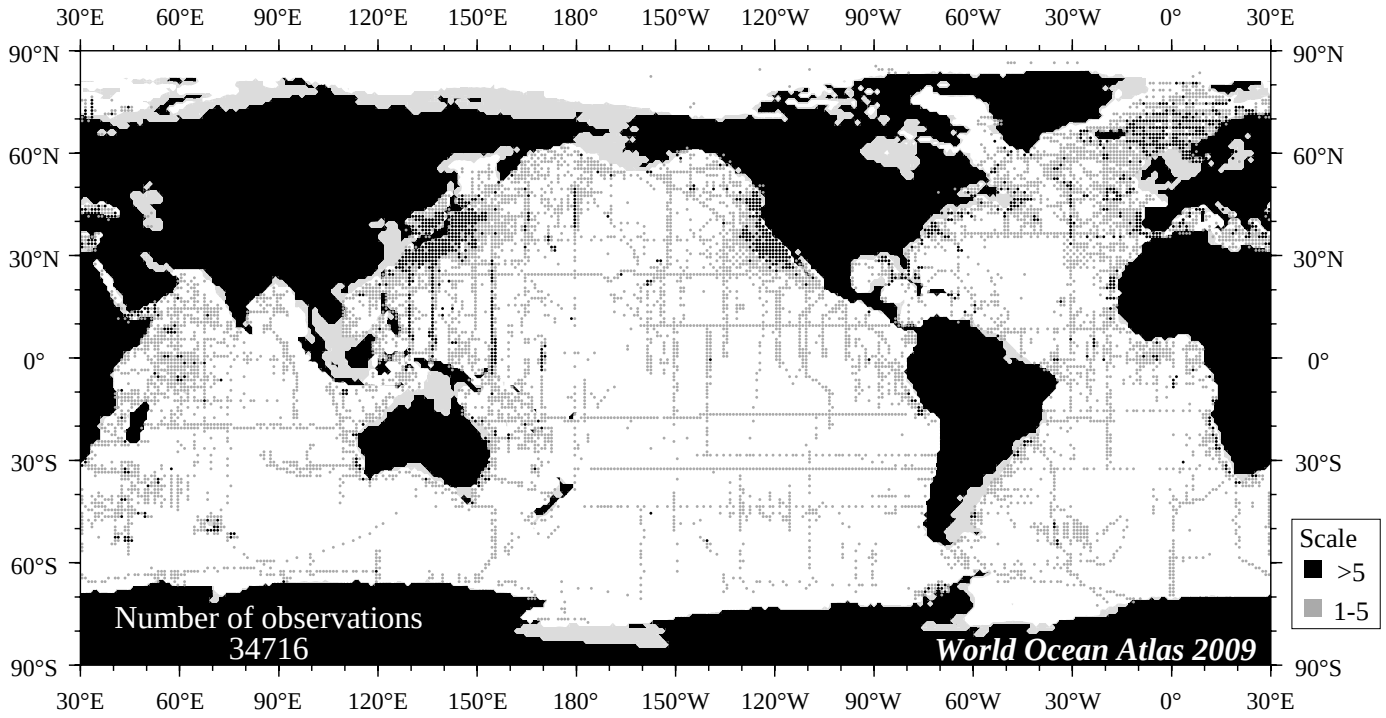

Fig B8 Spring (Apr.-Jun.) phosphate observations at 250 m. depth.

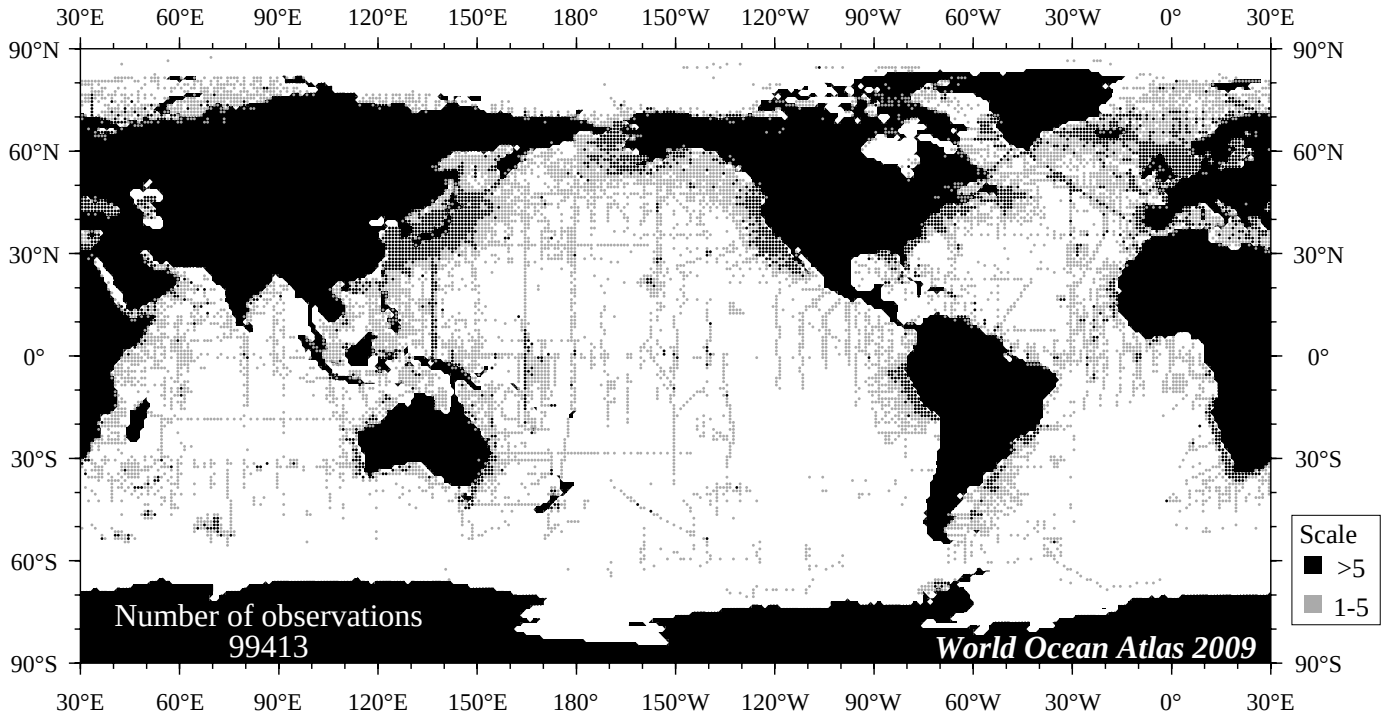

Fig B9 Summer (Jul.-Sep.) phosphate observations at the surface.

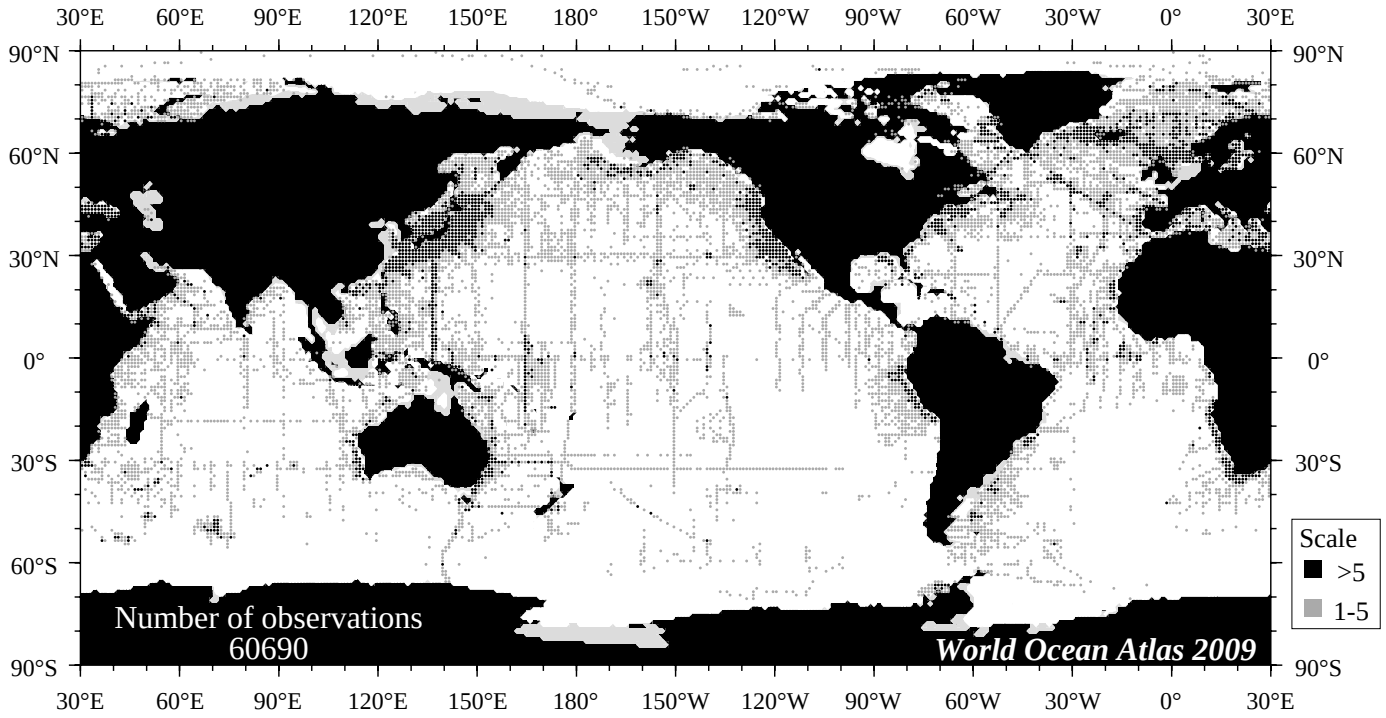

Fig B10 Summer (Jul.-Sep.) phosphate observations at 75 m. depth.

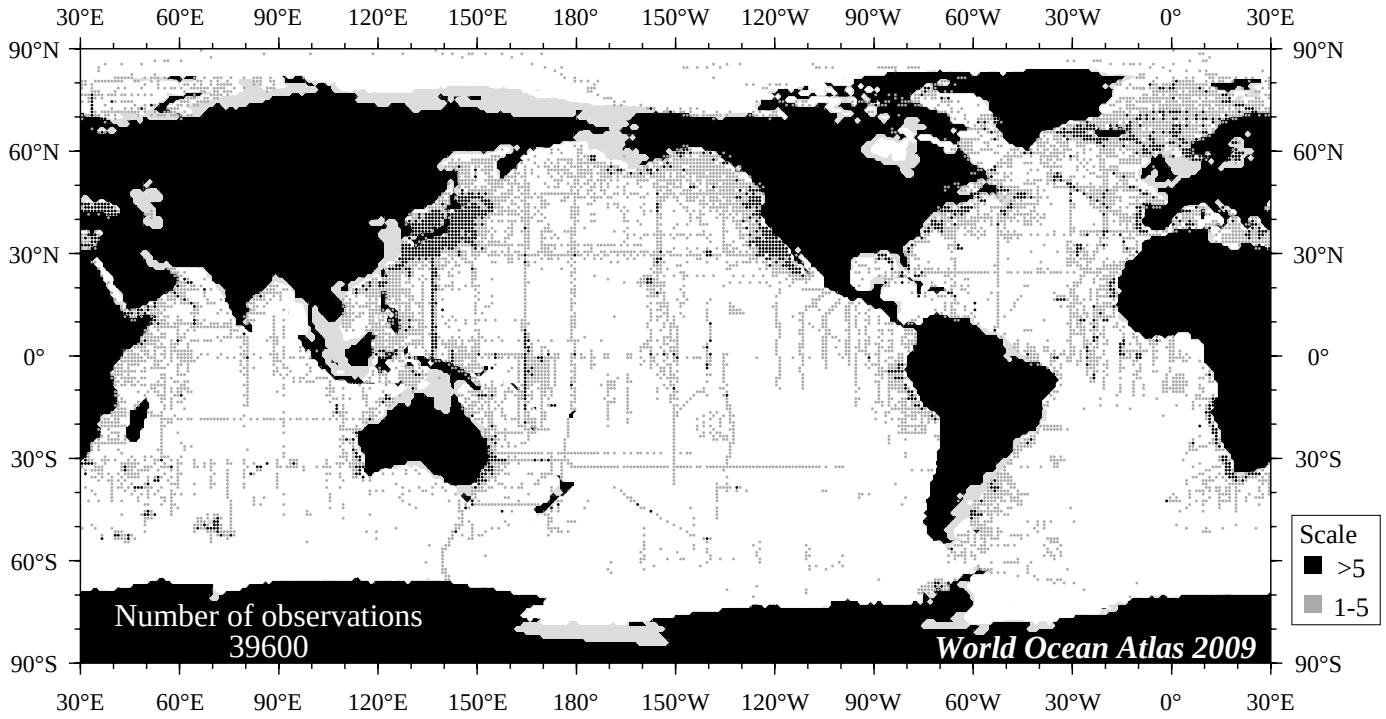

Fig B11 Summer (Jul.-Sep.) phosphate observations at 150 m. depth.

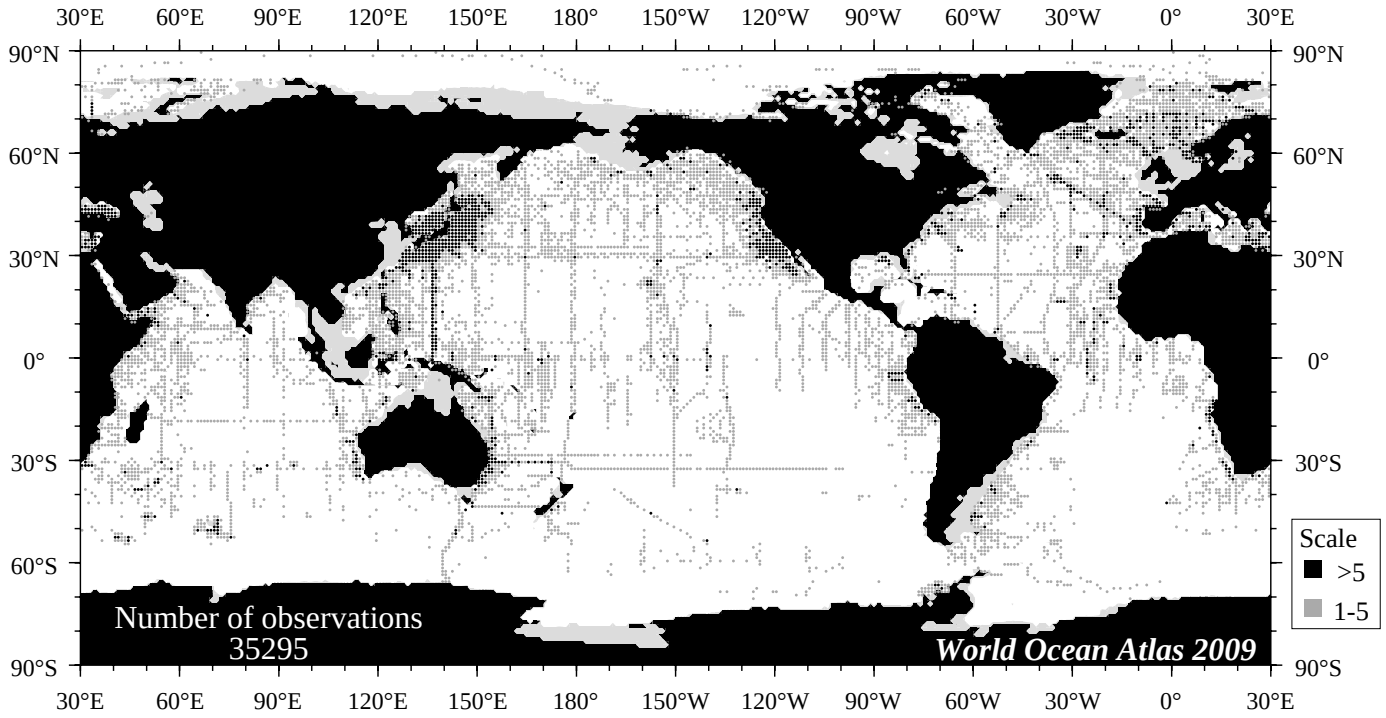

Fig B12 Summer (Jul.-Sep.) phosphate observations at 250 m. depth.

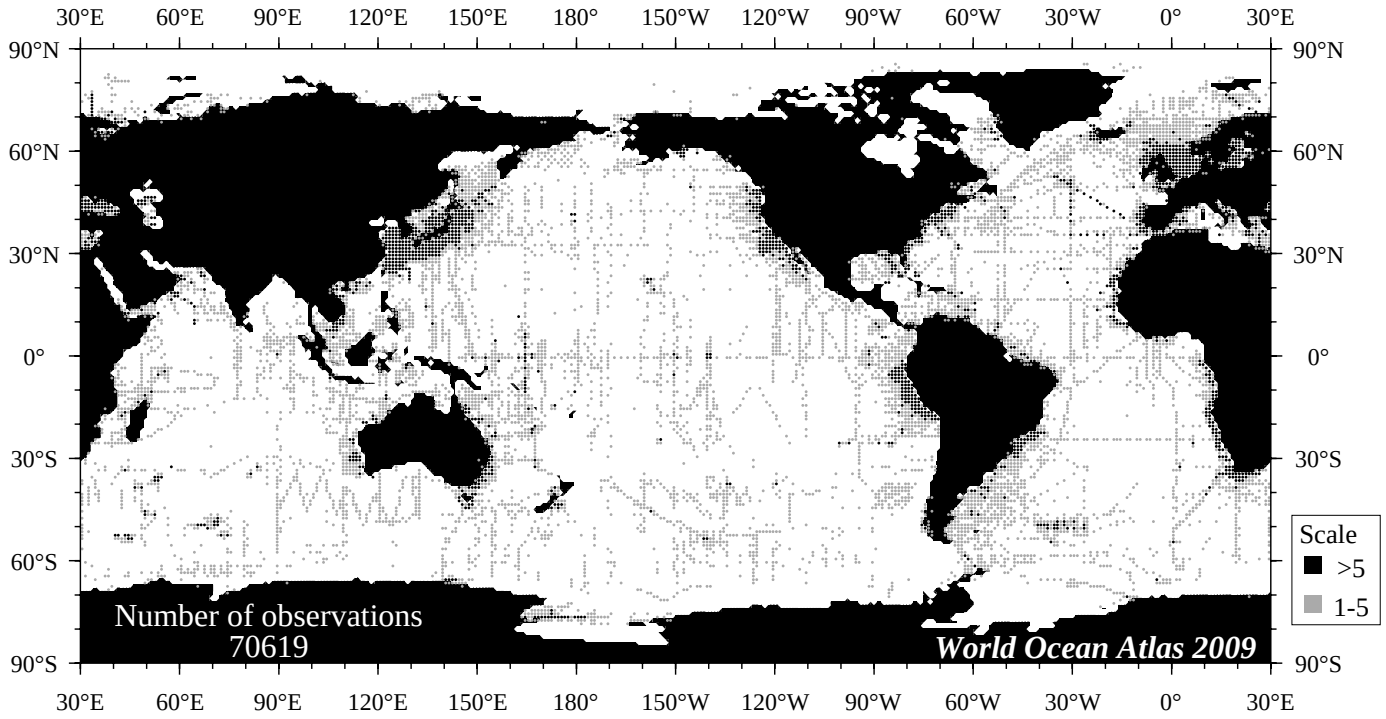

Fig B13 Fall (Oct.-Dec.) phosphate observations at the surface.

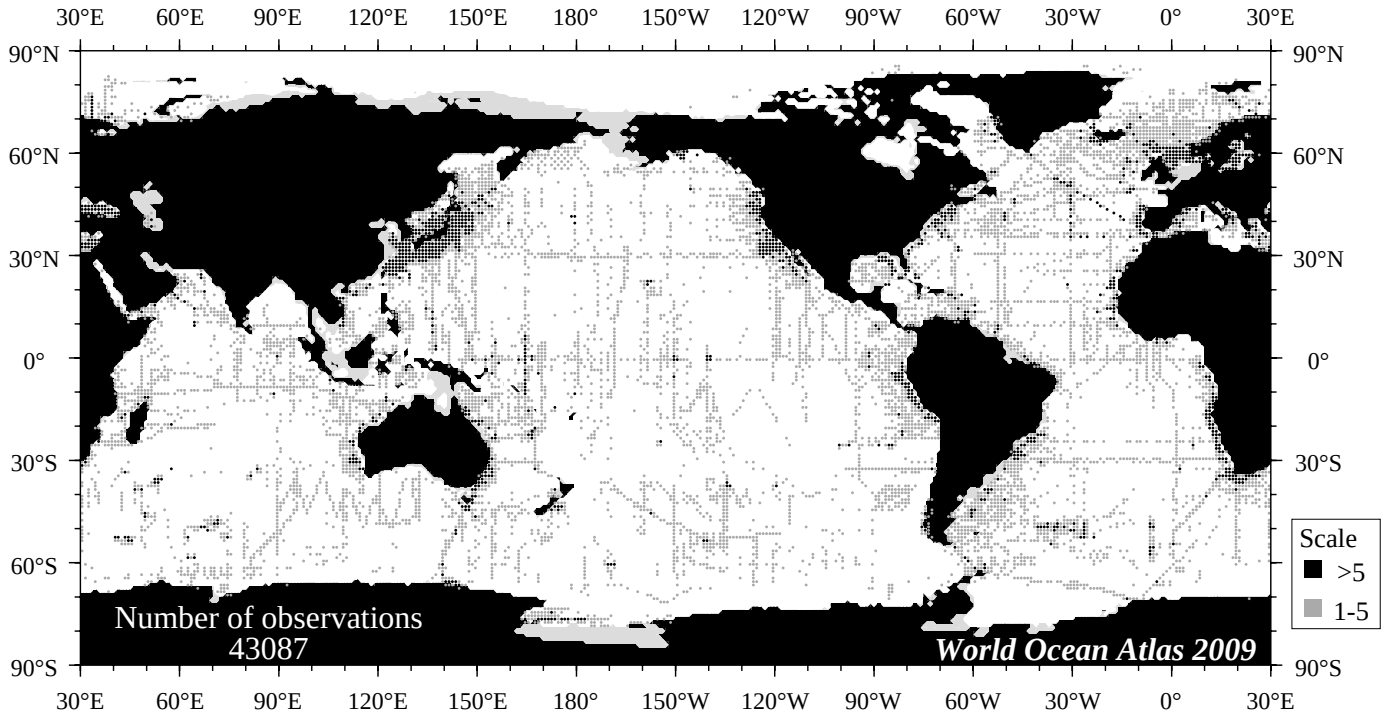

Fig B14 Fall (Oct.-Dec.) phosphate observations at 75 m. depth.

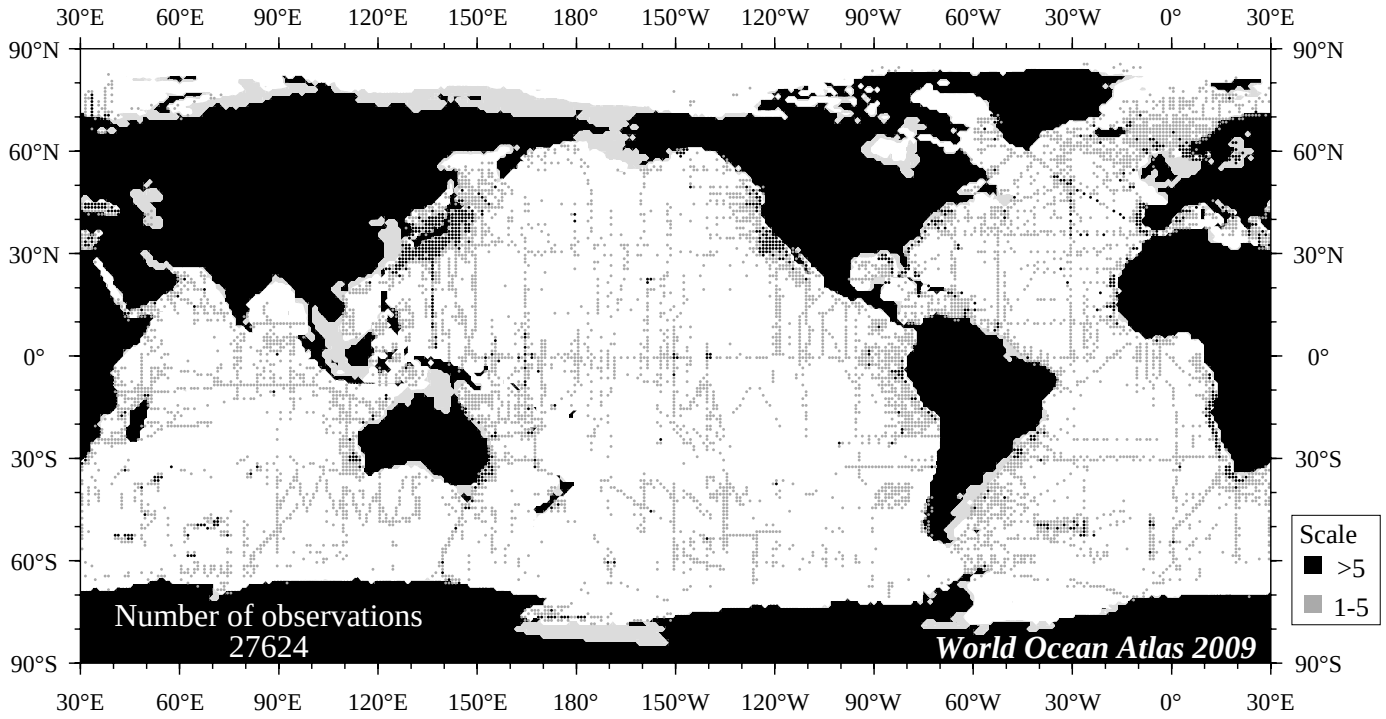

Fig B15 Fall (Oct.-Dec.) phosphate observations at 150 m. depth.

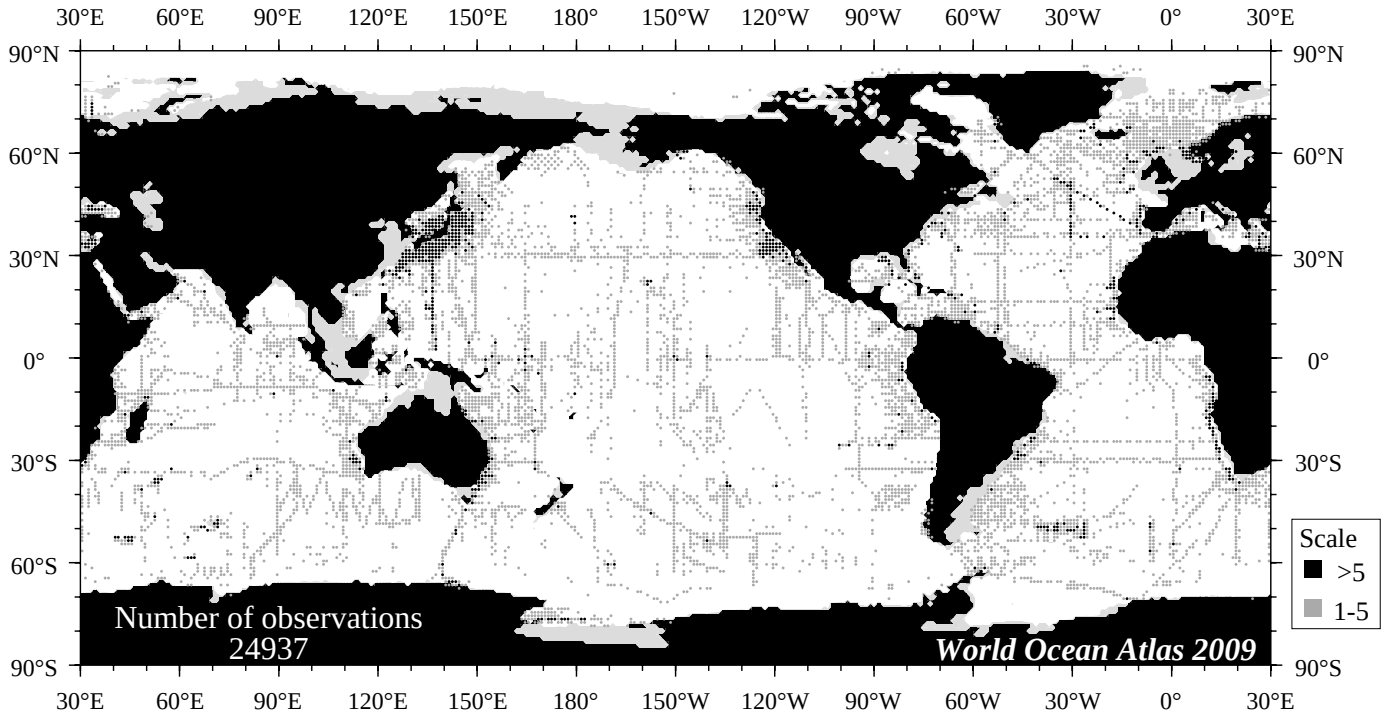

Fig B16 Fall (Oct.-Dec.) phosphate observations at 250 m. depth.

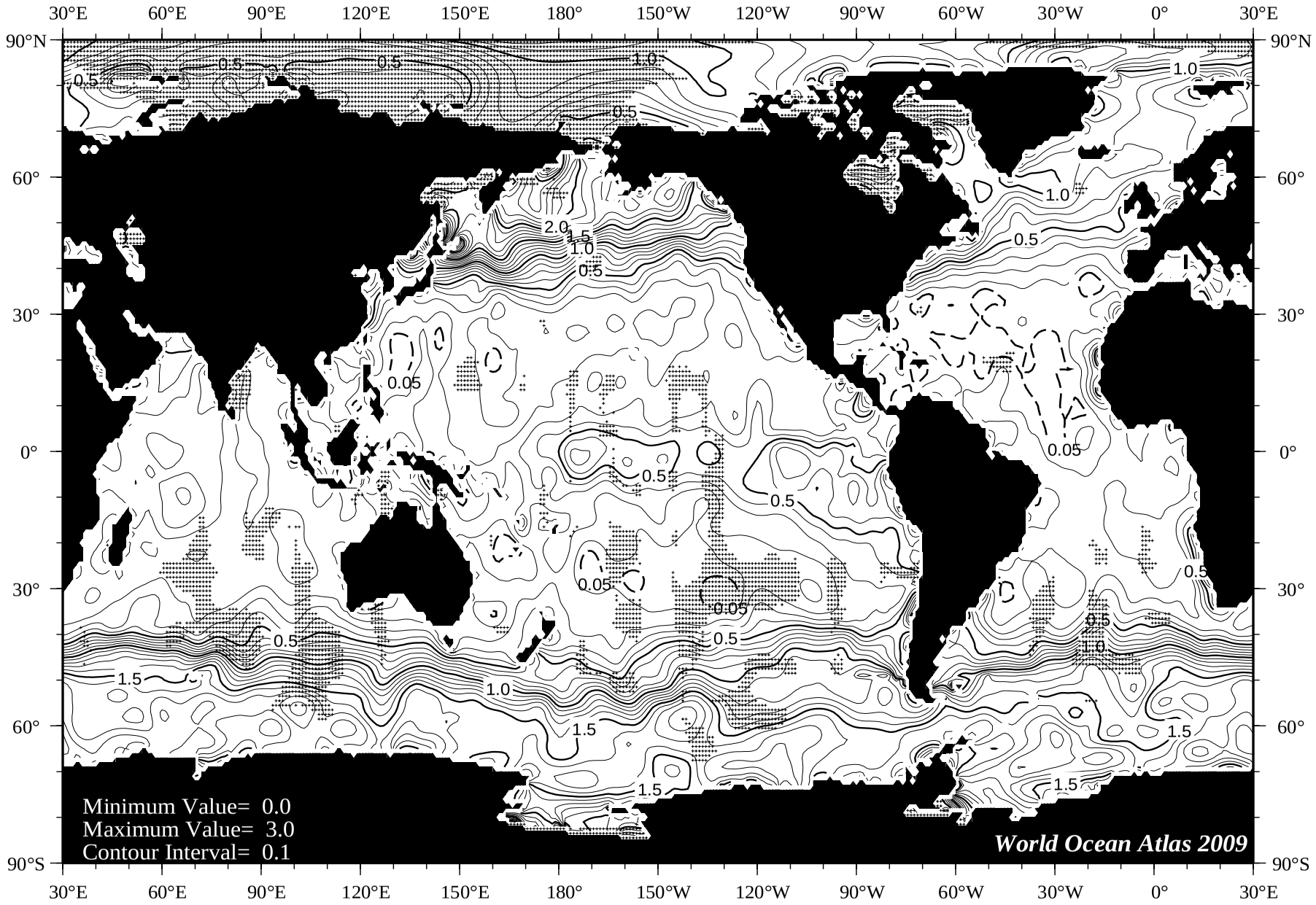

Fig B17 Winter (Jan.-Mar.) phosphate [umol/l] at the surface.

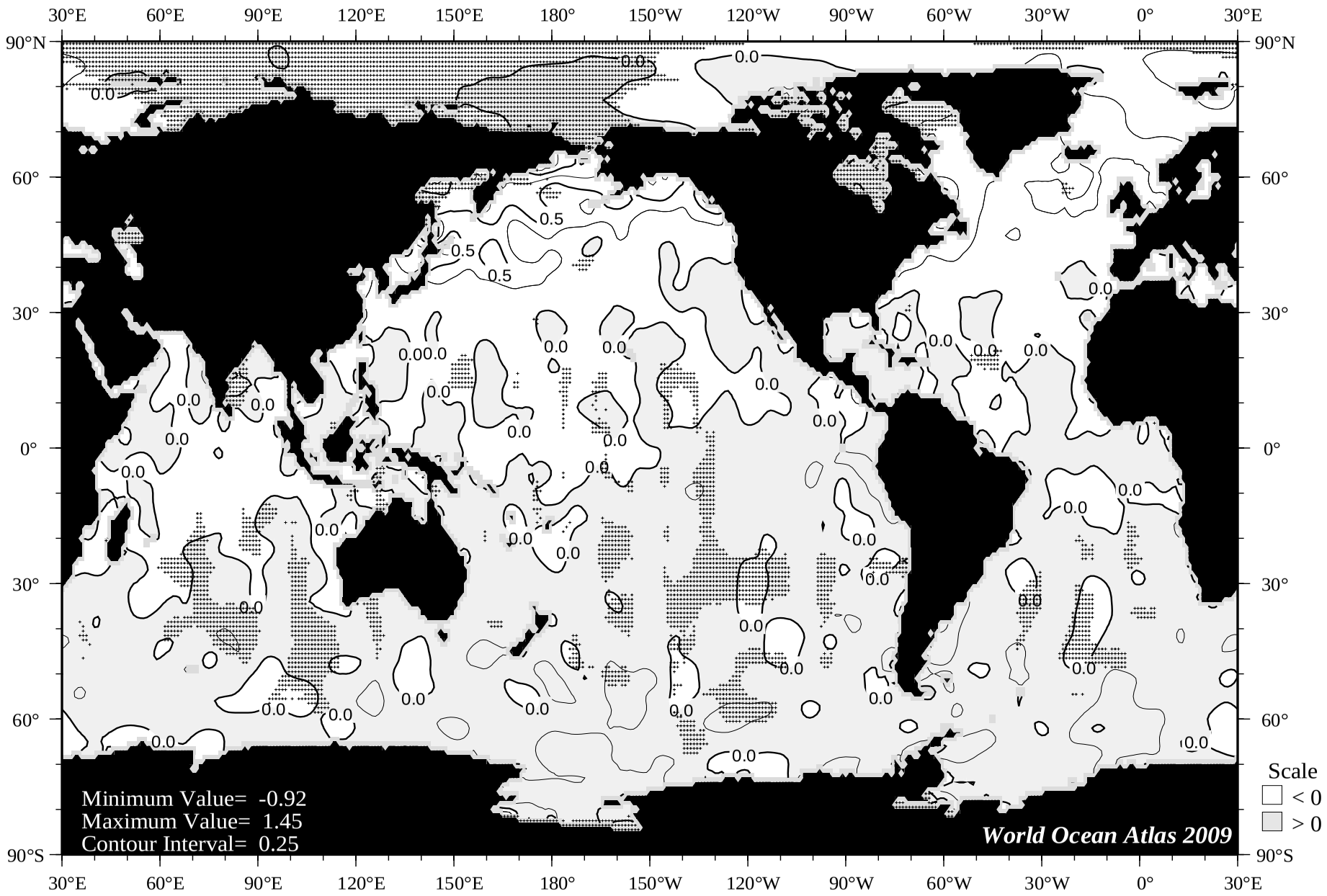

Fig B18 Winter (Jan.-Mar.) minus annual phosphate [umol/l] at the surface.

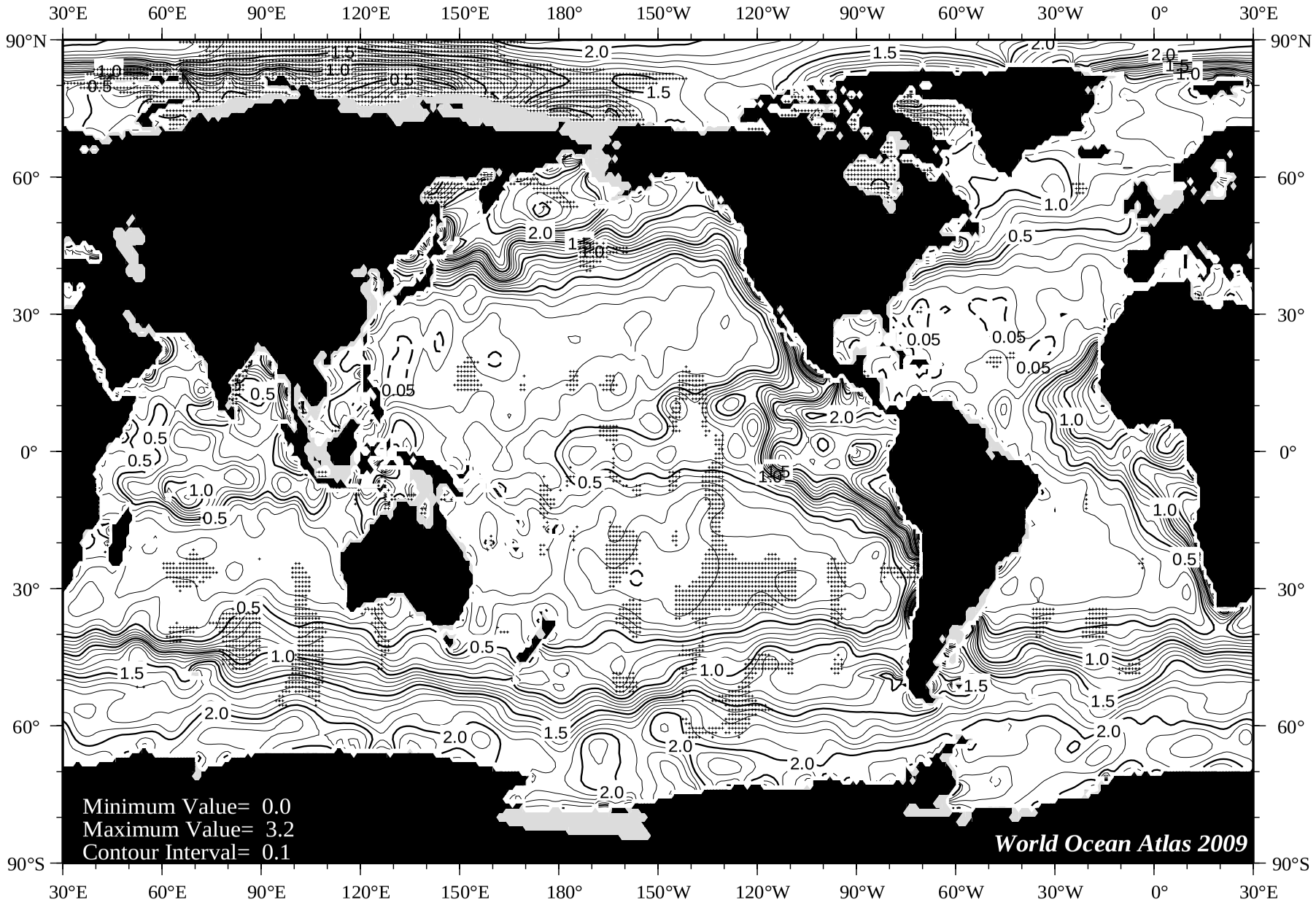

Fig B19 Winter (Jan.-Mar.) phosphate [umol/l] at 75 m. depth.

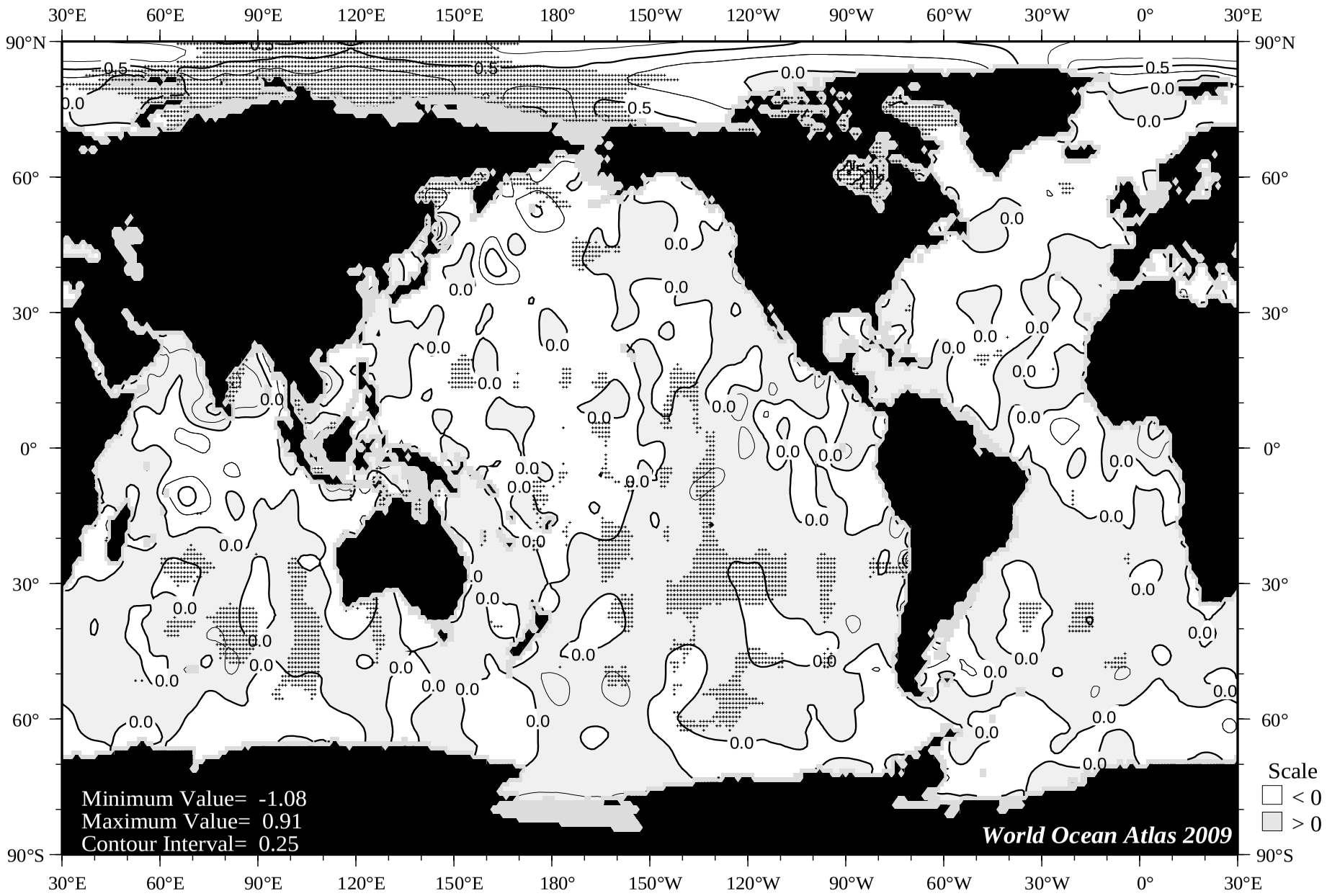

Fig B20 Winter (Jan.-Mar.) minus annual phosphate [umol/l] at 75 m. depth.

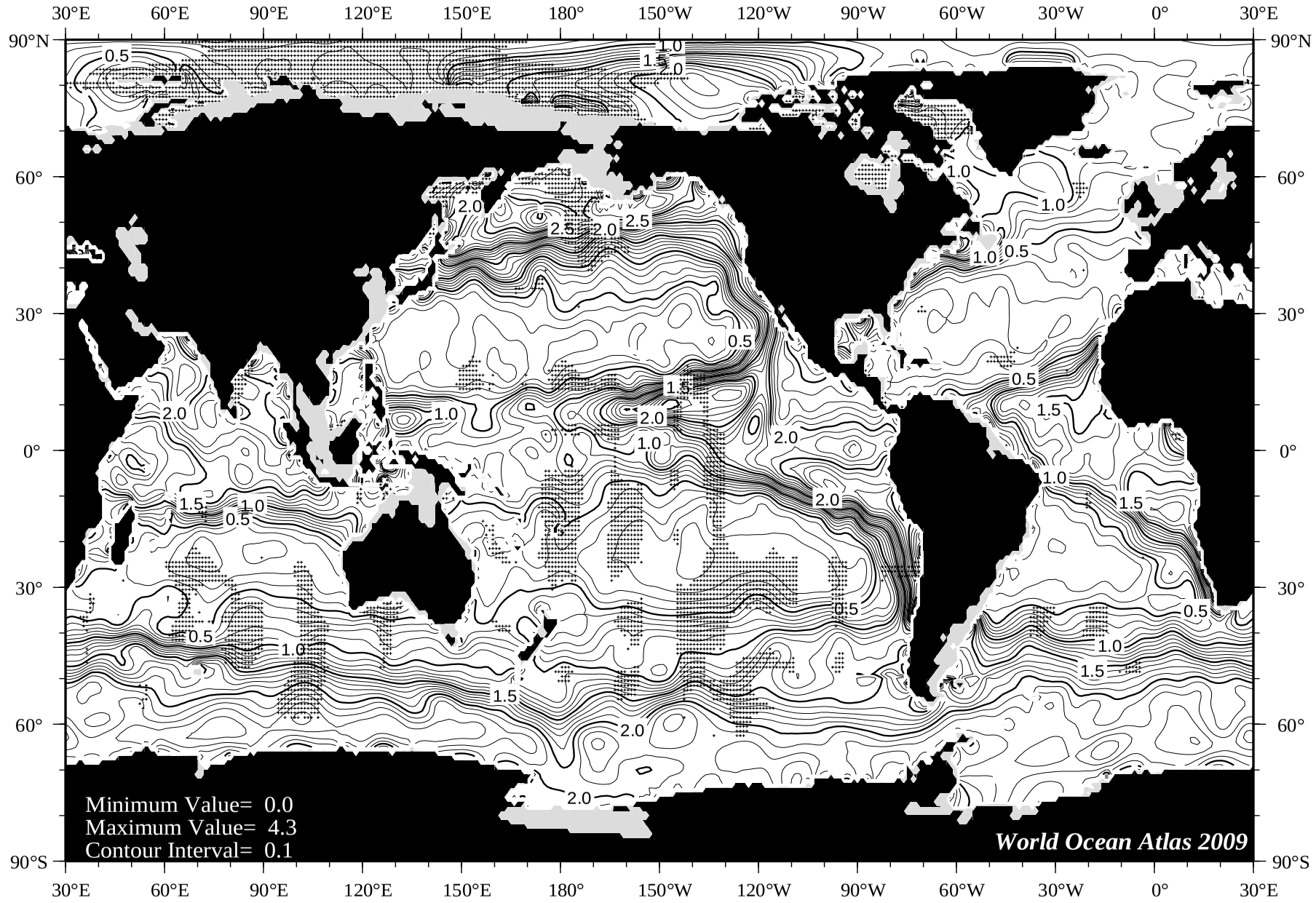

Fig B21 Winter (Jan.-Mar.) phosphate [umol/l] at 150 m. depth.

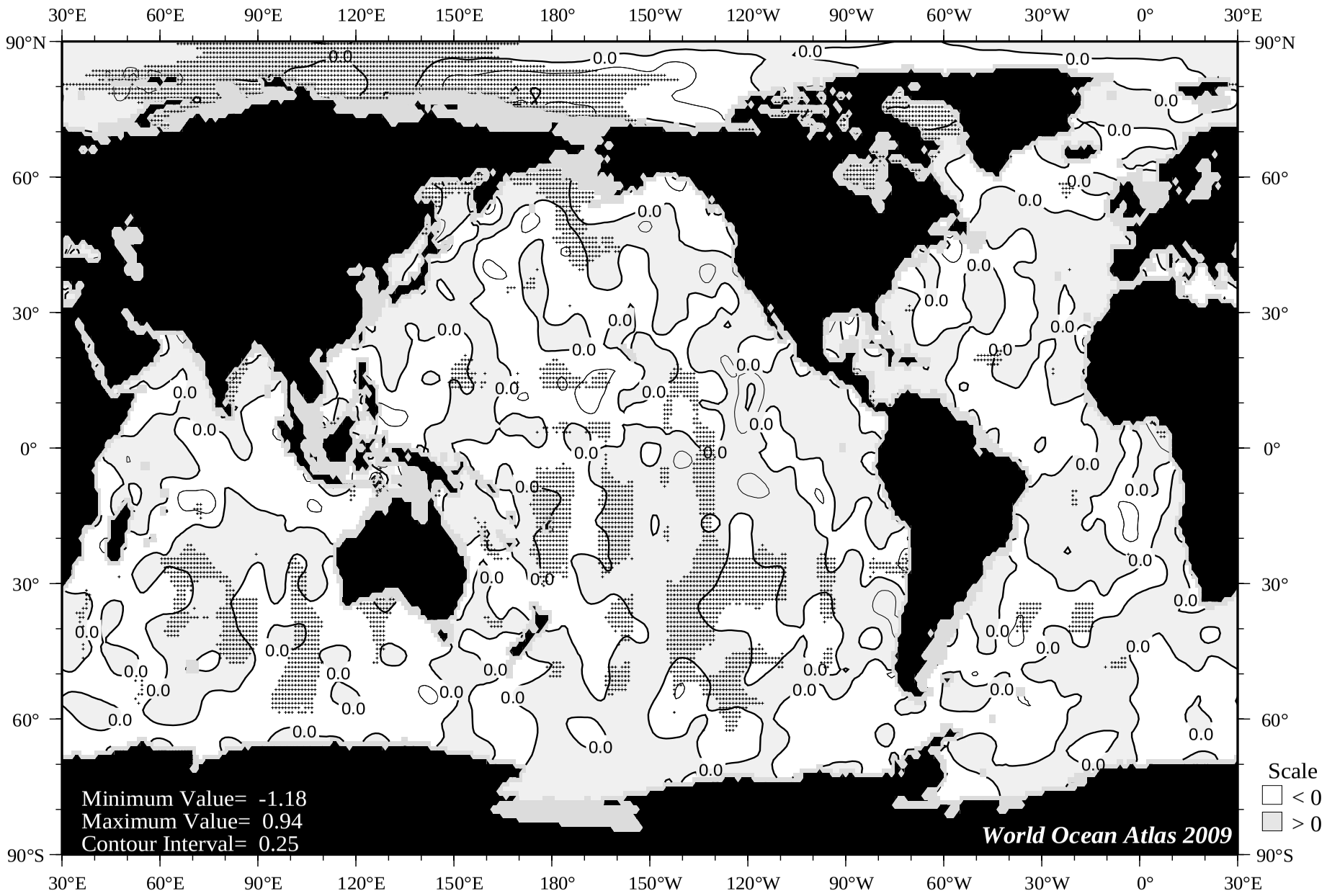

Fig B22 Winter (Jan.-Mar.) minus annual phosphate [umol/l] at 150 m. depth.

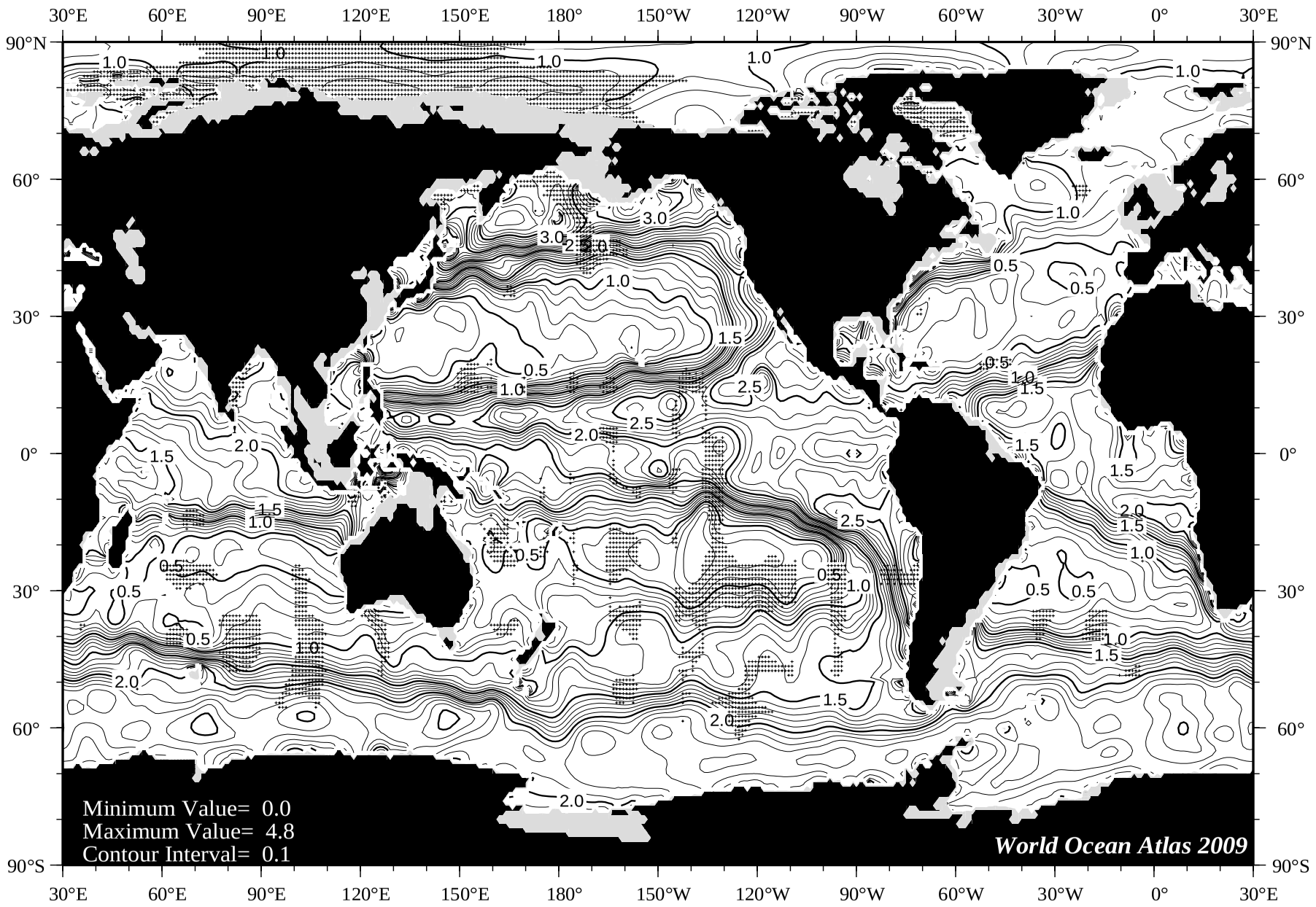

Fig B23 Winter (Jan.-Mar.) phosphate [umol/l] at 250 m. depth.

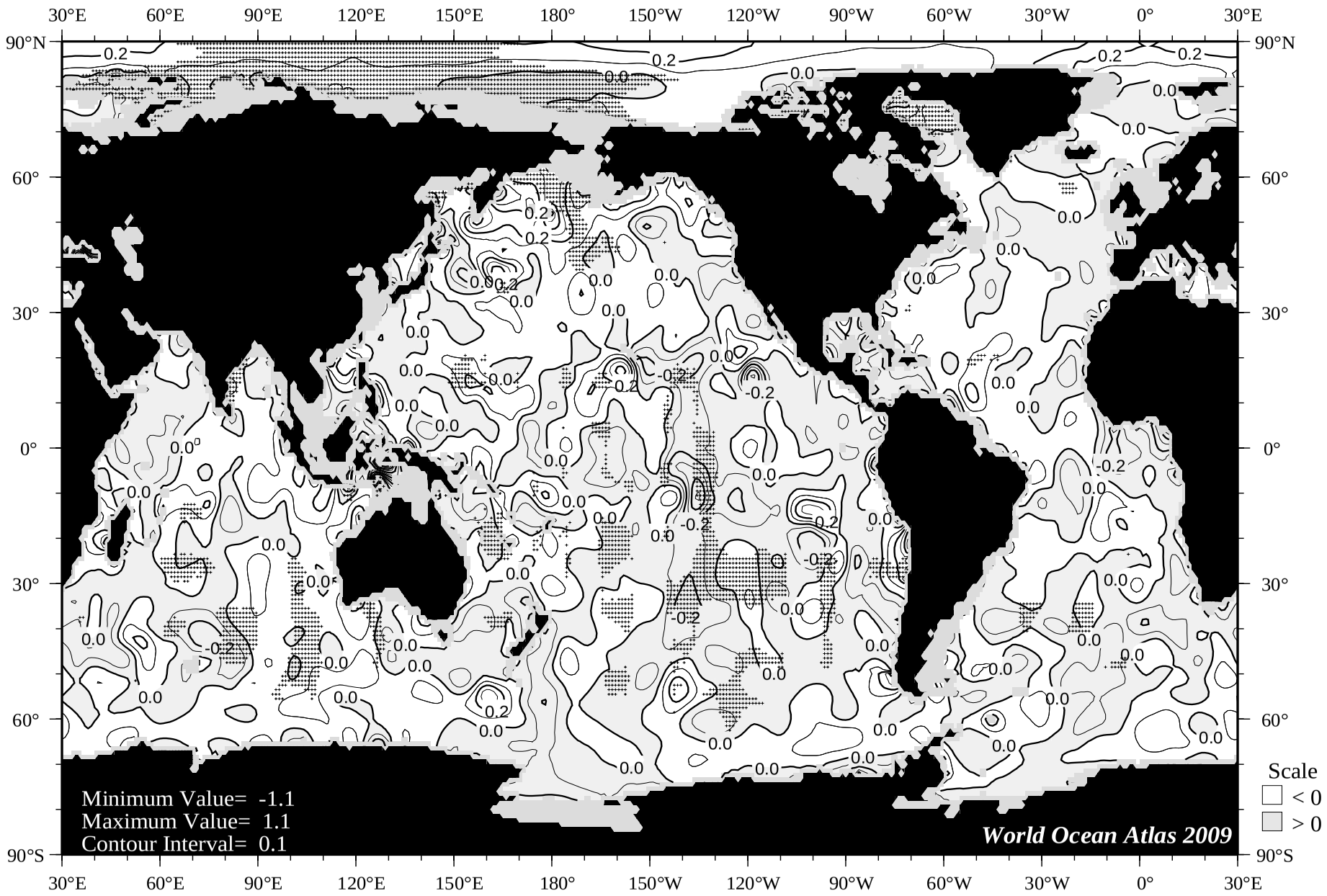

Fig B24 Winter (Jan.-Mar.) minus annual phosphate [umol/l] at 250 m. depth.

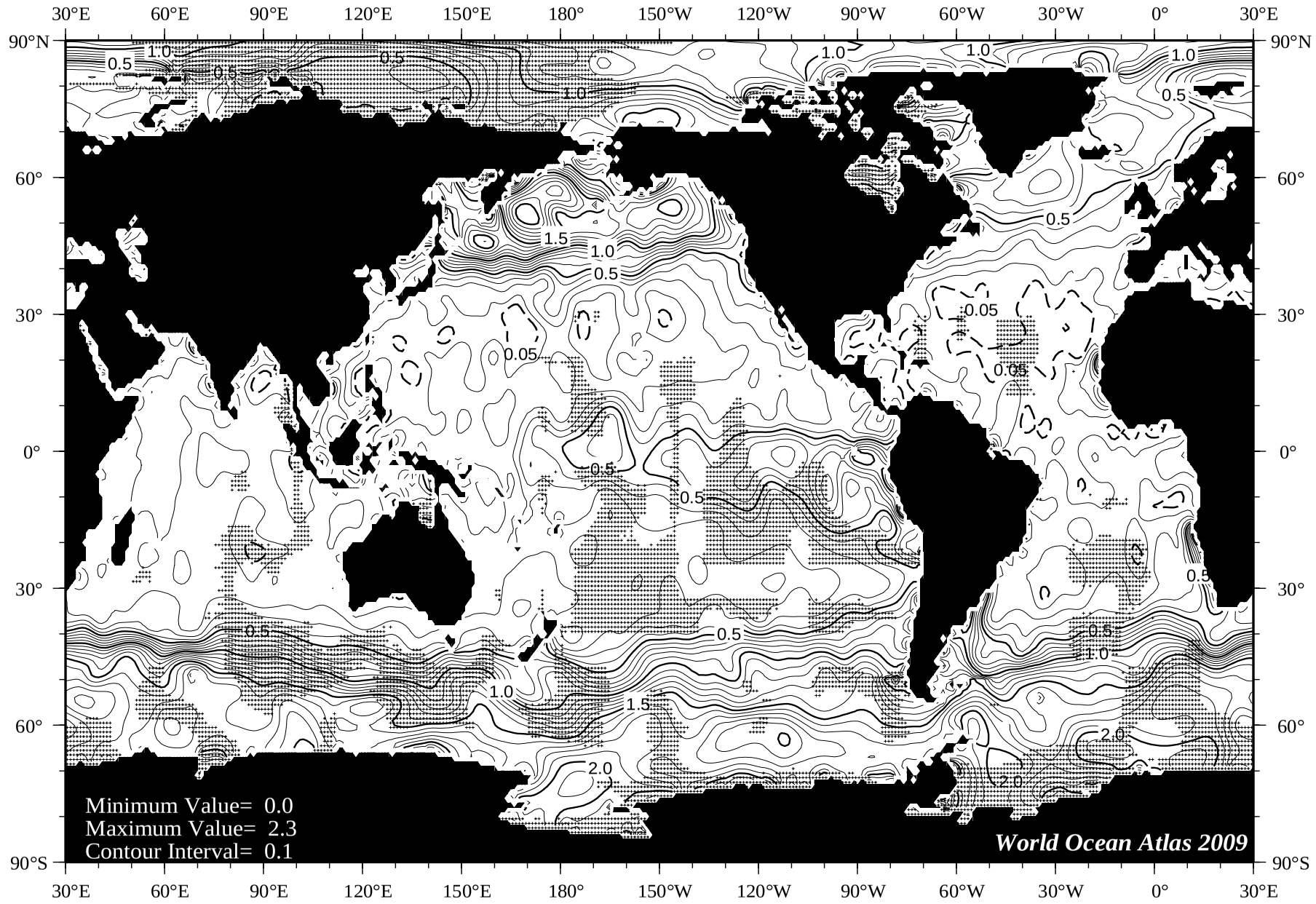

Fig B25 Spring (Apr.-Jun.) phosphate [umol/l] at the surface.

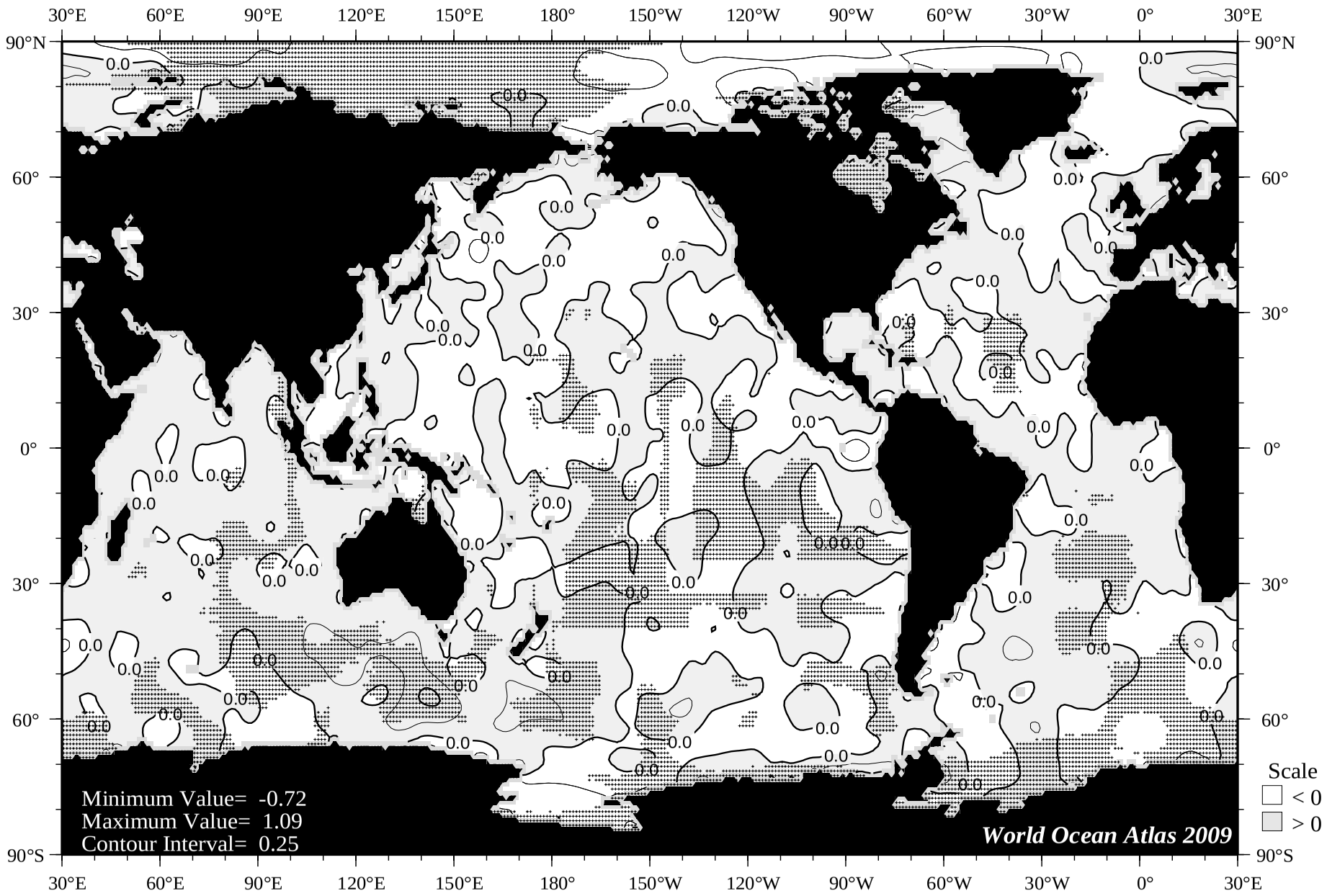

Fig B26 Spring (Apr.-Jun.) minus annual phosphate [umol/l] at the surface.

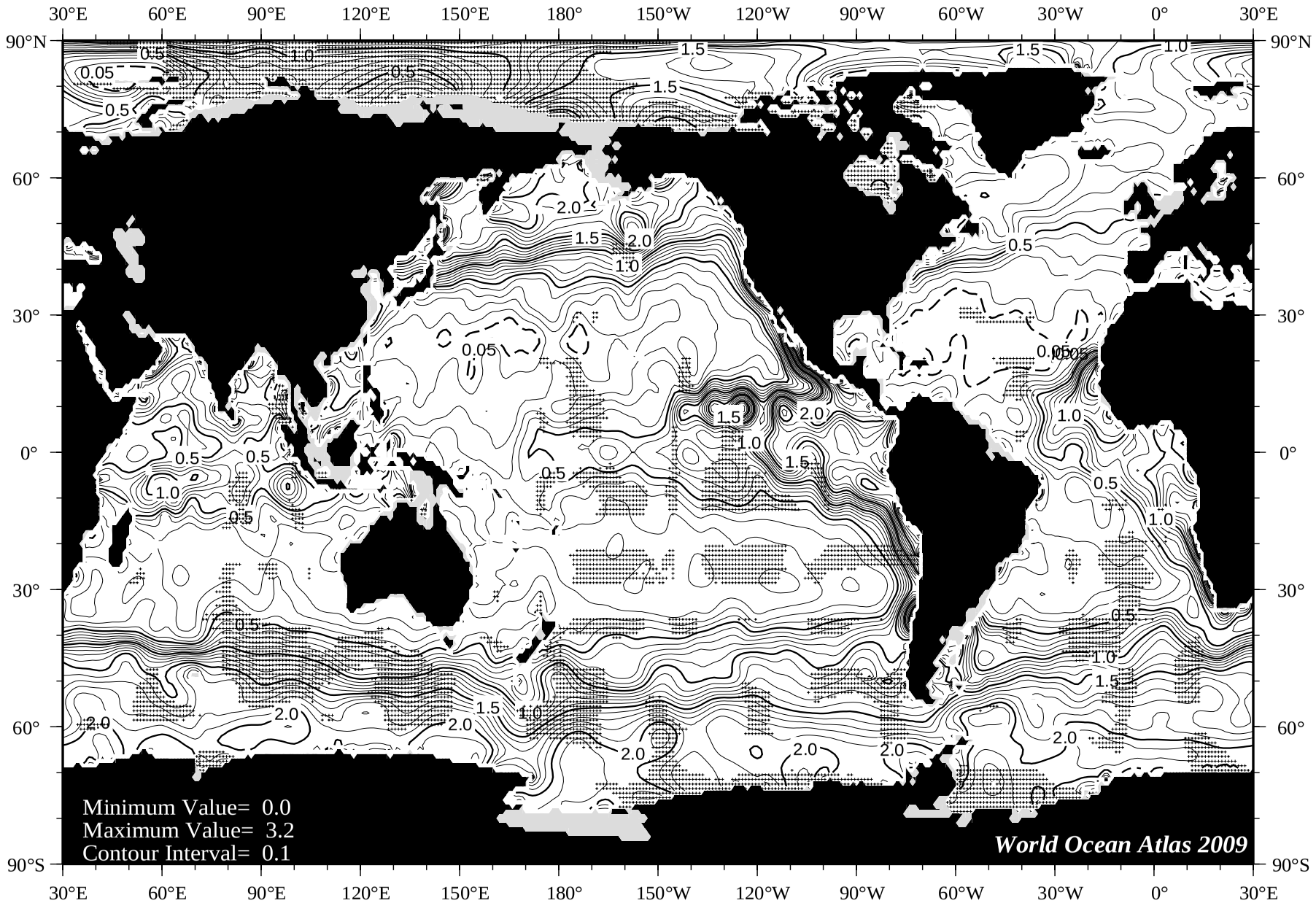

Fig B27 Spring (Apr.-Jun.) phosphate [umol/l] at 75 m. depth.

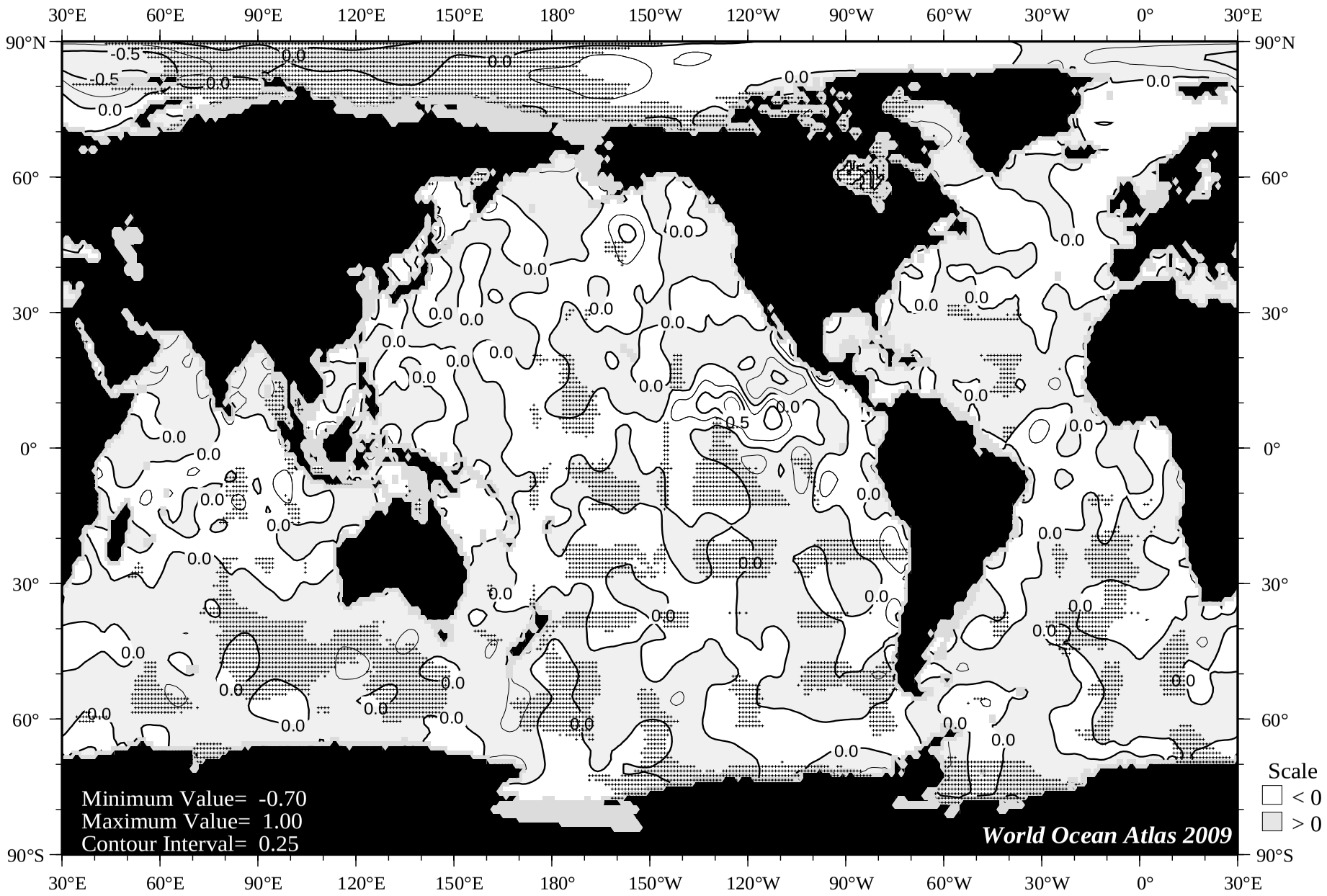

Fig B28 Spring (Apr.-Jun.) minus annual phosphate [umol/l] at 75 m. depth.

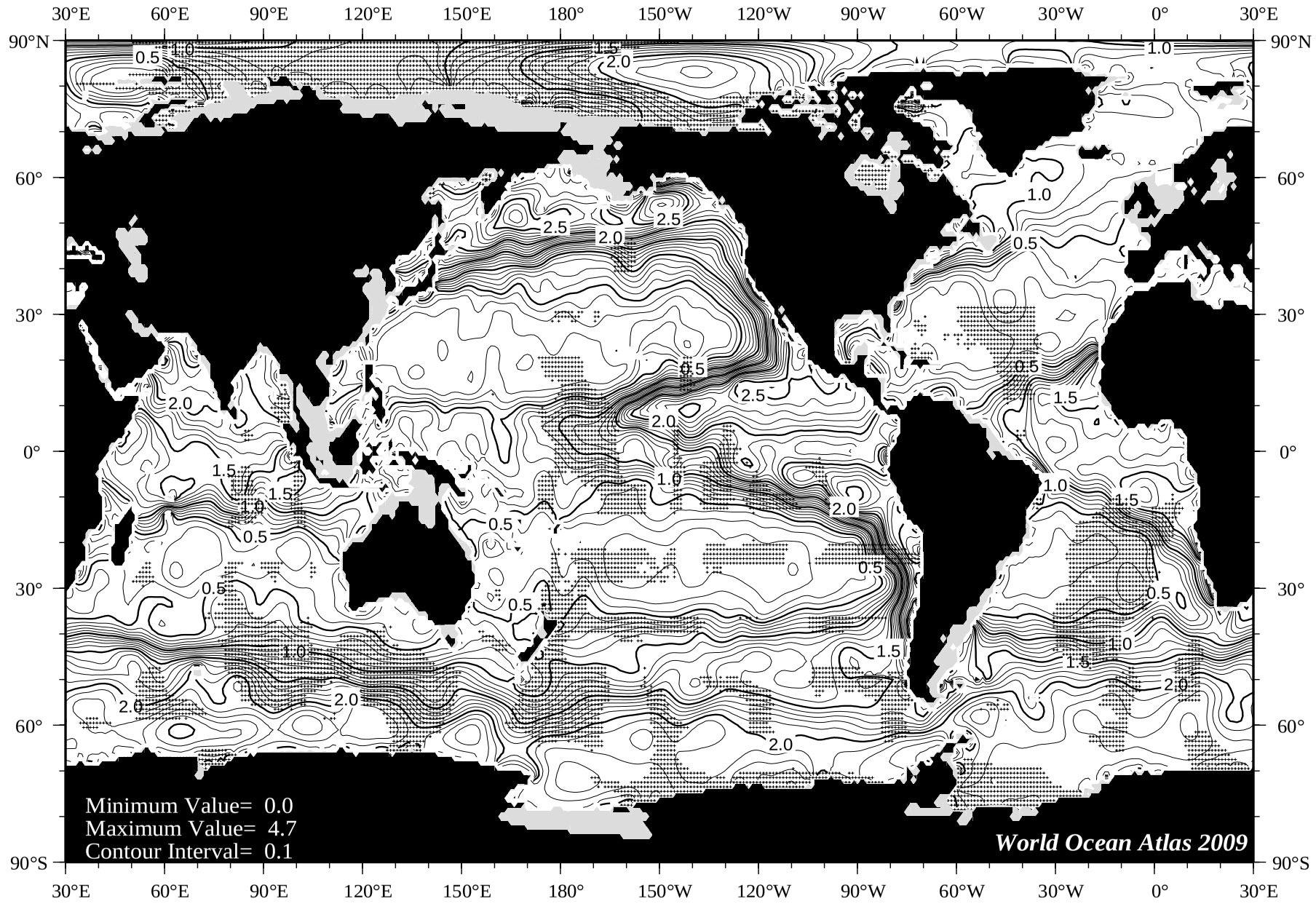

Fig B29 Spring (Apr.-Jun.) phosphate [umol/l] at 150 m. depth.

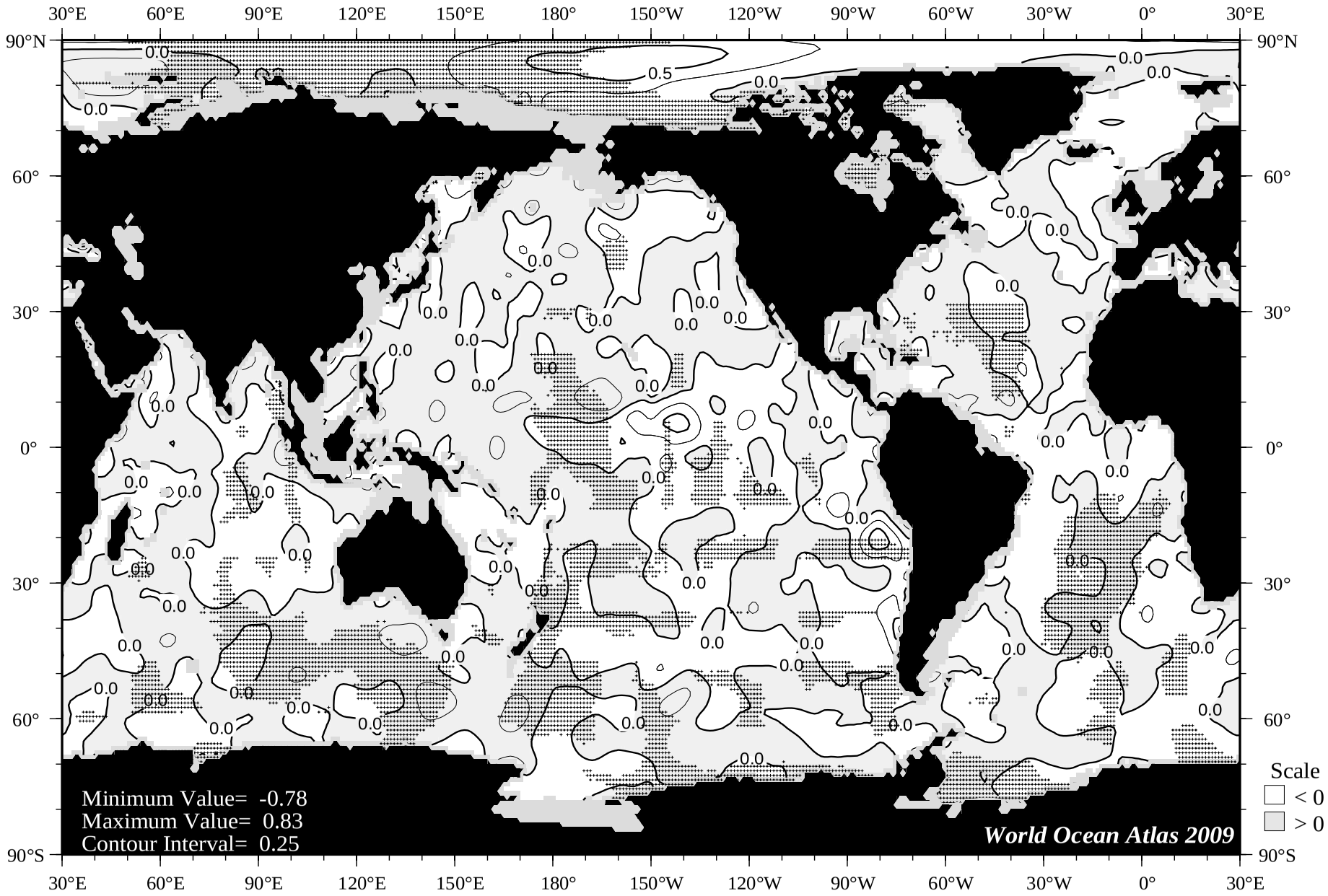

Fig B30 Spring (Apr.-Jun.) minus annual phosphate [umol/l] at 150 m. depth.

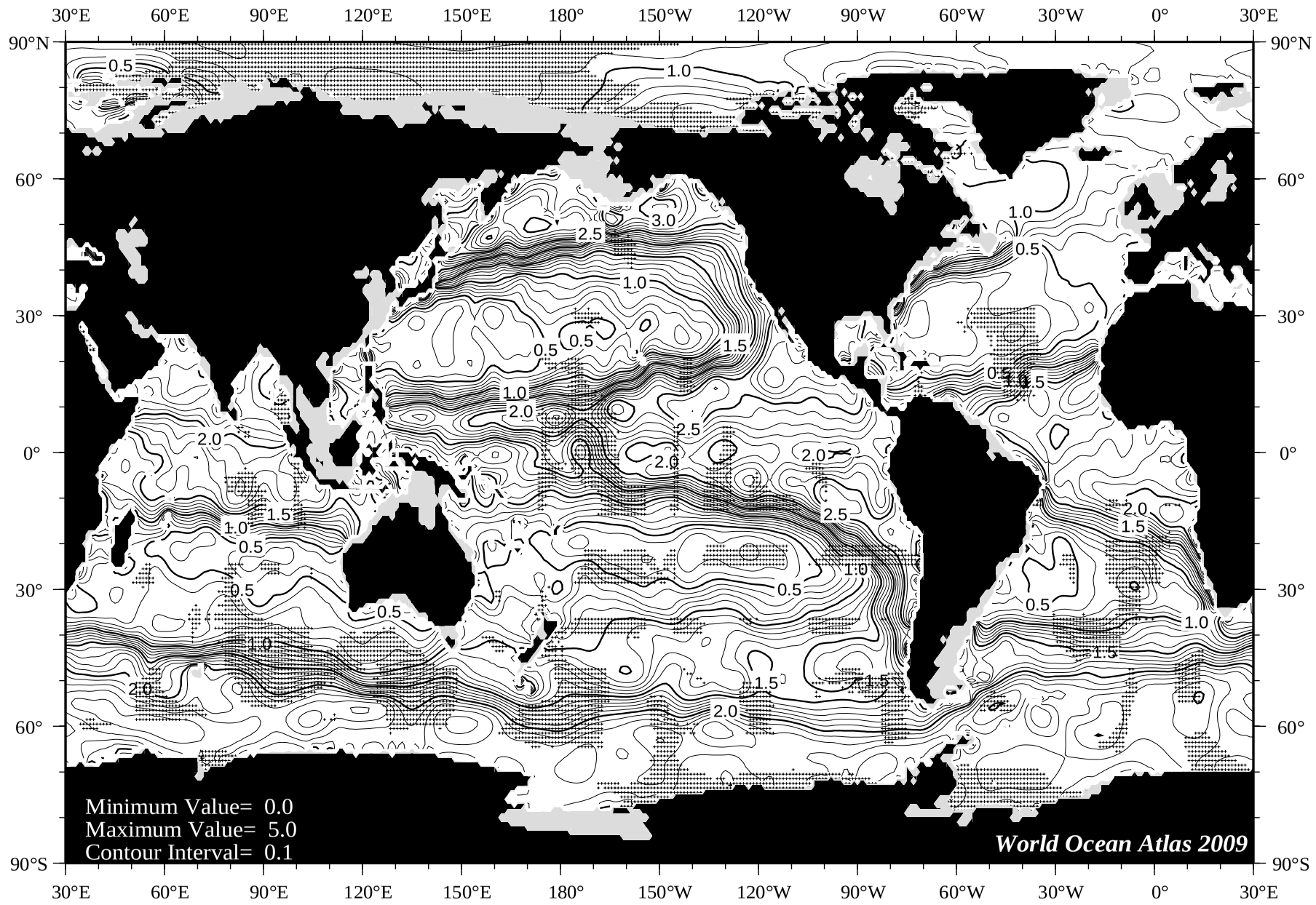

Fig B31 Spring (Apr.-Jun.) phosphate [umol/l] at 250 m. depth.

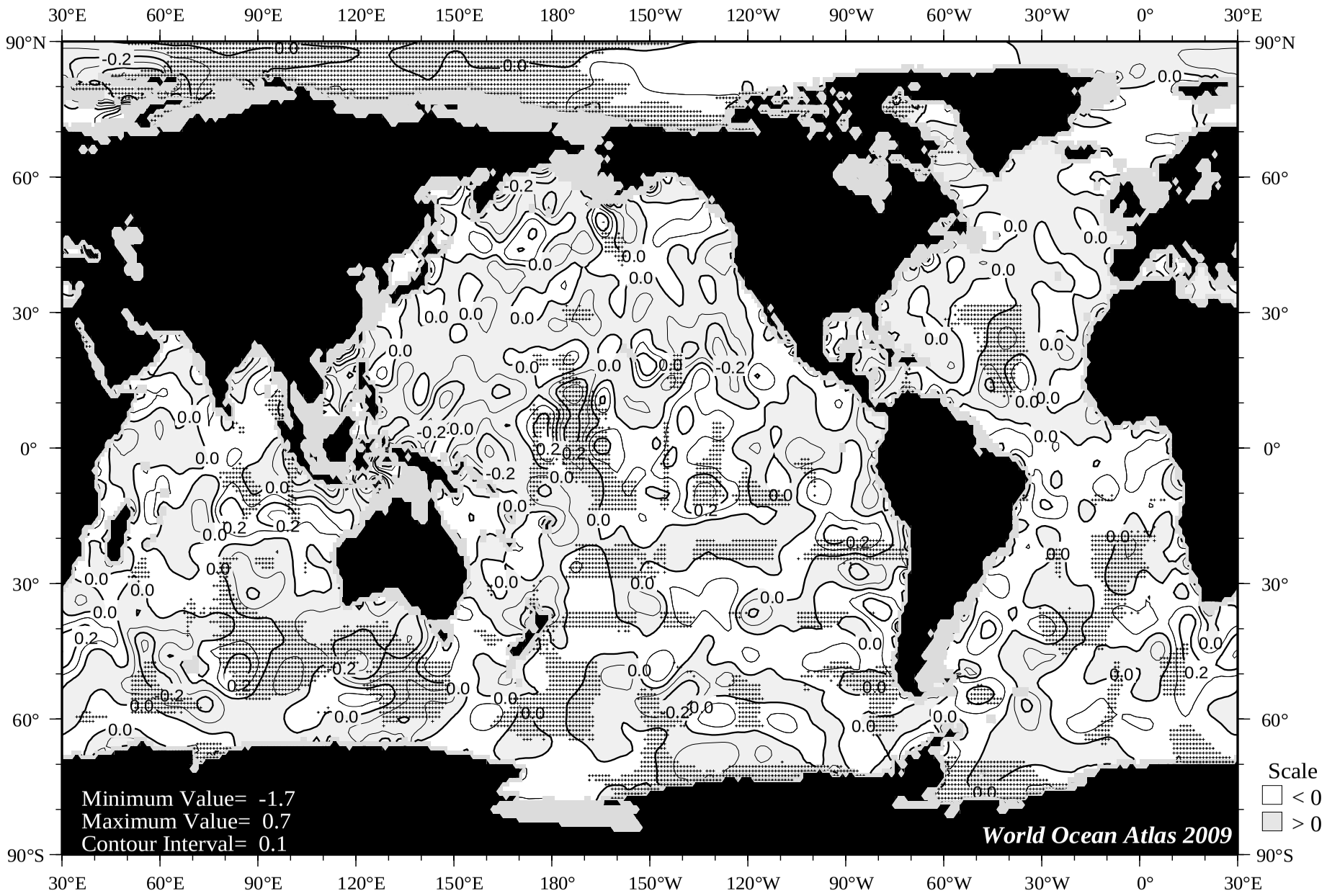

Fig B32 Spring (Apr.-Jun.) minus annual phosphate [umol/l] at 250 m. depth.

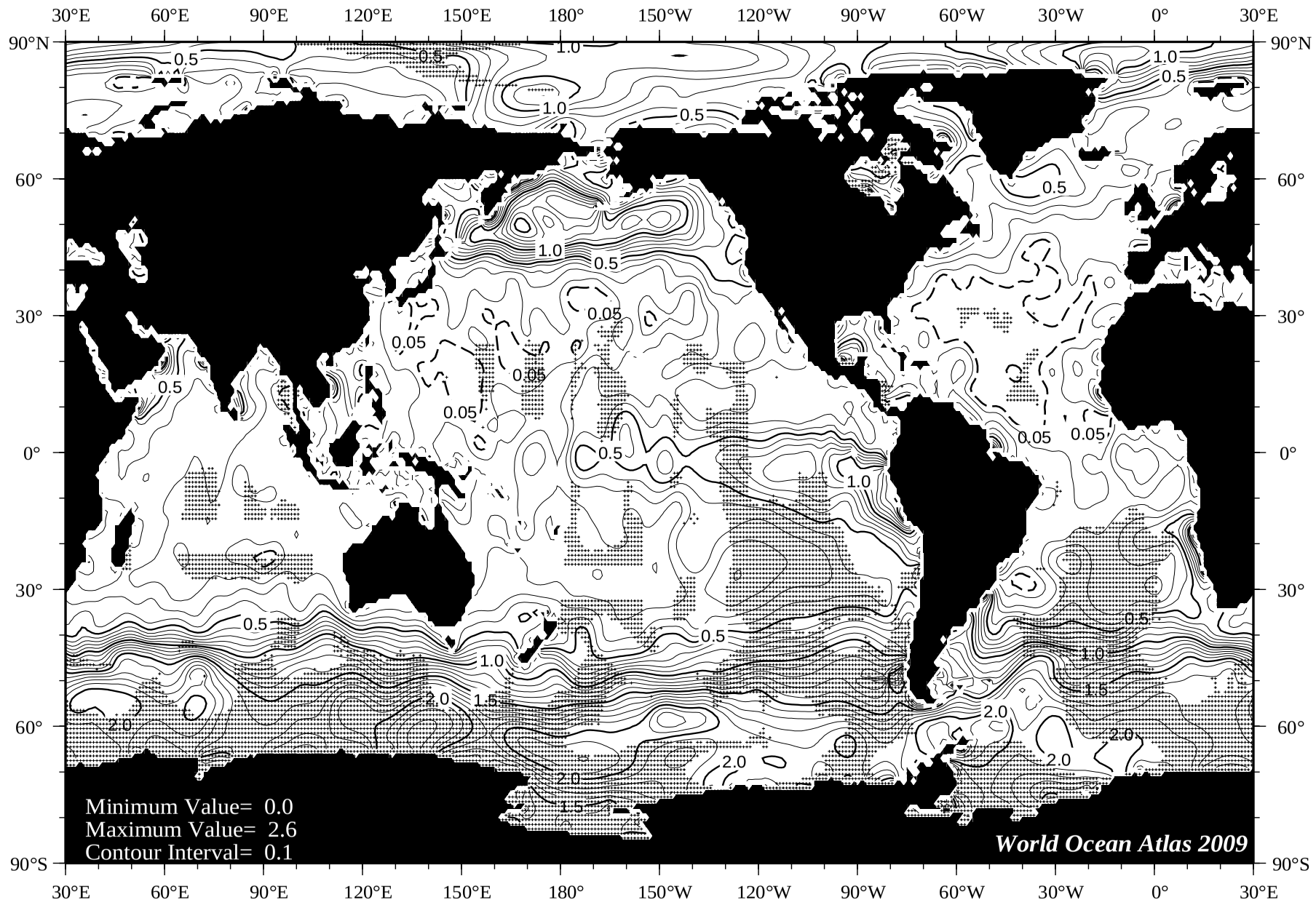

Fig B33 Summer (Jul.-Sep.) phosphate [umol/l] at the surface.

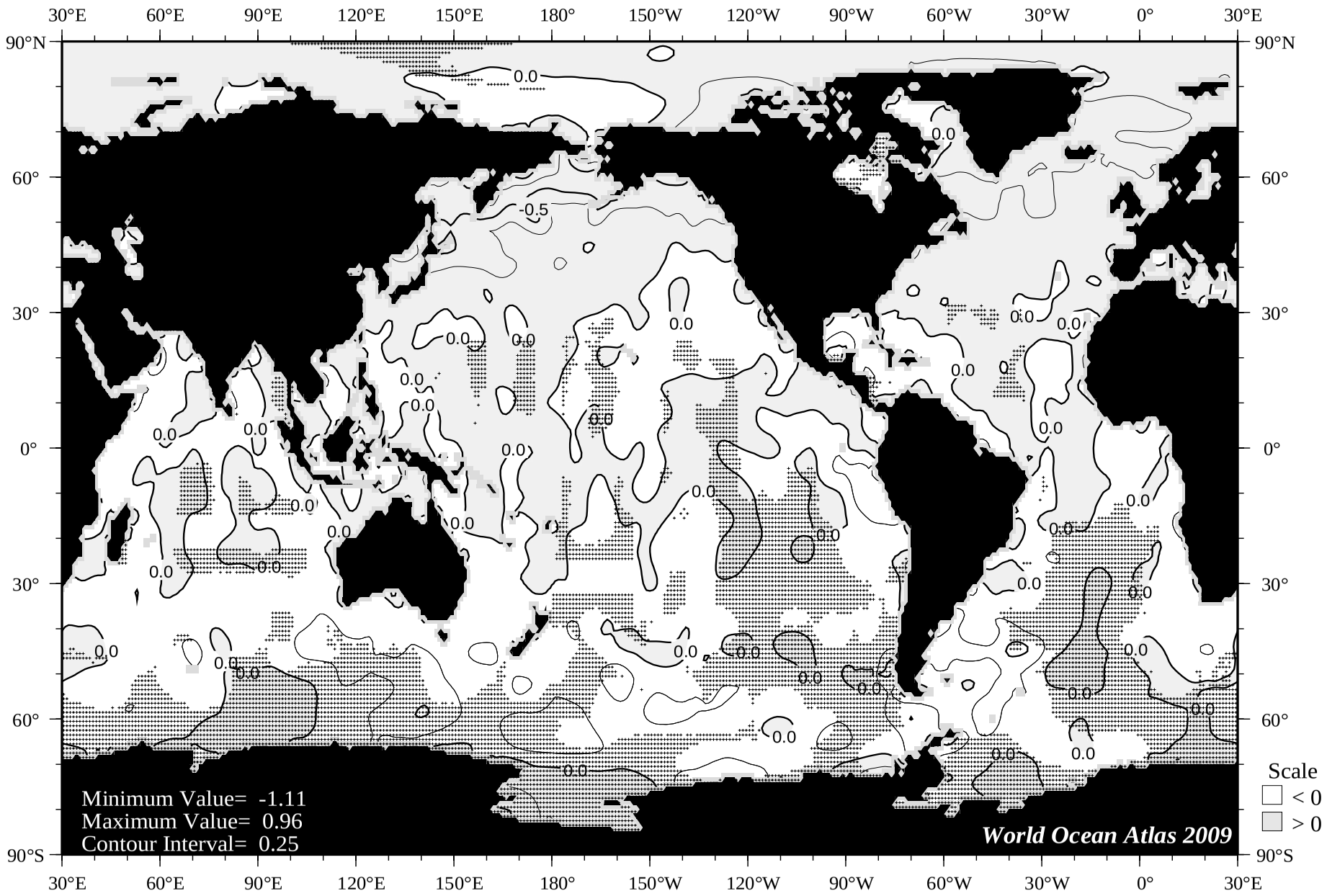

Fig B34 Summer (Jul.-Sep.) minus annual phosphate [umol/l] at the surface.

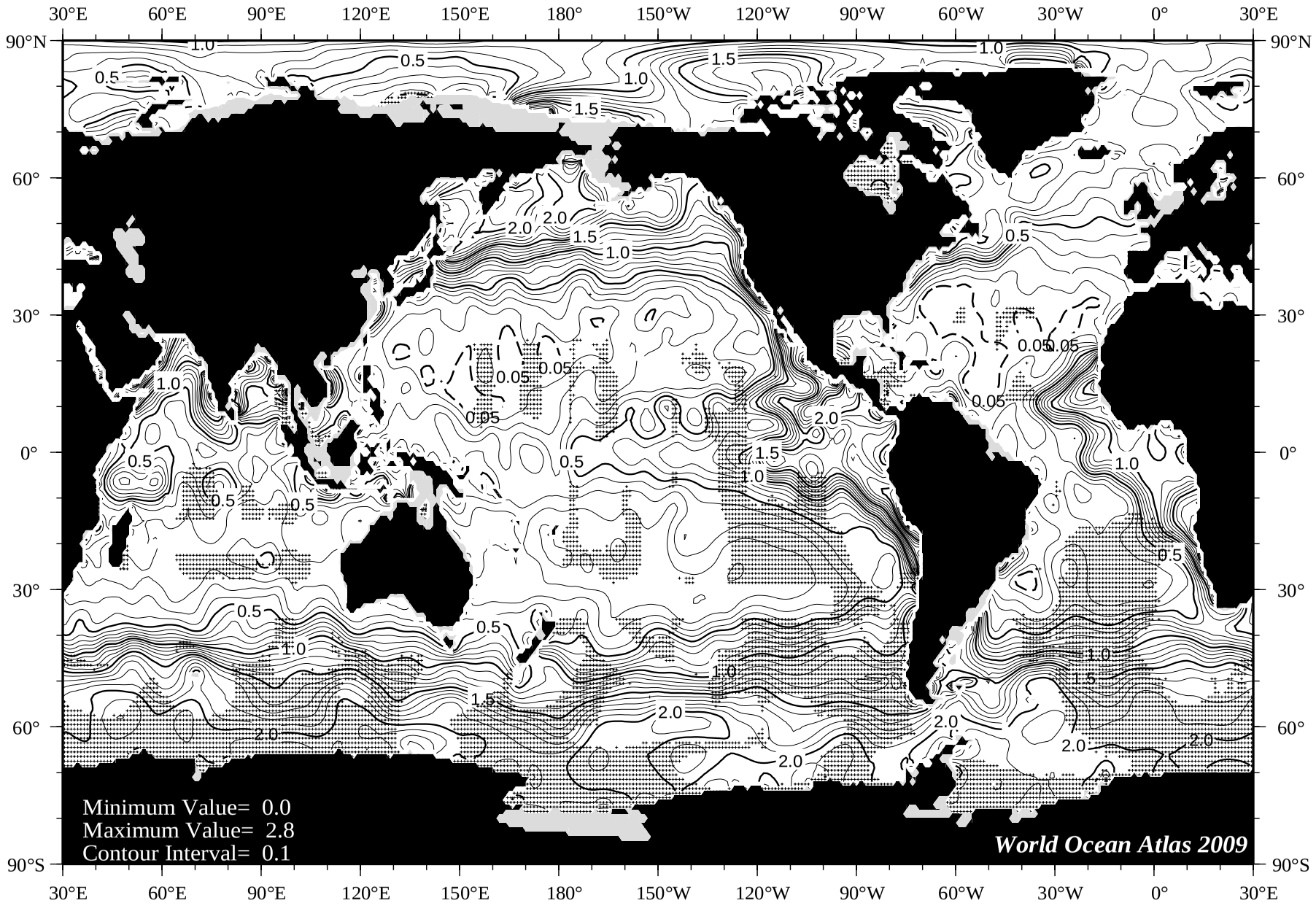

Fig B35 Summer (Jul.-Sep.) phosphate [umol/l] at 75 m. depth.

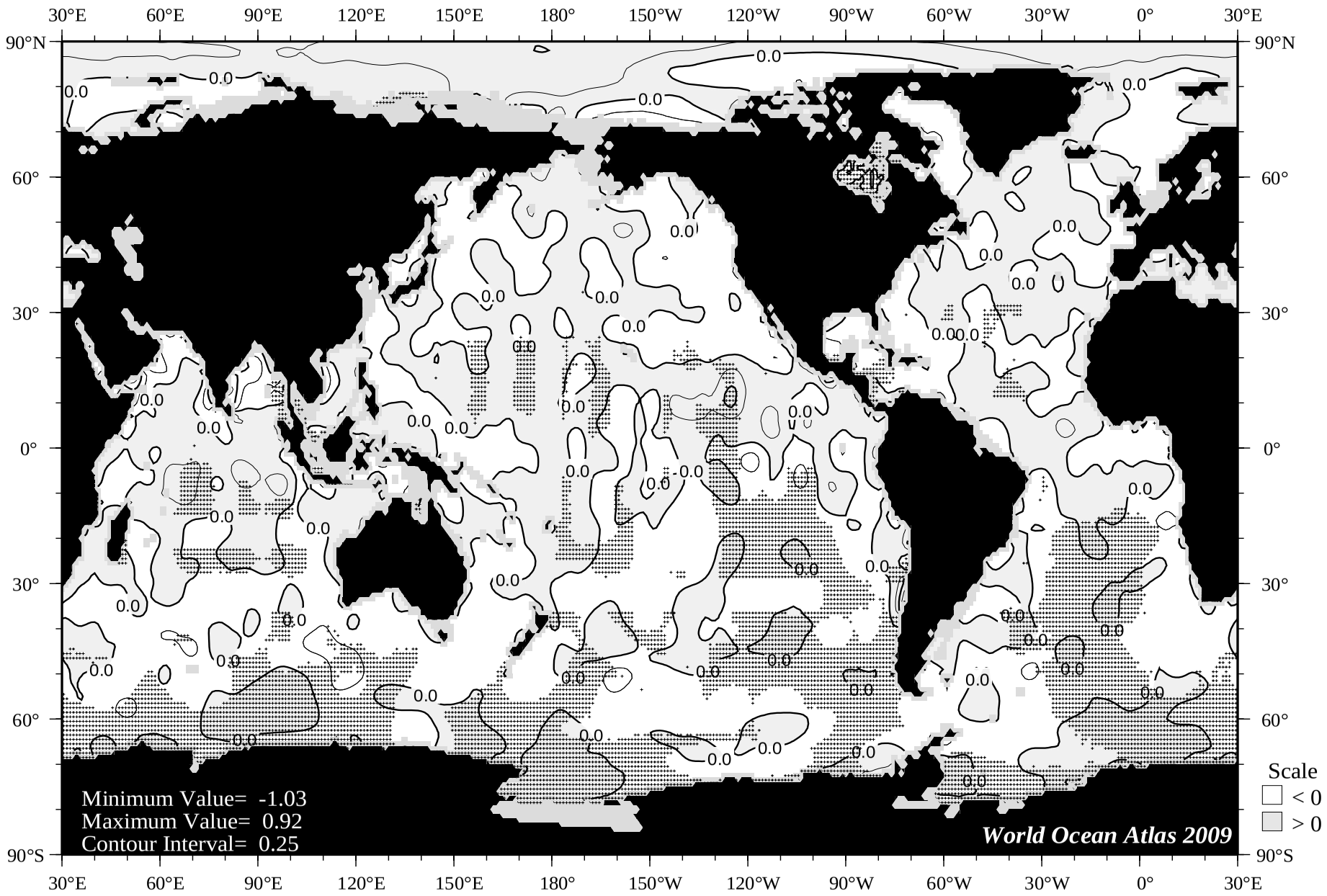

Fig B36 Summer (Jul.-Sep.) minus annual phosphate [umol/l] at 75 m. depth.

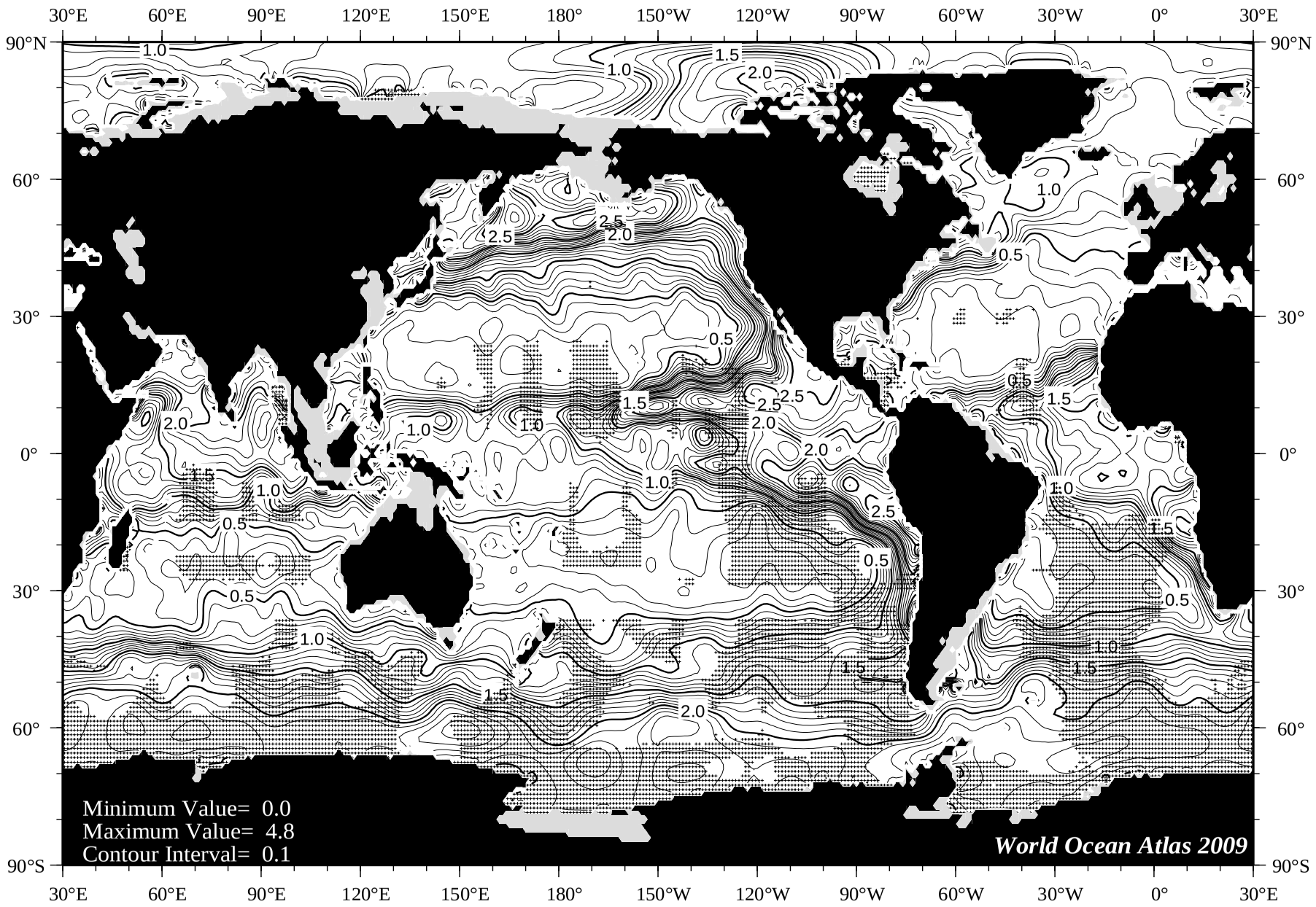

Fig B37 Summer (Jul.-Sep.) phosphate [umol/l] at 150 m. depth.

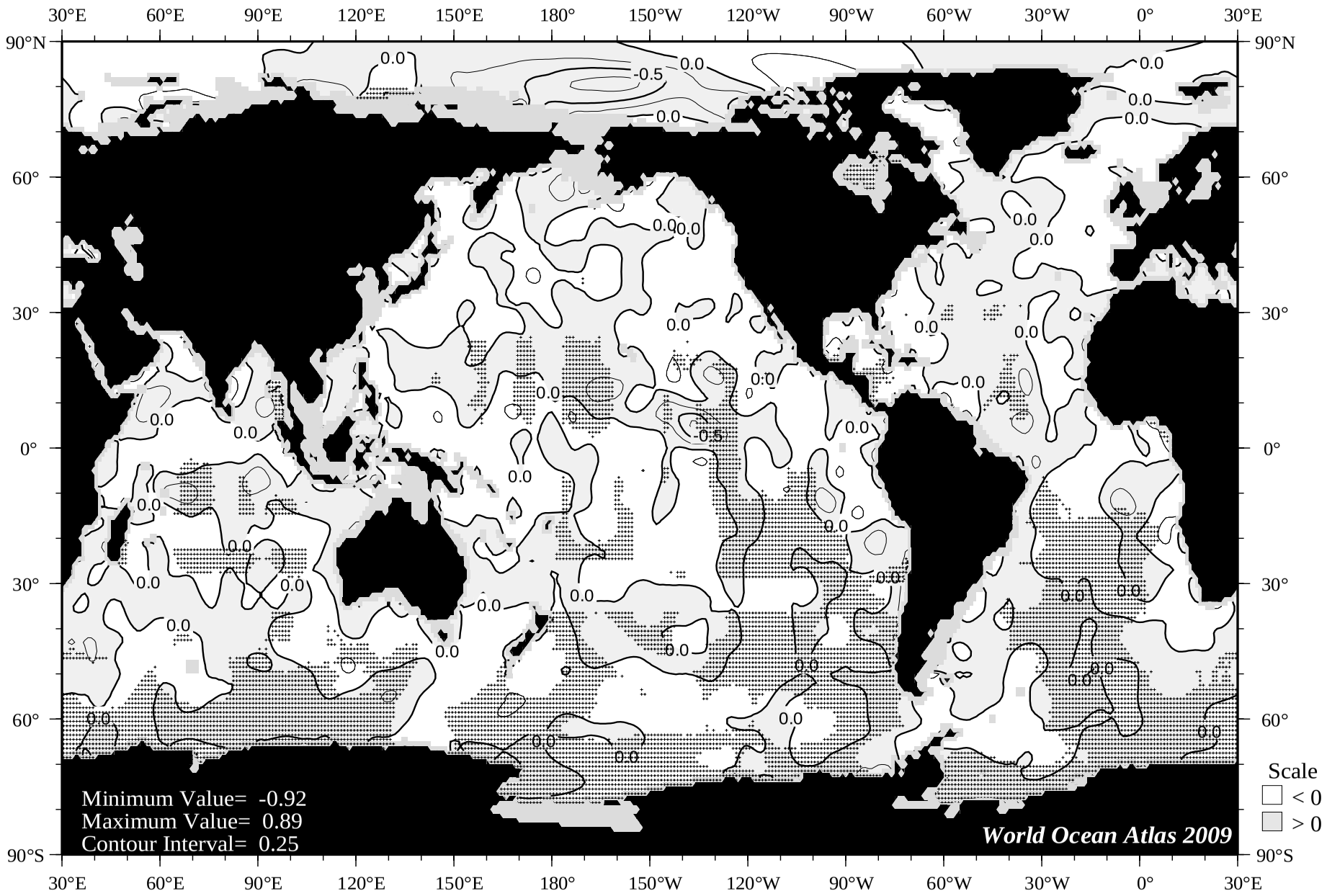

Fig B38 Summer (Jul.-Sep.) minus annual phosphate [umol/l] at 150 m. depth.

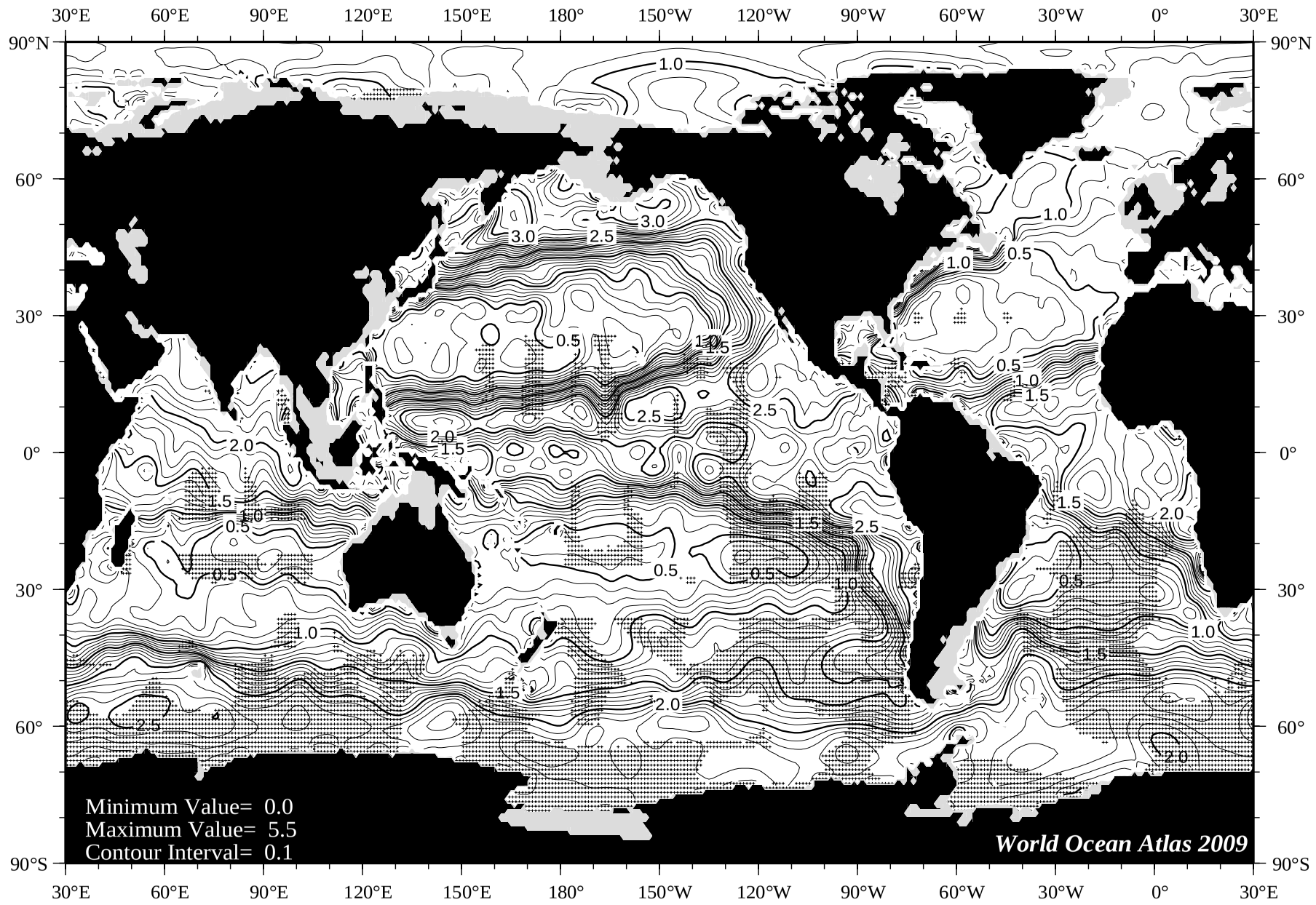

Fig B39 Summer (Jul.-Sep.) phosphate [umol/l] at 250 m. depth.

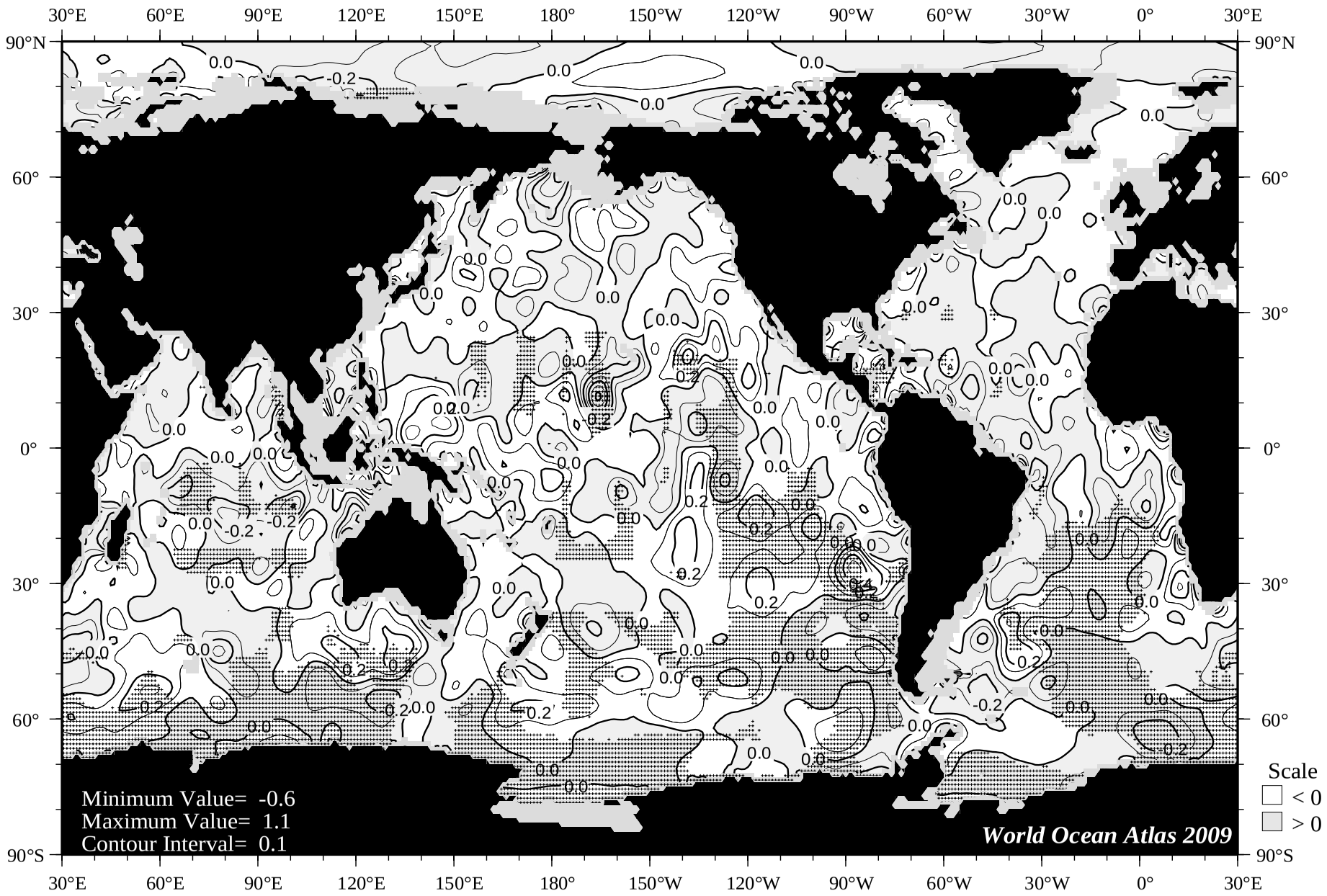

Fig B40 Summer (Jul.-Sep.) minus annual phosphate [umol/l] at 250 m. depth.

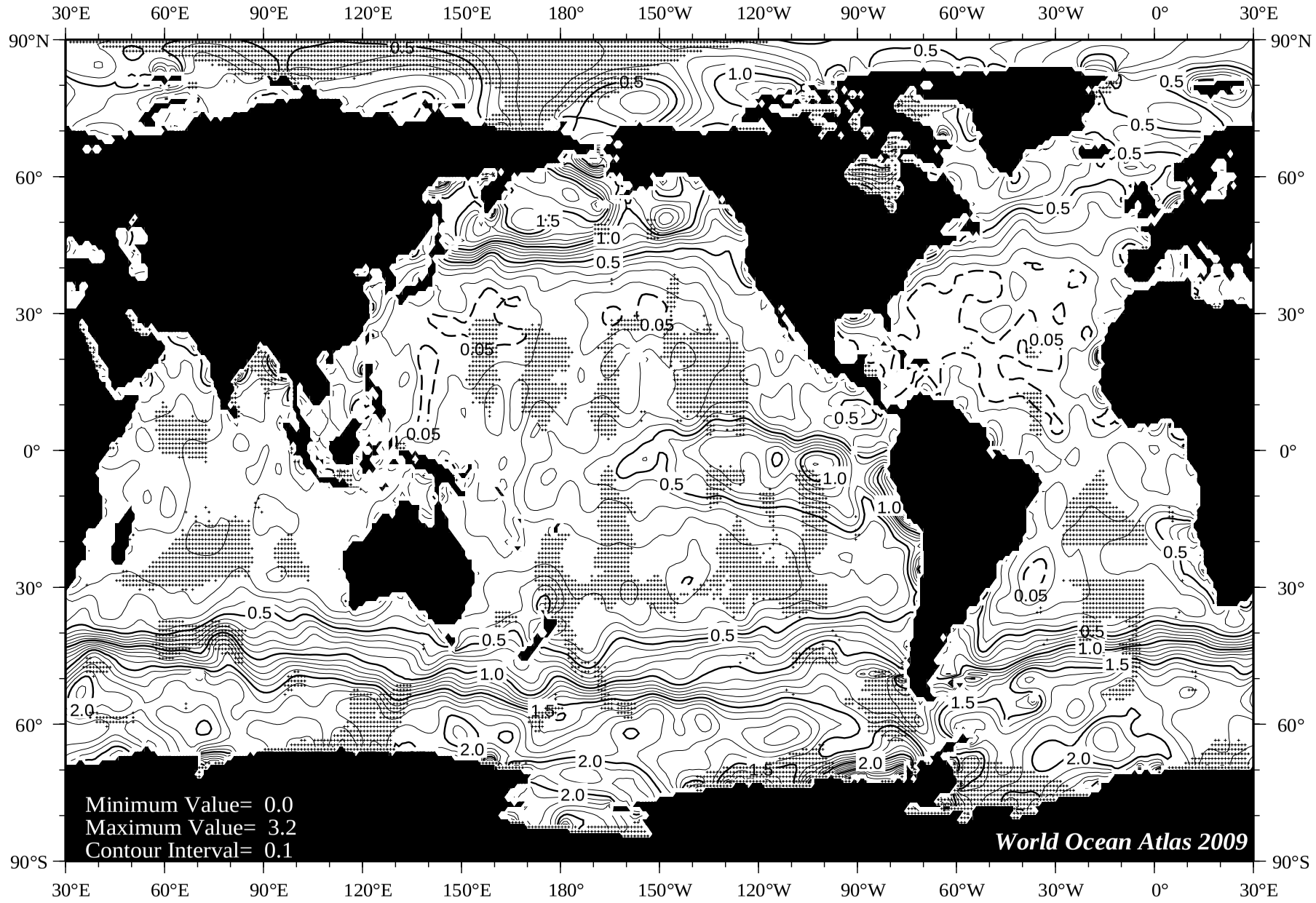

Fig B41 Fall (Oct.-Dec.) phosphate [umol/l] at the surface.

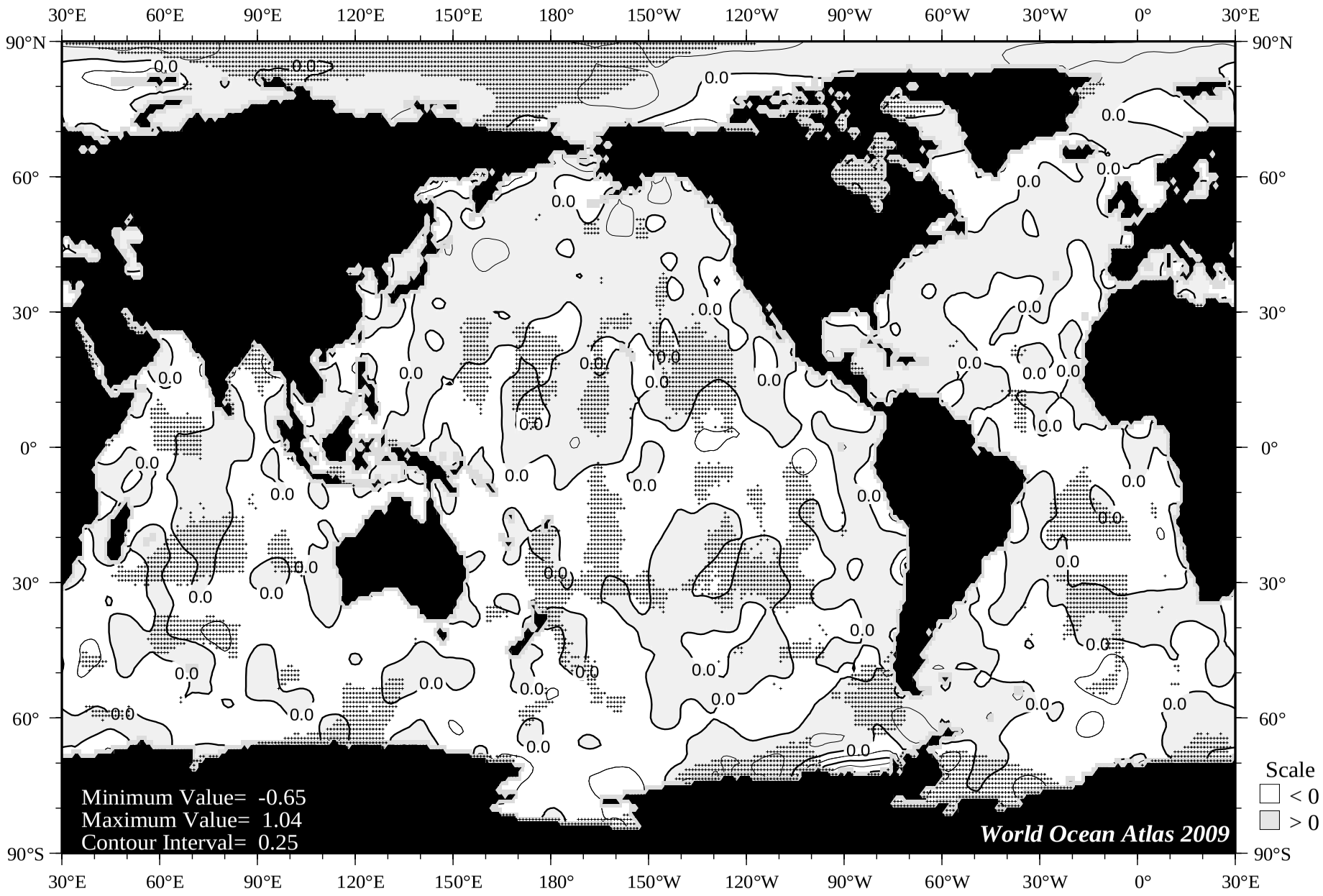

Fig B42 Fall (Oct.-Dec.) minus annual phosphate [umol/l] at the surface.

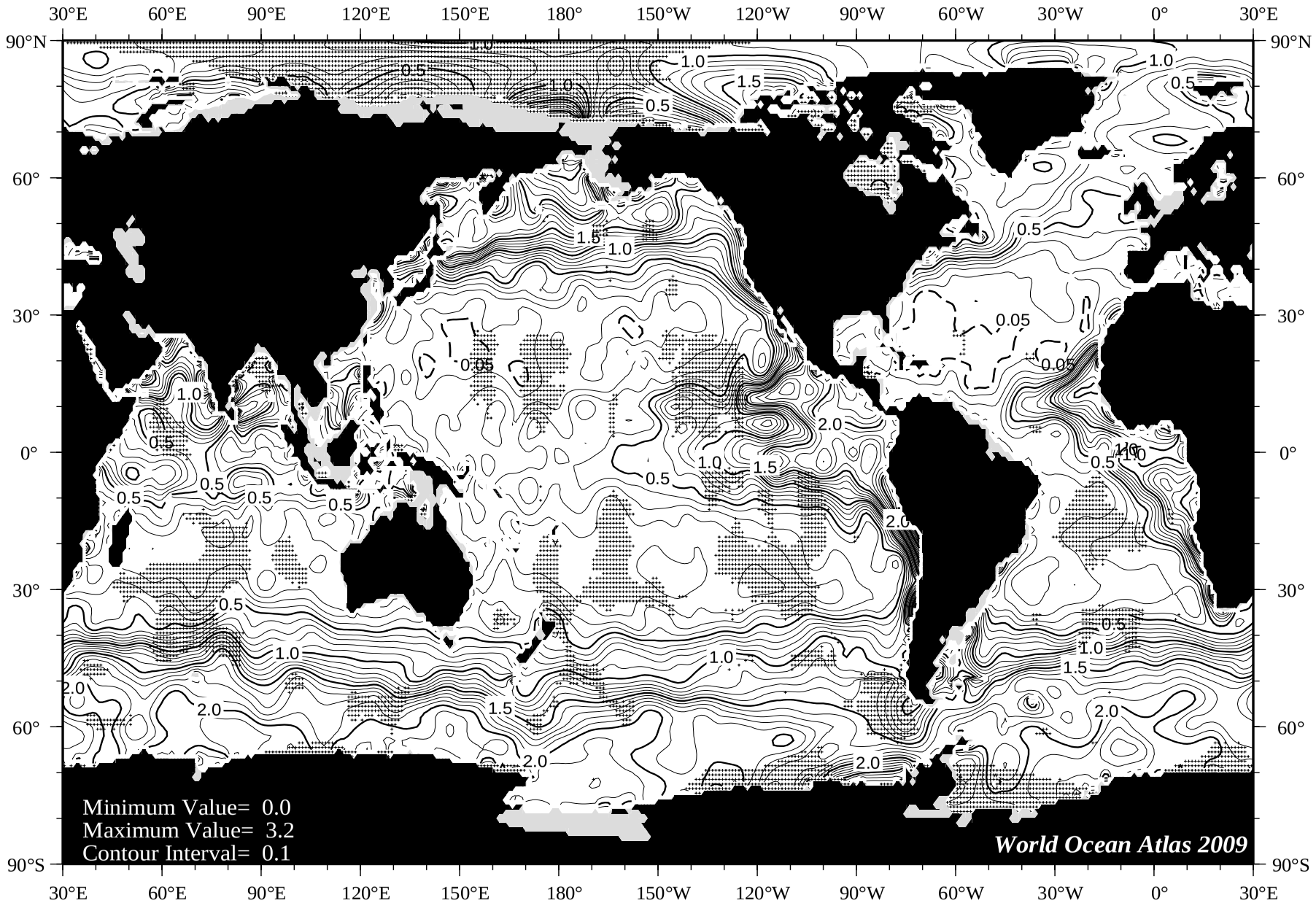

Fig B43 Fall (Oct.-Dec.) phosphate [umol/l] at 75 m. depth.

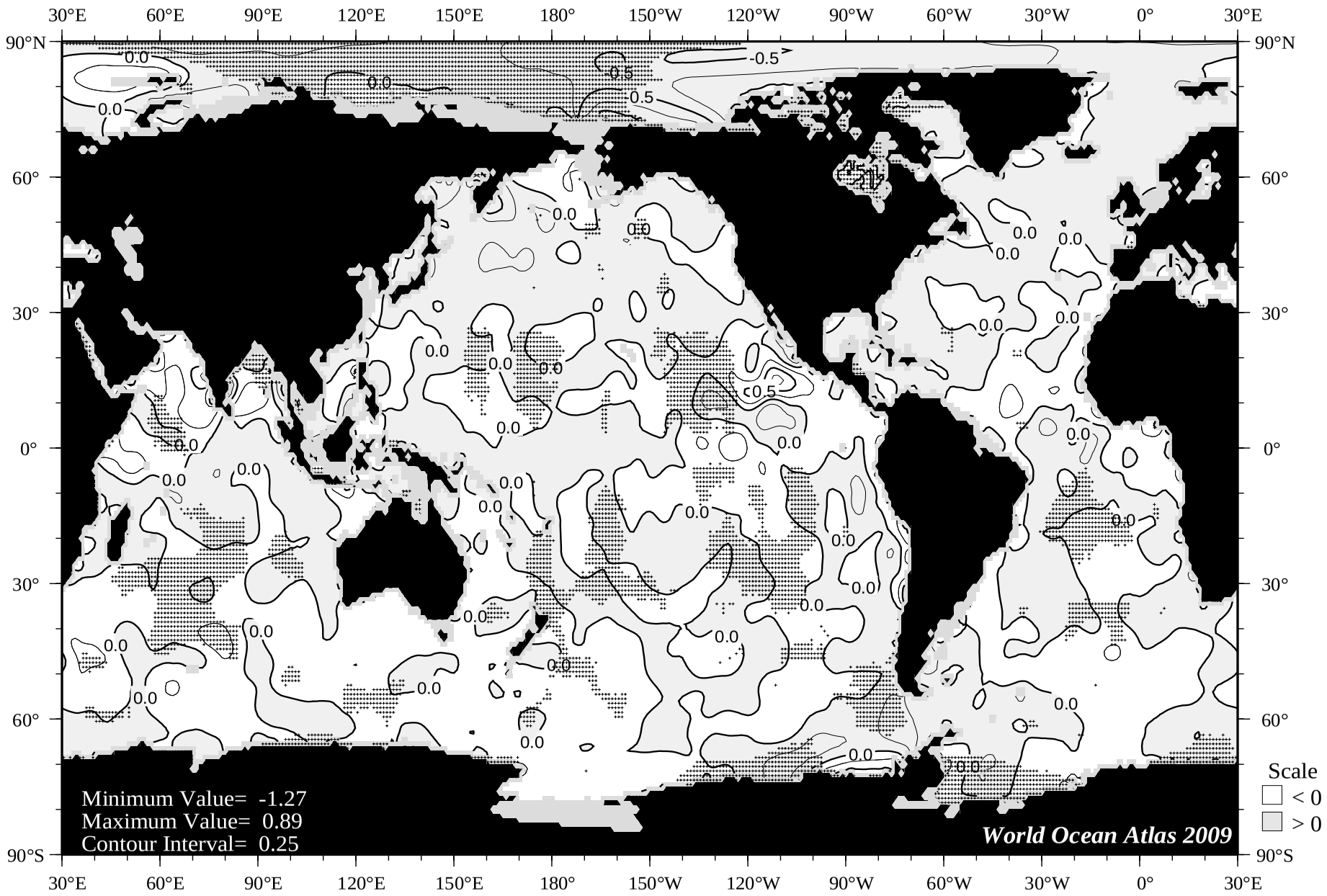

Fig B44 Fall (Oct.-Dec.) minus annual phosphate [umol/l] at 75 m. depth.

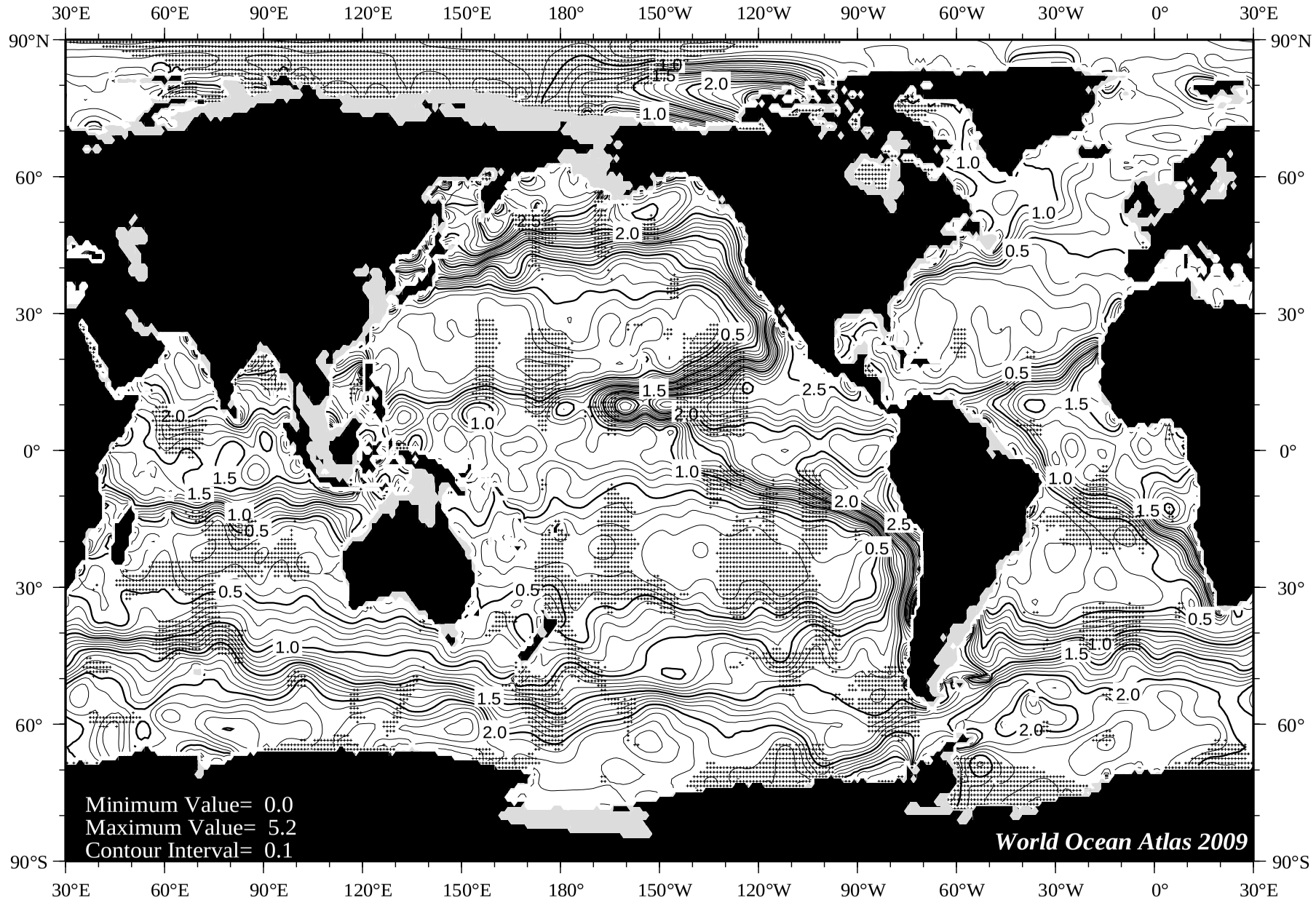

Fig B45 Fall (Oct.-Dec.) phosphate [umol/l] at 150 m. depth.

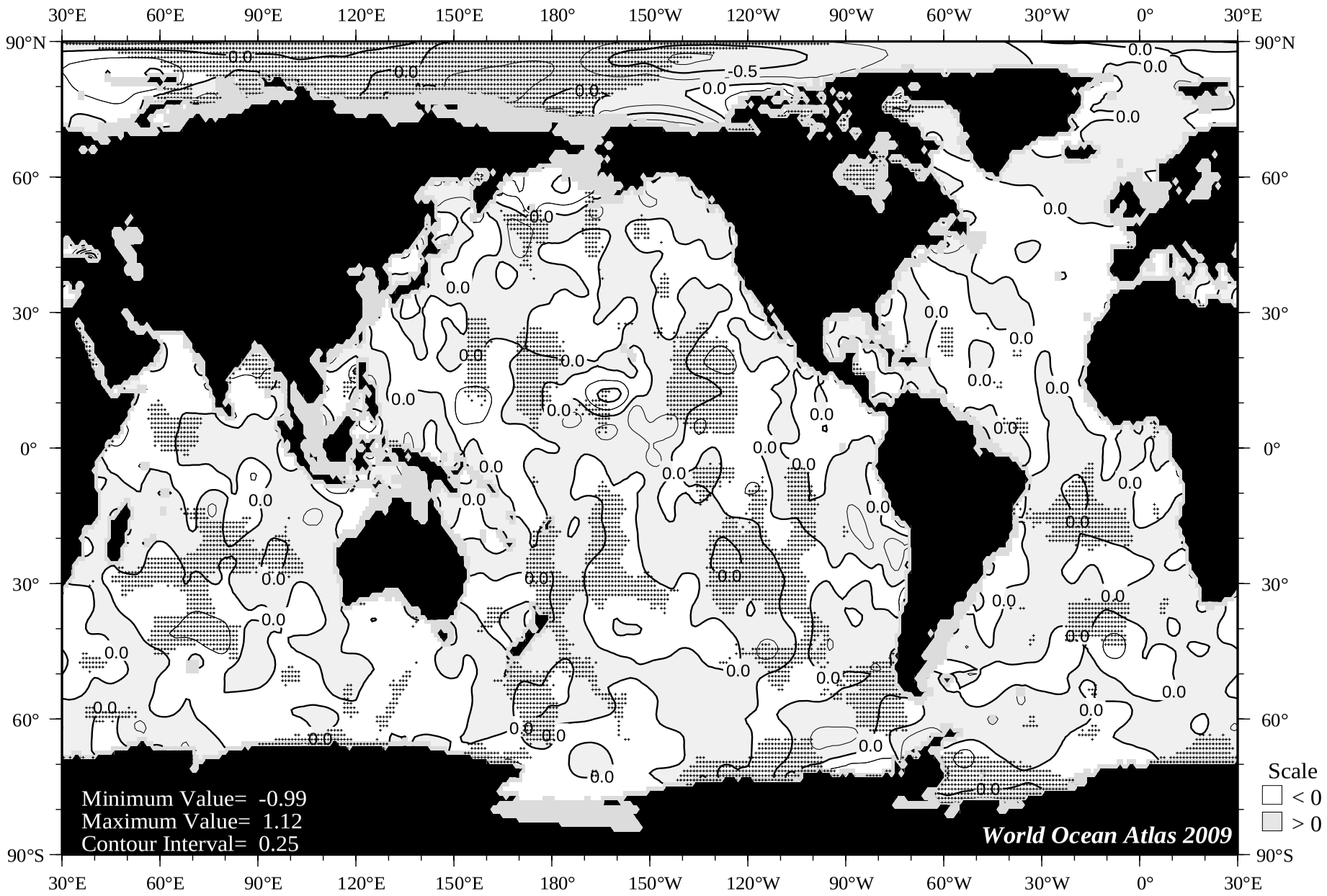

Fig B46 Fall (Oct.-Dec.) minus annual phosphate [umol/l] at 150 m. depth.

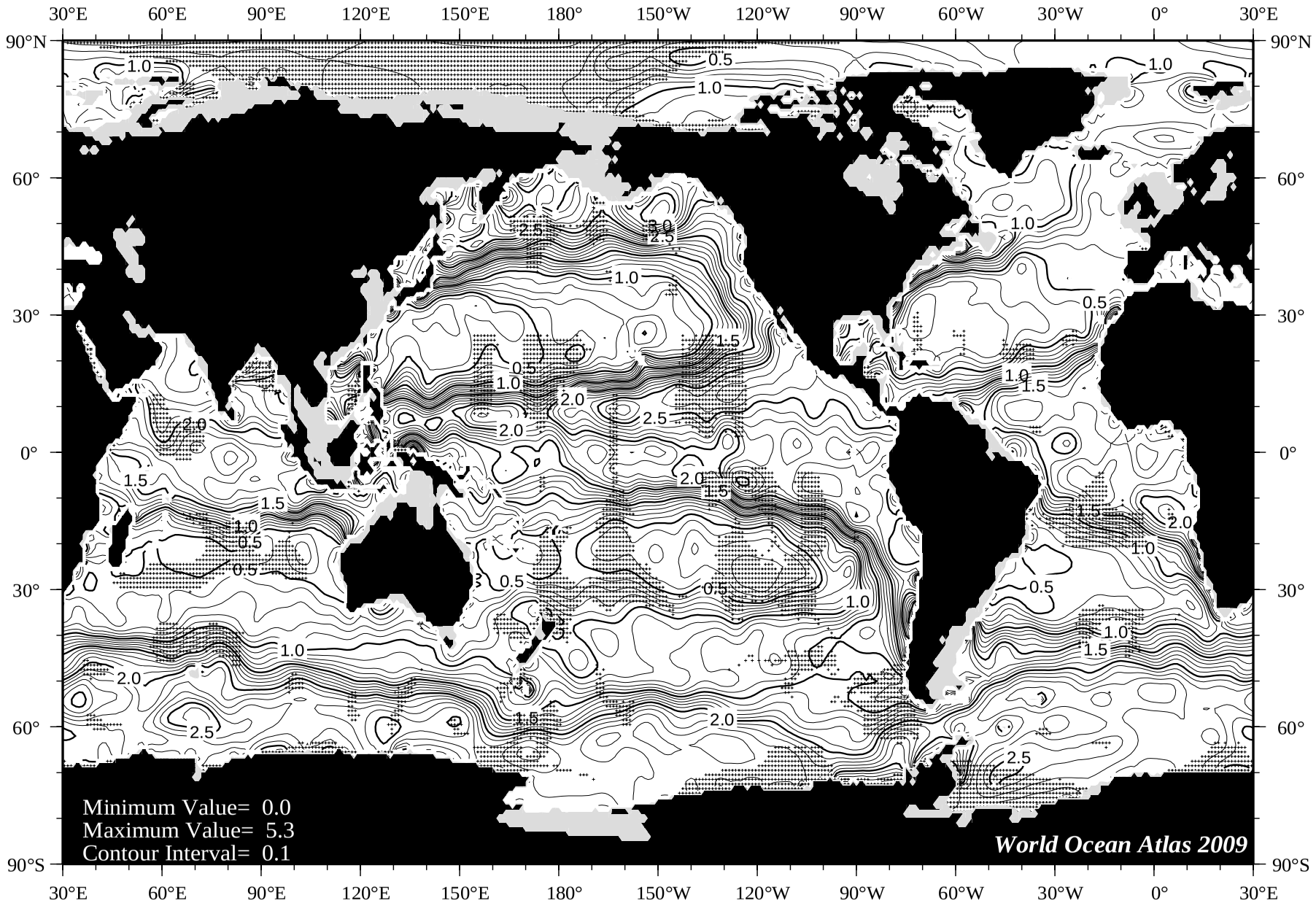

Fig B47 Fall (Oct.-Dec.) phosphate [umol/l] at 250 m. depth.

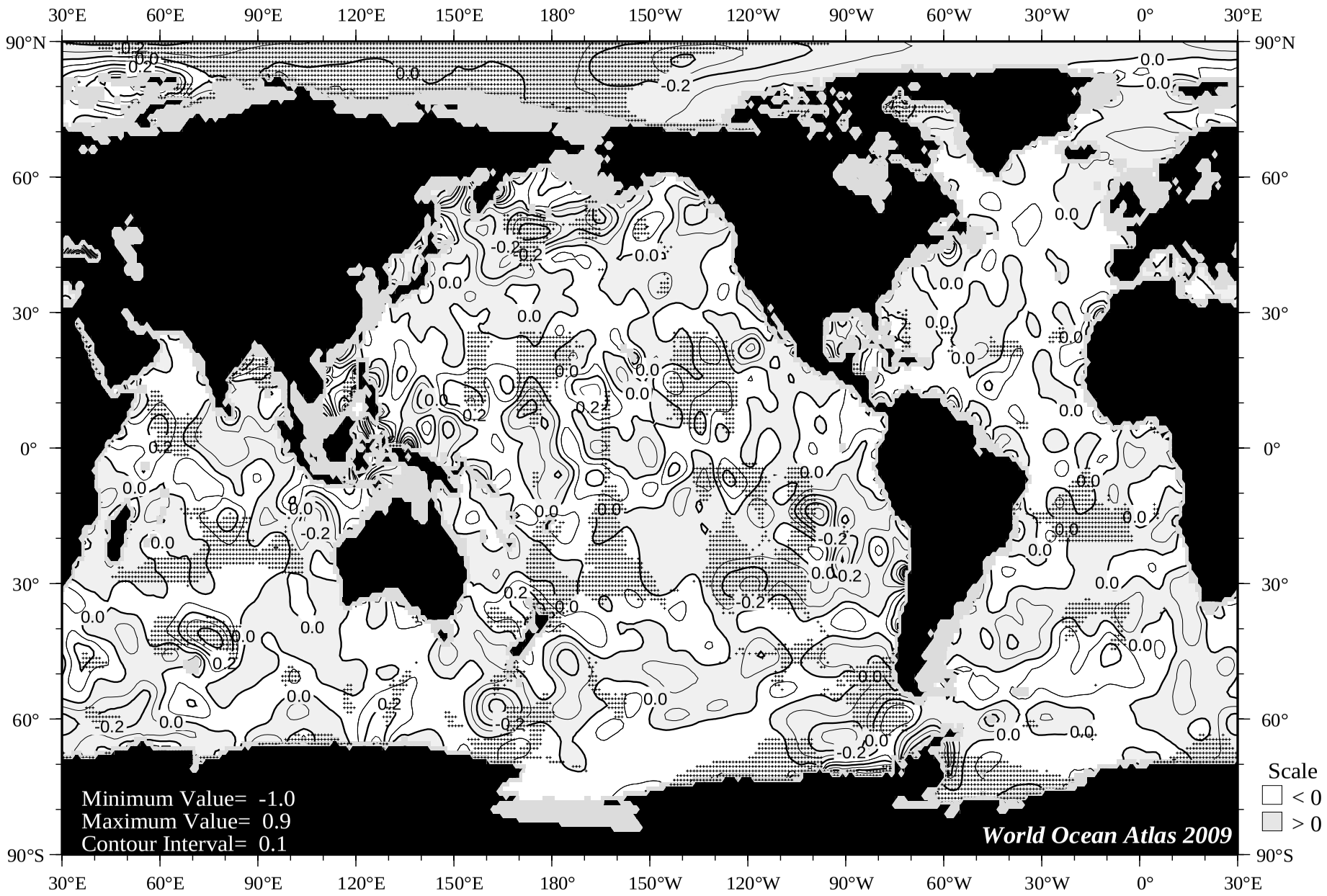

Fig B48 Fall (Oct.-Dec.) minus annual phosphate [umol/l] at 250 m. depth.

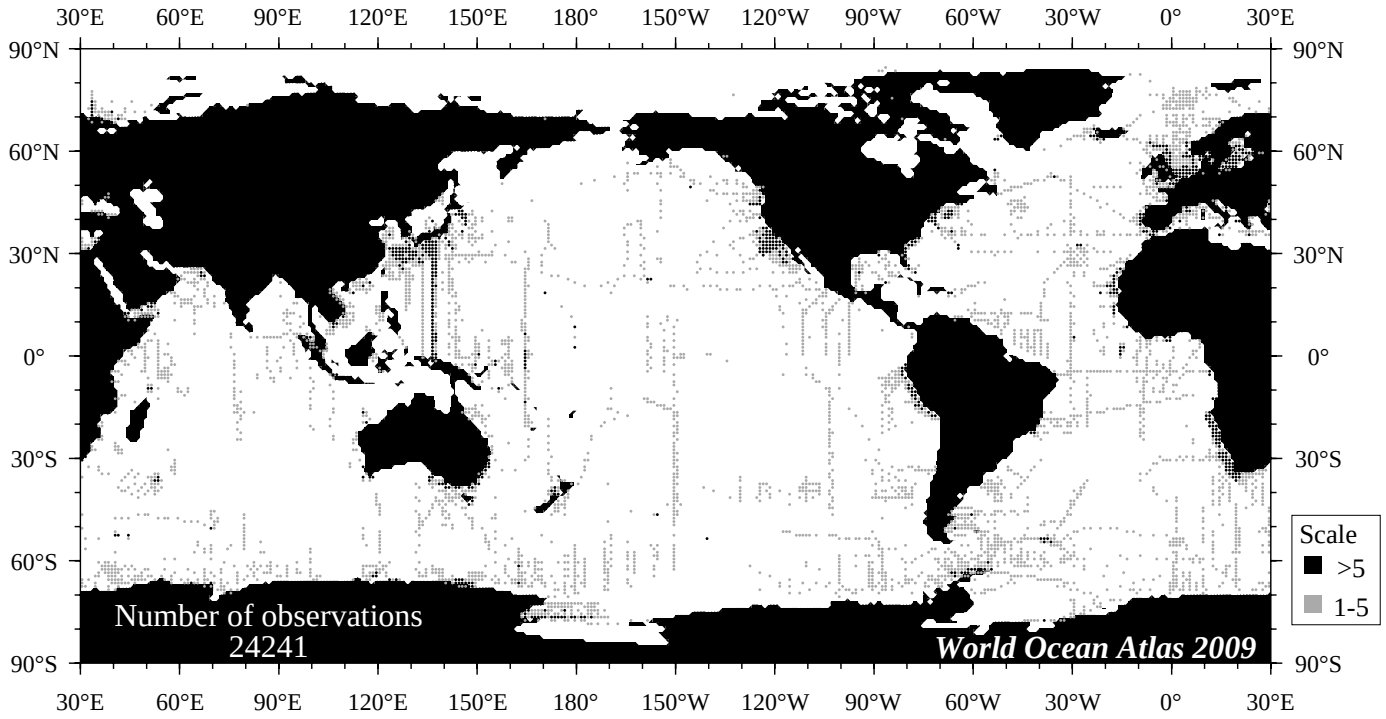

Fig C1 January phosphate observations at the surface.

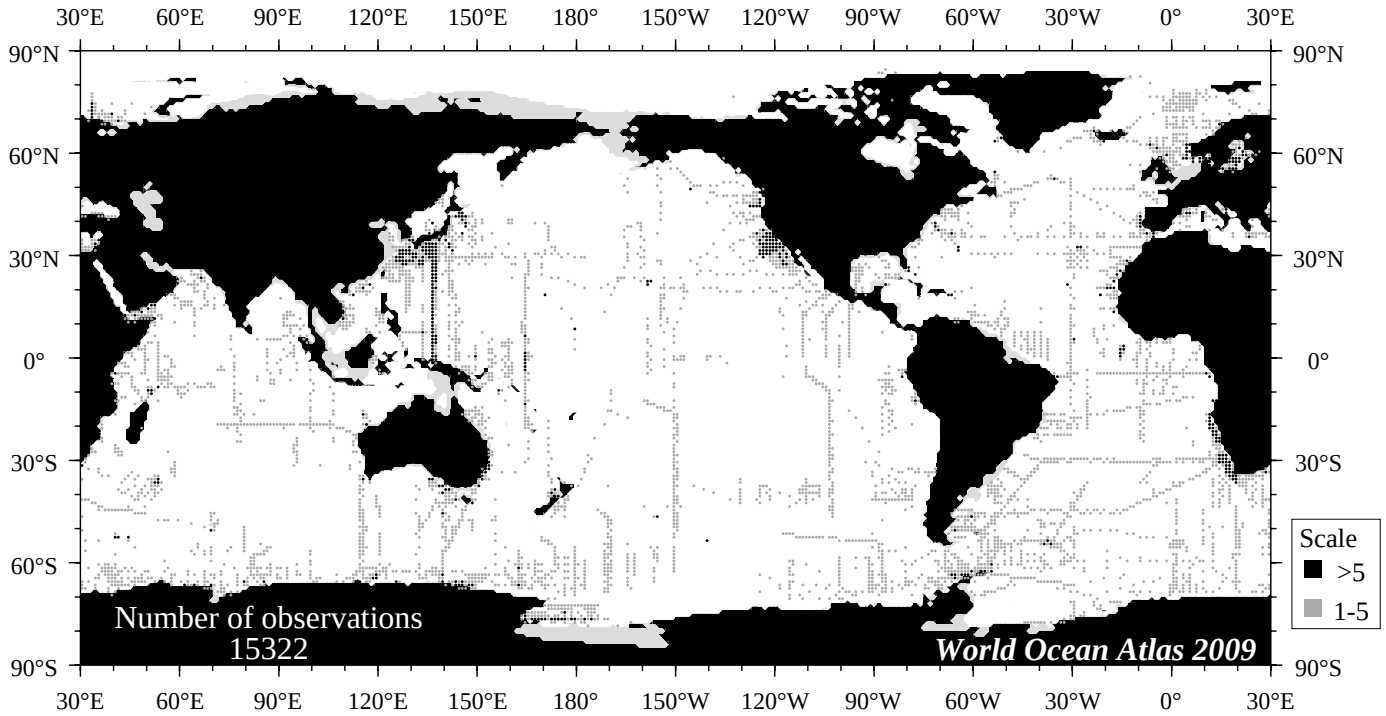

Fig C2 January phosphate observations at 75 m. depth.

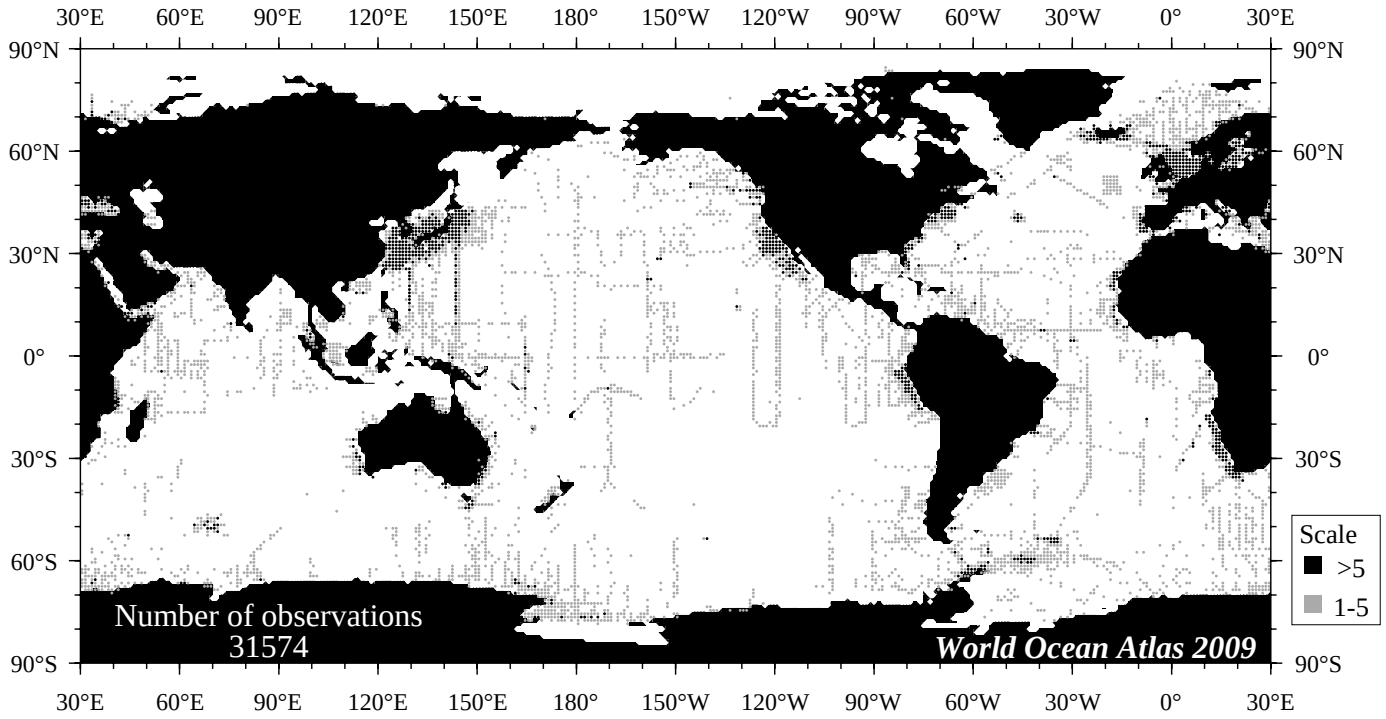

Fig C3 February phosphate observations at the surface.

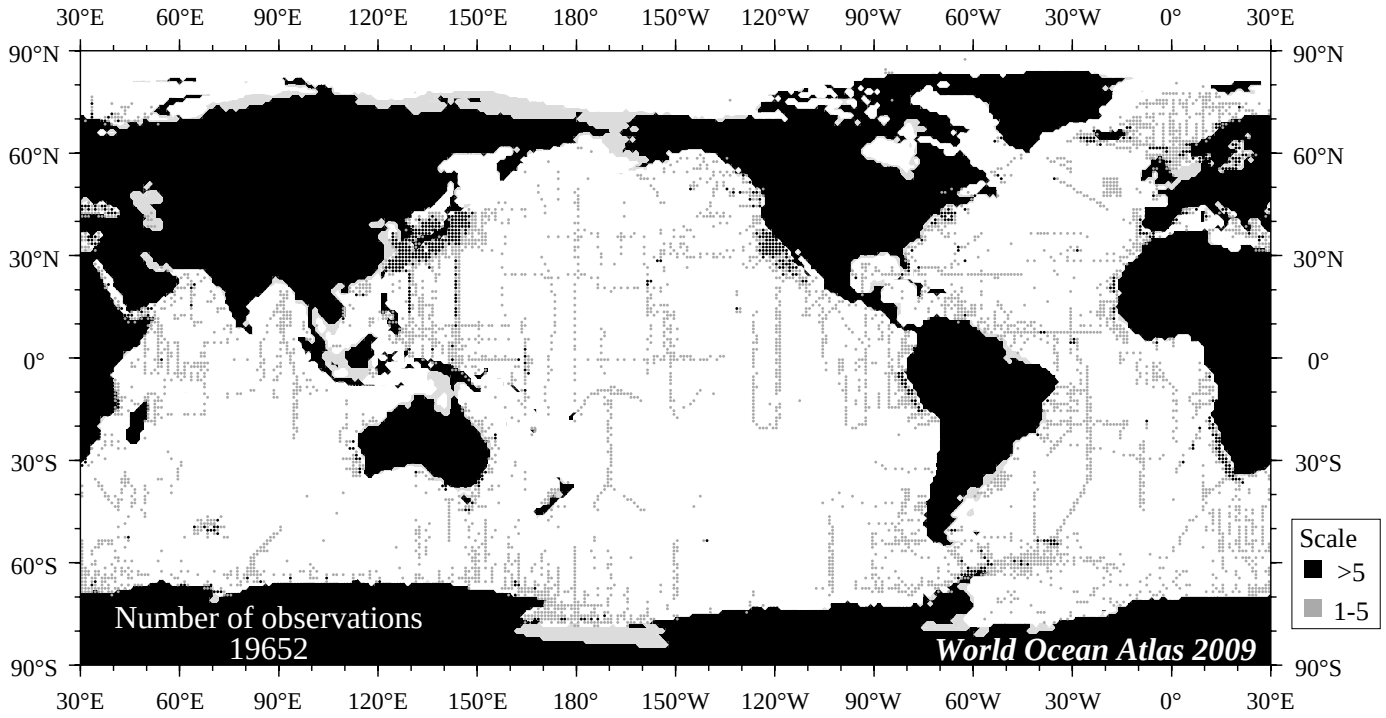

Fig C4 February phosphate observations at 75 m. depth.

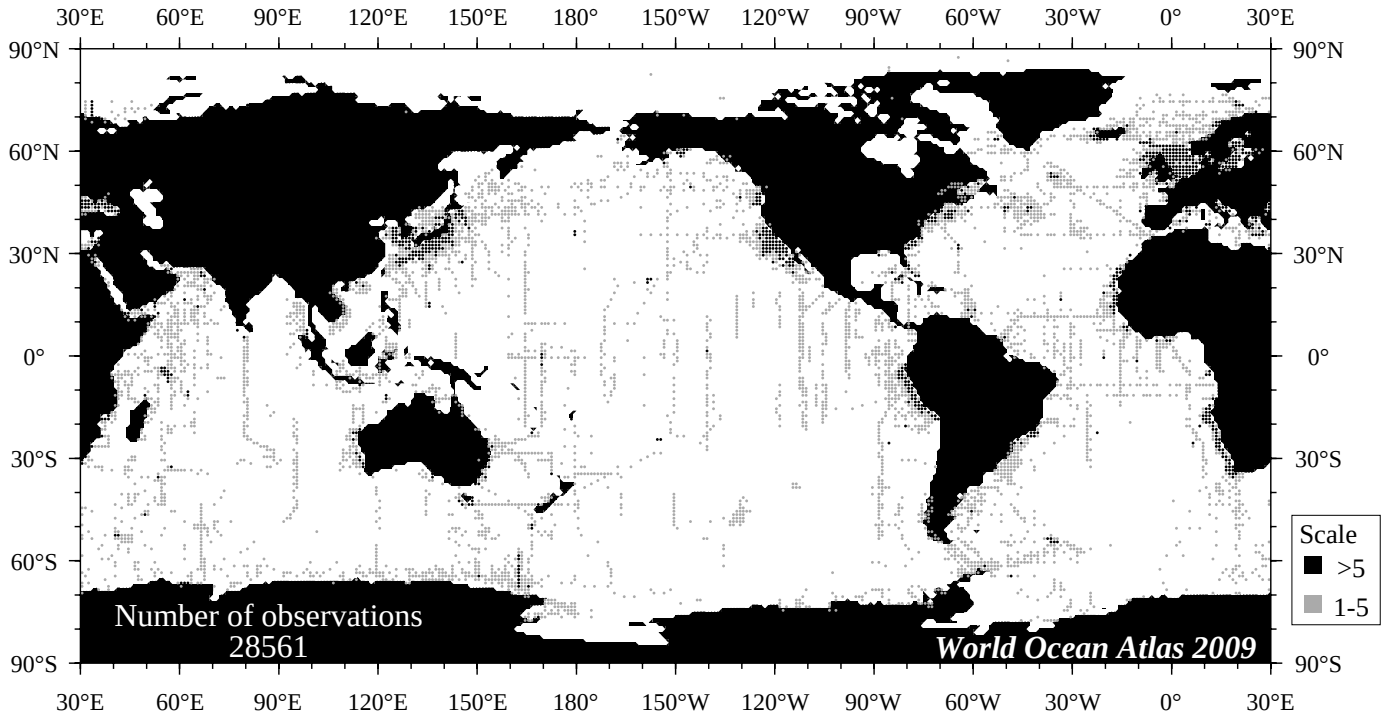

Fig C5 March phosphate observations at the surface.

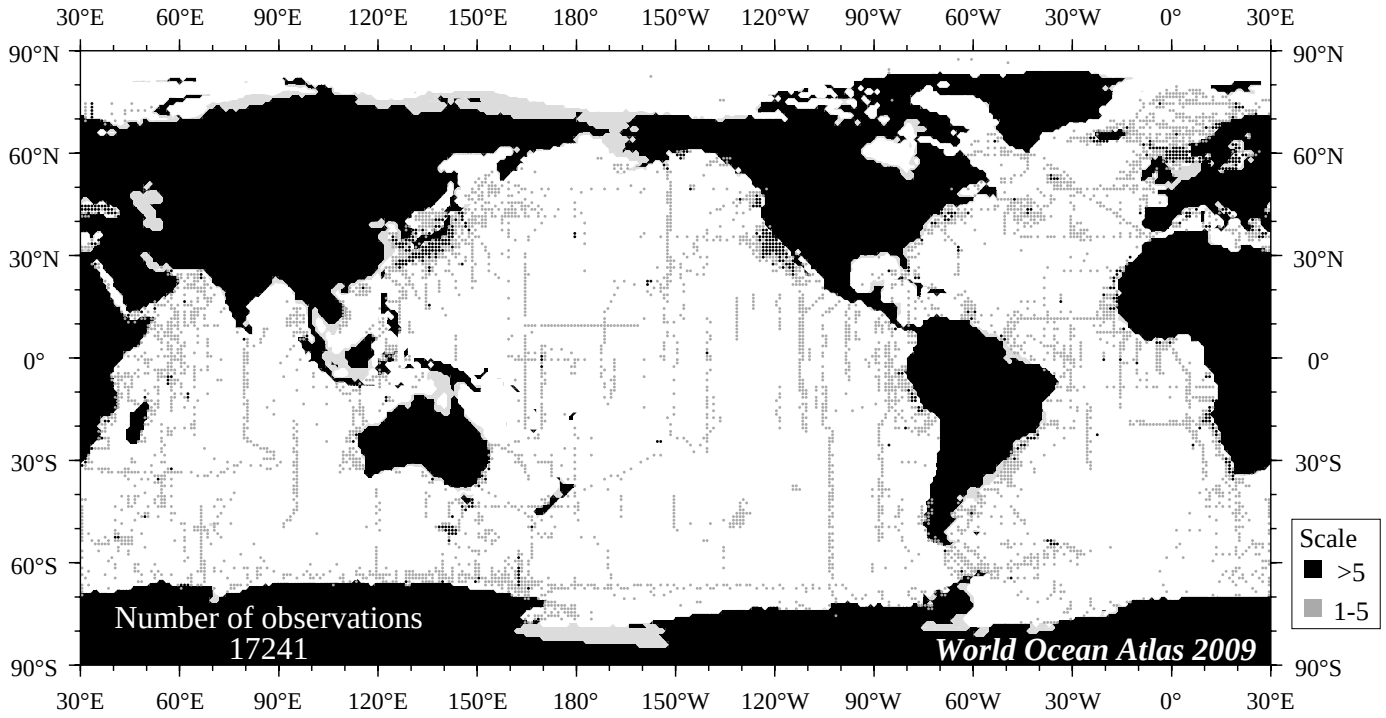

Fig C6 March phosphate observations at 75 m. depth.

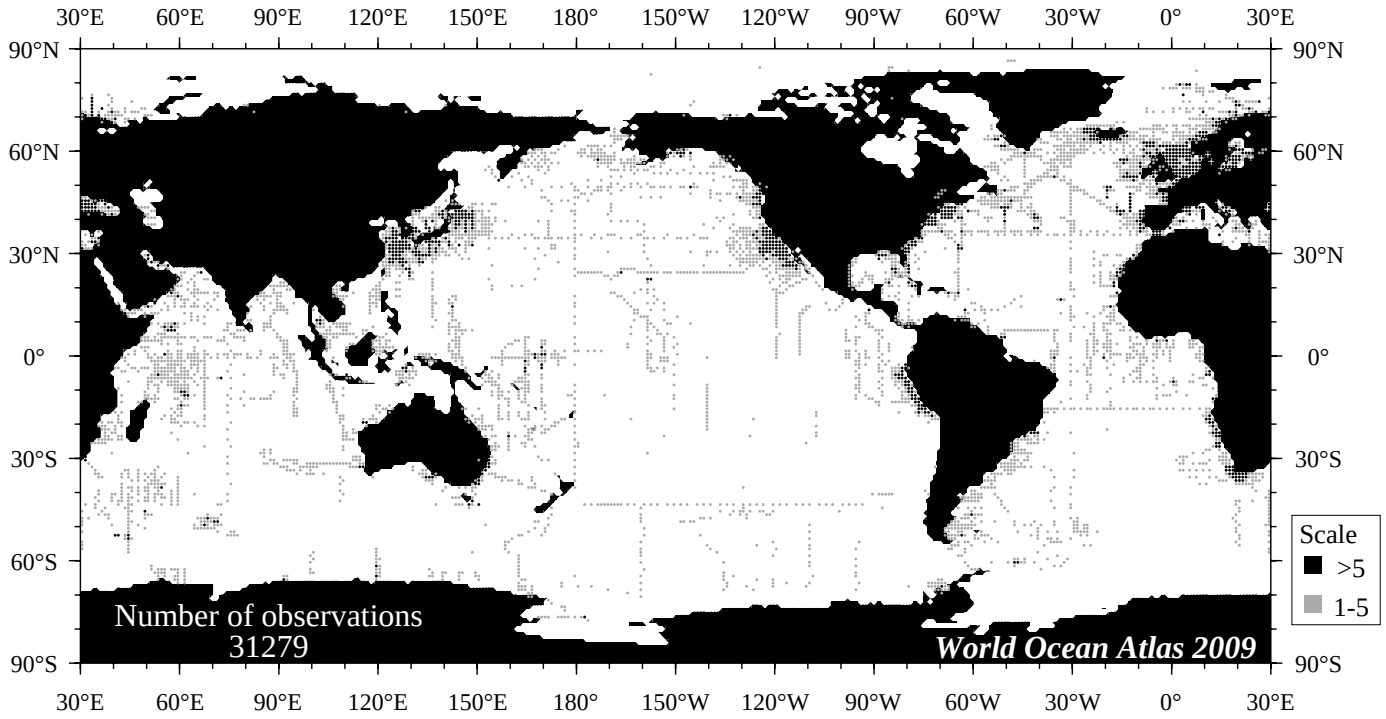

Fig C7 April phosphate observations at the surface.

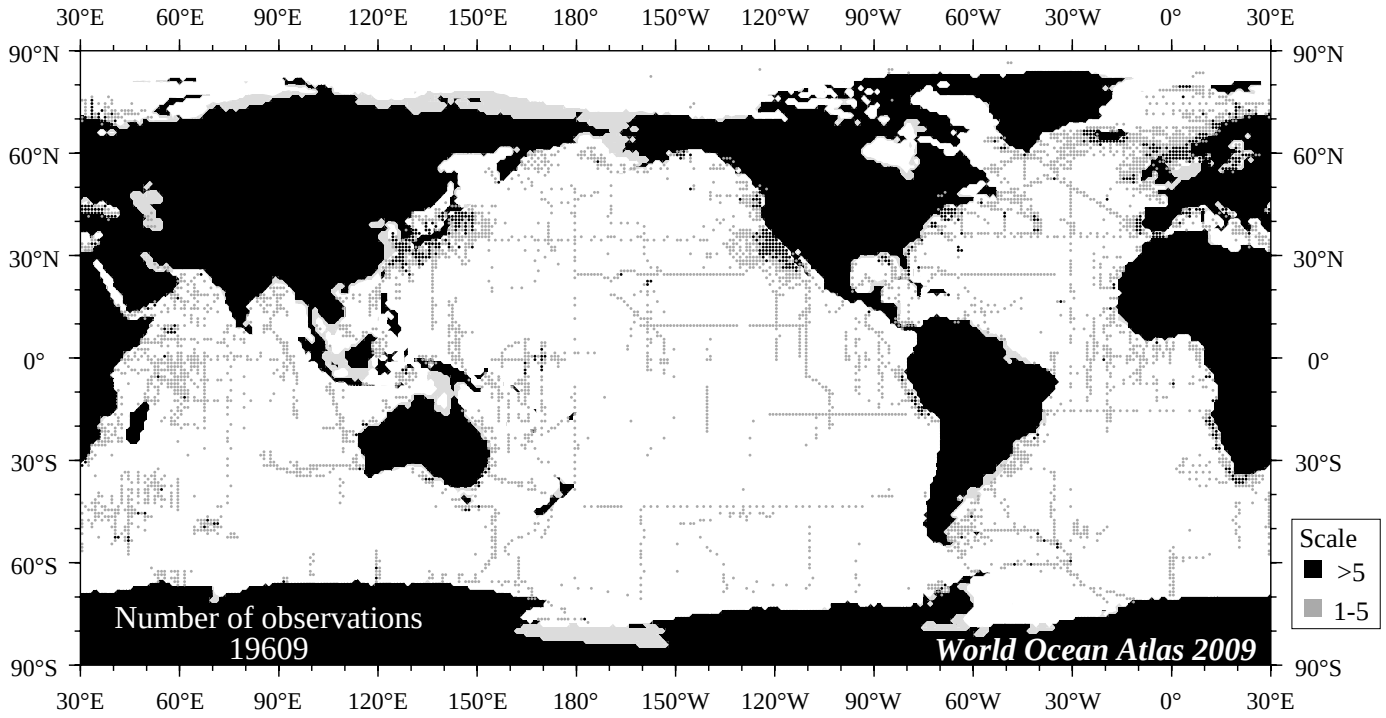

Fig C8 April phosphate observations at 75 m. depth.

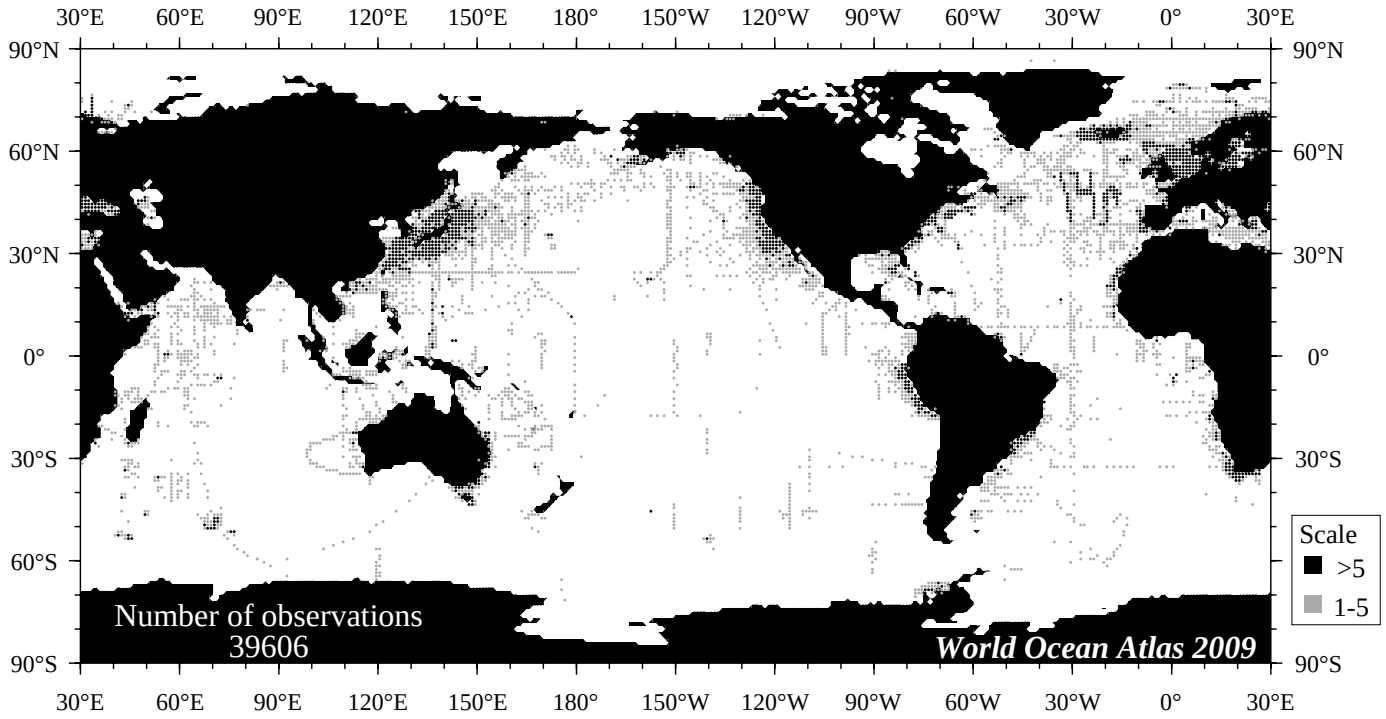

Fig C9 May phosphate observations at the surface.

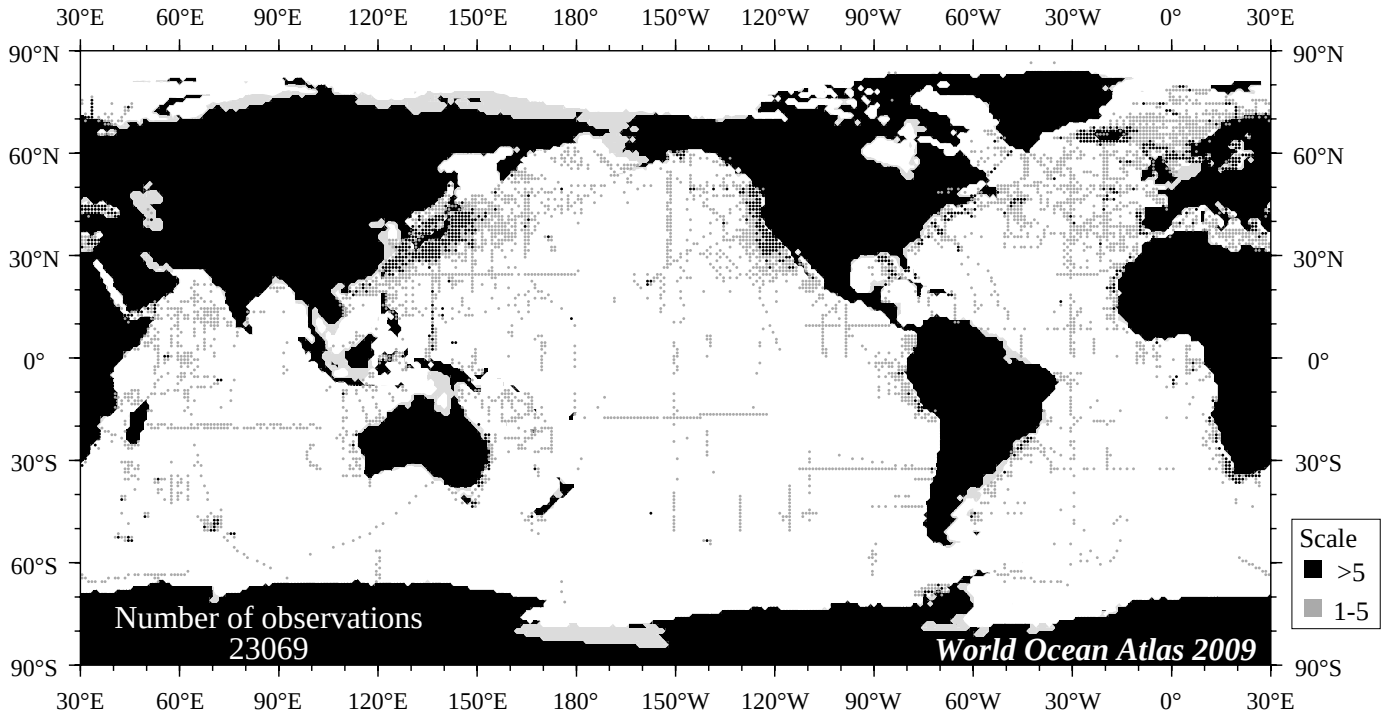

Fig C10 May phosphate observations at 75 m. depth.

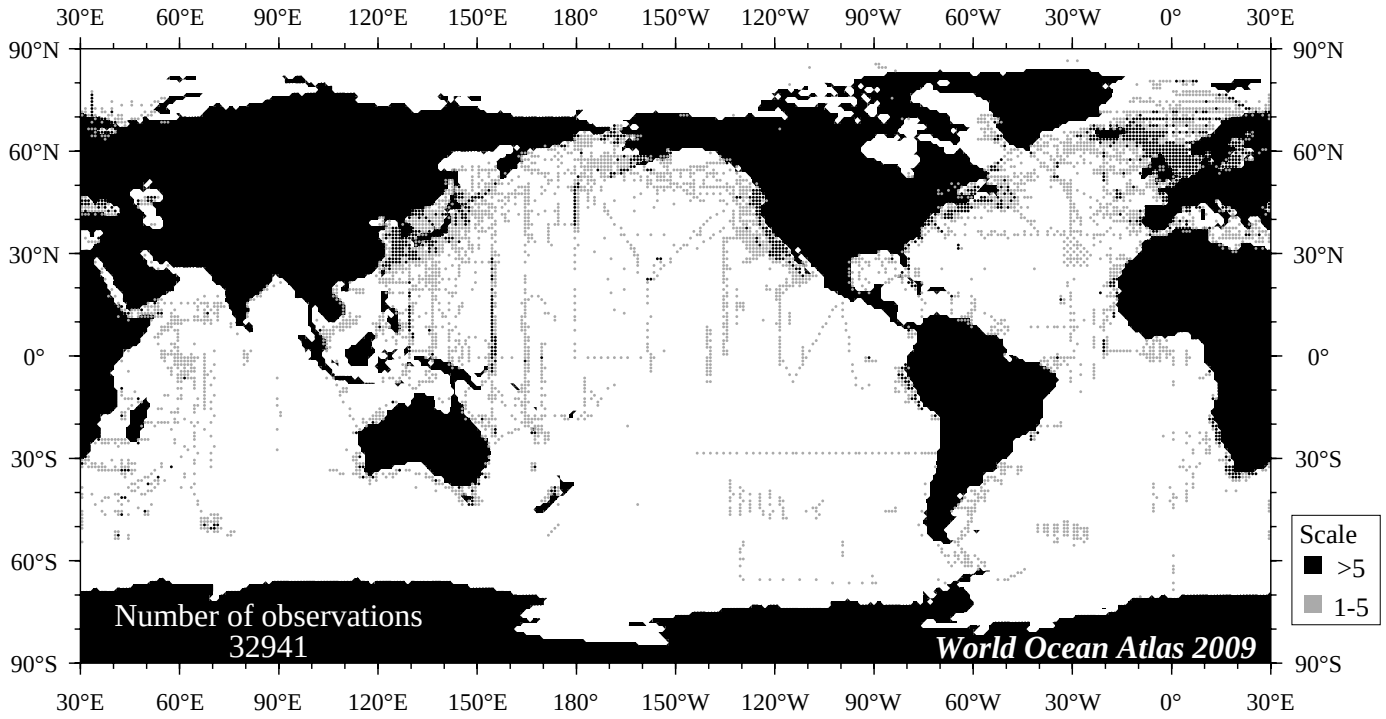

Fig C11 June phosphate observations at the surface.

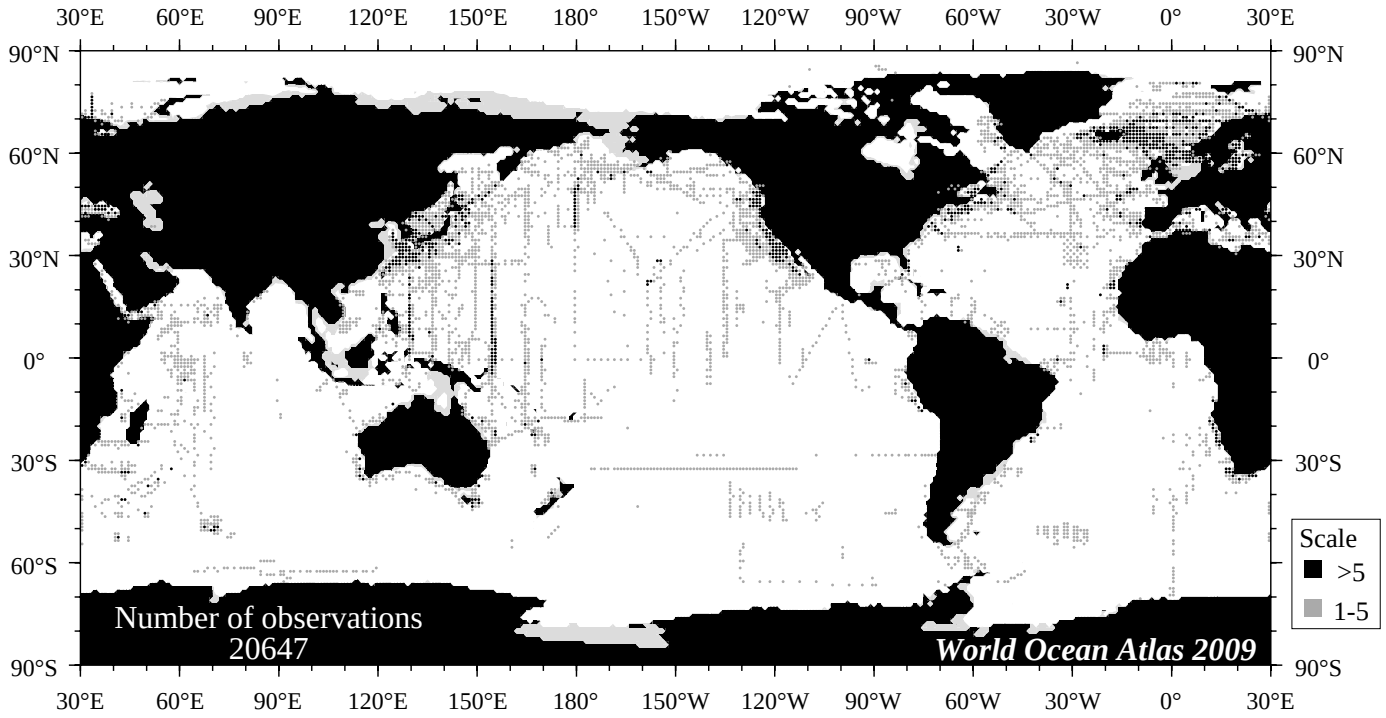

Fig C12 June phosphate observations at 75 m. depth.

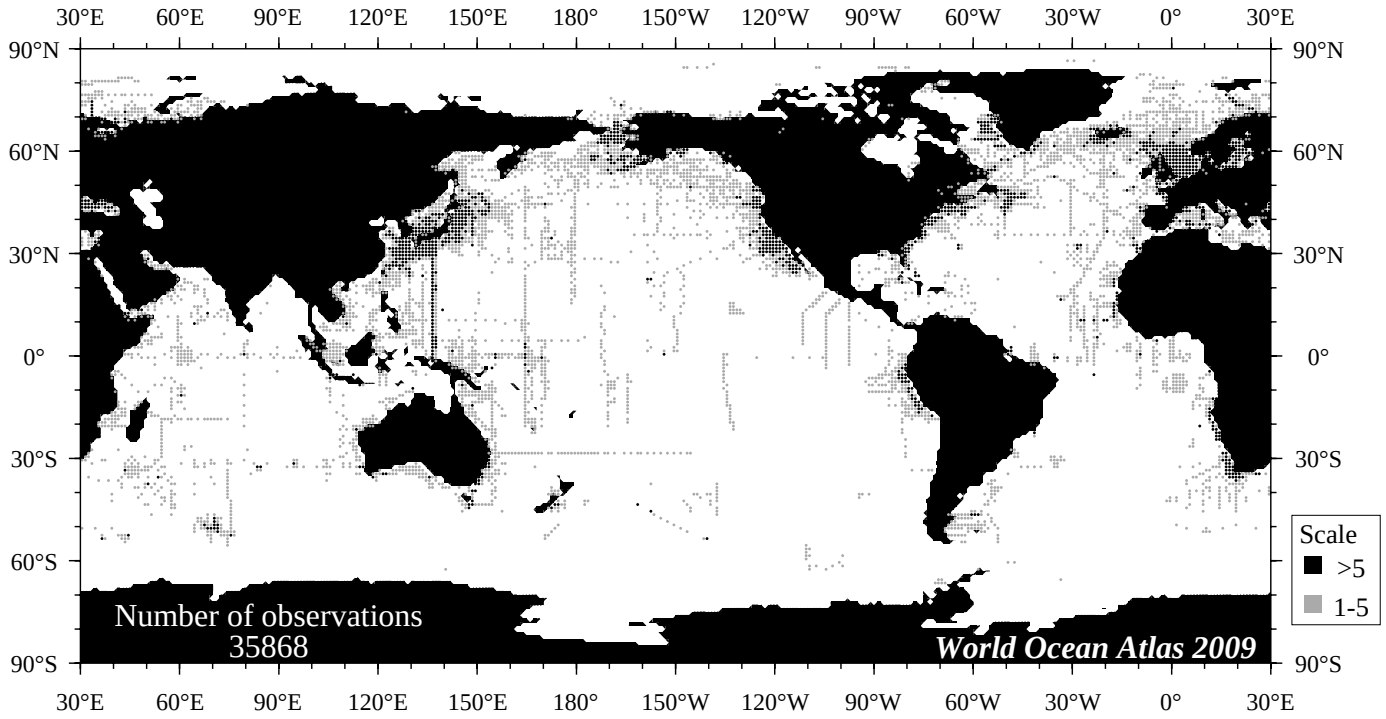

Fig C13 July phosphate observations at the surface.

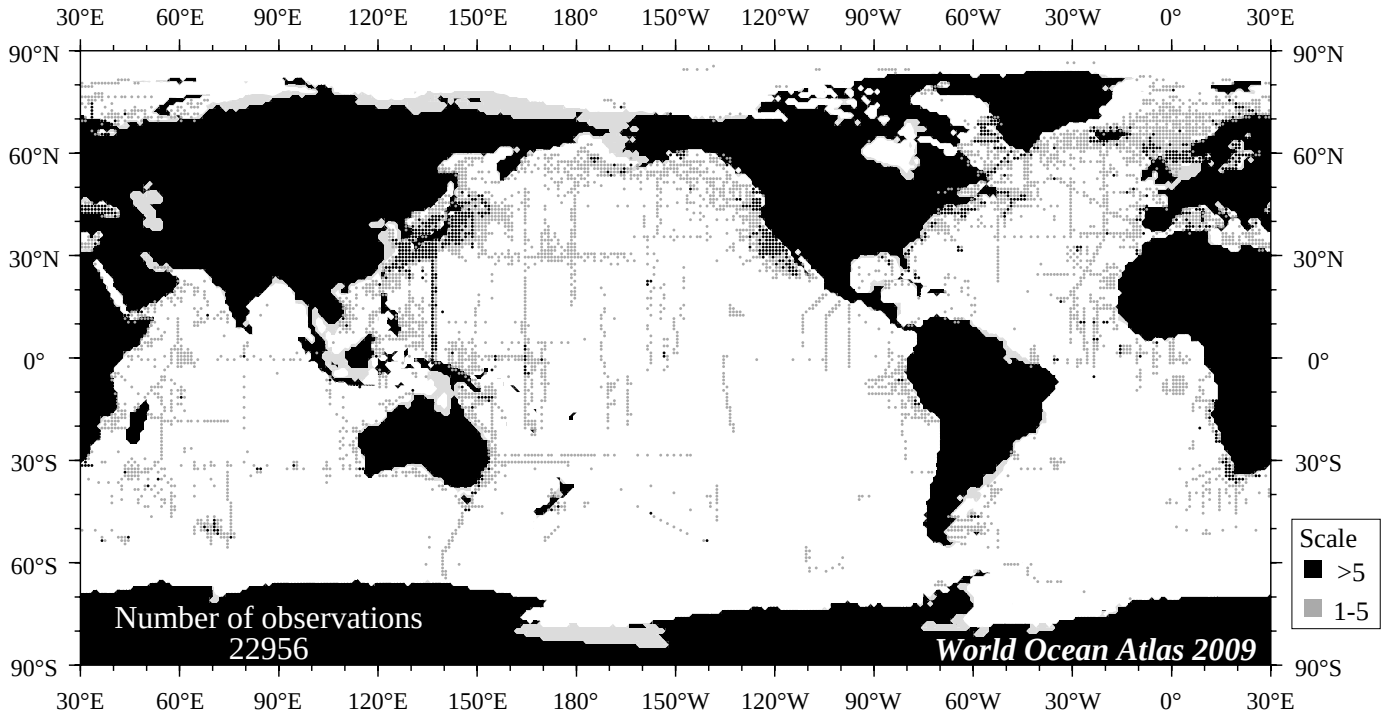

Fig C14 July phosphate observations at 75 m. depth.

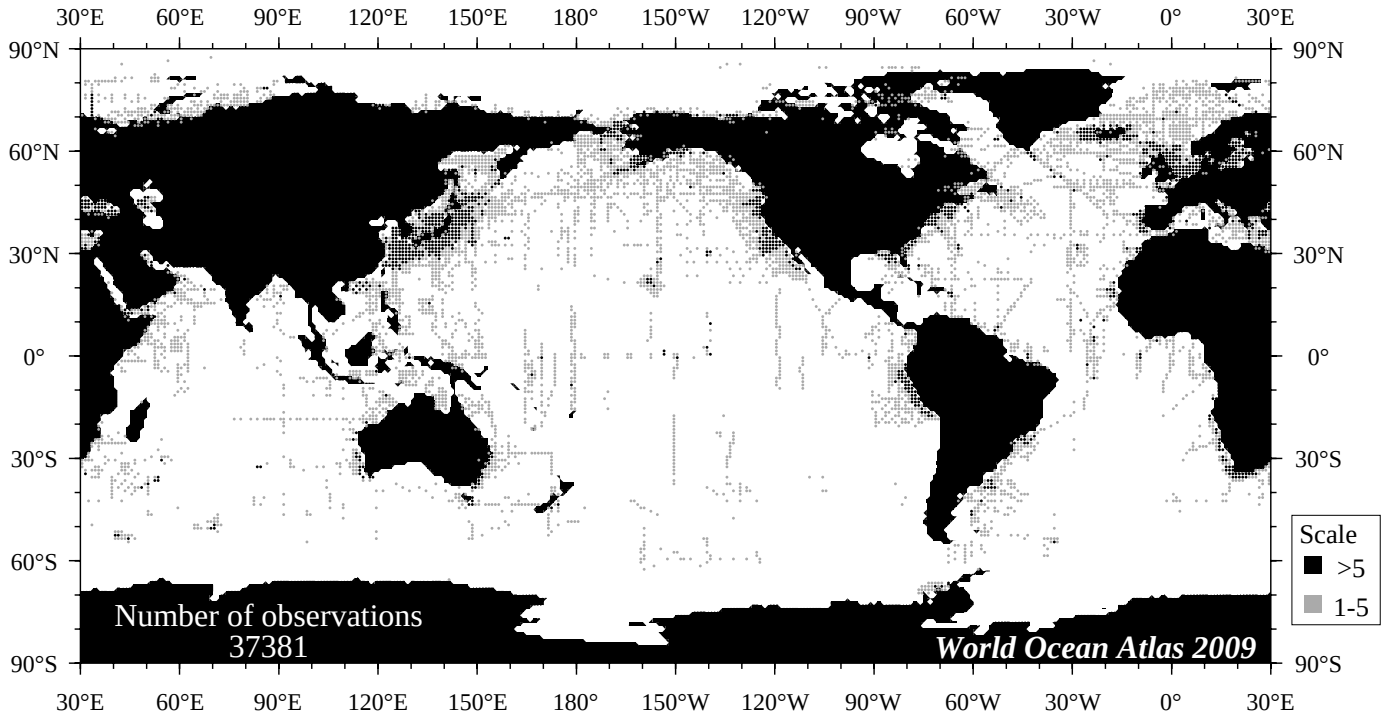

Fig C15 August phosphate observations at the surface.

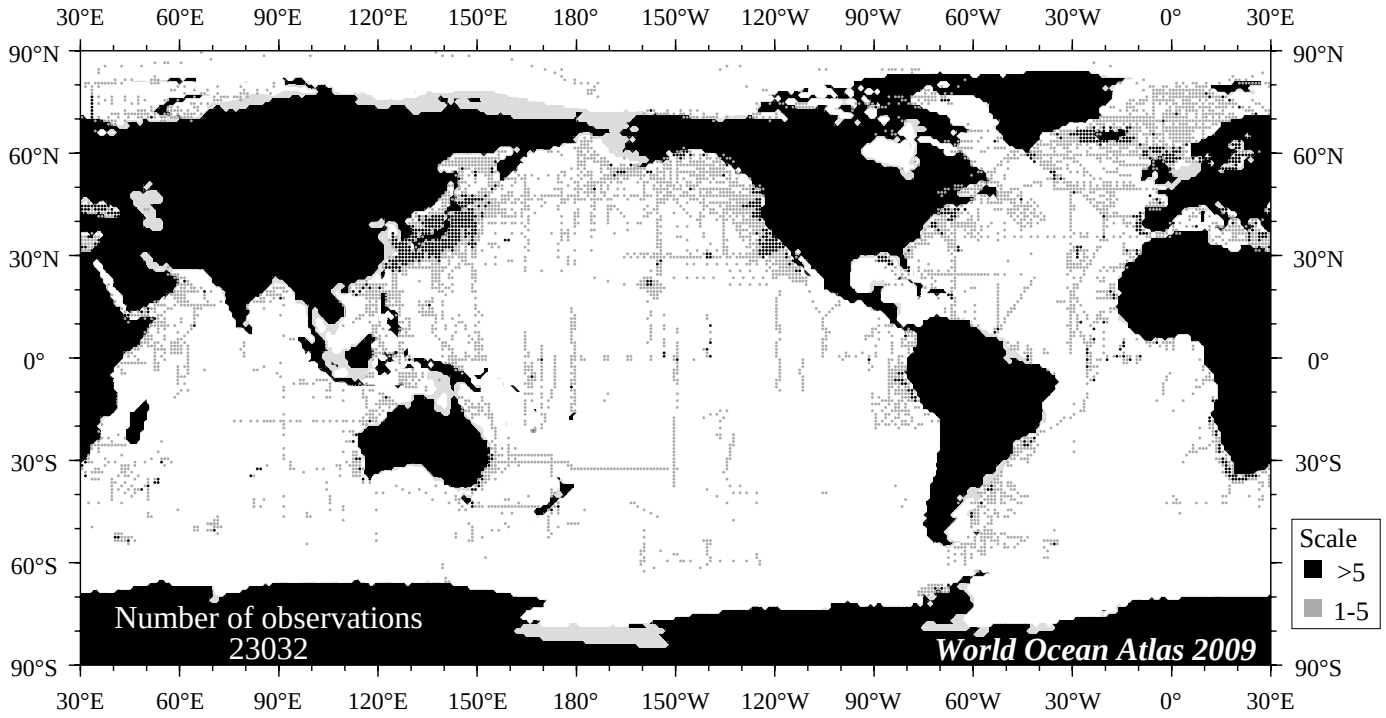

Fig C16 August phosphate observations at 75 m. depth.

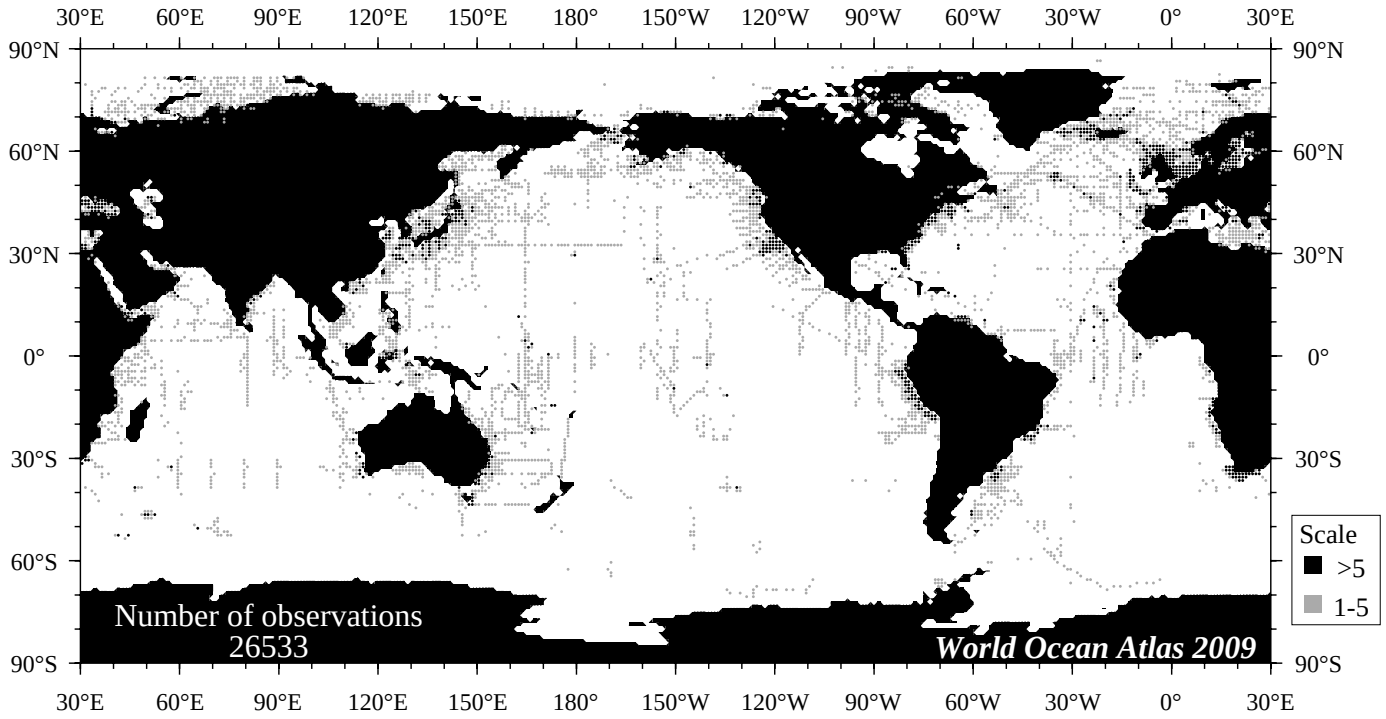

Fig C17 September phosphate observations at the surface.

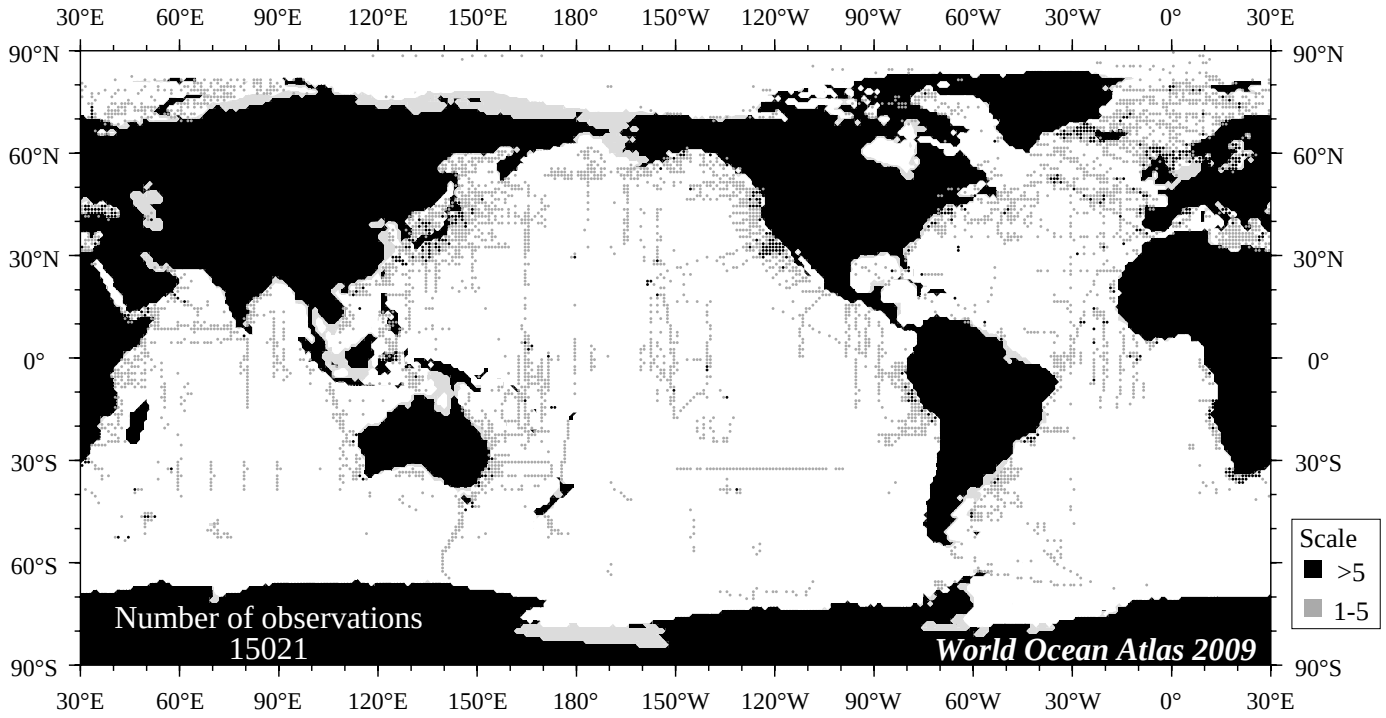

Fig C18 September phosphate observations at 75 m. depth.

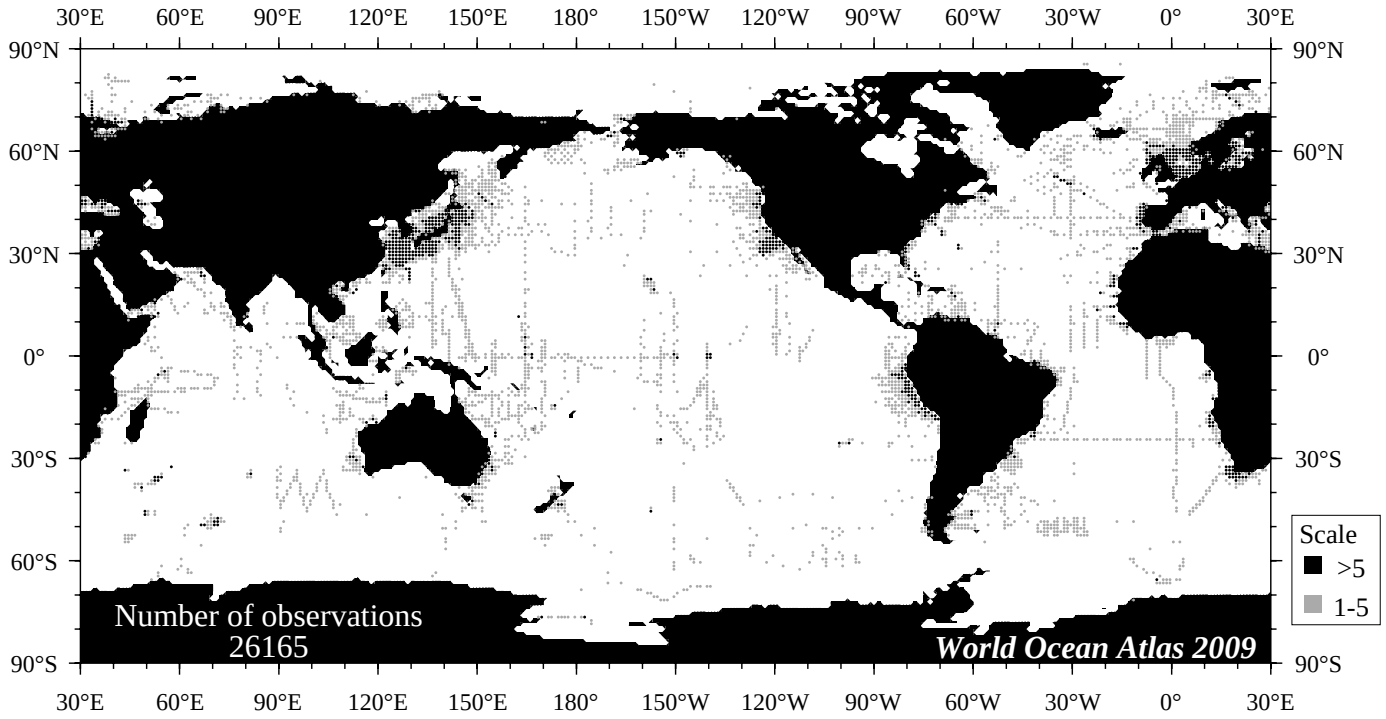

Fig C19 October phosphate observations at the surface.

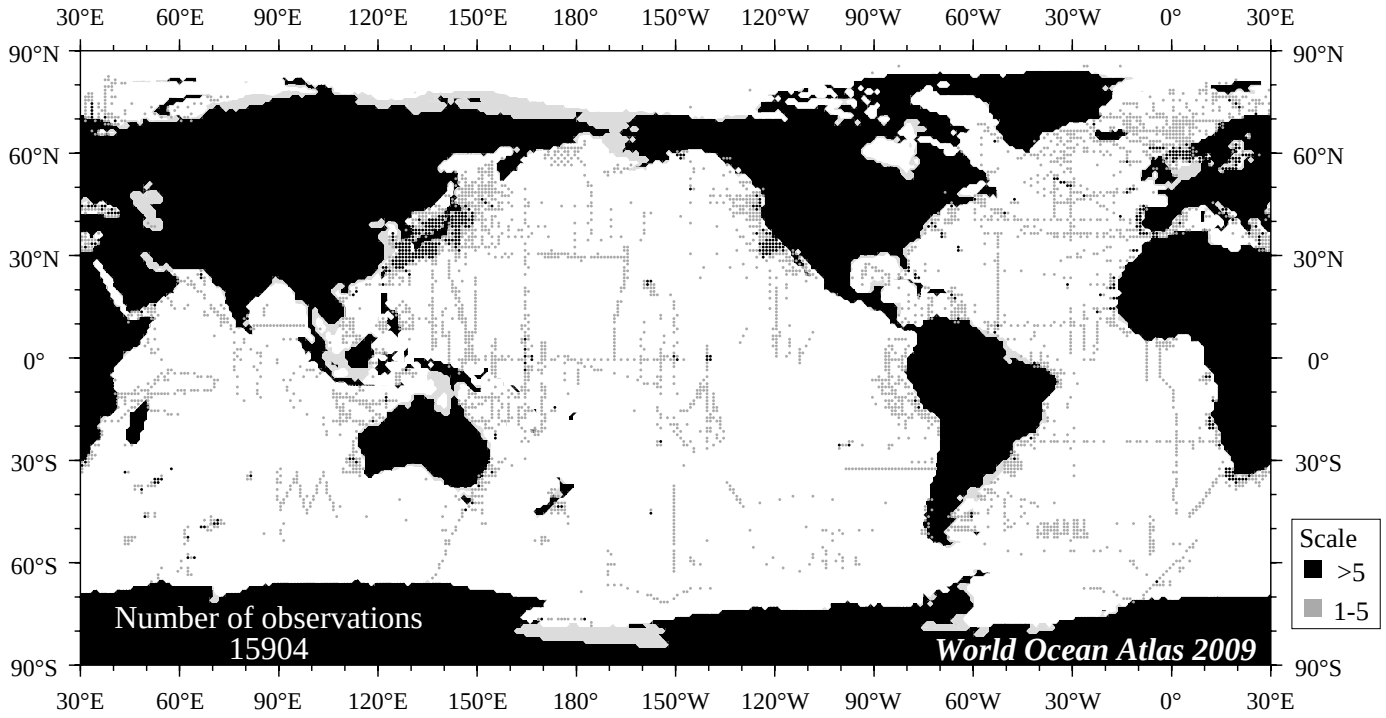

Fig C20 October phosphate observations at 75 m. depth.

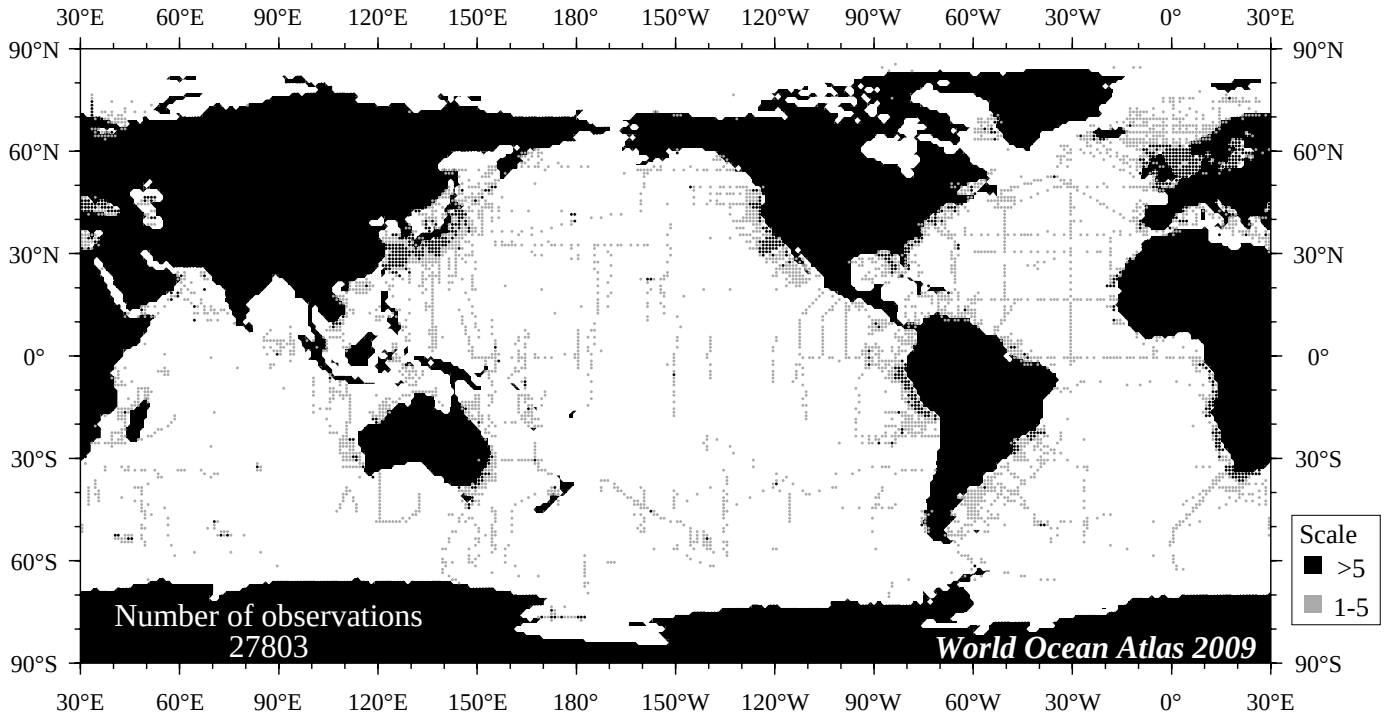

Fig C21 November phosphate observations at the surface.

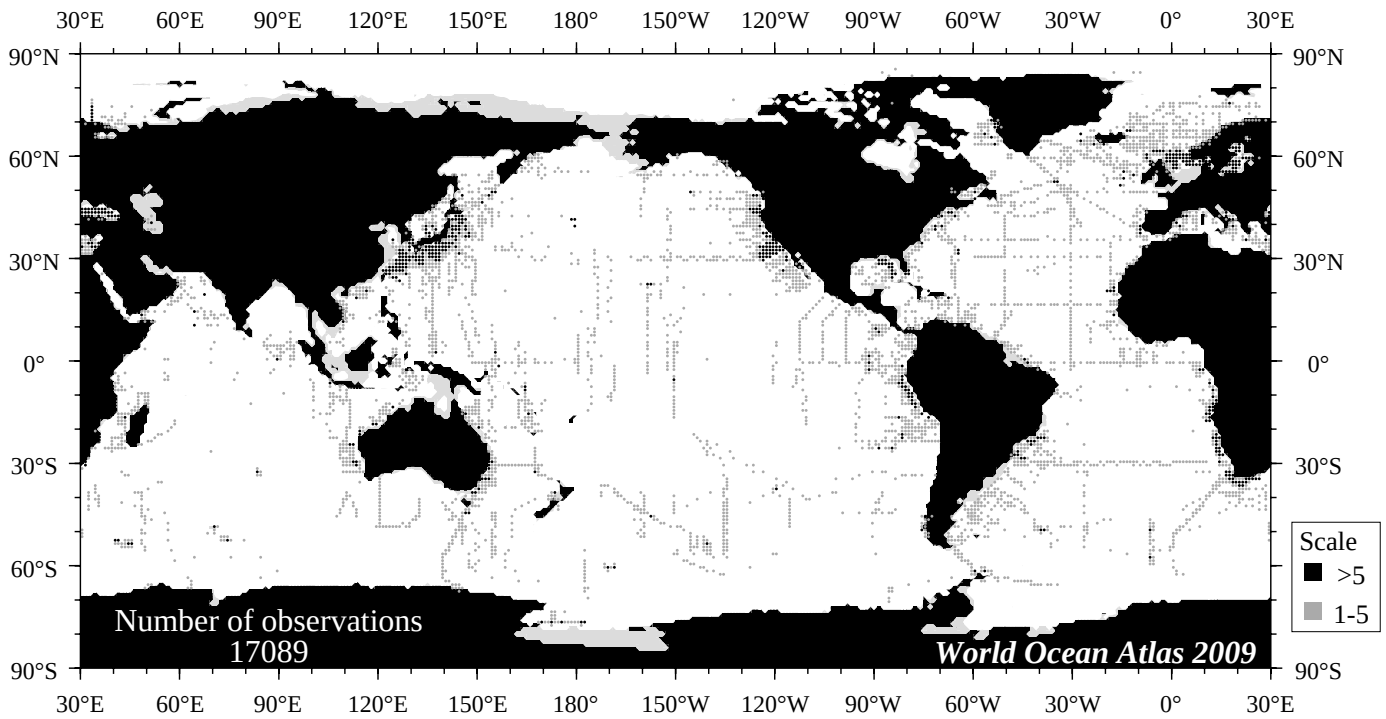

Fig C22 November phosphate observations at 75 m. depth.

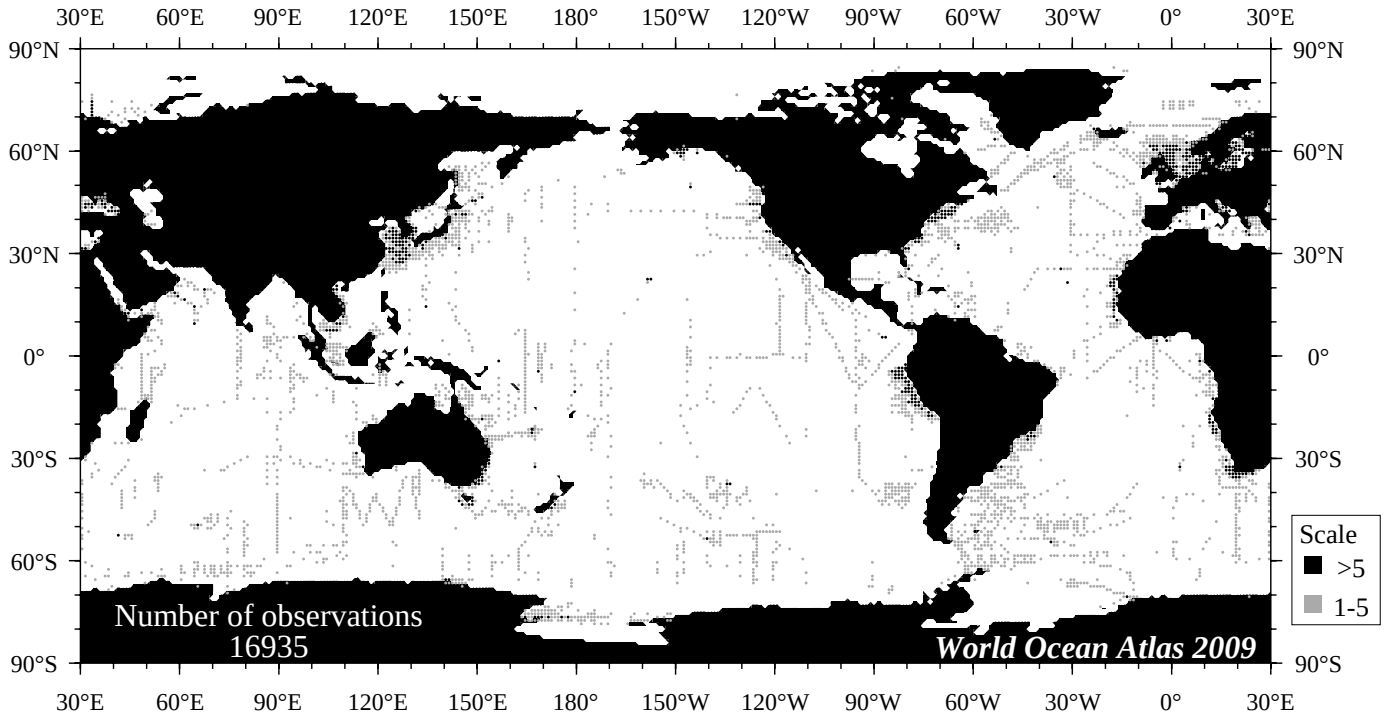

Fig C23 December phosphate observations at the surface.

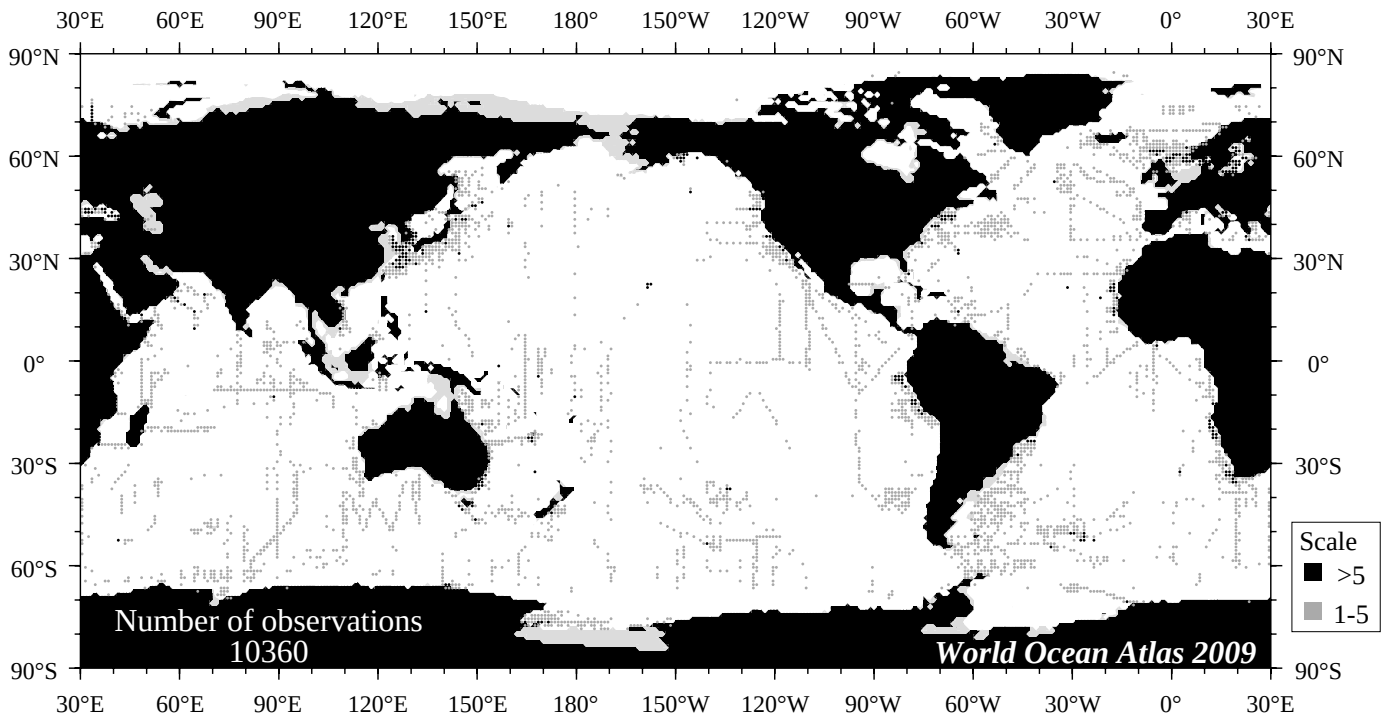

Fig C24 December phosphate observations at 75 m. depth.

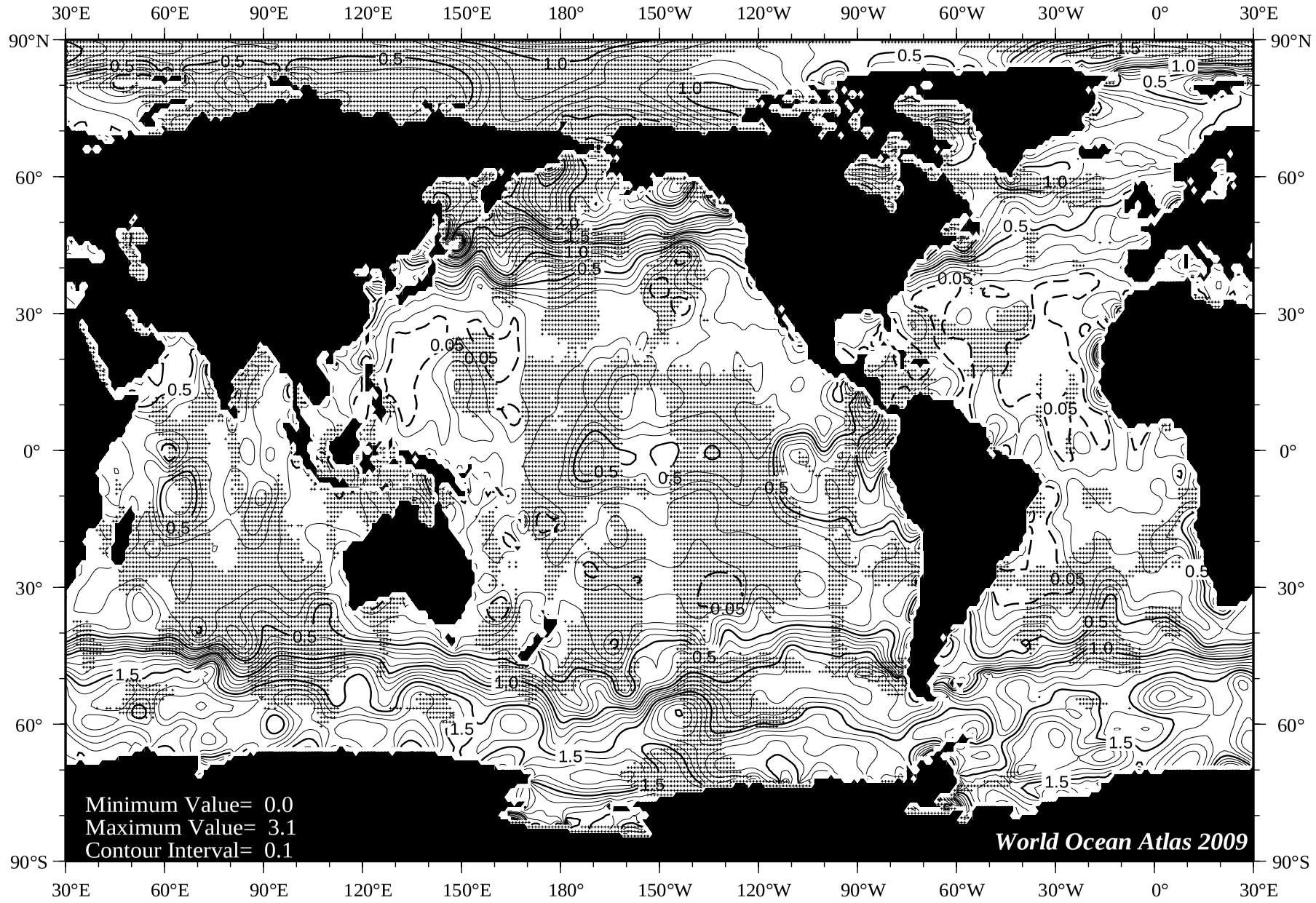

Fig C25 January mean phosphate [umol/l] at the surface.

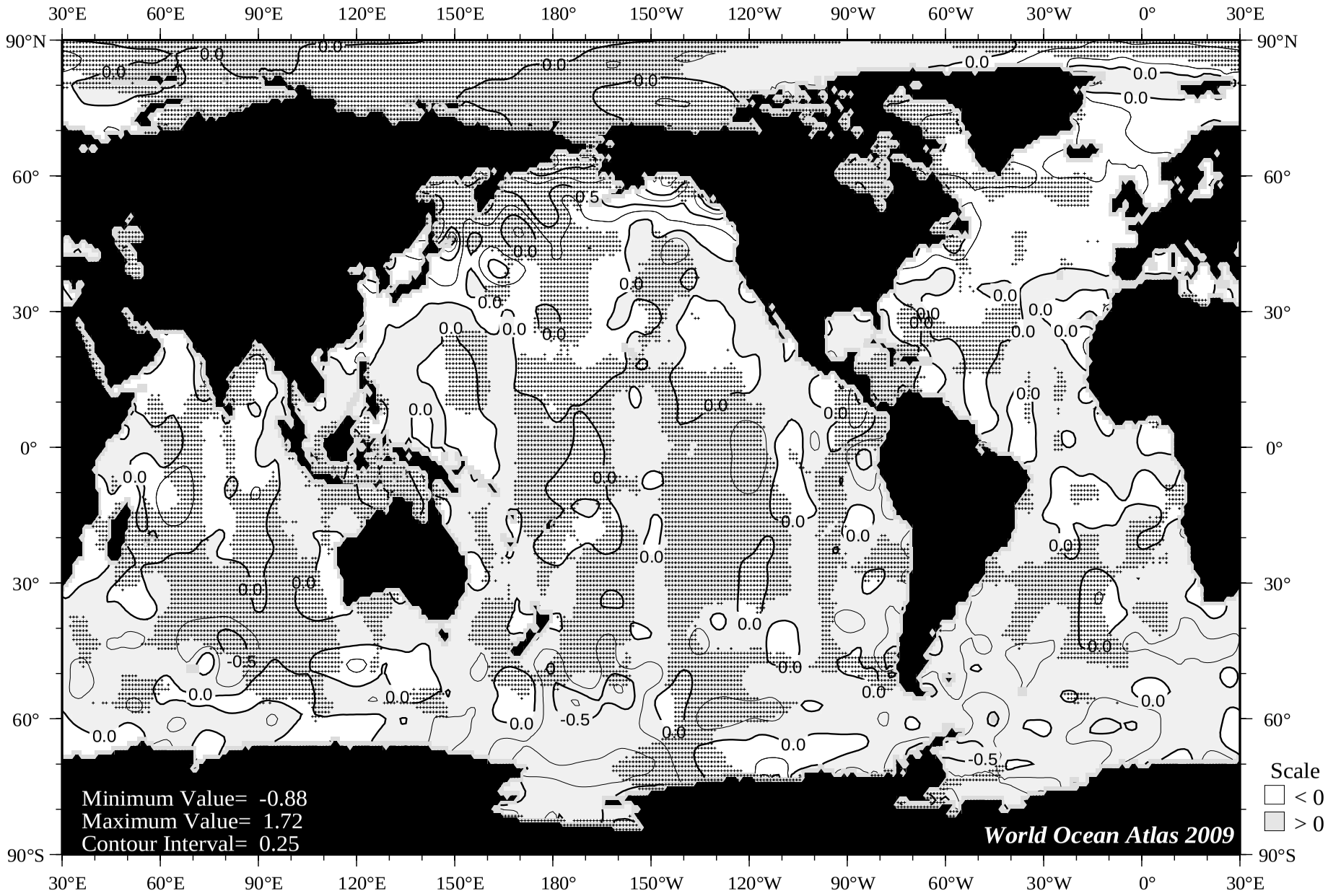

Fig C26 January minus annual phosphate [umol/l] at the surface.

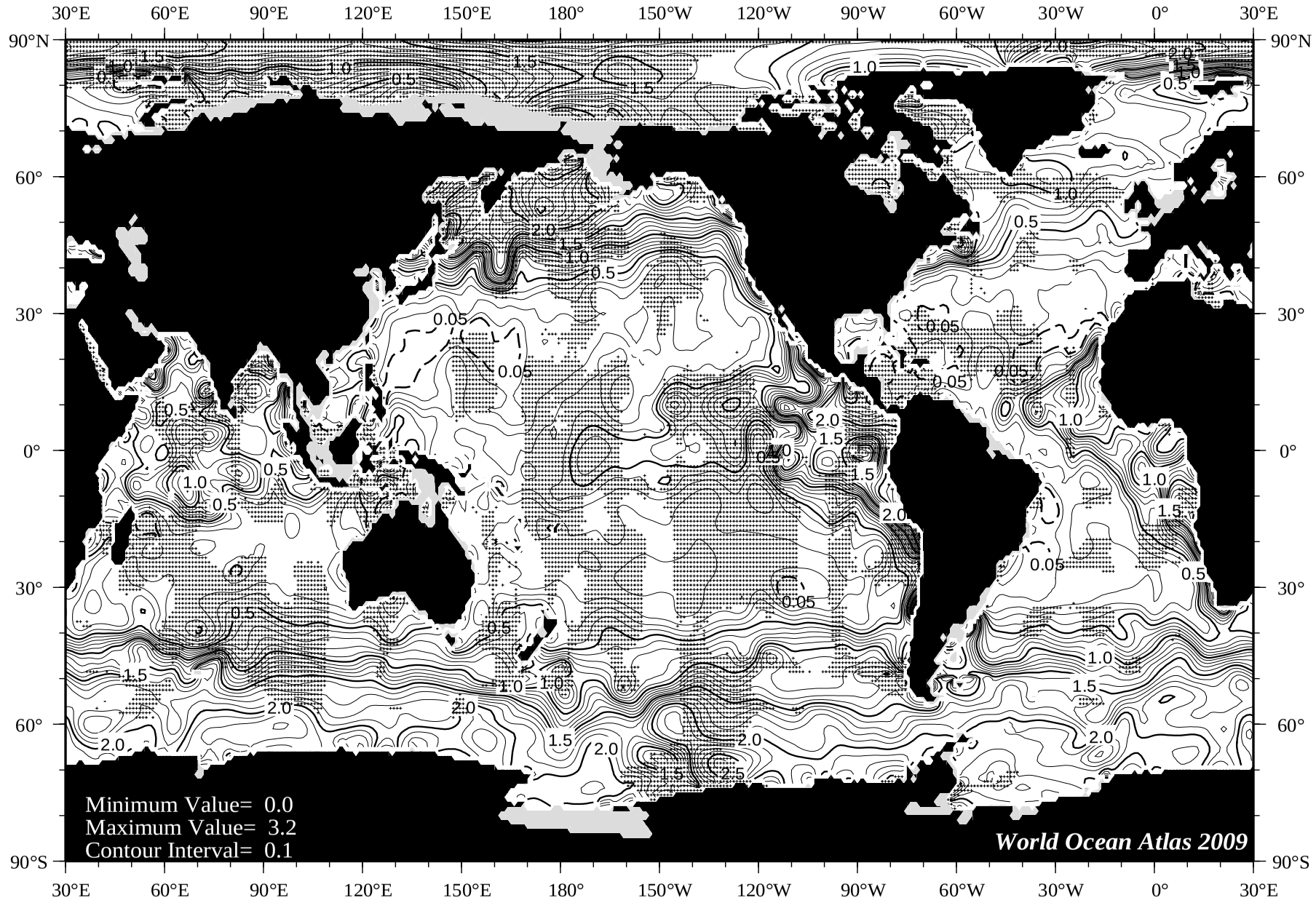

Fig C27 January mean phosphate [umol/l] at 75 m. depth.

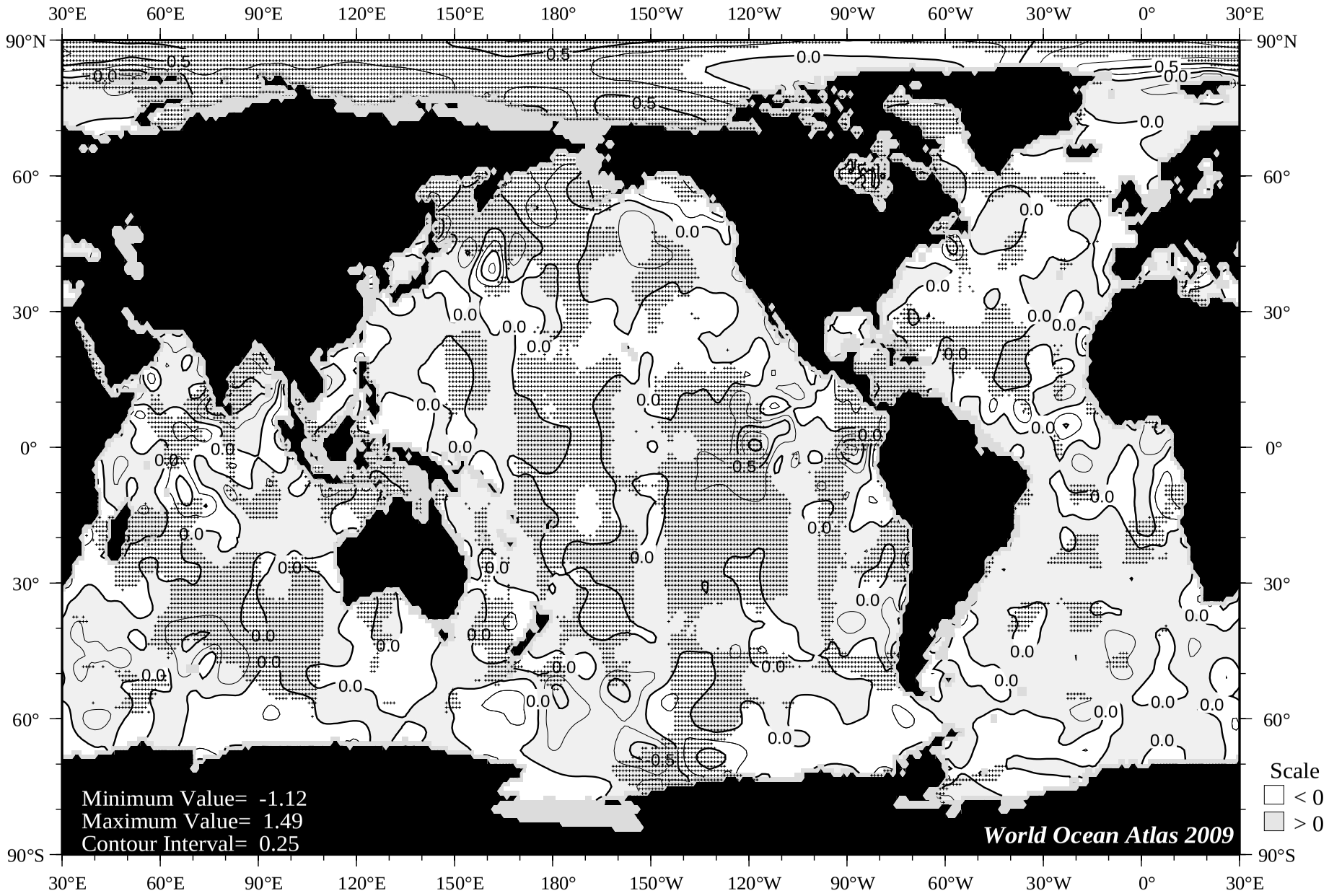

Fig C28 January minus annual phosphate [umol/l] at 75 m. depth.

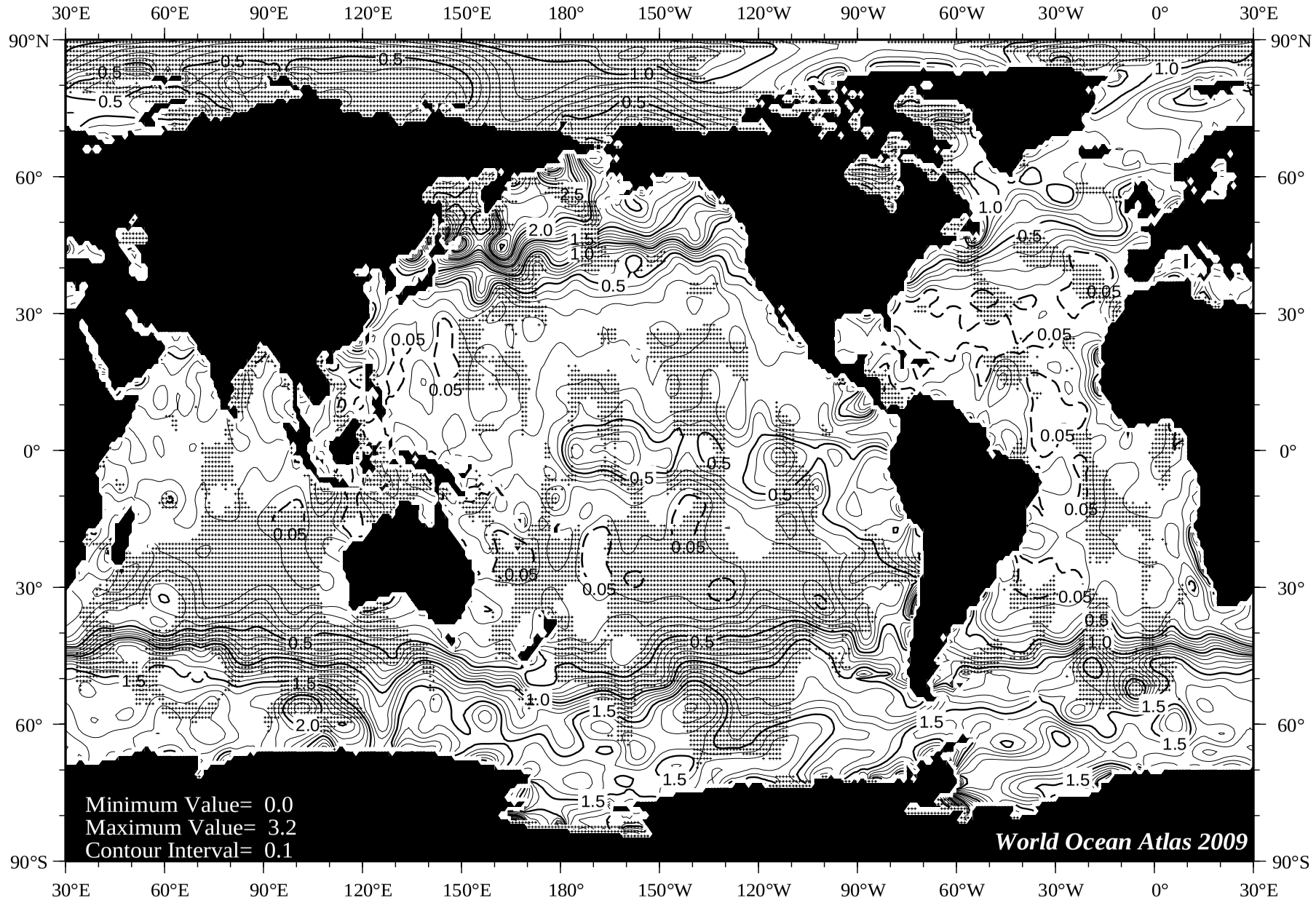

Fig C29 February mean phosphate [umol/l] at the surface.

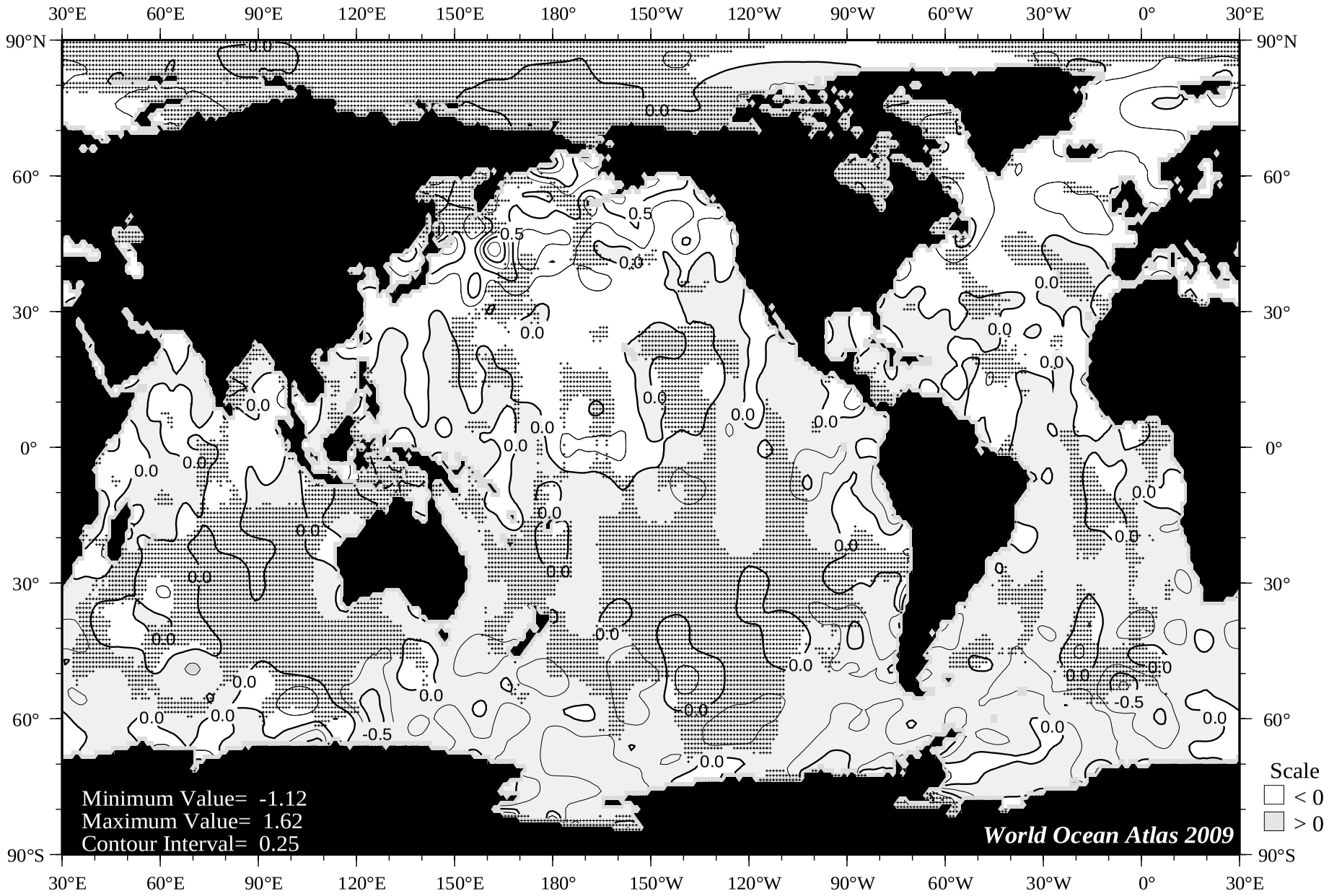

Fig C30 February minus annual phosphate [umol/l] at the surface.

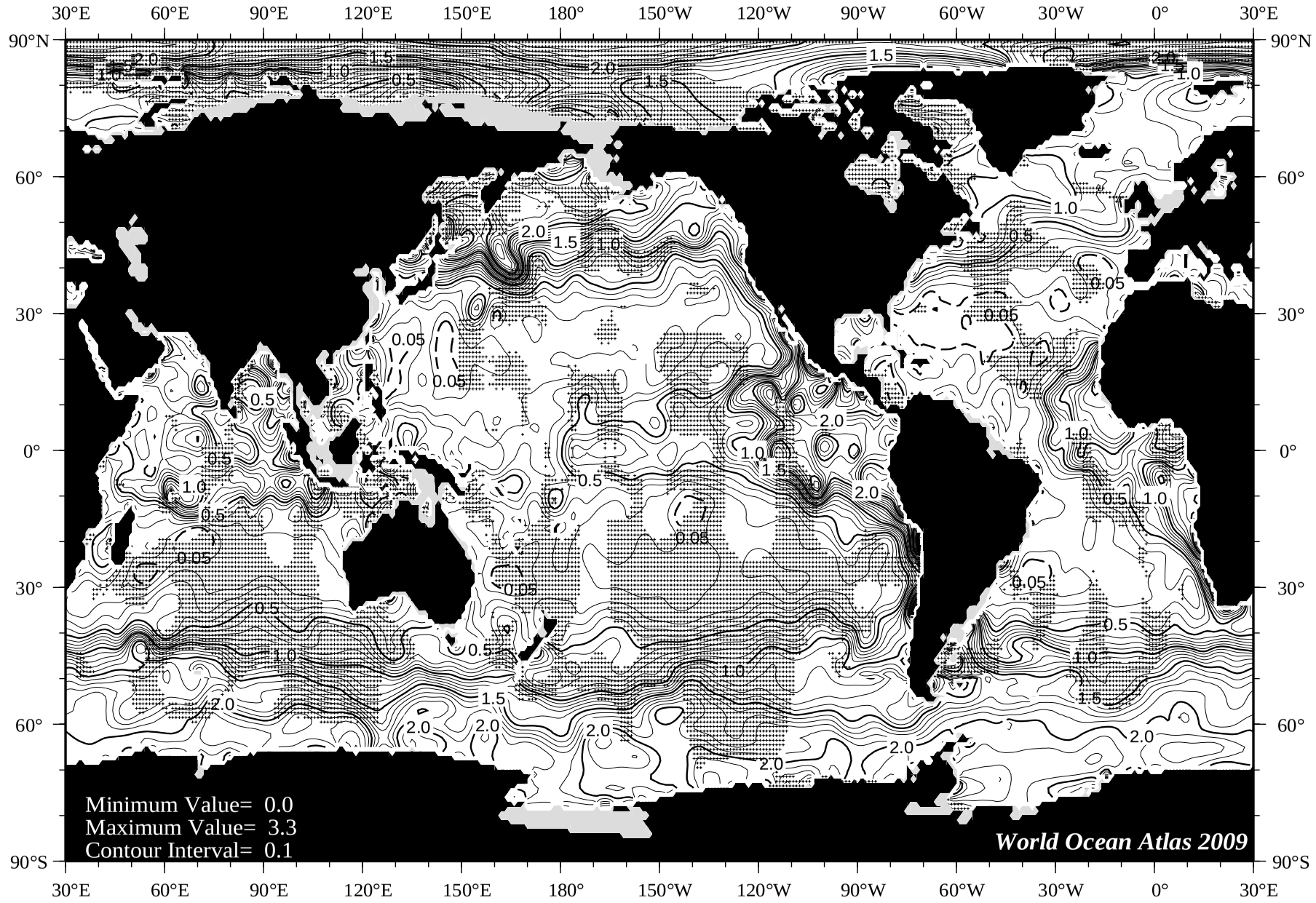

Fig C31 February mean phosphate [umol/l] at 75 m. depth.

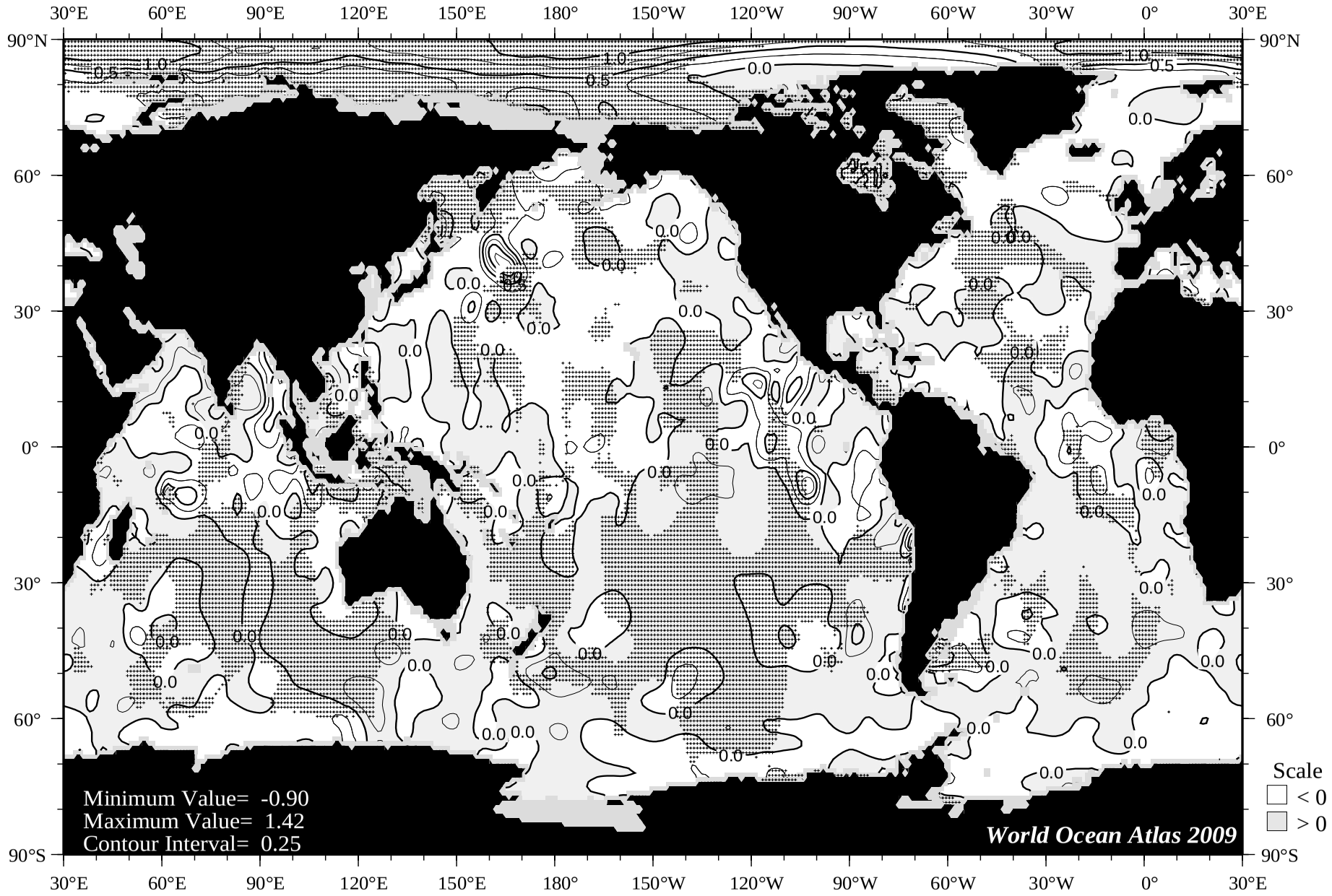

Fig C32 February minus annual phosphate [umol/l] at 75 m. depth.

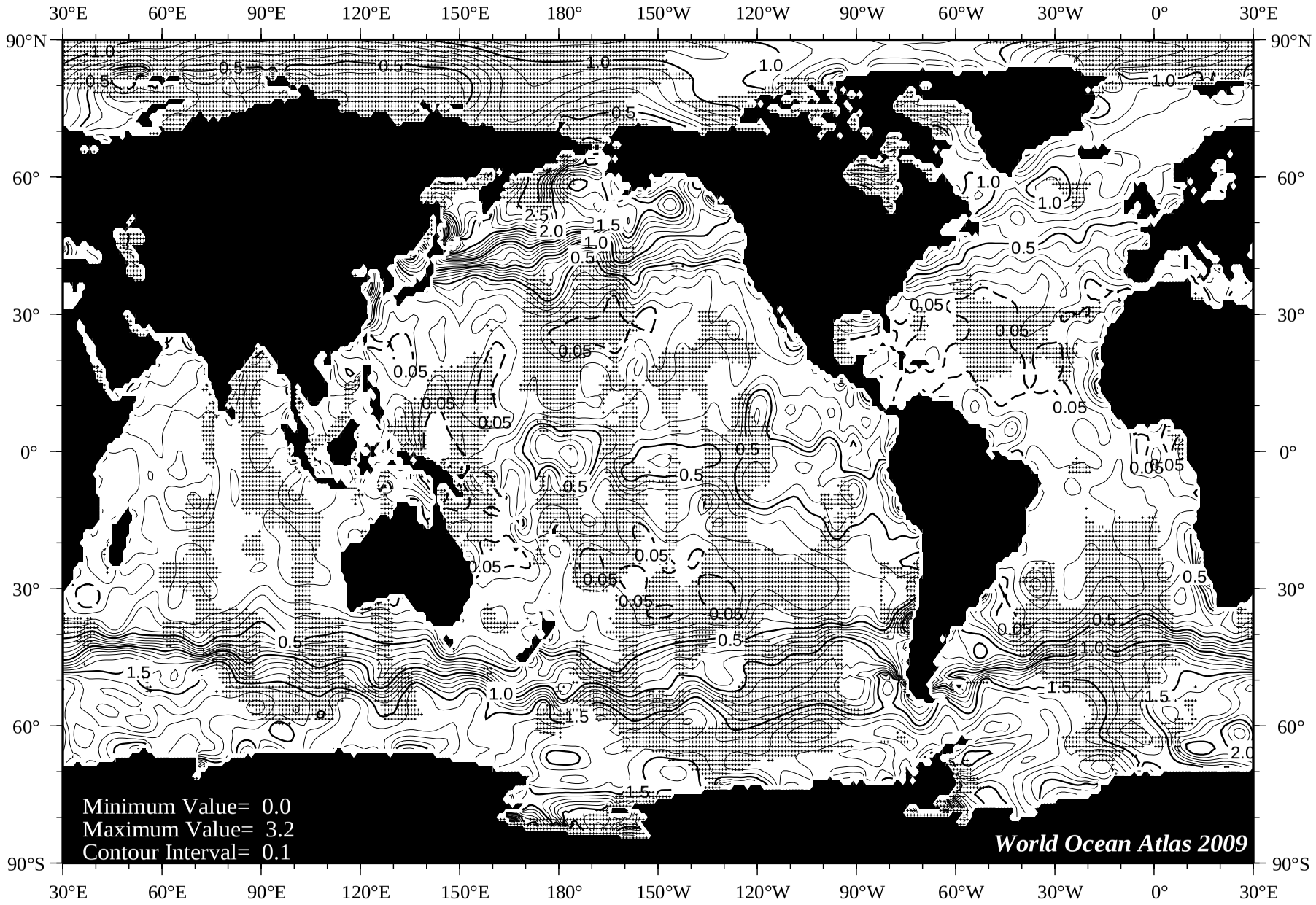

Fig C33 March mean phosphate [umol/l] at the surface.

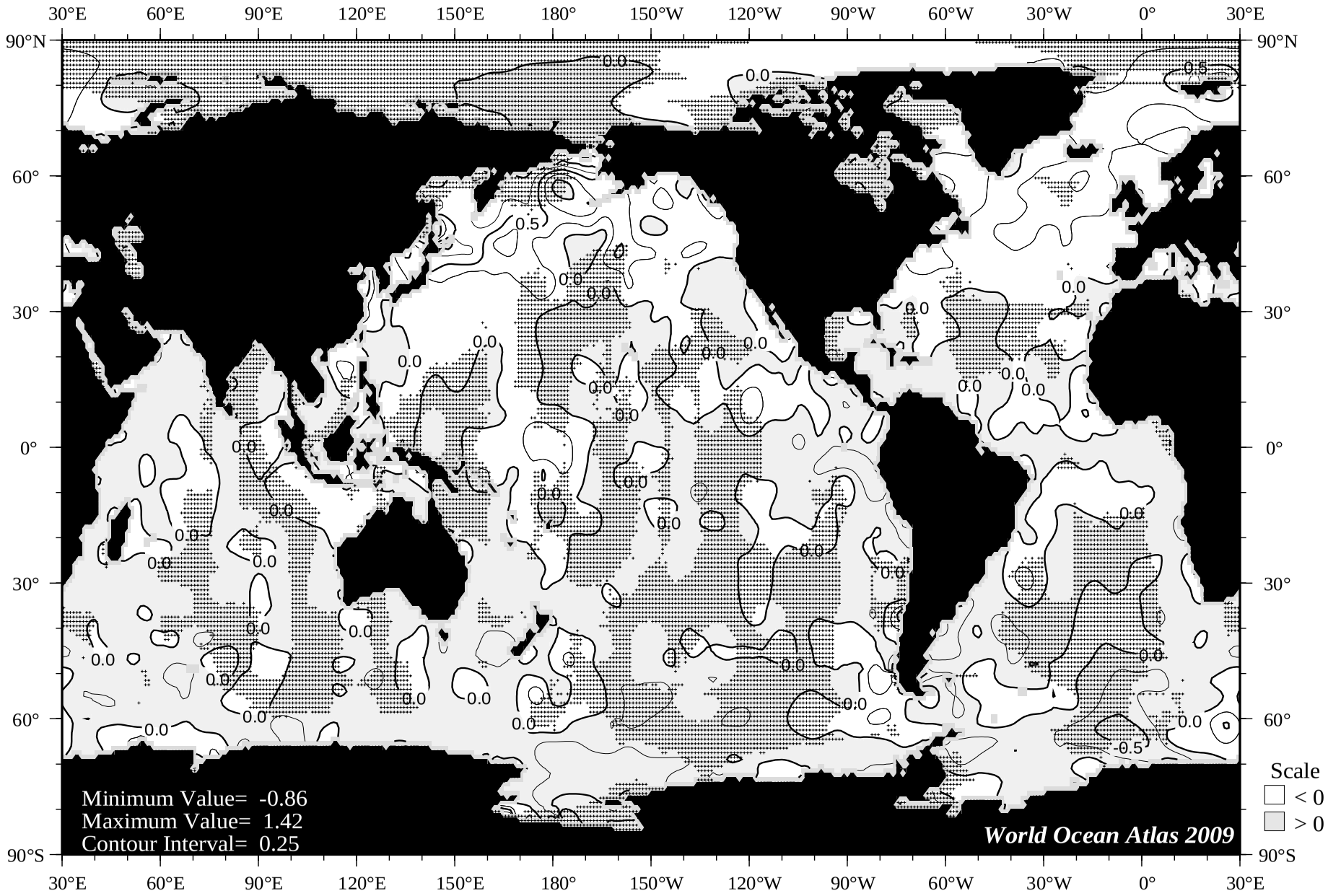

Fig C34 March minus annual phosphate [umol/l] at the surface.

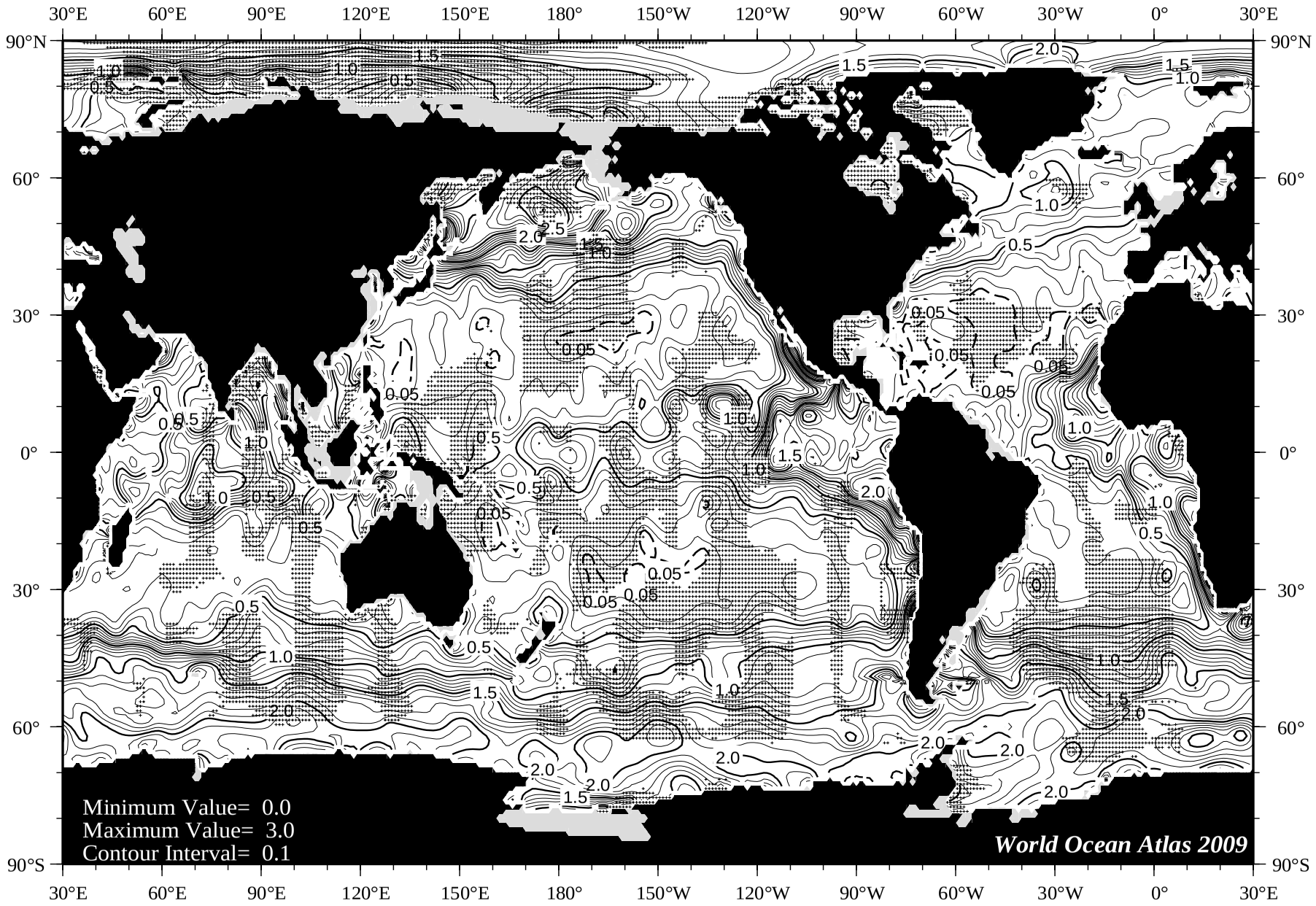

Fig C35 March mean phosphate [umol/l] at 75 m. depth.

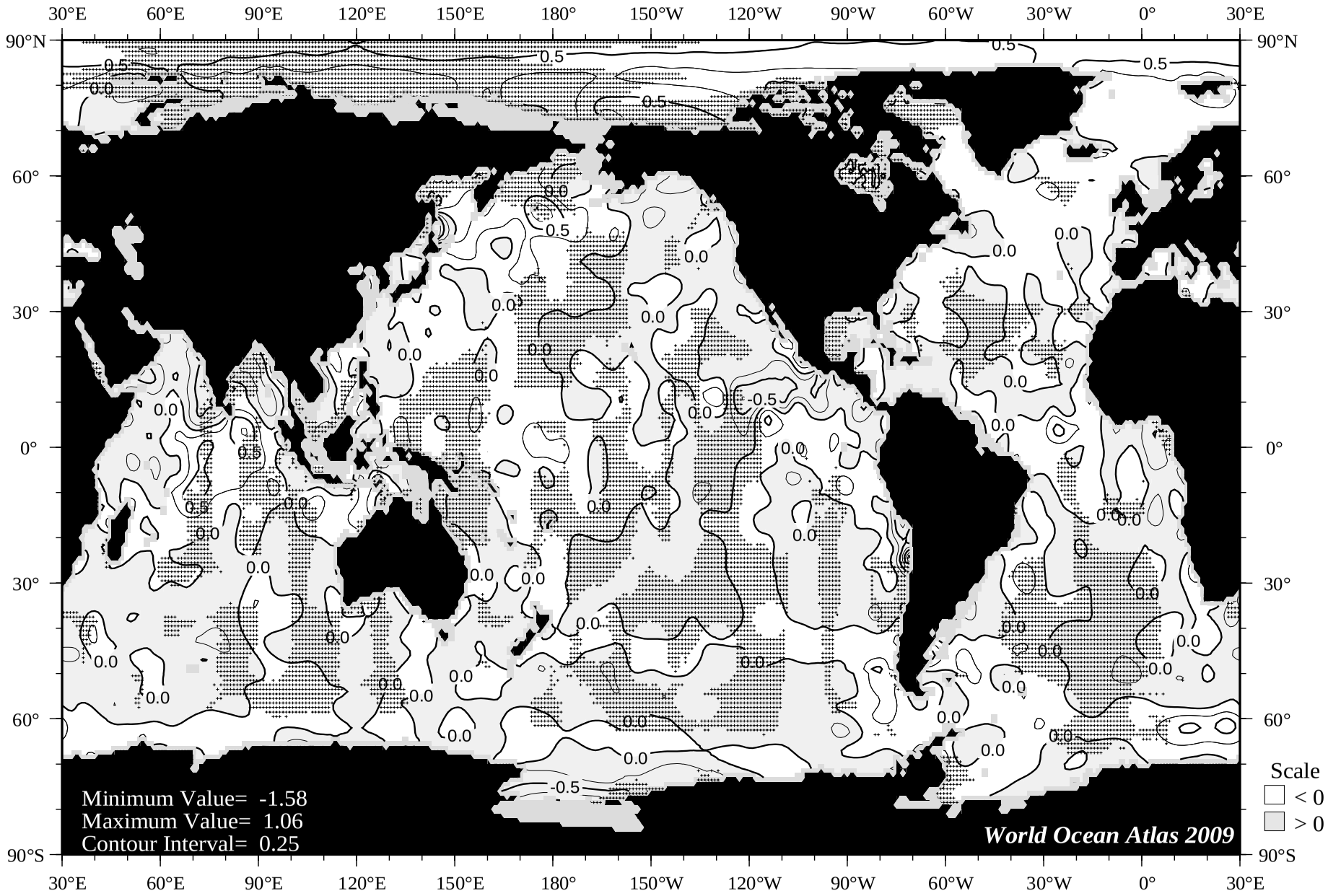

Fig C36 March minus annual phosphate [umol/l] at 75 m. depth.

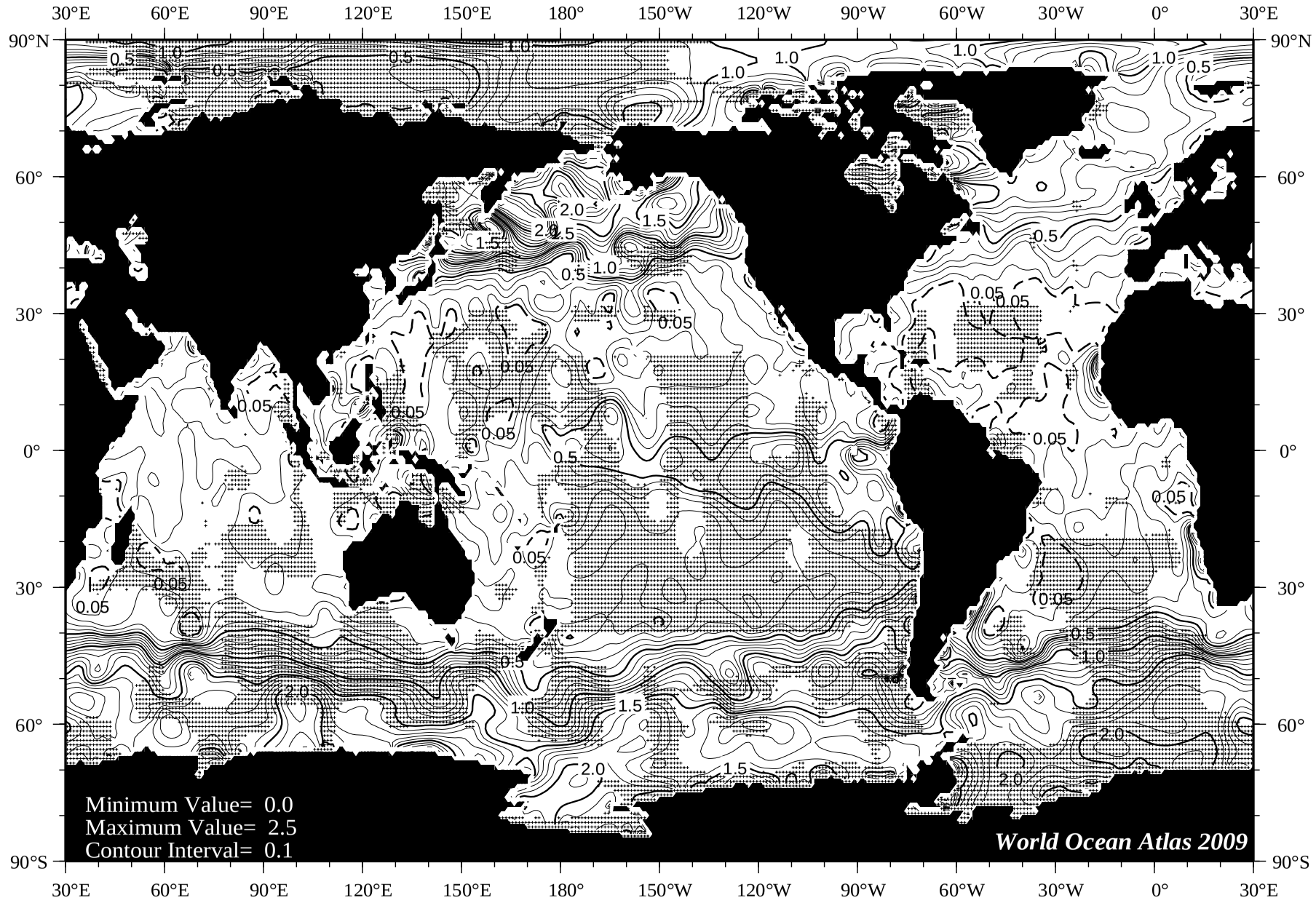

Fig C37 April mean phosphate [umol/l] at the surface.

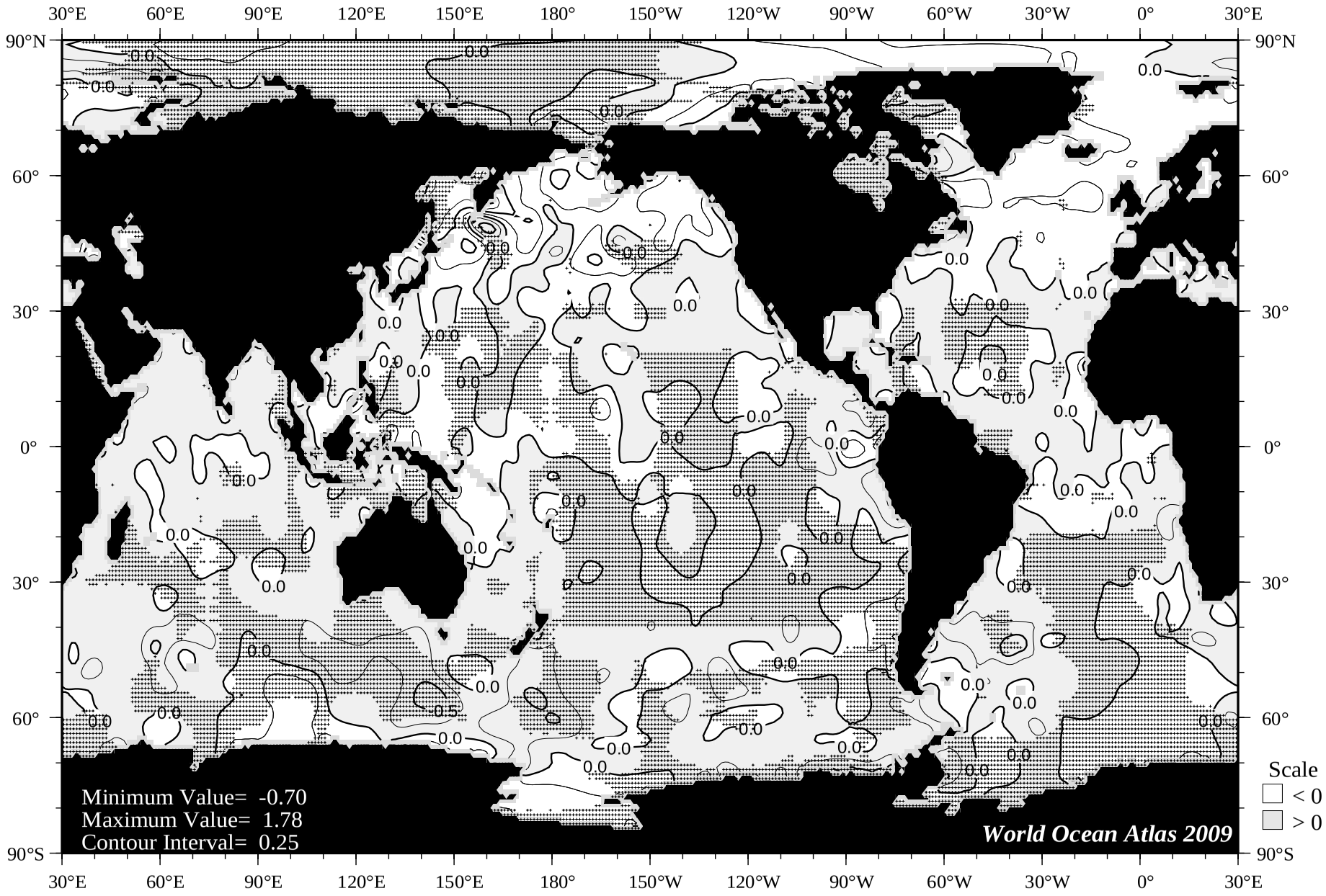

Fig C38 April minus annual phosphate [umol/l] at the surface.

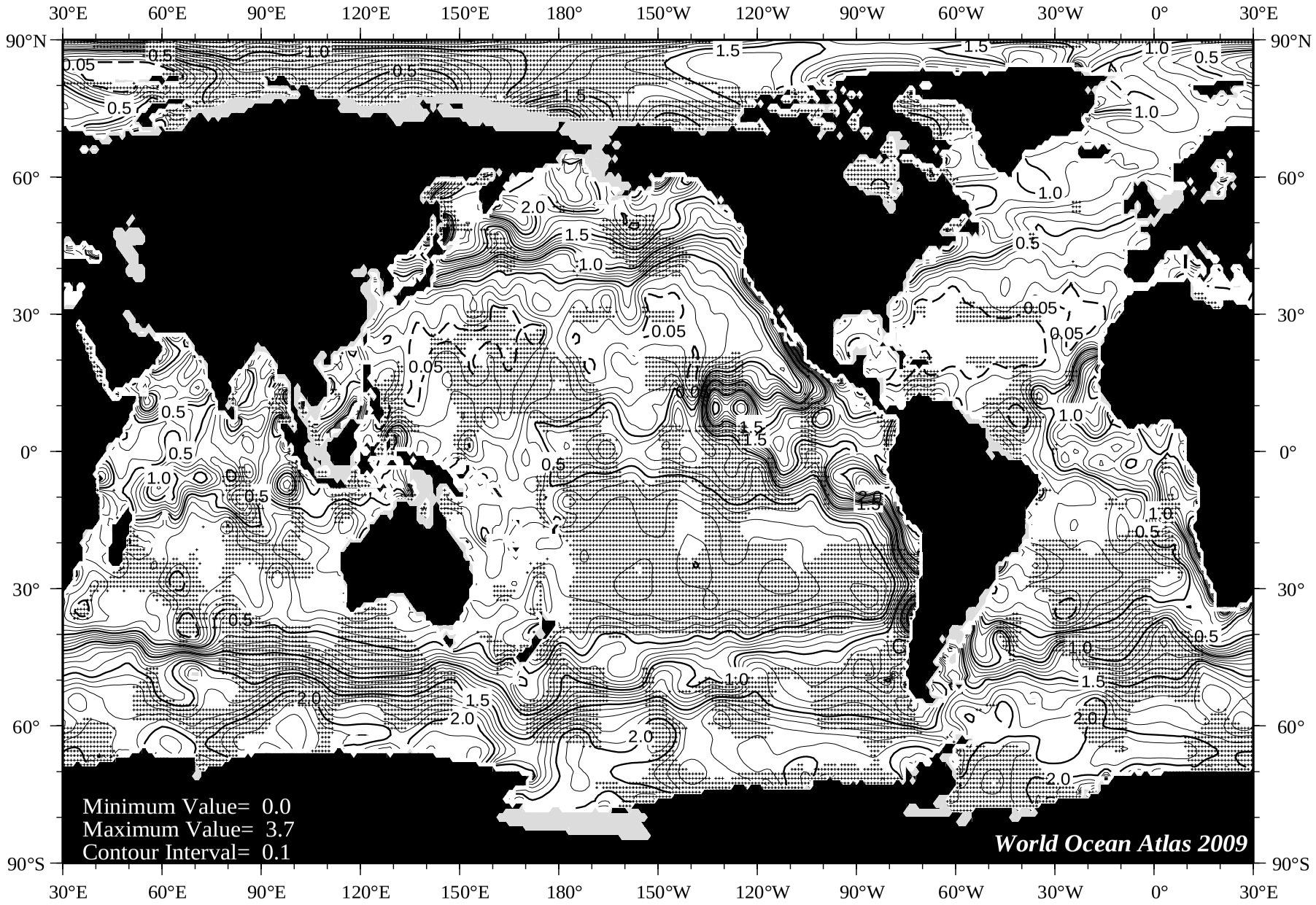

Fig C39 April mean phosphate [umol/l] at 75 m. depth.

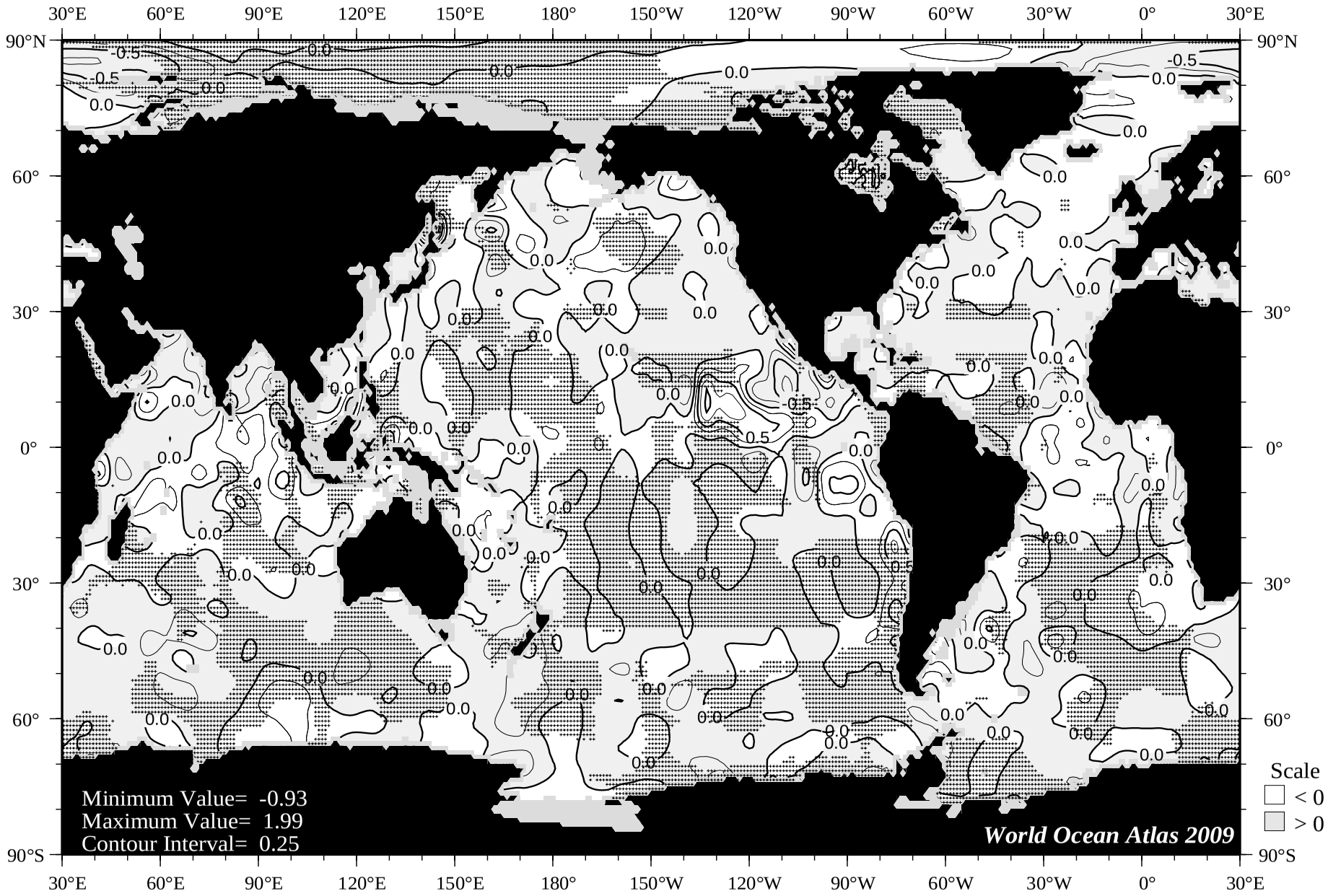

Fig C40 April minus annual phosphate [umol/l] at 75 m. depth.

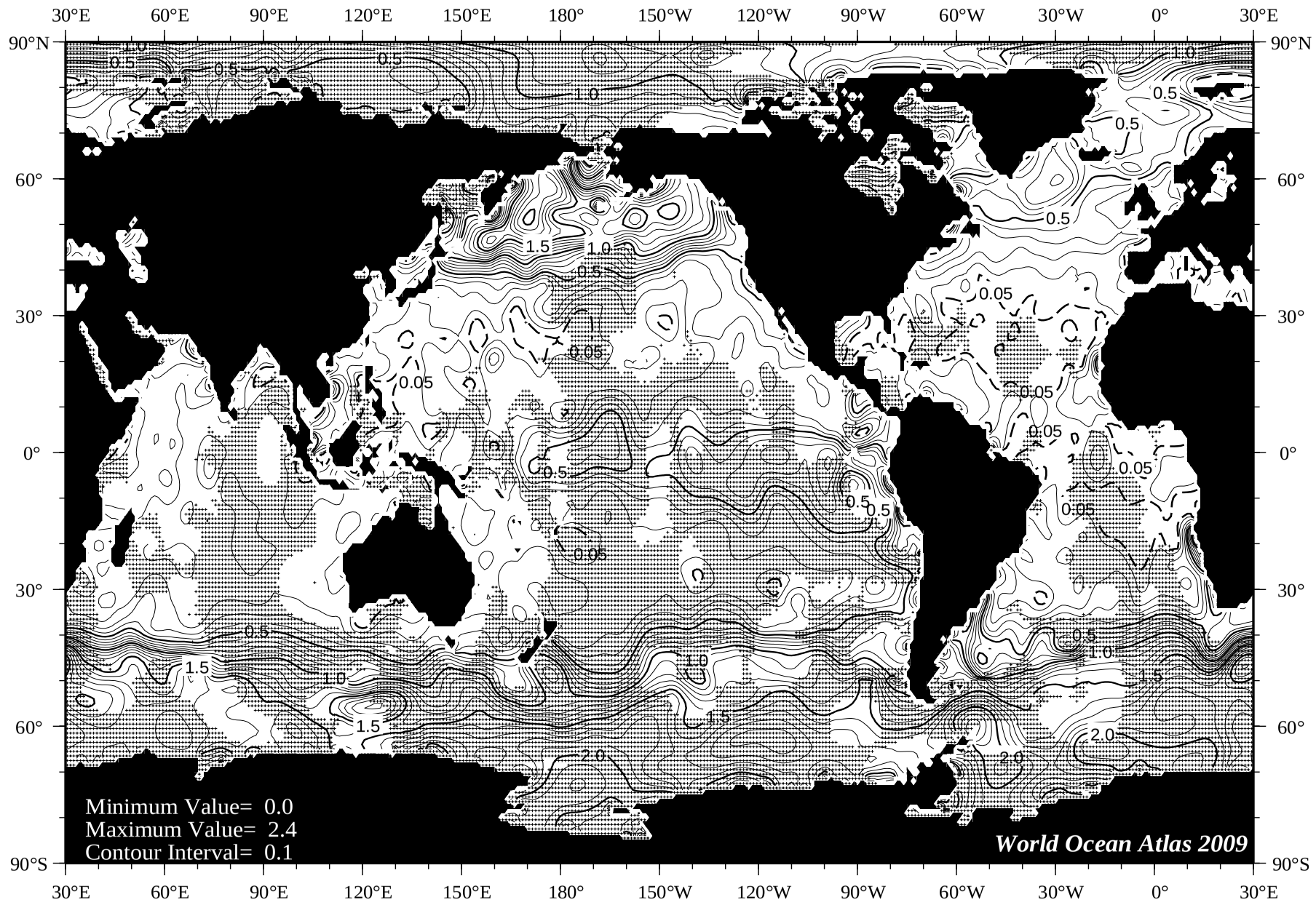

Fig C41 May mean phosphate [umol/l] at the surface.

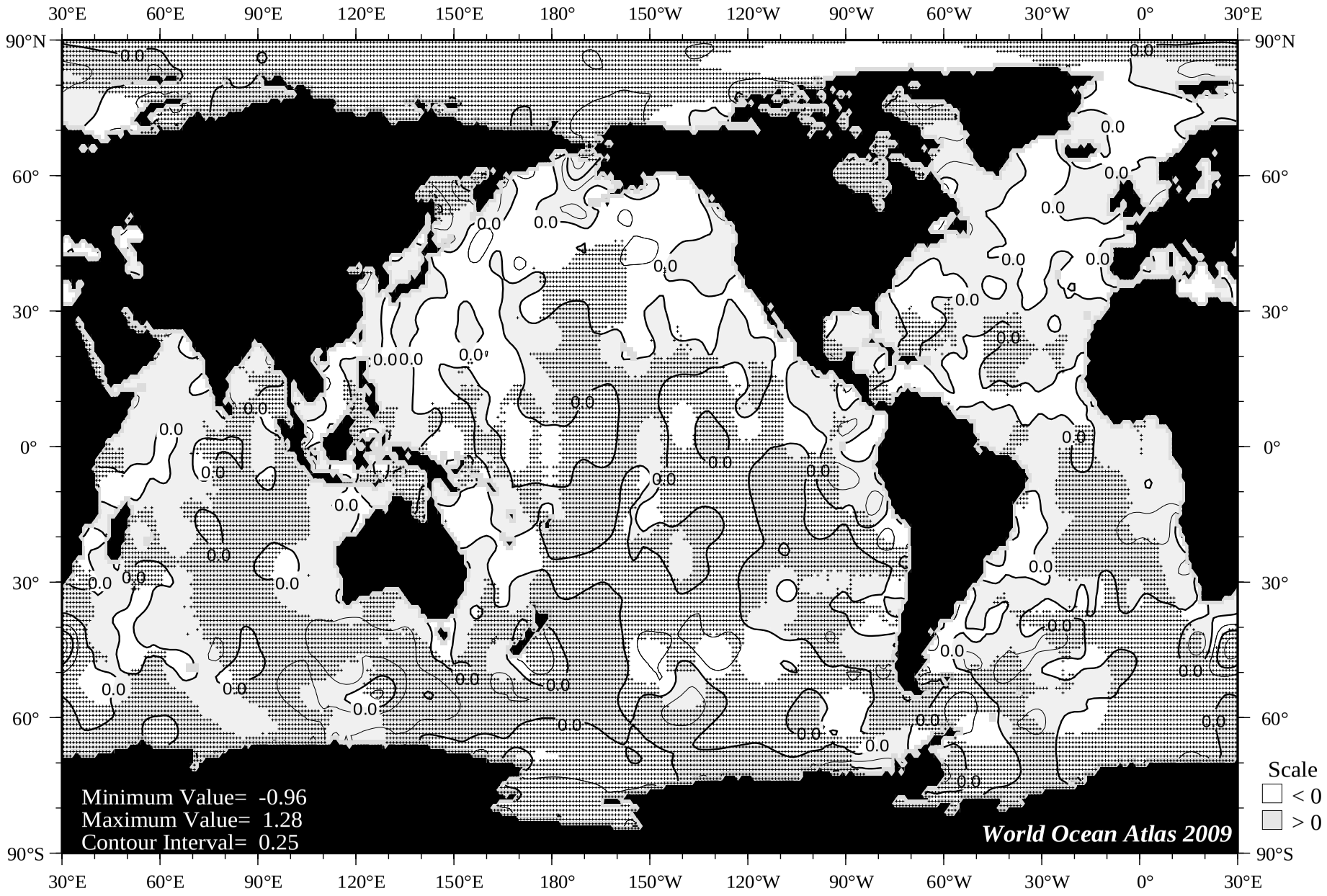

Fig C42 May minus annual phosphate [umol/l] at the surface.

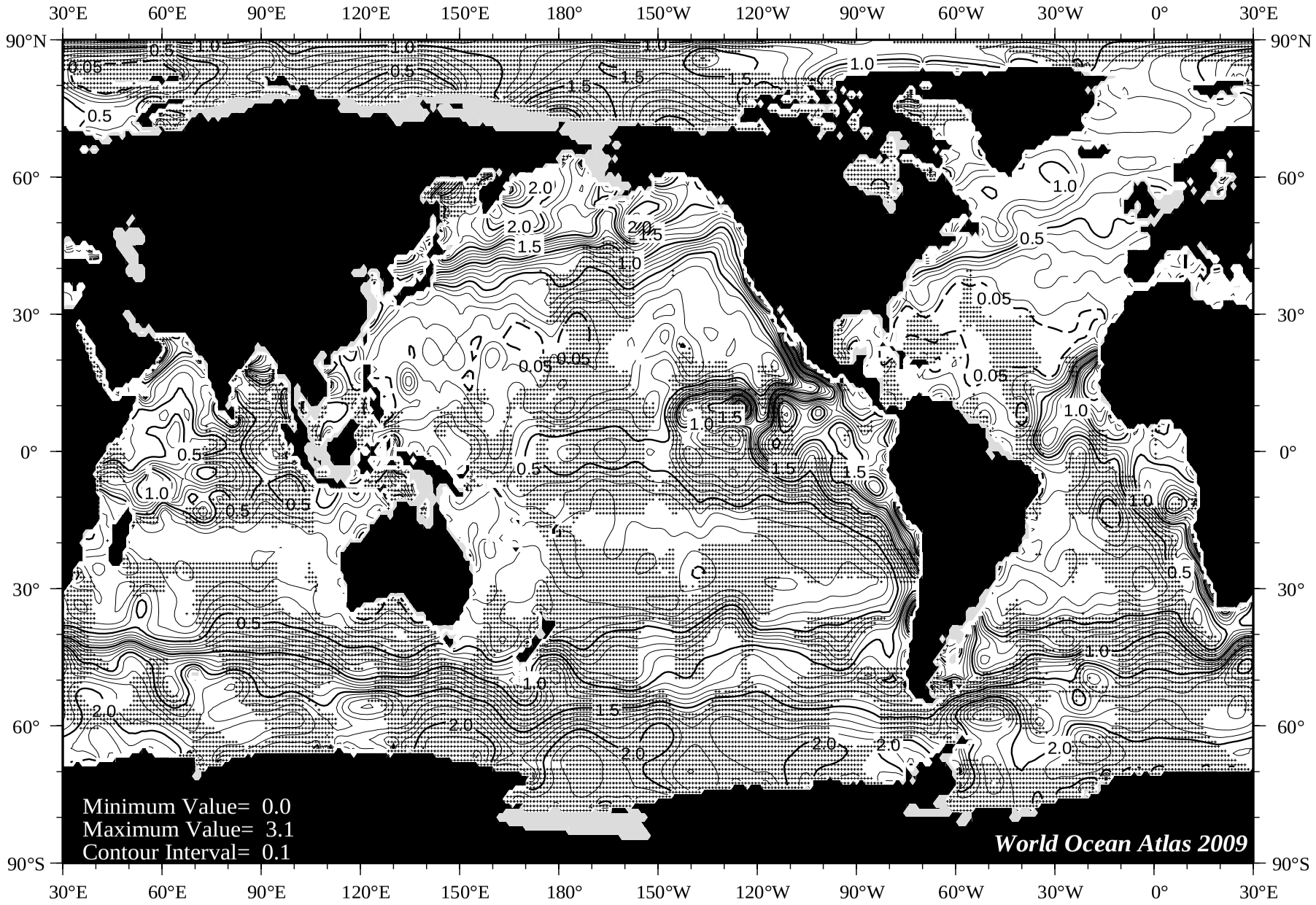

Fig C43 May mean phosphate [umol/l] at 75 m. depth.

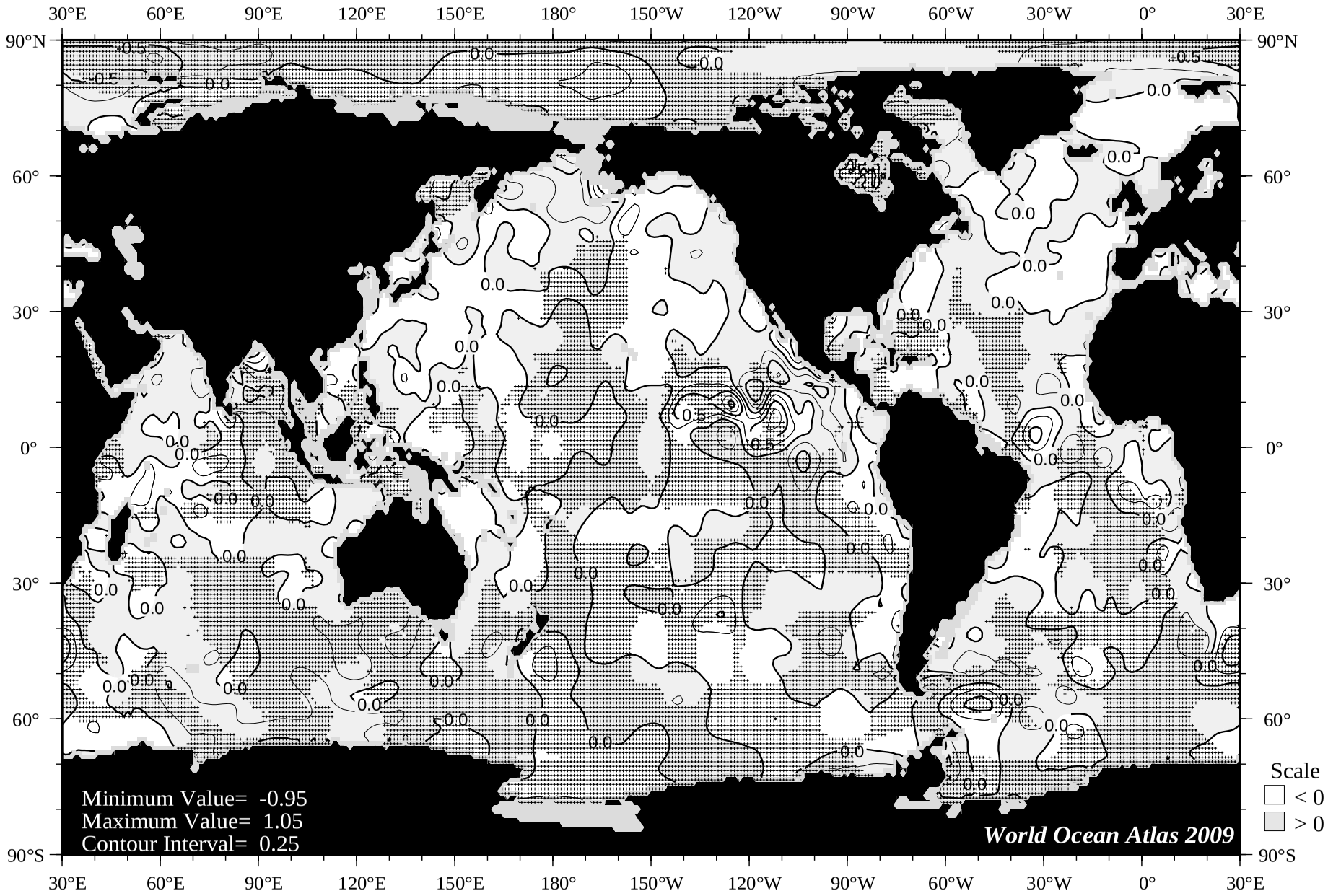

Fig C44 May minus annual phosphate [umol/l] at 75 m. depth.

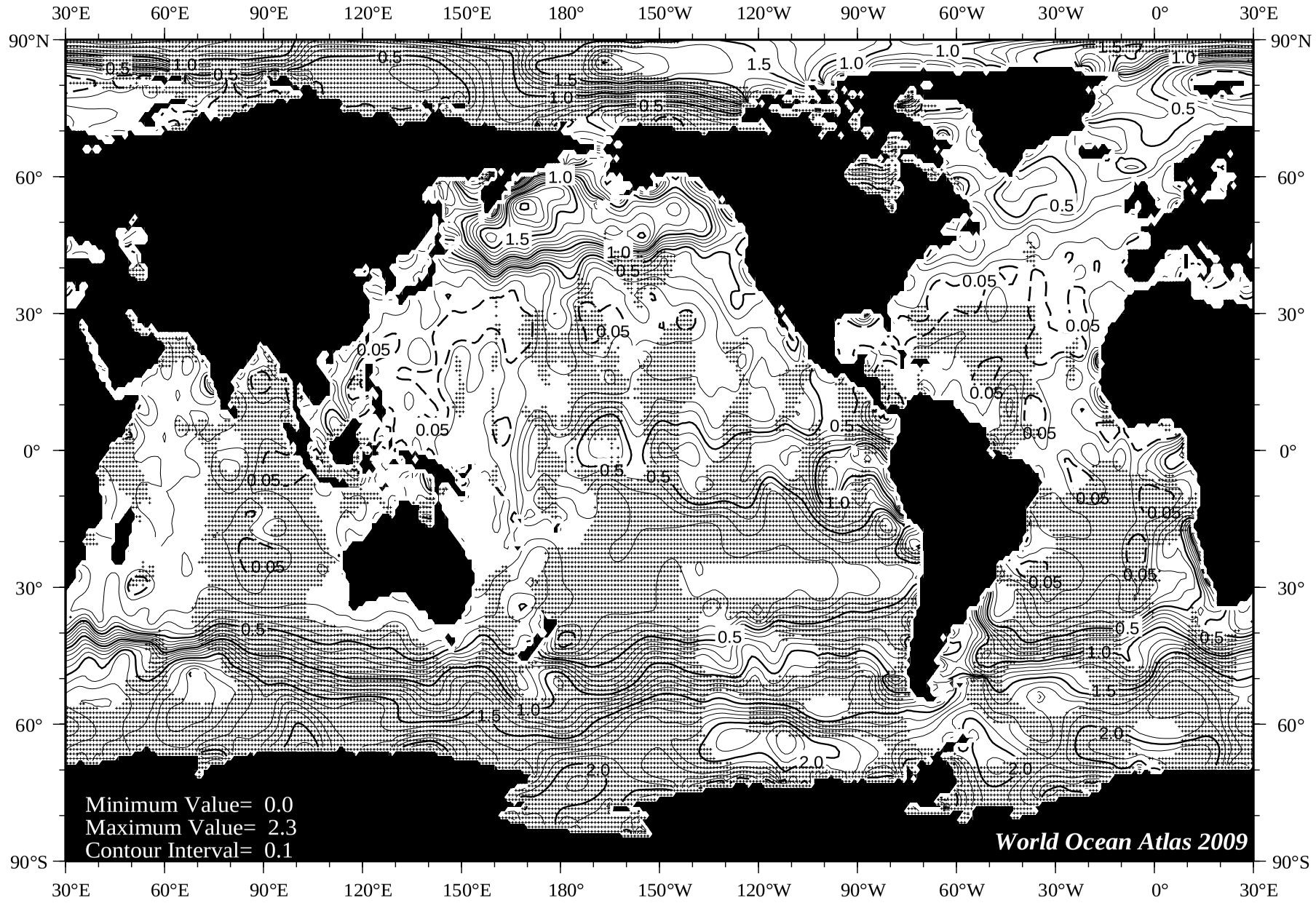

Fig C45 June mean phosphate [umol/l] at the surface.

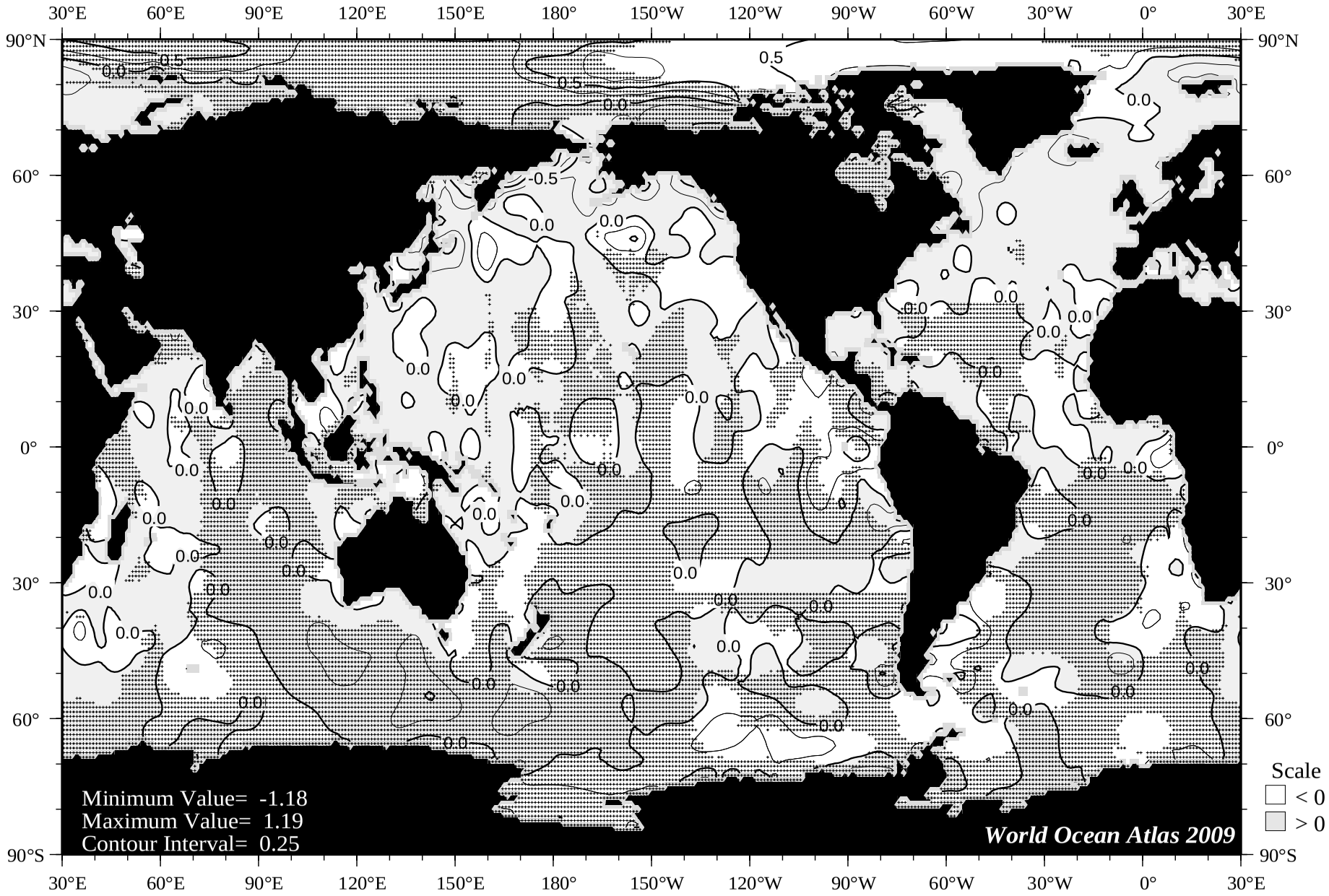

Fig C46 June minus annual phosphate [umol/l] at the surface.

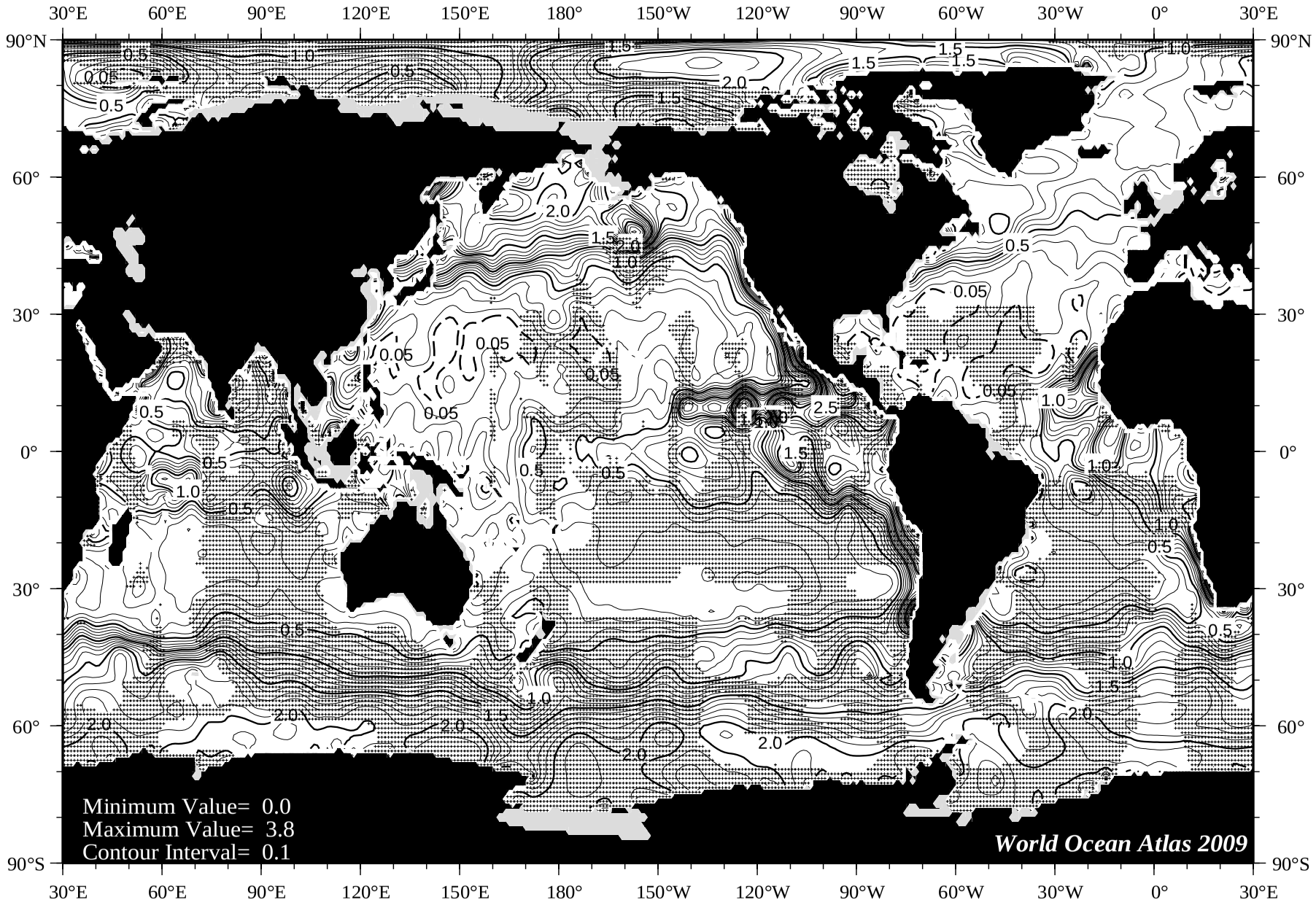

Fig C47 June mean phosphate [umol/l] at 75 m. depth.

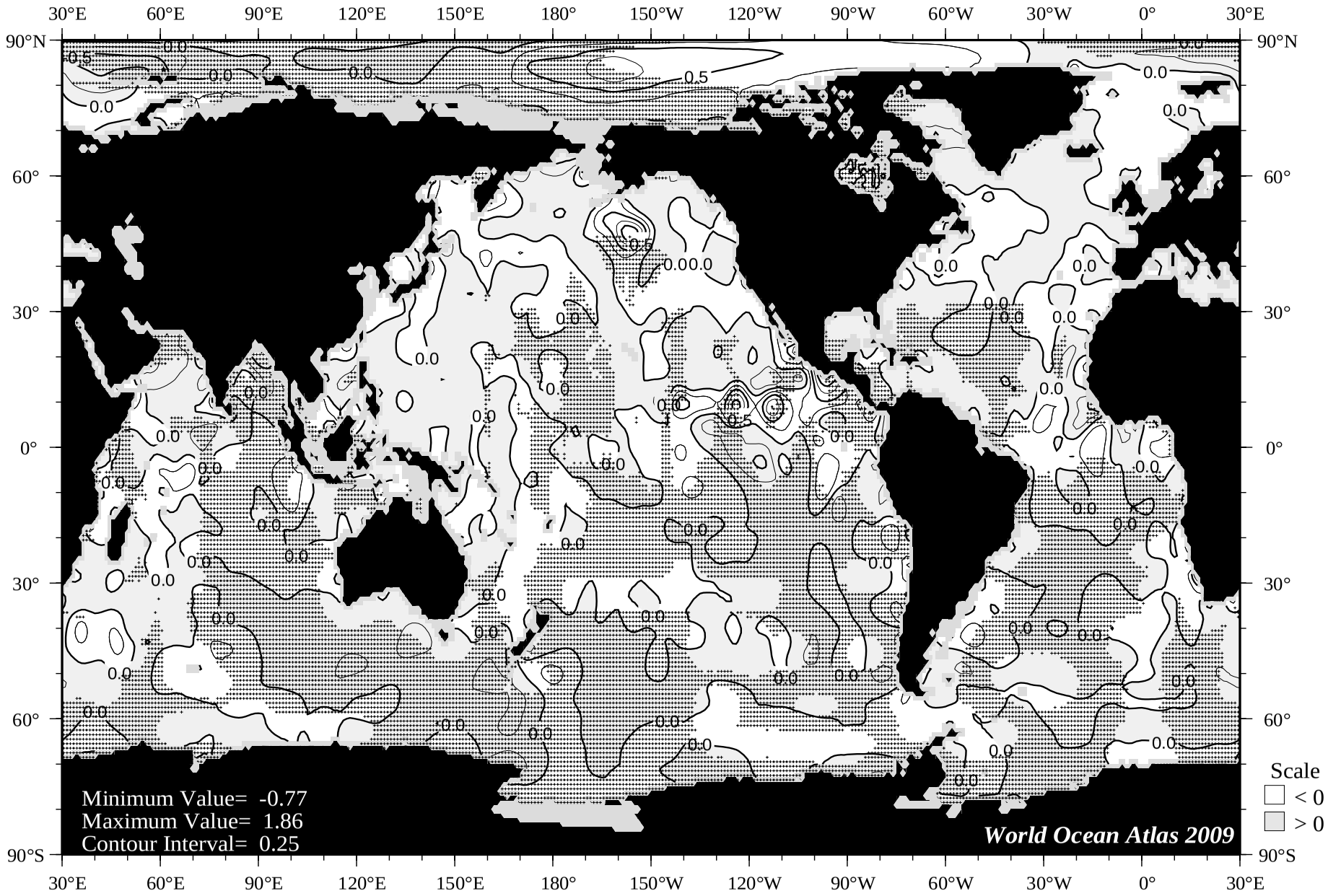

Fig C48 June minus annual phosphate [umol/l] at 75 m. depth.

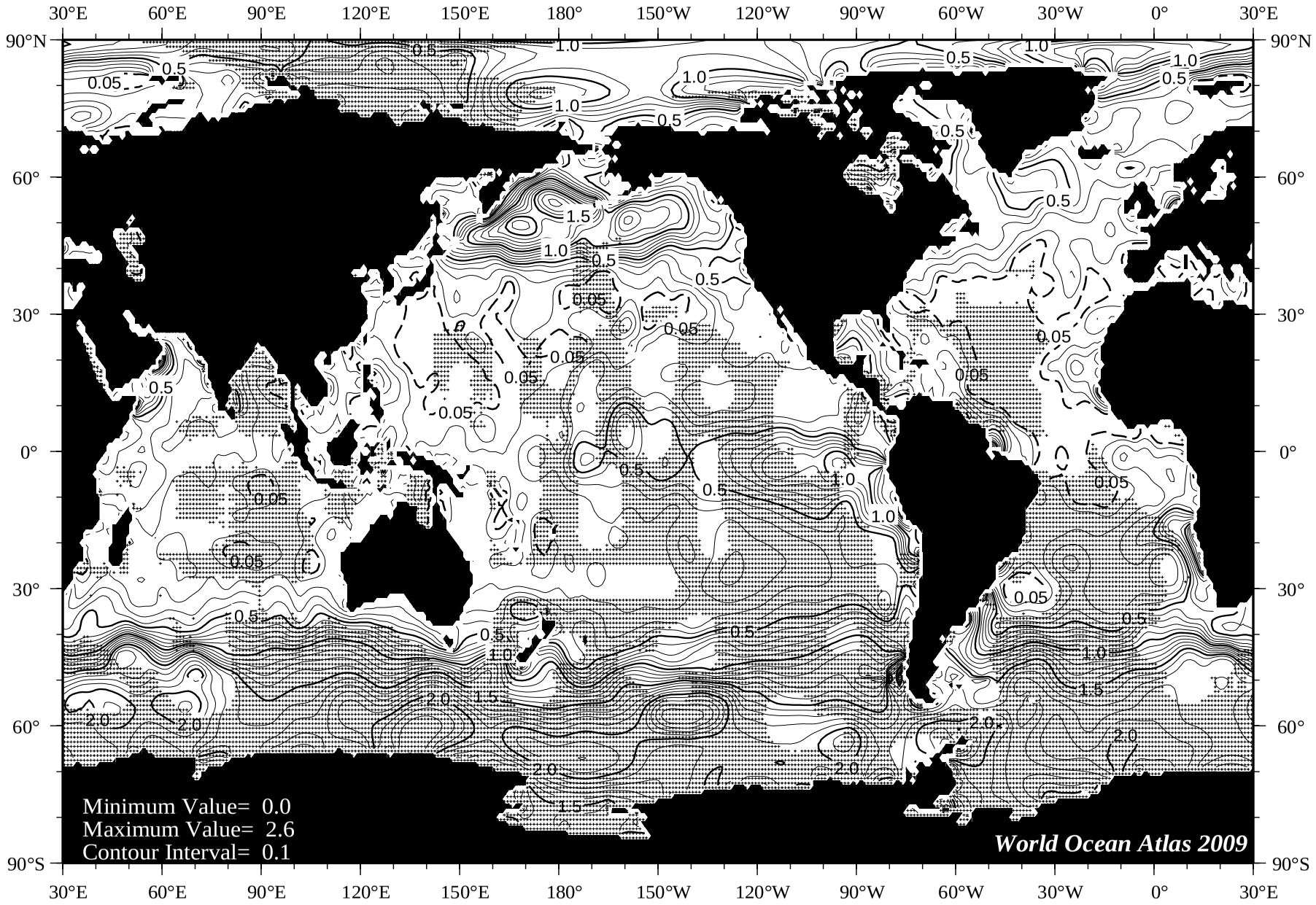

Fig C49 July mean phosphate [umol/l] at the surface.

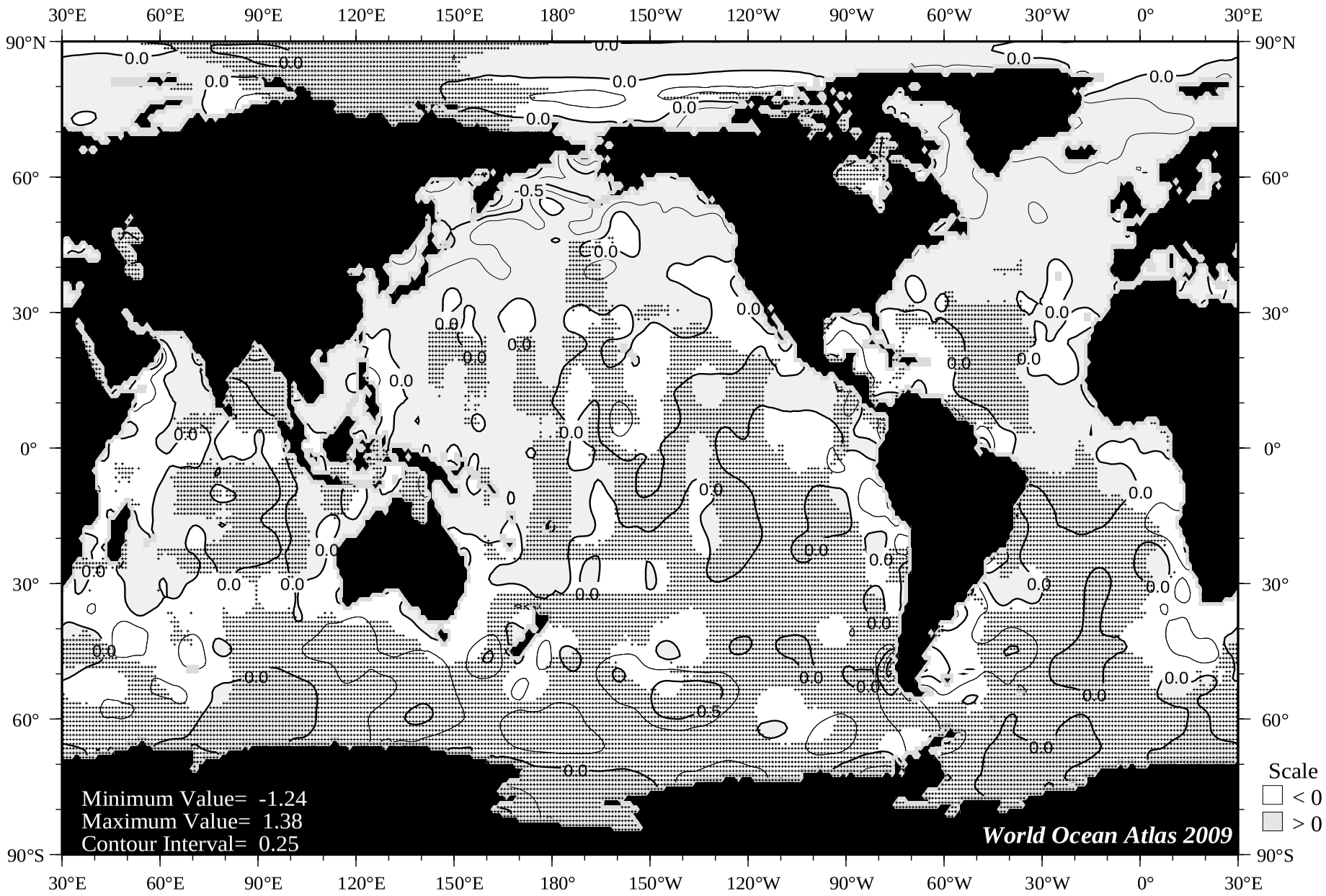

Fig C50 July minus annual phosphate [umol/l] at the surface.

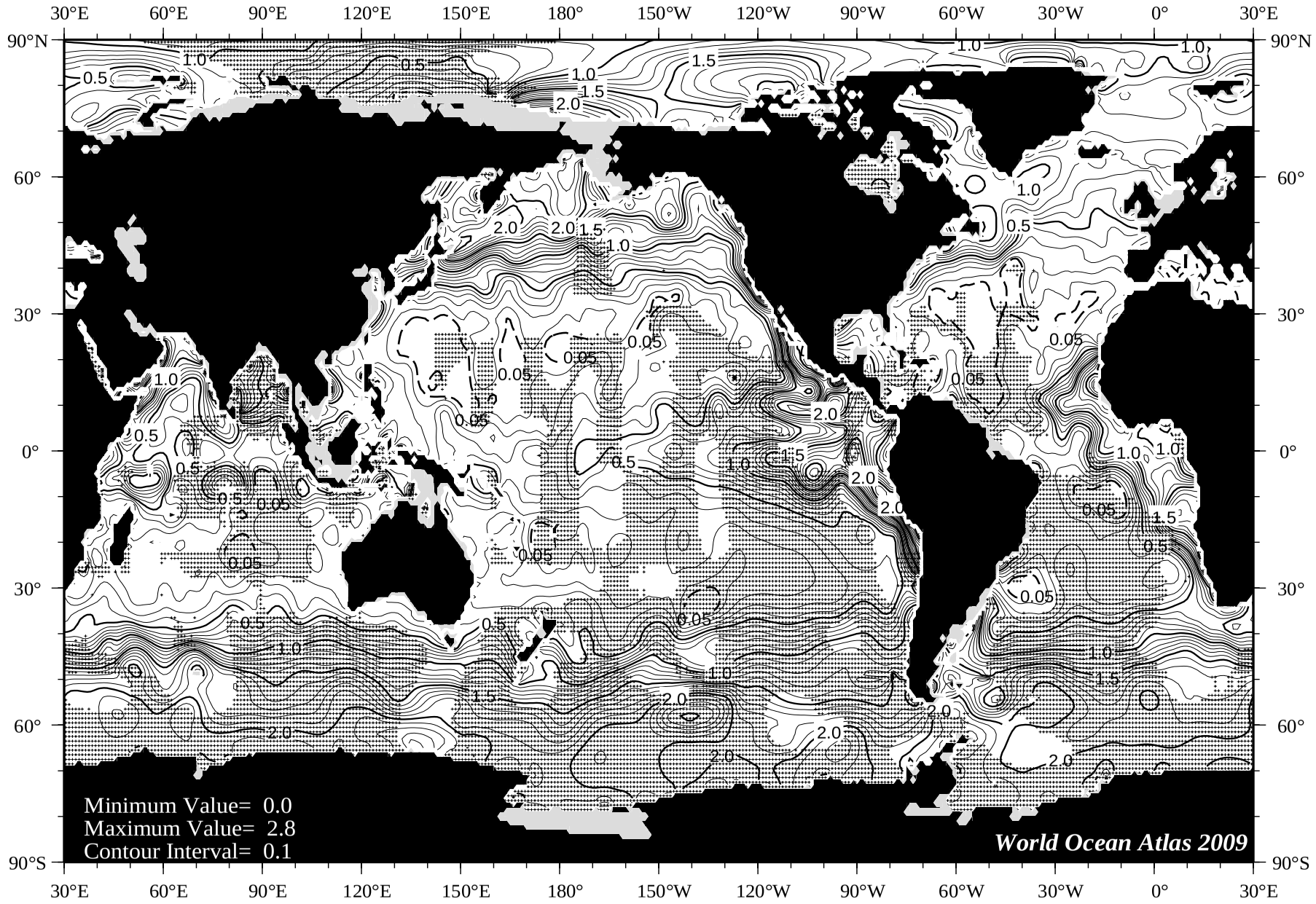

Fig C51 July mean phosphate [umol/l] at 75 m. depth.

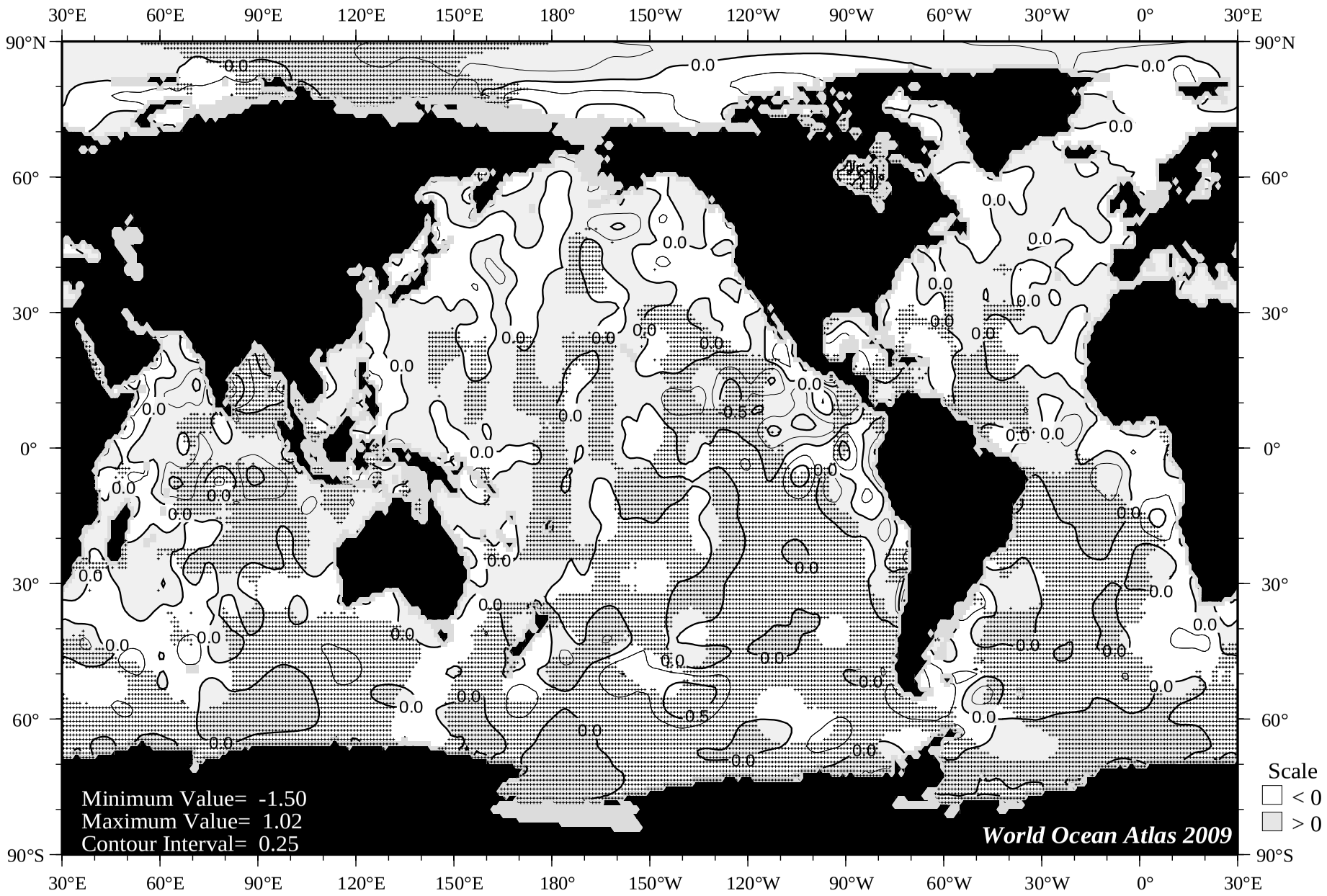

Fig C52 July minus annual phosphate [umol/l] at 75 m. depth.

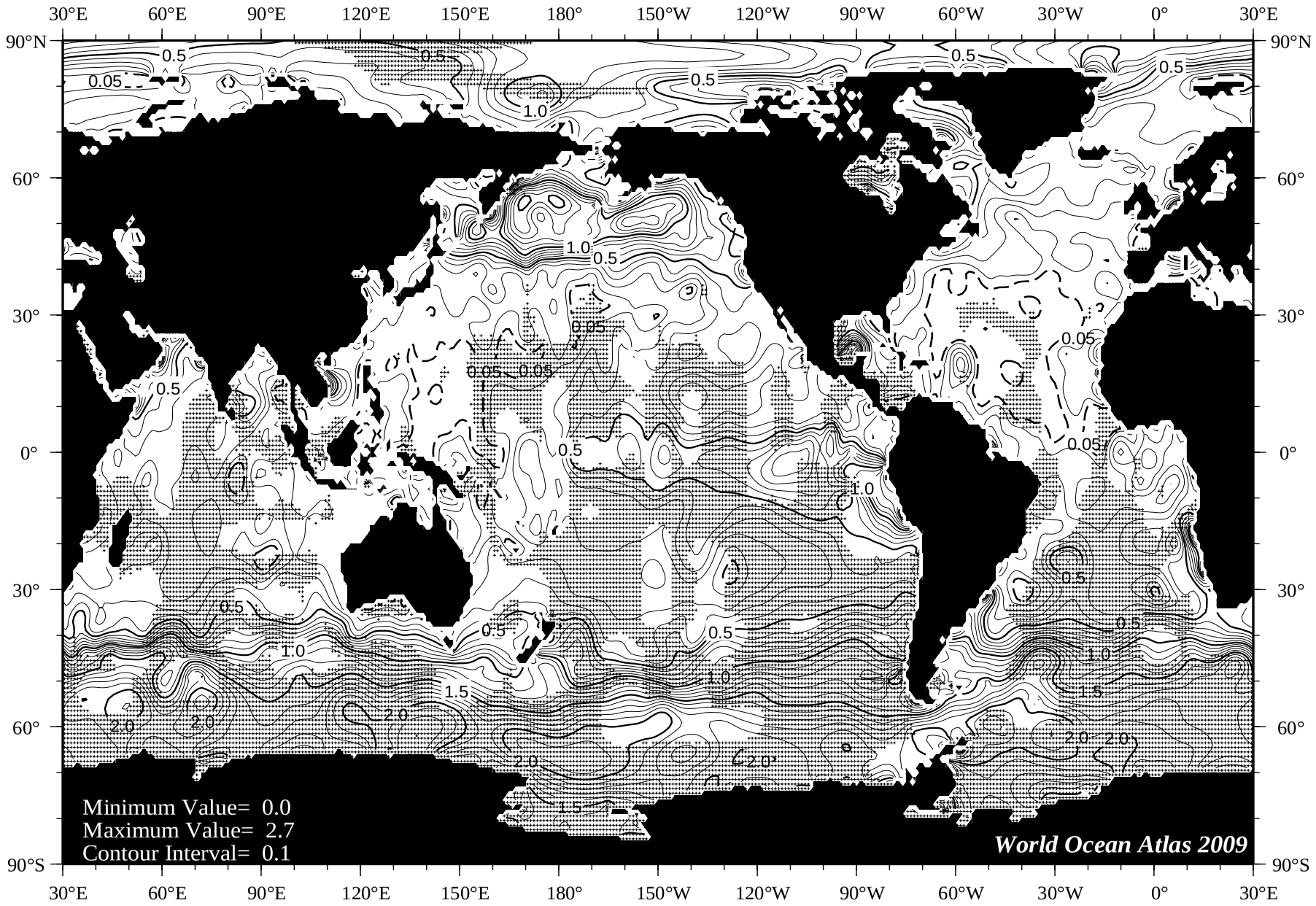

Fig C53 August mean phosphate [umol/l] at the surface.

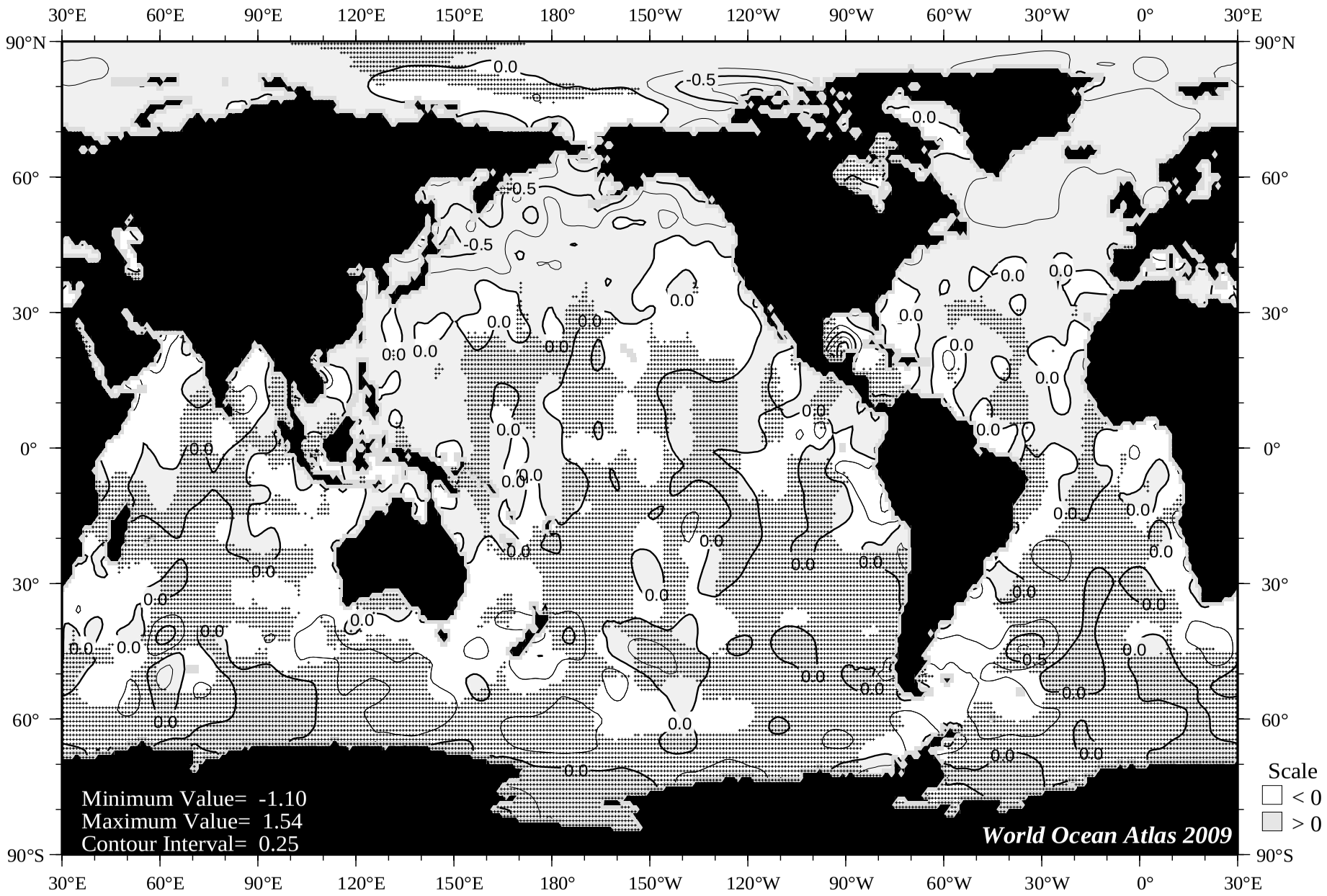

Fig C54 August minus annual phosphate [umol/l] at the surface.

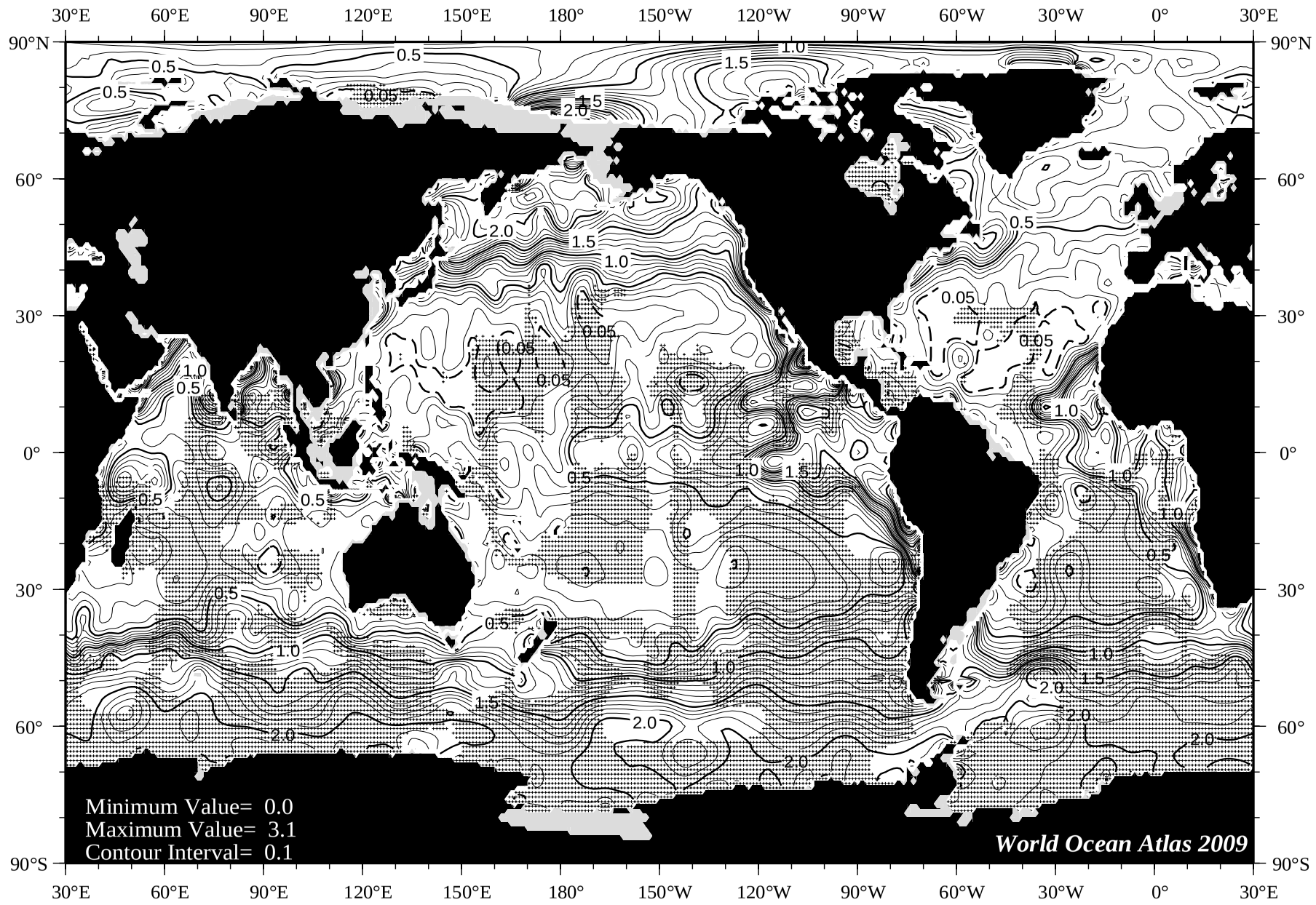

Fig C55 August mean phosphate [umol/l] at 75 m. depth.

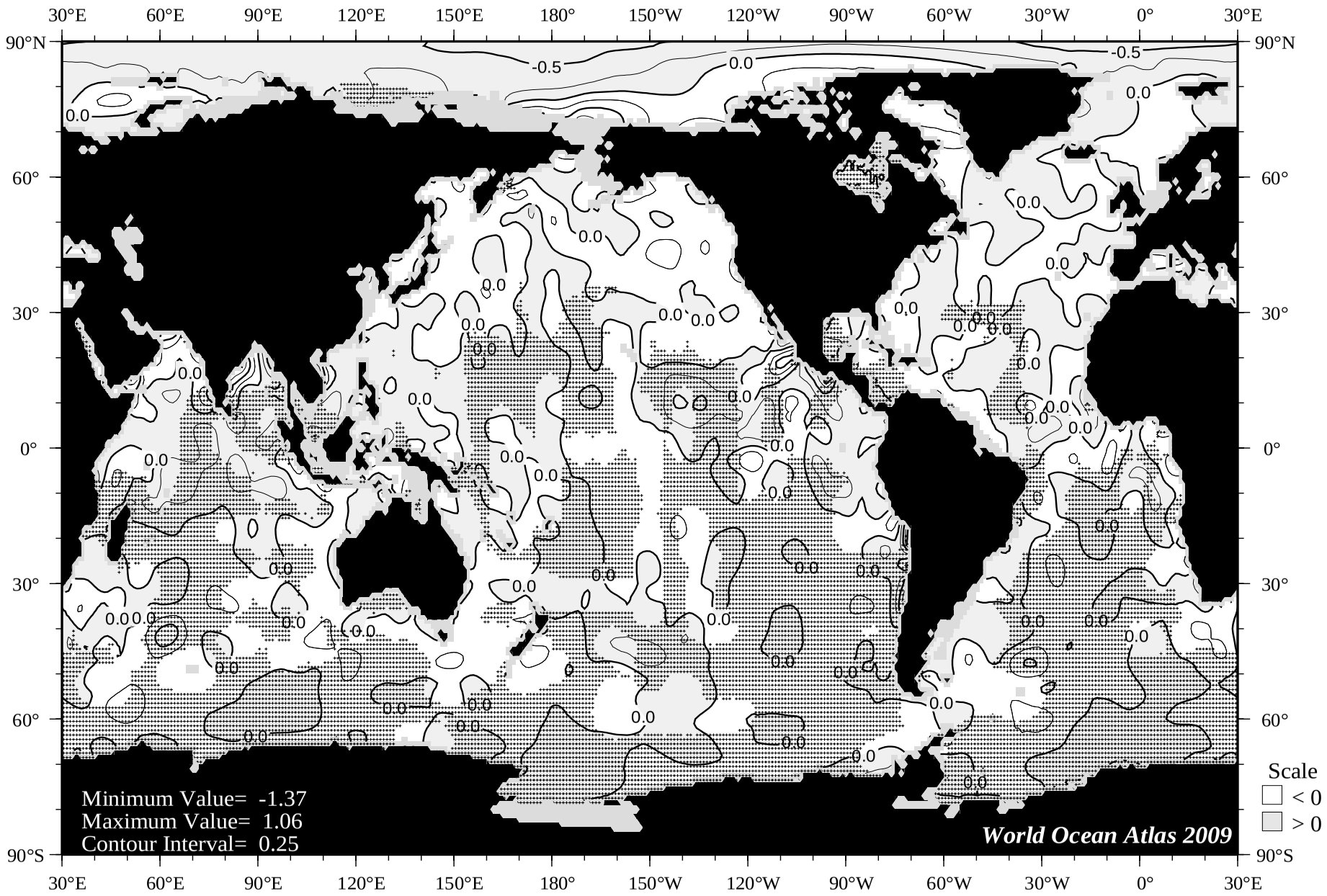

Fig C56 August minus annual phosphate [umol/l] at 75 m. depth.

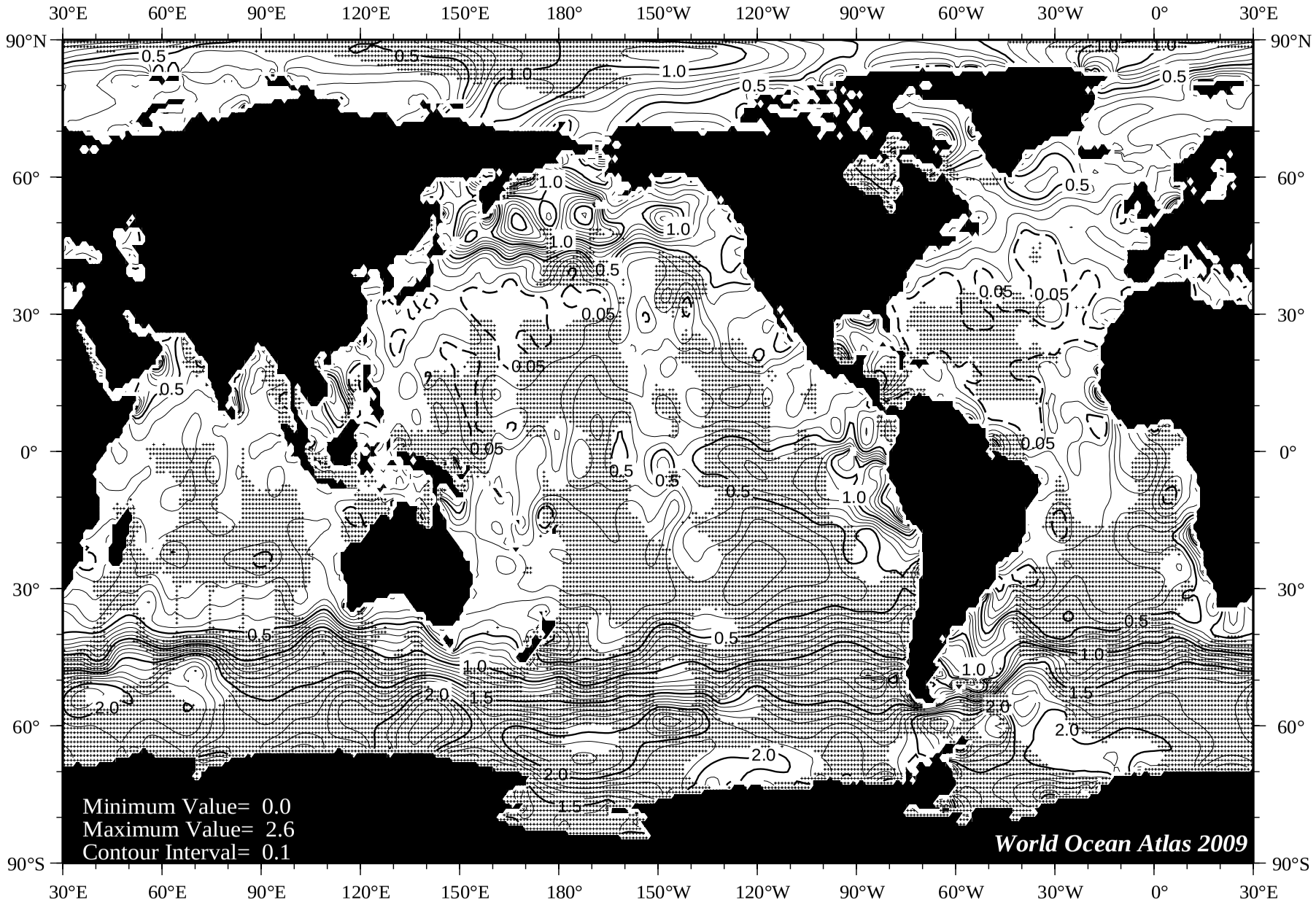

Fig C57 September mean phosphate [umol/l] at the surface.

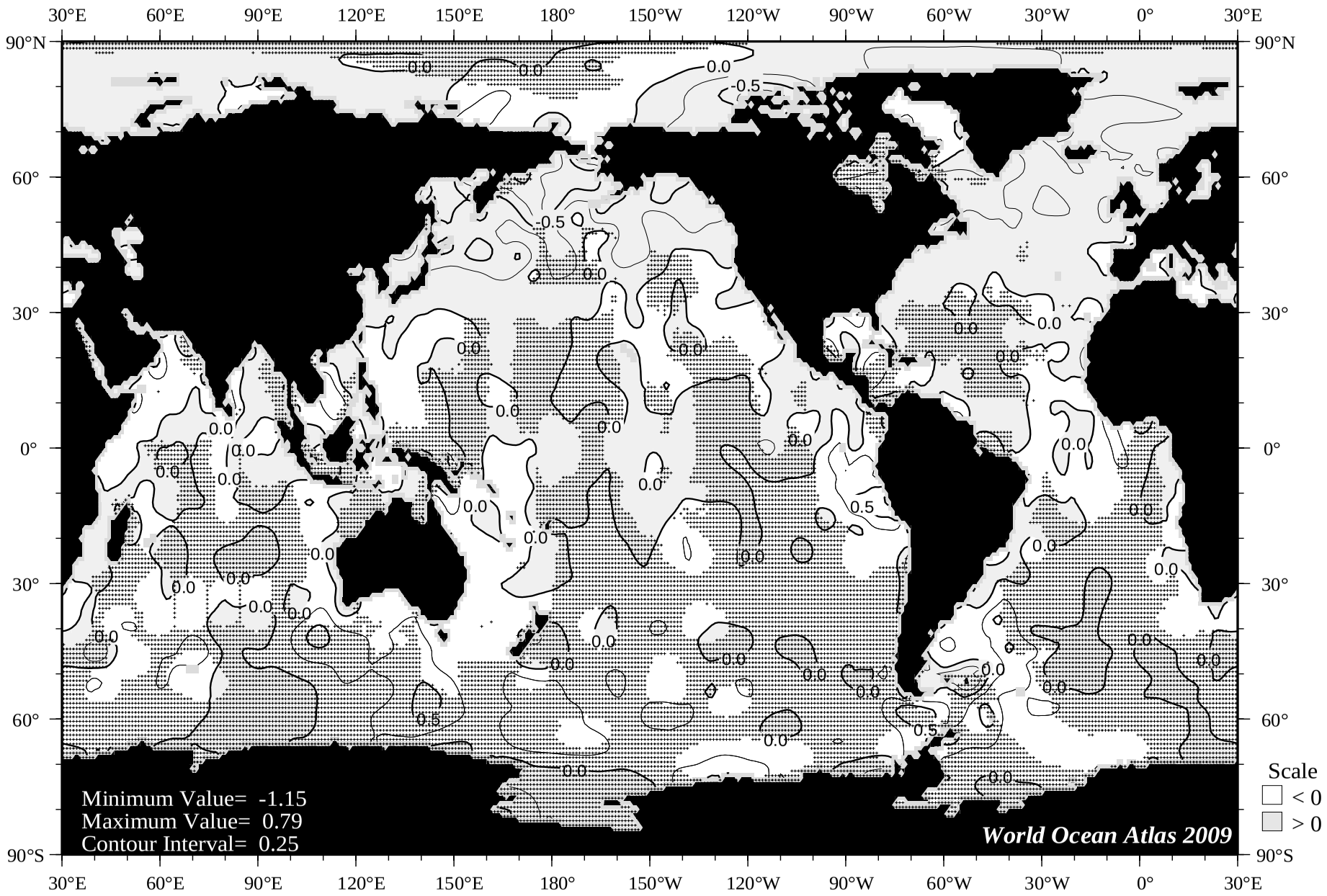

Fig C58 September minus annual phosphate [umol/l] at the surface.

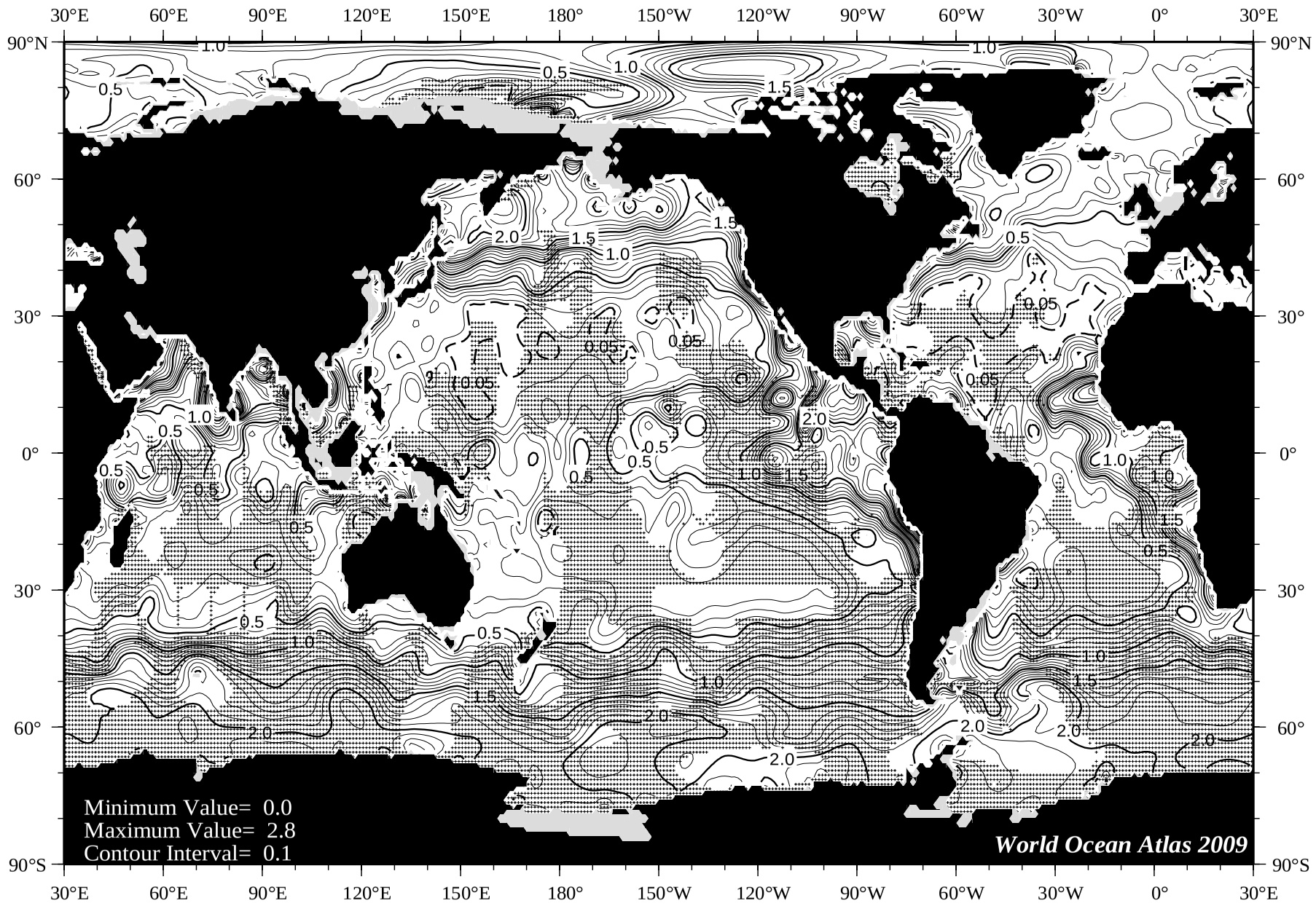

Fig C59 September mean phosphate [umol/l] at 75 m. depth.

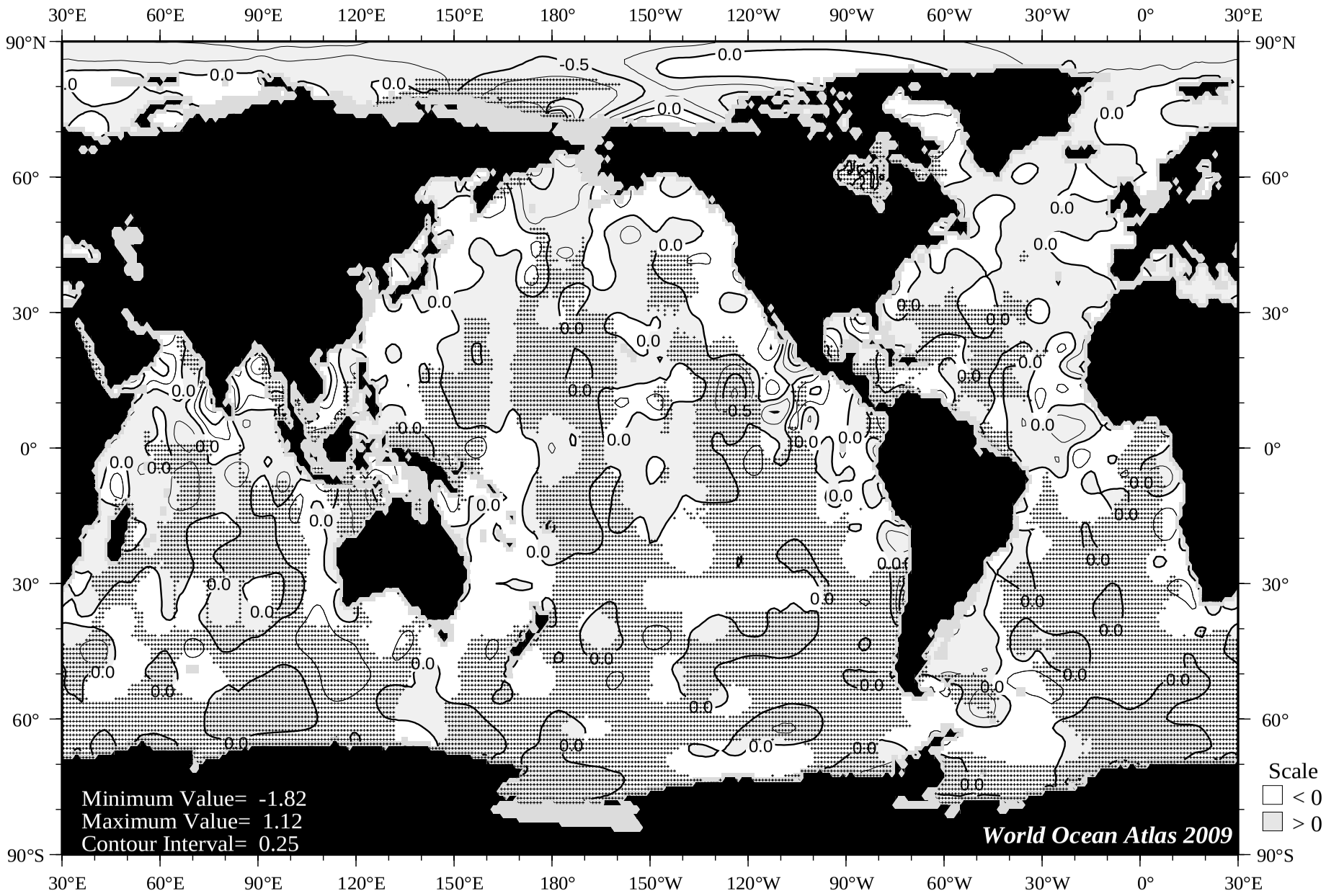

Fig C60 September minus annual phosphate [umol/l] at 75 m. depth.

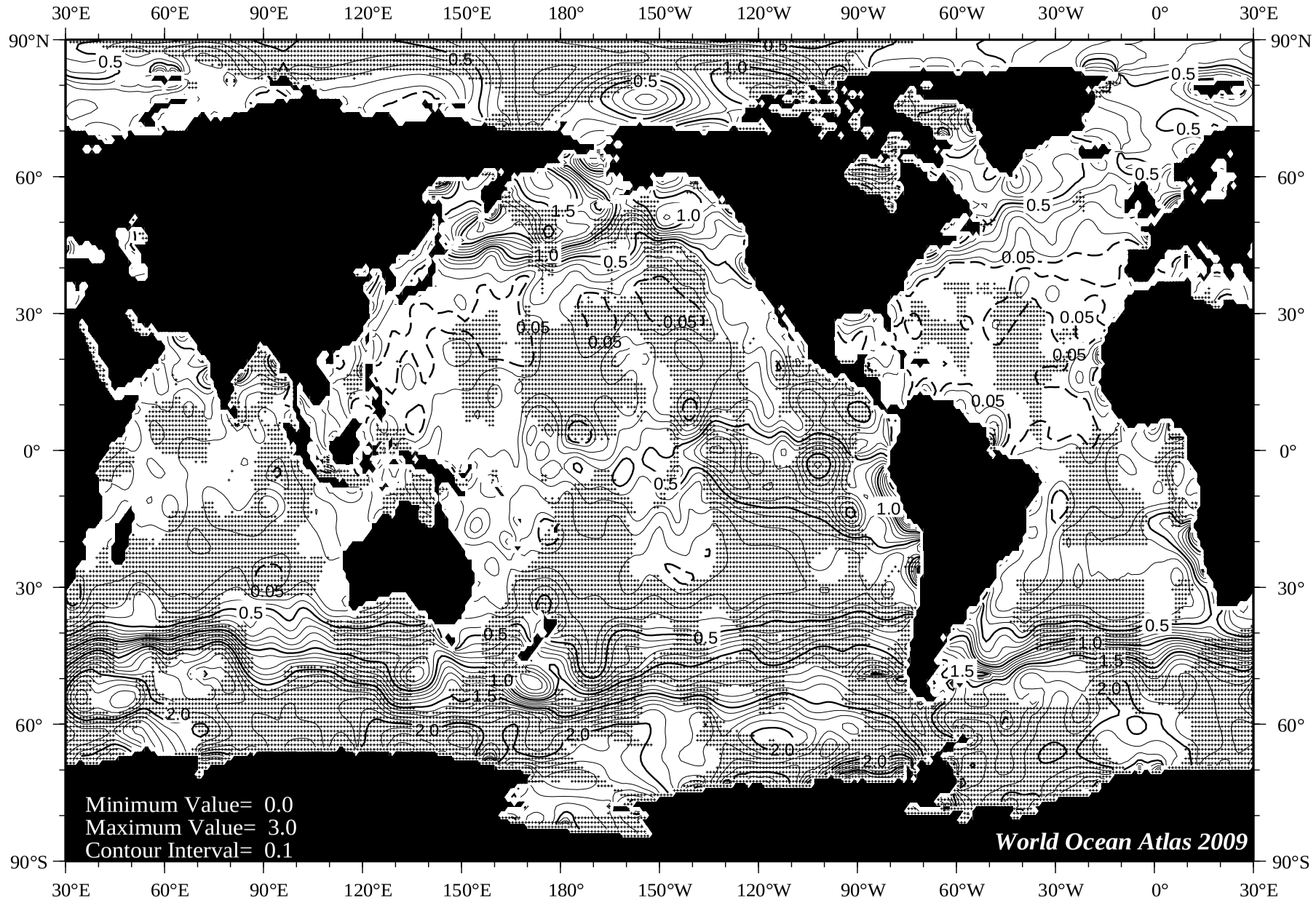

Fig C61 October mean phosphate [umol/l] at the surface.

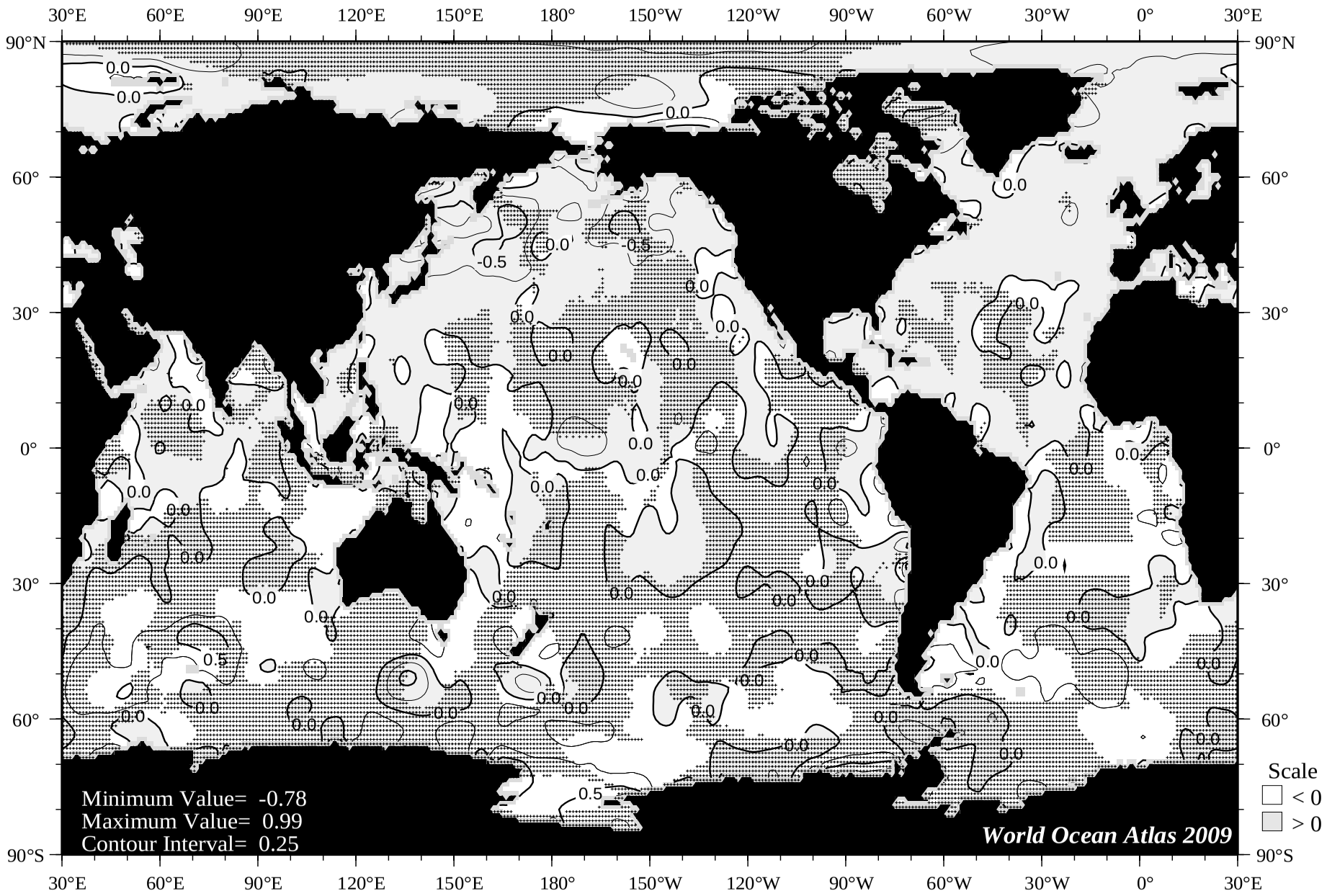

Fig C62 October minus annual phosphate [umol/l] at the surface.

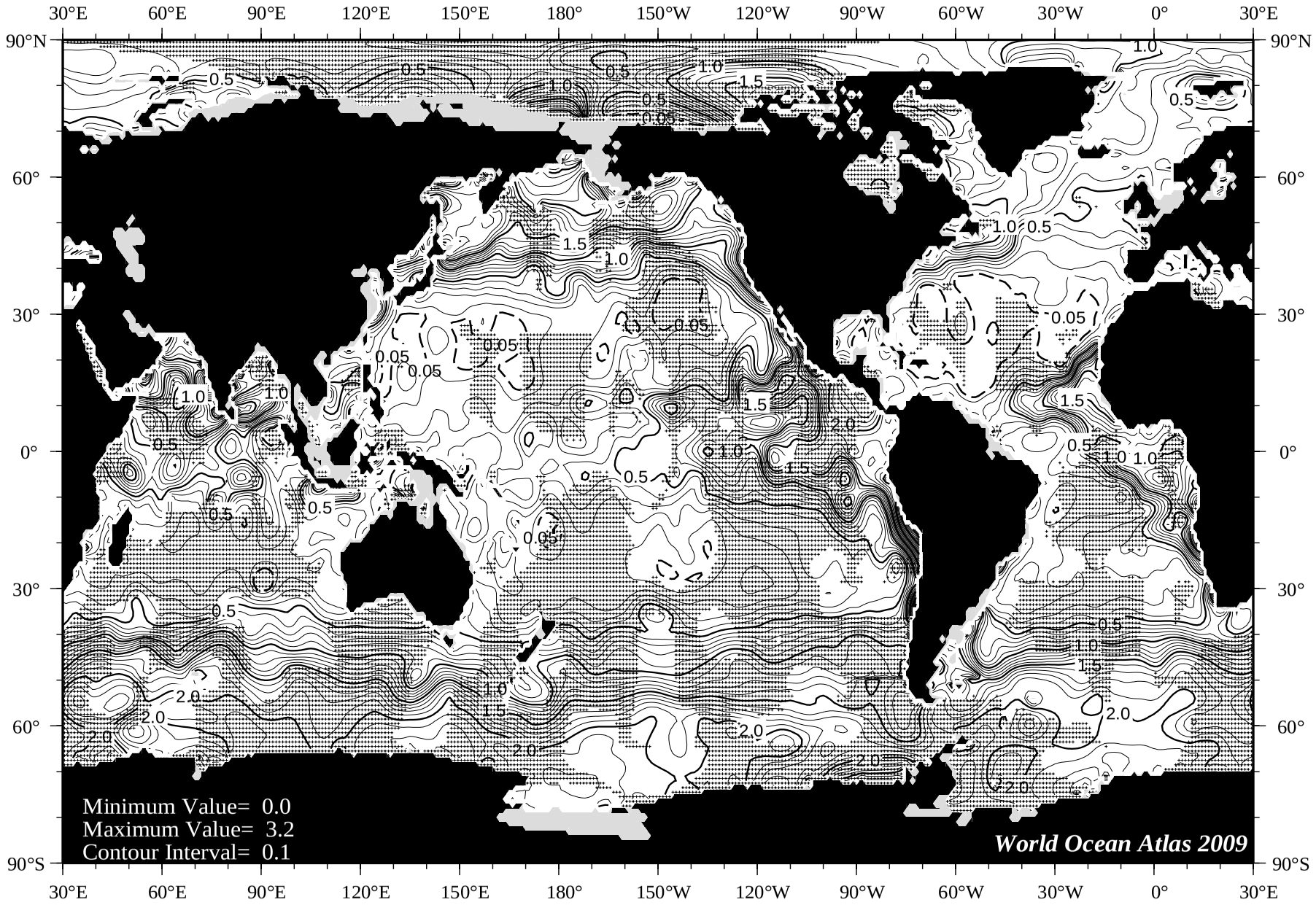

Fig C63 October mean phosphate [umol/l] at 75 m. depth.

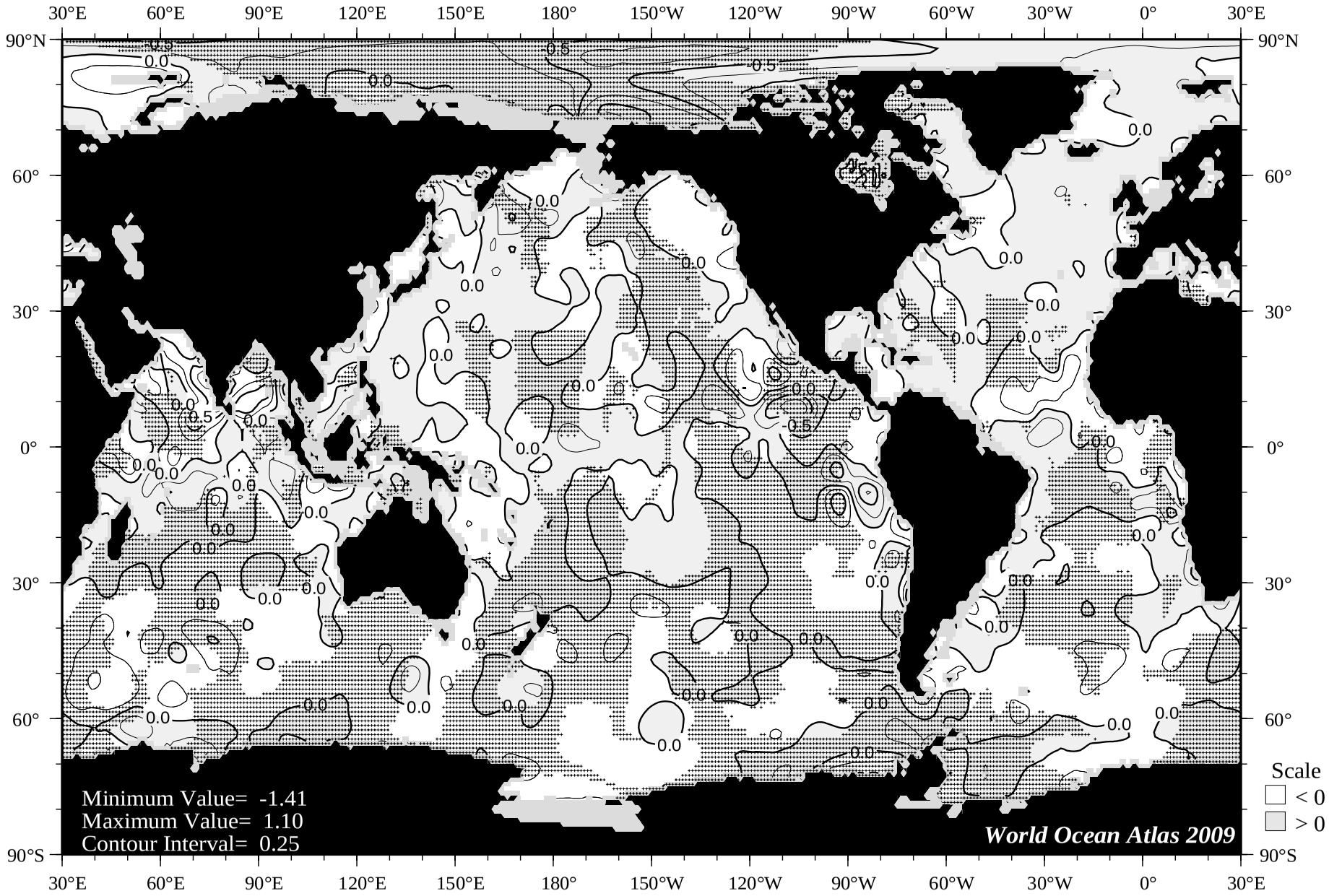

Fig C64 October minus annual phosphate [umol/l] at 75 m. depth.

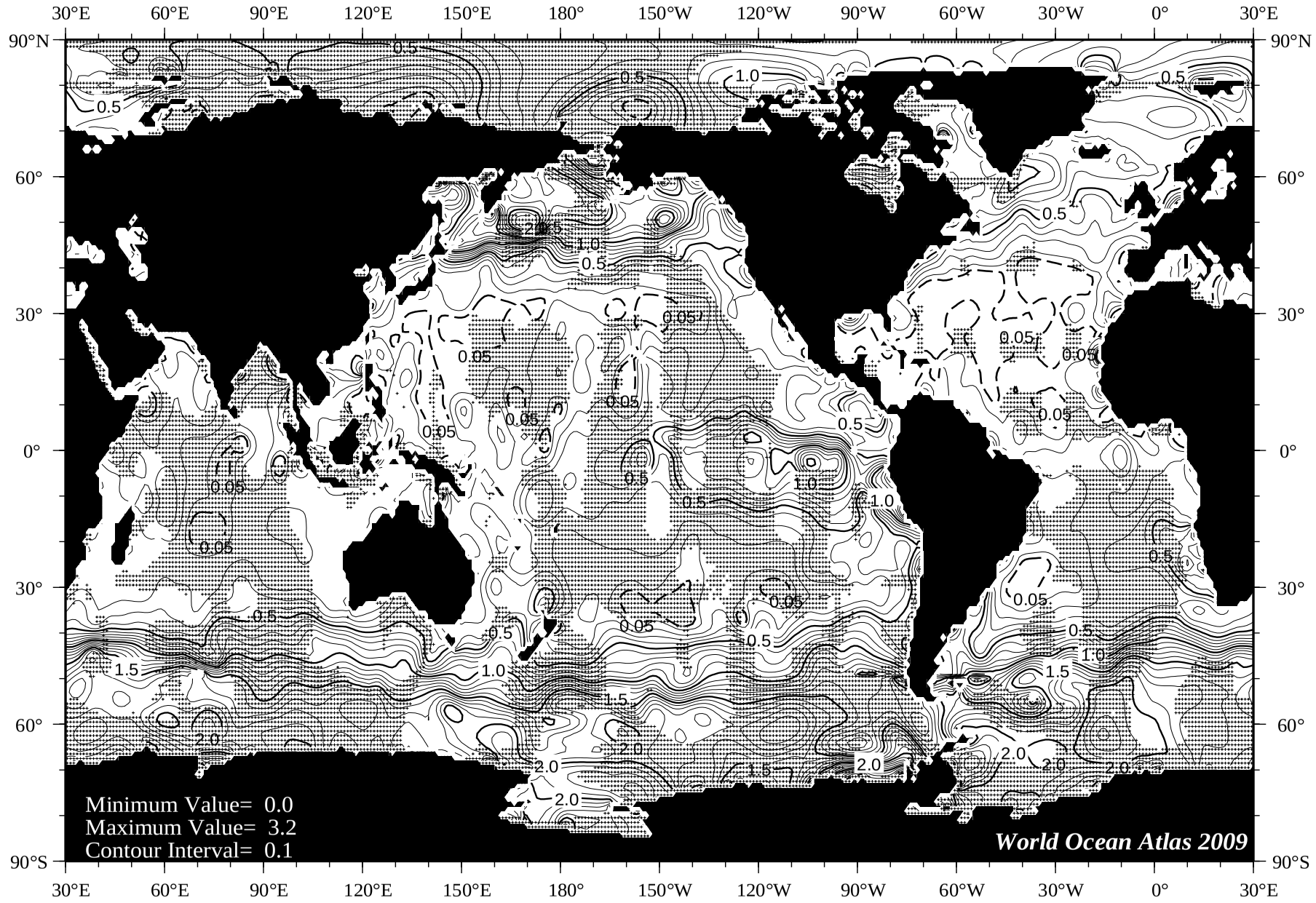

Fig C65 November mean phosphate [umol/l] at the surface.

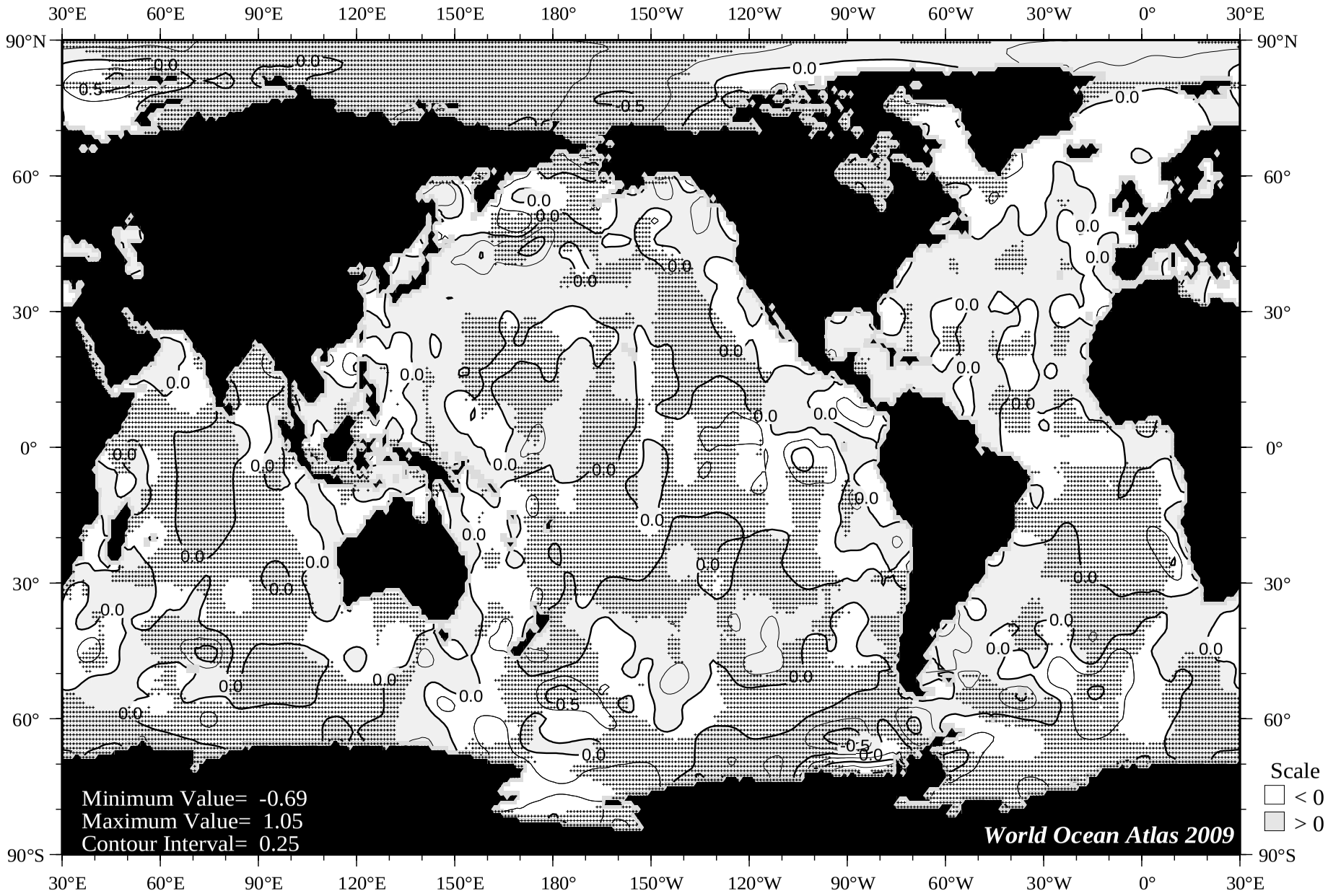

Fig C66 November minus annual phosphate [umol/l] at the surface.

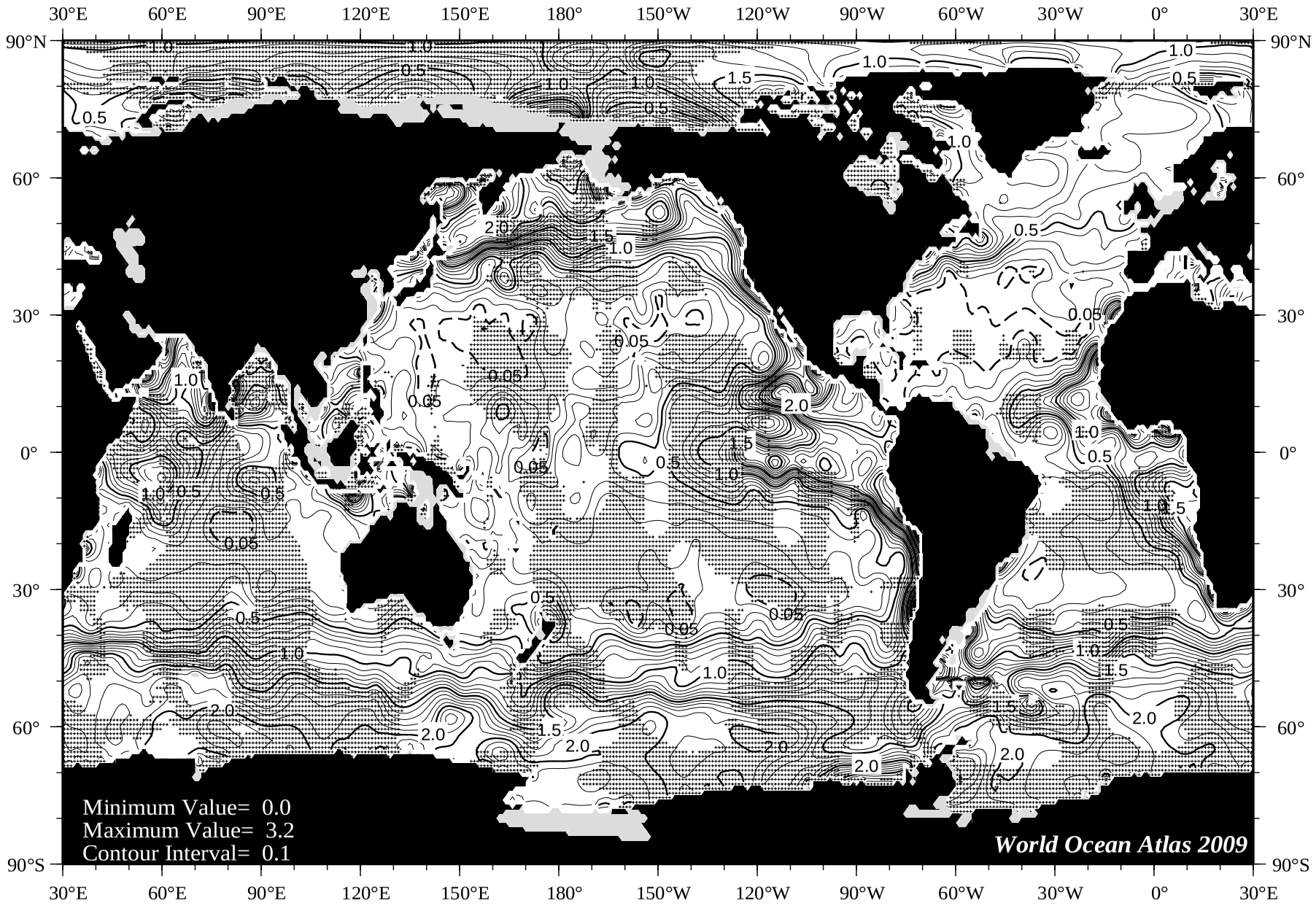

Fig C67 November mean phosphate [umol/l] at 75 m. depth.

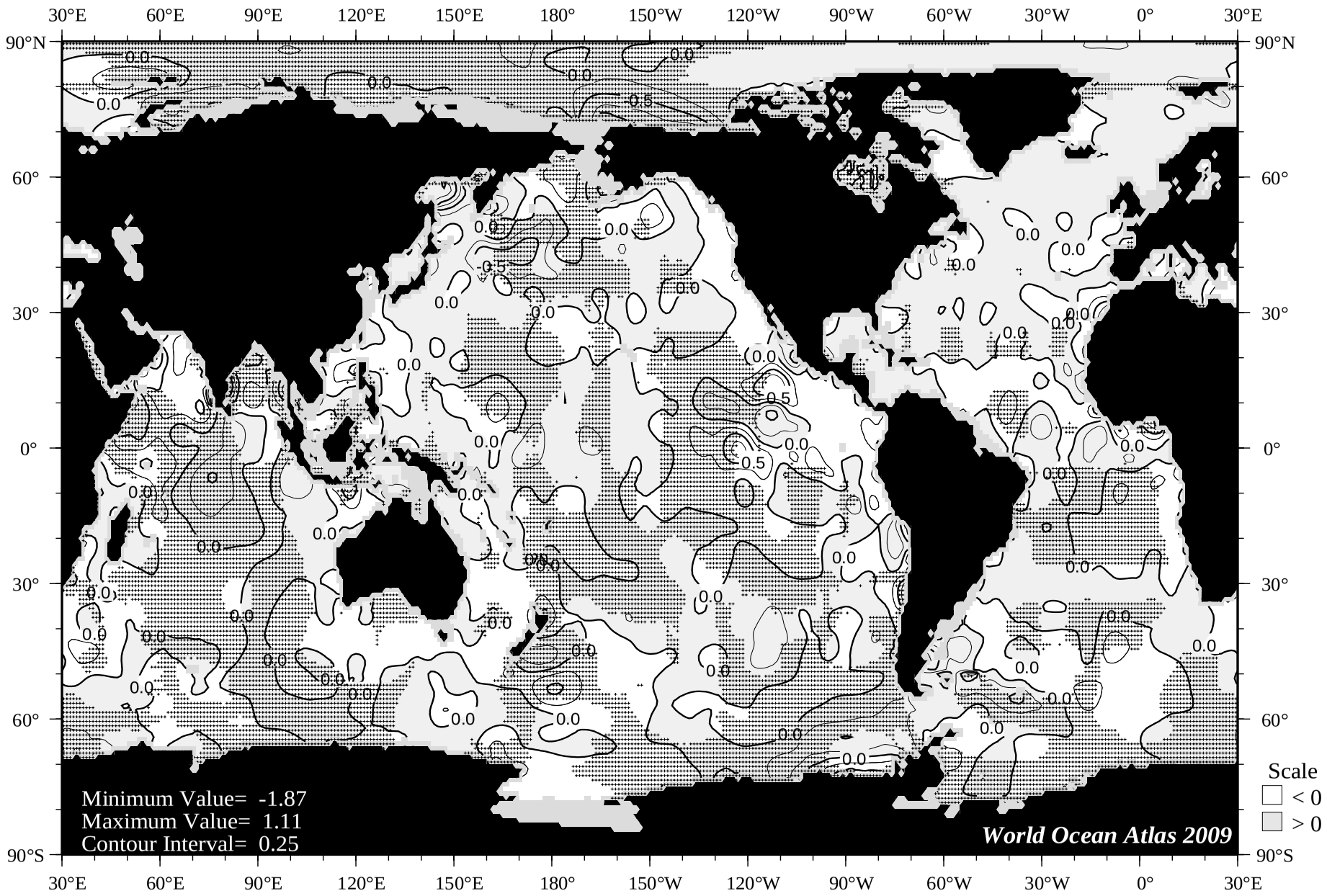

Fig C68 November minus annual phosphate [umol/l] at 75 m. depth.

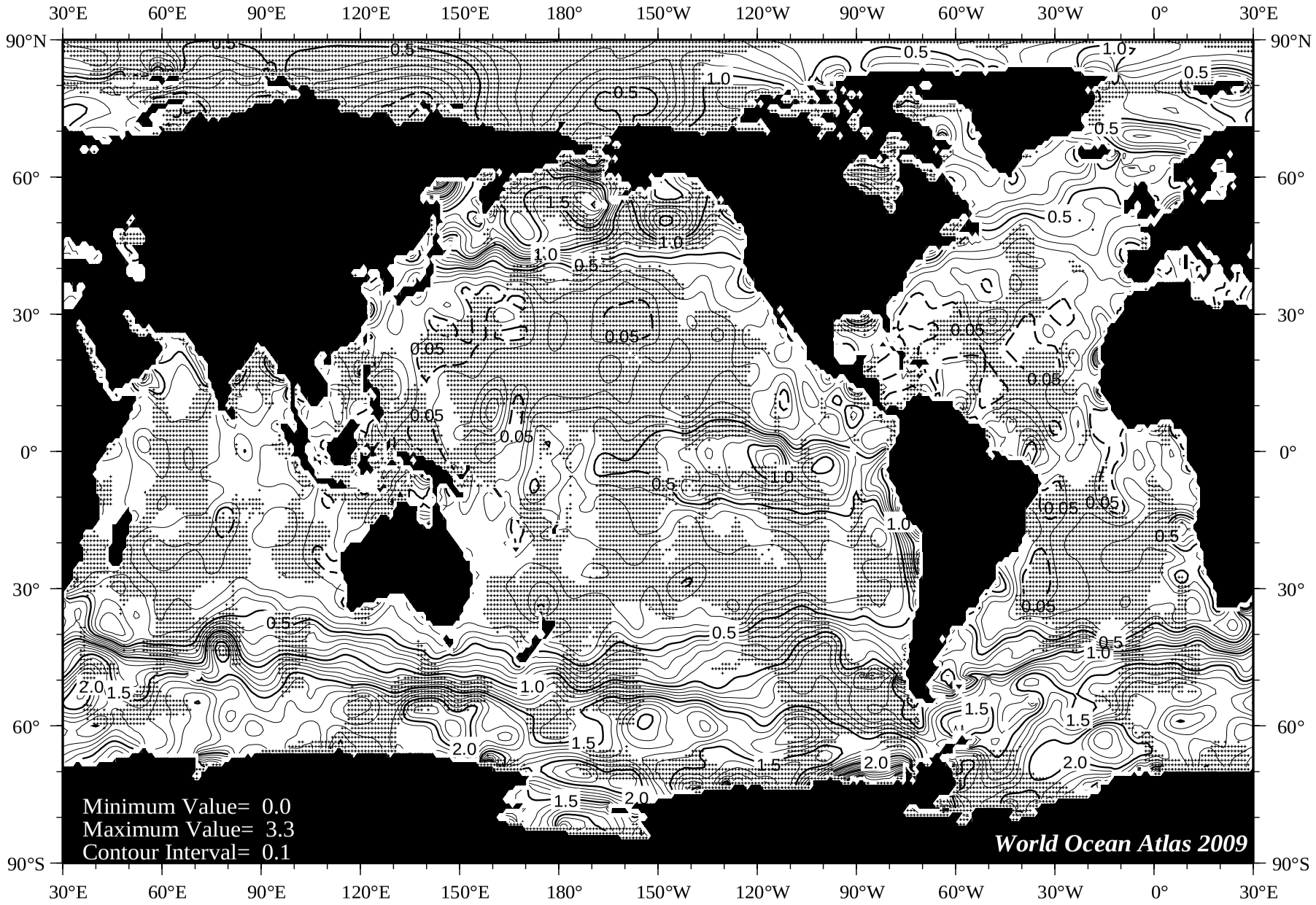

Fig C69 December mean phosphate [umol/l] at the surface.

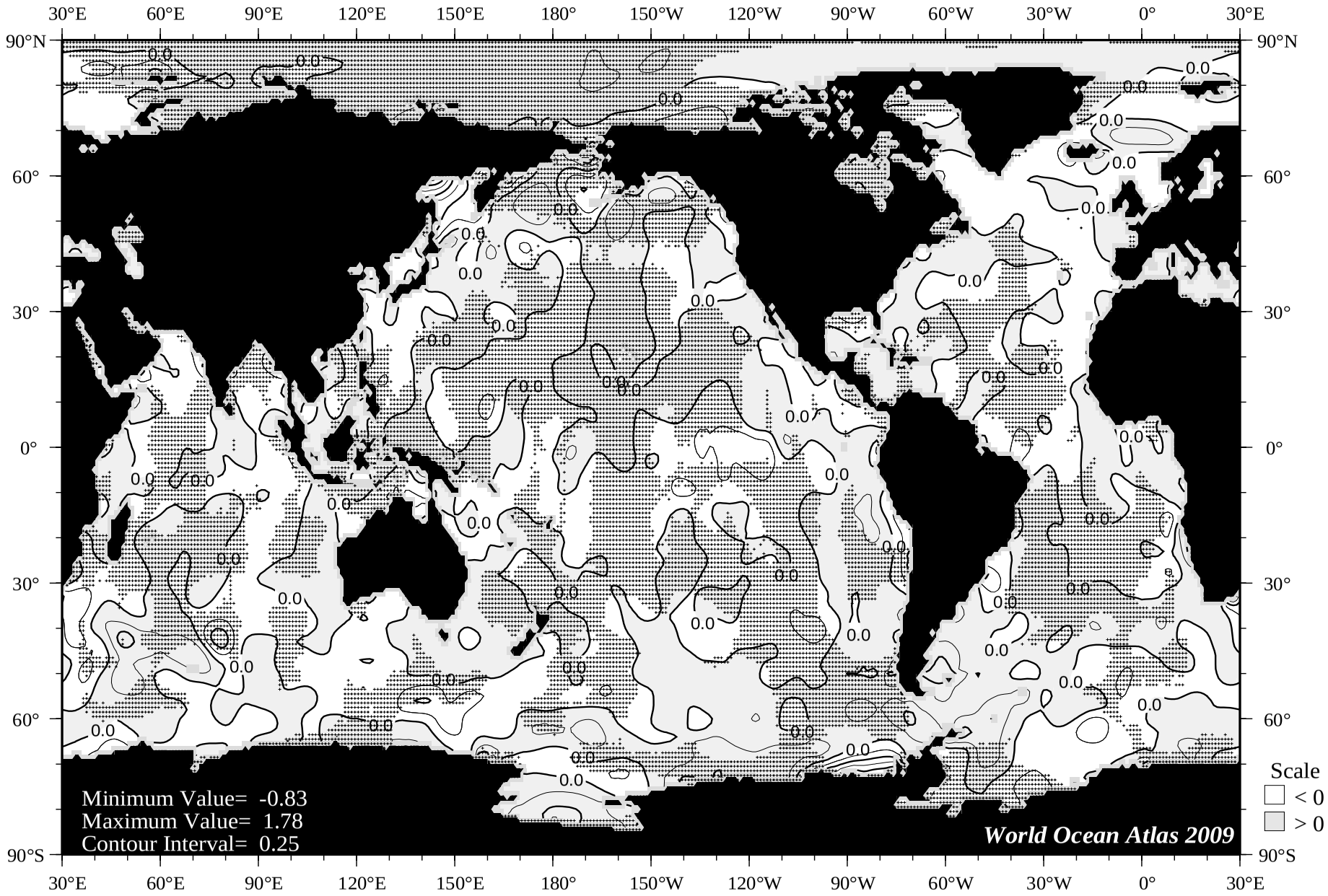

Fig C70 December minus annual phosphate [umol/l] at the surface.

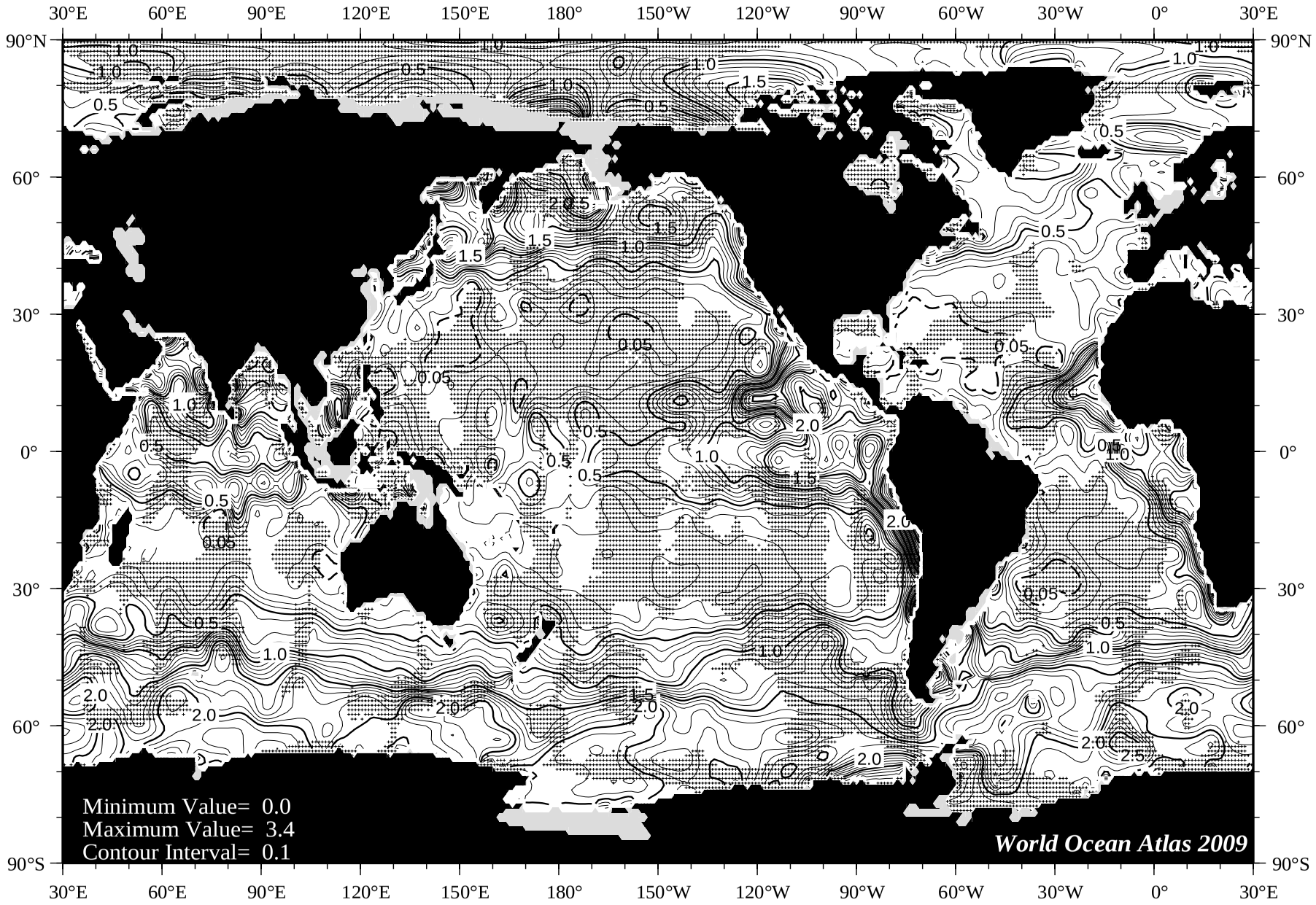

Fig C71 December mean phosphate [umol/l] at 75 m. depth.

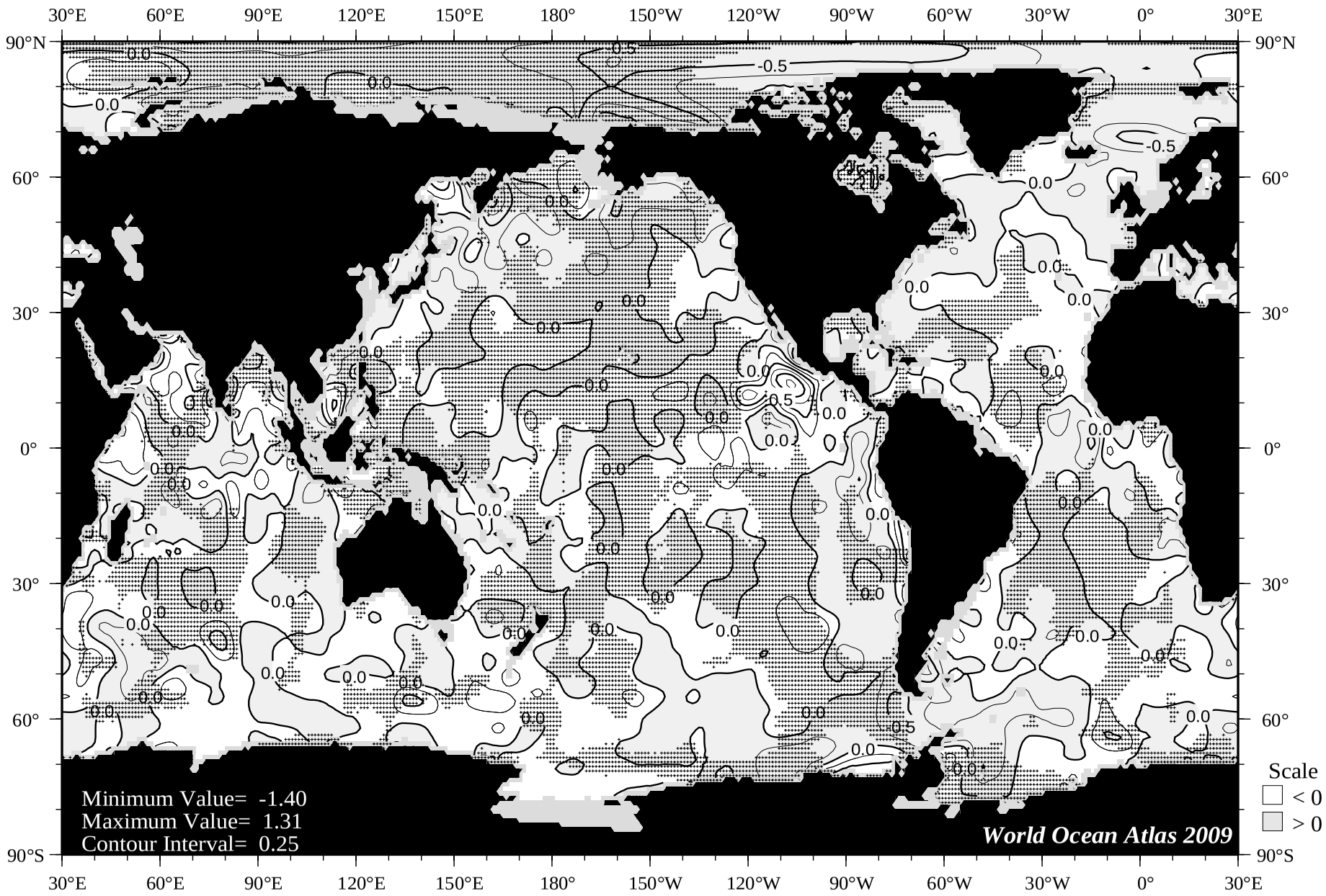

Fig C72 December minus annual phosphate [umol/l] at 75 m. depth.

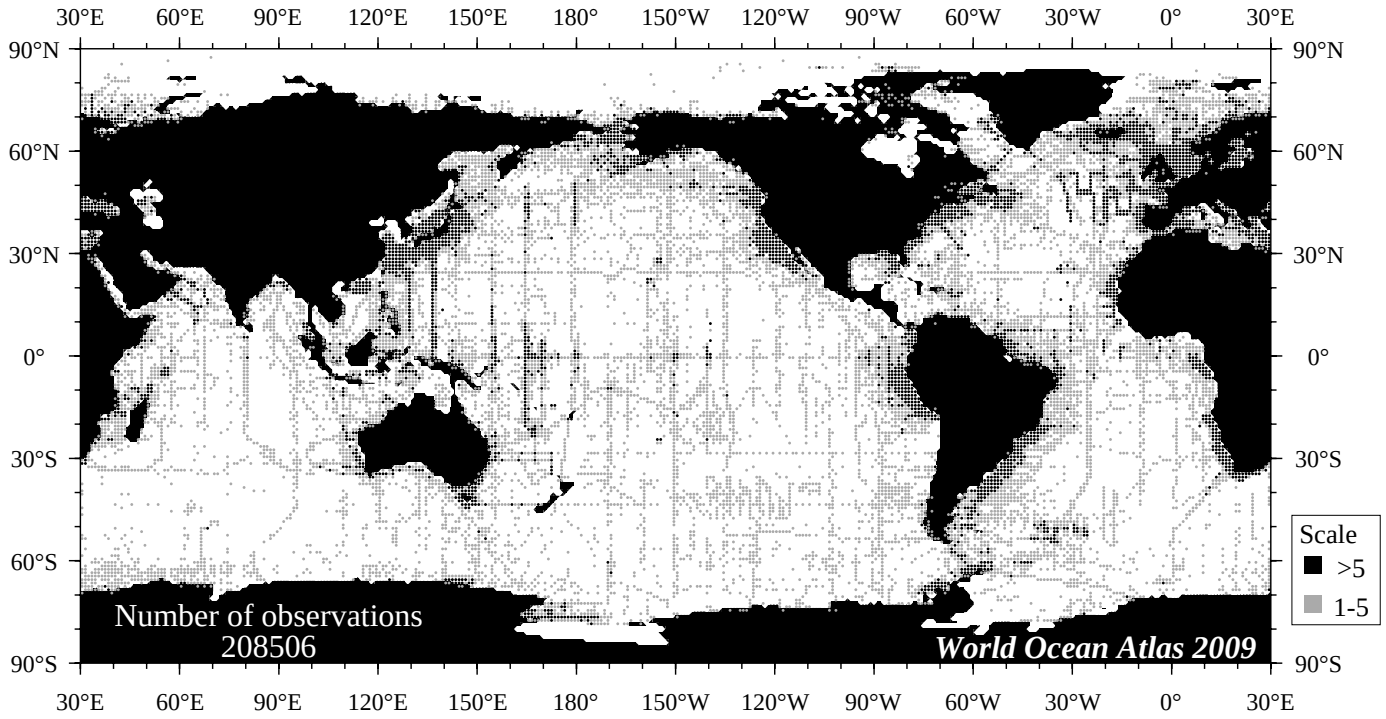

Fig D1 Annual nitrate observations at the surface.

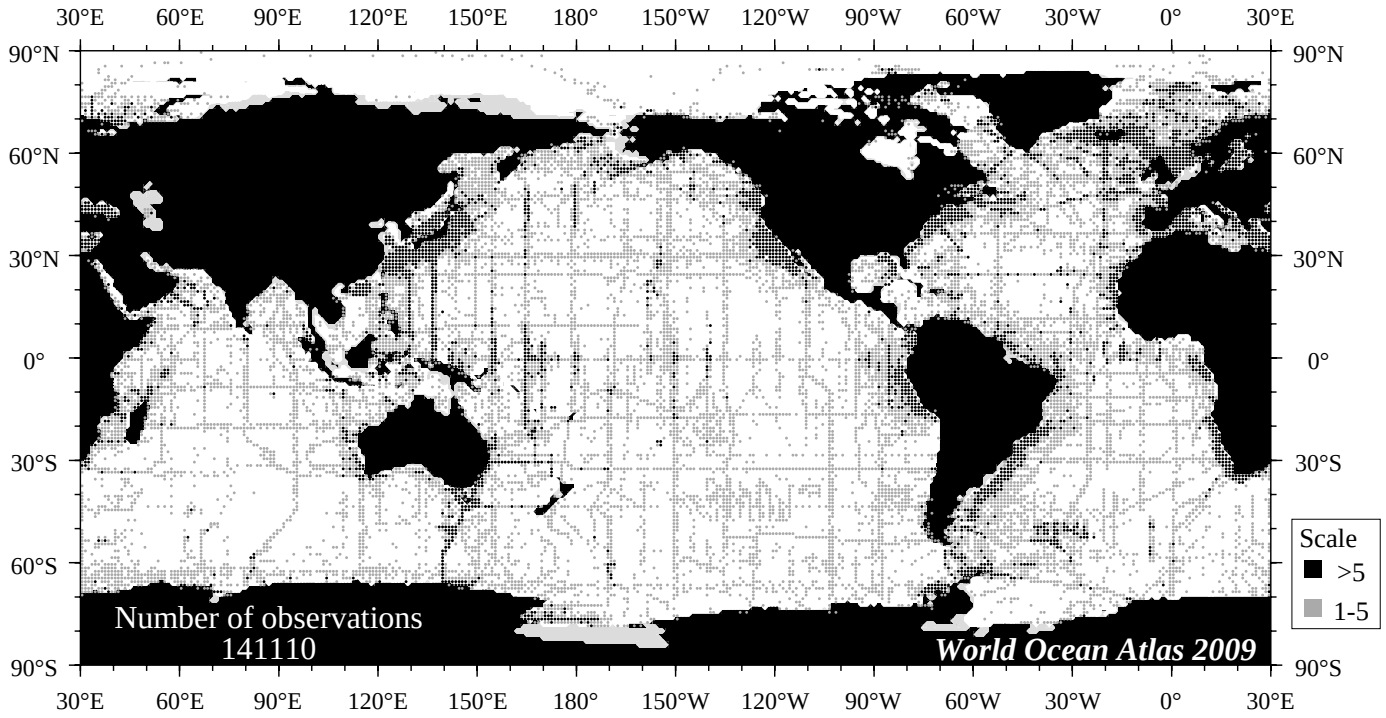

Fig D2 Annual nitrate observations at 50 m. depth.

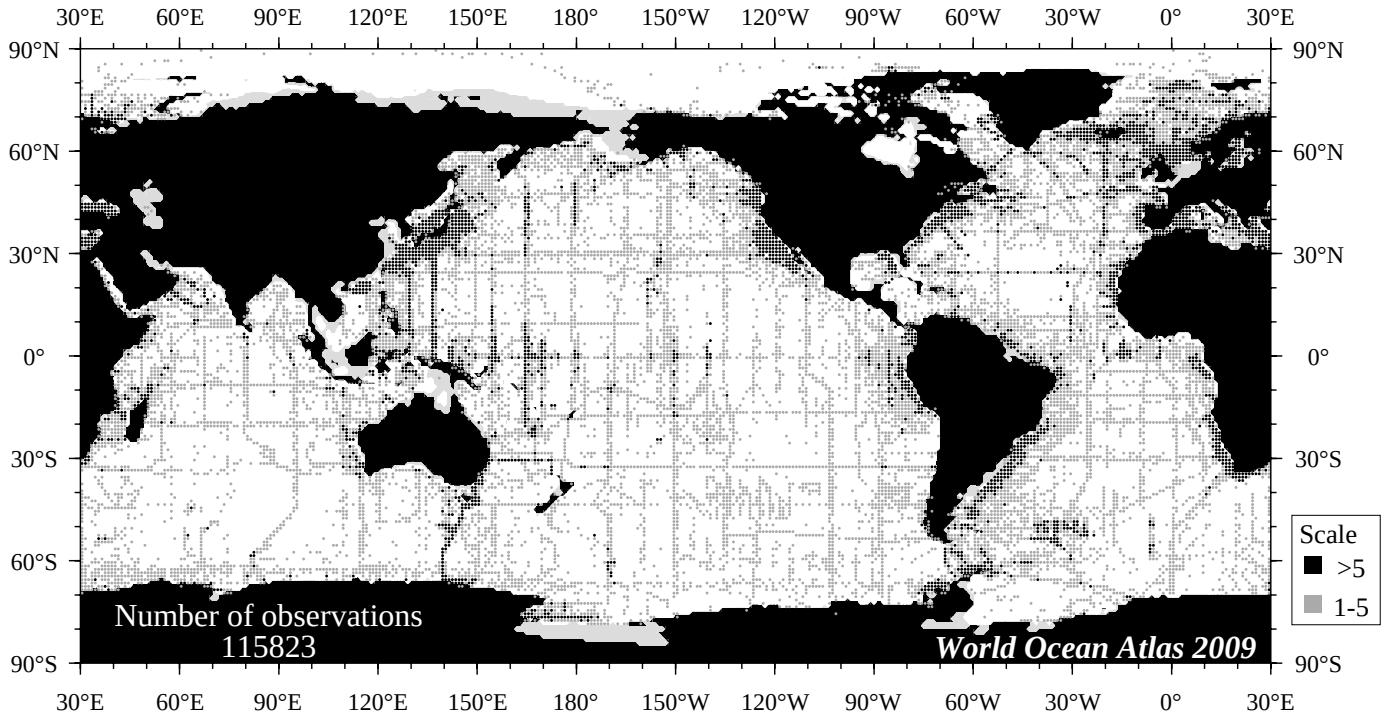

Fig D3 Annual nitrate observations at 75 m. depth.

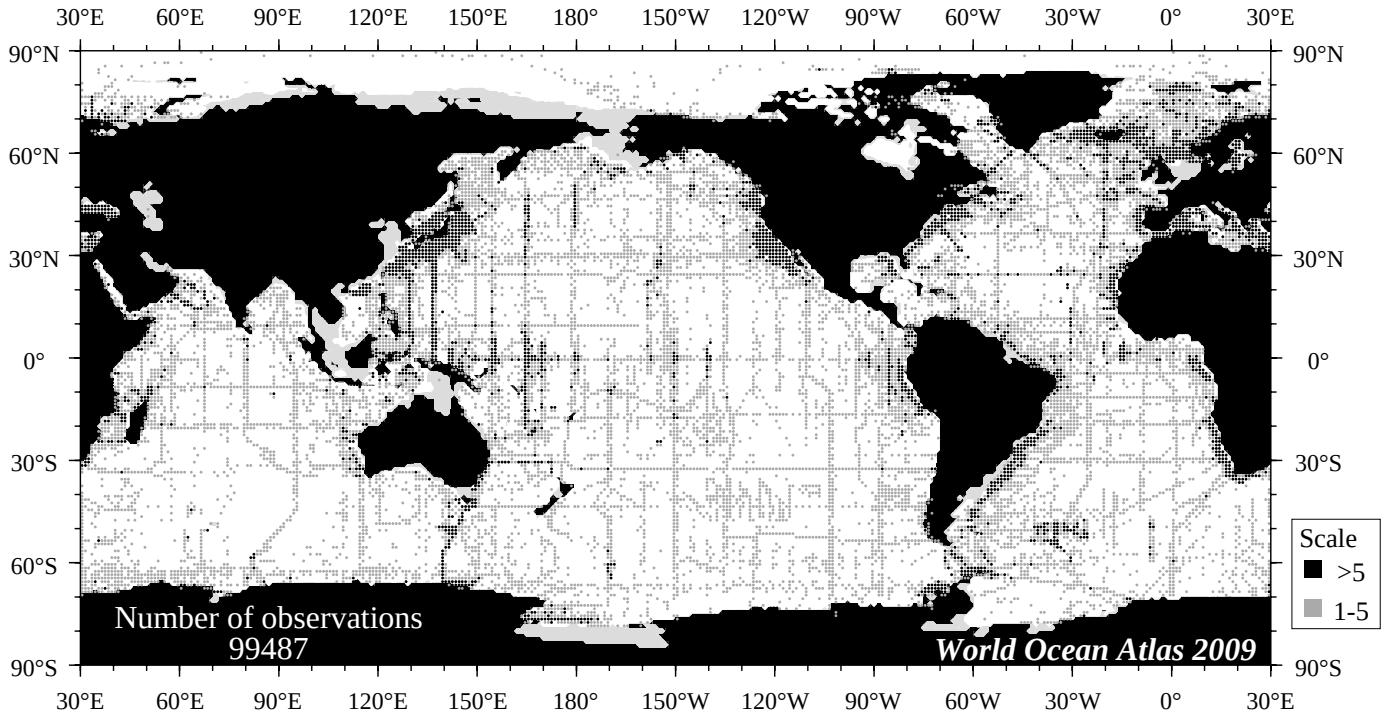

Fig D4 Annual nitrate observations at 100 m. depth.

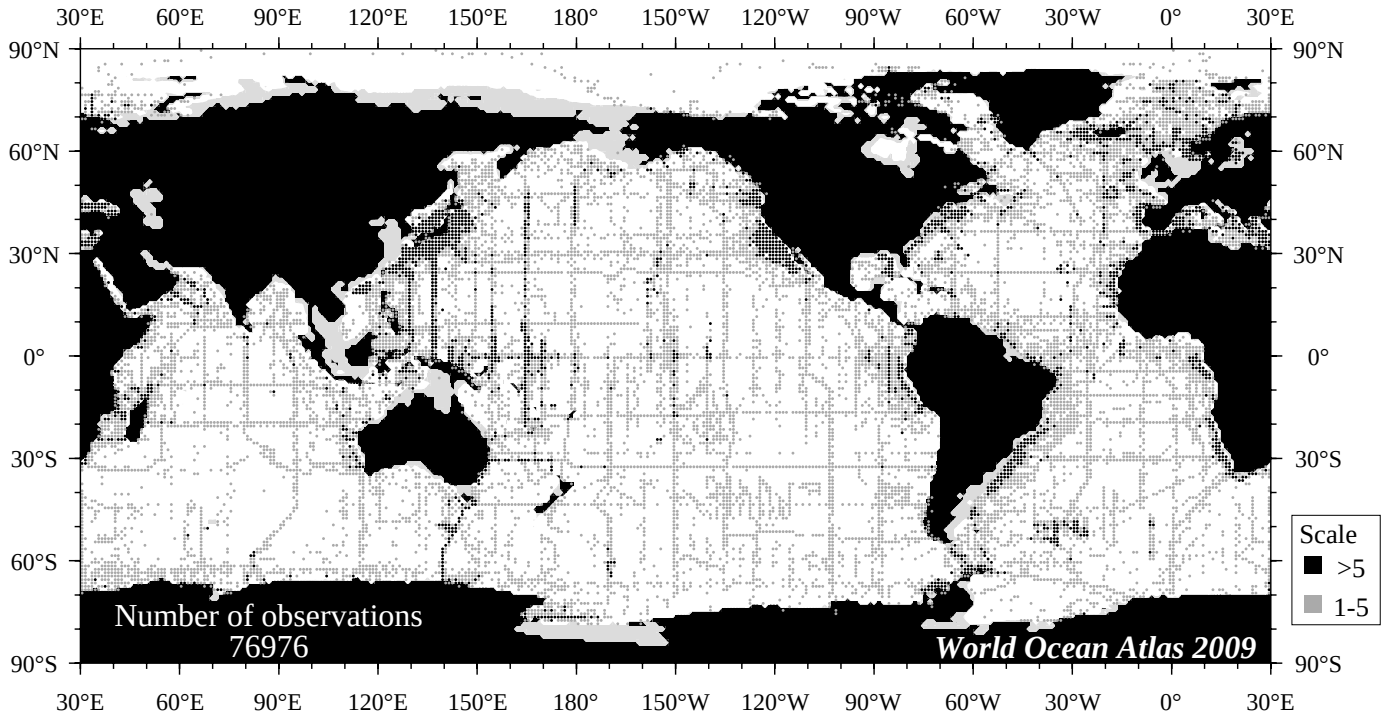

Fig D5 Annual nitrate observations at 150 m. depth.

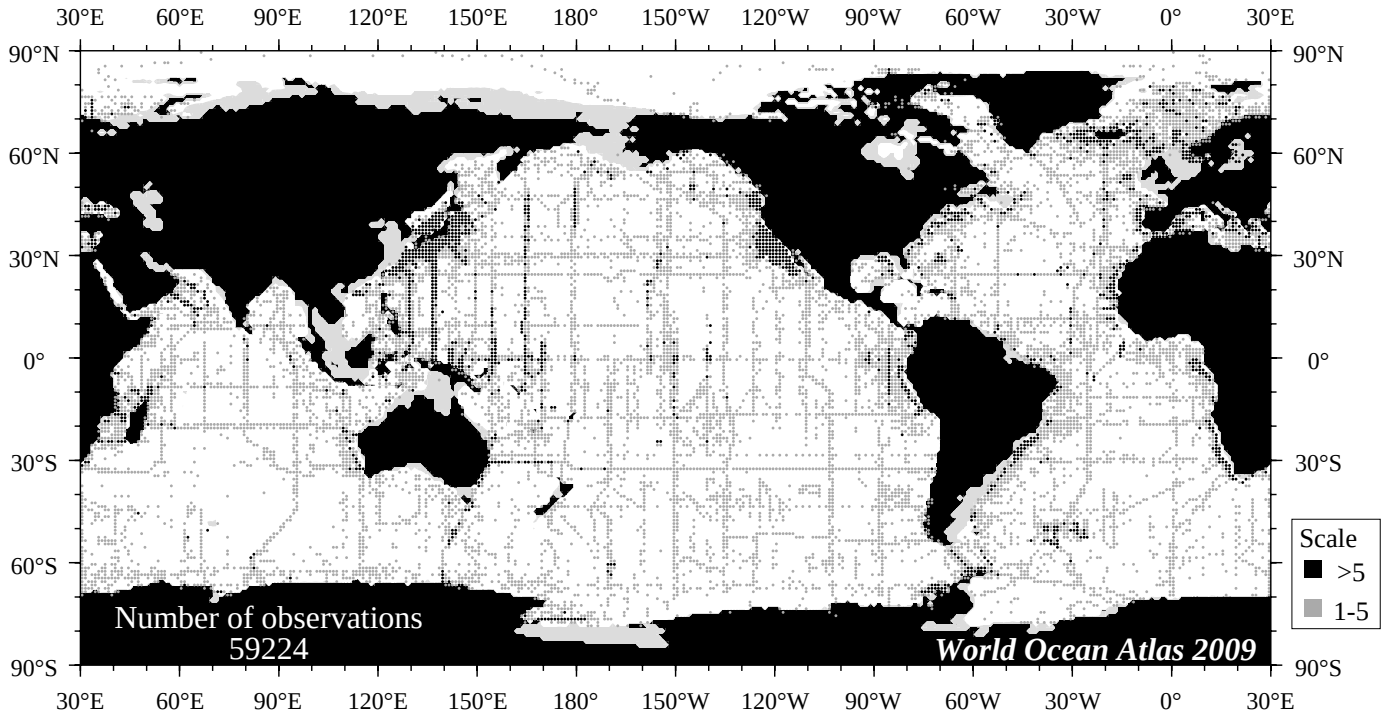

Fig D6 Annual nitrate observations at 200 m. depth.

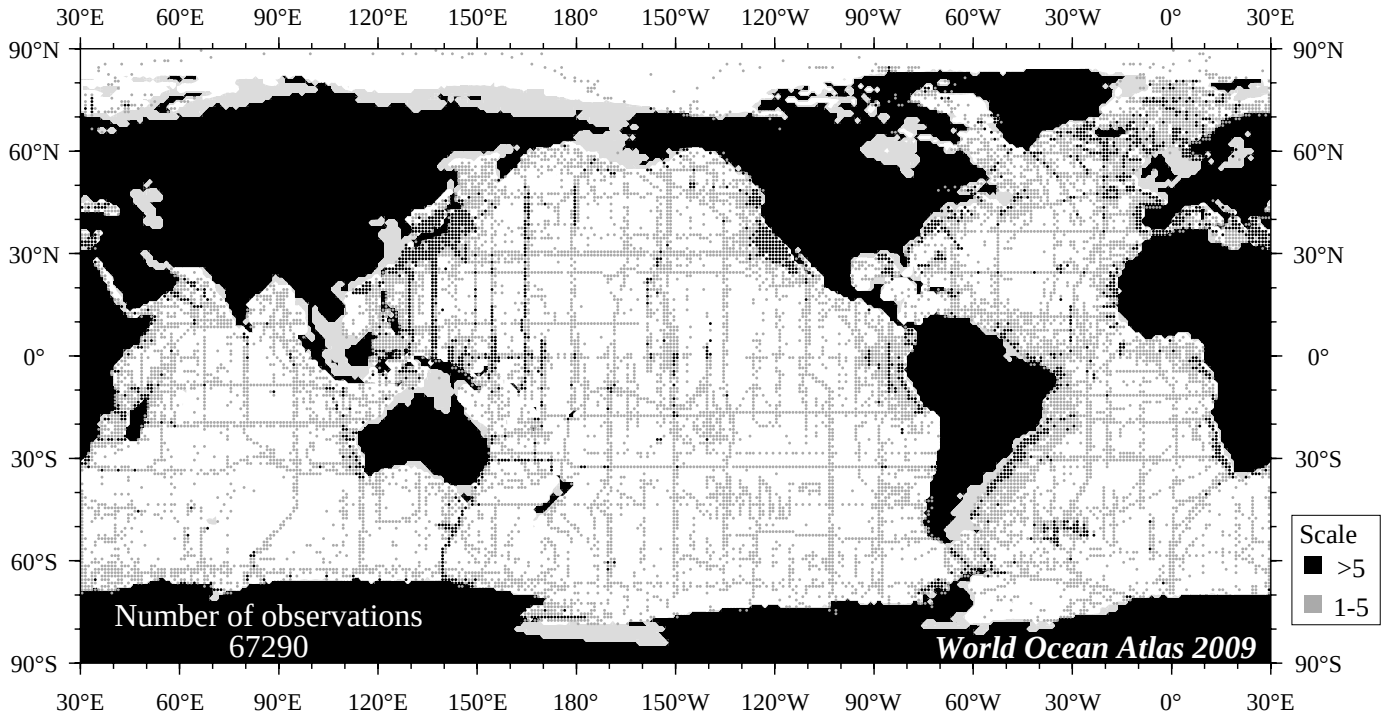

Fig D7 Annual nitrate observations at 250 m. depth.

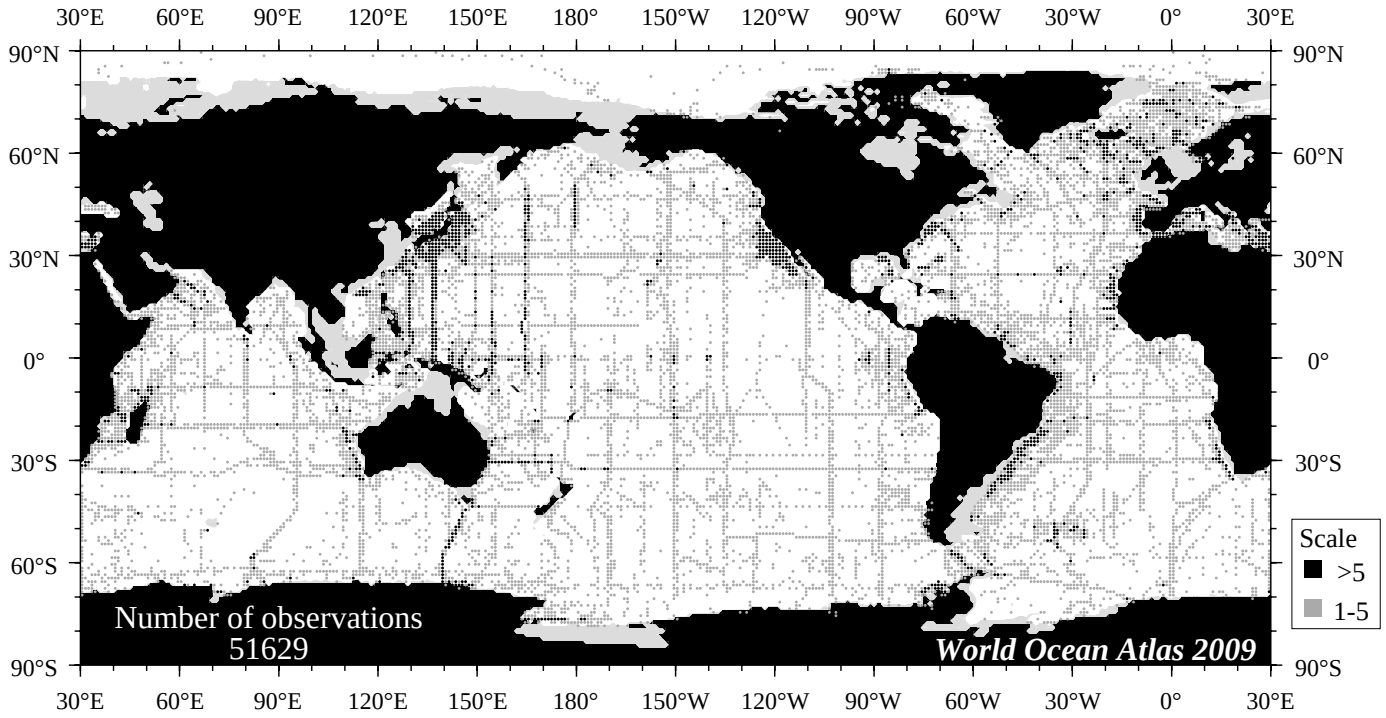

Fig D8 Annual nitrate observations at 400 m. depth.

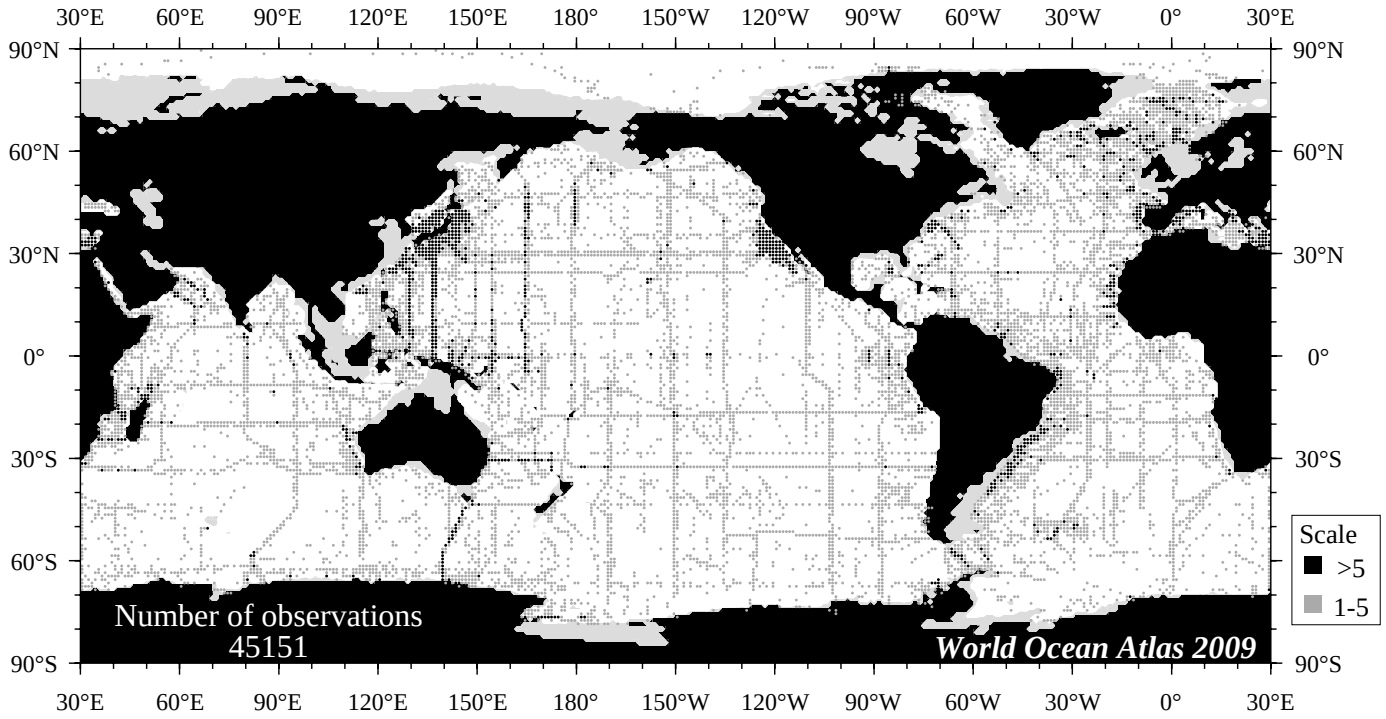

Fig D9 Annual nitrate observations at 500 m. depth.

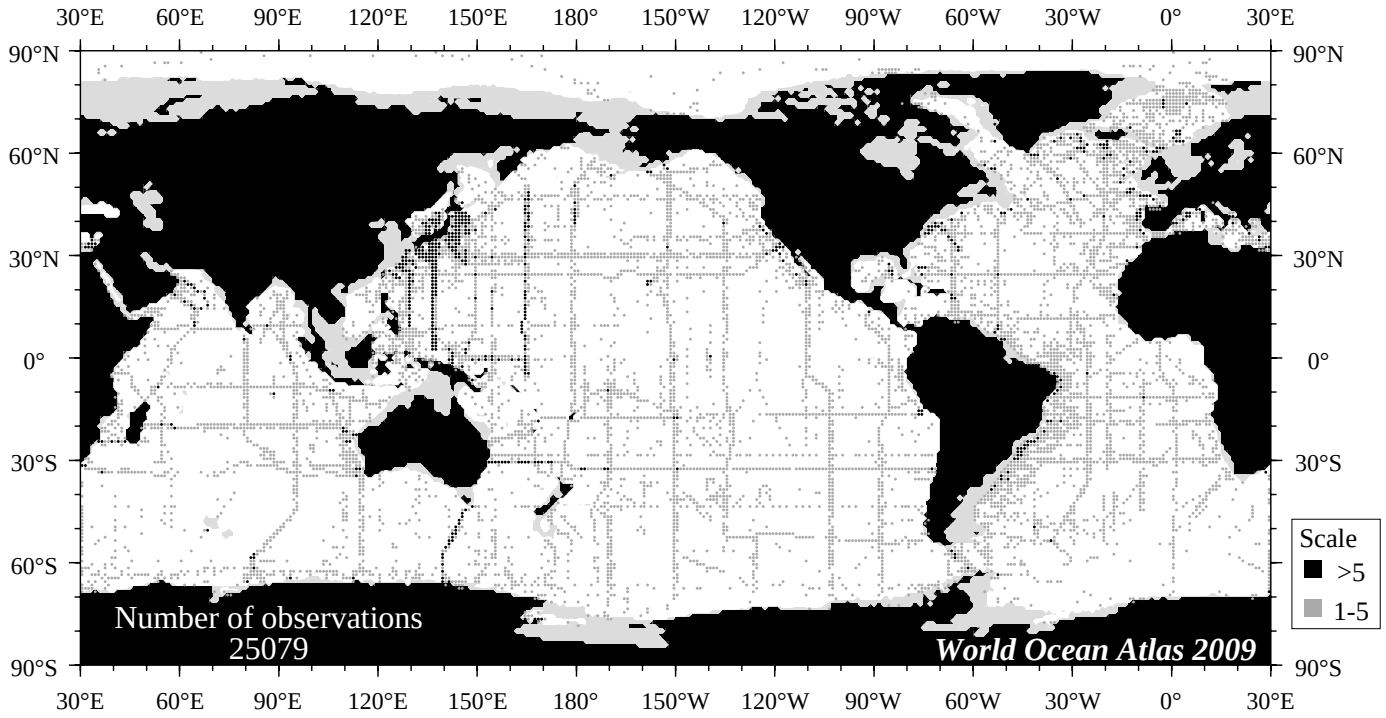

Fig D10 Annual nitrate observations at 700 m. depth.

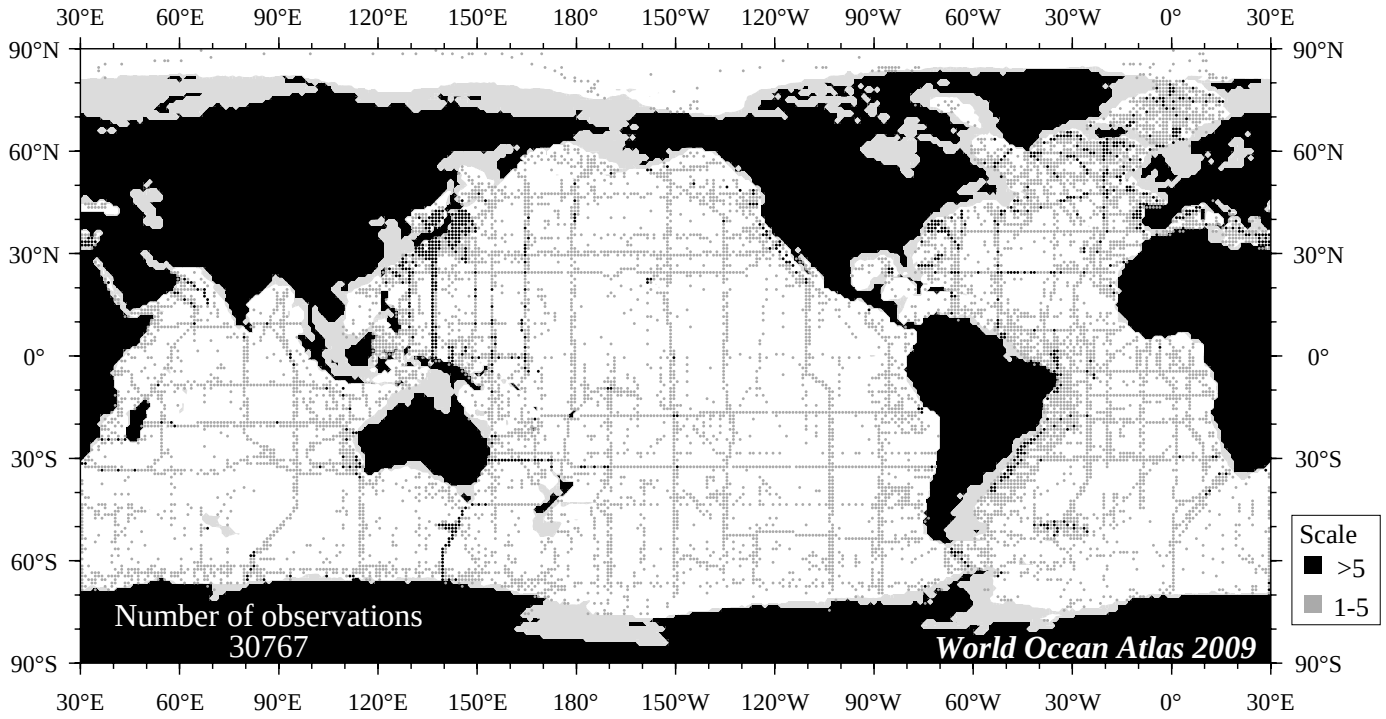

Fig D11 Annual nitrate observations at 1000 m. depth.

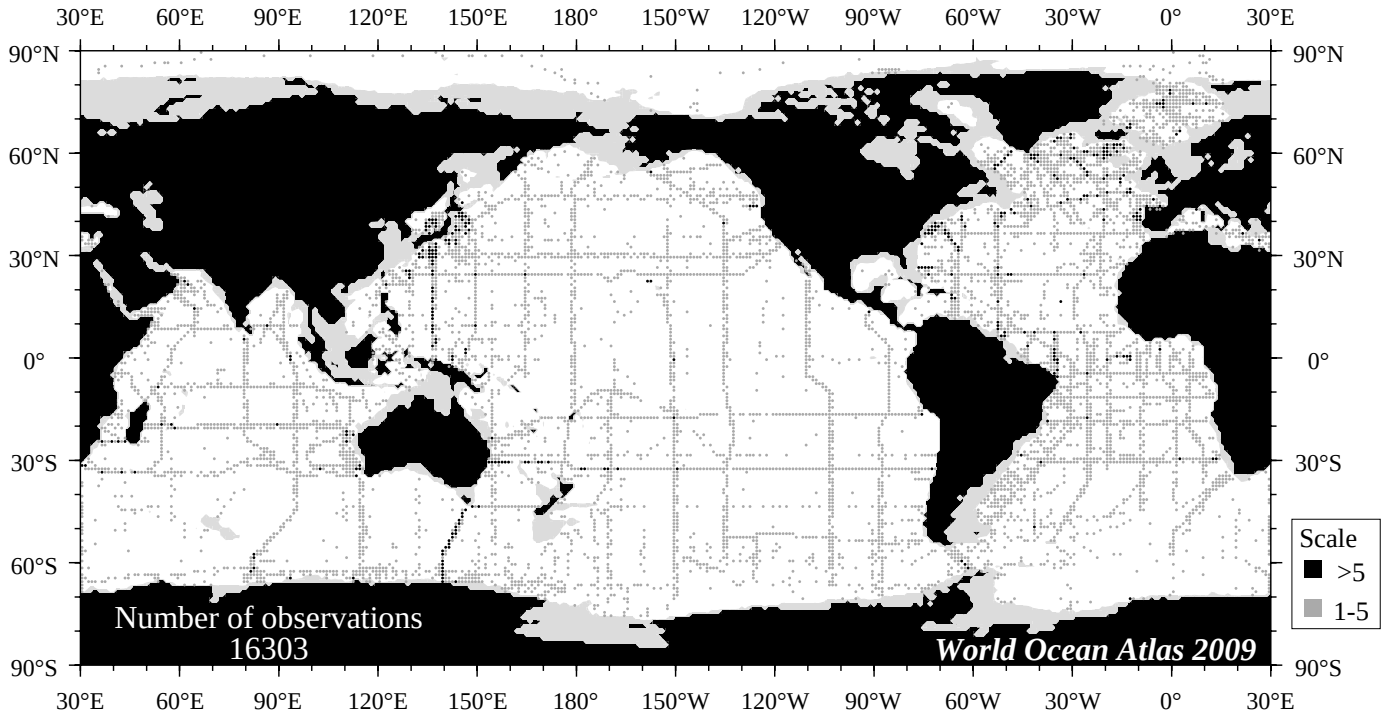

Fig D12 Annual nitrate observations at 1500 m. depth.

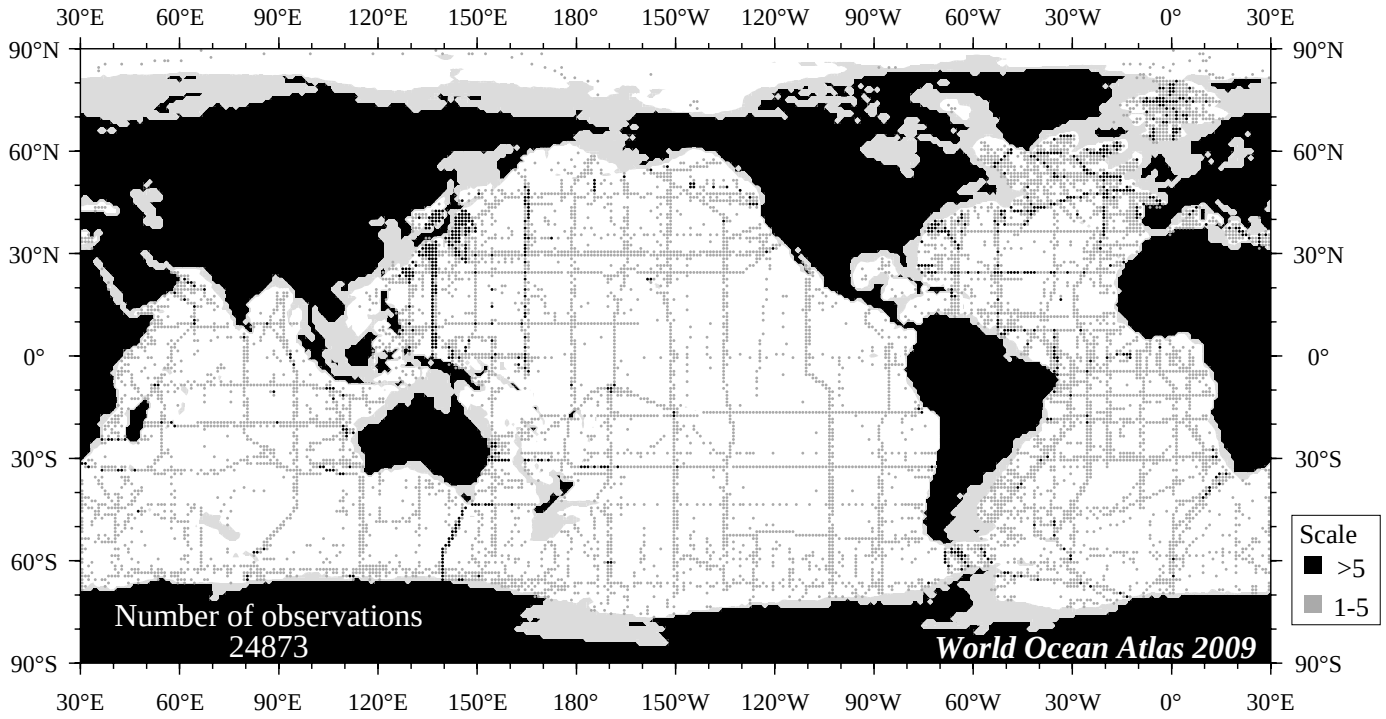

Fig D13 Annual nitrate observations at 2000 m. depth.

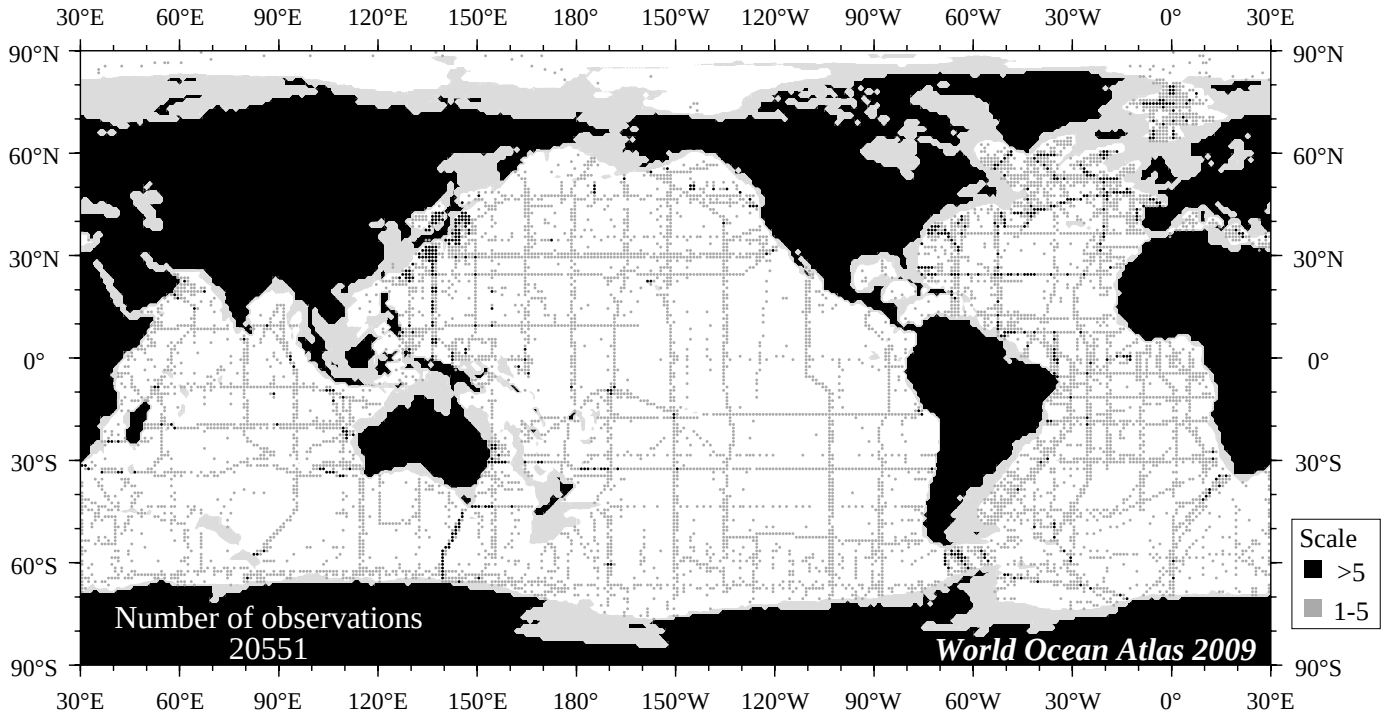

Fig D14 Annual nitrate observations at 2500 m. depth.

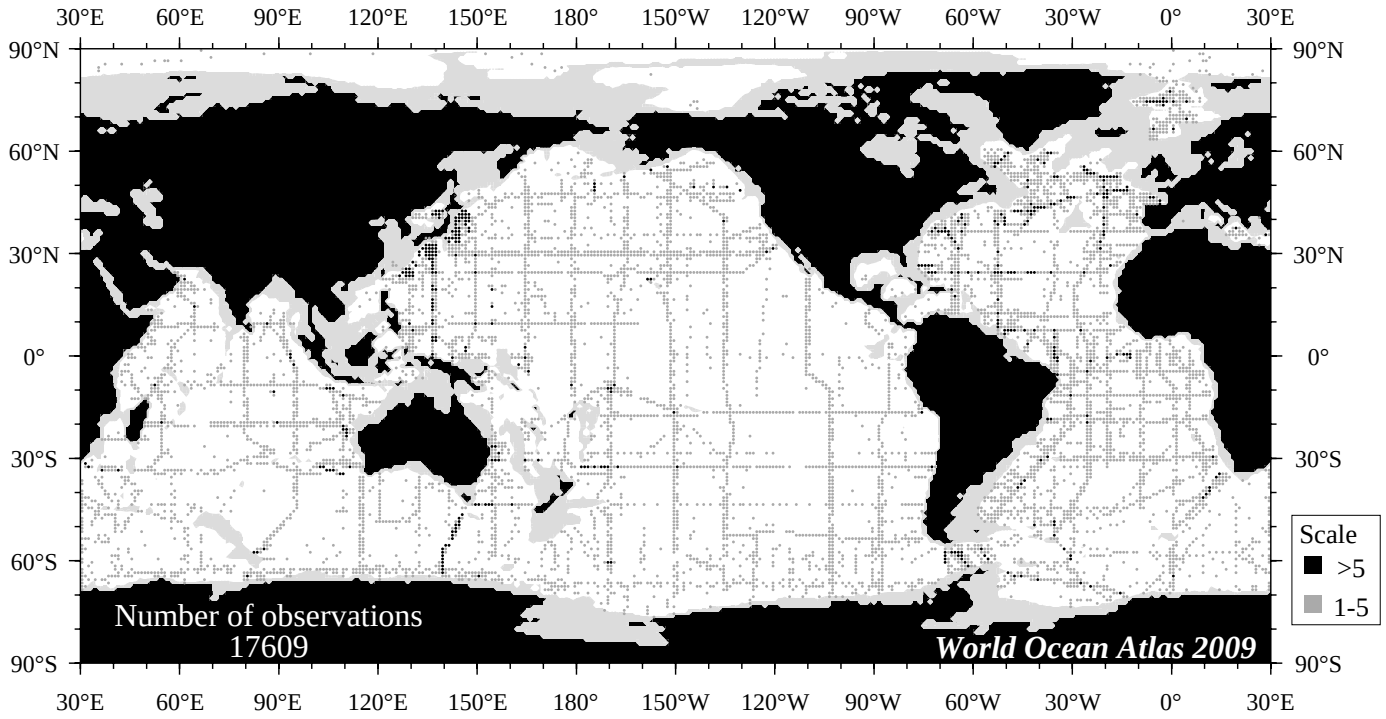

Fig D15 Annual nitrate observations at 3000 m. depth.

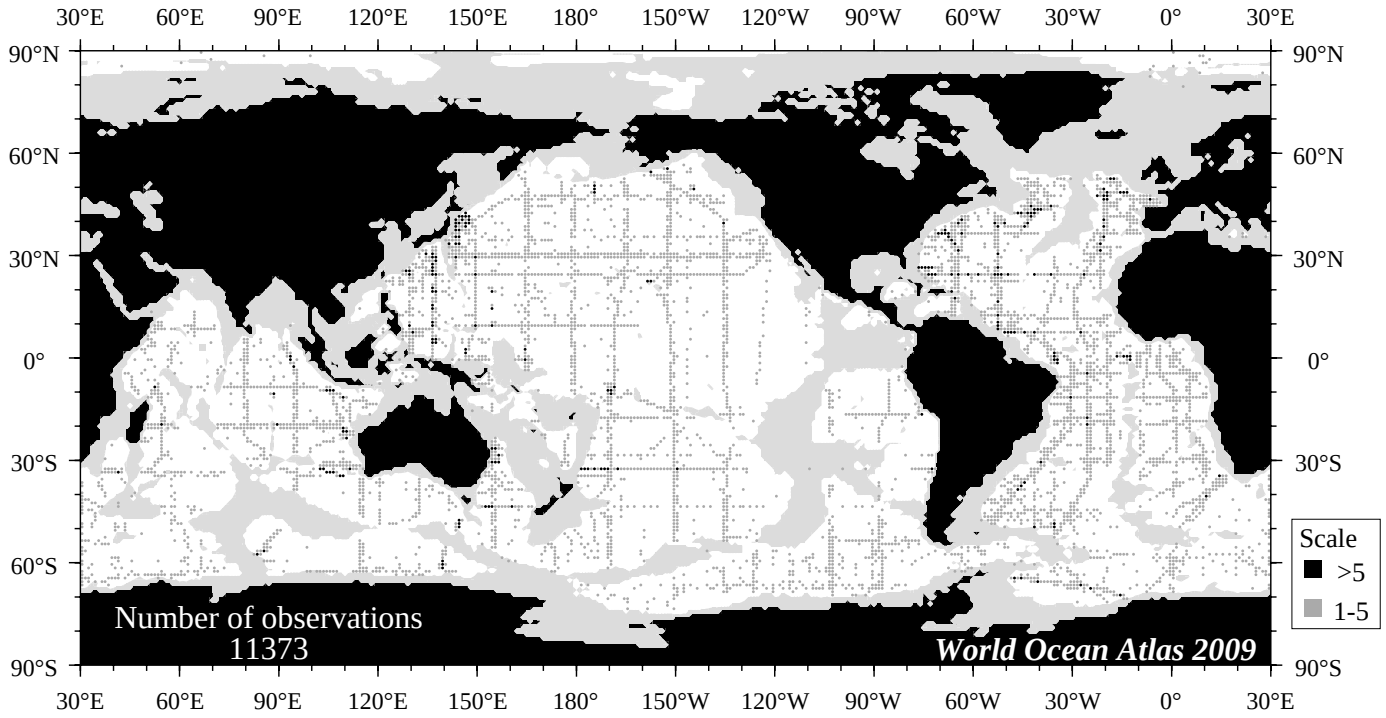

Fig D16 Annual nitrate observations at 4000 m. depth.

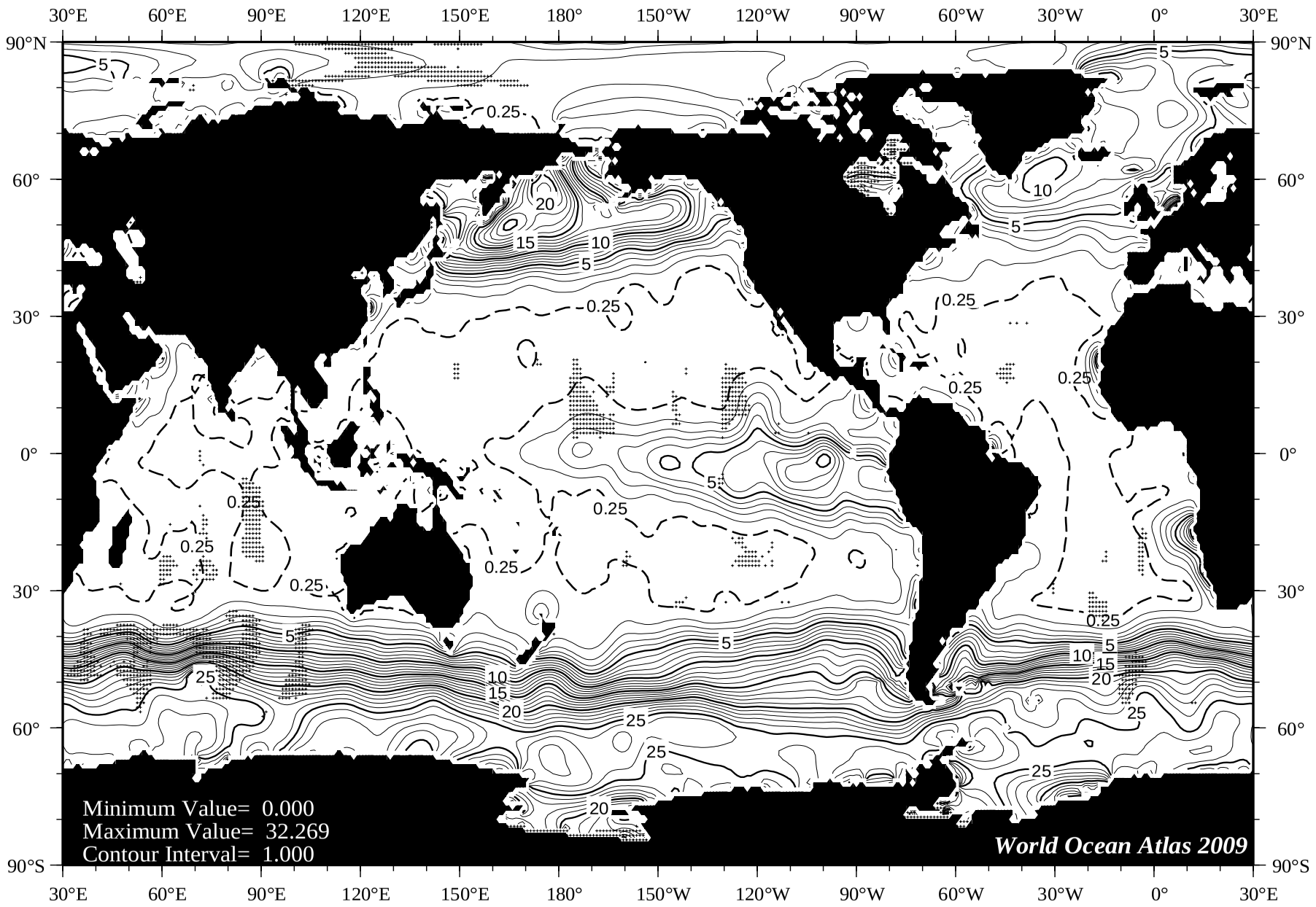

Fig D17 Annual nitrate [umol/l] at the surface.

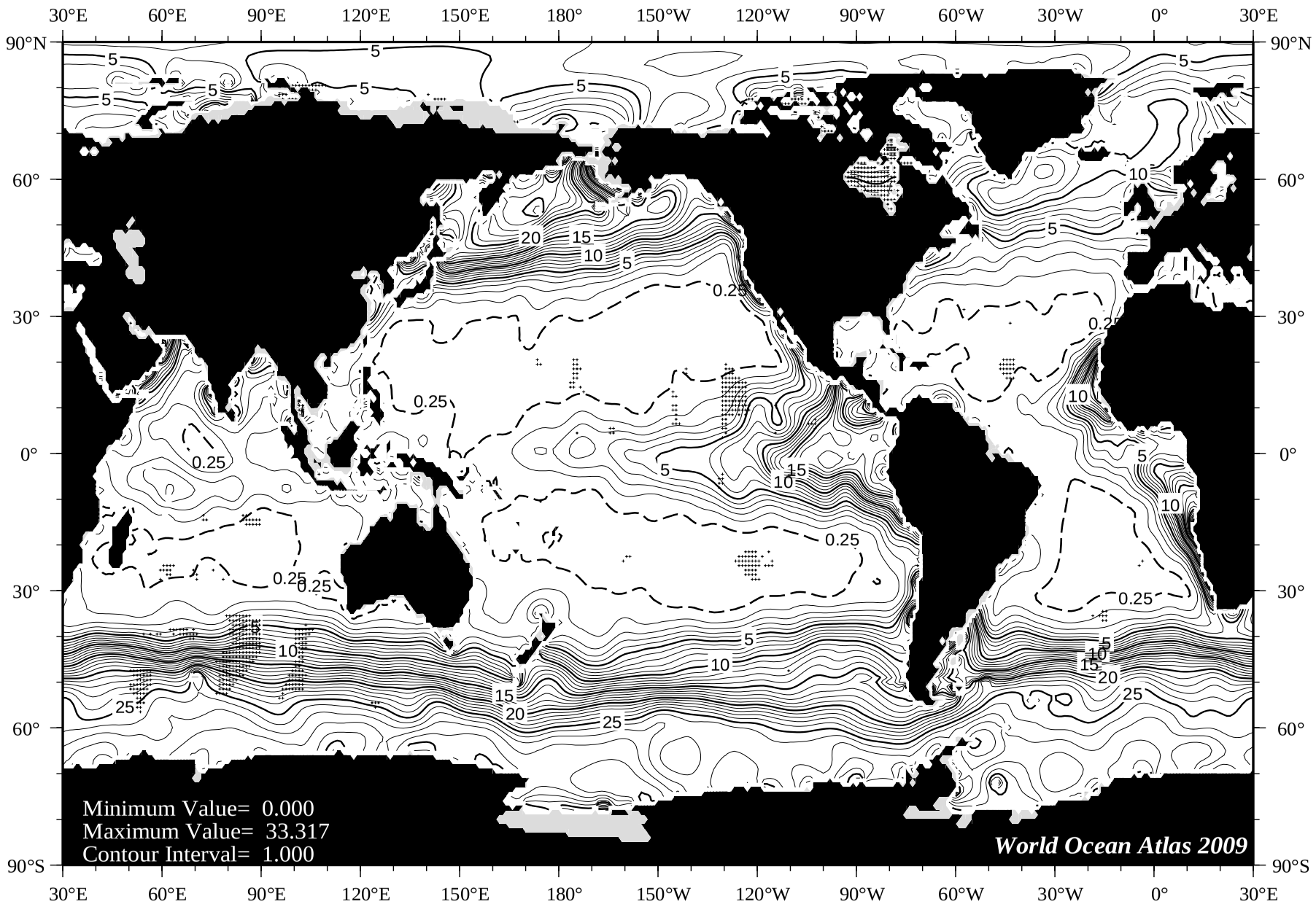

Fig D18 Annual nitrate [umol/l] at 50 m. depth.

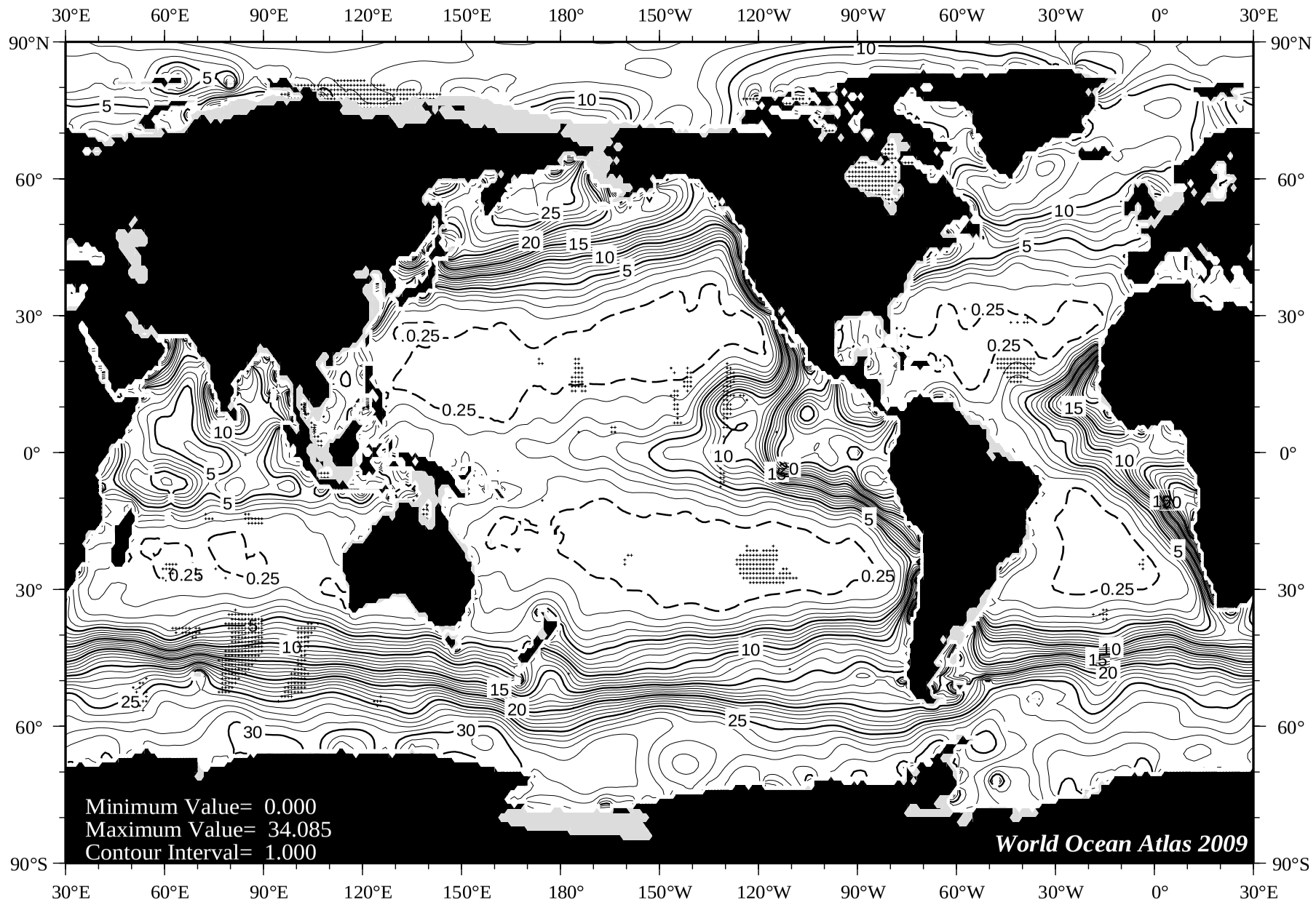

Fig D19 Annual nitrate [umol/l] at 75 m. depth.

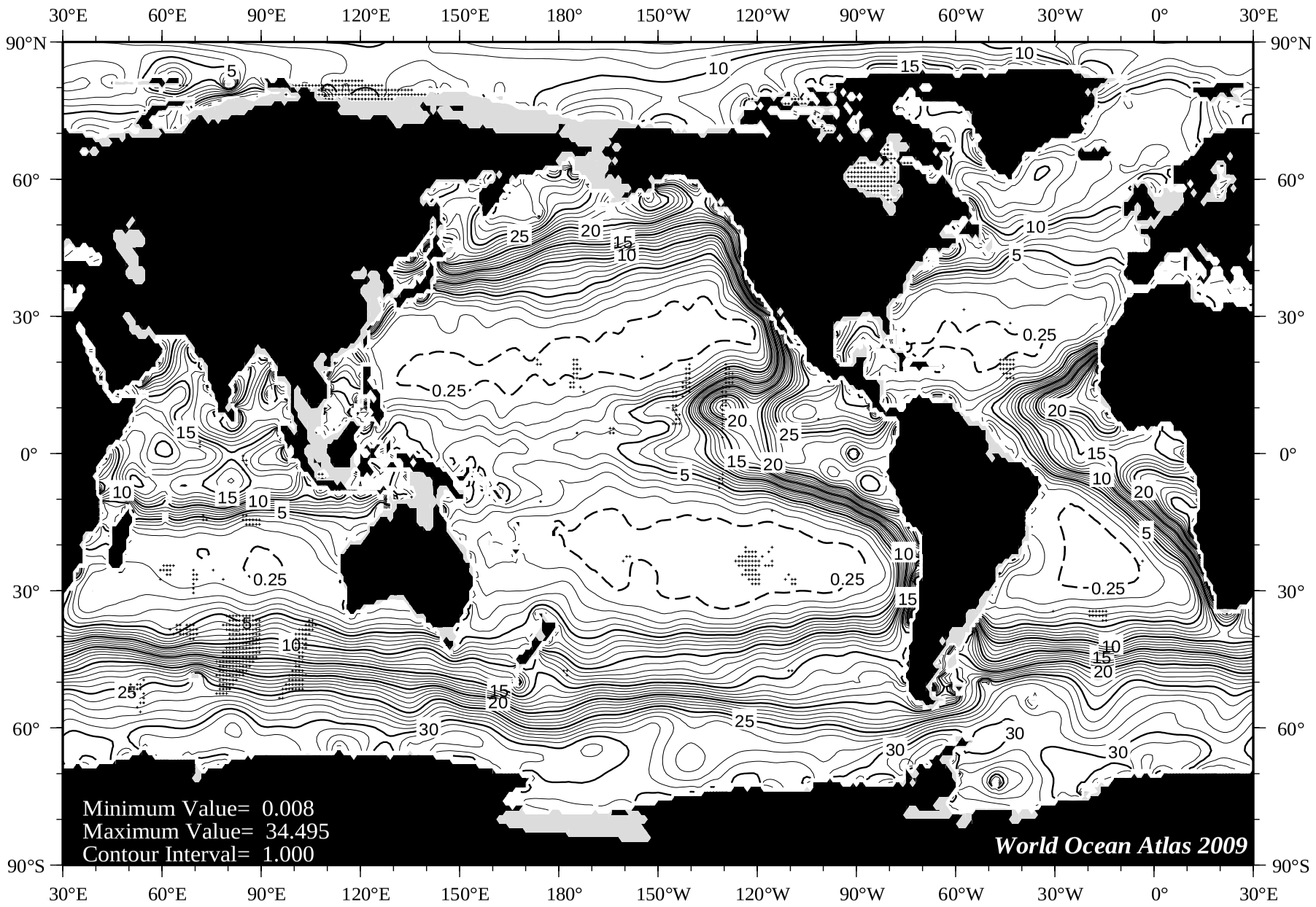

Fig D20 Annual nitrate [umol/l] at 100 m. depth.

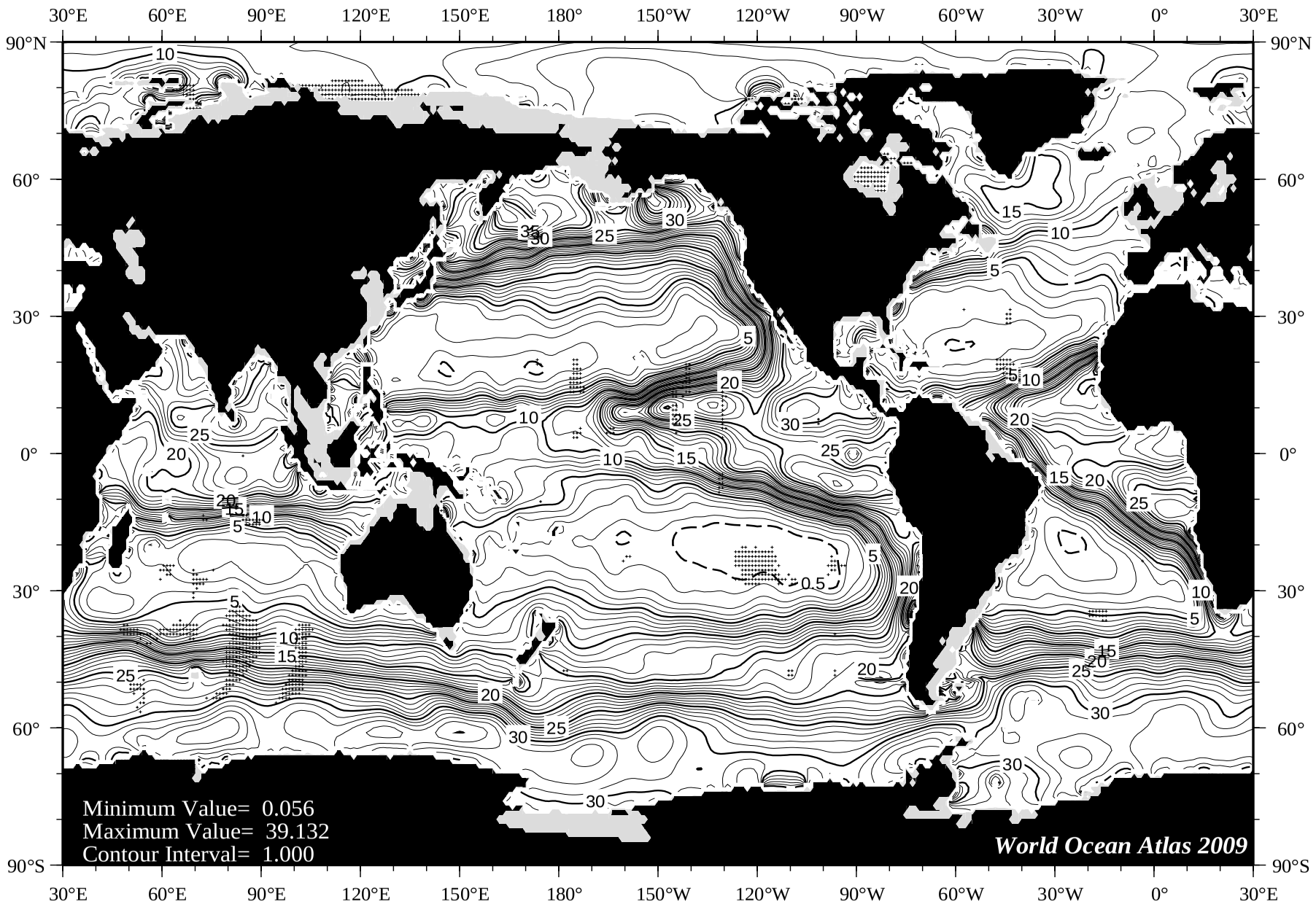

Fig D21 Annual nitrate [umol/l] at 150 m. depth.

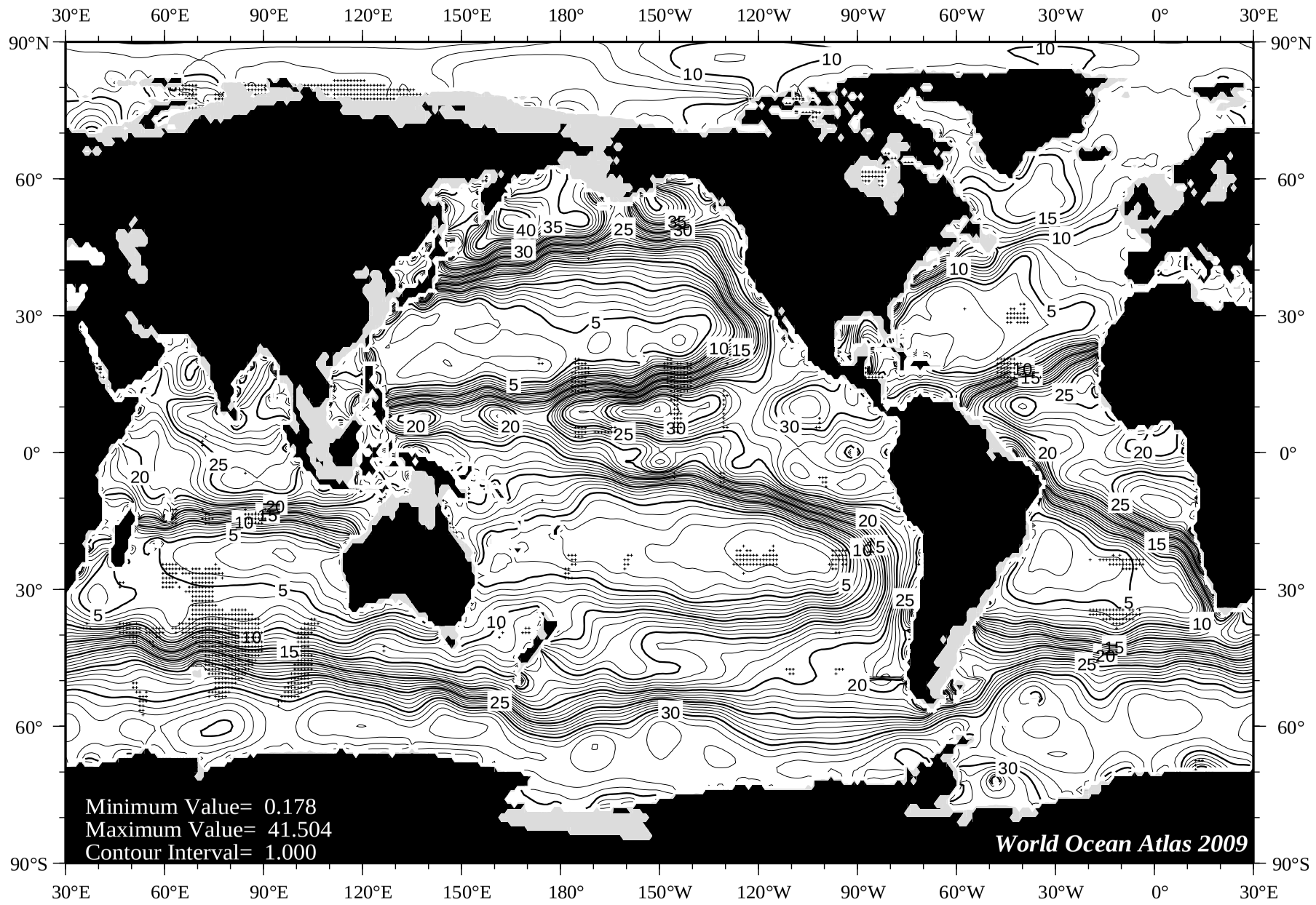

Fig D22 Annual nitrate [umol/l] at 200 m. depth.

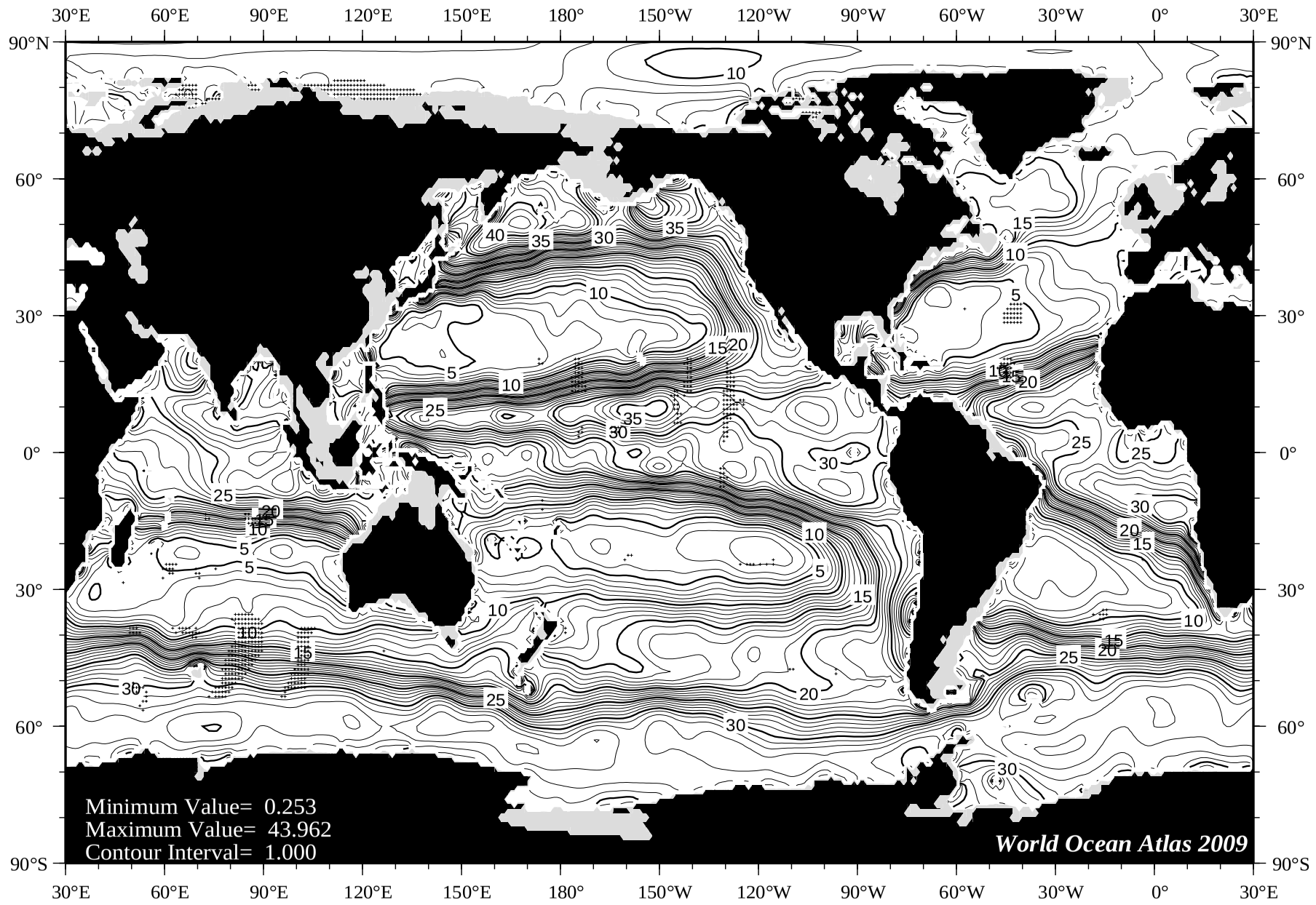

Fig D23 Annual nitrate [umol/l] at 250 m. depth.

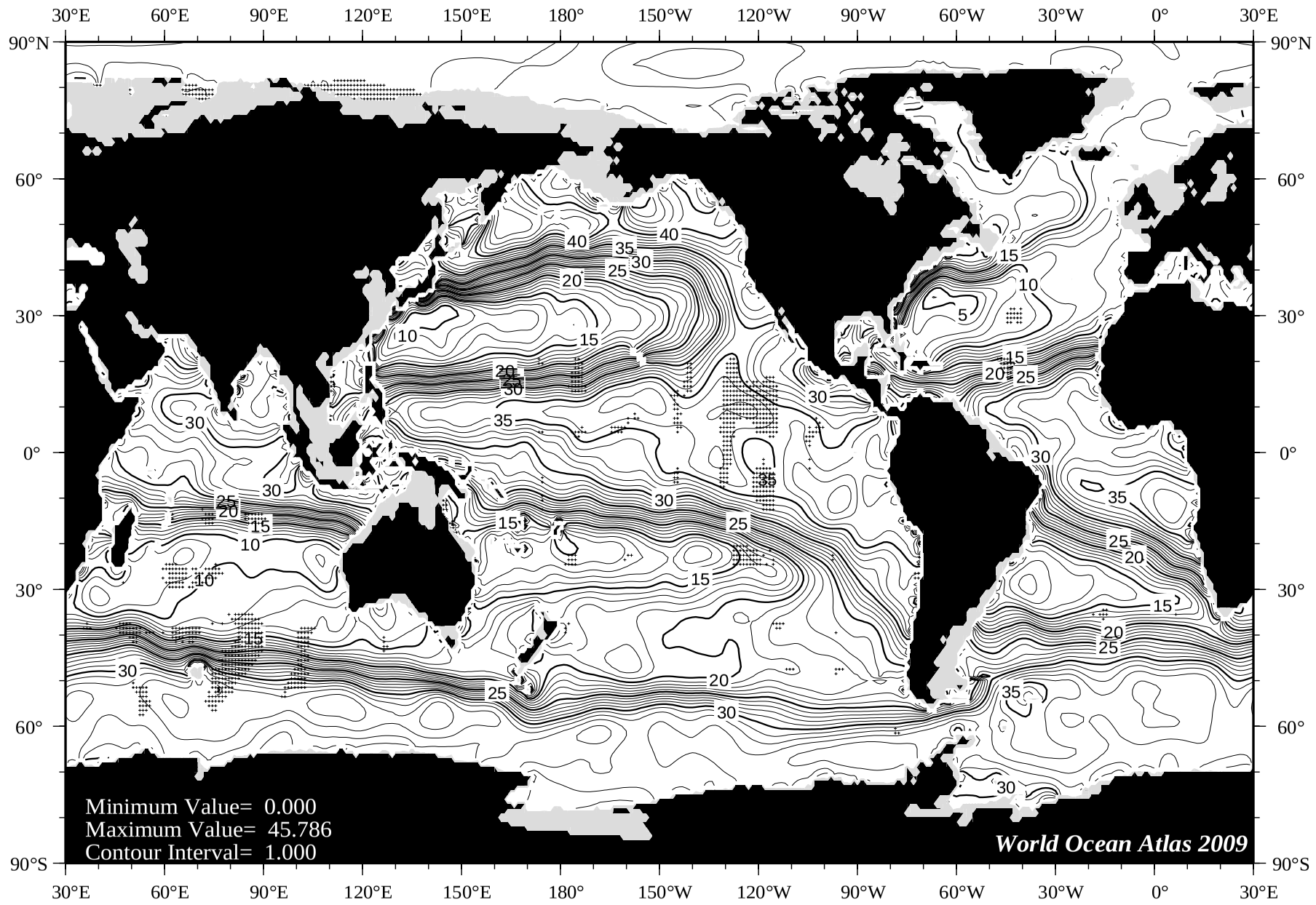

Fig D24 Annual nitrate [umol/l] at 400 m. depth.

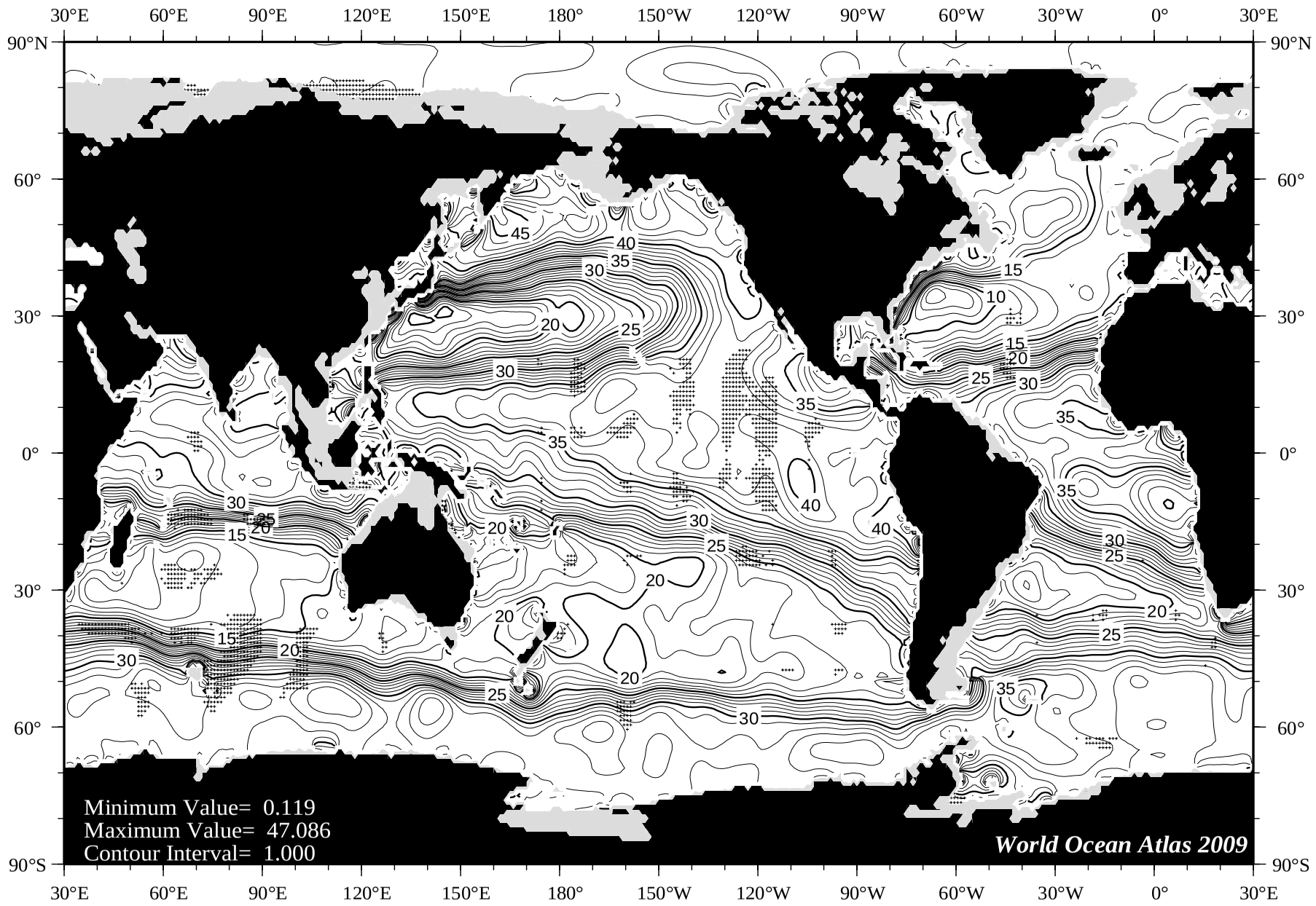

Fig D25 Annual nitrate [umol/l] at 500 m. depth.

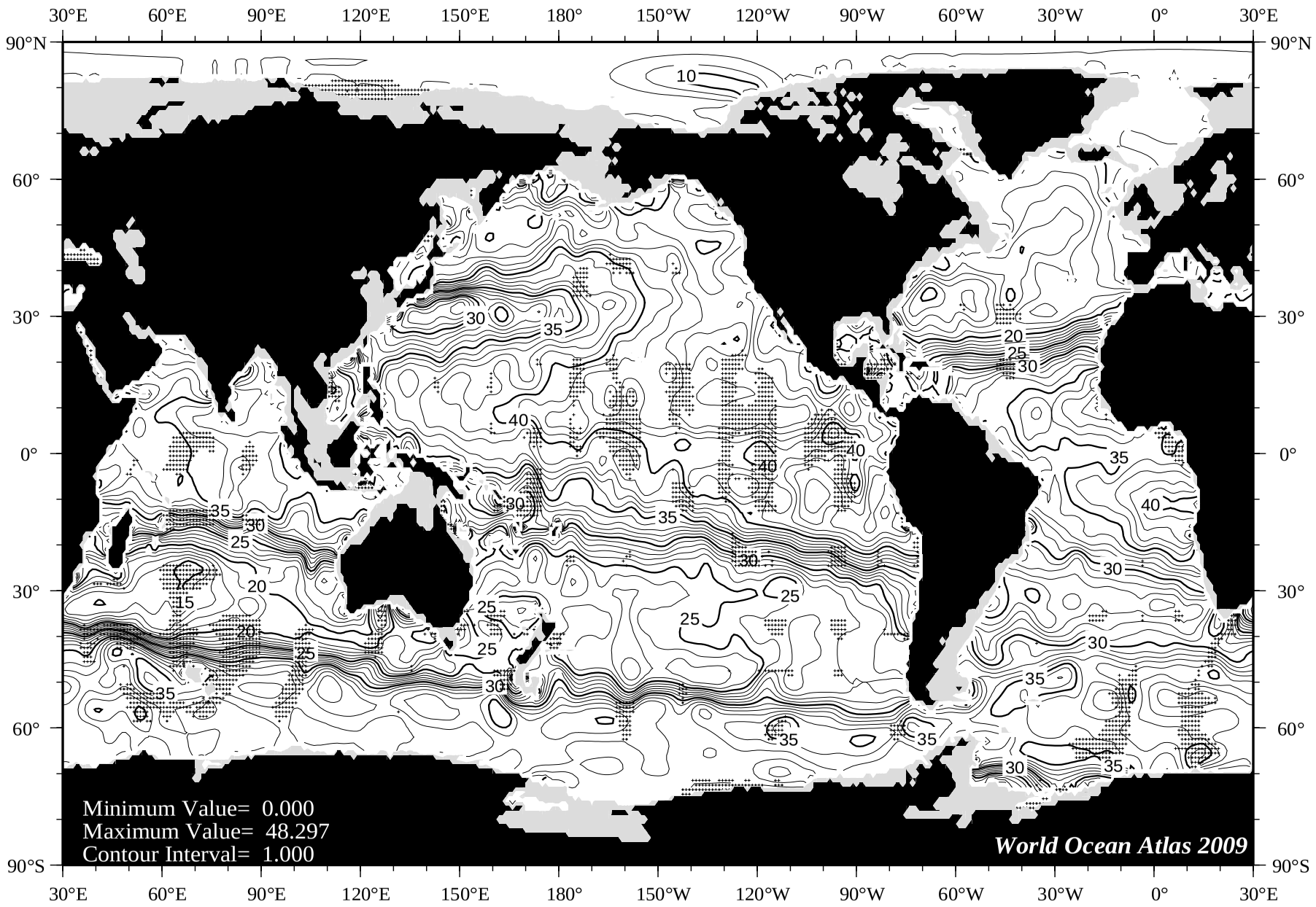

Fig D26 Annual nitrate [umol/l] at 700 m. depth.

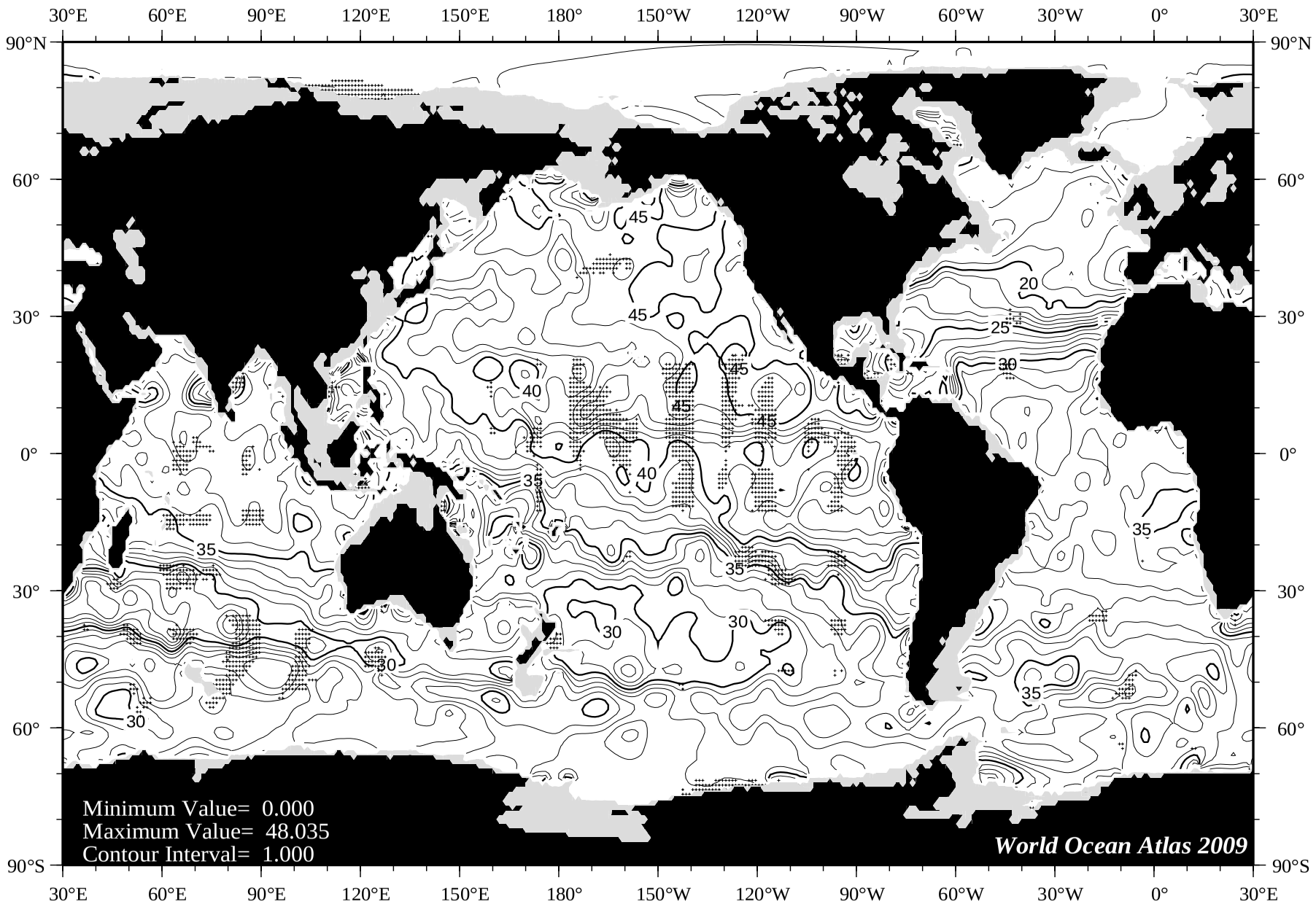

Fig D27 Annual nitrate [umol/l] at 1000 m. depth.

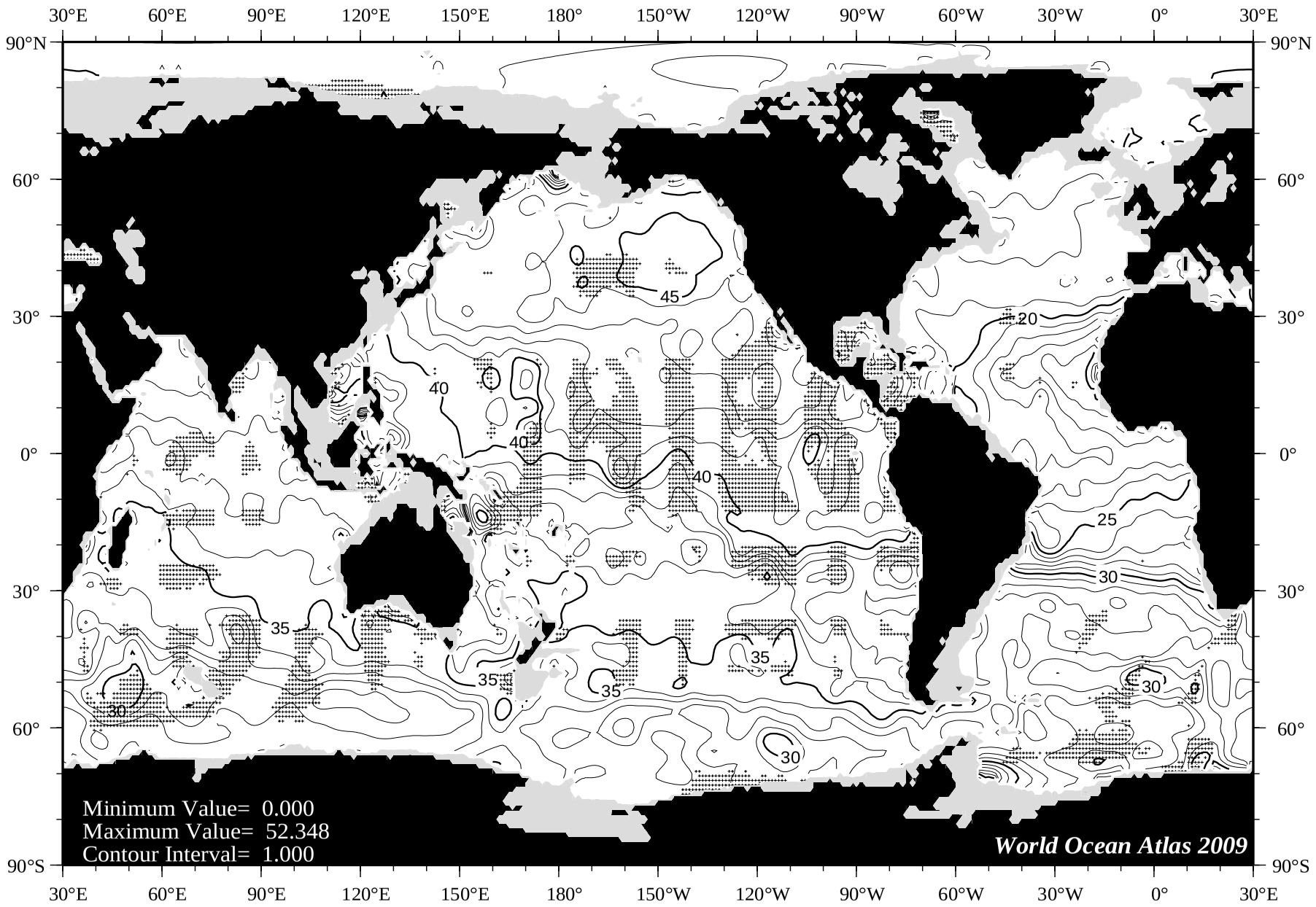

Fig D28 Annual nitrate [umol/l] at 1500 m. depth.

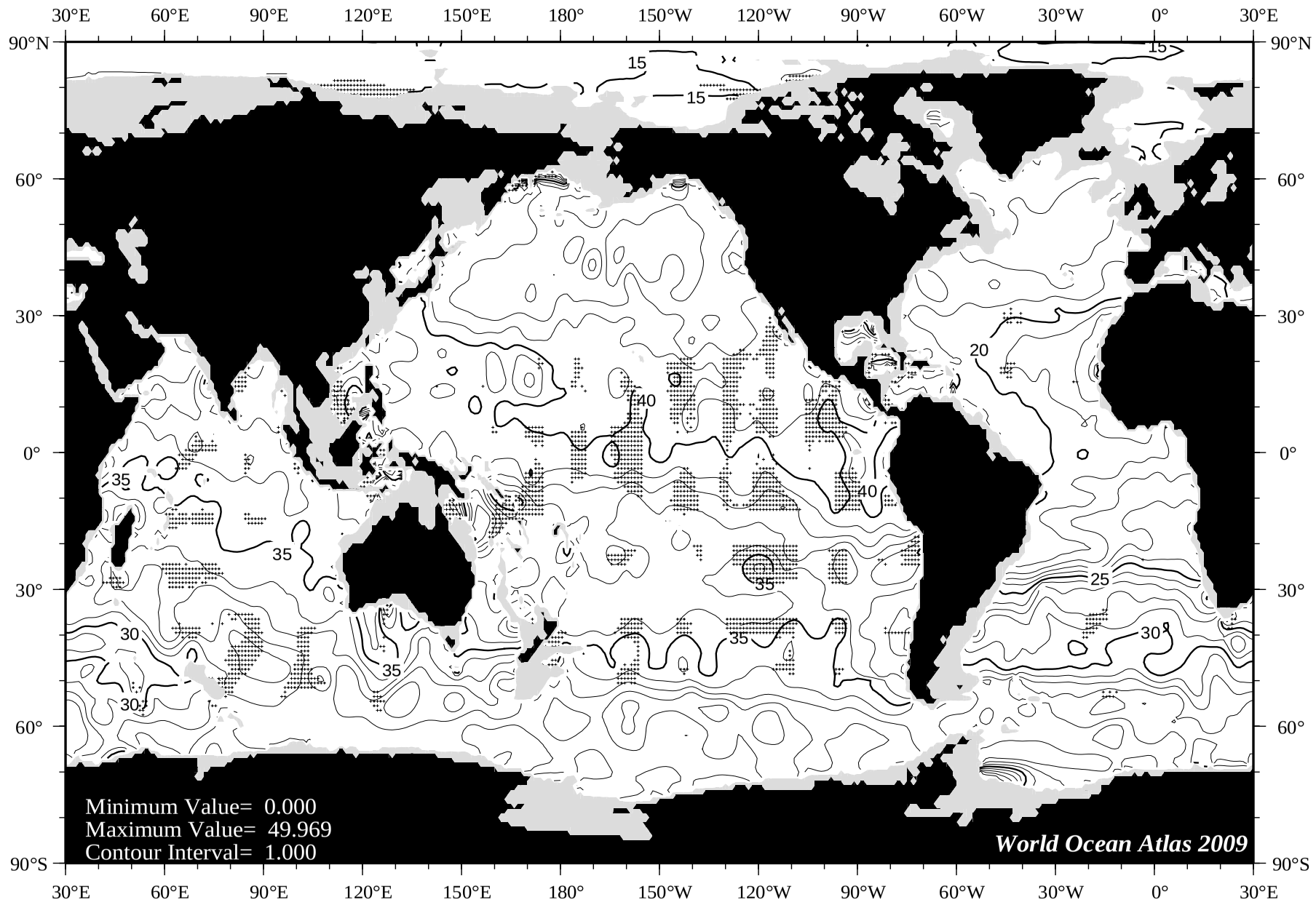

Fig D29 Annual nitrate [umol/l] at 2000 m. depth.

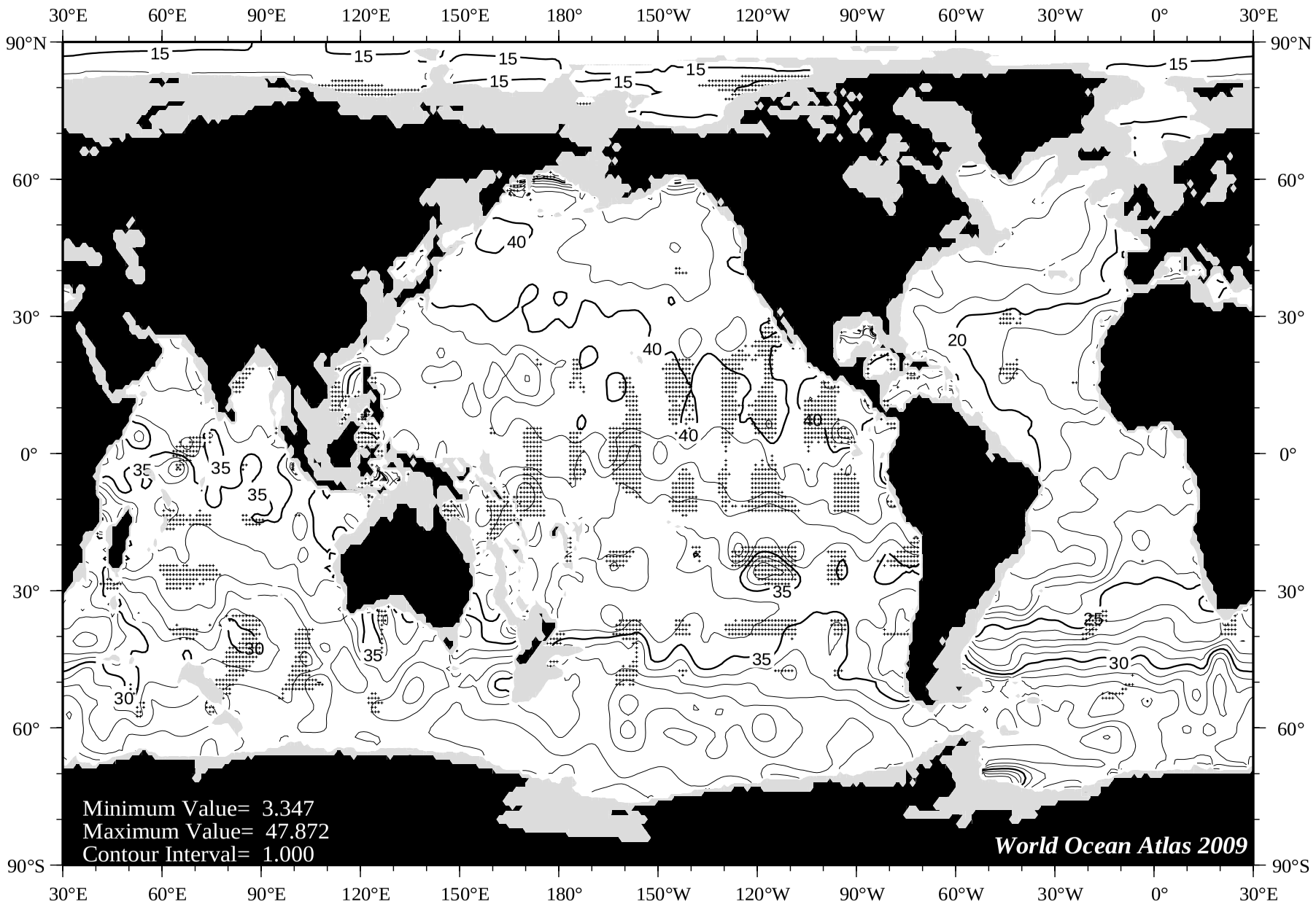

Fig D30 Annual nitrate [umol/l] at 2500 m. depth.

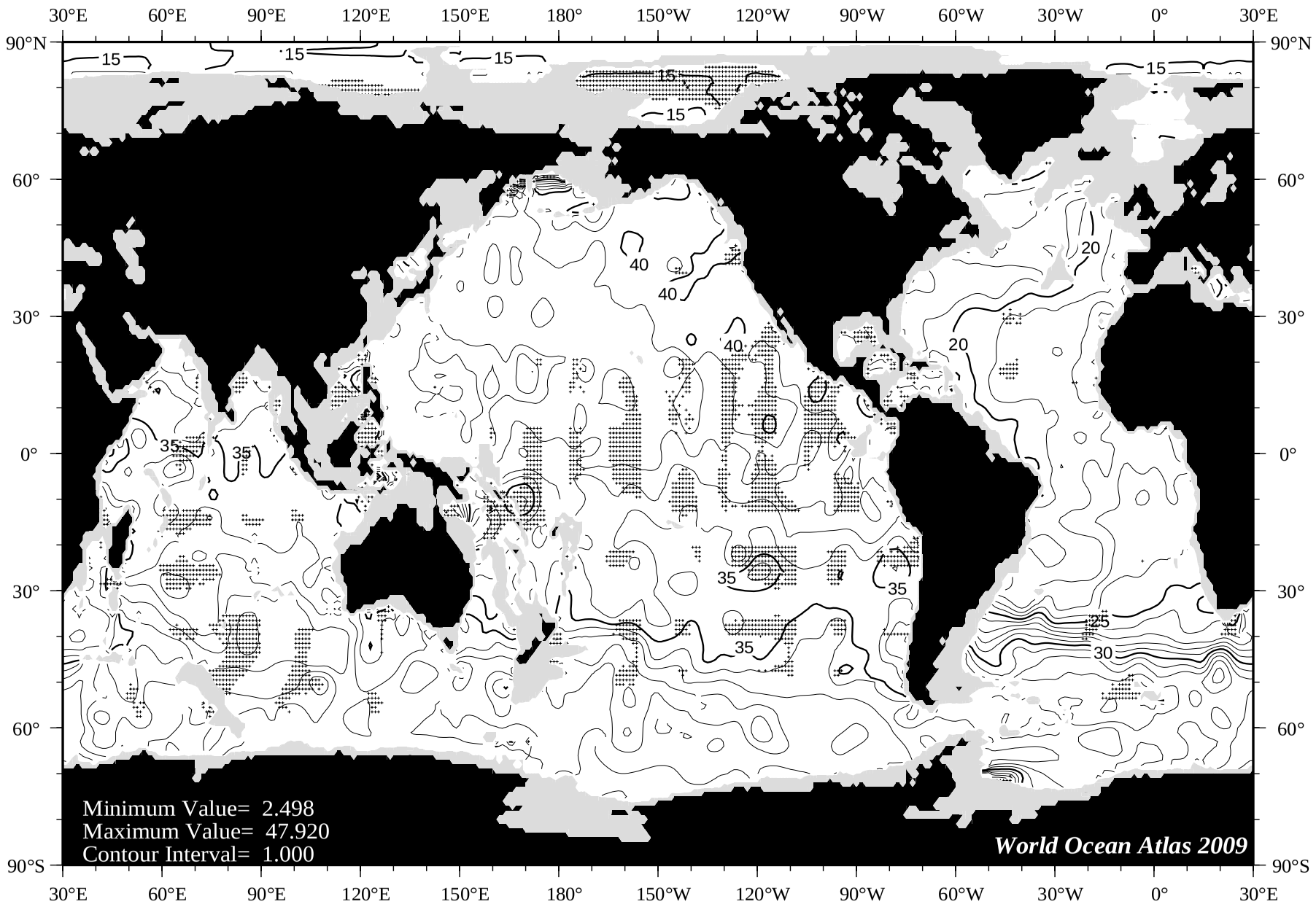

Fig D31 Annual nitrate [umol/l] at 3000 m. depth.

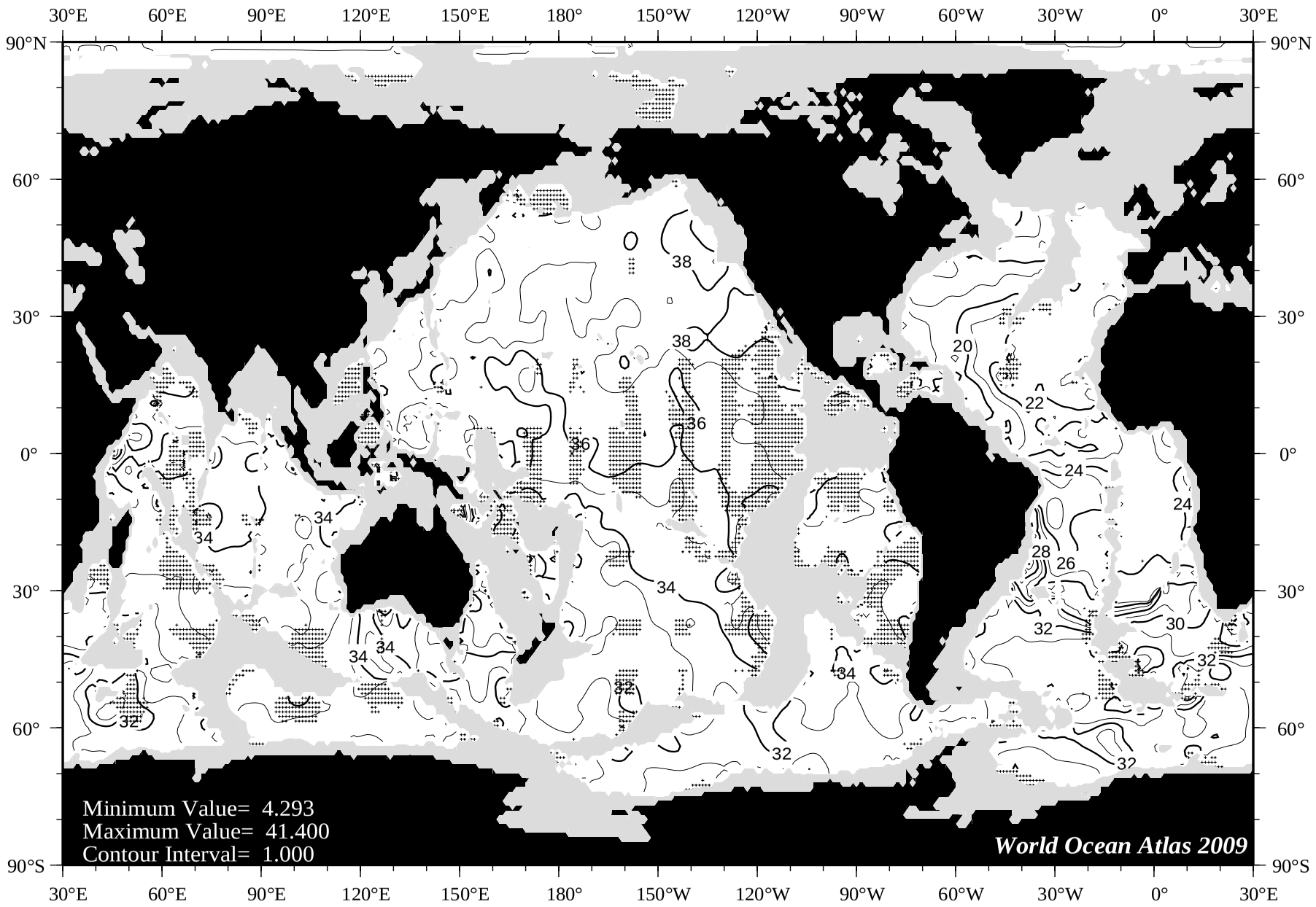

Fig D32 Annual nitrate [umol/l] at 4000 m. depth.

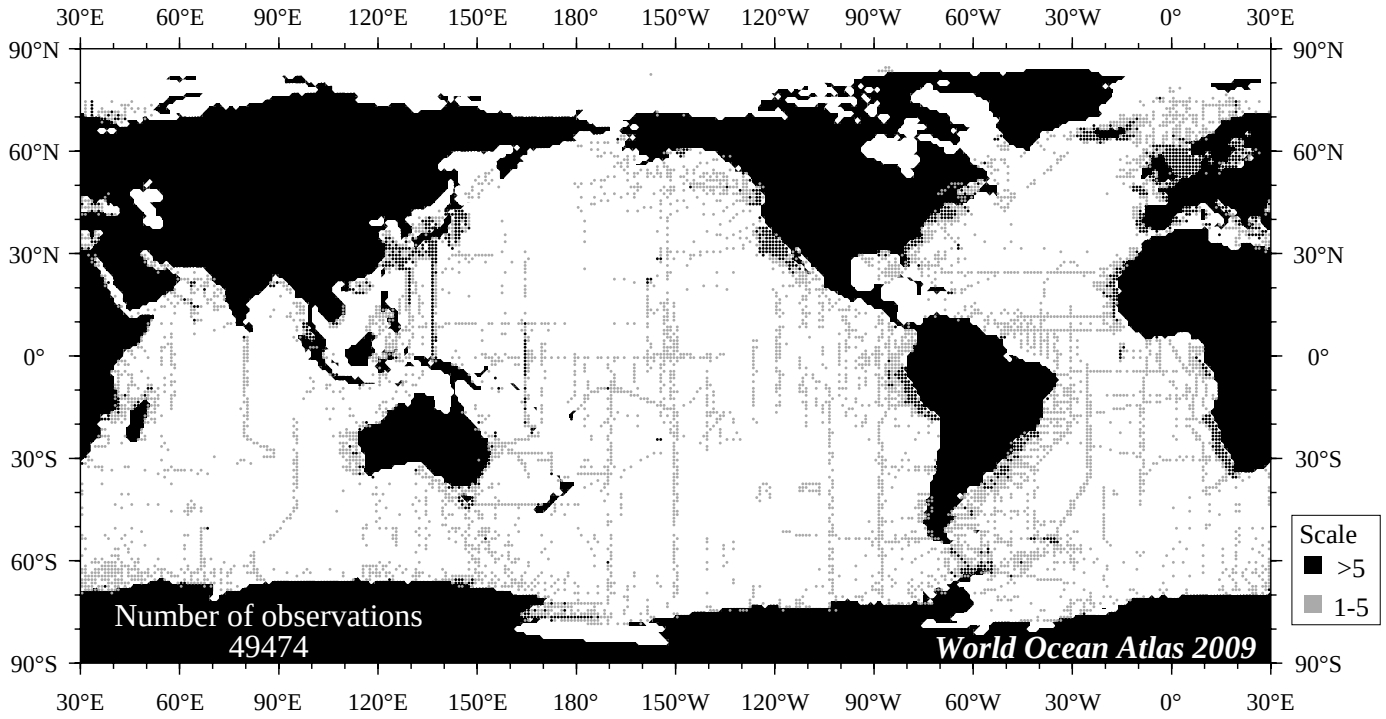

Fig E1 Winter (Jan.-Mar.) nitrate observations at the surface.

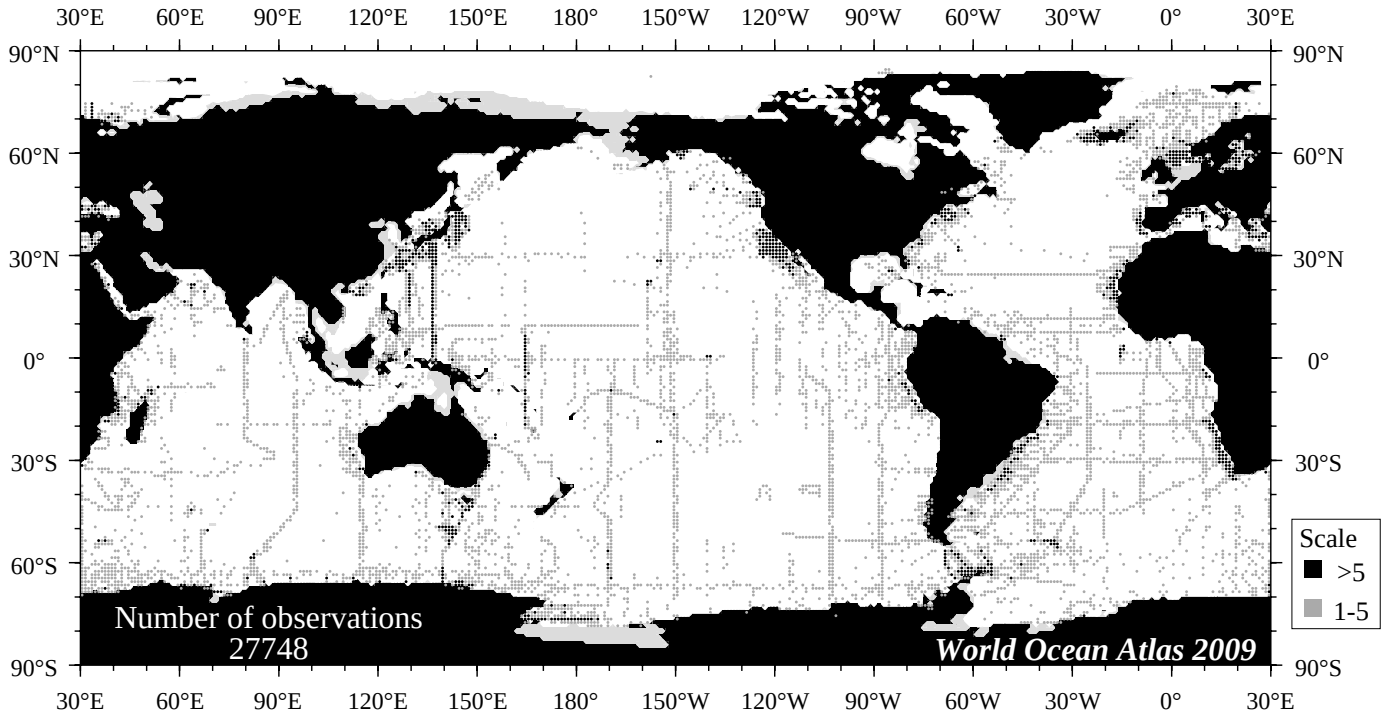

Fig E2 Winter (Jan.-Mar.) nitrate observations at 75 m. depth.

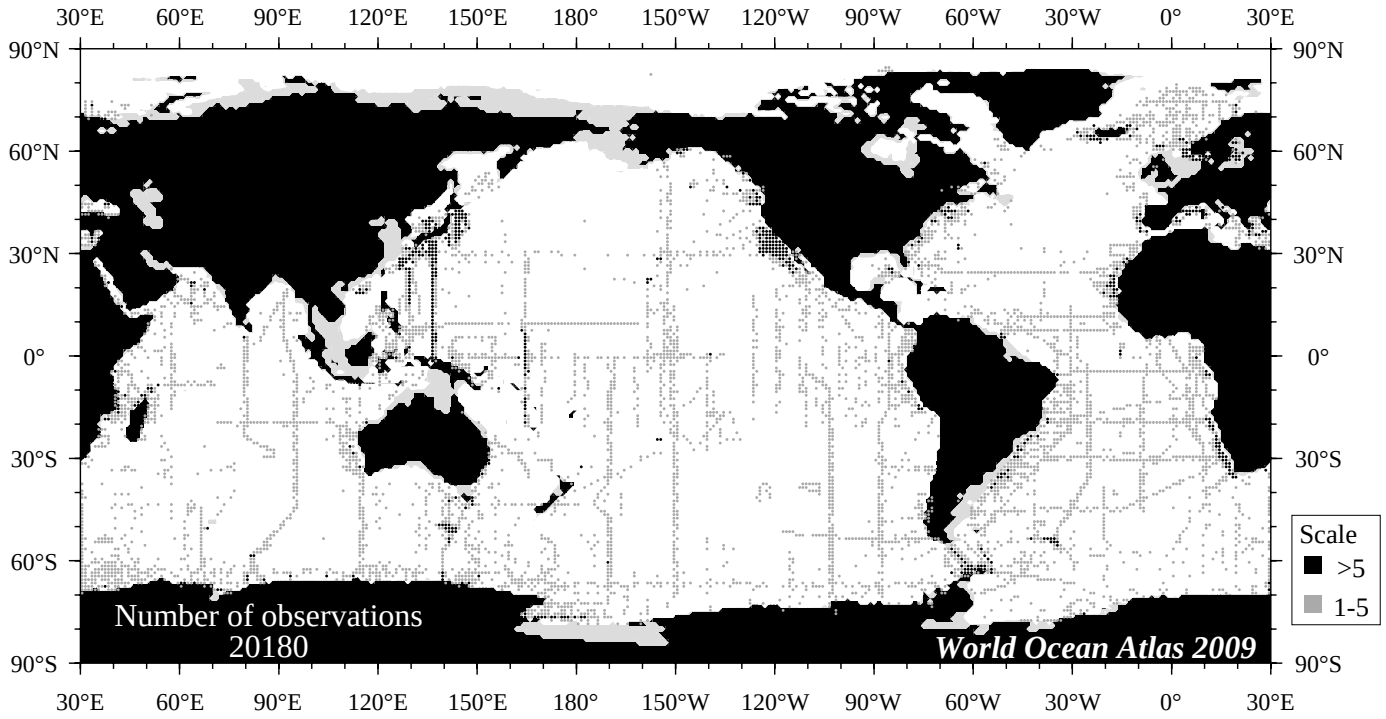

Fig E3 Winter (Jan.-Mar.) nitrate observations at 150 m. depth.

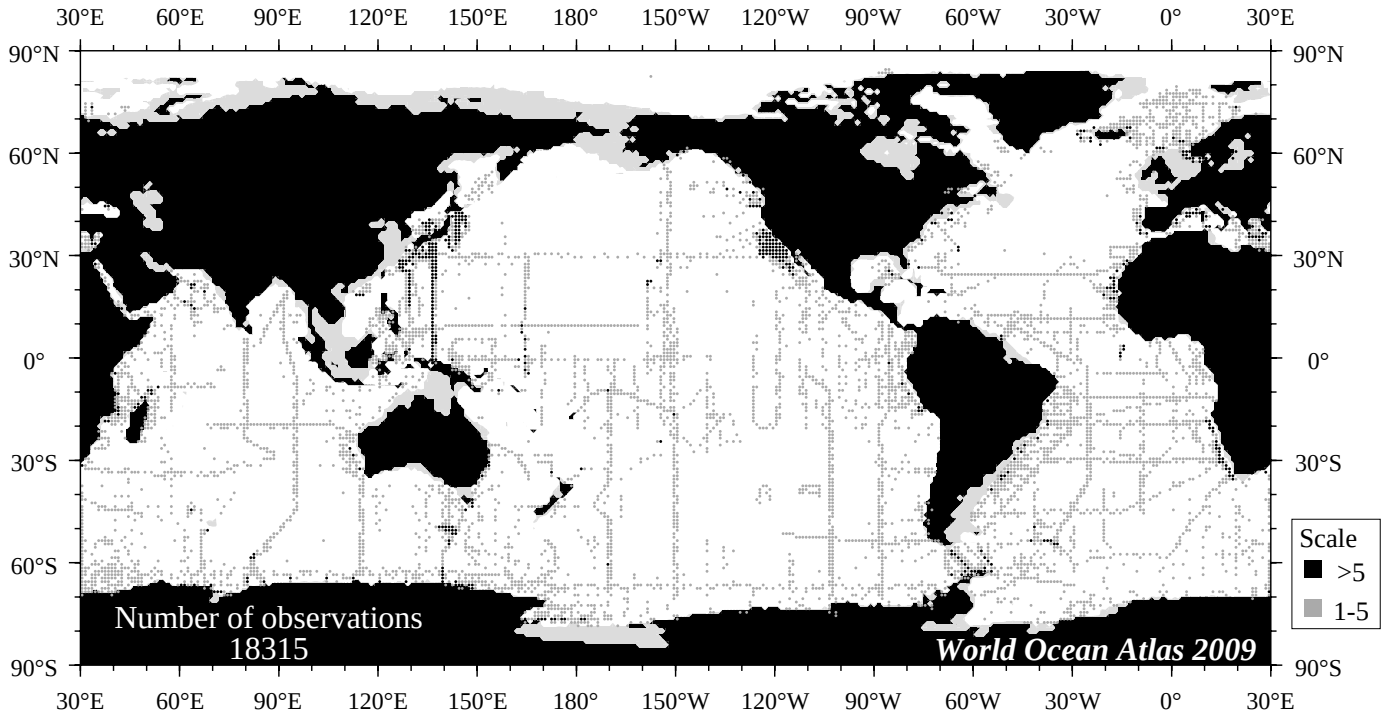

Fig E4 Winter (Jan.-Mar.) nitrate observations at 250 m. depth.

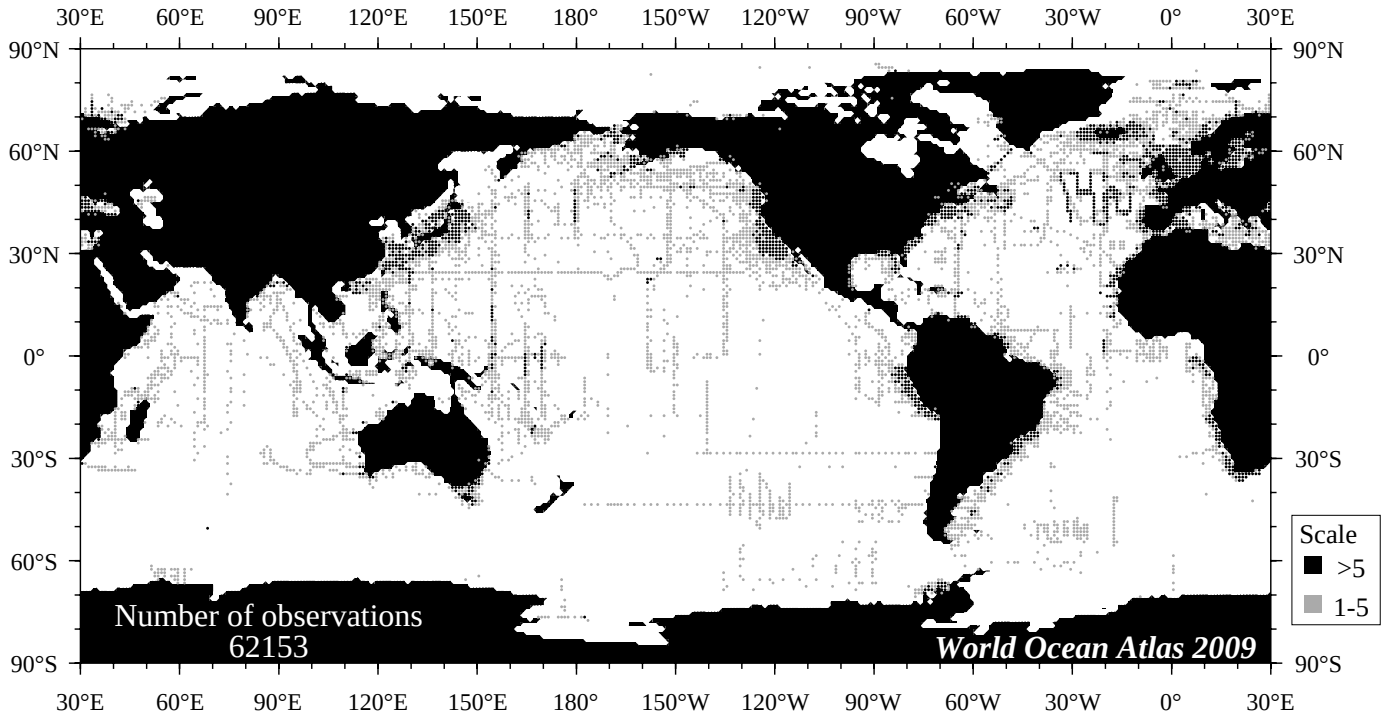

Fig E5 Spring (Apr.-Jun.) nitrate observations at the surface.

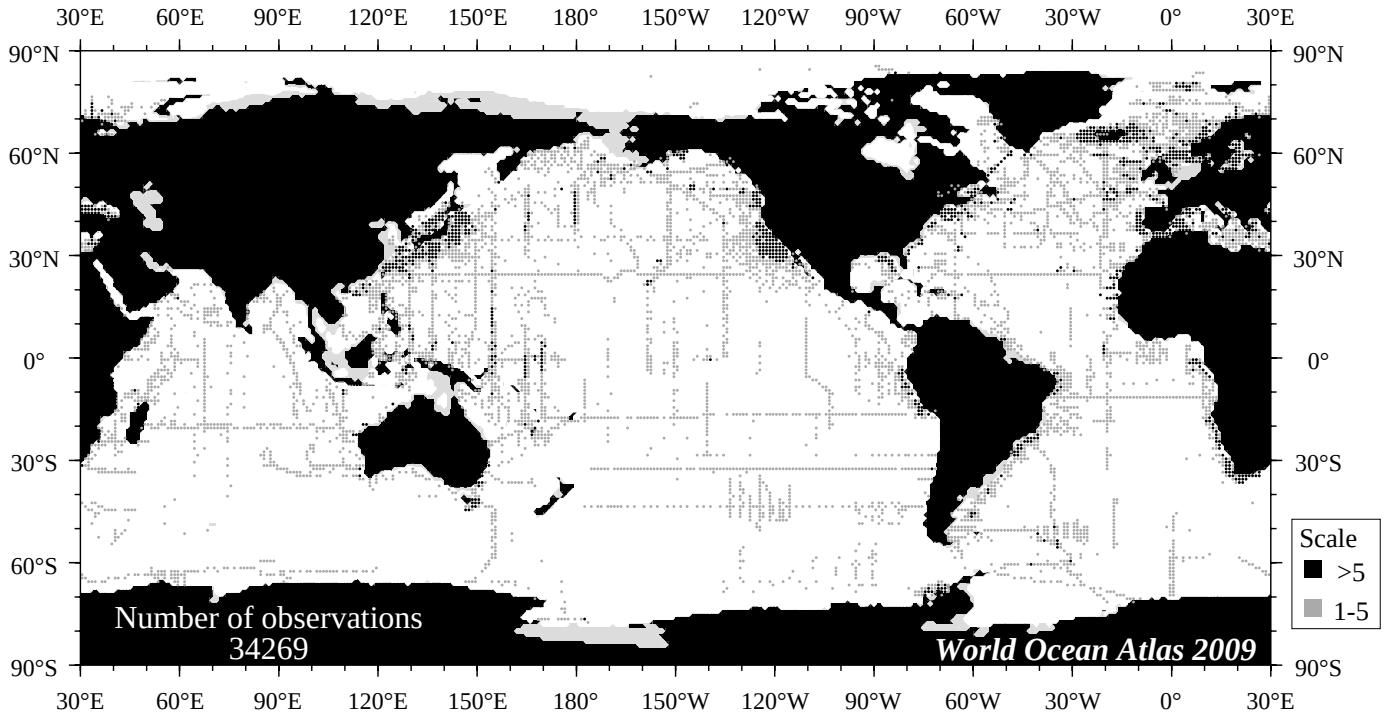

Fig E6 Spring (Apr.-Jun.) nitrate observations at 75 m. depth.

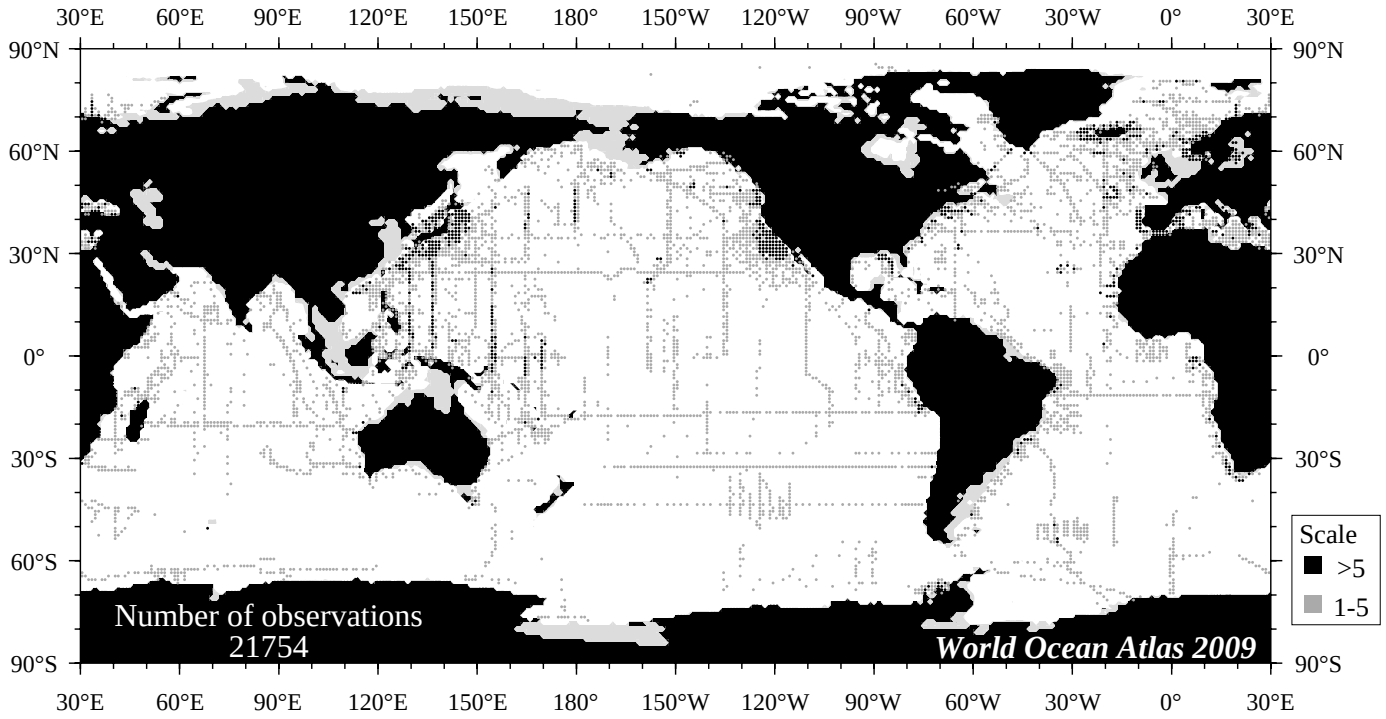

Fig E7 Spring (Apr.-Jun.) nitrate observations at 150 m. depth.

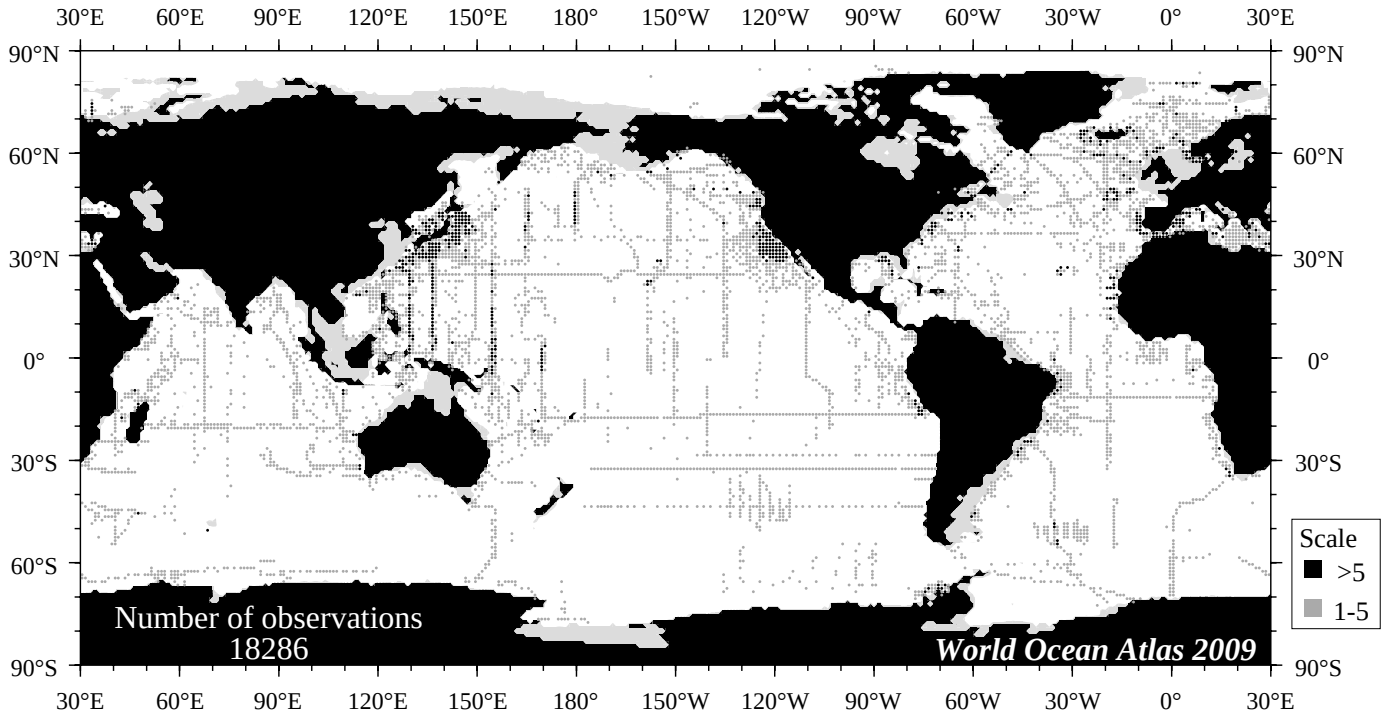

Fig E8 Spring (Apr.-Jun.) nitrate observations at 250 m. depth.

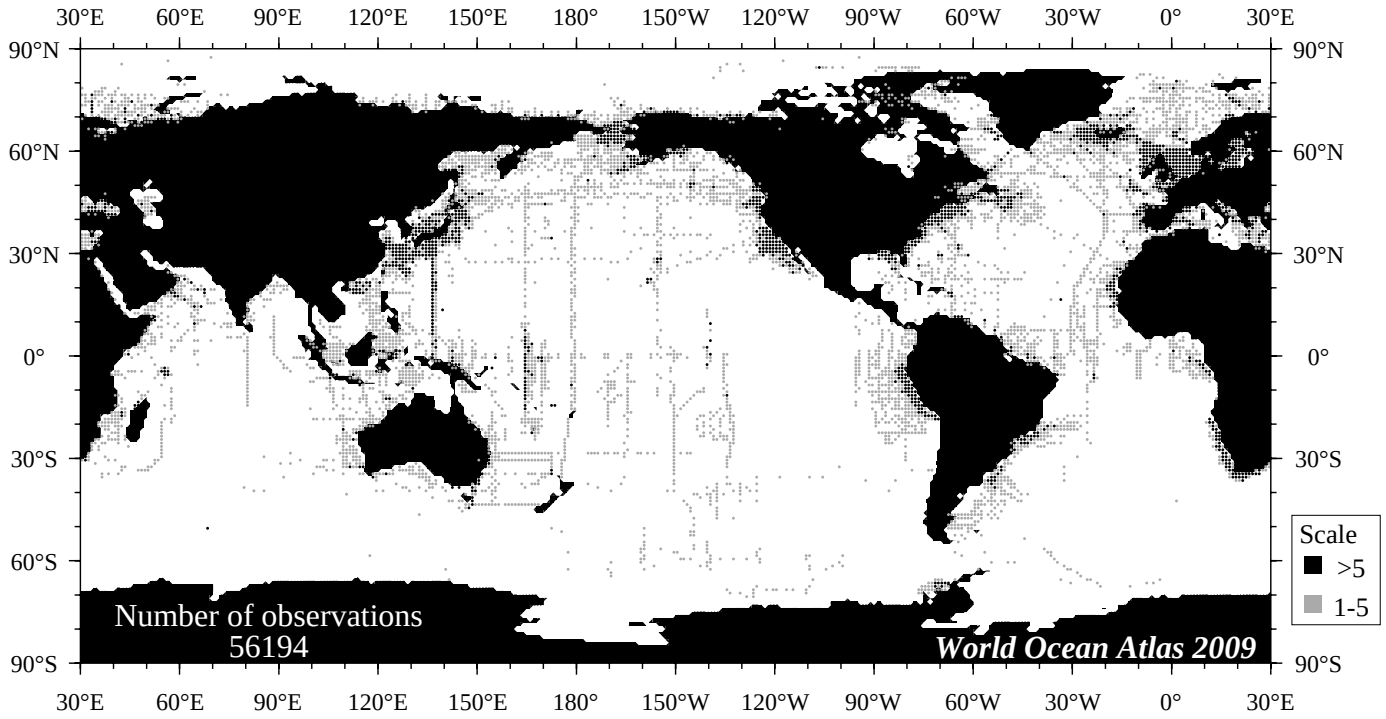

Fig E9 Summer (Jul.-Sep.) nitrate observations at the surface.

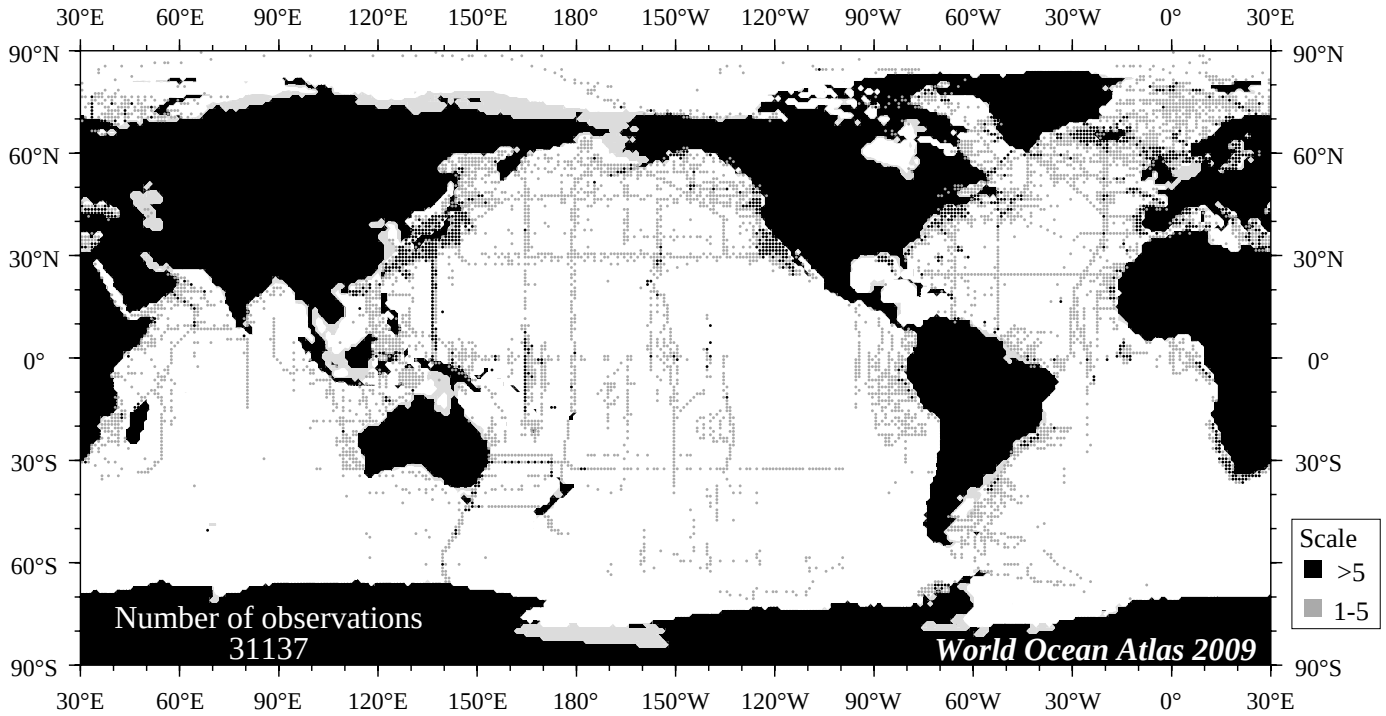

Fig E10 Summer (Jul.-Sep.) nitrate observations at 75 m. depth.

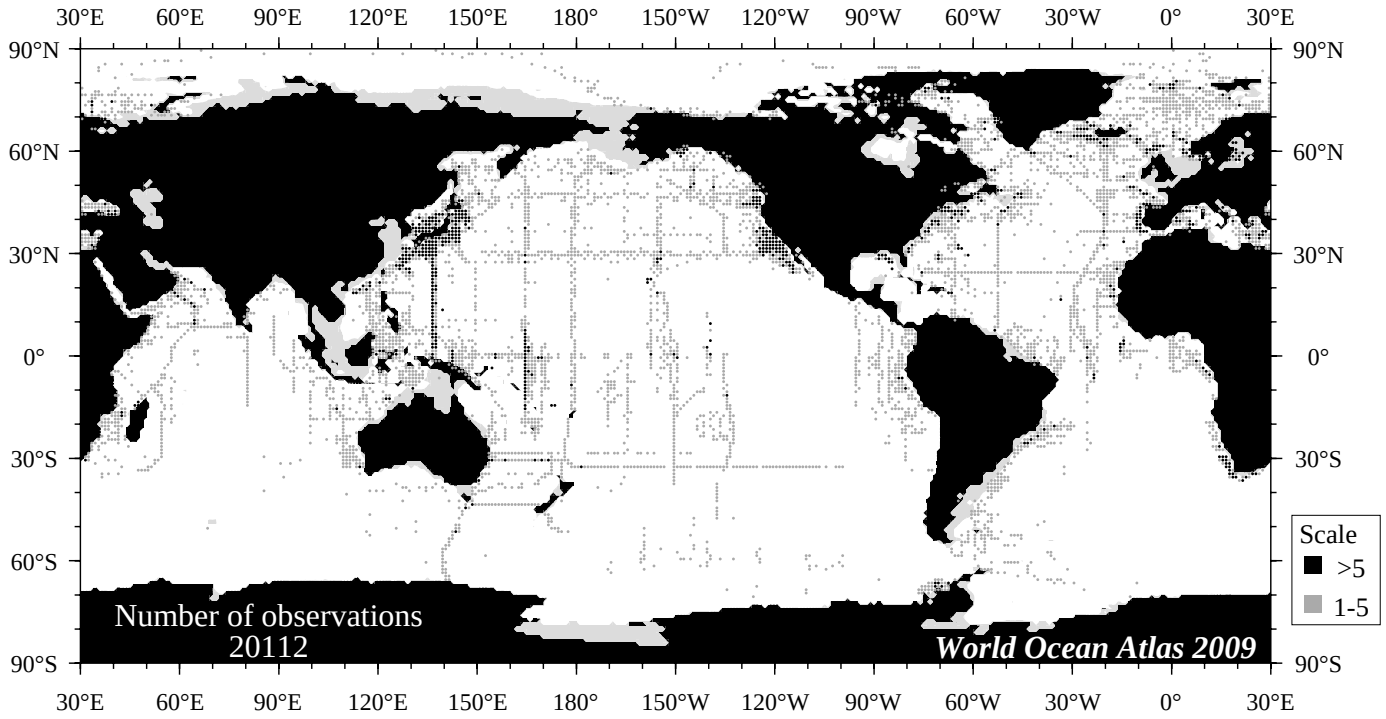

Fig E11 Summer (Jul.-Sep.) nitrate observations at 150 m. depth.

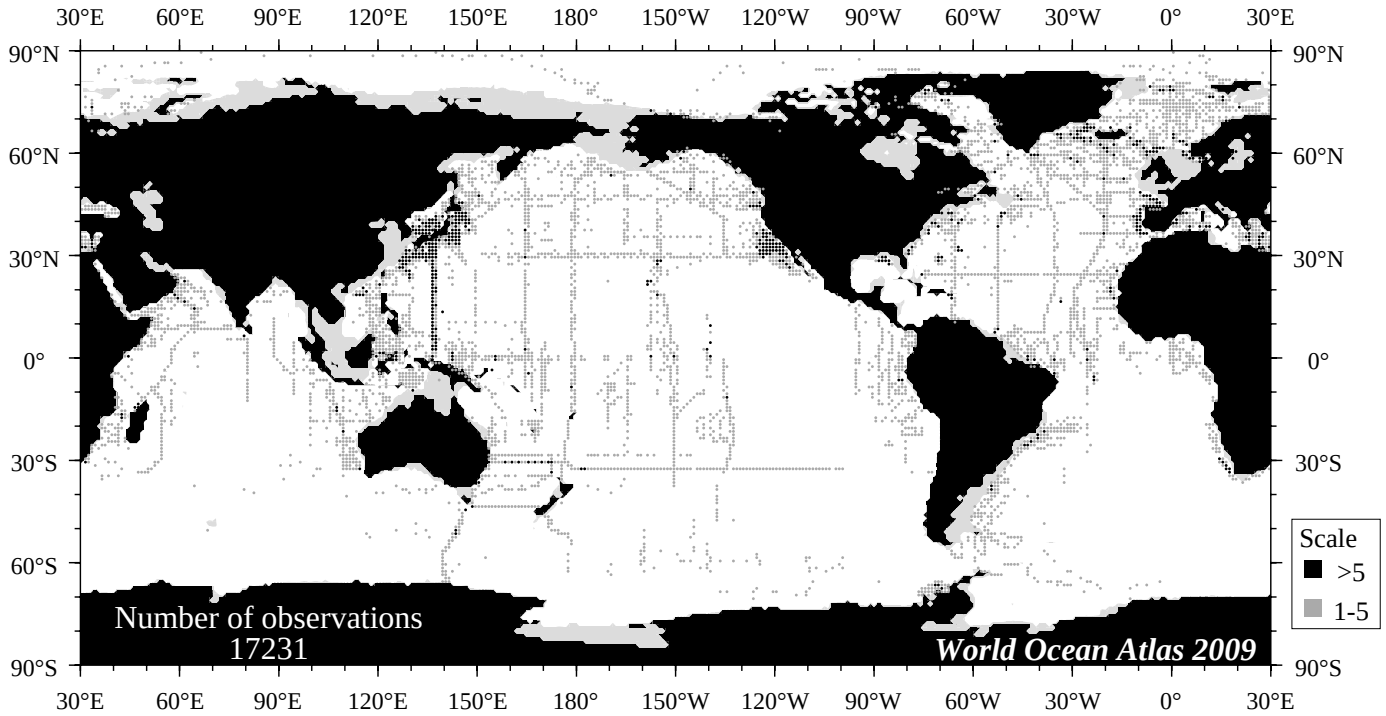

Fig E12 Summer (Jul.-Sep.) nitrate observations at 250 m. depth.

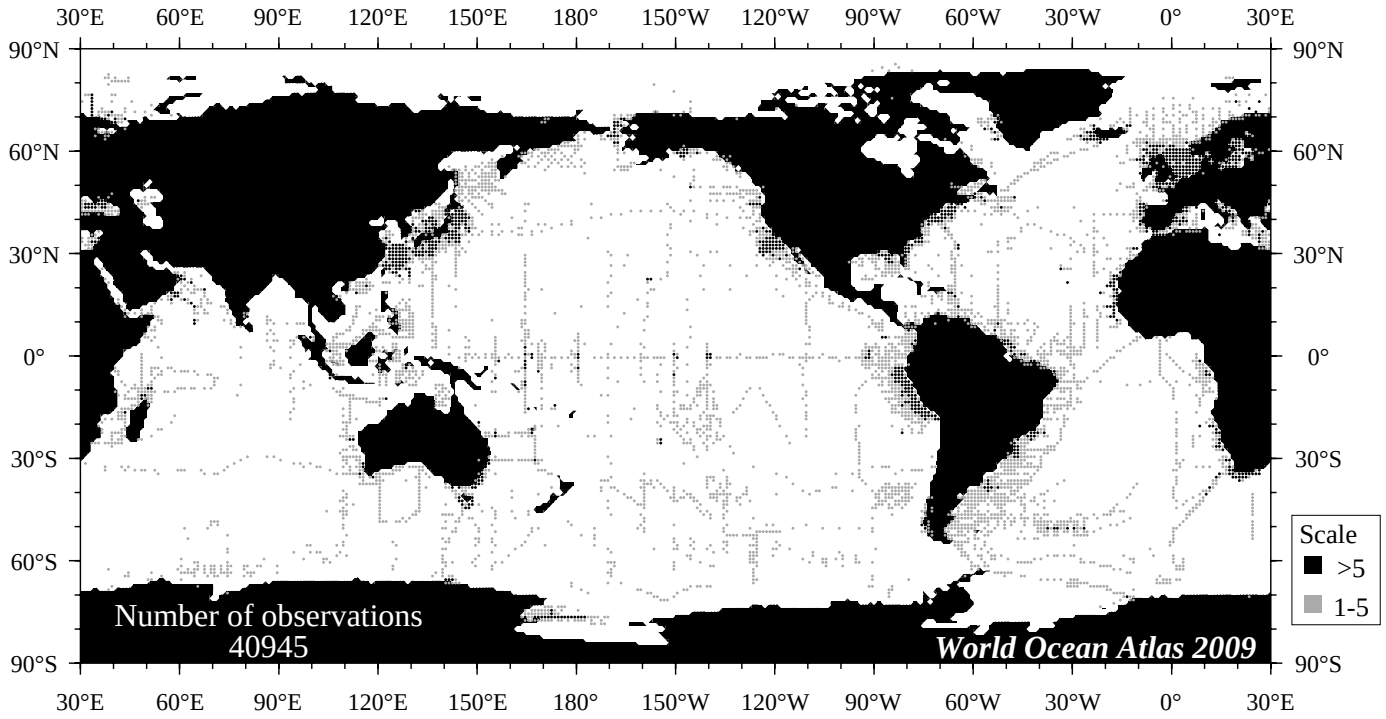

Fig E13 Fall (Oct.-Dec.) nitrate observations at the surface.

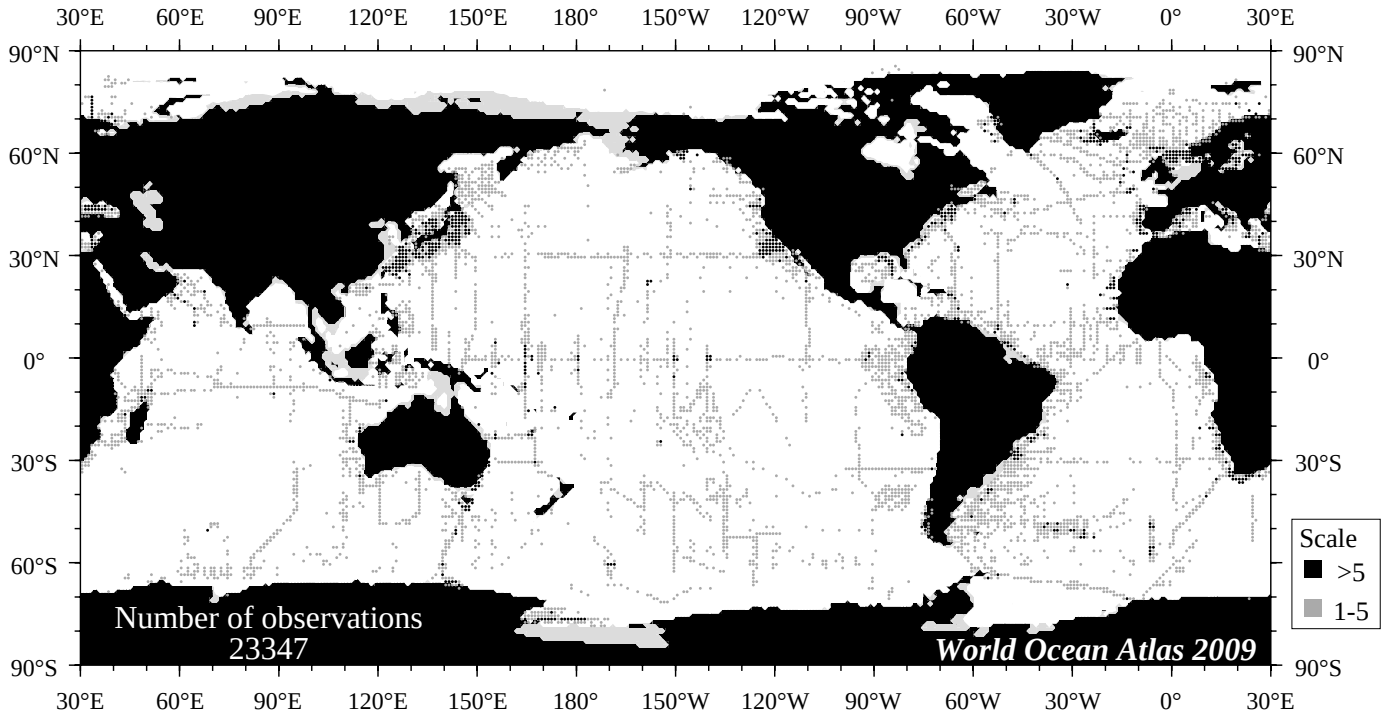

Fig E14 Fall (Oct.-Dec.) nitrate observations at 75 m. depth.

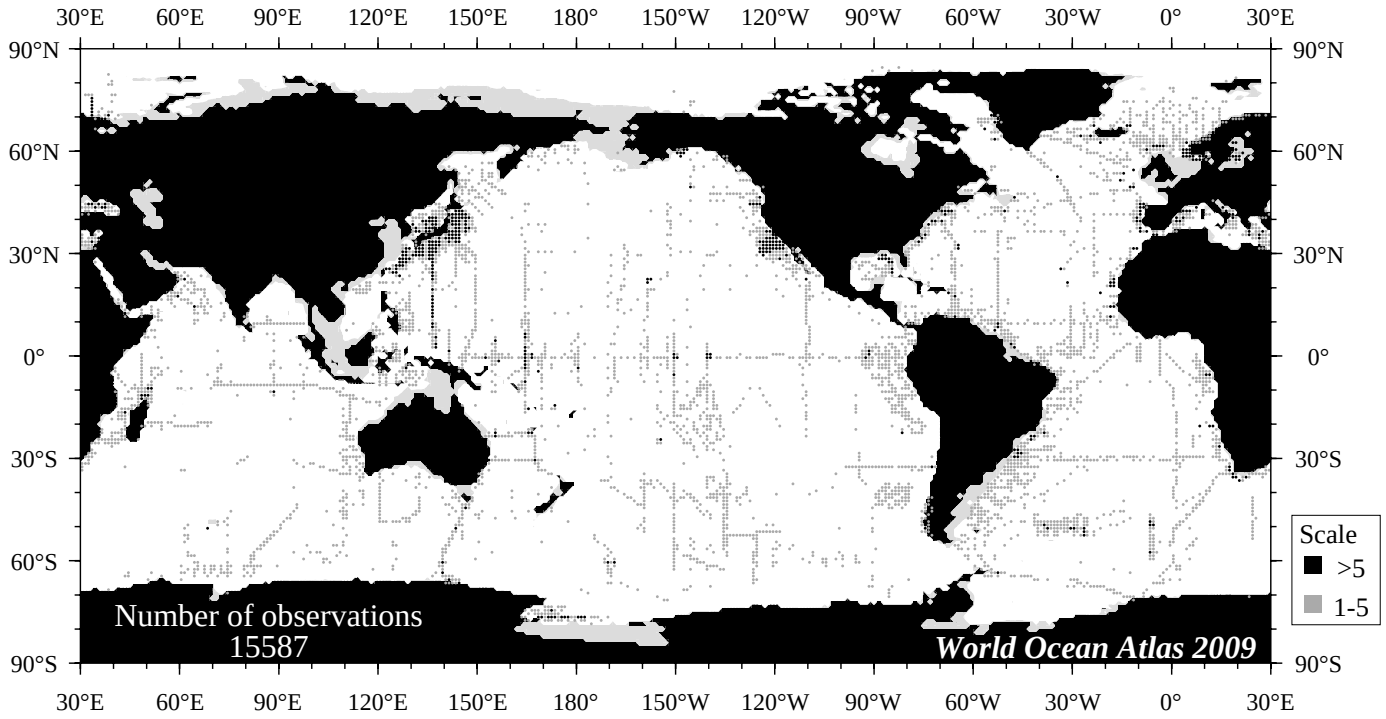

Fig E15 Fall (Oct.-Dec.) nitrate observations at 150 m. depth.

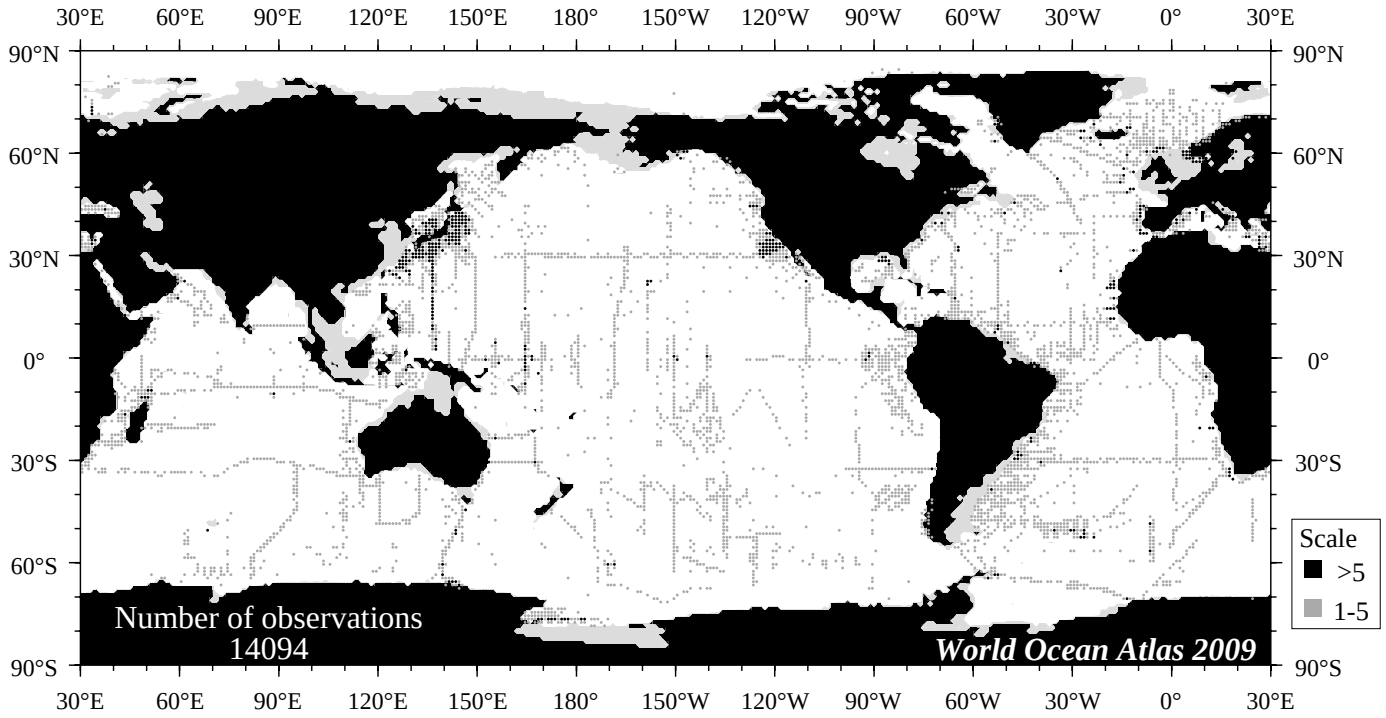

Fig E16 Fall (Oct.-Dec.) nitrate observations at 250 m. depth.

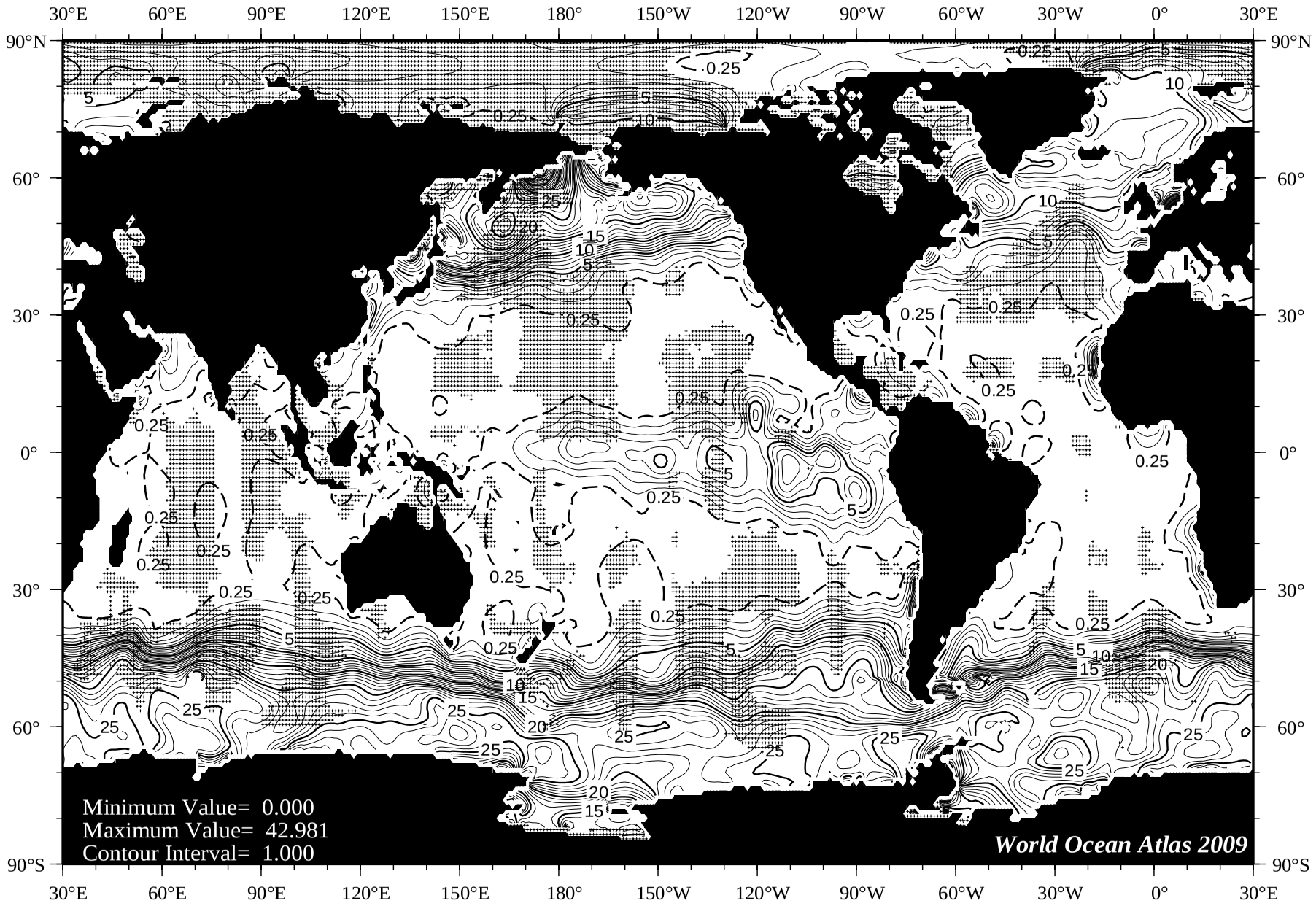

Fig E17 Winter (Jan.-Mar.) nitrate [umol/l] at the surface.

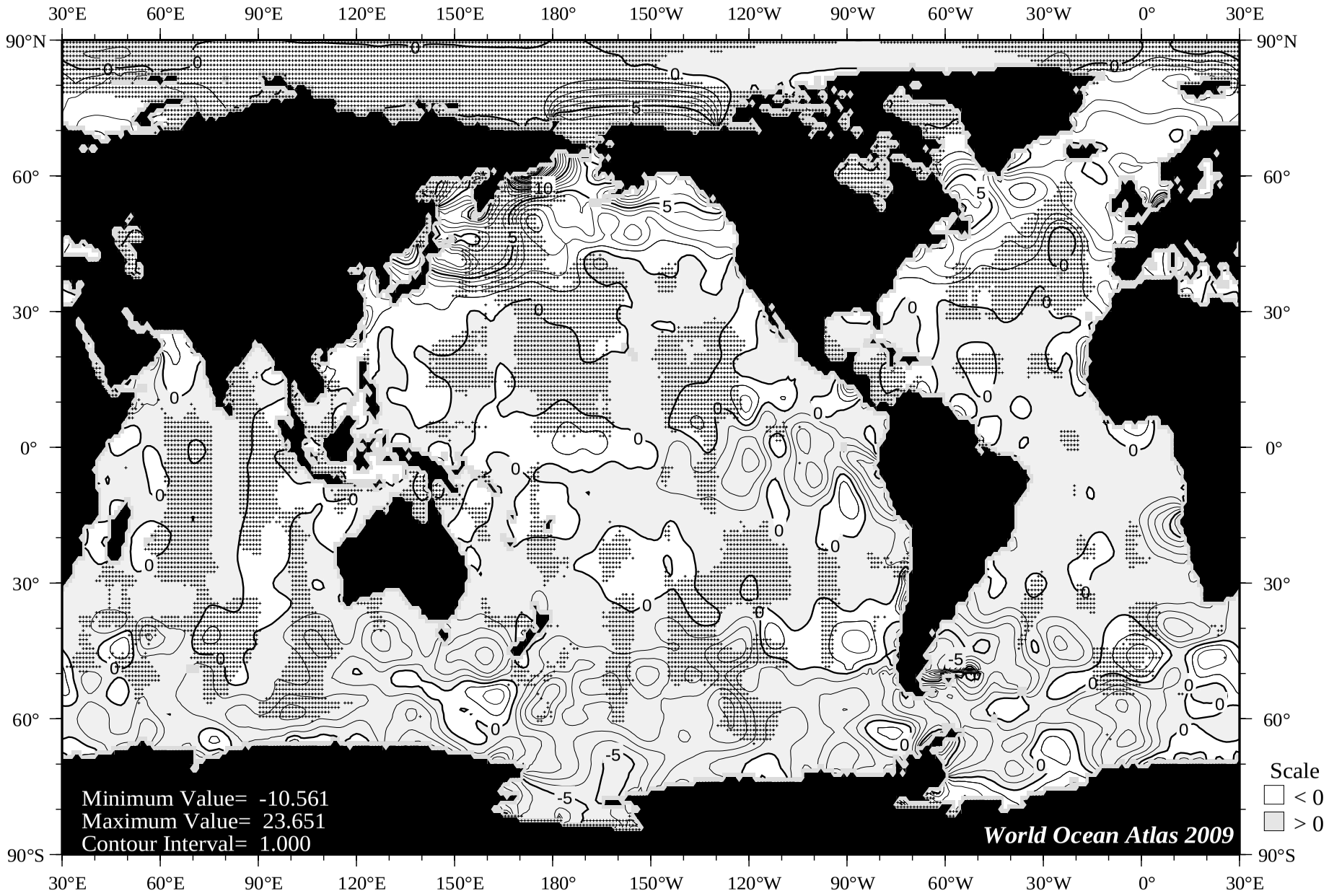

Fig E18 Winter (Jan.-Mar.) minus annual nitrate [umol/l] at the surface.

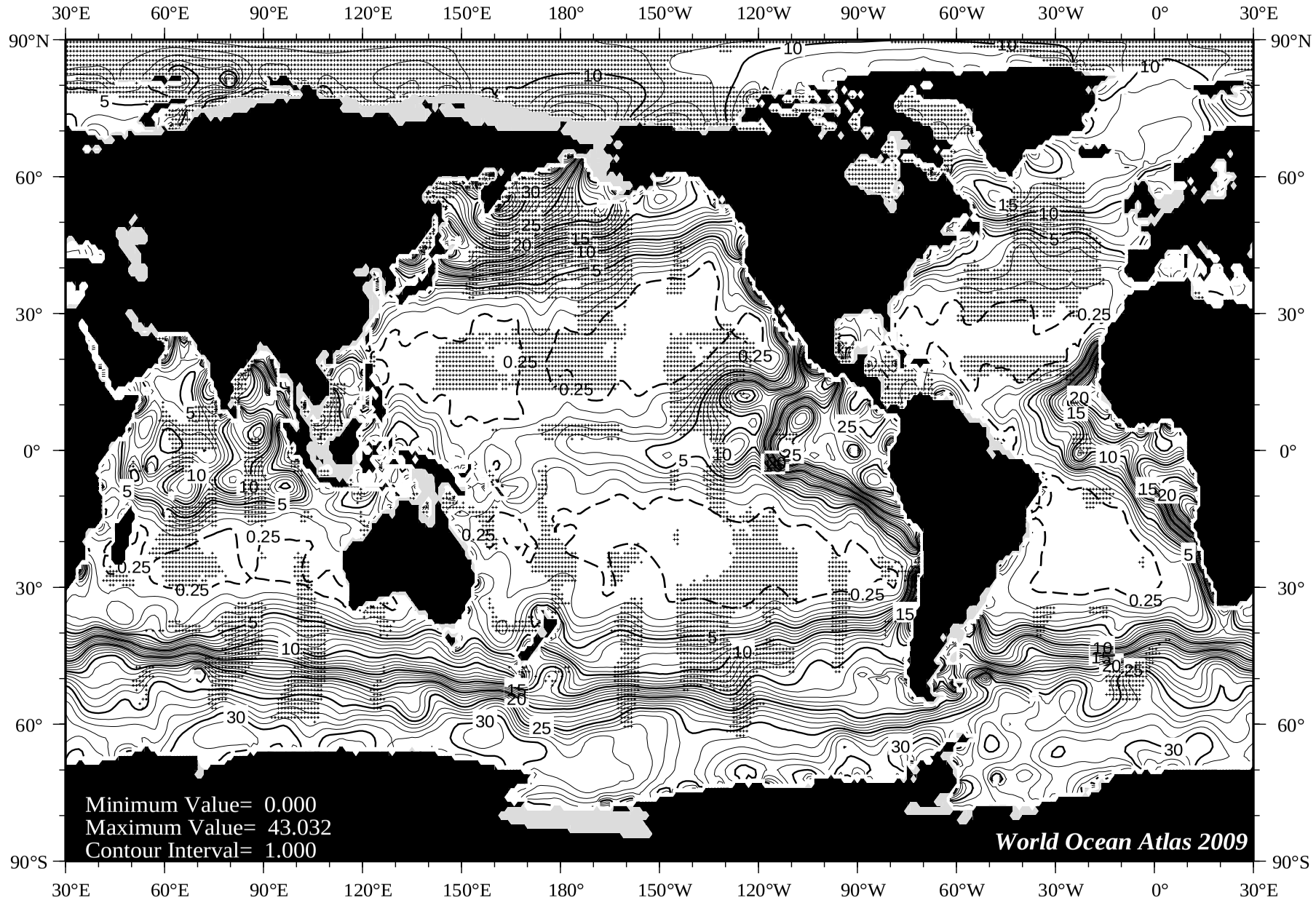

Fig E19 Winter (Jan.-Mar.) nitrate [umol/l] at 75 m. depth.

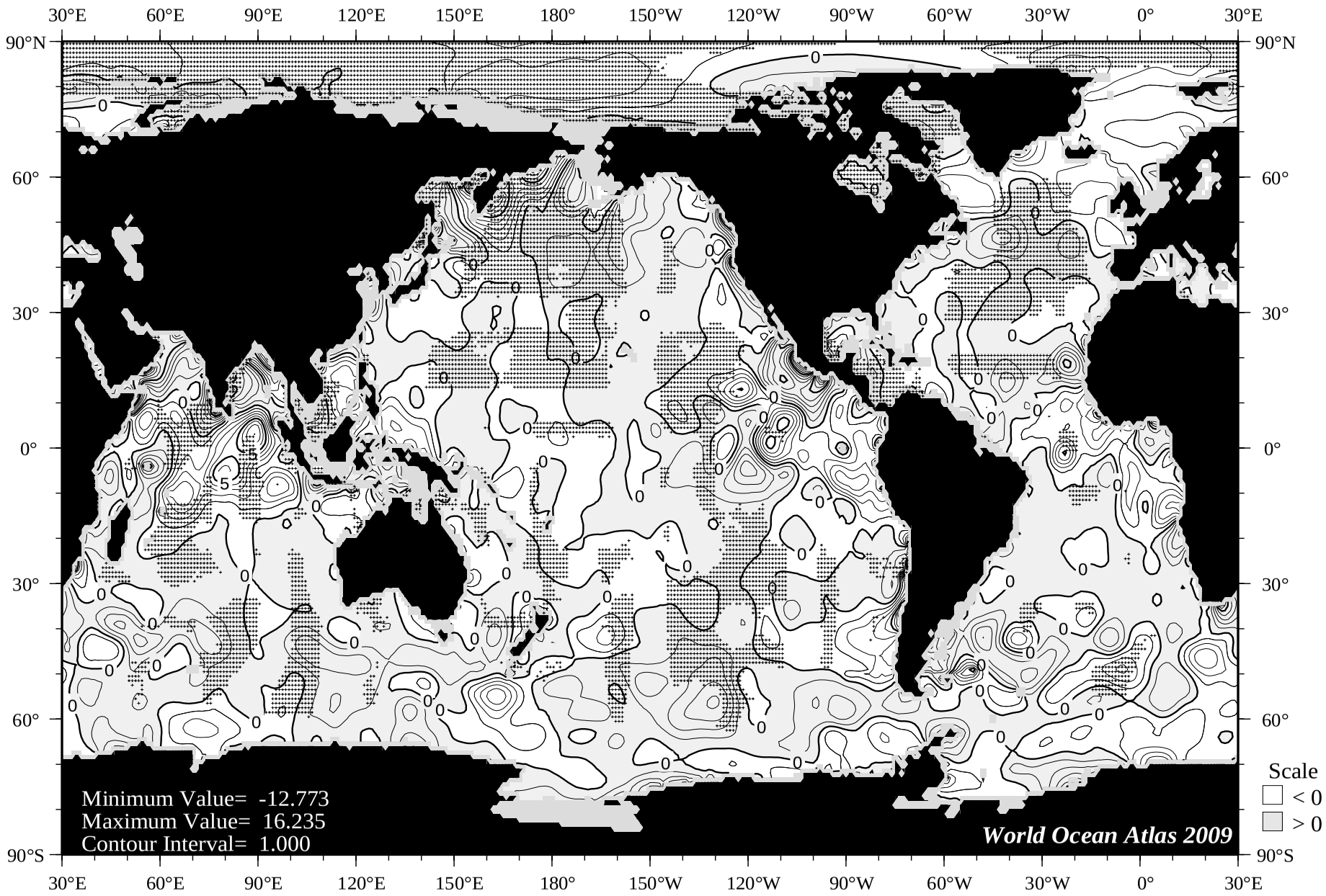

Fig E20 Winter (Jan.-Mar.) minus annual nitrate [umol/l] at 75 m. depth.

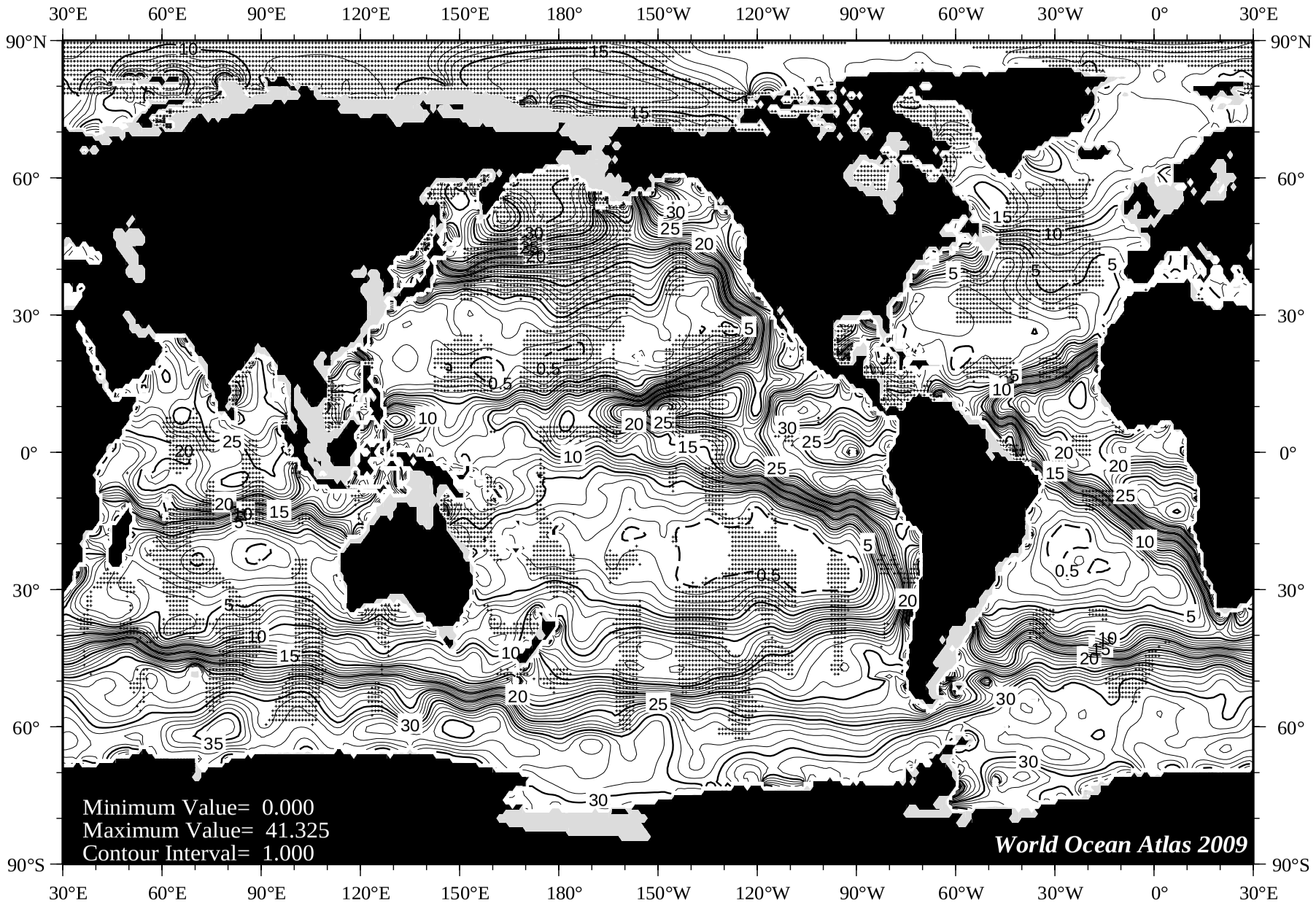

Fig E21 Winter (Jan.-Mar.) nitrate [umol/l] at 150 m. depth.

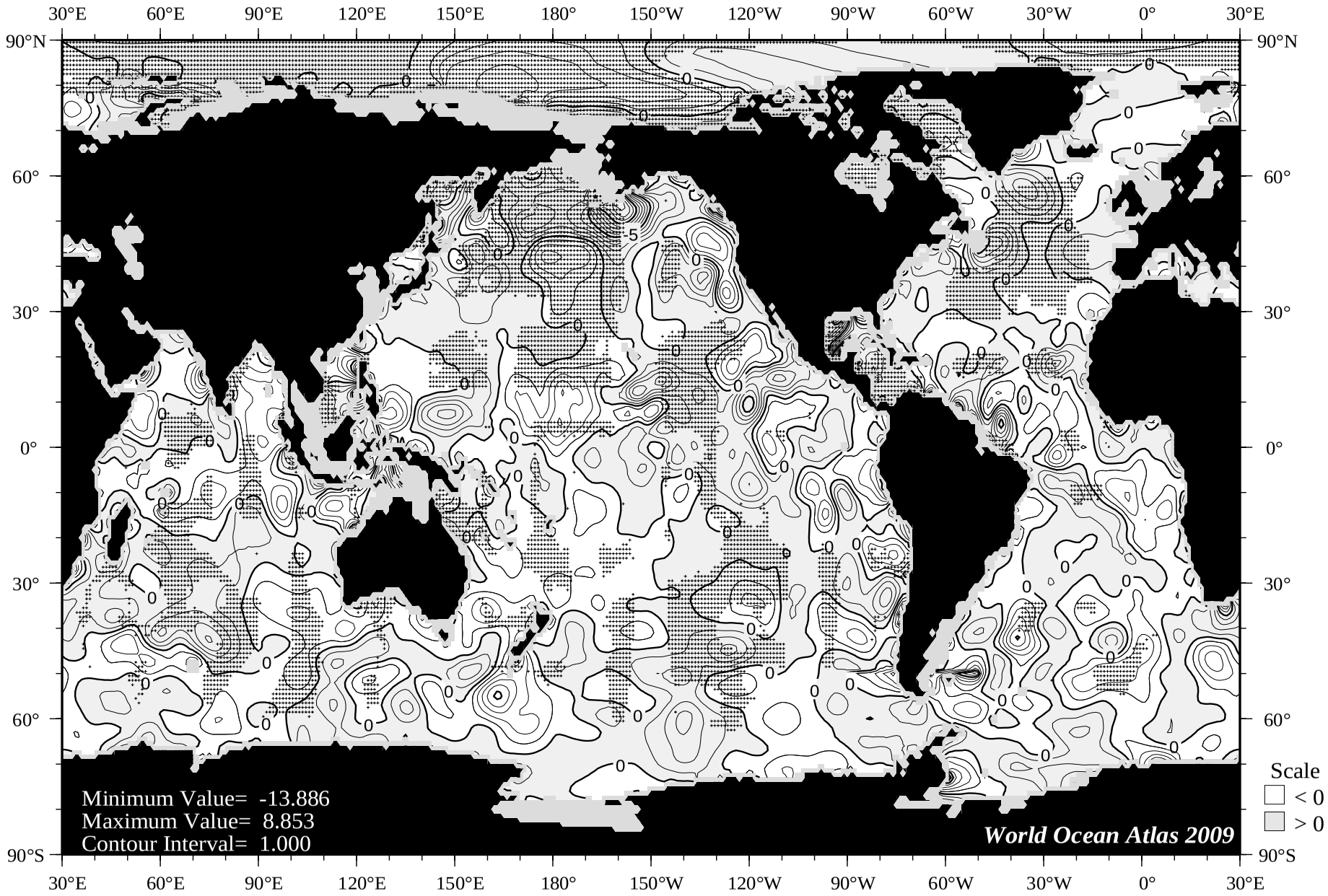

Fig E22 Winter (Jan.-Mar.) minus annual nitrate [umol/l] at 150 m. depth.

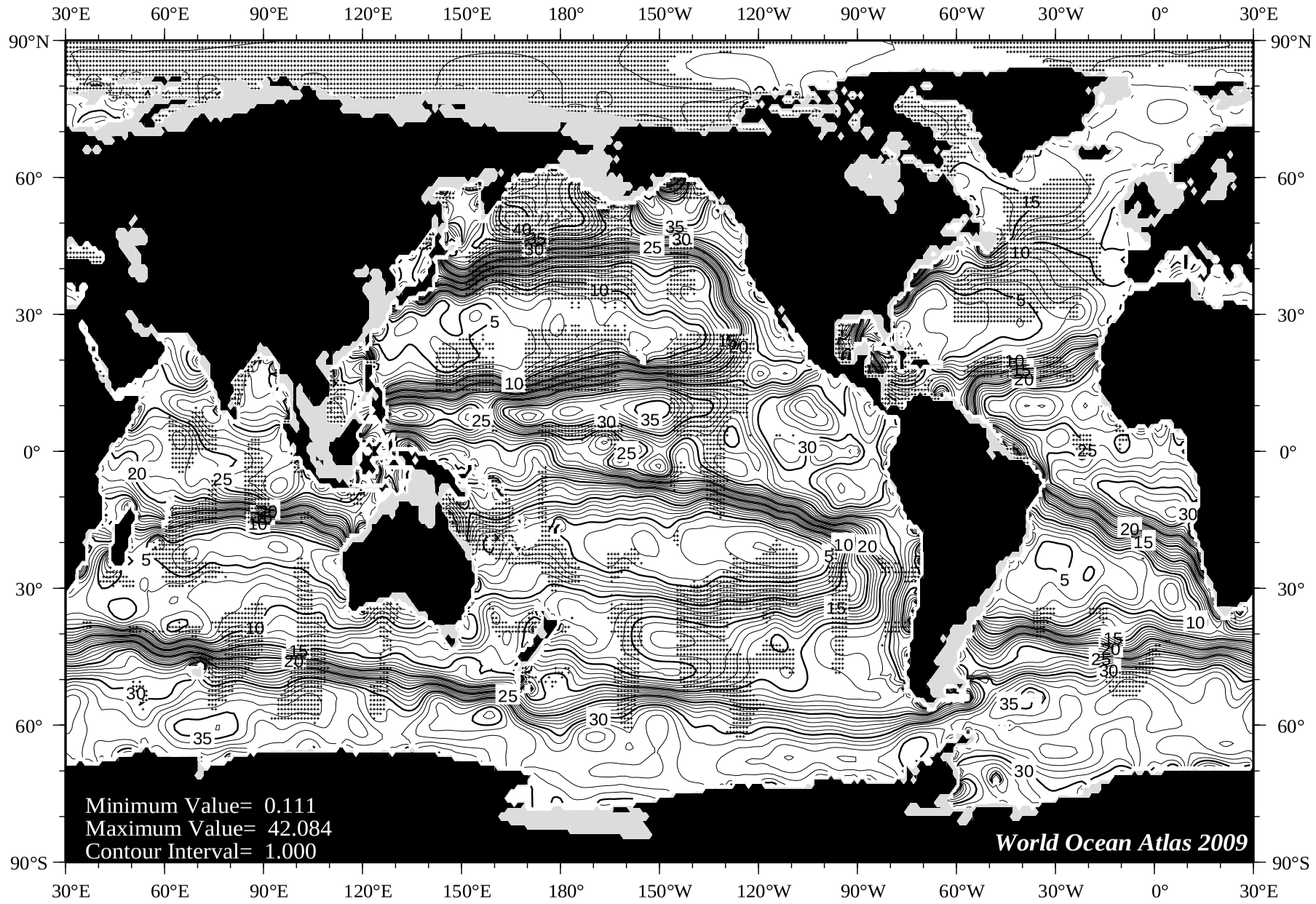

Fig E23 Winter (Jan.-Mar.) nitrate [umol/l] at 250 m. depth.

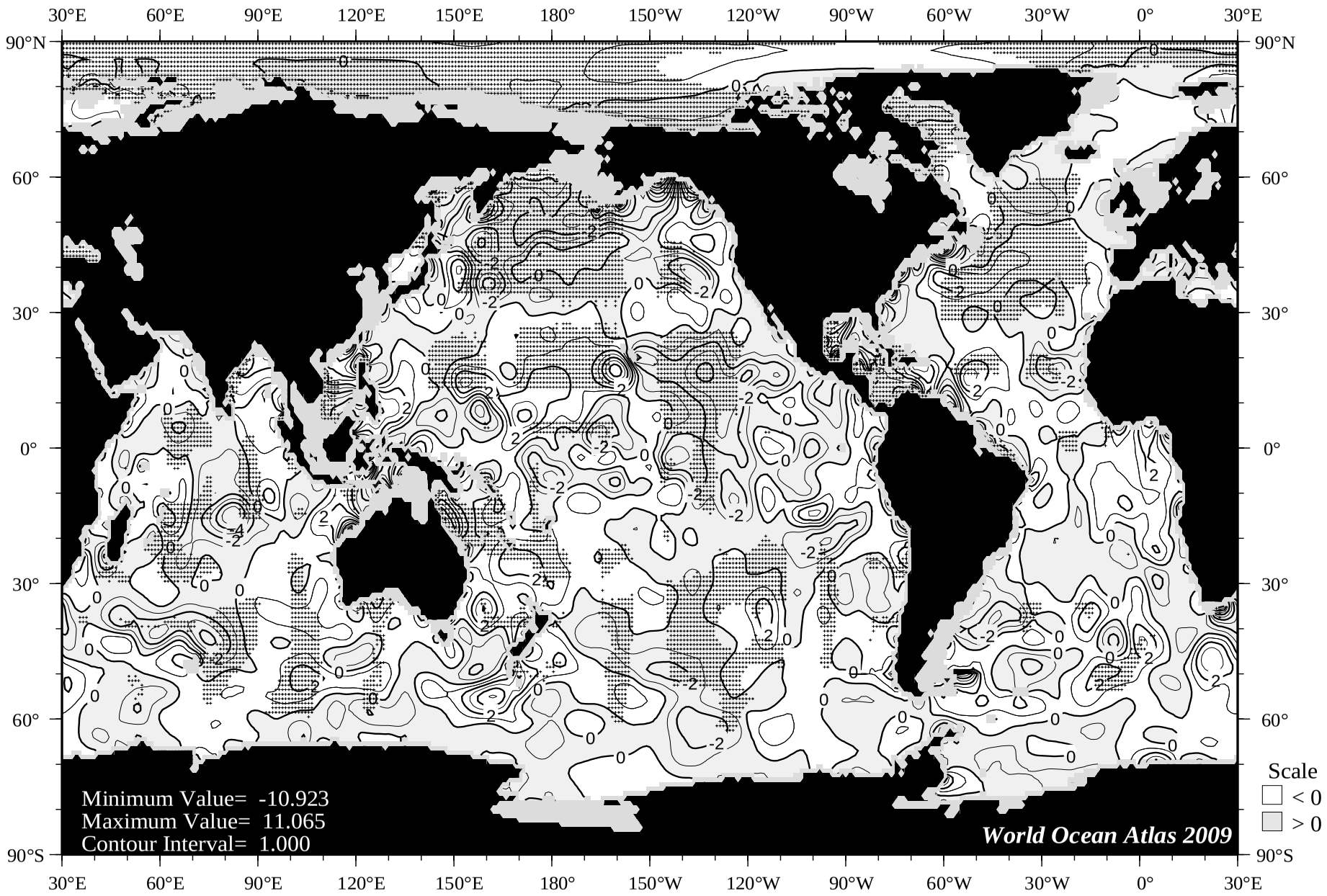

Fig E24 Winter (Jan.-Mar.) minus annual nitrate [umol/l] at 250 m. depth.

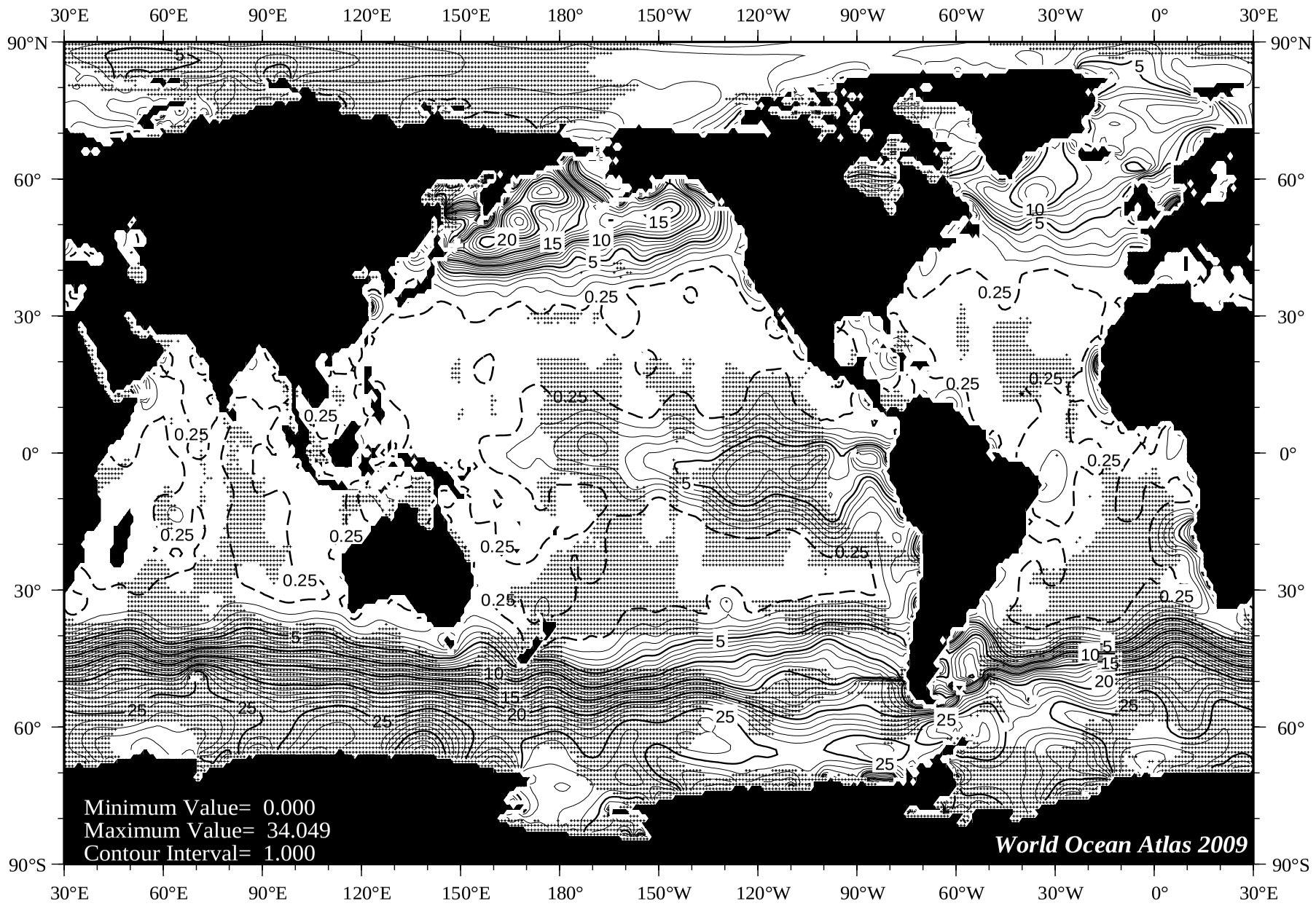

Fig E25 Spring (Apr.-Jun.) nitrate [umol/l] at the surface.

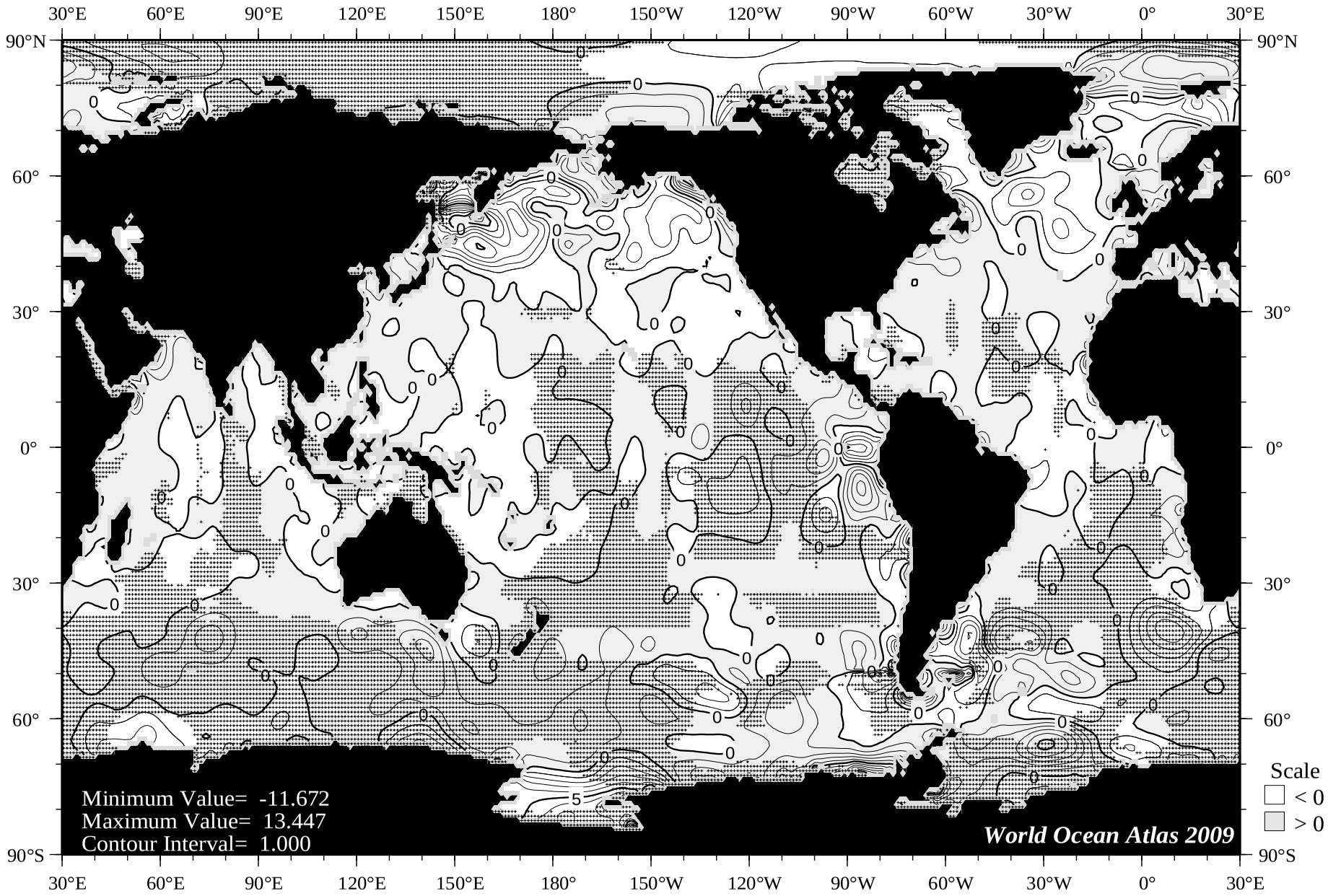

Fig E26 Spring (Apr.-Jun.) minus annual nitrate [umol/l] at the surface.

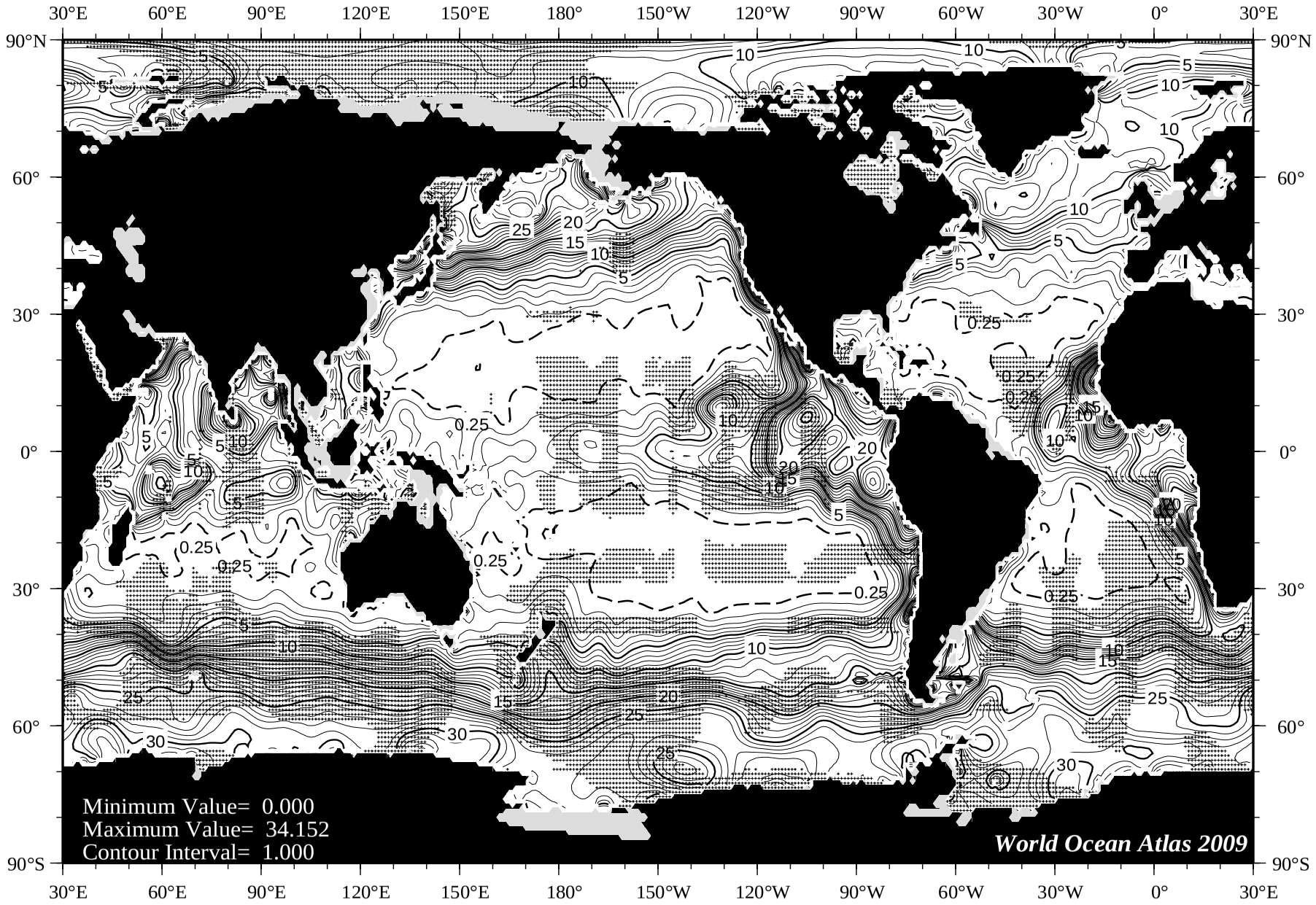

Fig E27 Spring (Apr.-Jun.) nitrate [umol/l] at 75 m. depth.

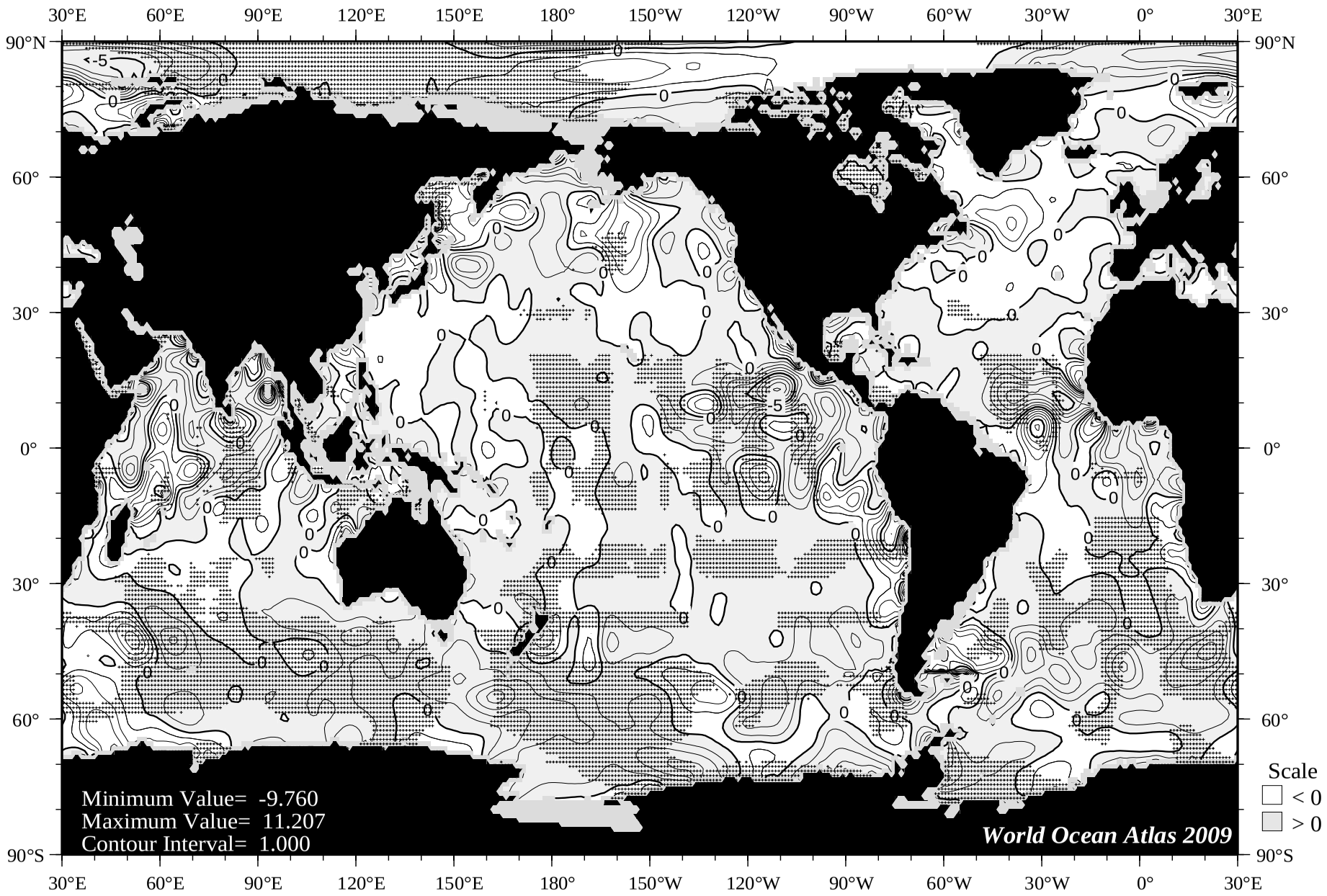

Fig E28 Spring (Apr.-Jun.) minus annual nitrate [umol/l] at 75 m. depth.

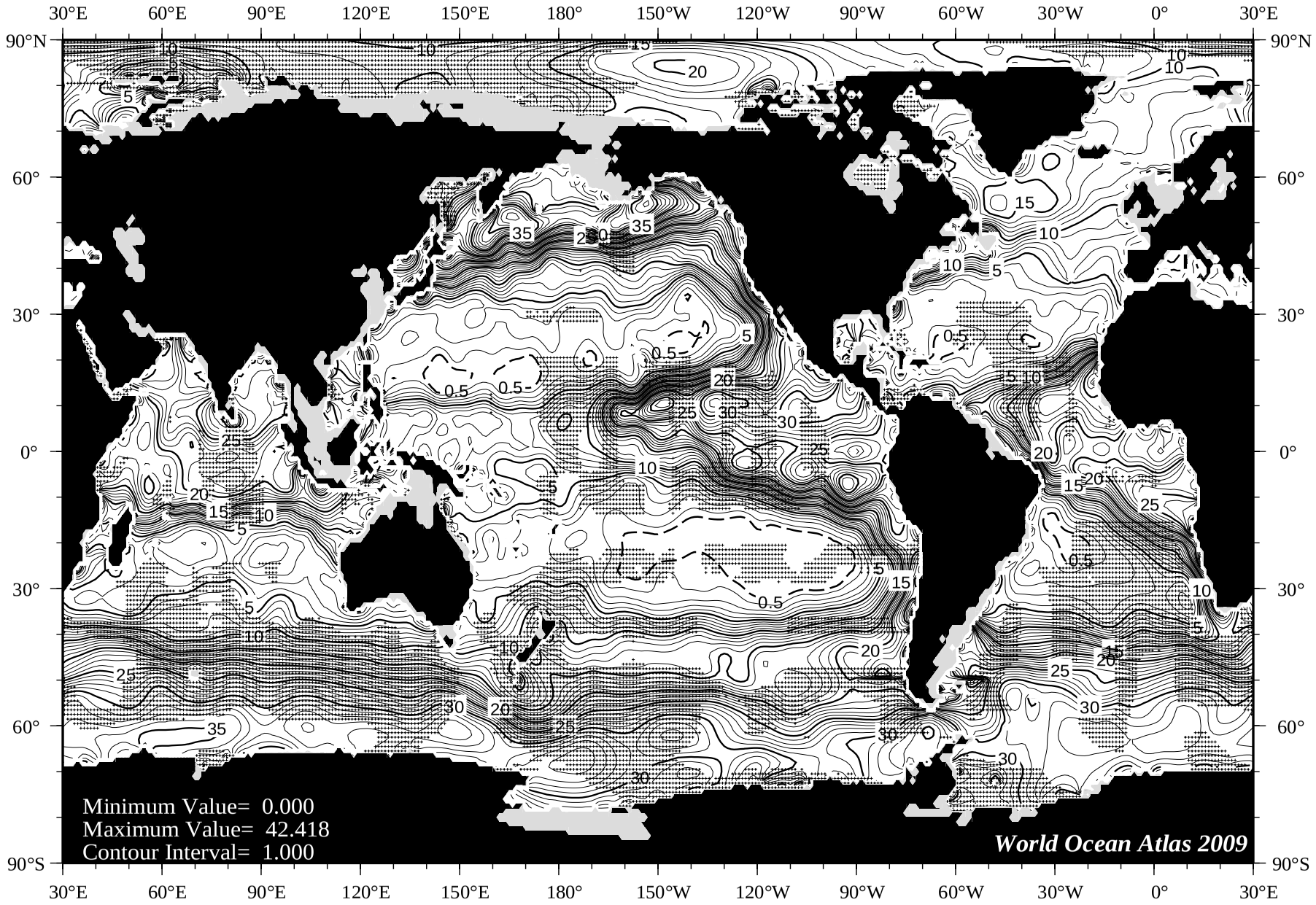

Fig E29 Spring (Apr.-Jun.) nitrate [umol/l] at 150 m. depth.

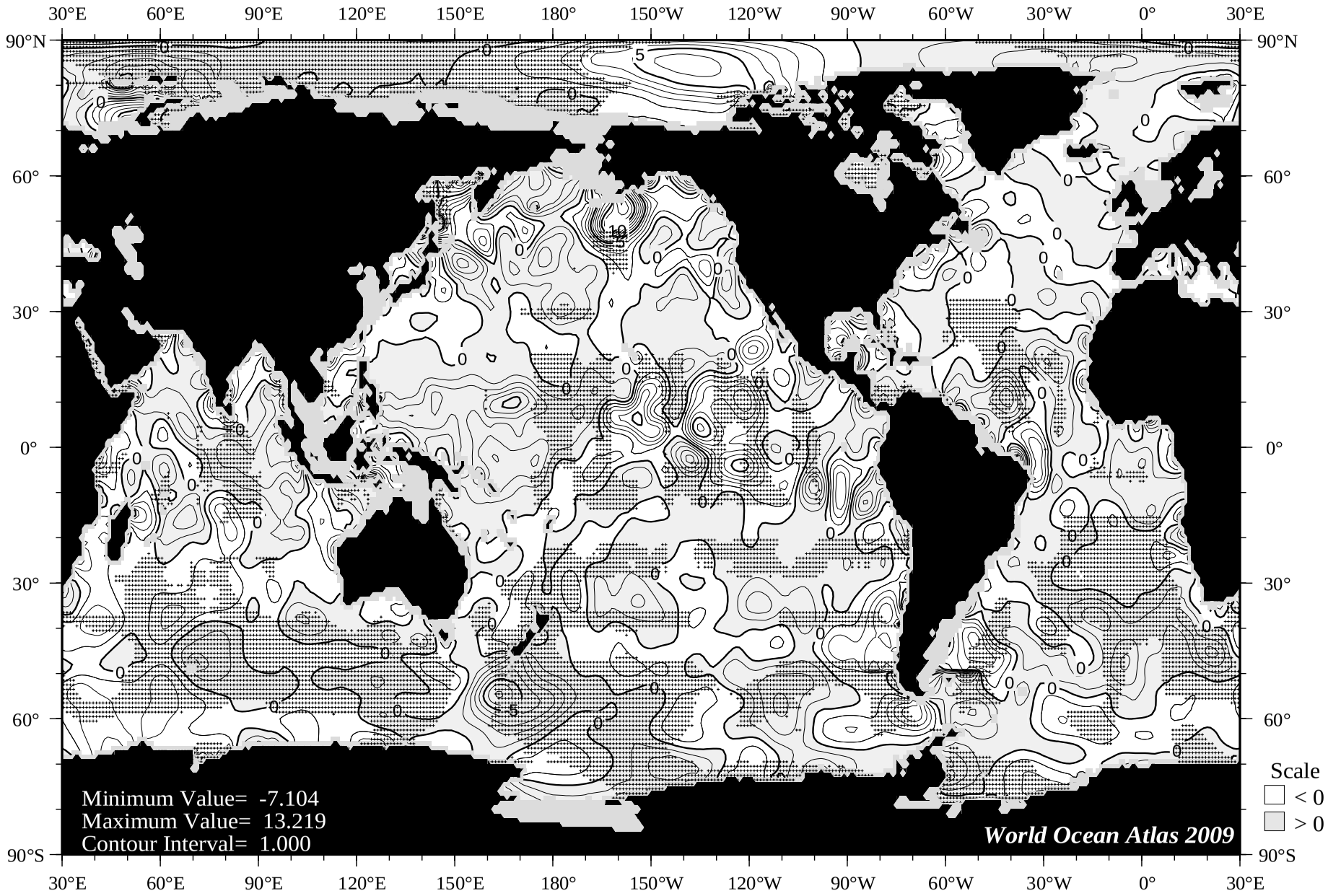

Fig E30 Spring (Apr.-Jun.) minus annual nitrate [umol/l] at 150 m. depth.

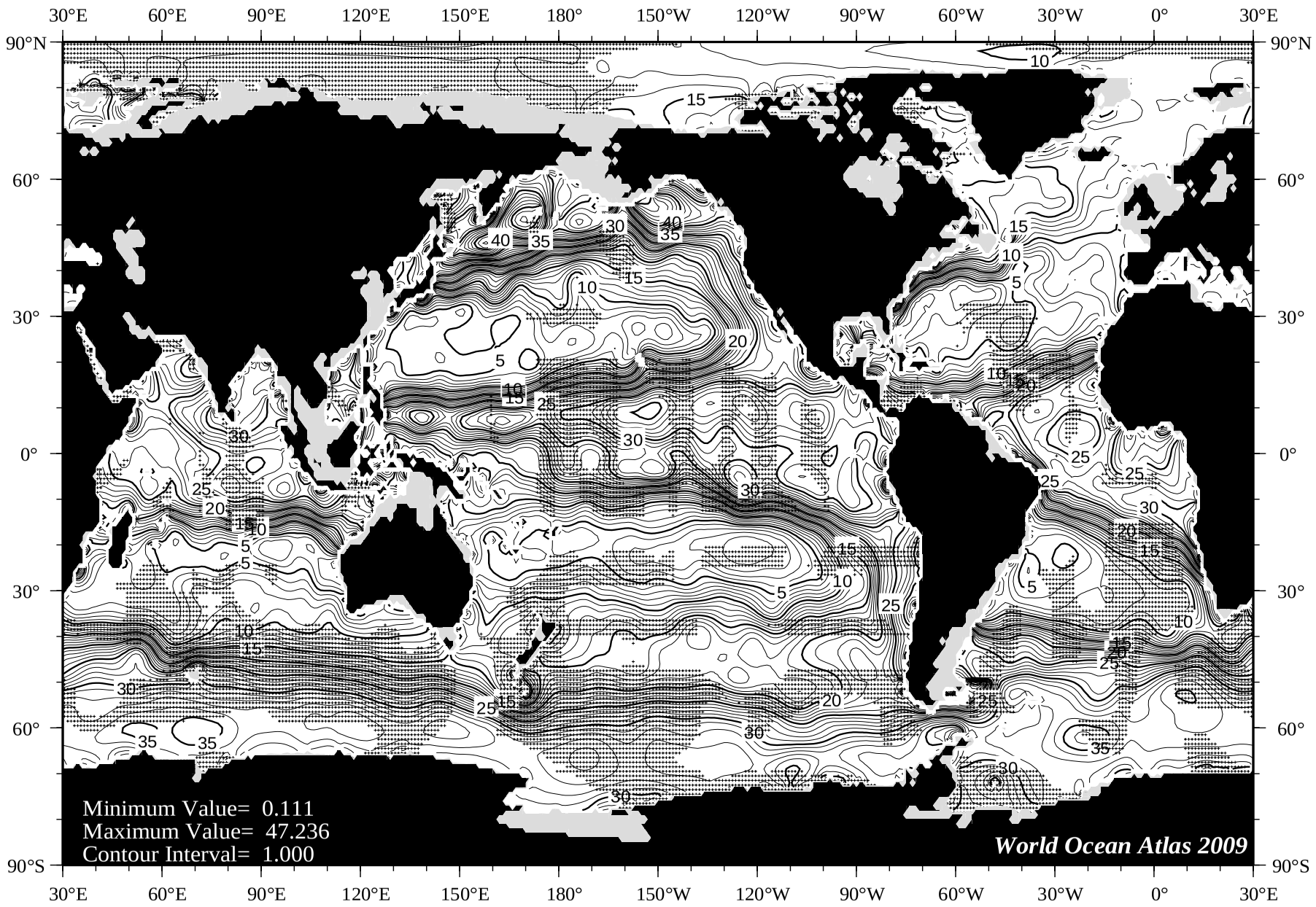

Fig E31 Spring (Apr.-Jun.) nitrate [umol/l] at 250 m. depth.

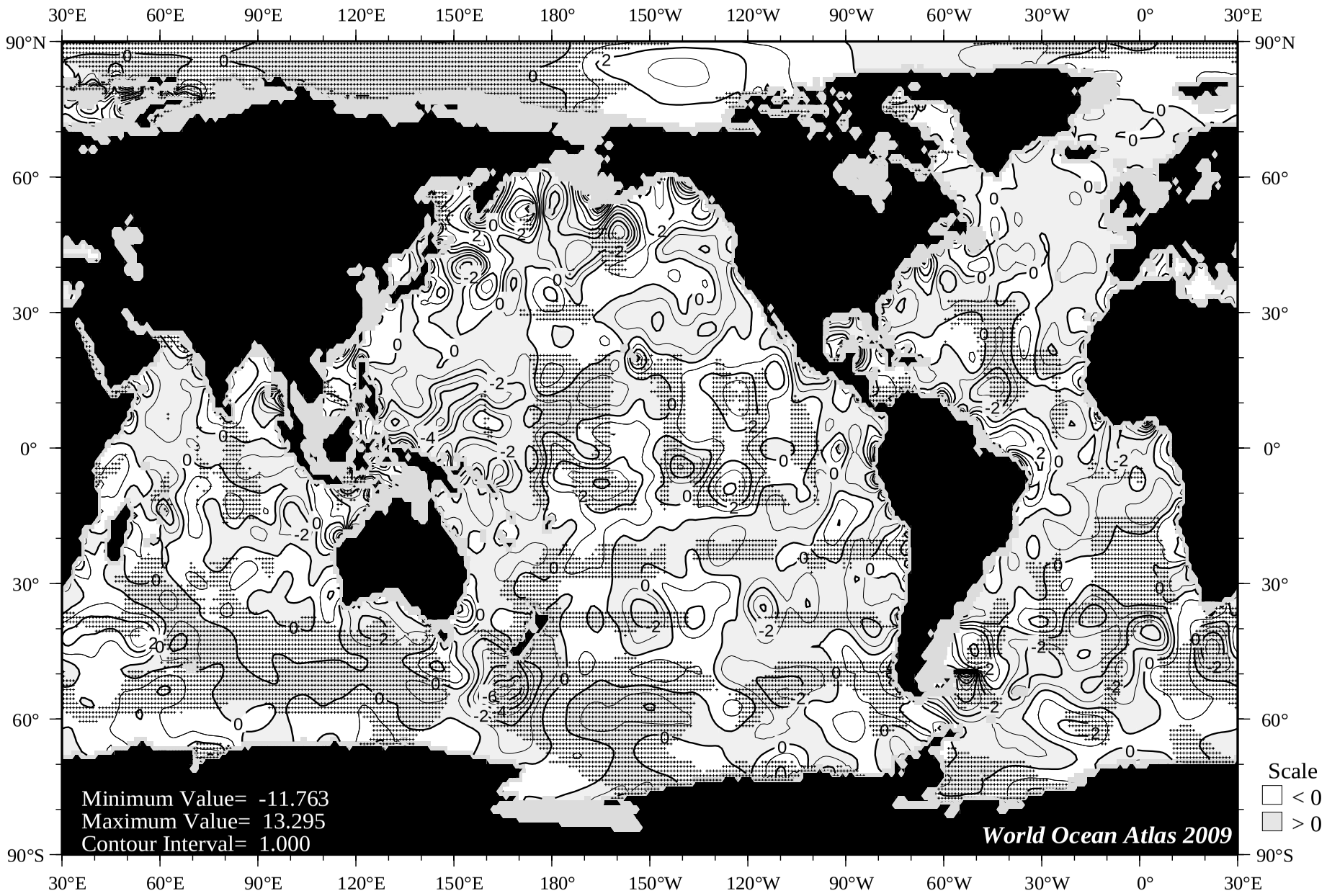

Fig E32 Spring (Apr.-Jun.) minus annual nitrate [umol/l] at 250 m. depth.

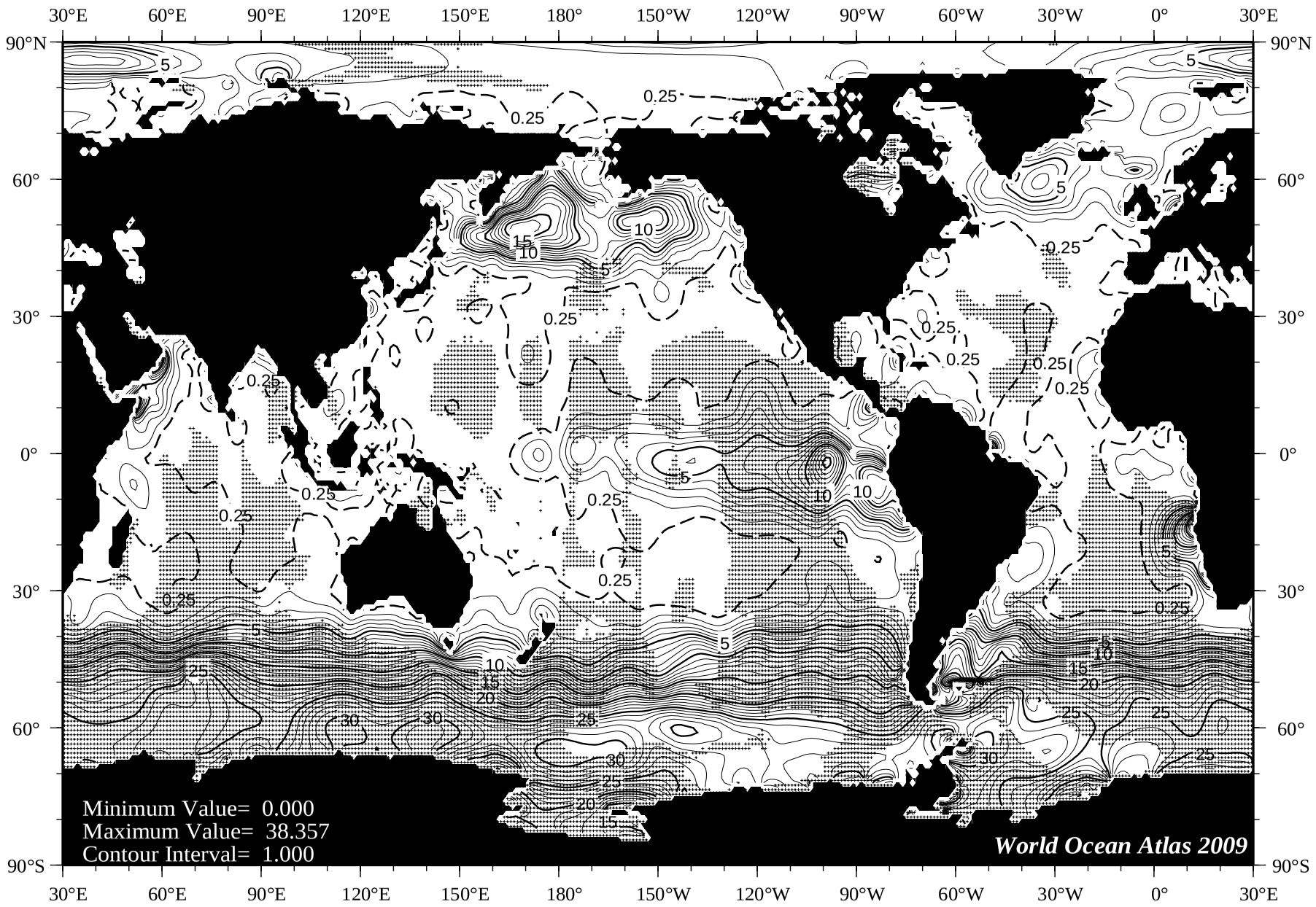

Fig E33 Summer (Jul.-Sep.) nitrate [umol/l] at the surface.

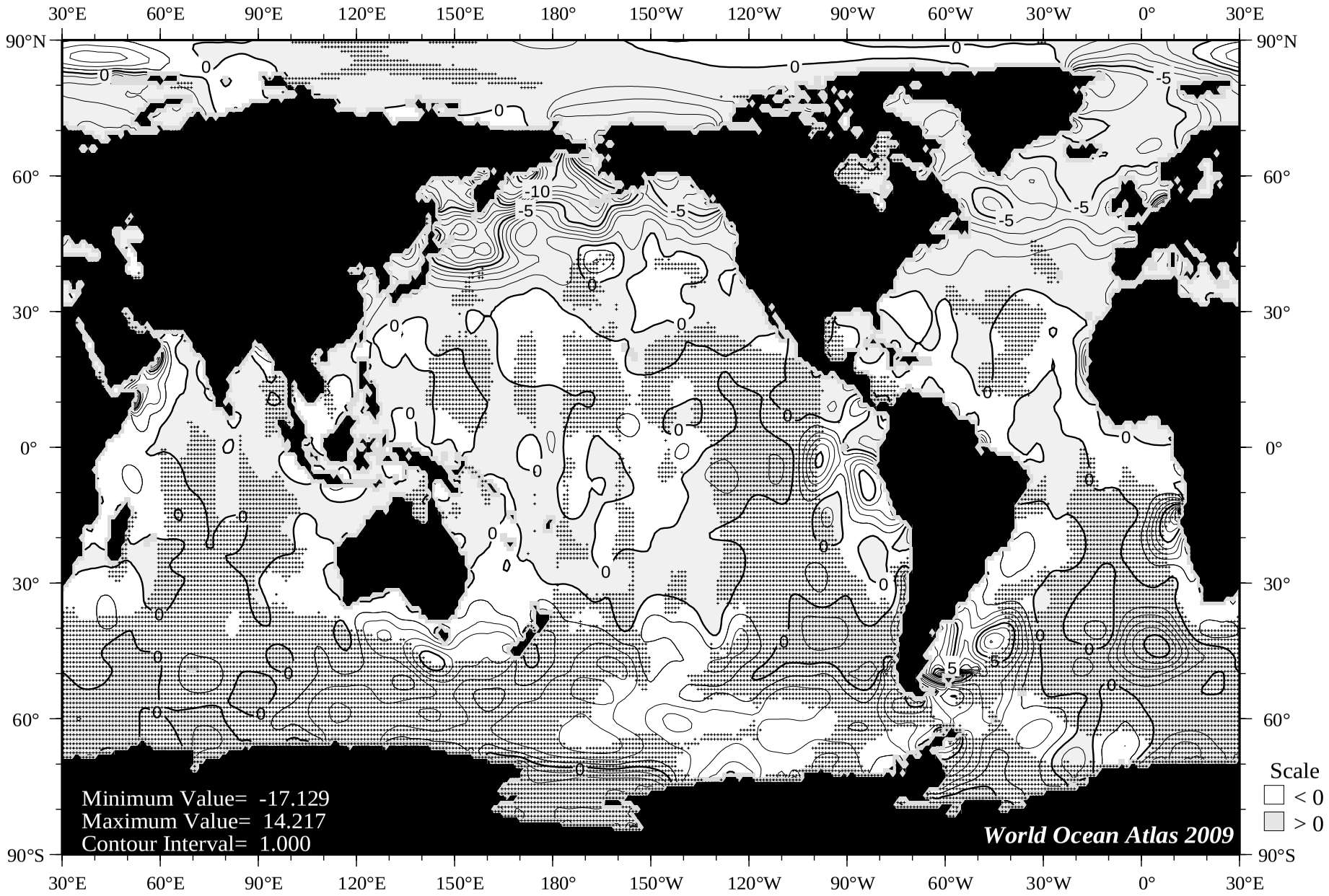

Fig E34 Summer (Jul.-Sep.) minus annual nitrate [umol/l] at the surface.

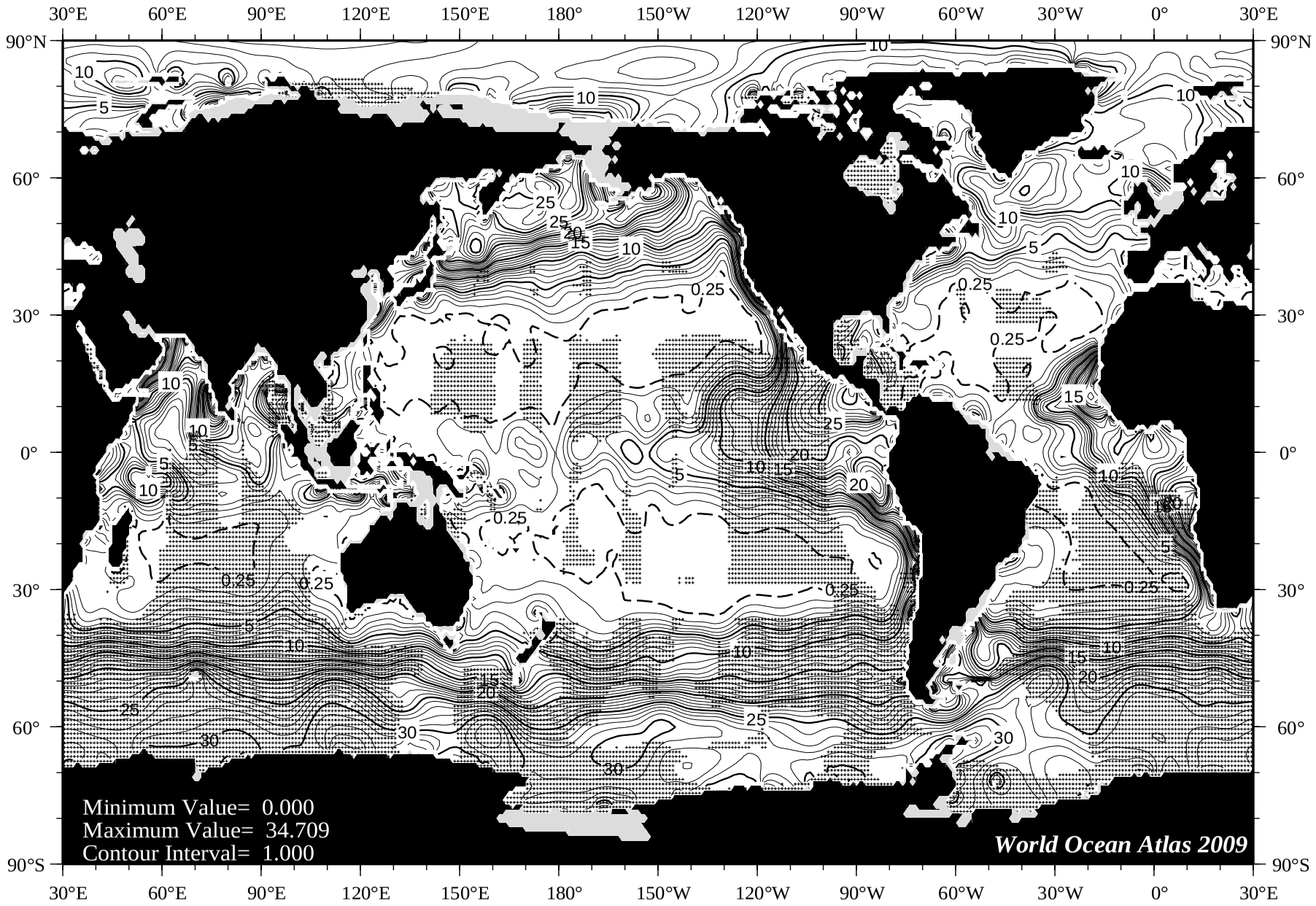

Fig E35 Summer (Jul.-Sep.) nitrate [umol/l] at 75 m. depth.

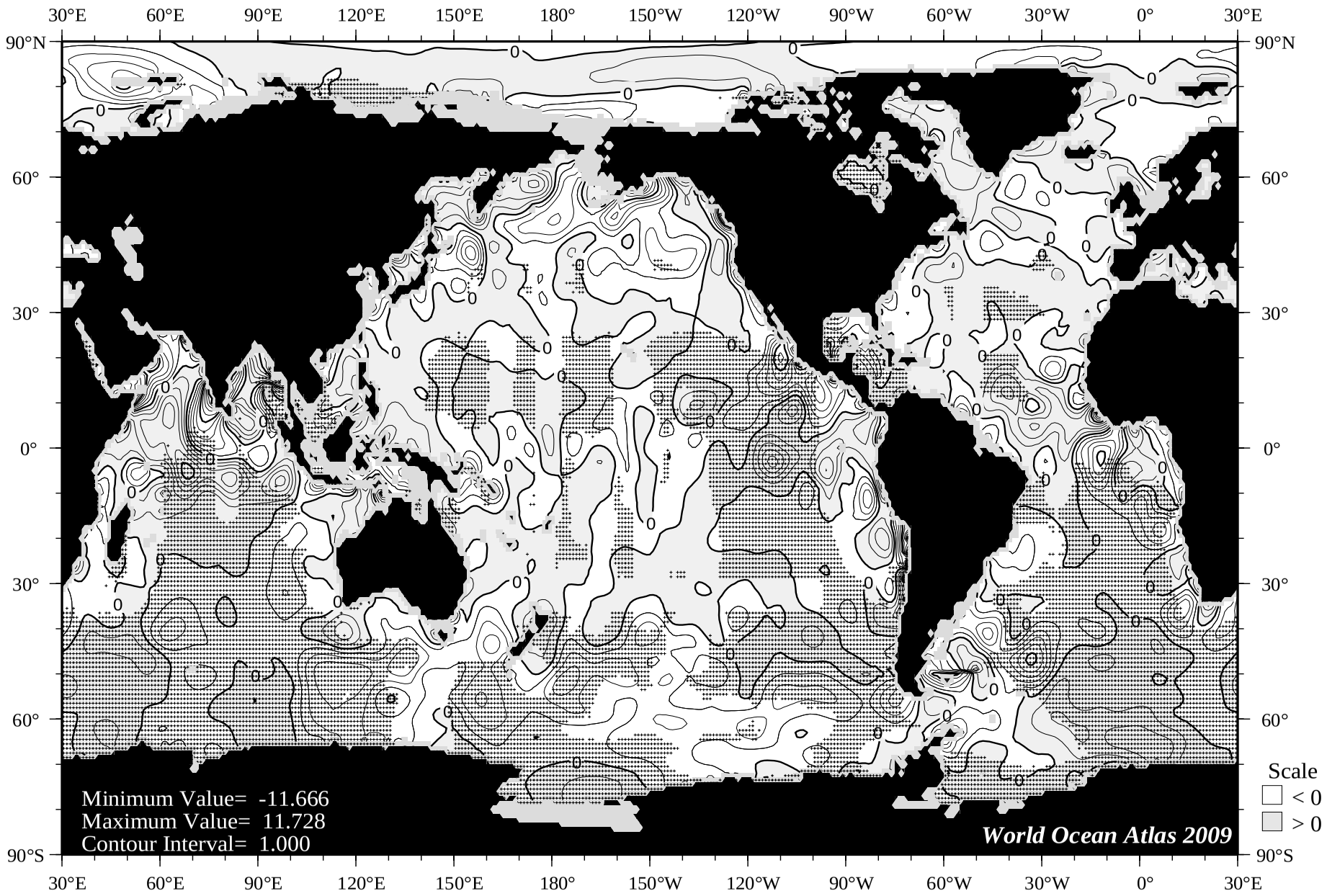

Fig E36 Summer (Jul.-Sep.) minus annual nitrate [umol/l] at 75 m. depth.

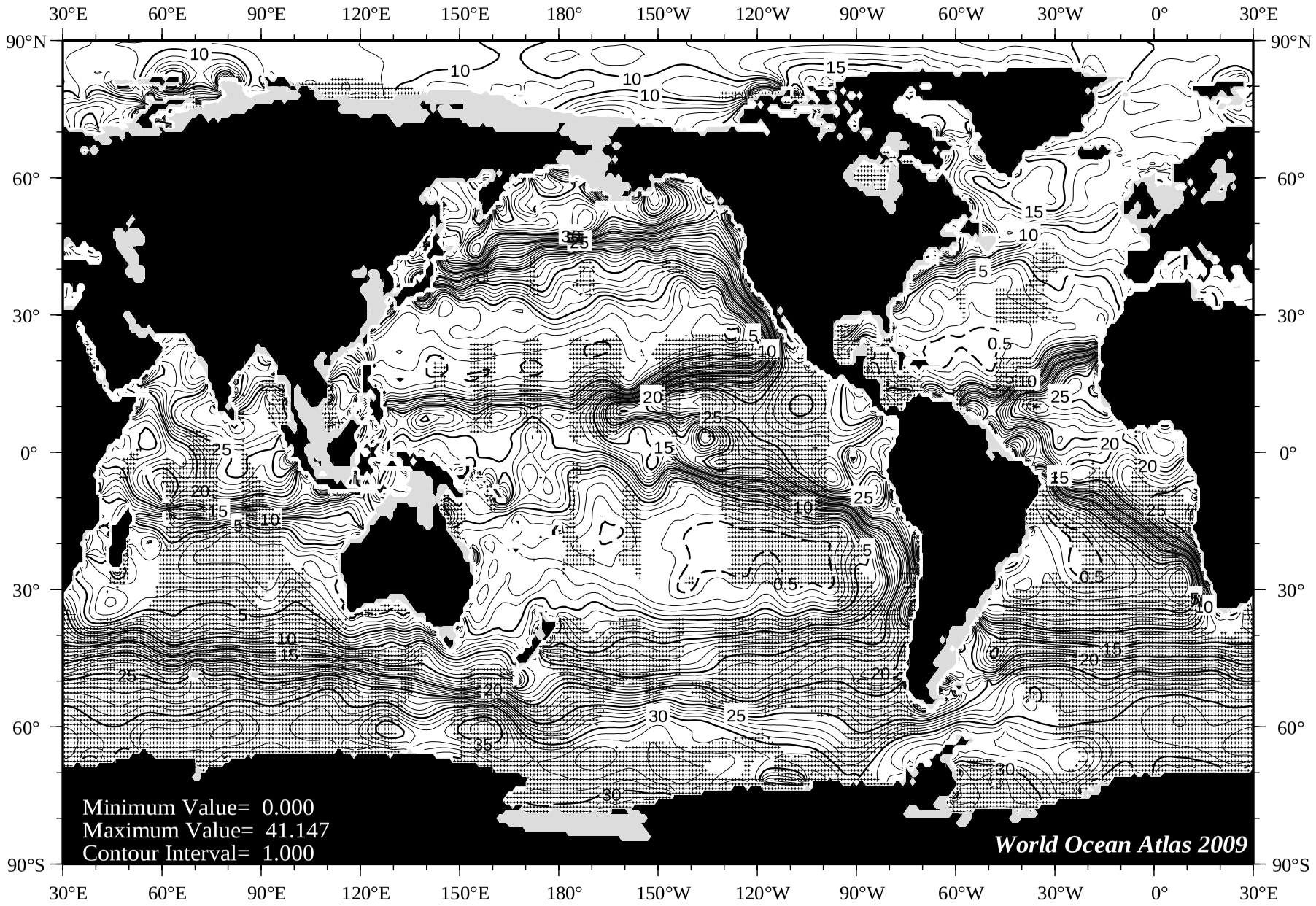

Fig E37 Summer (Jul.-Sep.) nitrate [umol/l] at 150 m. depth.

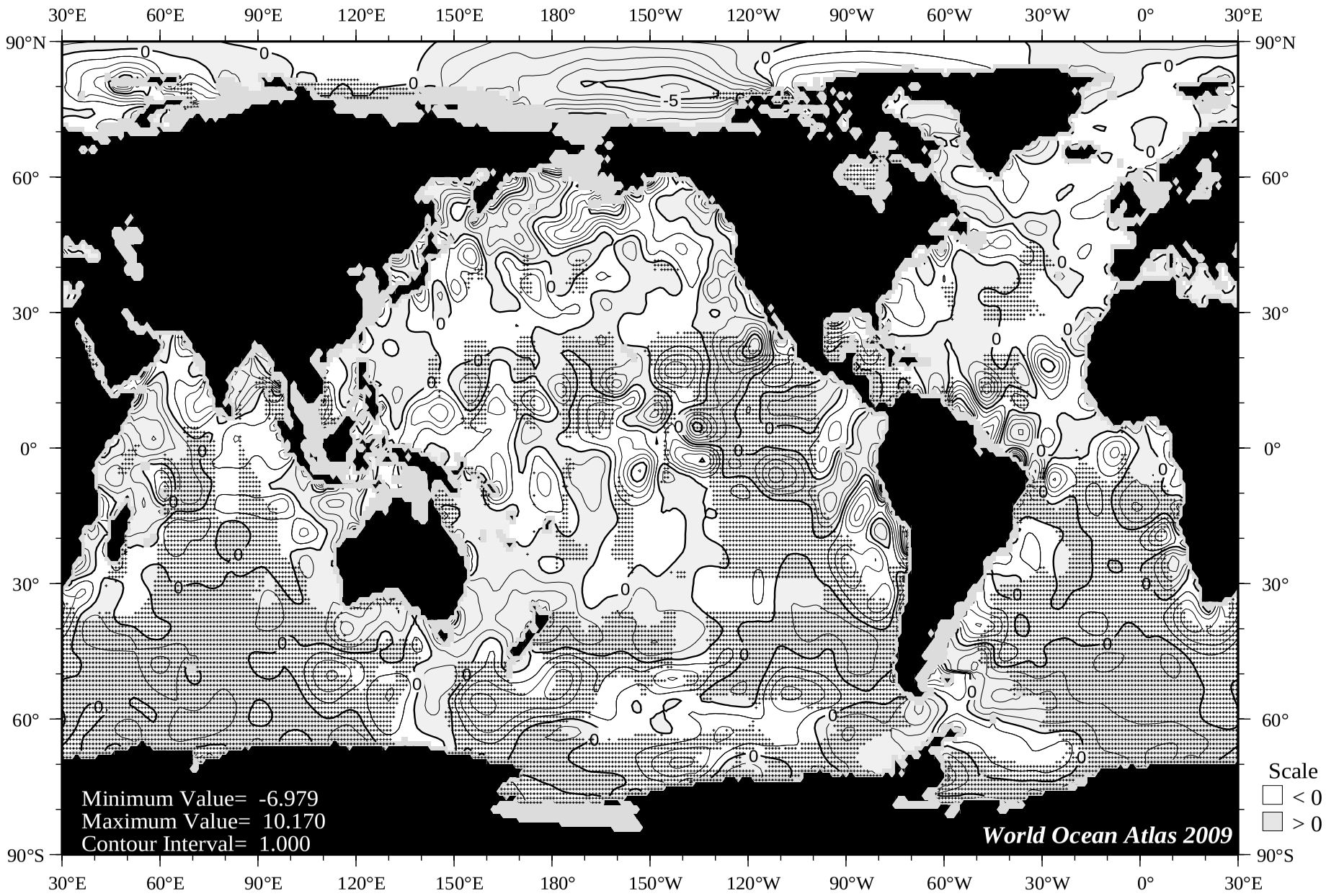

Fig E38 Summer (Jul.-Sep.) minus annual nitrate [umol/l] at 150 m. depth.

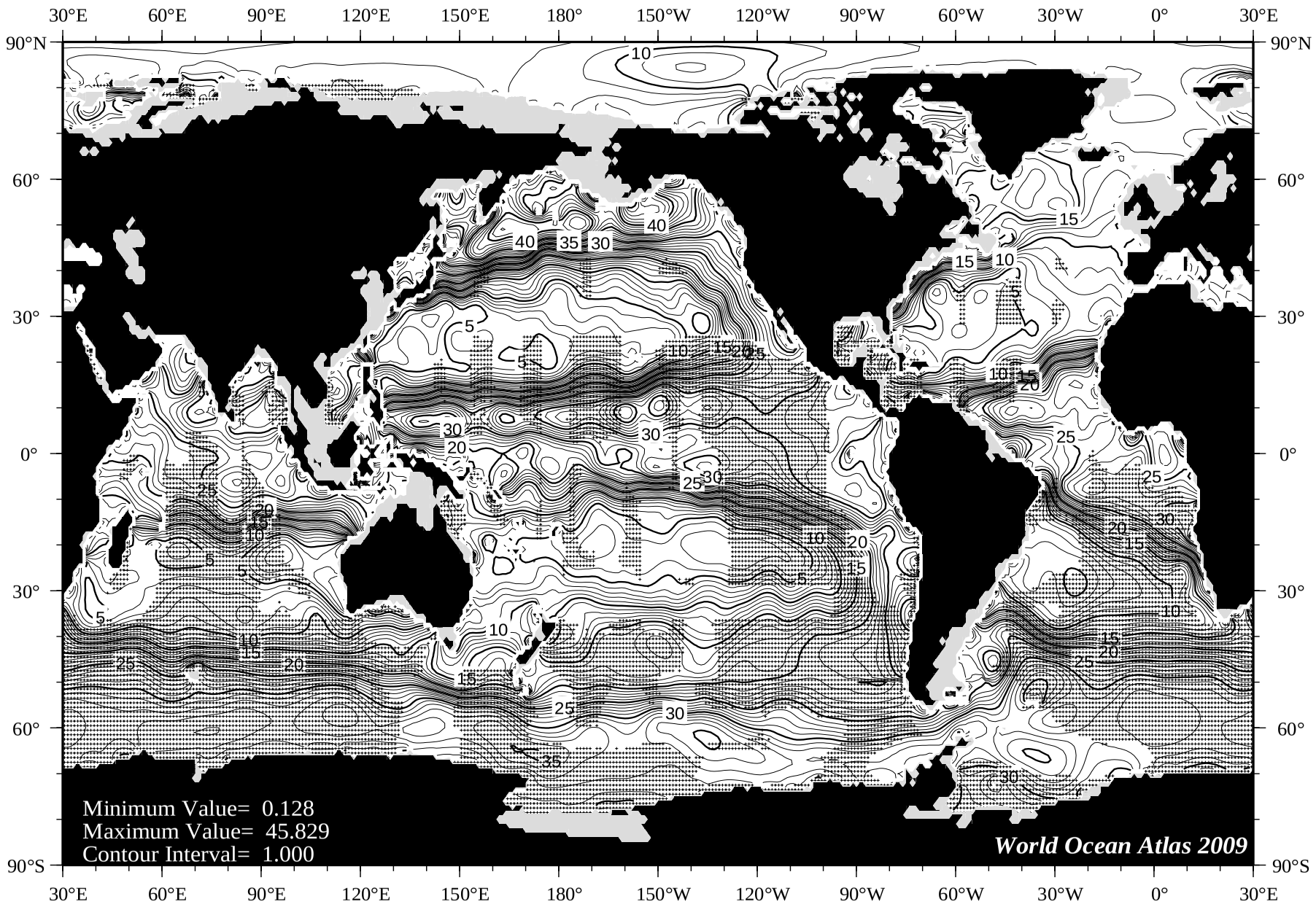

Fig E39 Summer (Jul.-Sep.) nitrate [umol/l] at 250 m. depth.

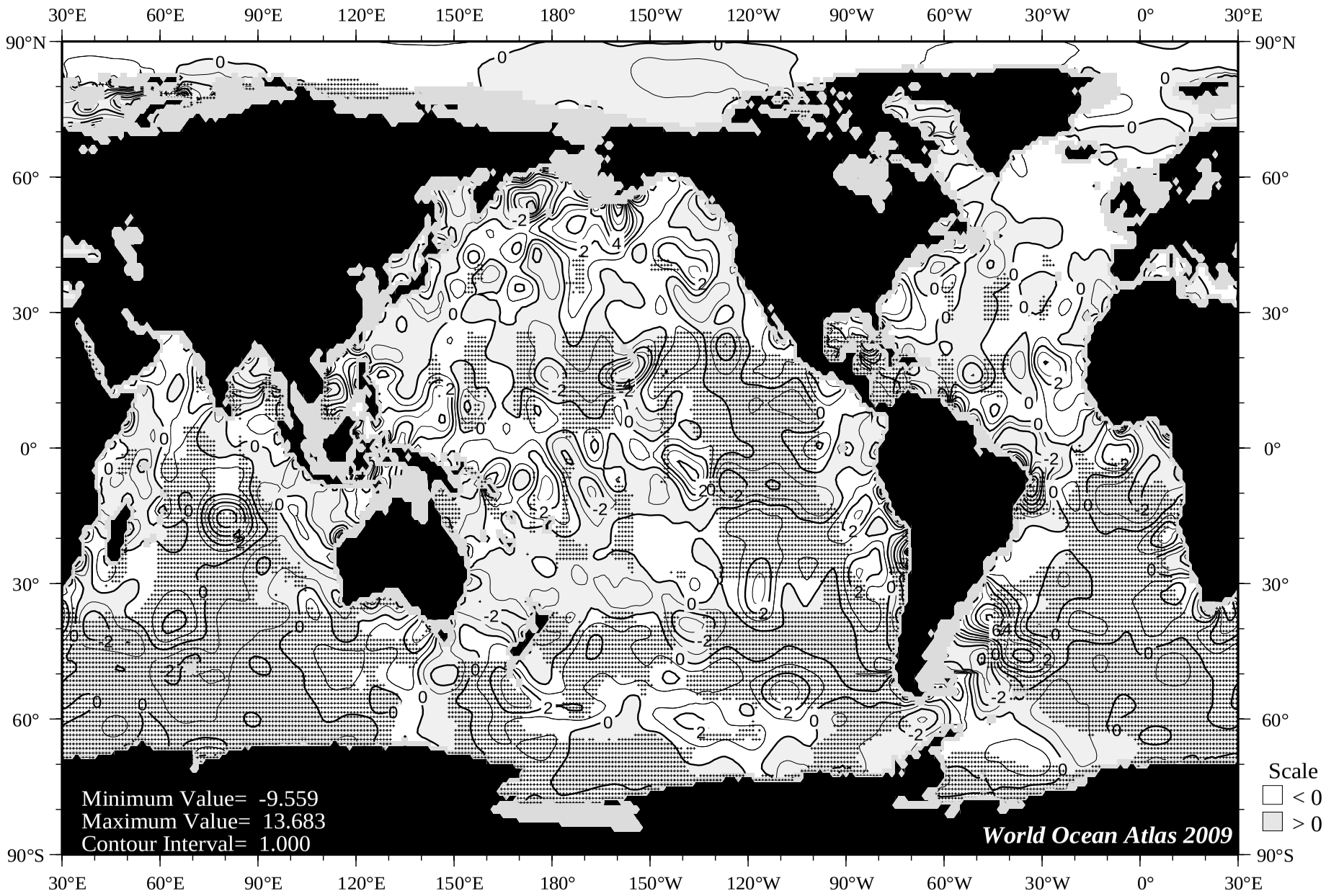

Fig E40 Summer (Jul.-Sep.) minus annual nitrate [umol/l] at 250 m. depth.

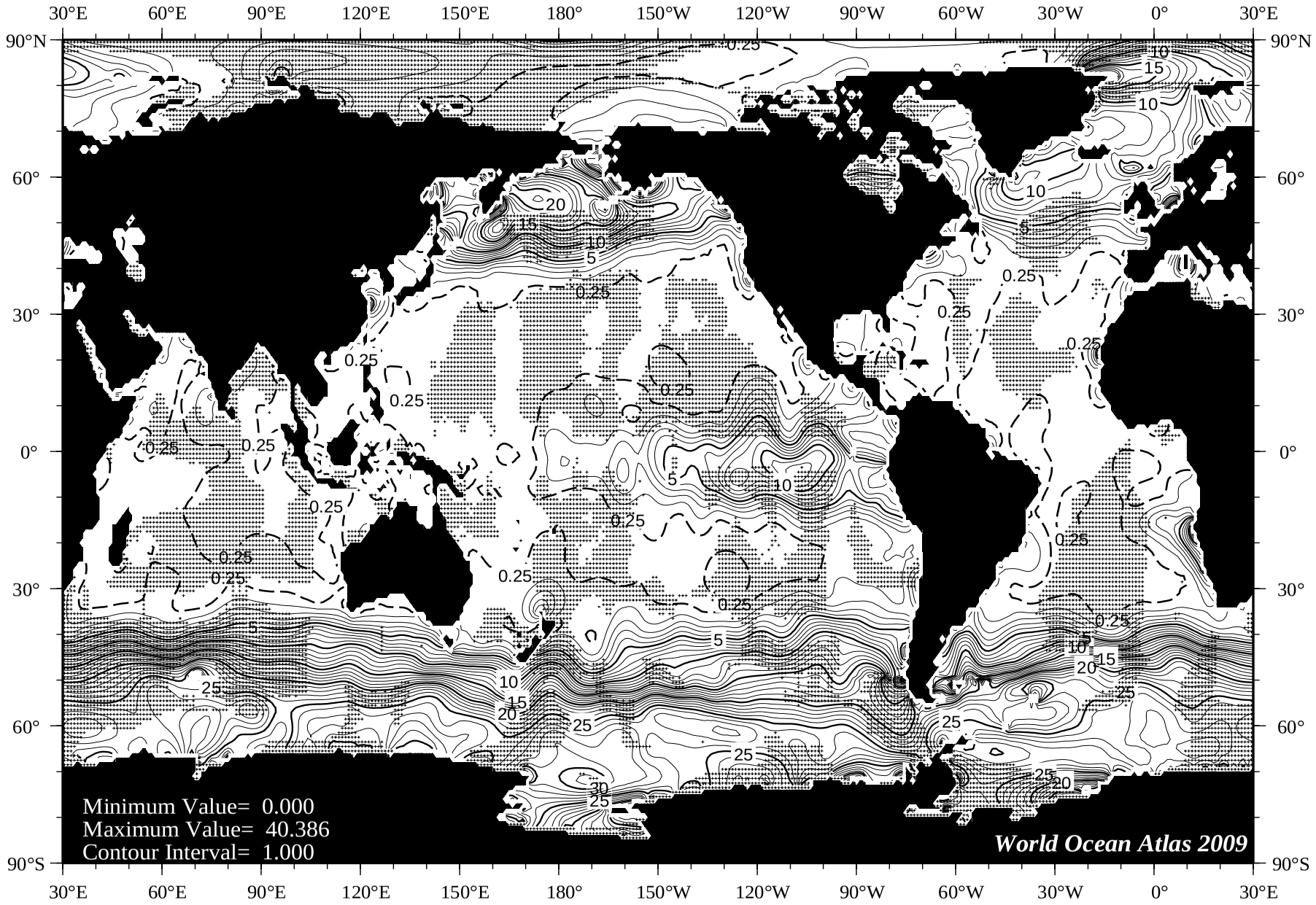

Fig E41 Fall (Oct.-Dec.) nitrate [umol/l] at the surface.

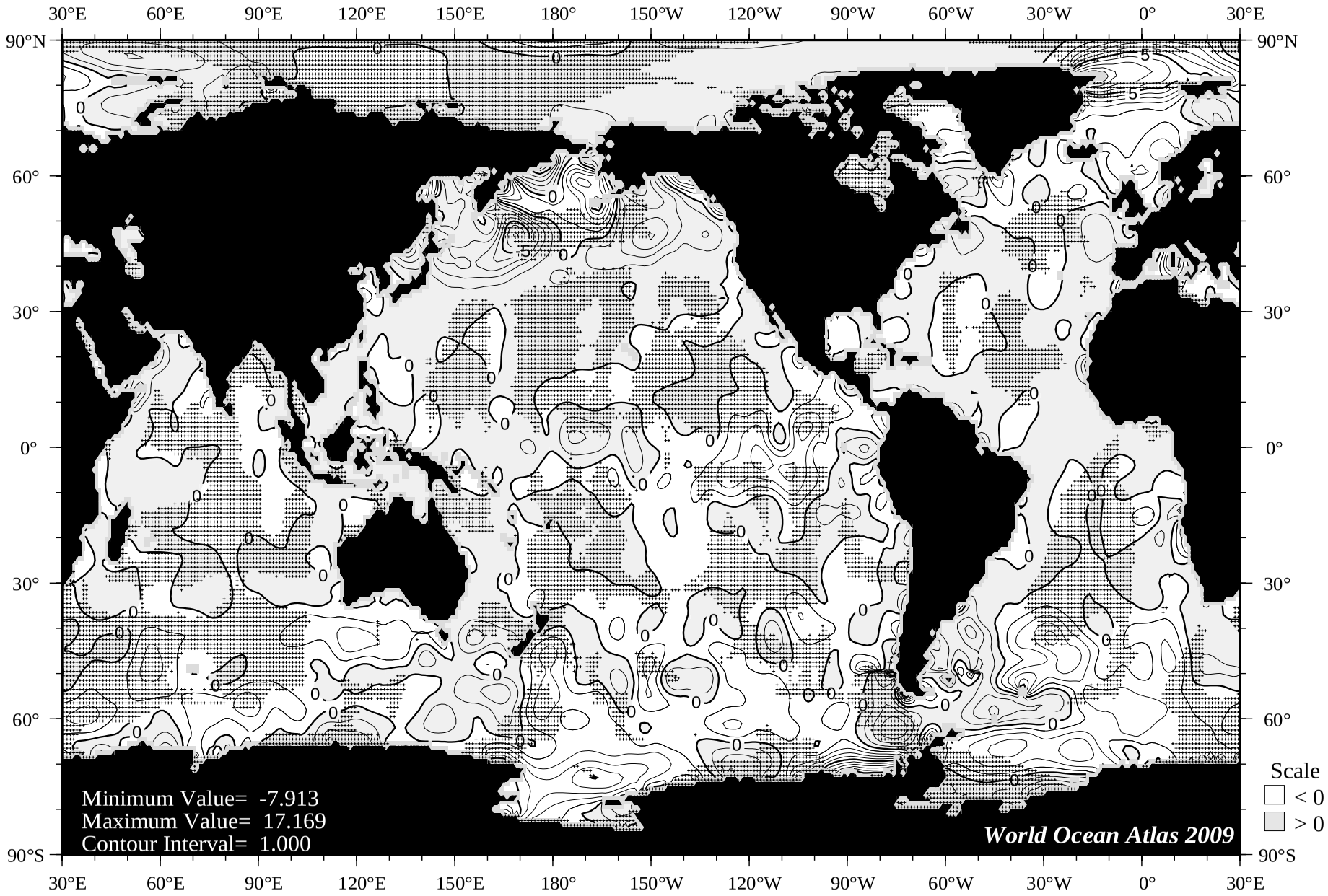

Fig E42 Fall (Oct.-Dec.) minus annual nitrate [umol/l] at the surface.

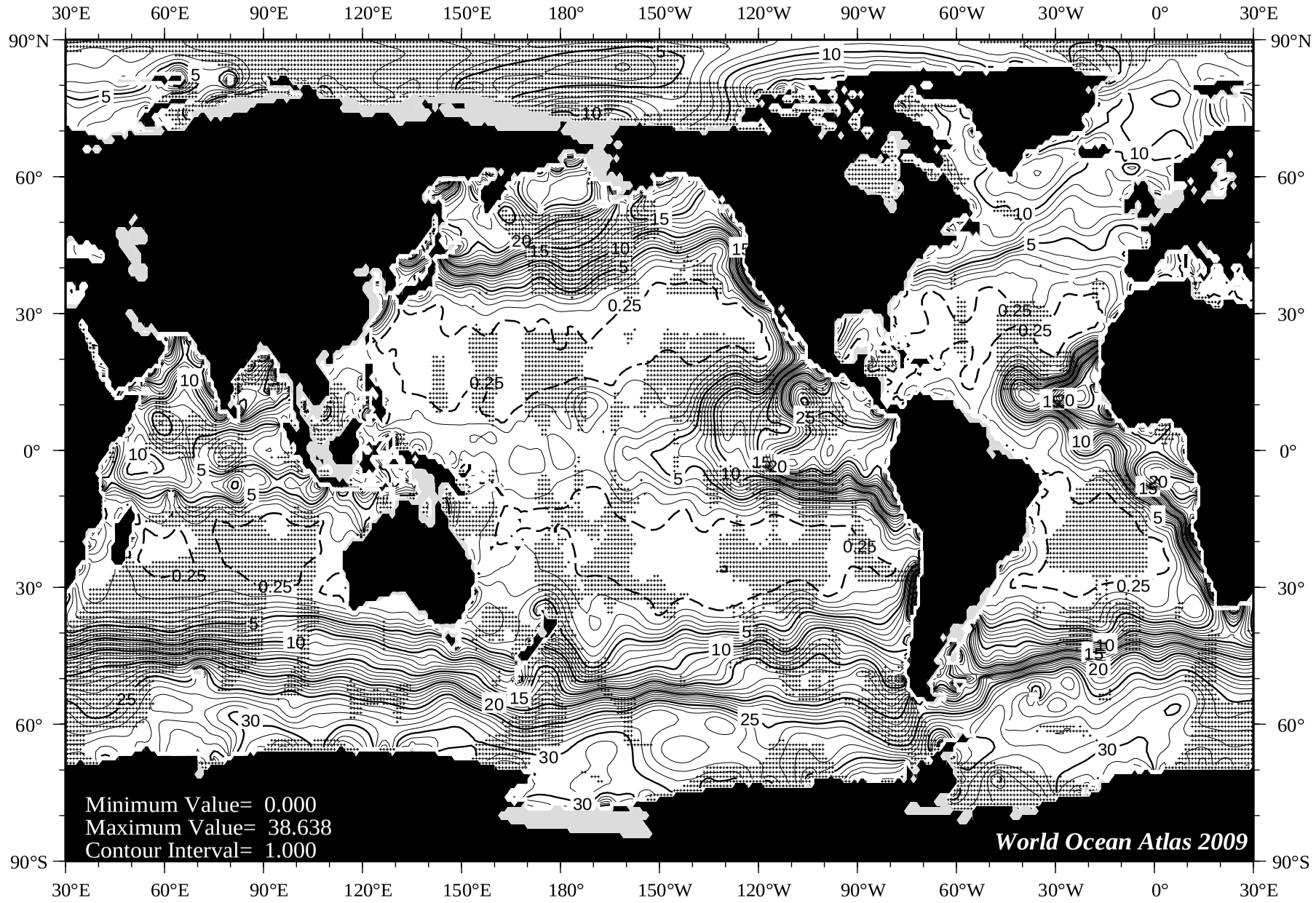

Fig E43 Fall (Oct.-Dec.) nitrate [umol/l] at 75 m. depth.

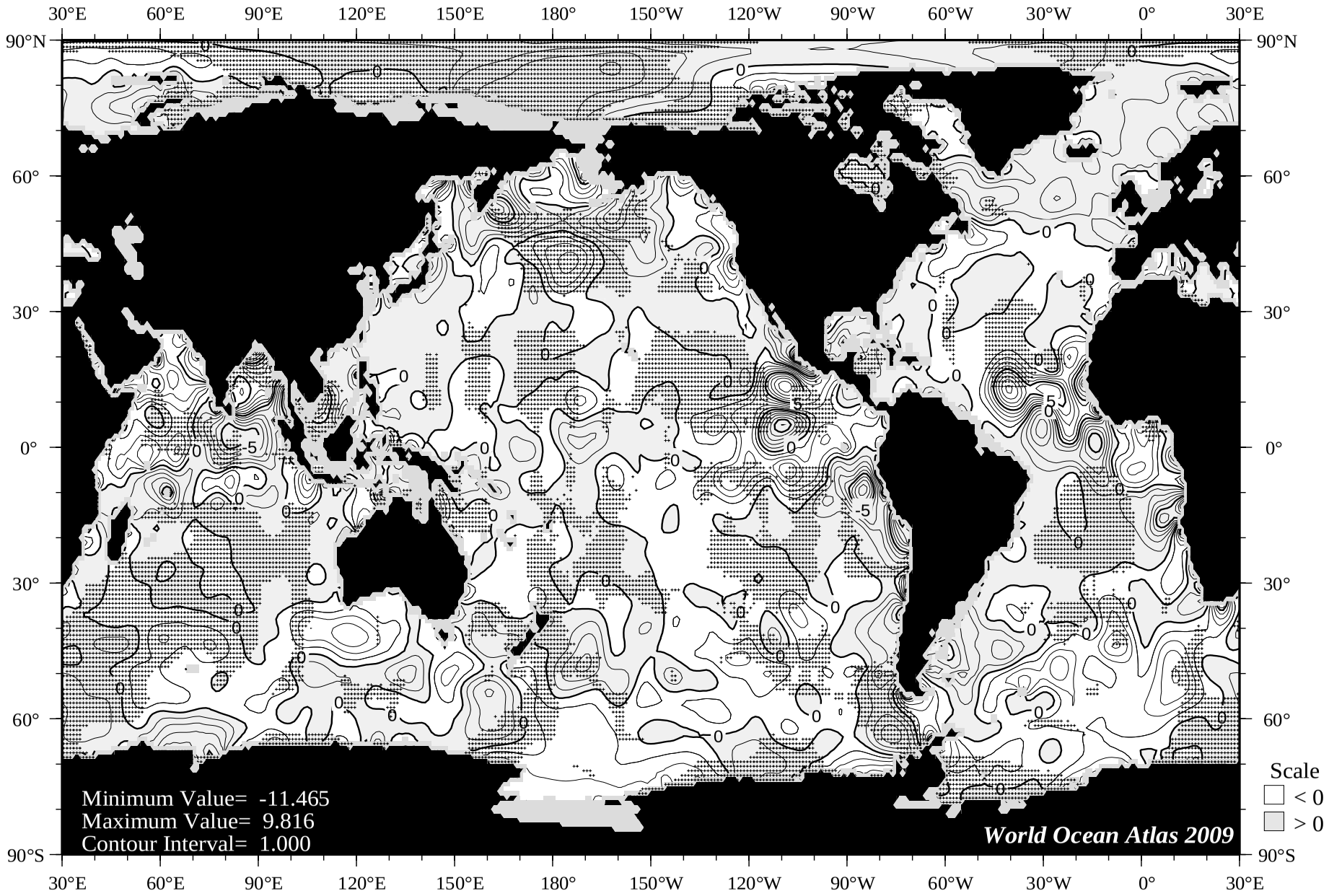

Fig E44 Fall (Oct.-Dec.) minus annual nitrate [umol/l] at 75 m. depth.

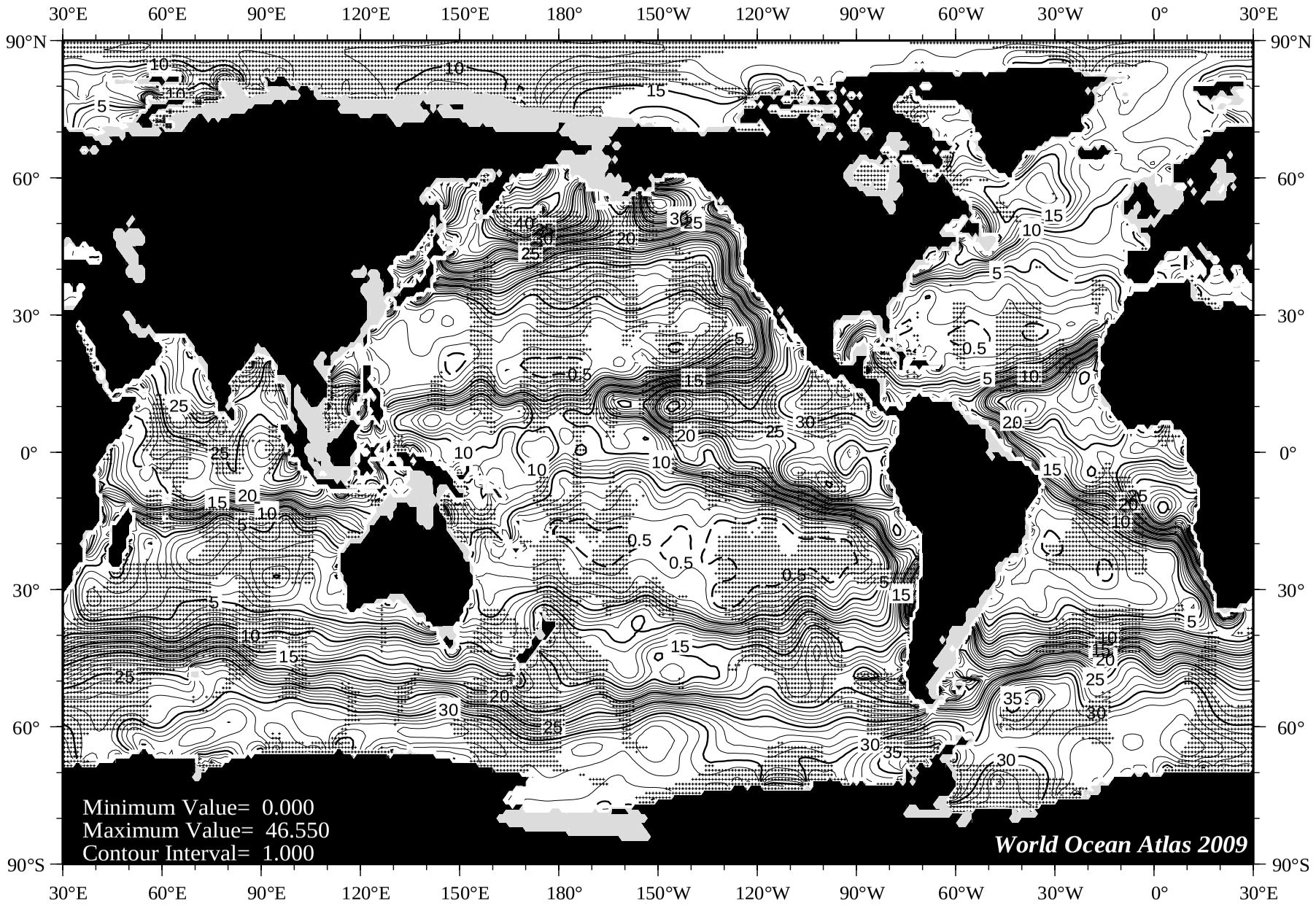

Fig E45 Fall (Oct.-Dec.) nitrate [umol/l] at 150 m. depth.

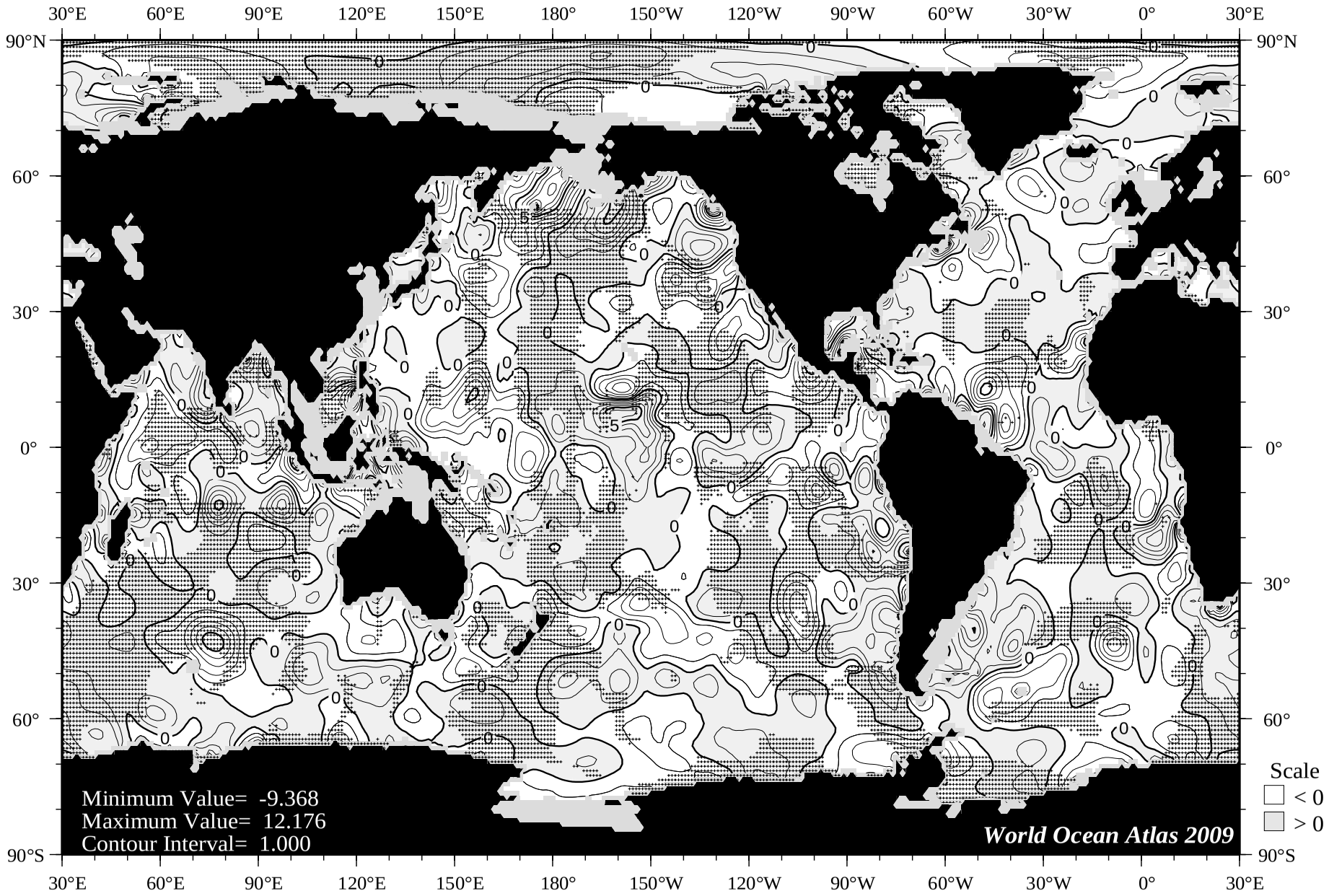

Fig E46 Fall (Oct.-Dec.) minus annual nitrate [umol/l] at 150 m. depth.

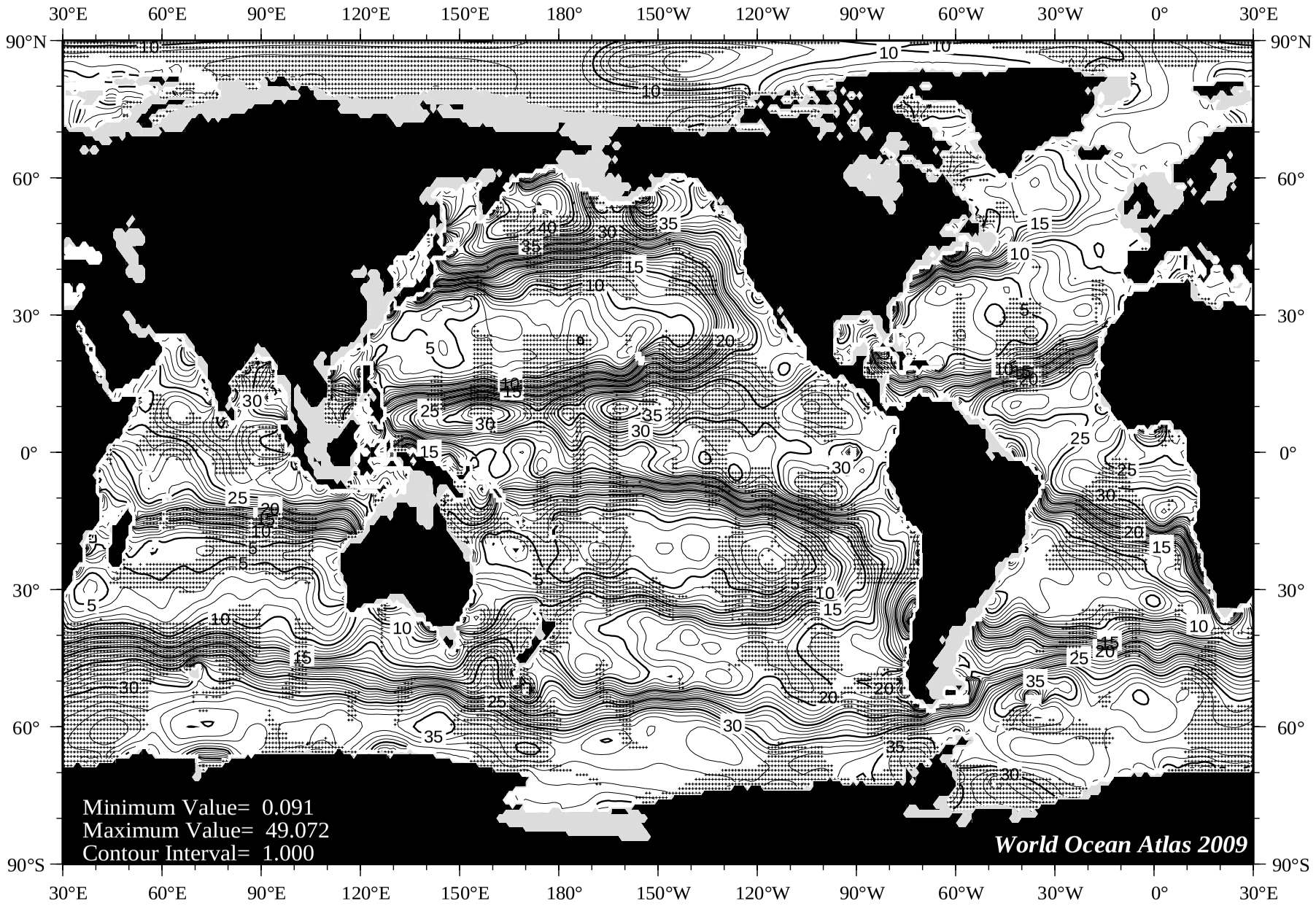

Fig E47 Fall (Oct.-Dec.) nitrate [umol/l] at 250 m. depth.

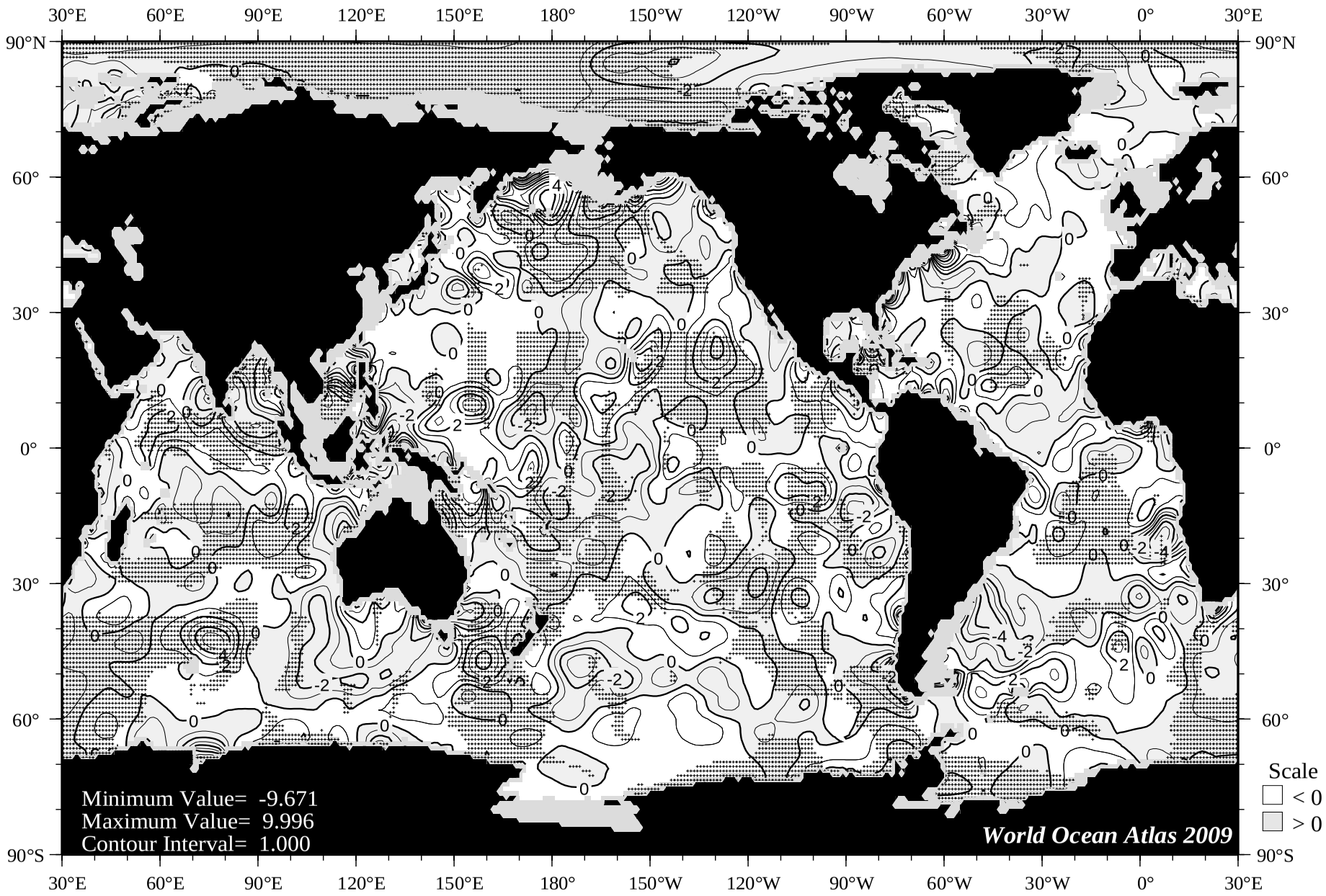

Fig E48 Fall (Oct.-Dec.) minus annual nitrate [umol/l] at 250 m. depth.

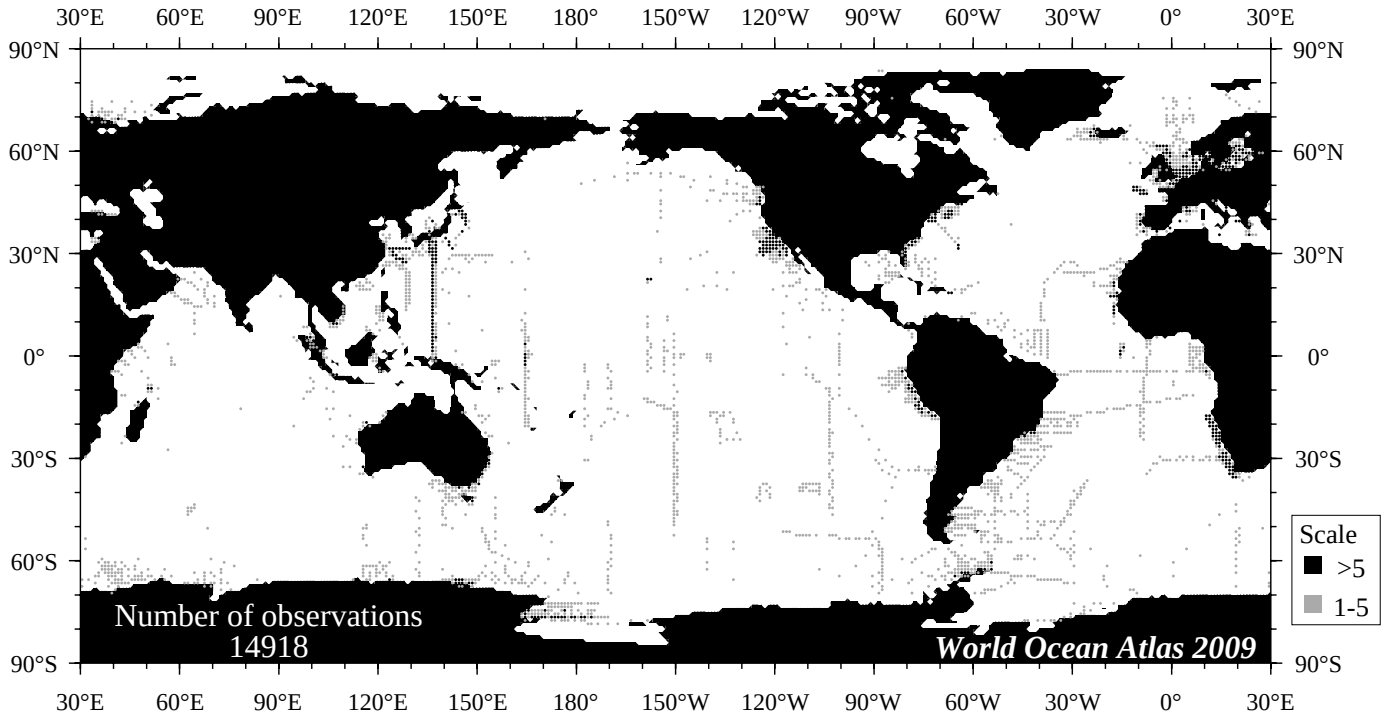

Fig F1 January nitrate observations at the surface.

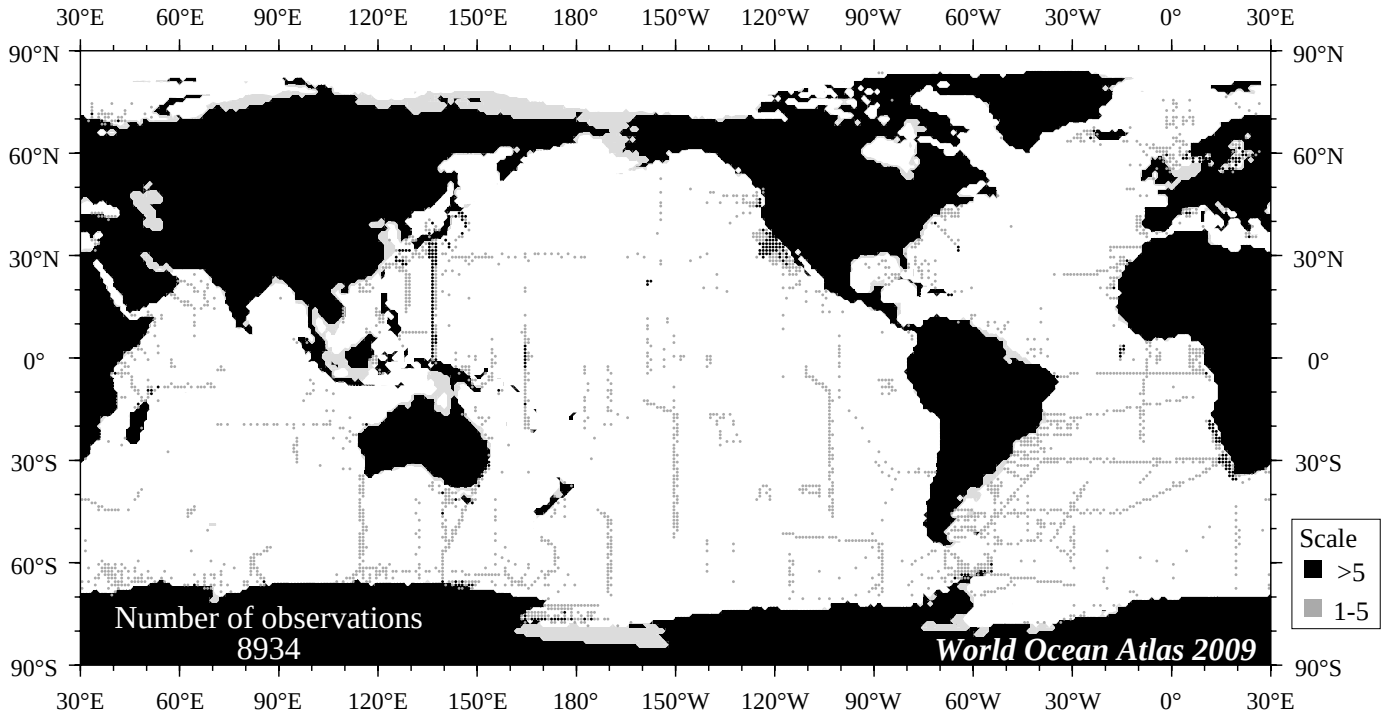

Fig F2 January nitrate observations at 75 m. depth.

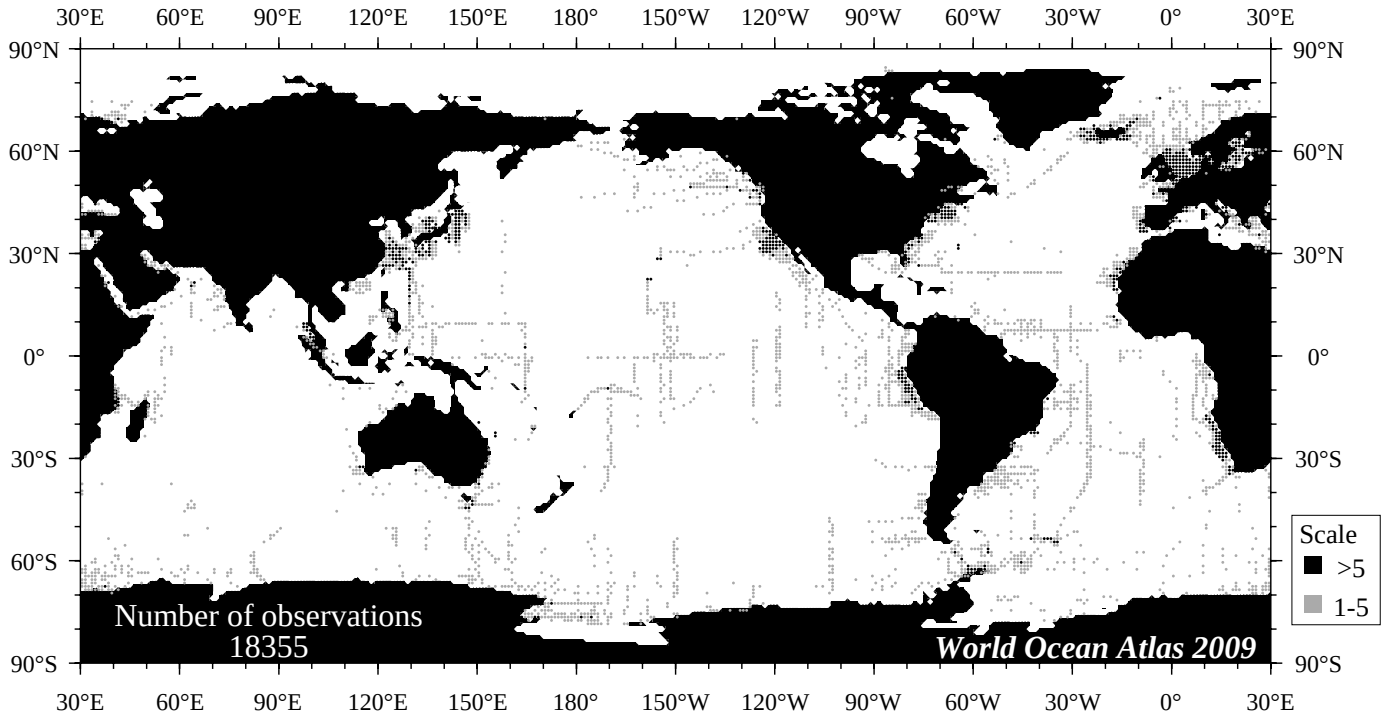

Fig F3 February nitrate observations at the surface.

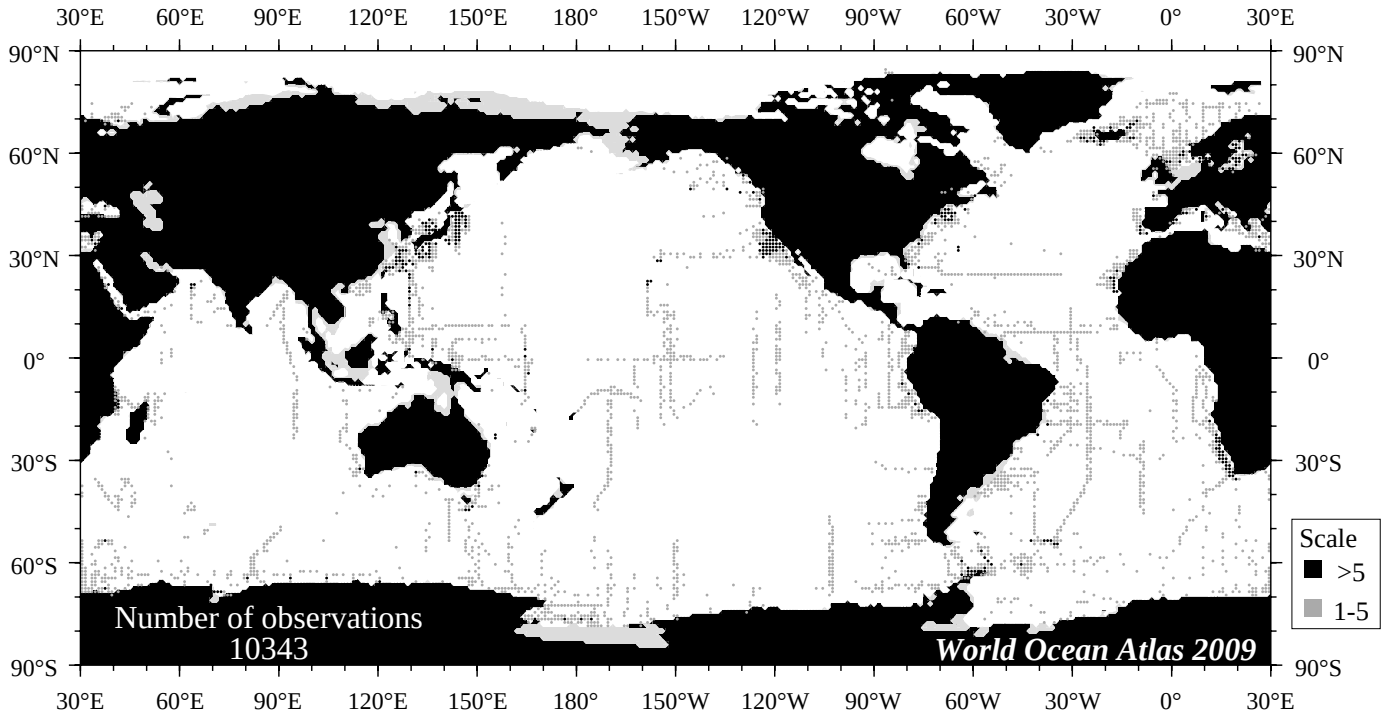

Fig F4 February nitrate observations at 75 m. depth.

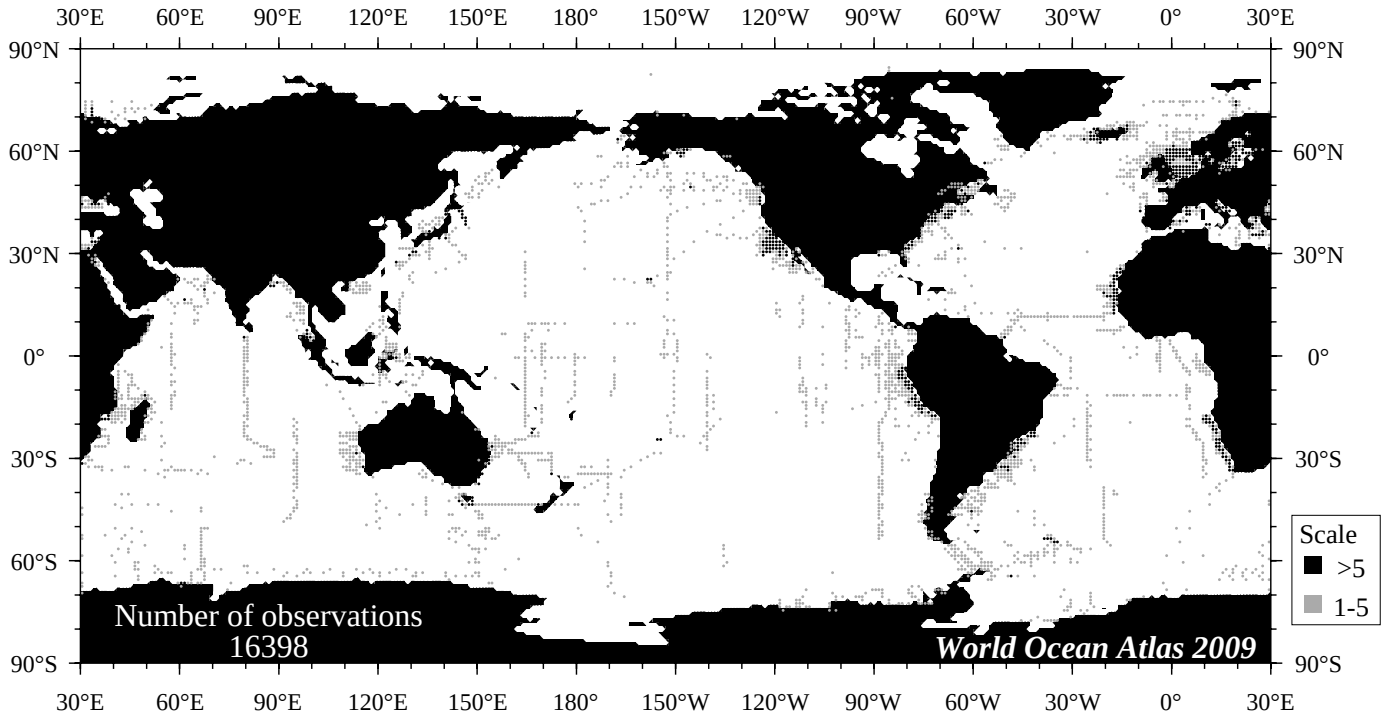

Fig F5 March nitrate observations at the surface.

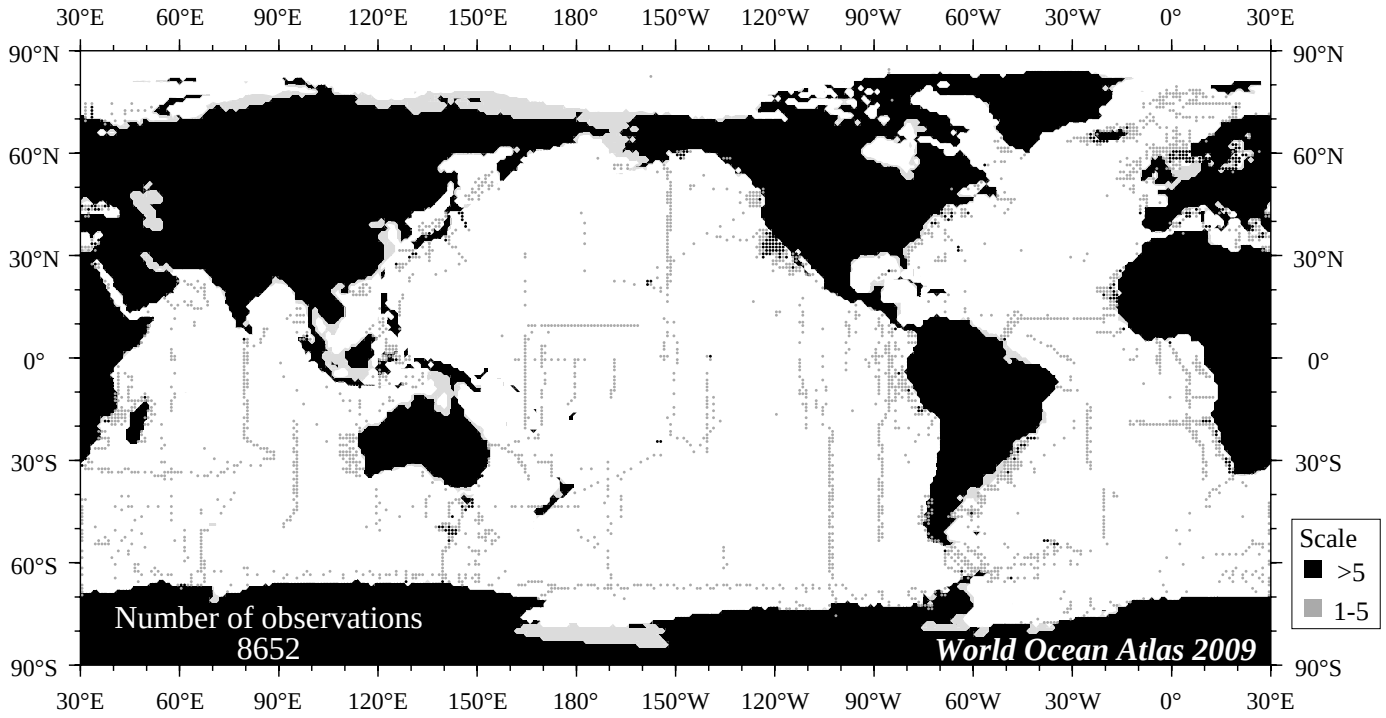

Fig F6 March nitrate observations at 75 m. depth.

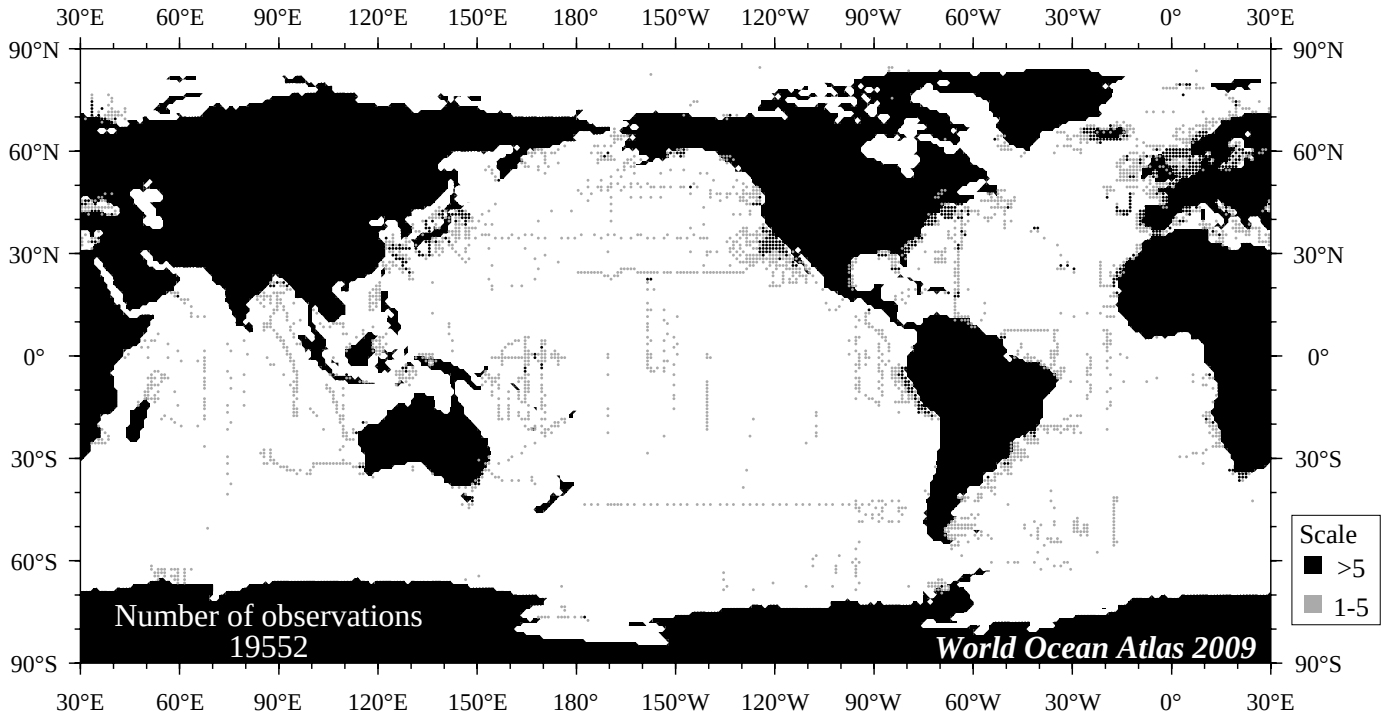

Fig F7 April nitrate observations at the surface.

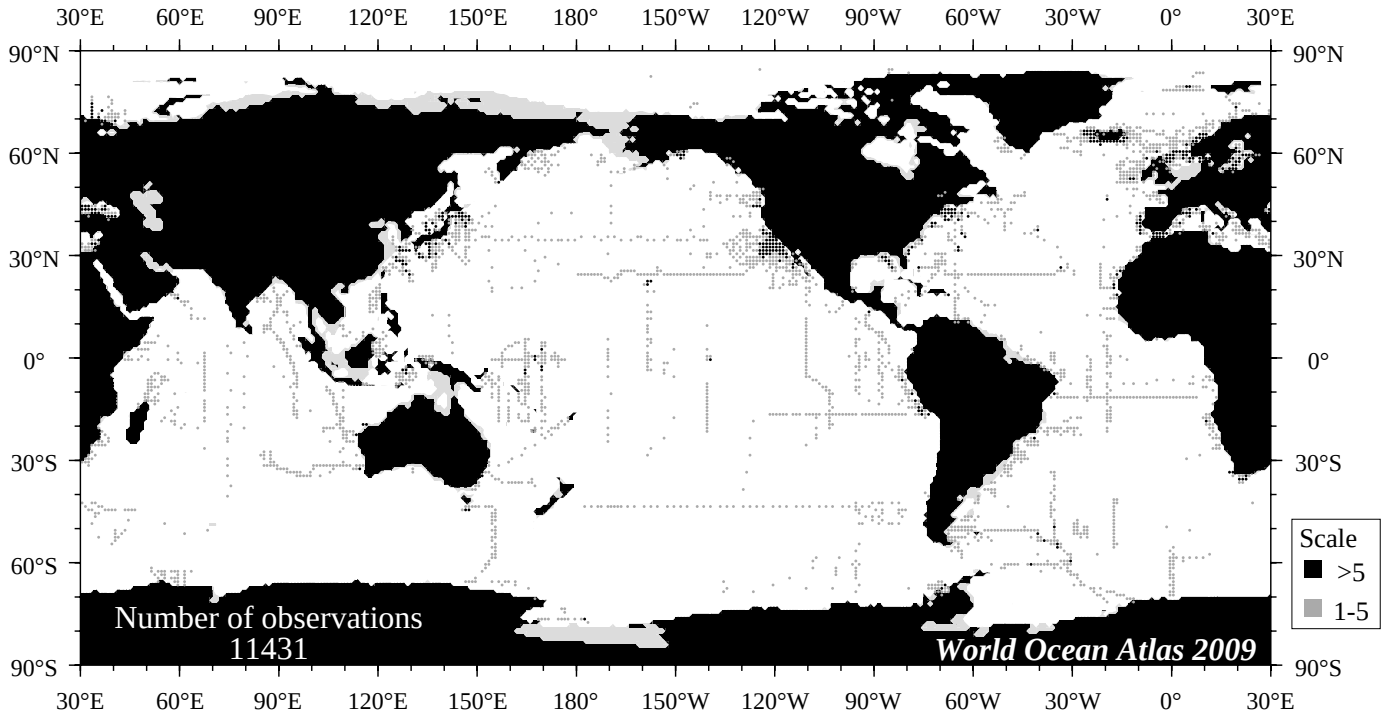

Fig F8 April nitrate observations at 75 m. depth.

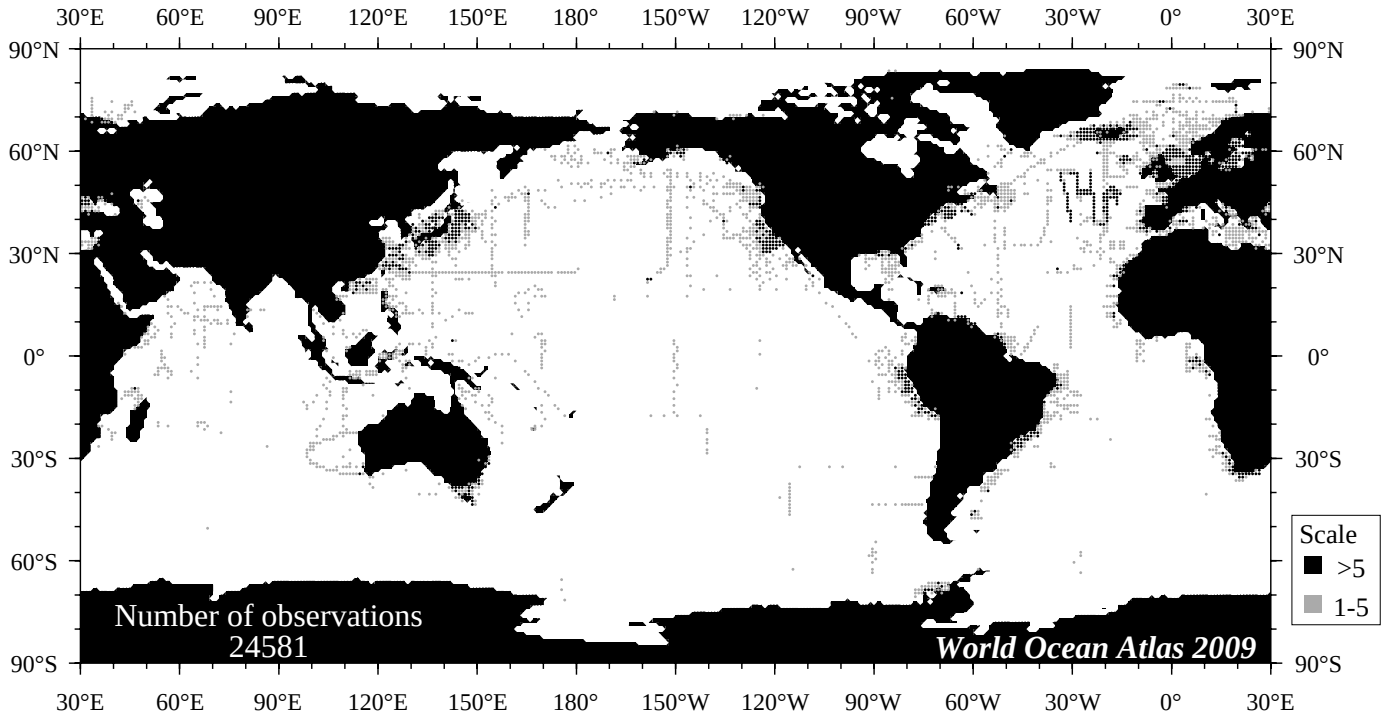

Fig F9 May nitrate observations at the surface.

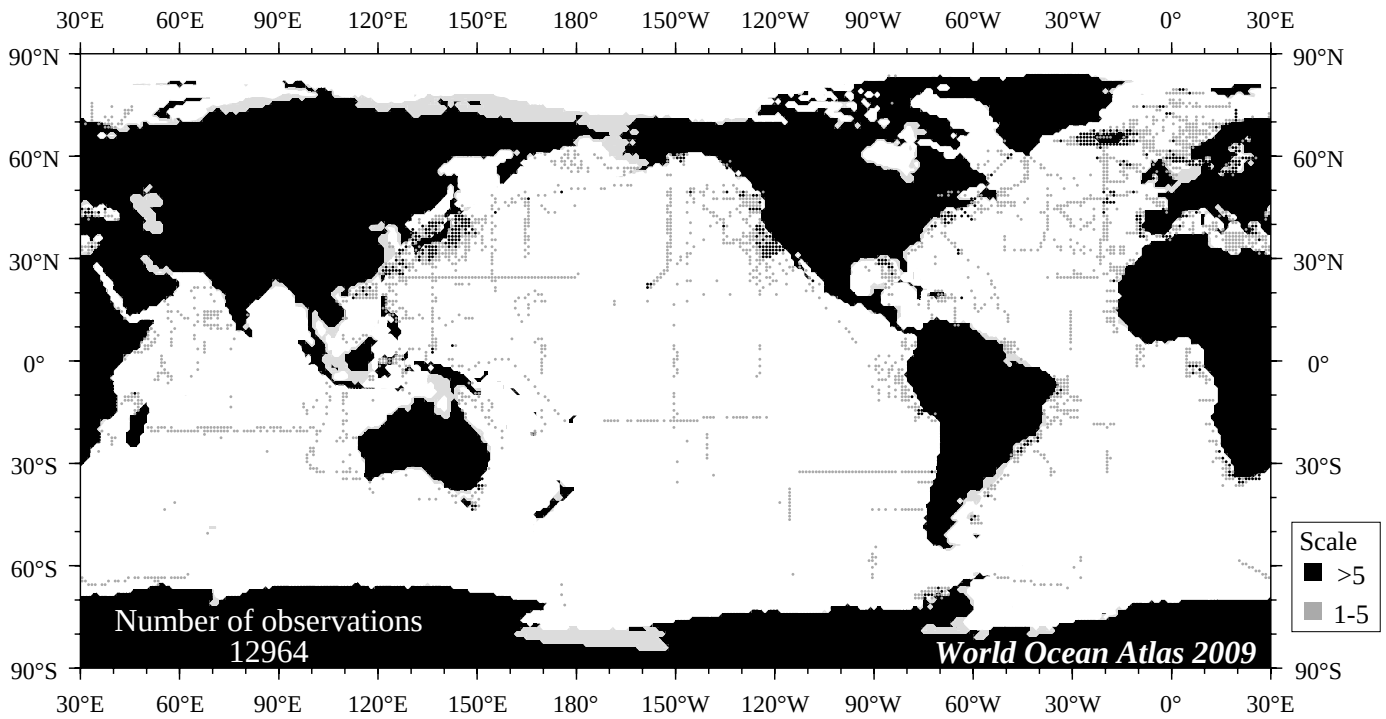

Fig F10 May nitrate observations at 75 m. depth.

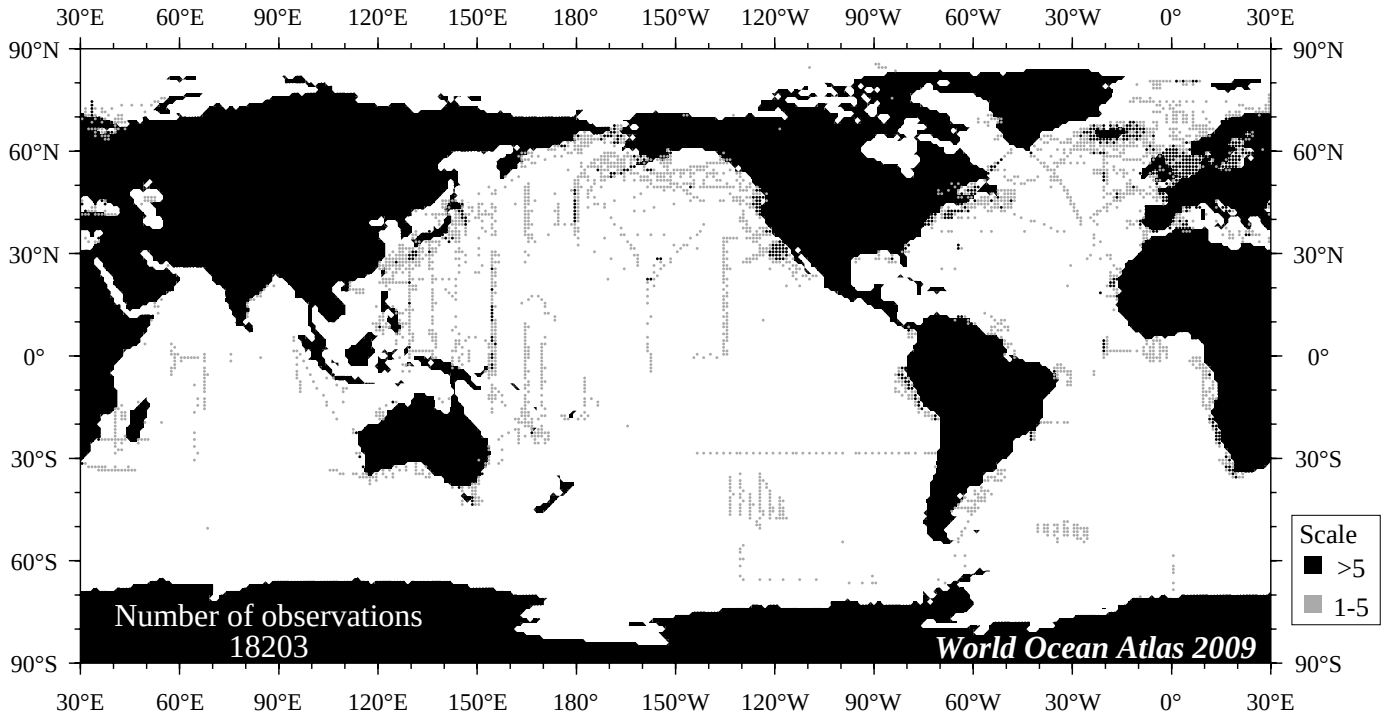

Fig F11 June nitrate observations at the surface.

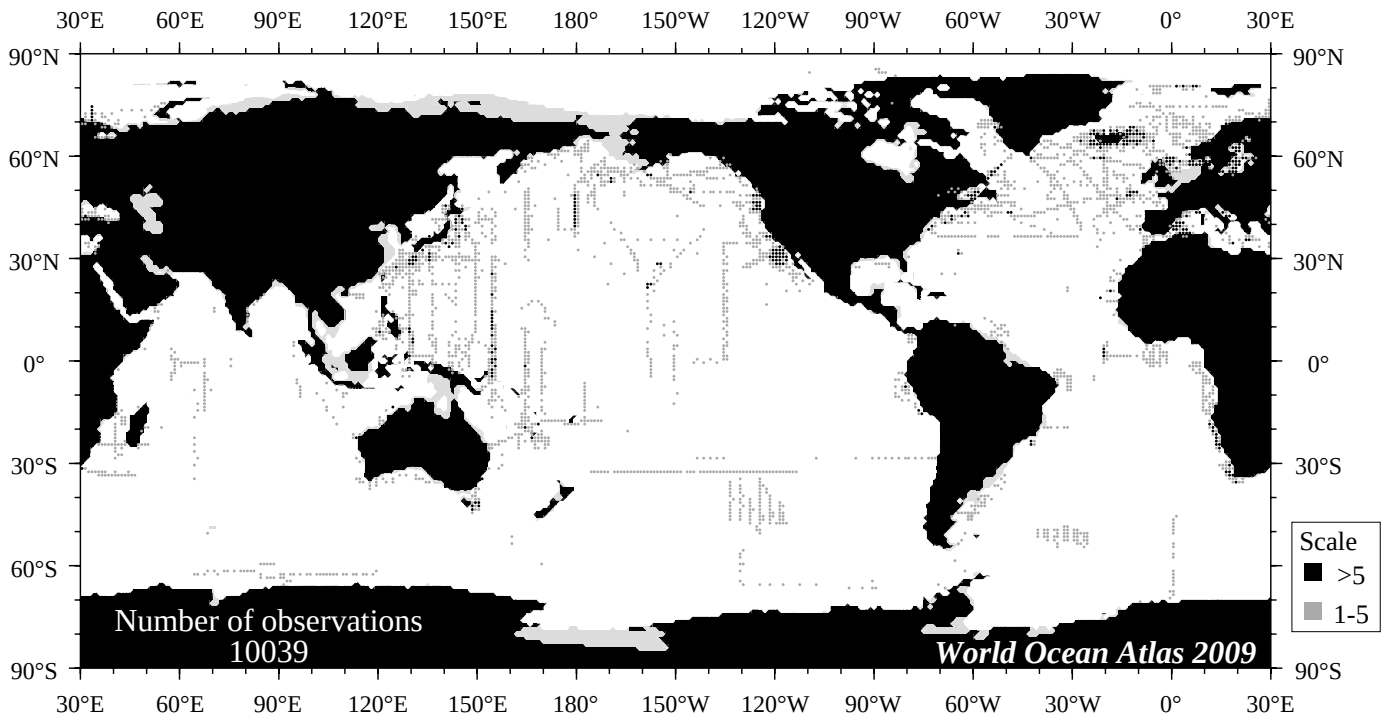

Fig F12 June nitrate observations at 75 m. depth.

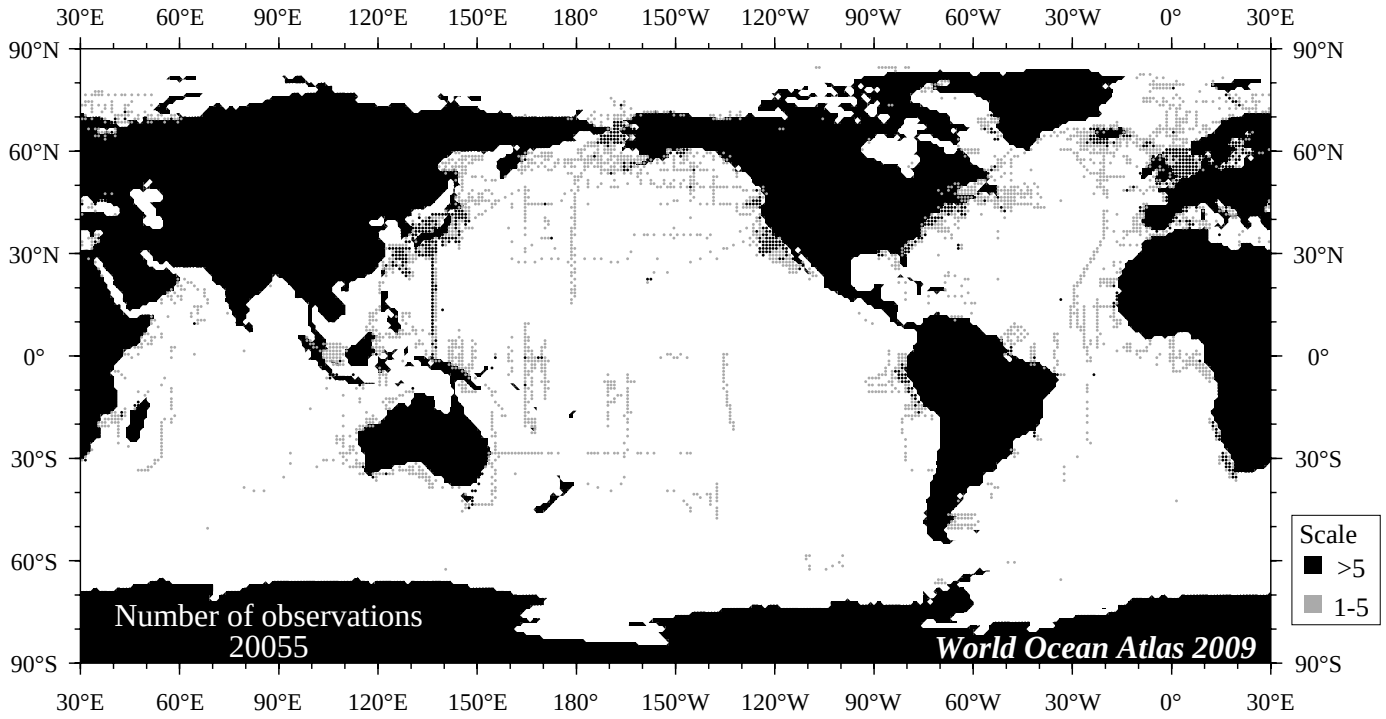

Fig F13 July nitrate observations at the surface.

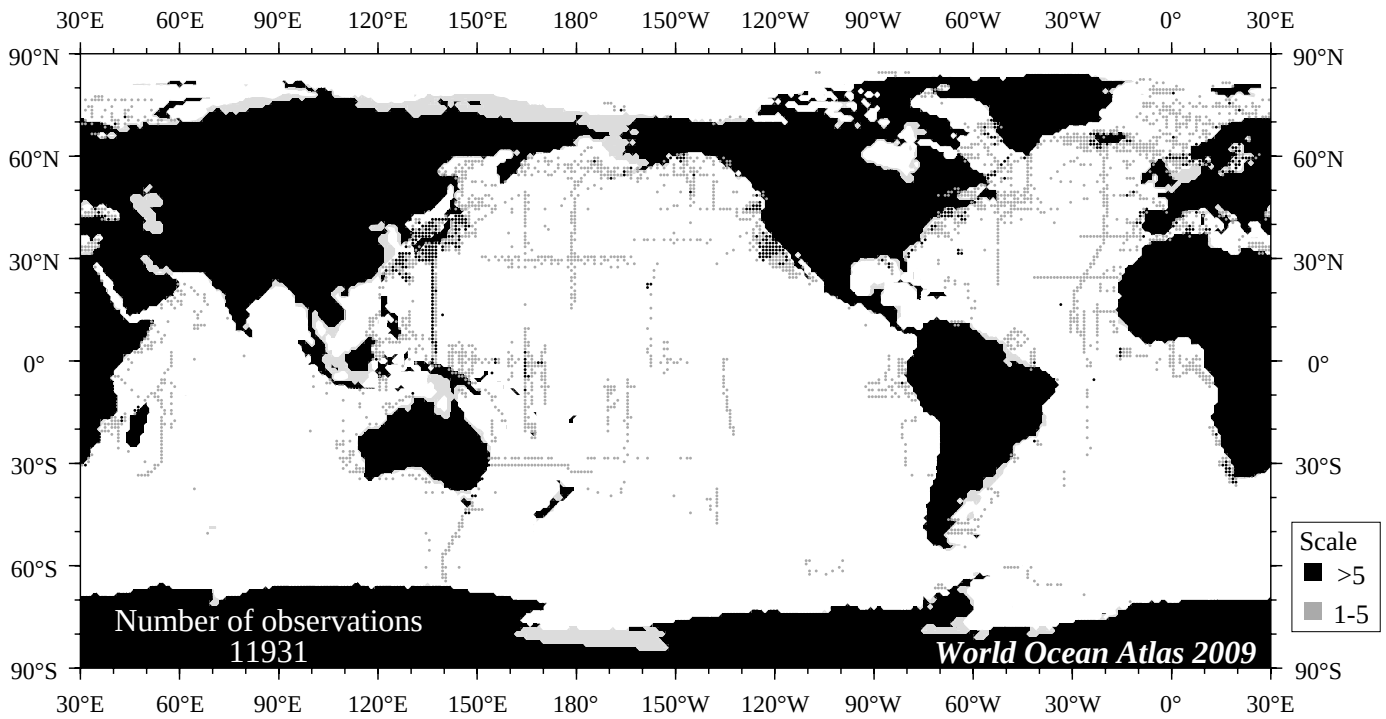

Fig F14 July nitrate observations at 75 m. depth.

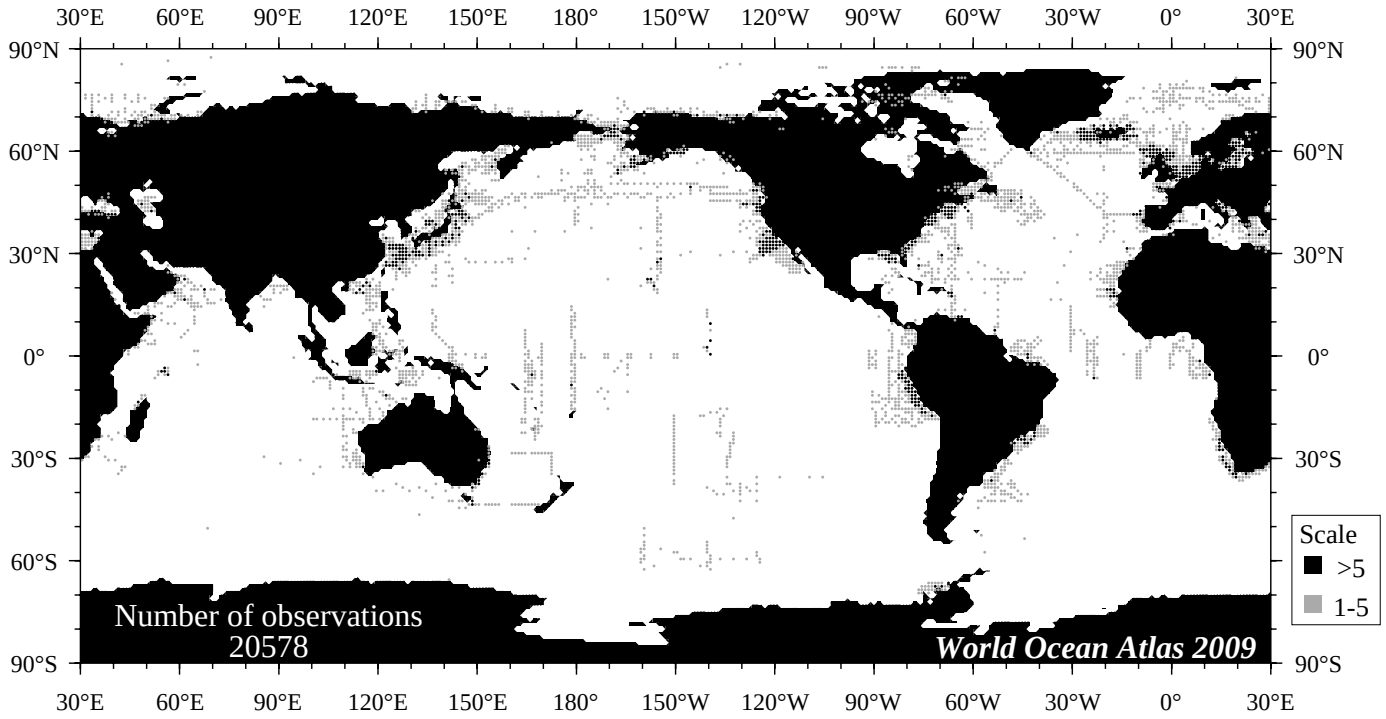

Fig F15 August nitrate observations at the surface.

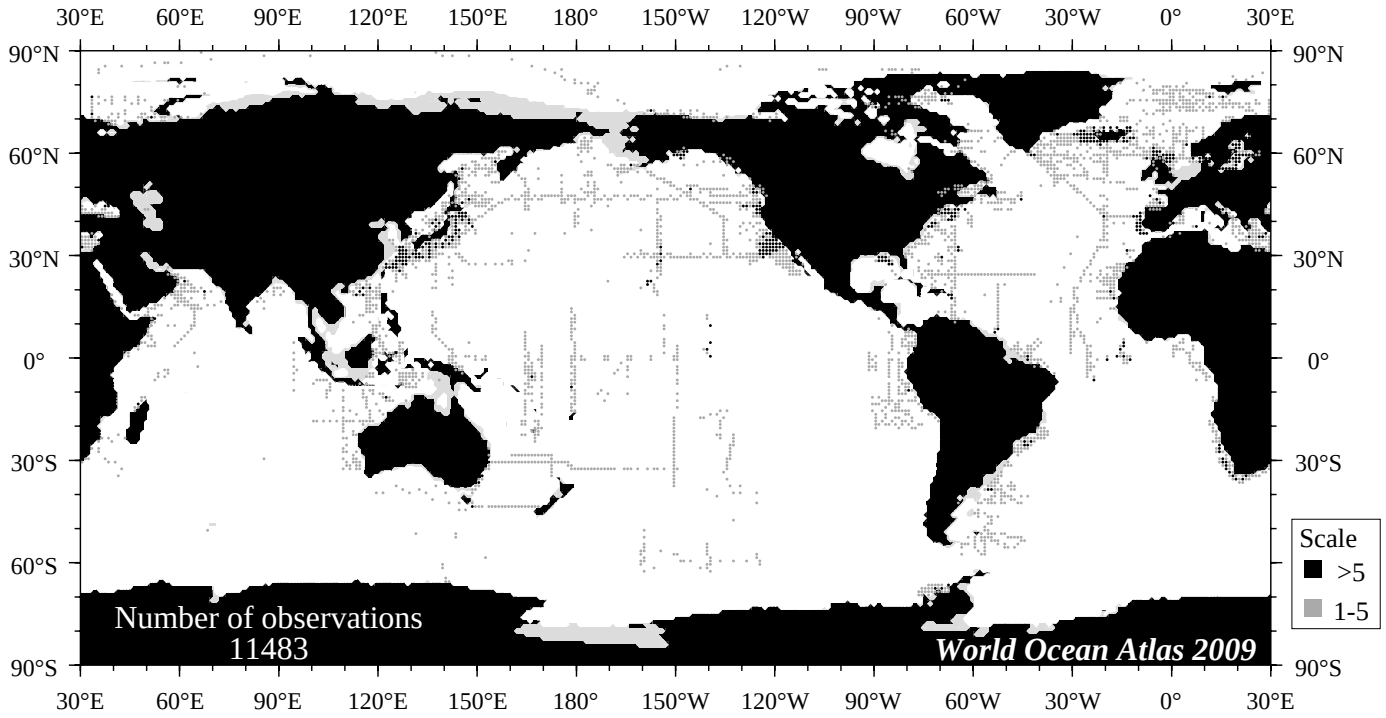

Fig F16 August nitrate observations at 75 m. depth.

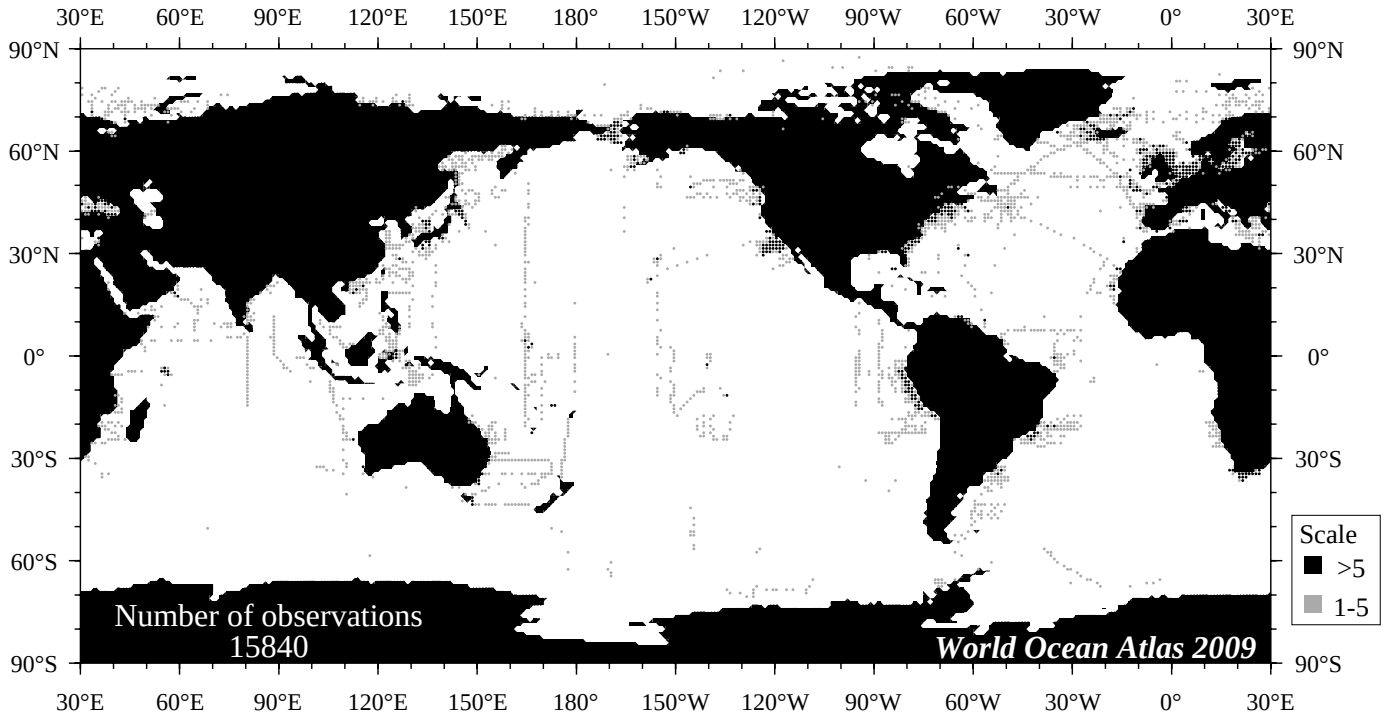

Fig F17 September nitrate observations at the surface.

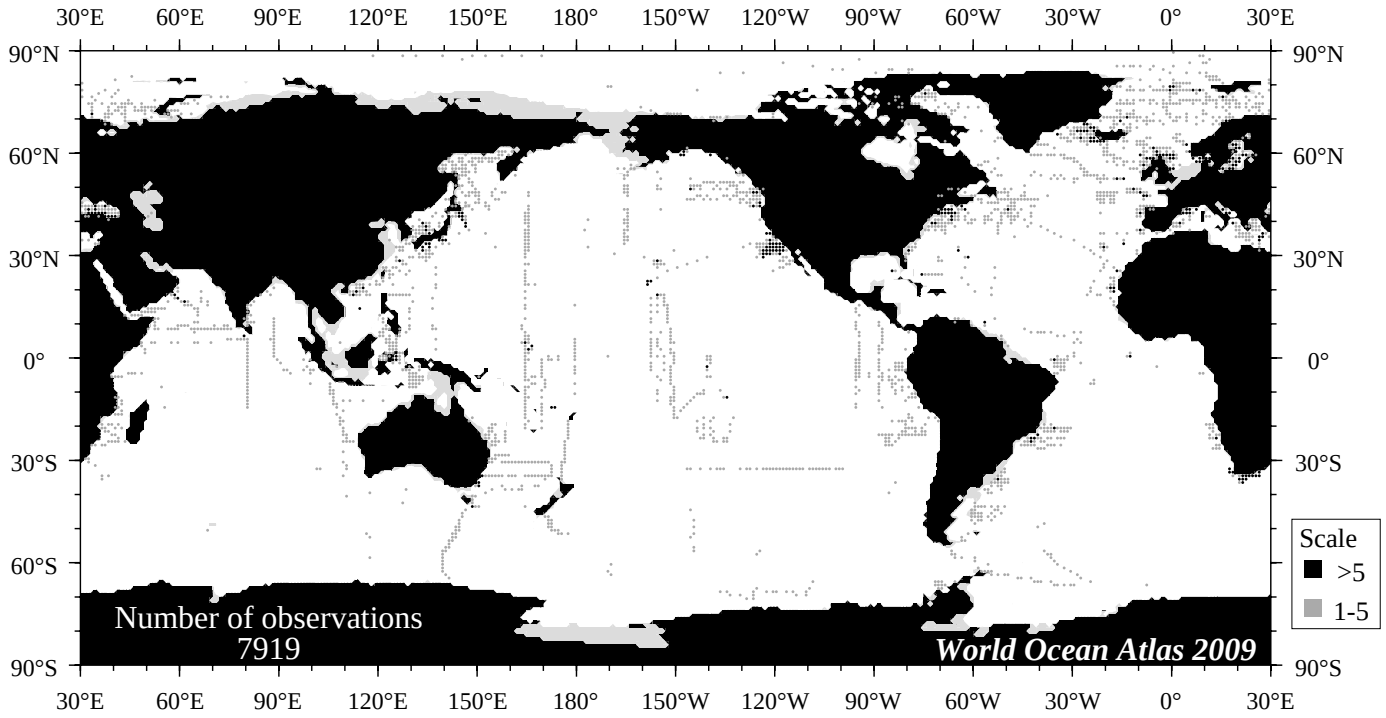

Fig F18 September nitrate observations at 75 m. depth.

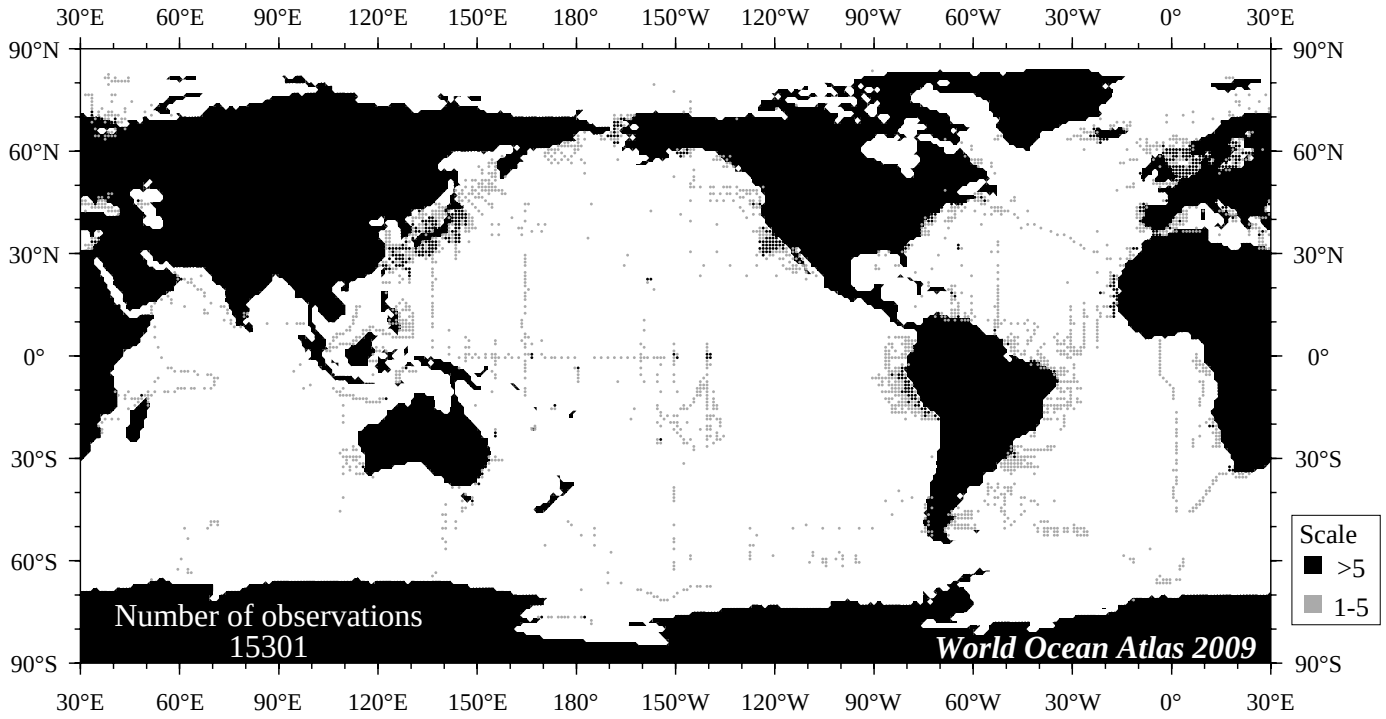

Fig F19 October nitrate observations at the surface.

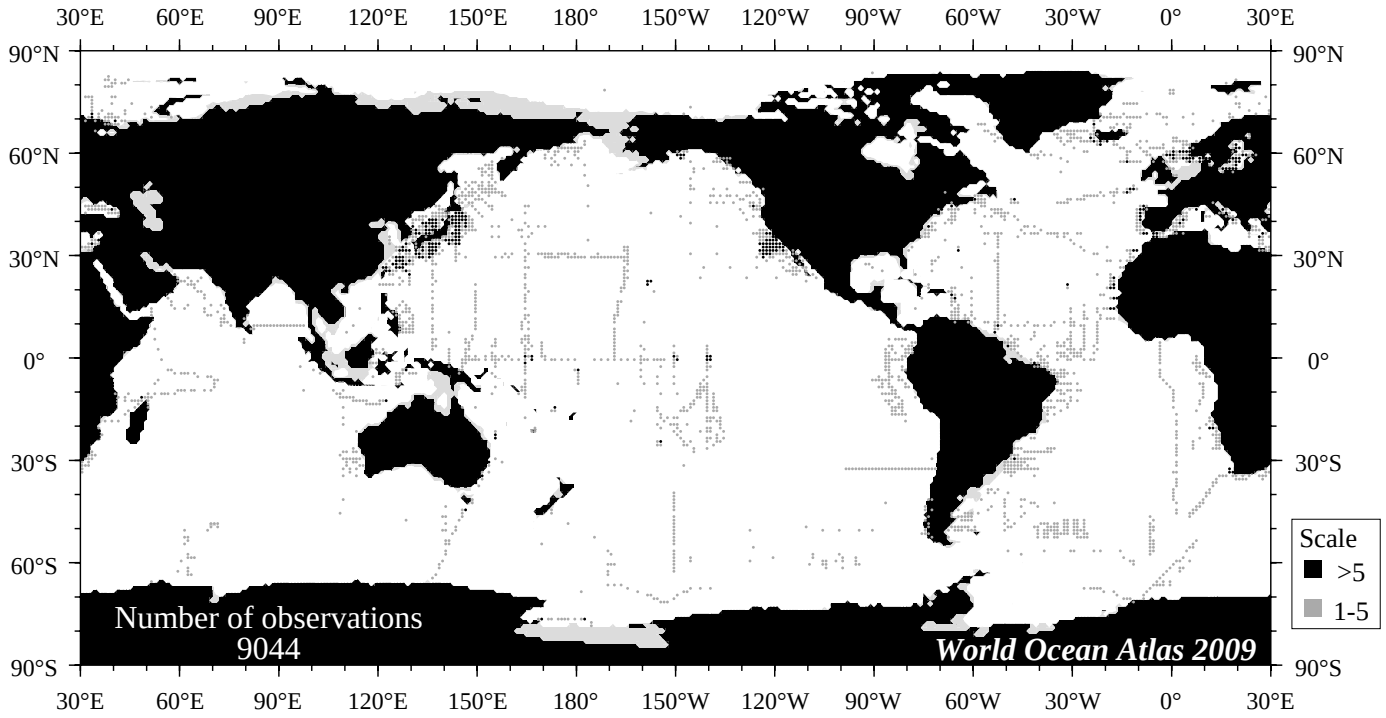

Fig F20 October nitrate observations at 75 m. depth.

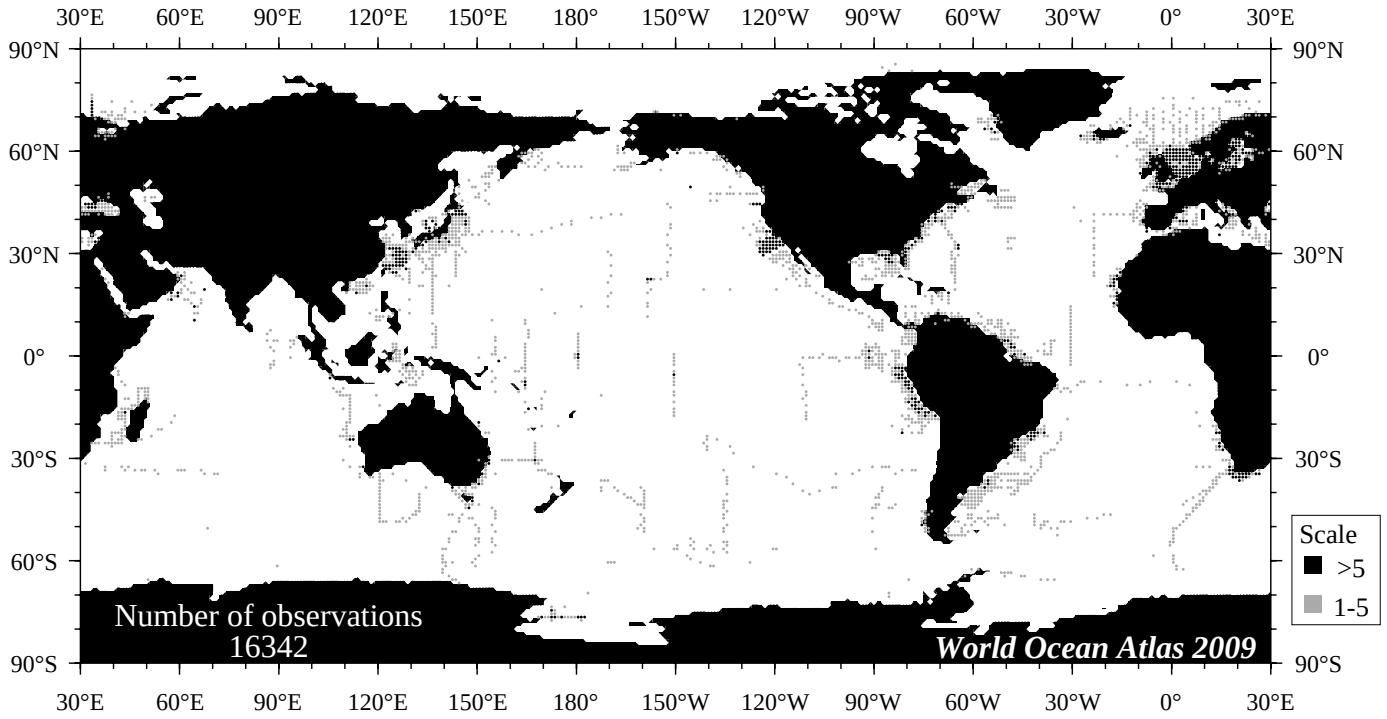

Fig F21 November nitrate observations at the surface.

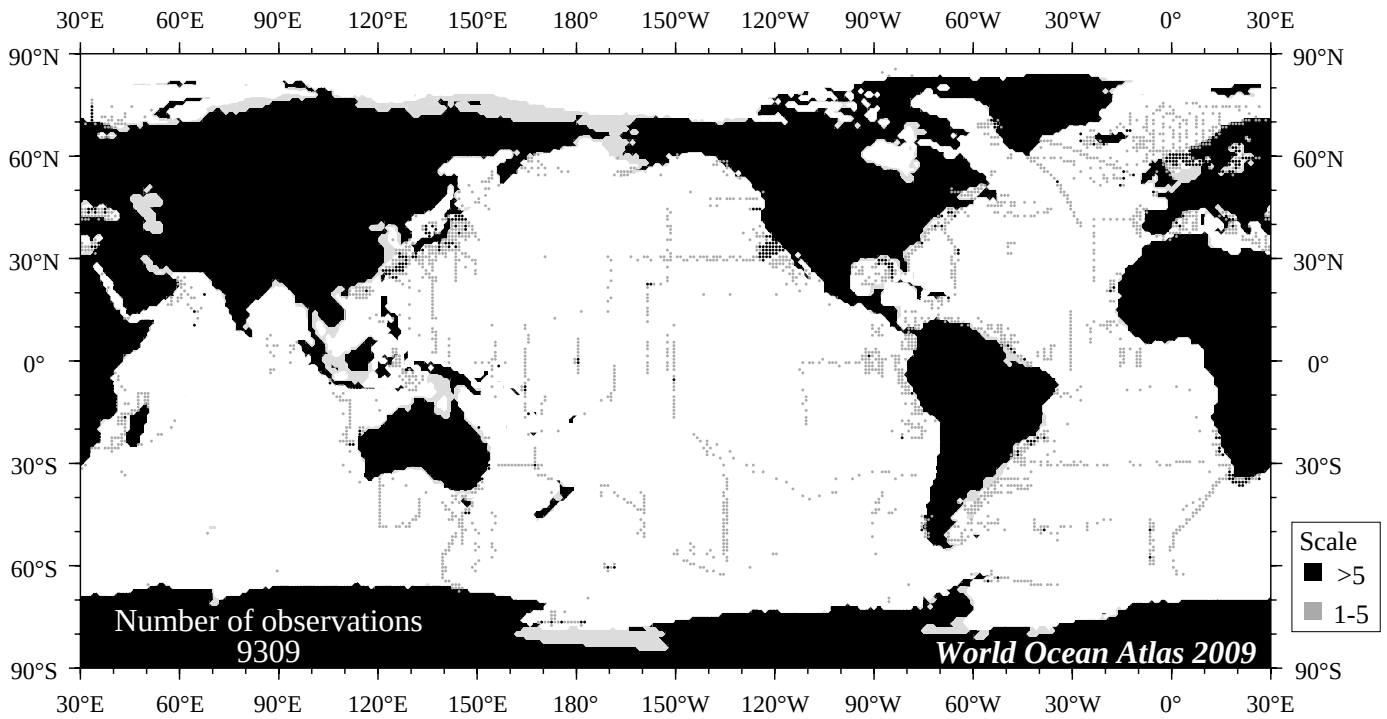

Fig F22 November nitrate observations at 75 m. depth.

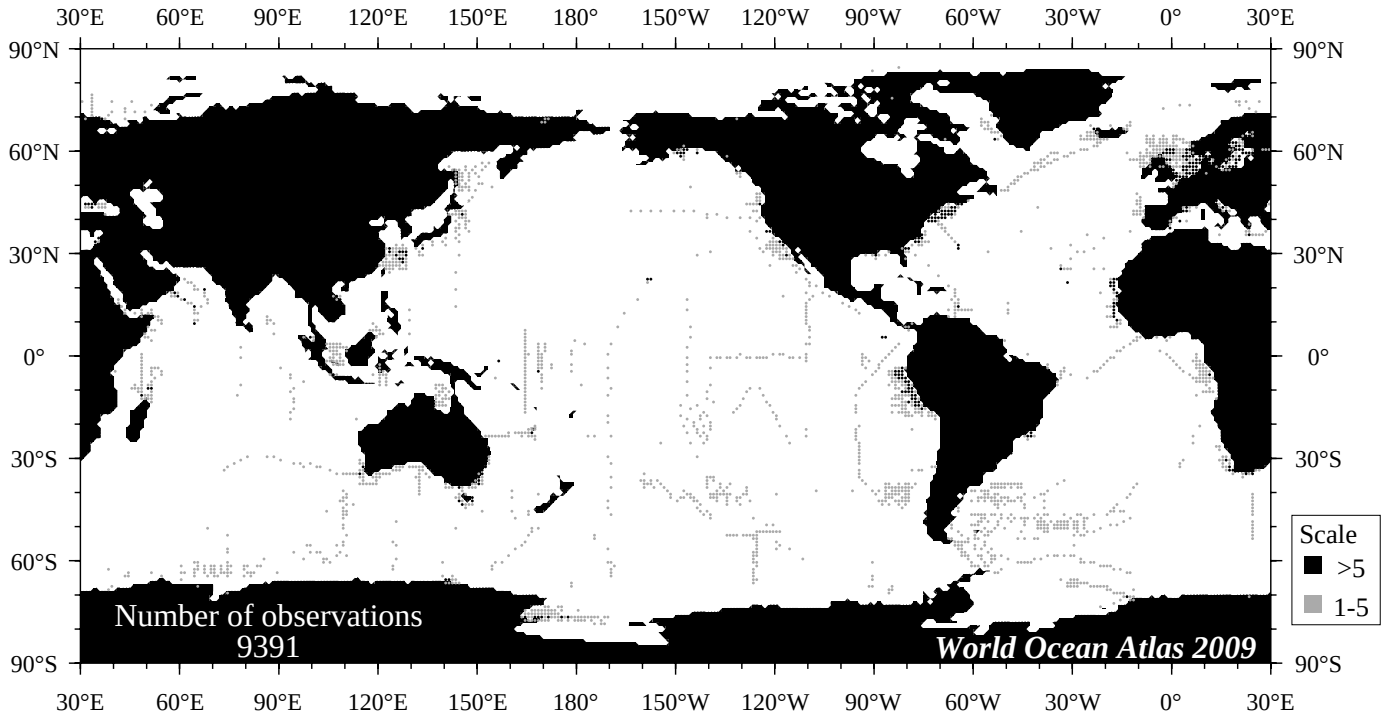

Fig F23 December nitrate observations at the surface.

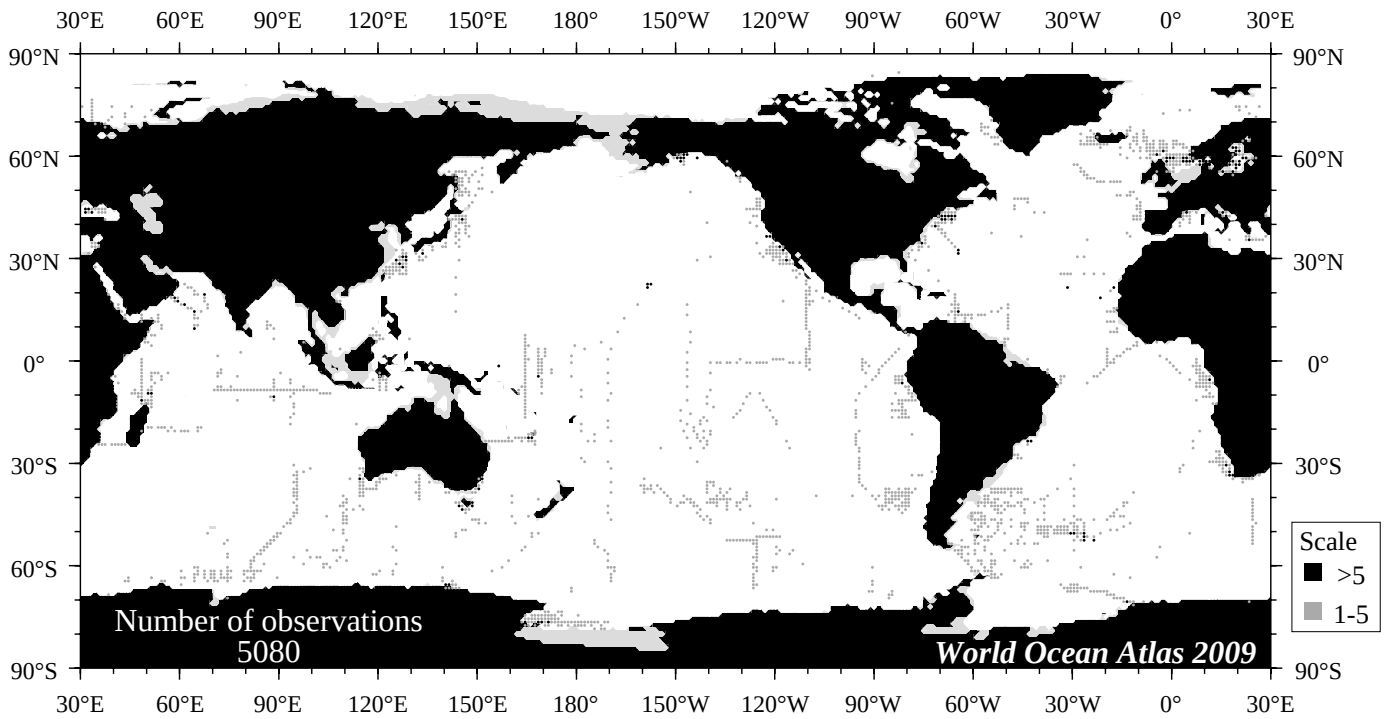

Fig F24 December nitrate observations at 75 m. depth.

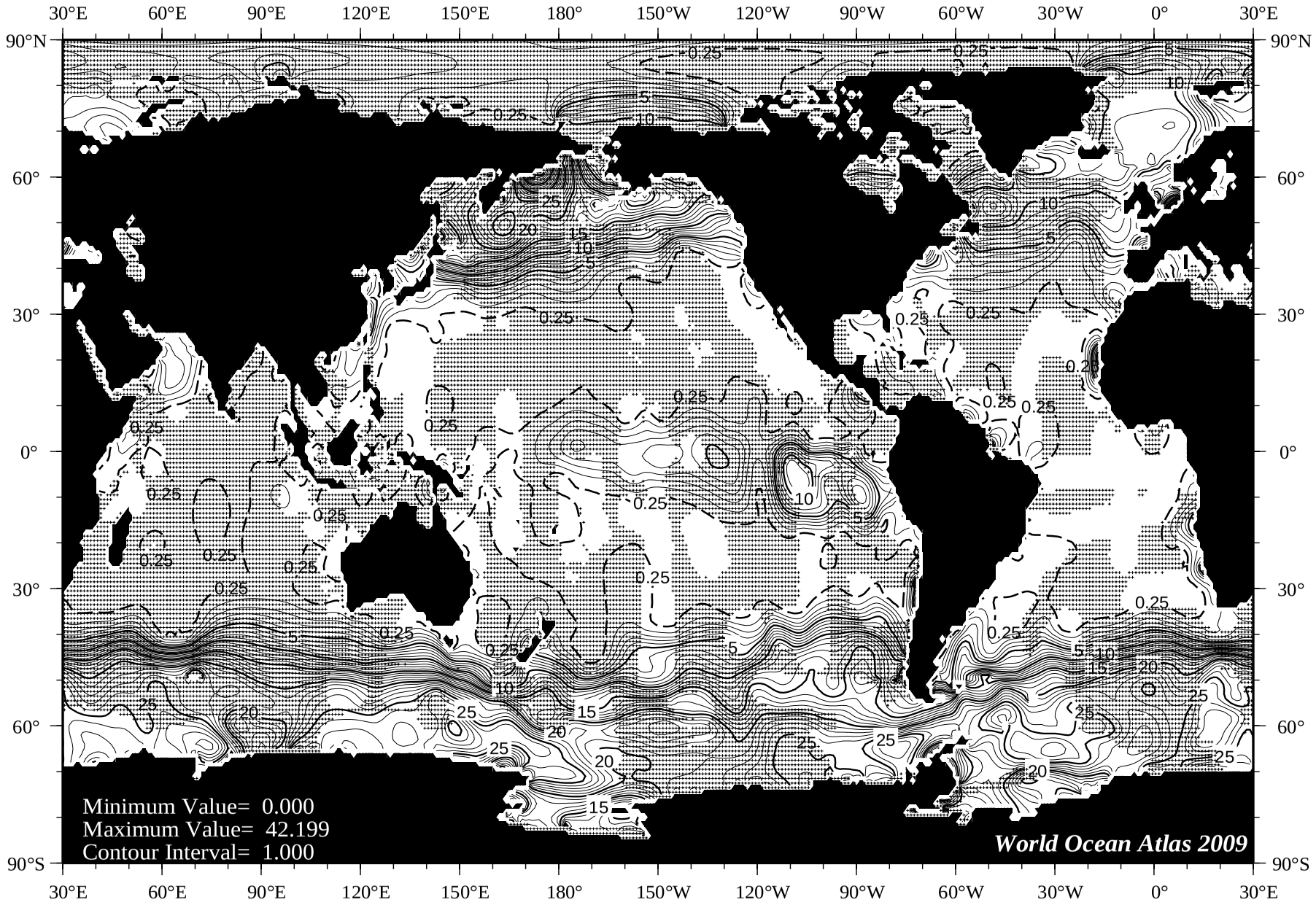

Fig F25 January mean nitrate [umol/l] at the surface.

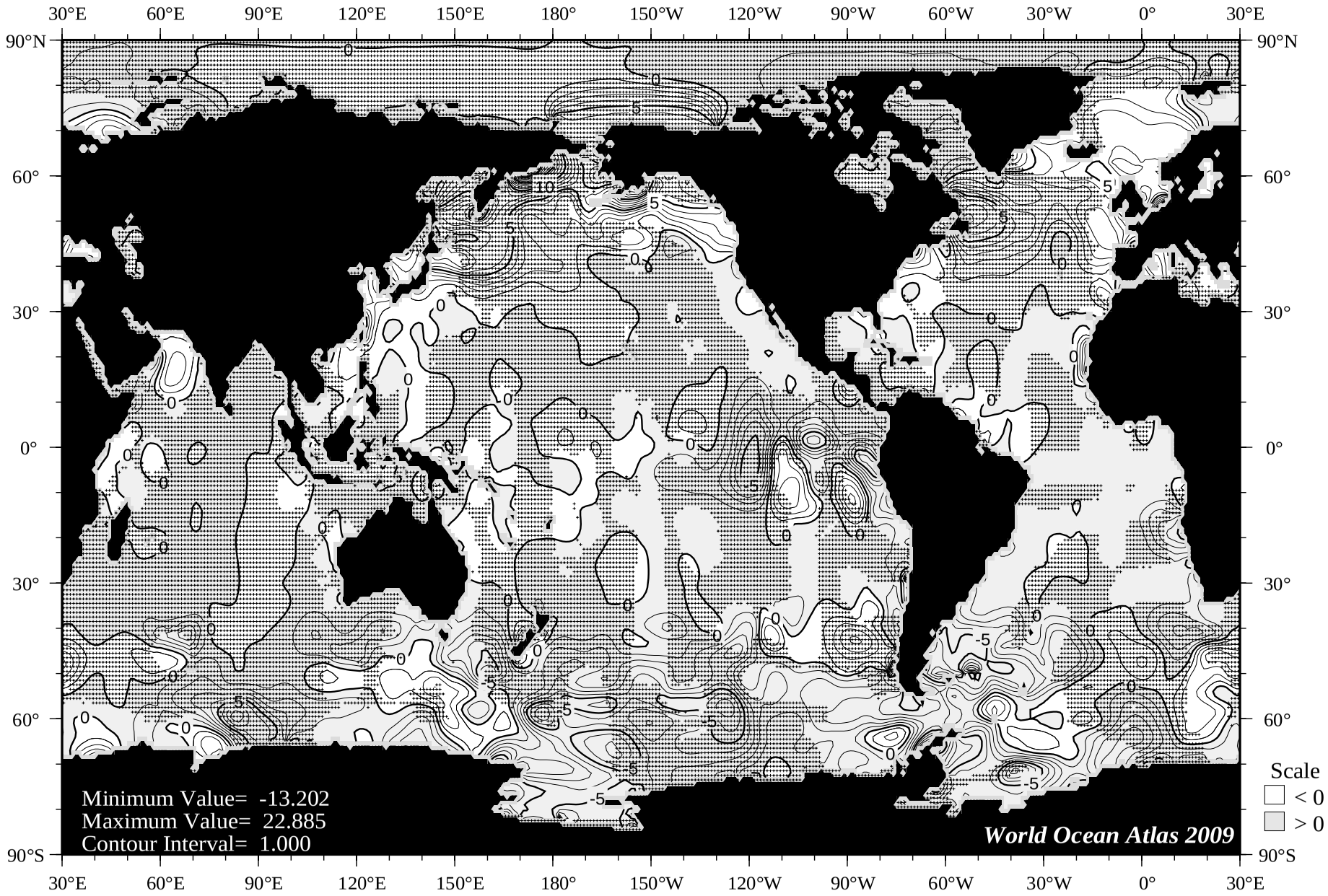

Fig F26 January minus annual nitrate [umol/l] at the surface.

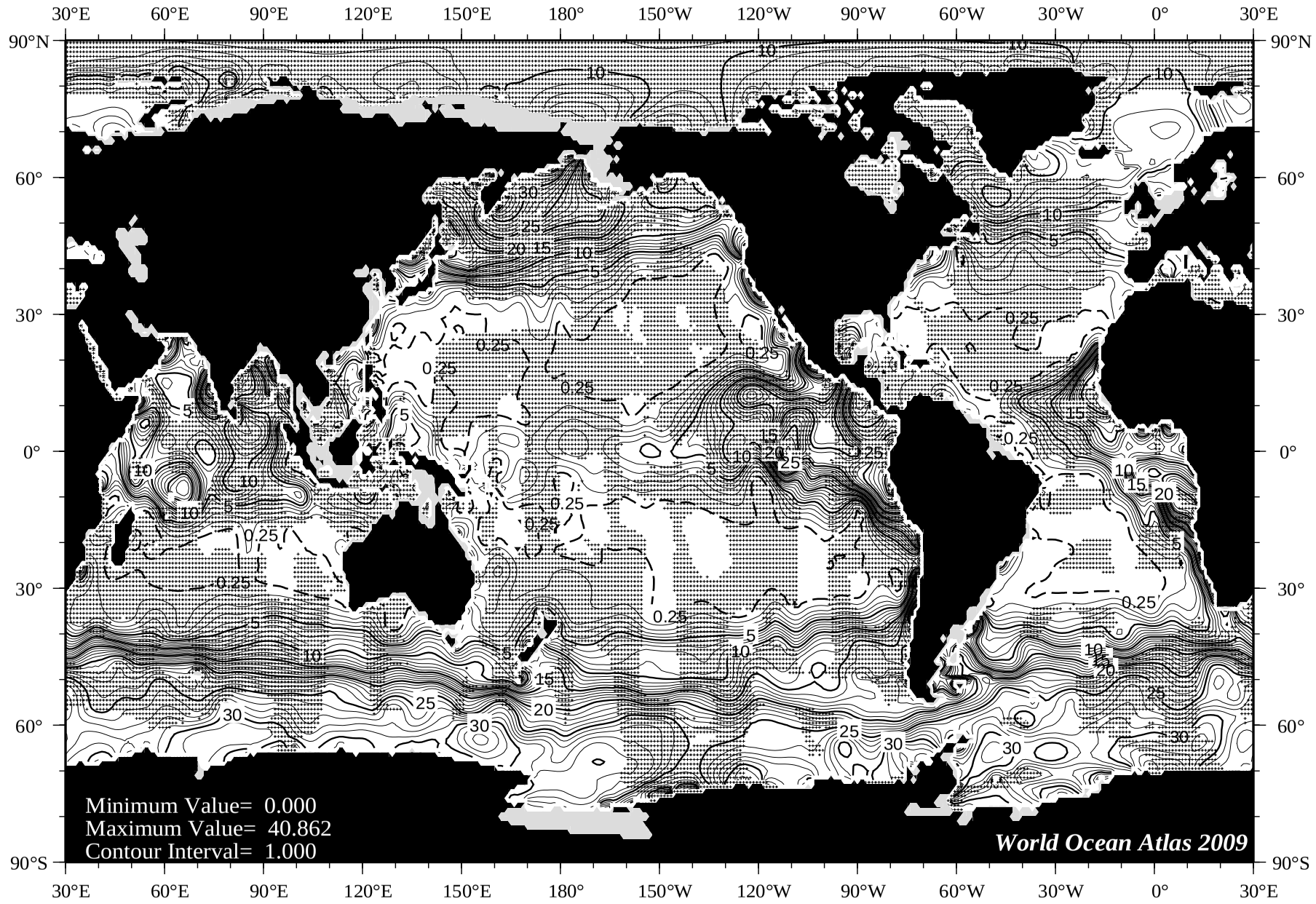

Fig F27 January mean nitrate [umol/l] at 75 m. depth.

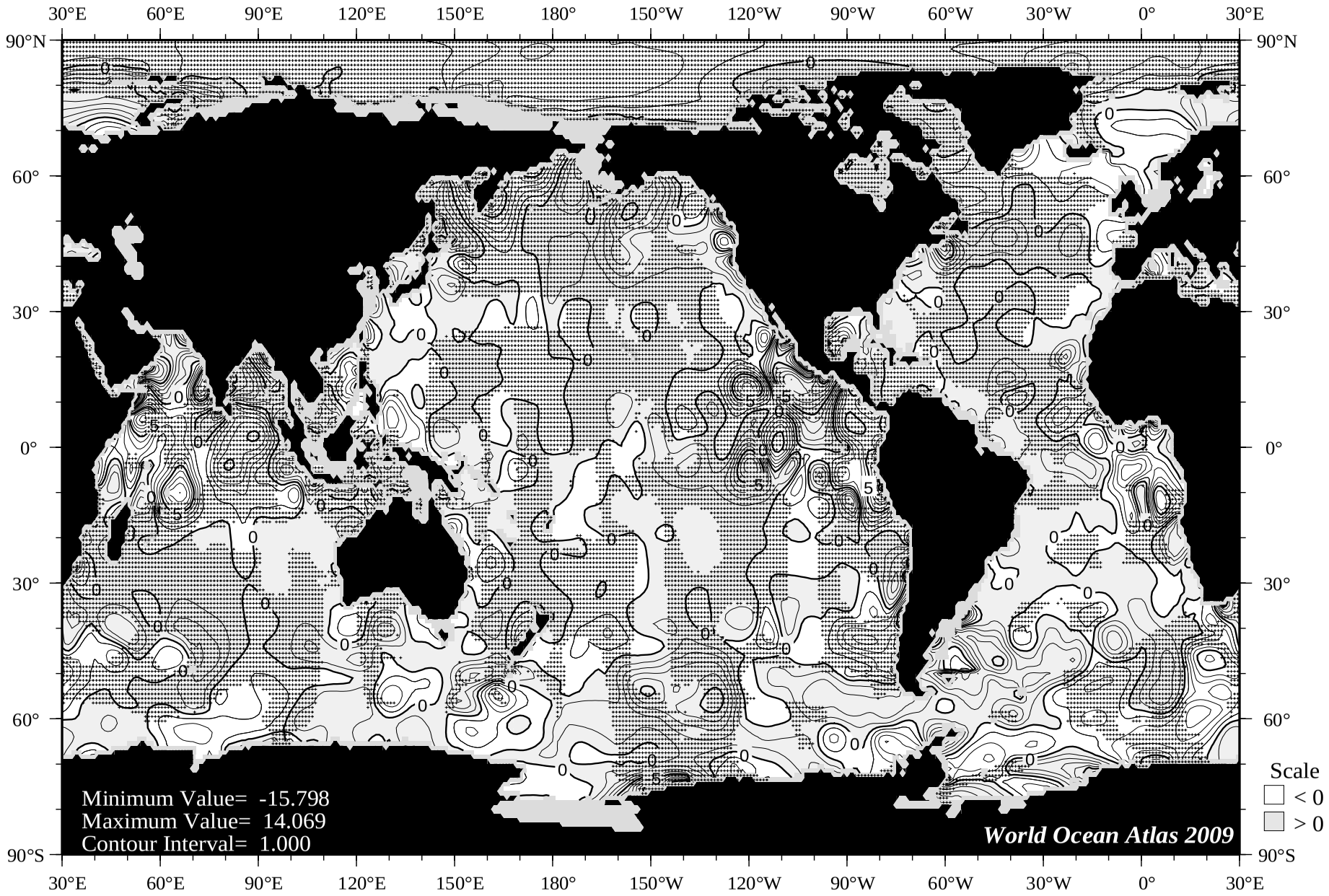

Fig F28 January minus annual nitrate [umol/l] at 75 m. depth.

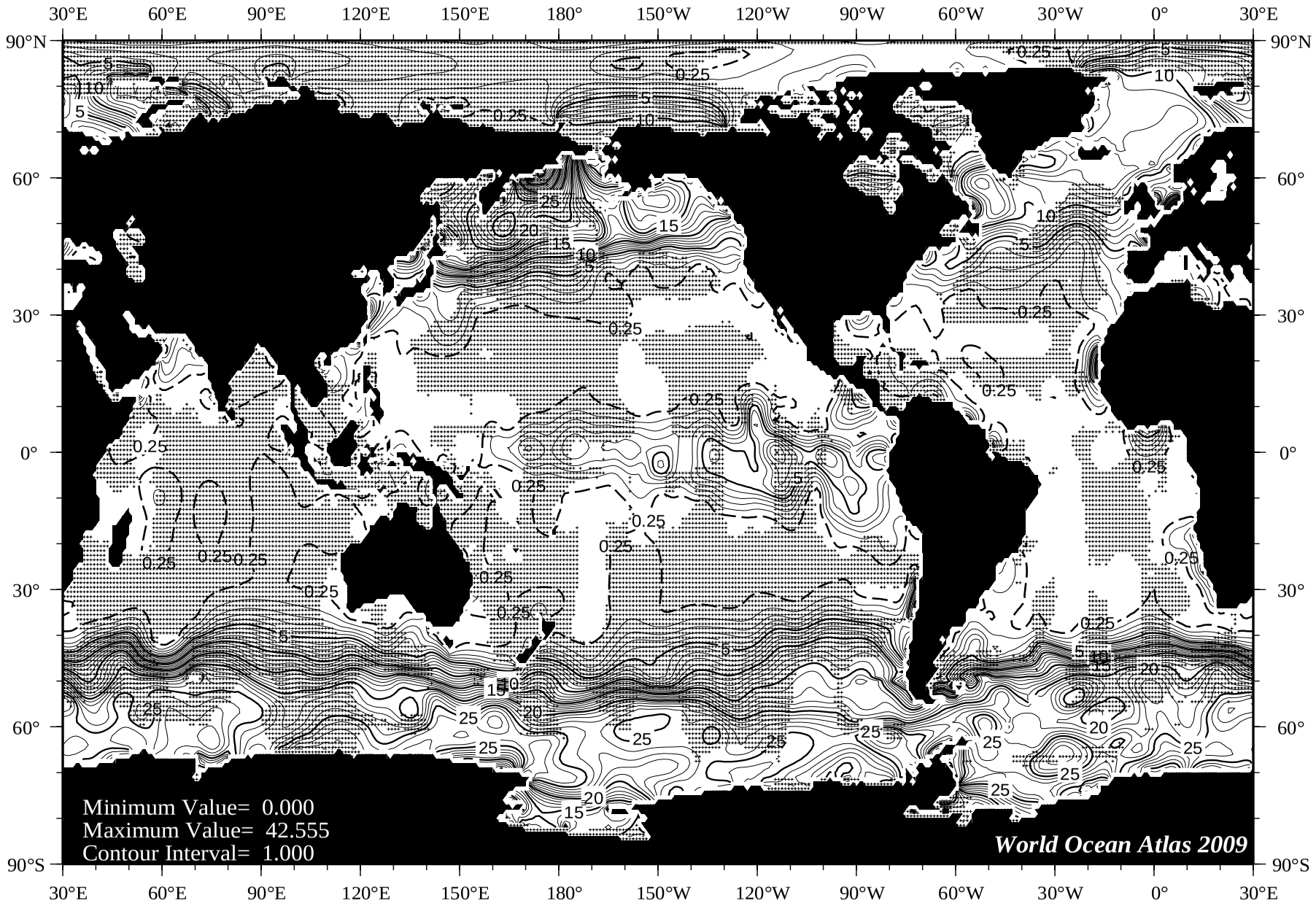

Fig F29 February mean nitrate [umol/l] at the surface.

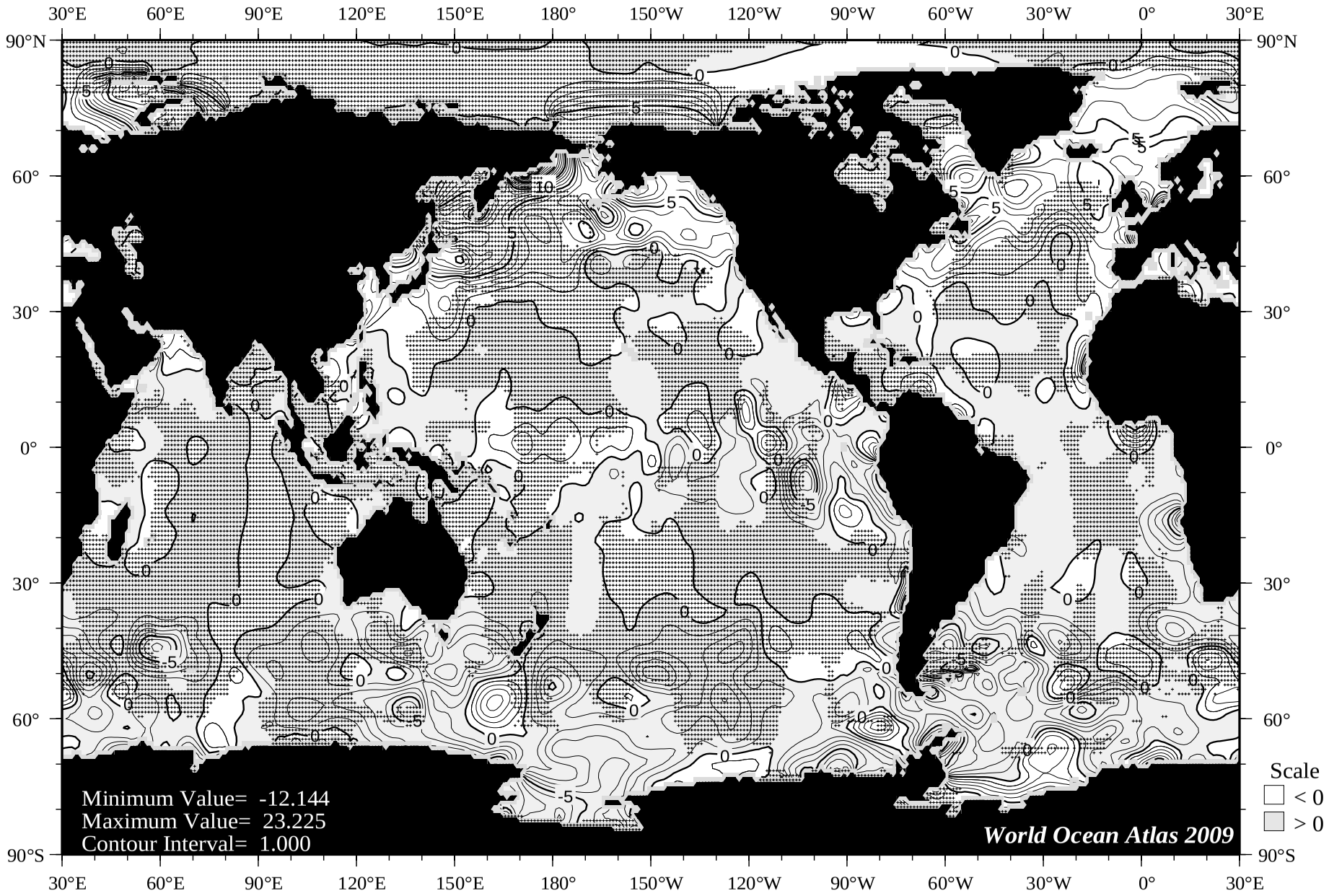

Fig F30 February minus annual nitrate [umol/l] at the surface.

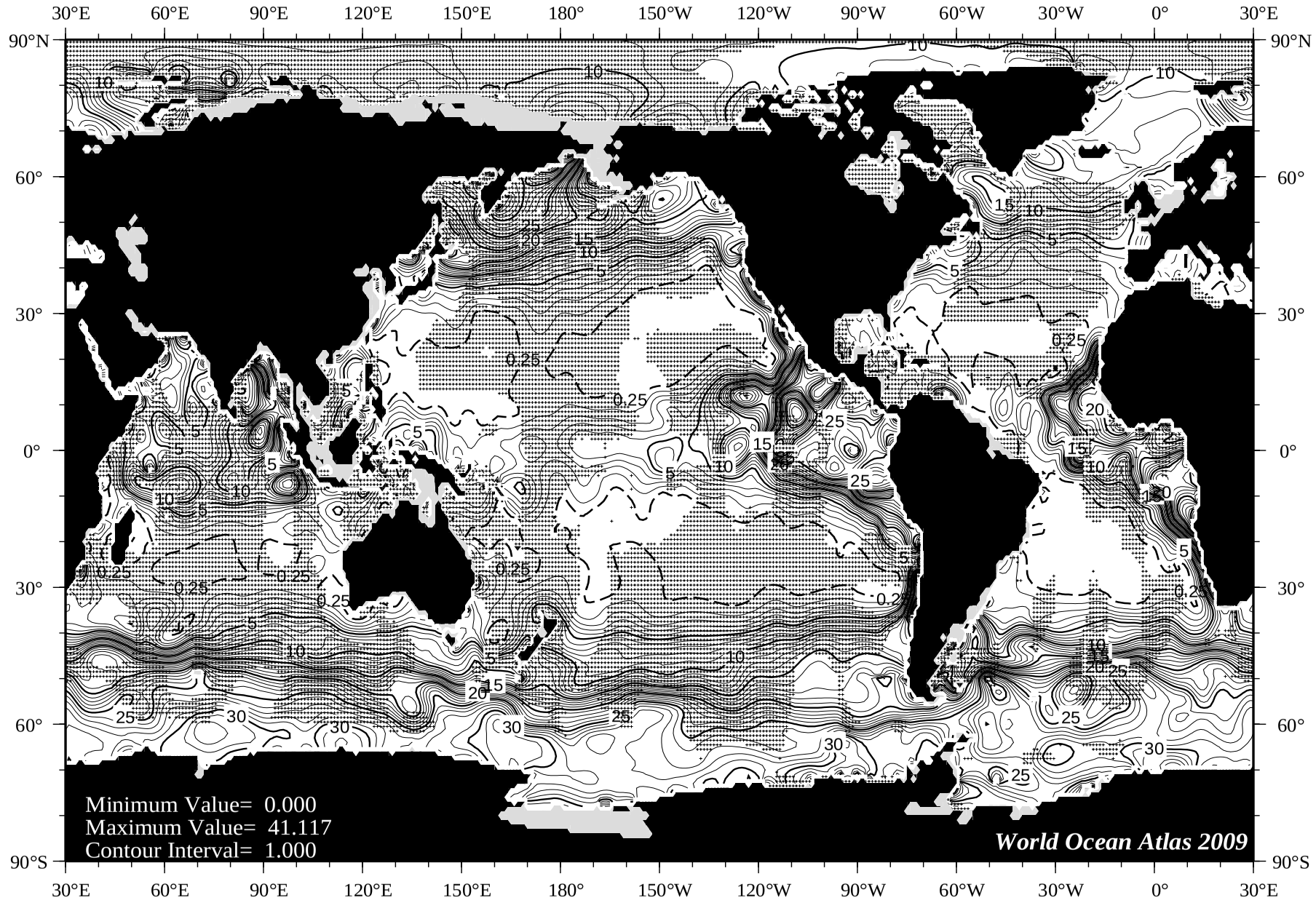

Fig F31 February mean nitrate [umol/l] at 75 m. depth.

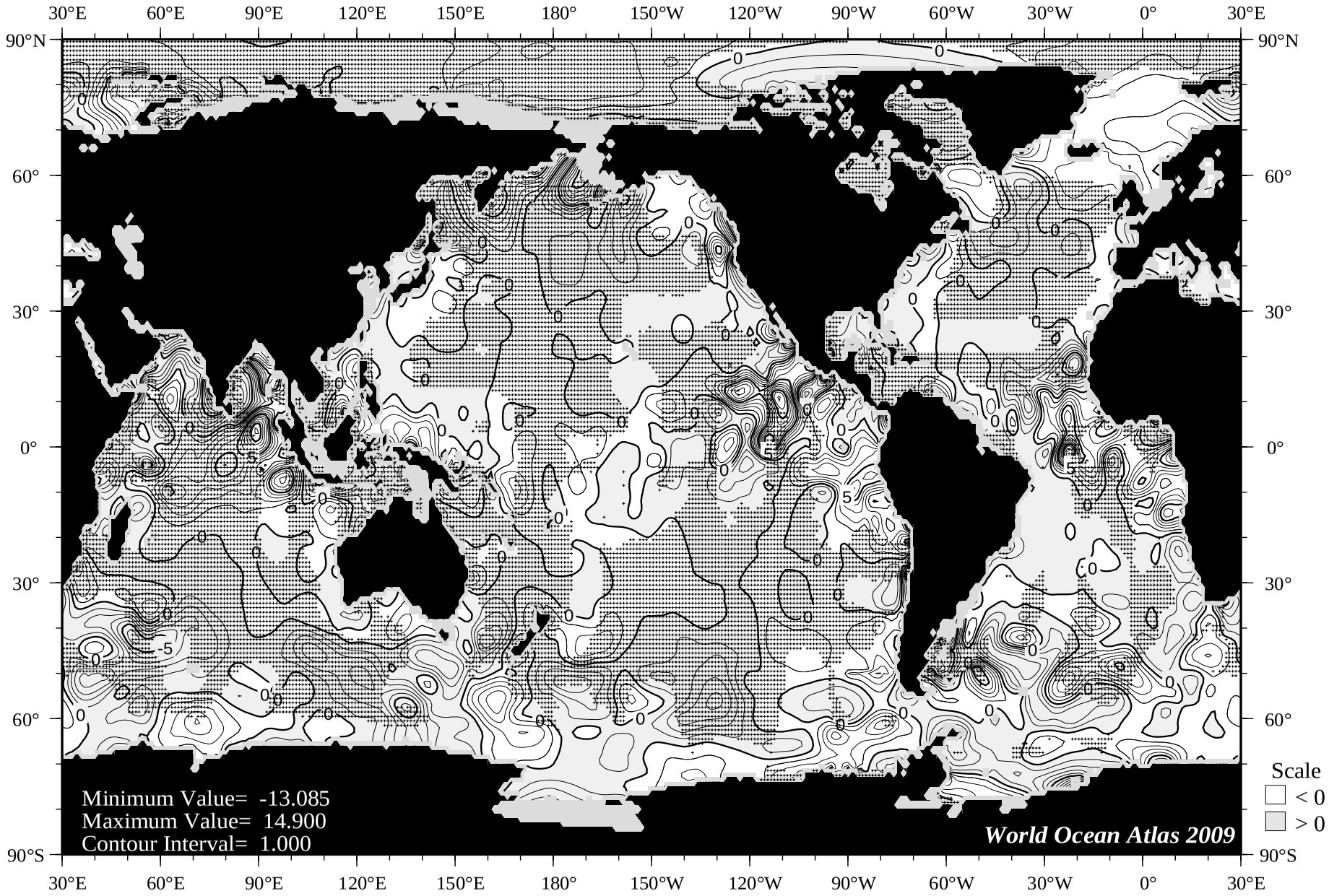

Fig F32 February minus annual nitrate [umol/l] at 75 m. depth.

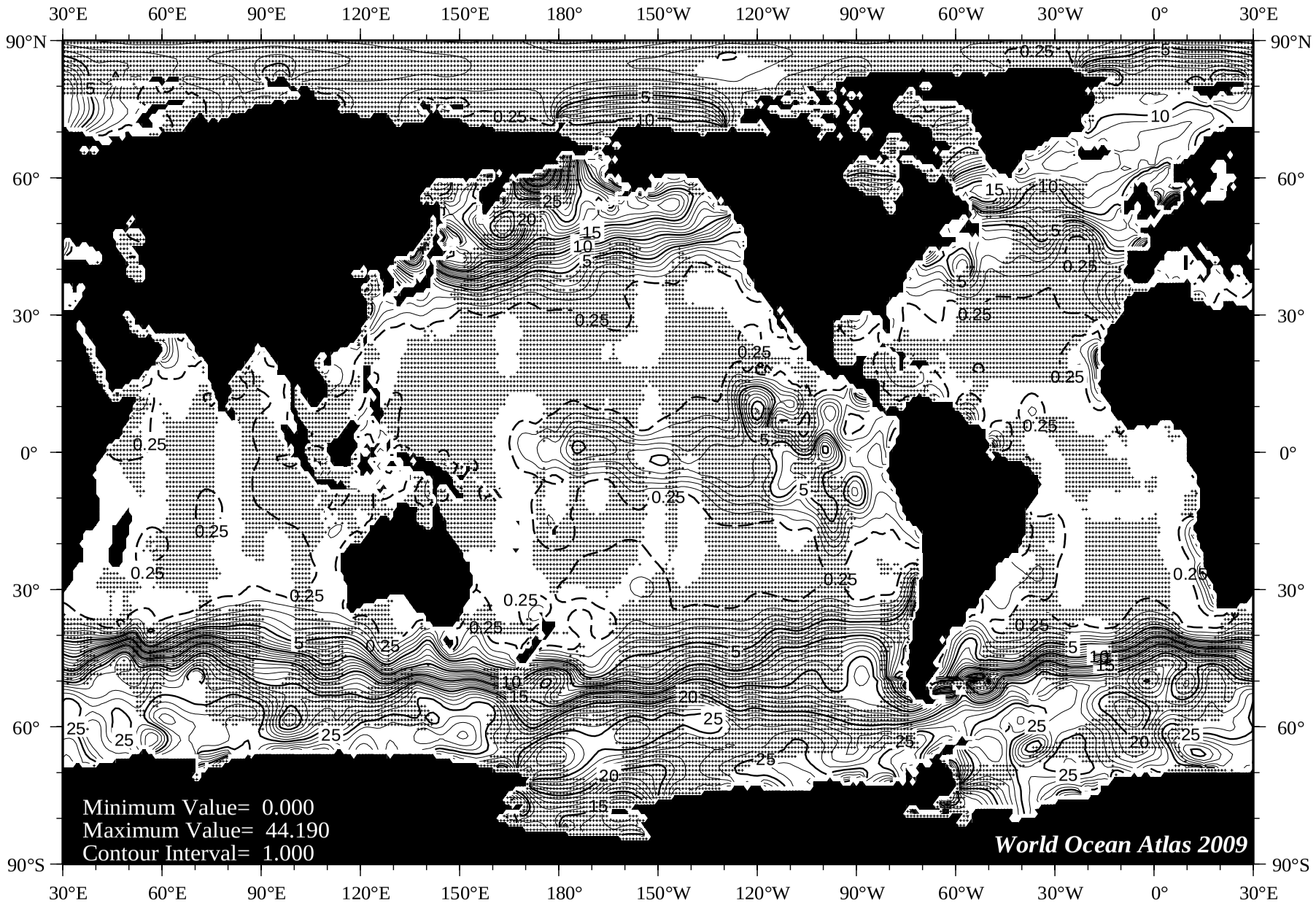

Fig F33 March mean nitrate [umol/l] at the surface.

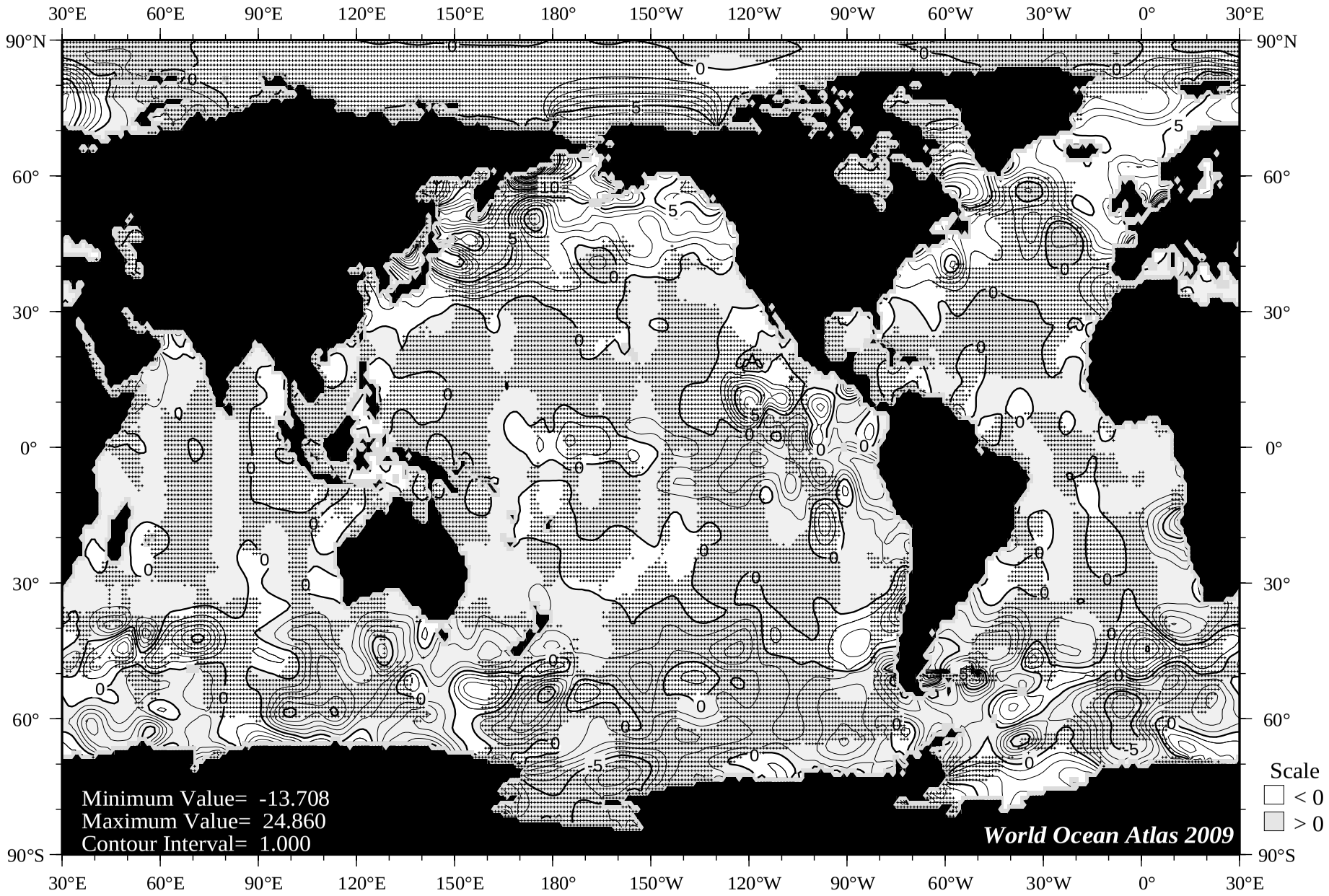

Fig F34 March minus annual nitrate [umol/l] at the surface.

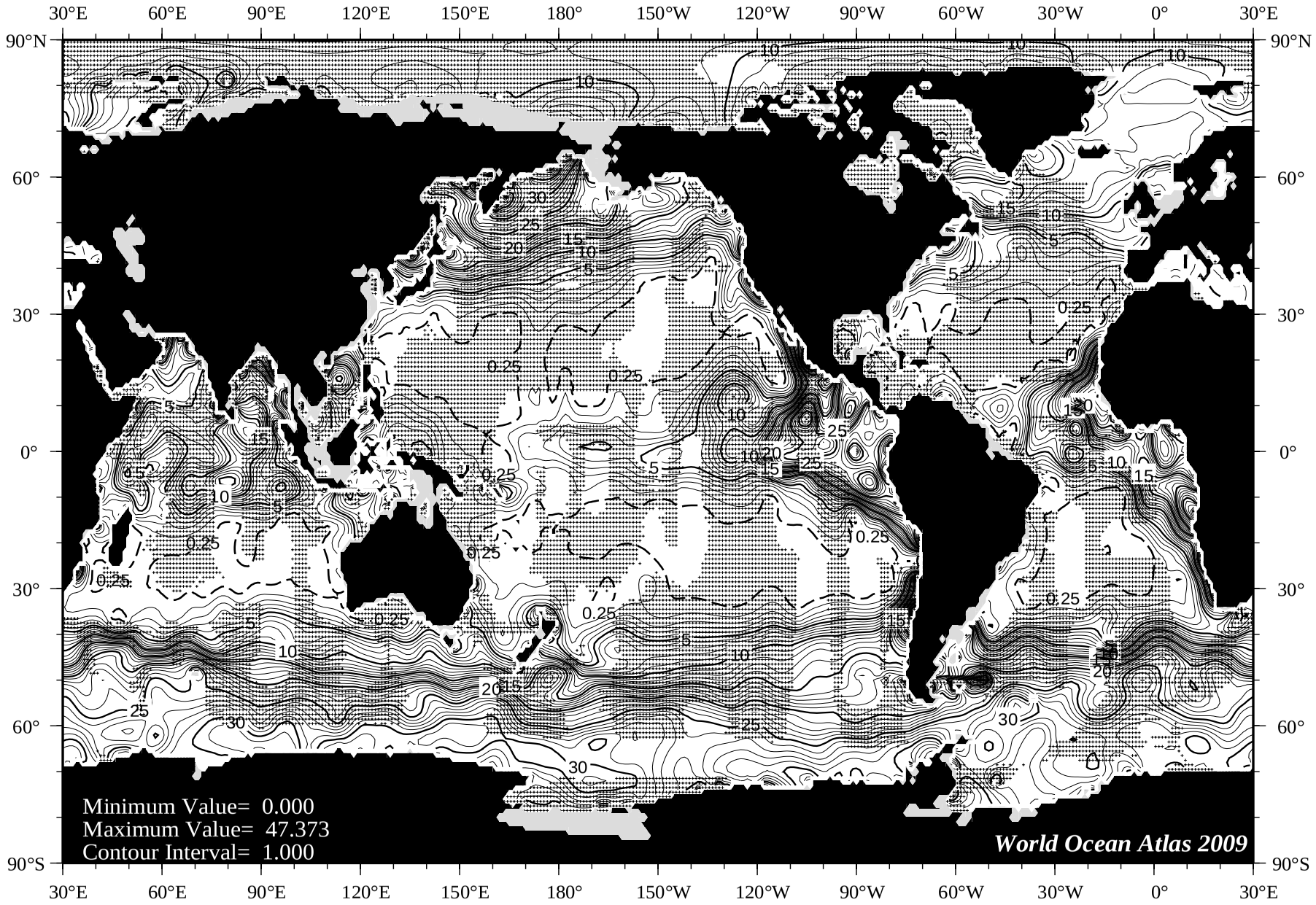

Fig F35 March mean nitrate [umol/l] at 75 m. depth.

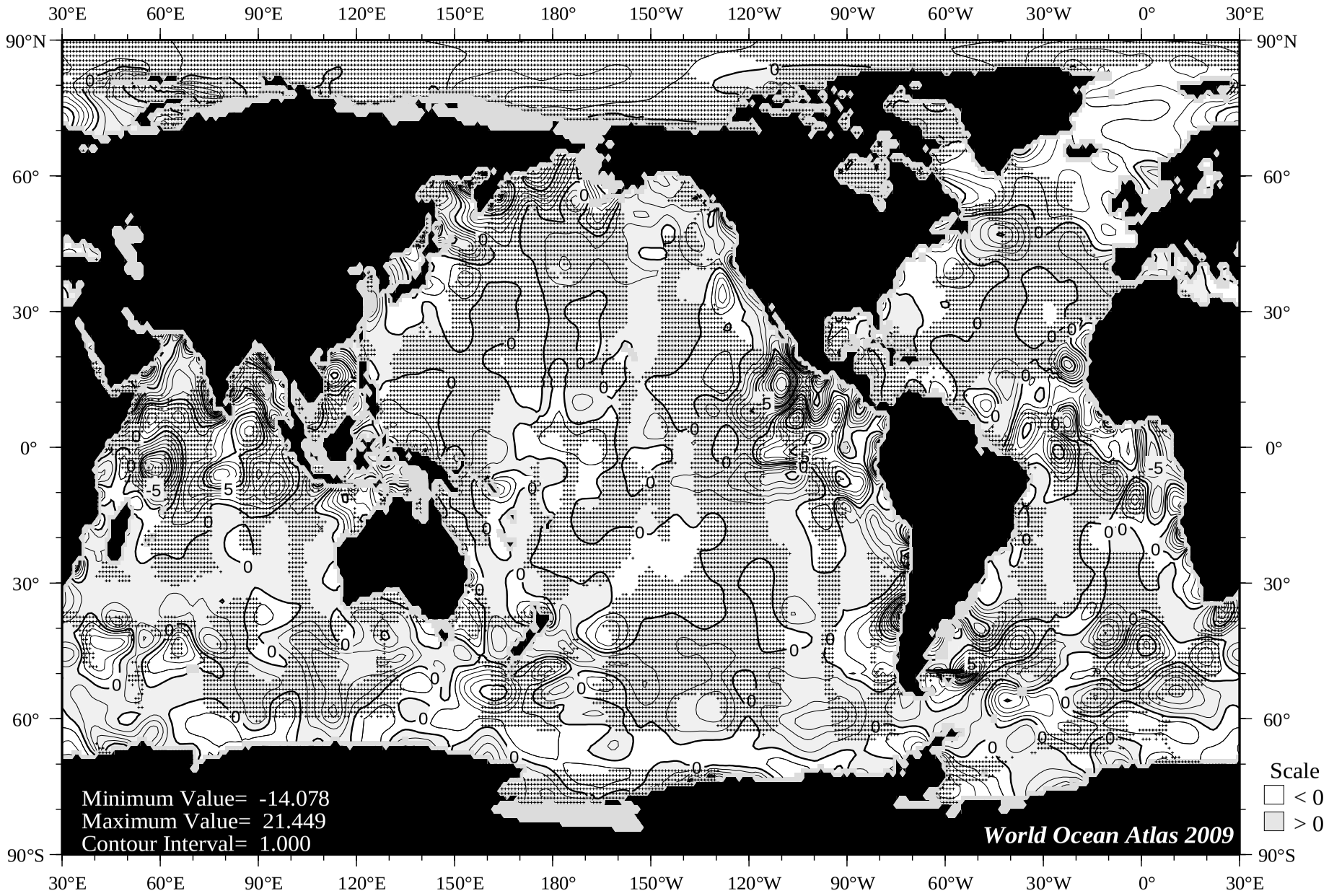

Fig F36 March minus annual nitrate [umol/l] at 75 m. depth.

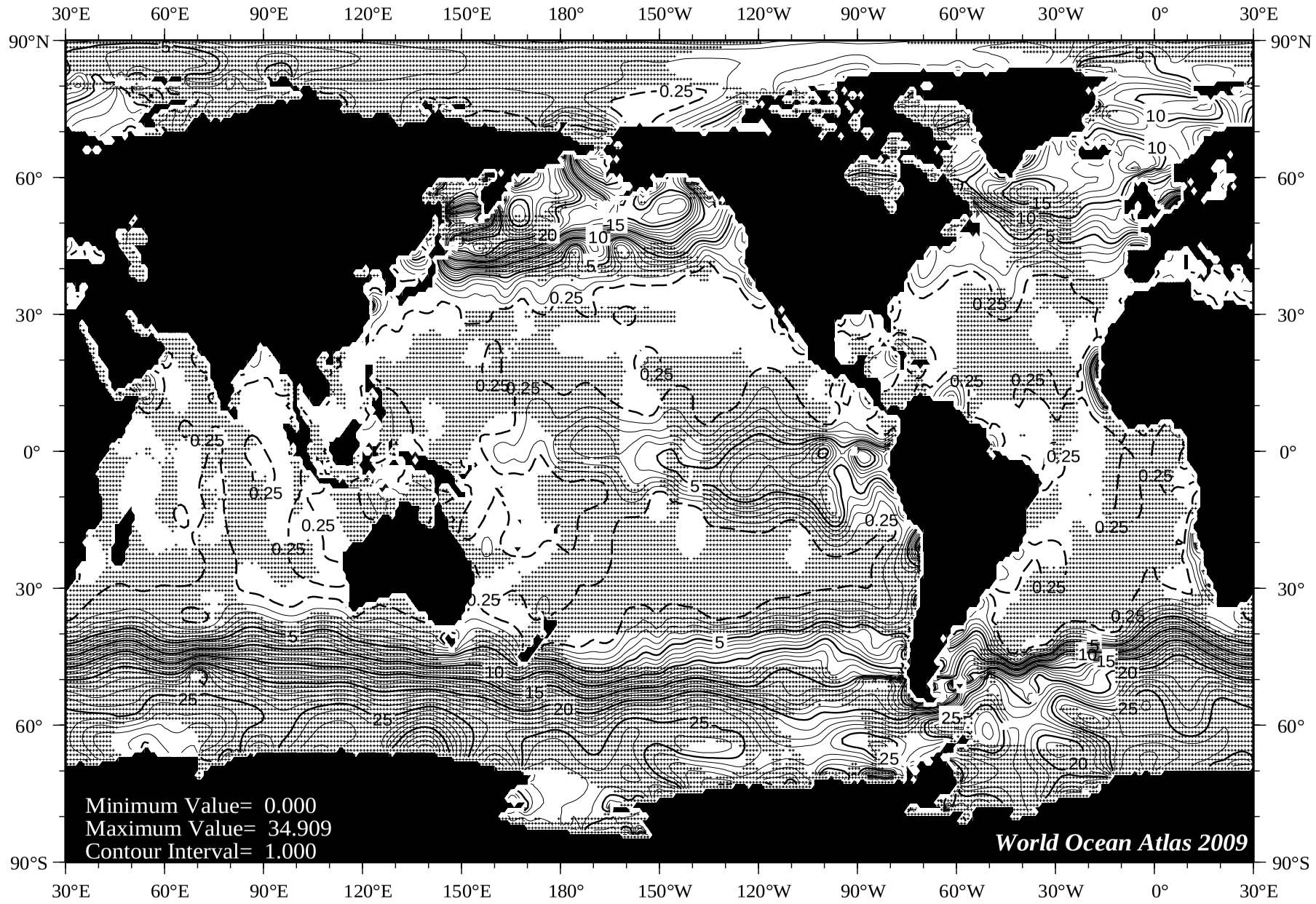

Fig F37 April mean nitrate [umol/l] at the surface.

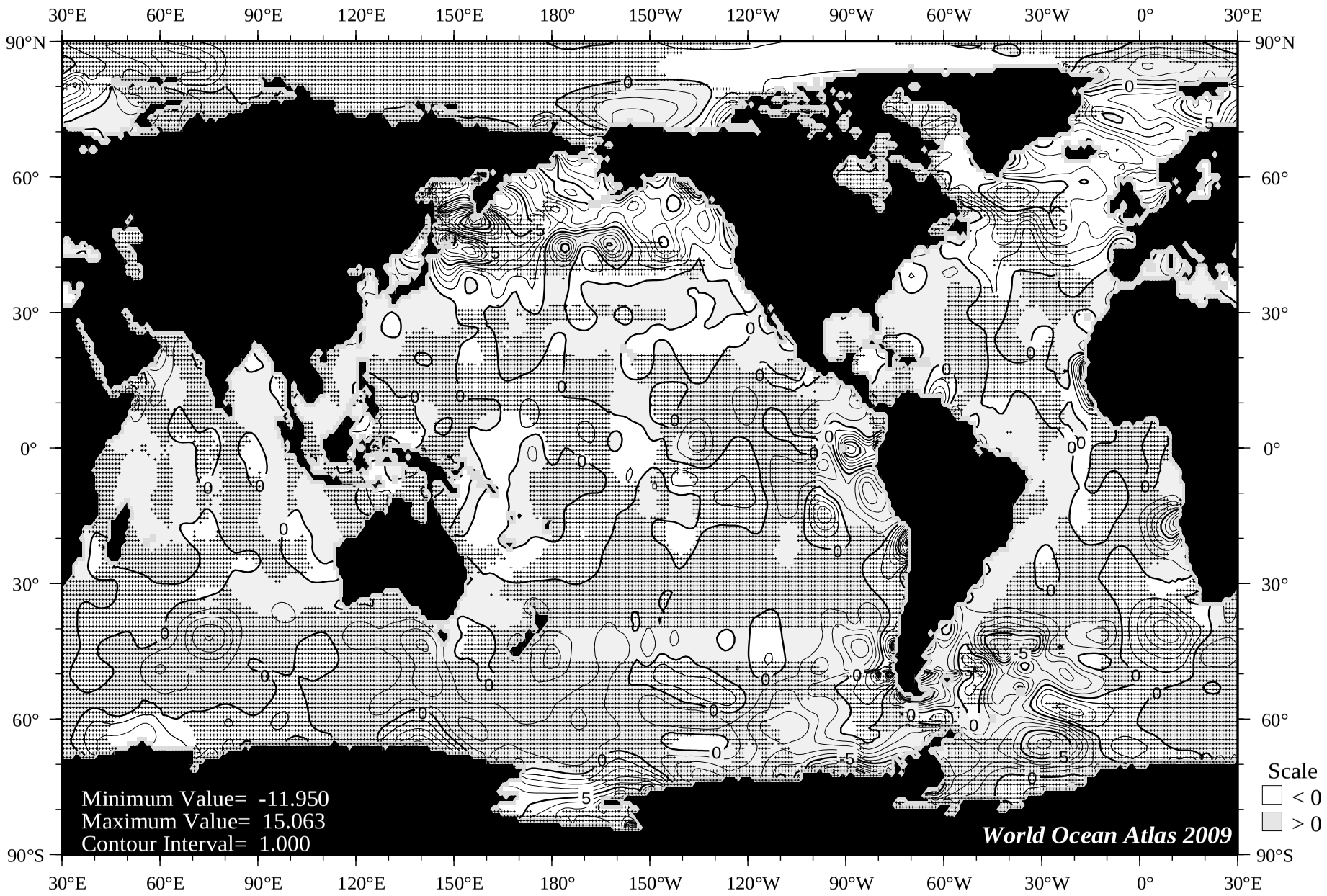

Fig F38 April minus annual nitrate [umol/l] at the surface.

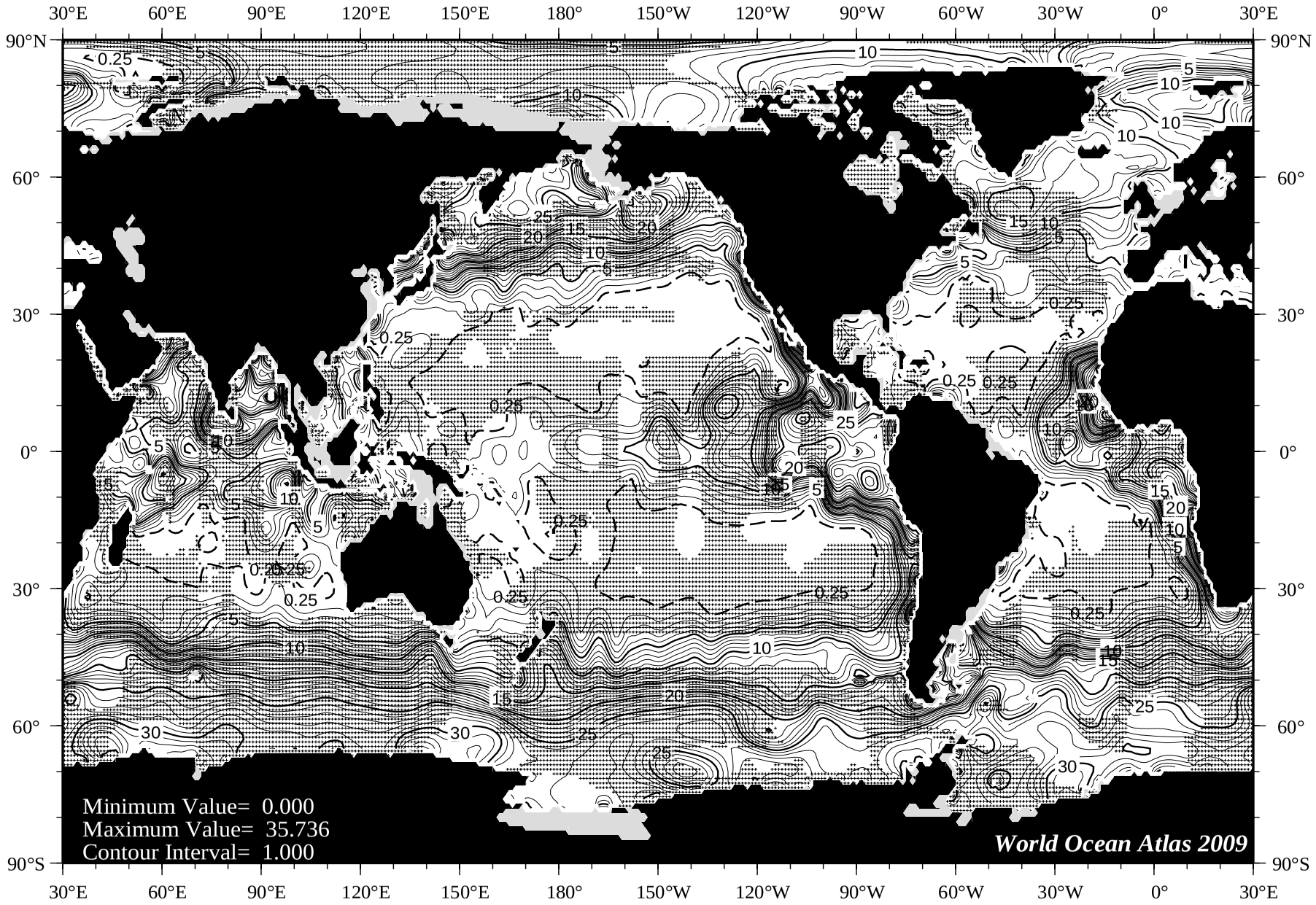

Fig F39 April mean nitrate [umol/l] at 75 m. depth.

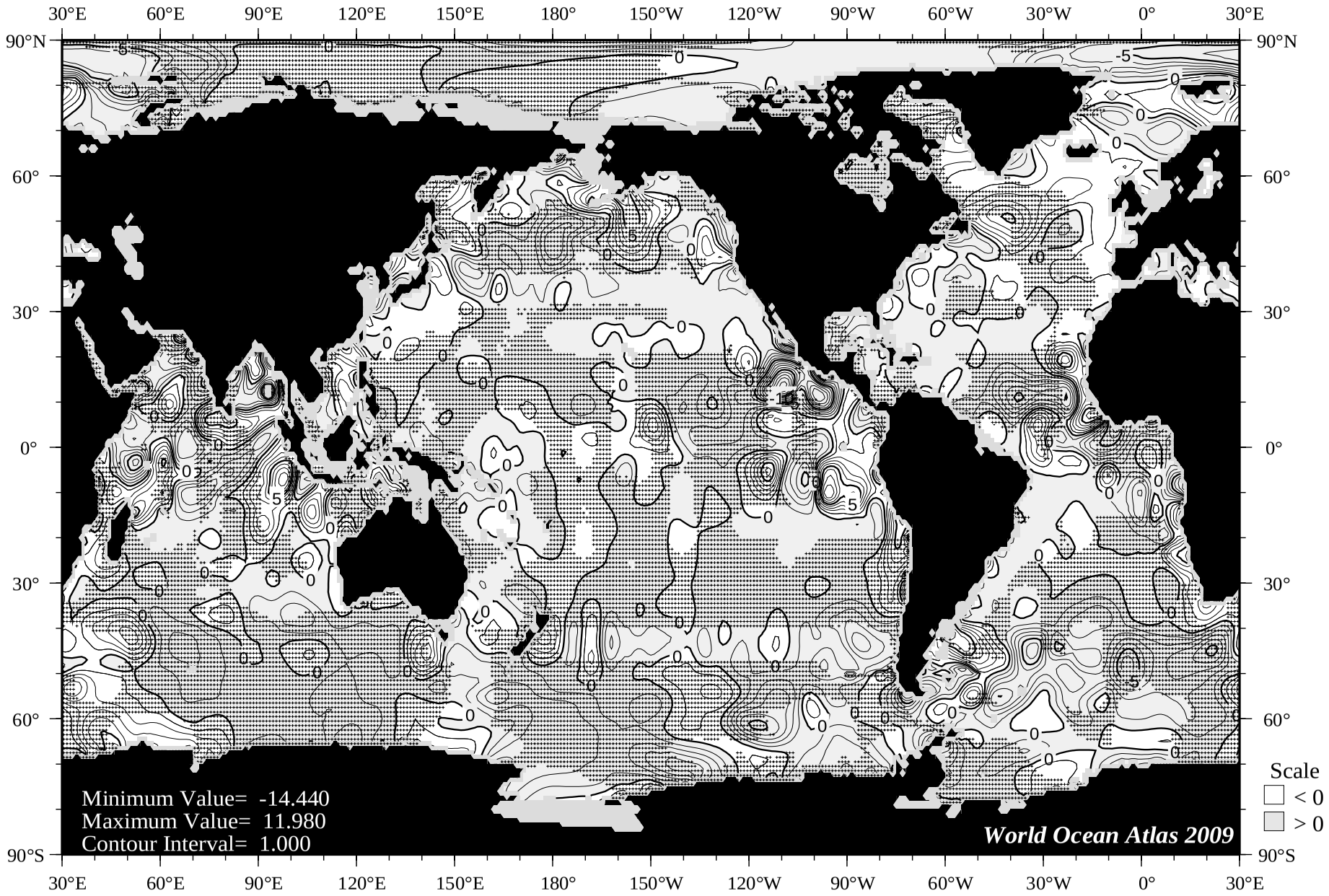

Fig F40 April minus annual nitrate [umol/l] at 75 m. depth.

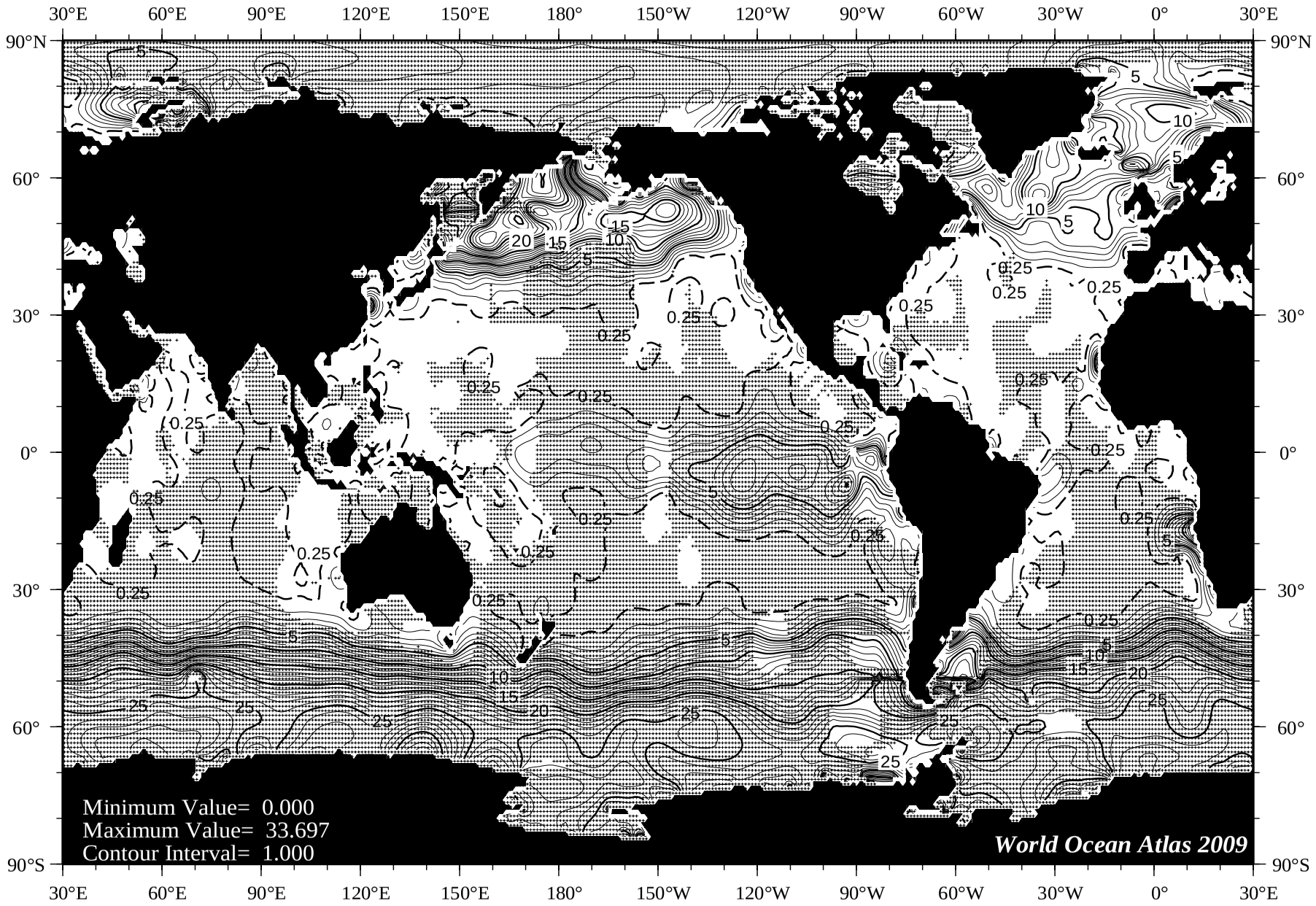

Fig F41 May mean nitrate [umol/l] at the surface.

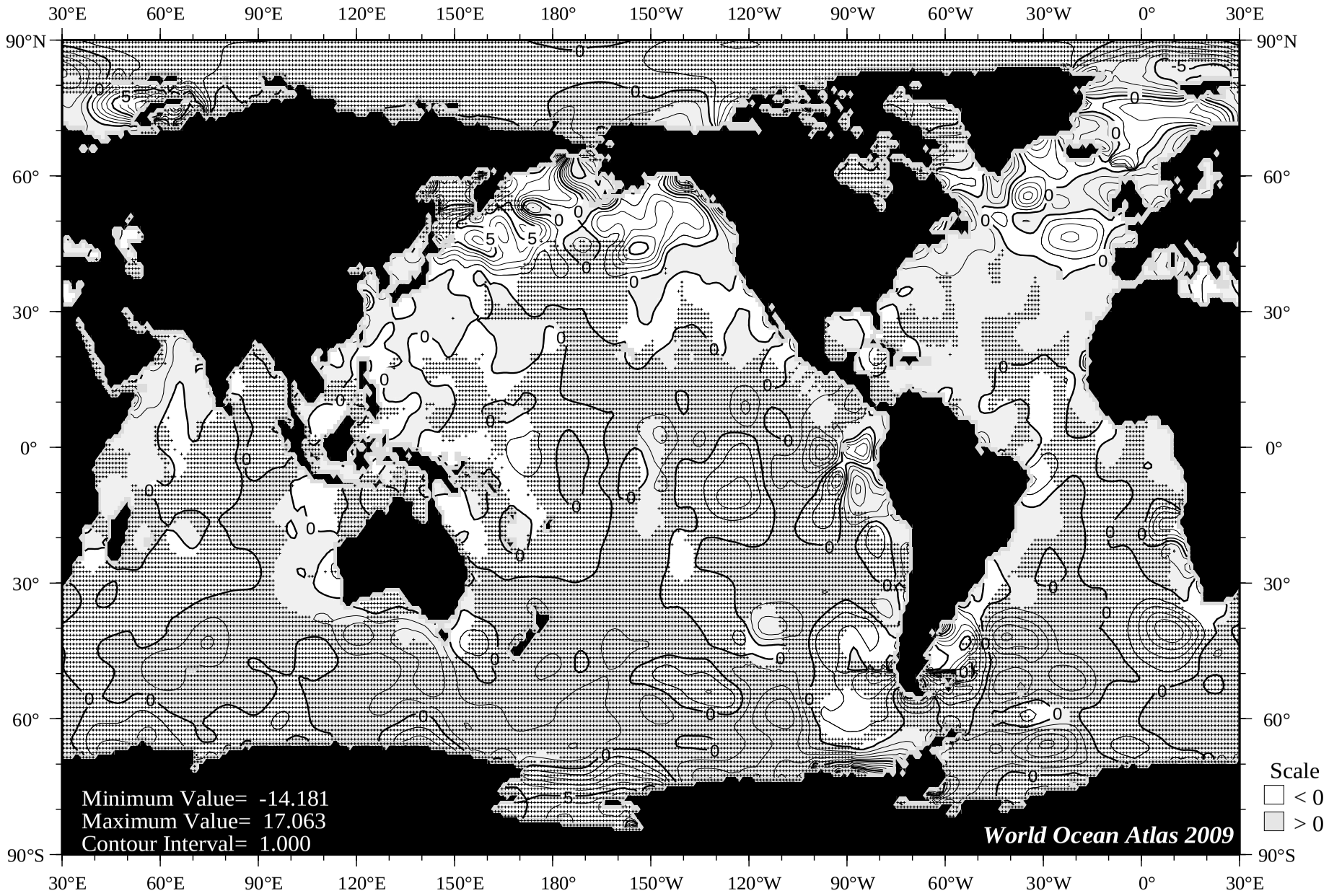

Fig F42 May minus annual nitrate [umol/l] at the surface.

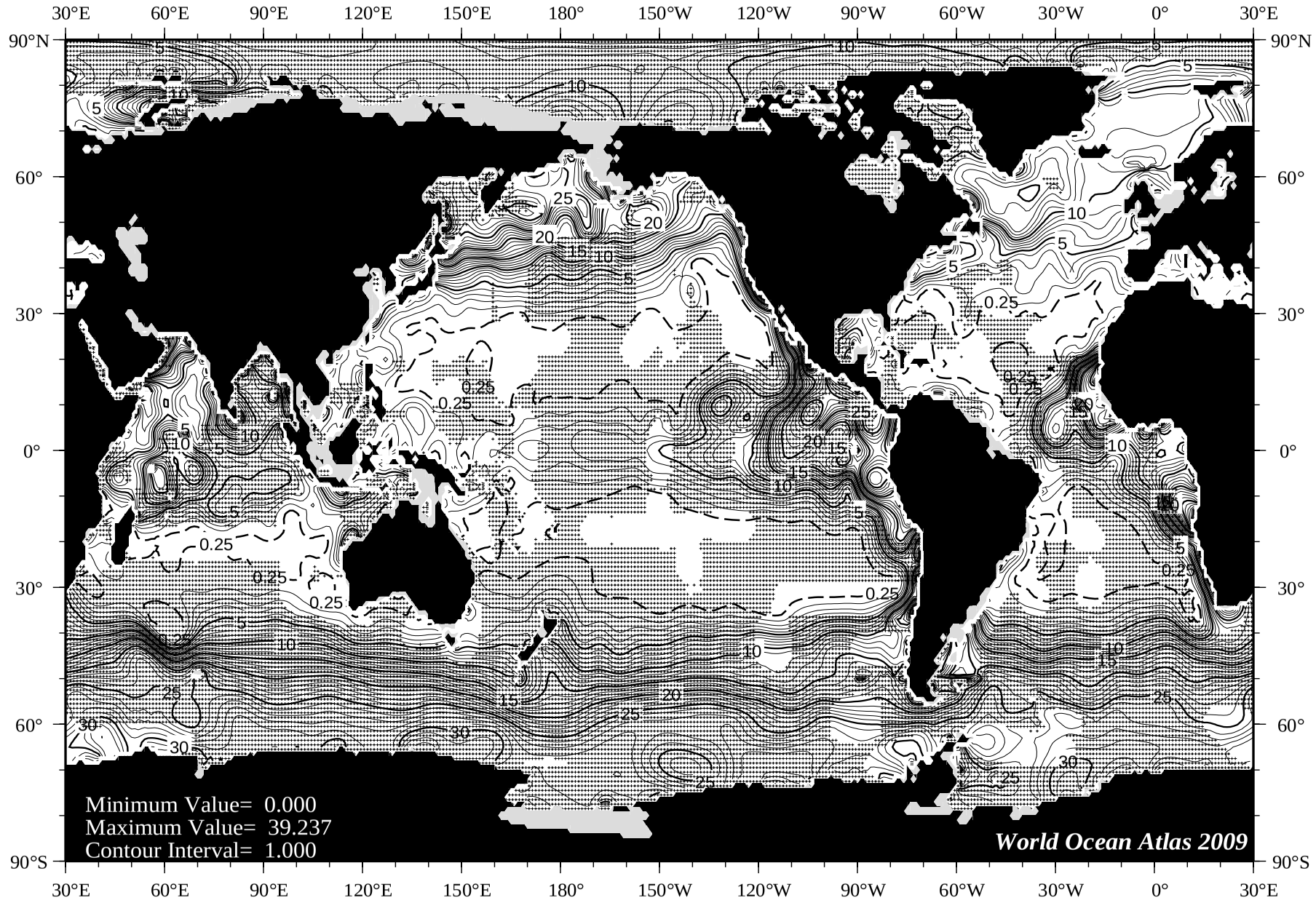

Fig F43 May mean nitrate [umol/l] at 75 m. depth.

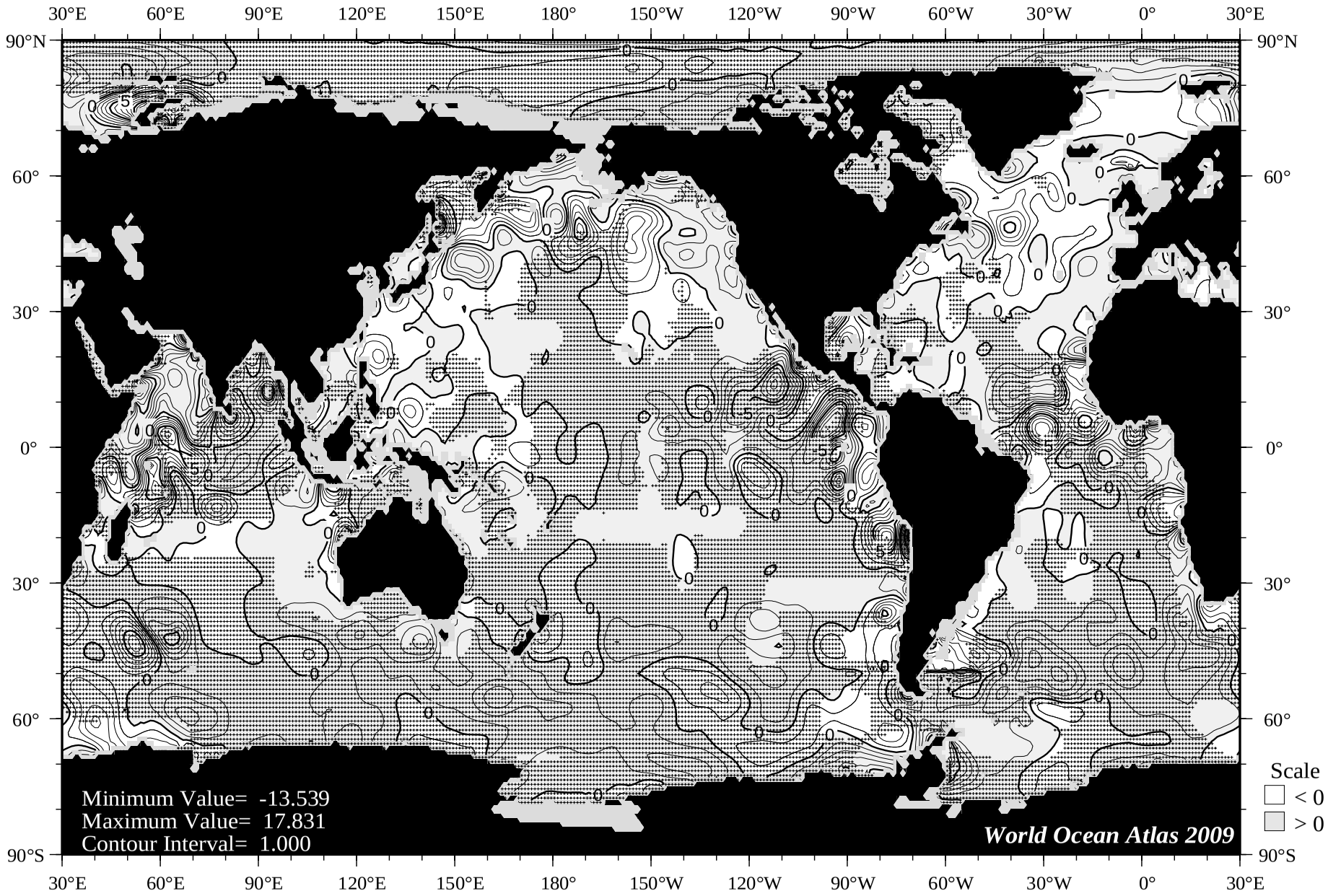

Fig F44 May minus annual nitrate [umol/l] at 75 m. depth.

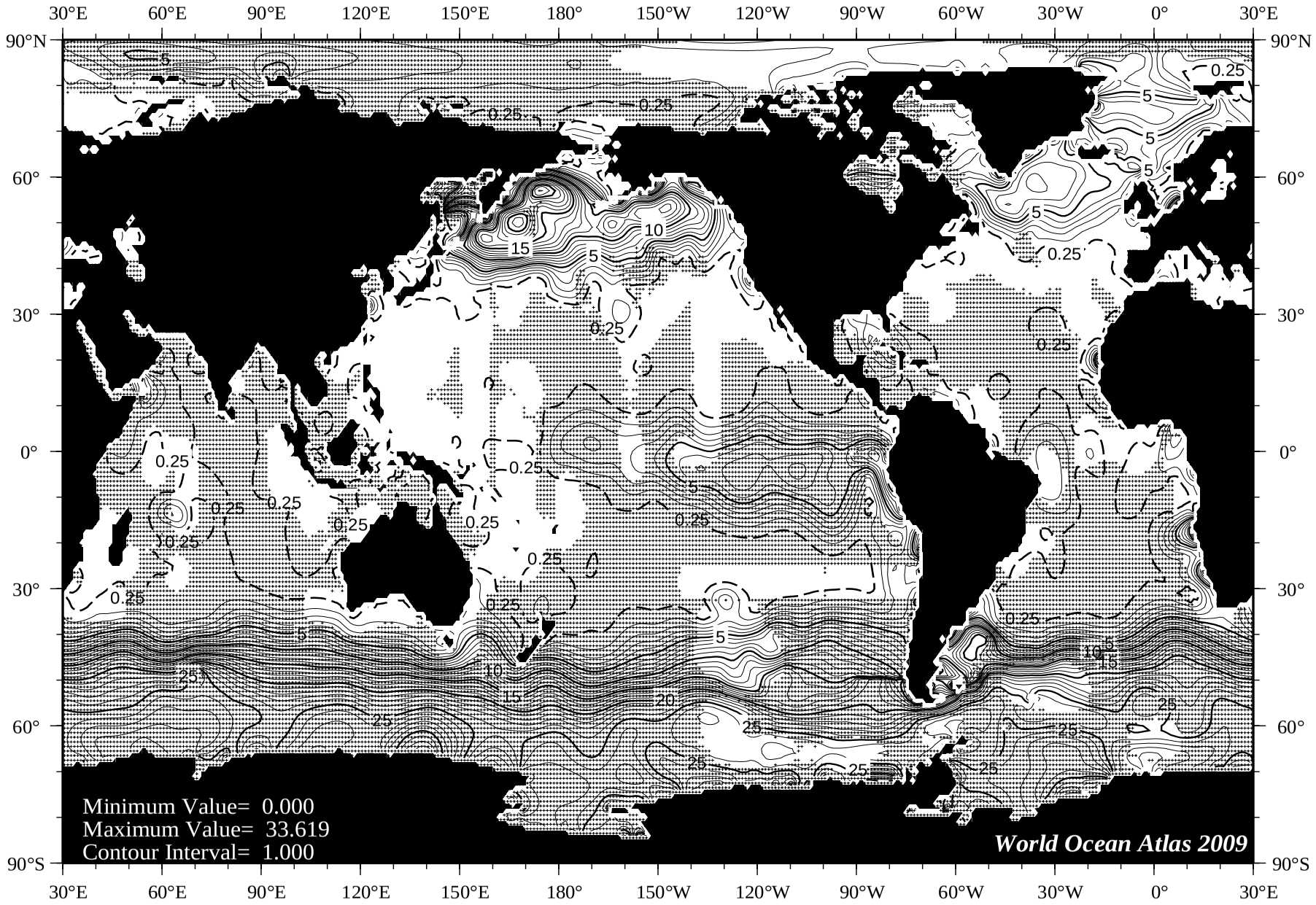

Fig F45 June mean nitrate [umol/l] at the surface.

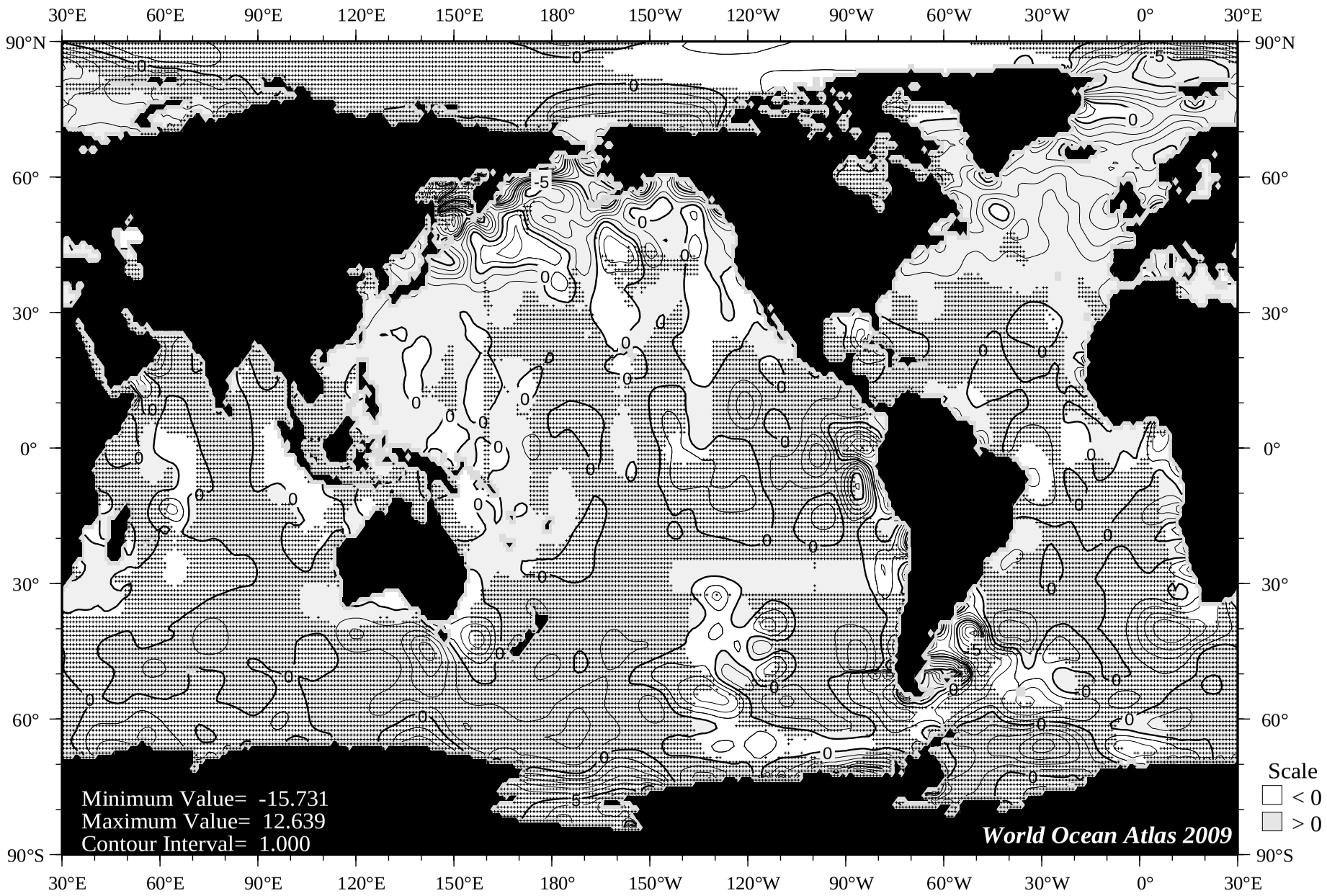

Fig F46 June minus annual nitrate [umol/l] at the surface.

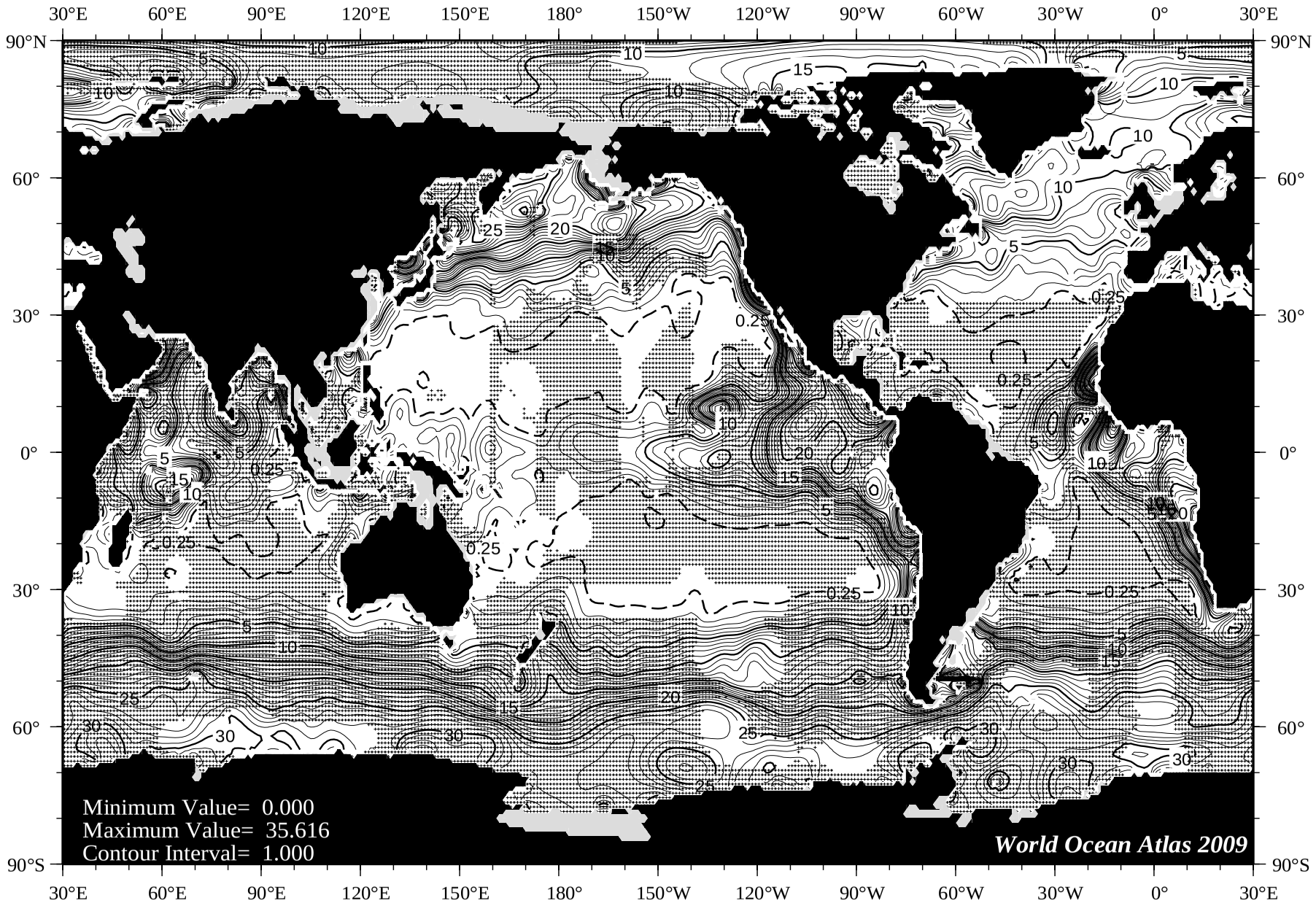

Fig F47 June mean nitrate [umol/l] at 75 m. depth.

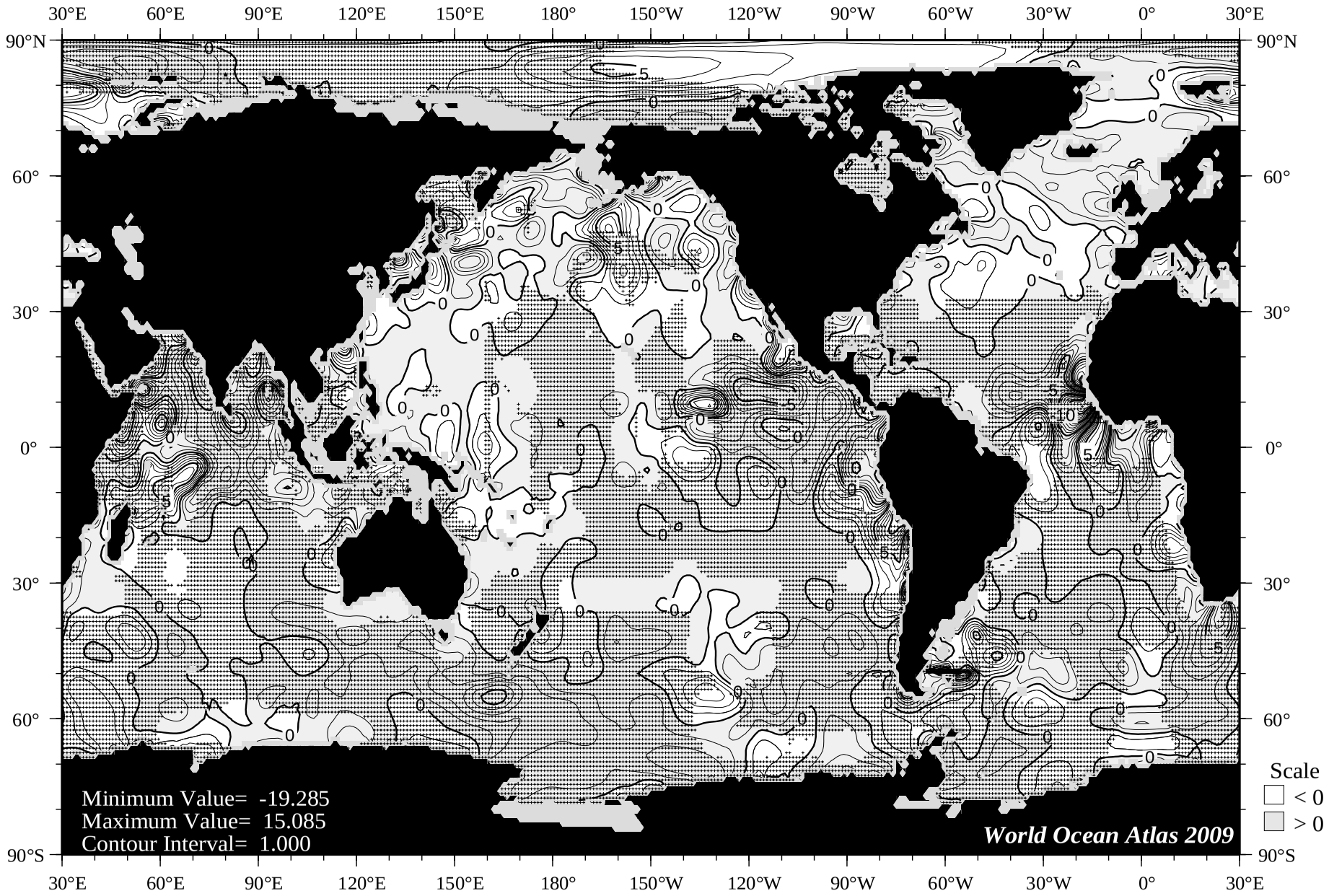

Fig F48 June minus annual nitrate [umol/l] at 75 m. depth.

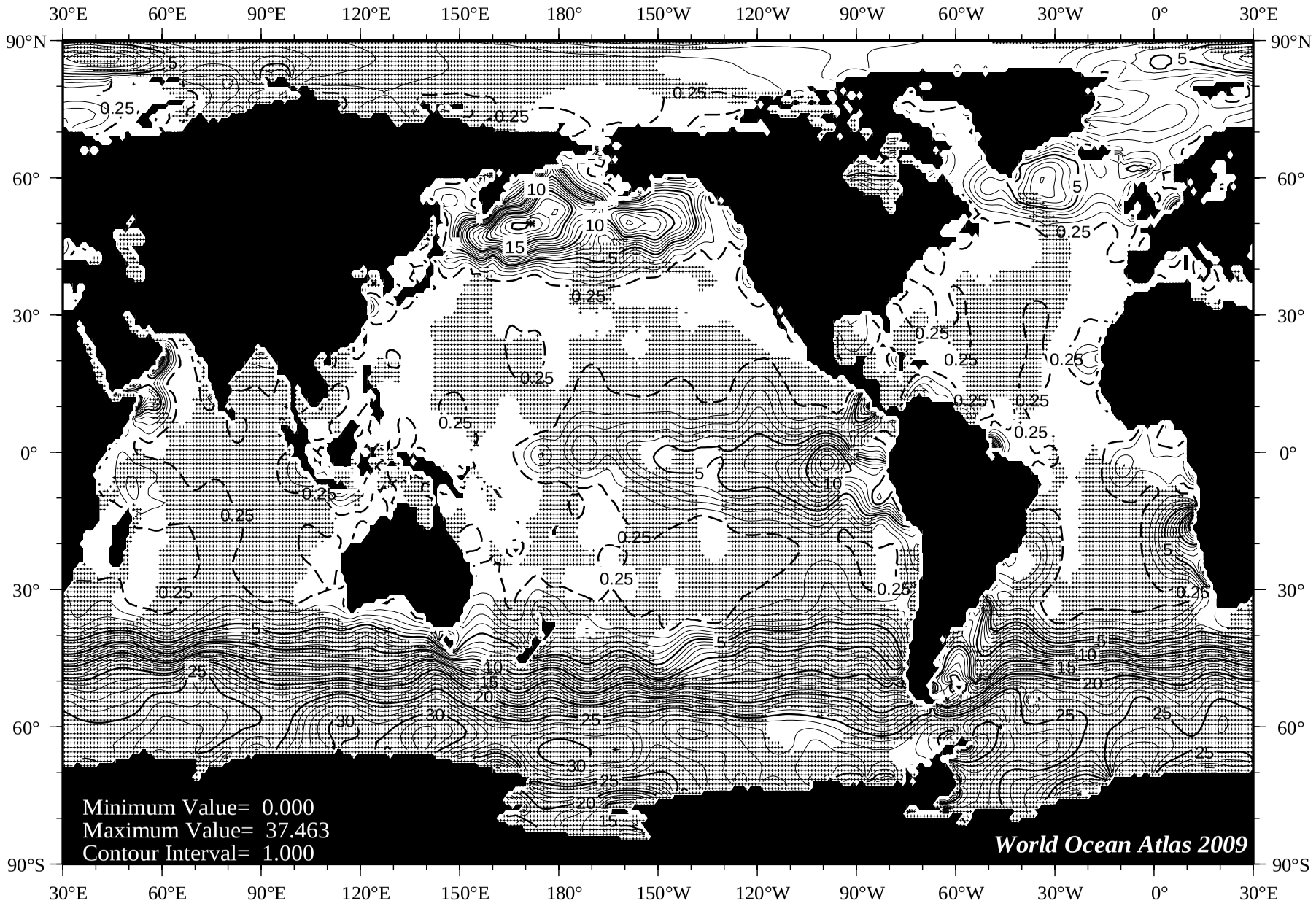

Fig F49 July mean nitrate [umol/l] at the surface.

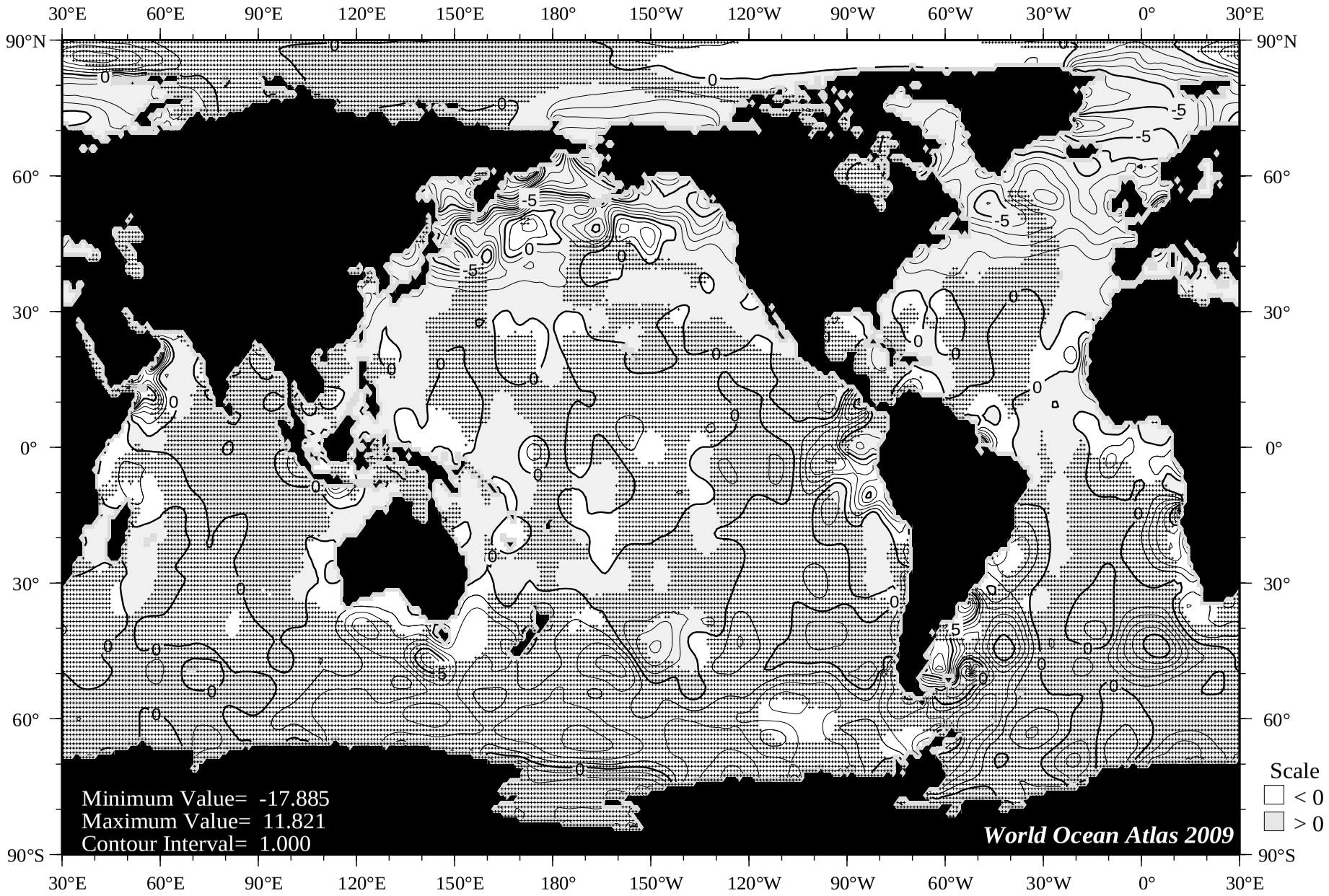

Fig F50 July minus annual nitrate [umol/l] at the surface.

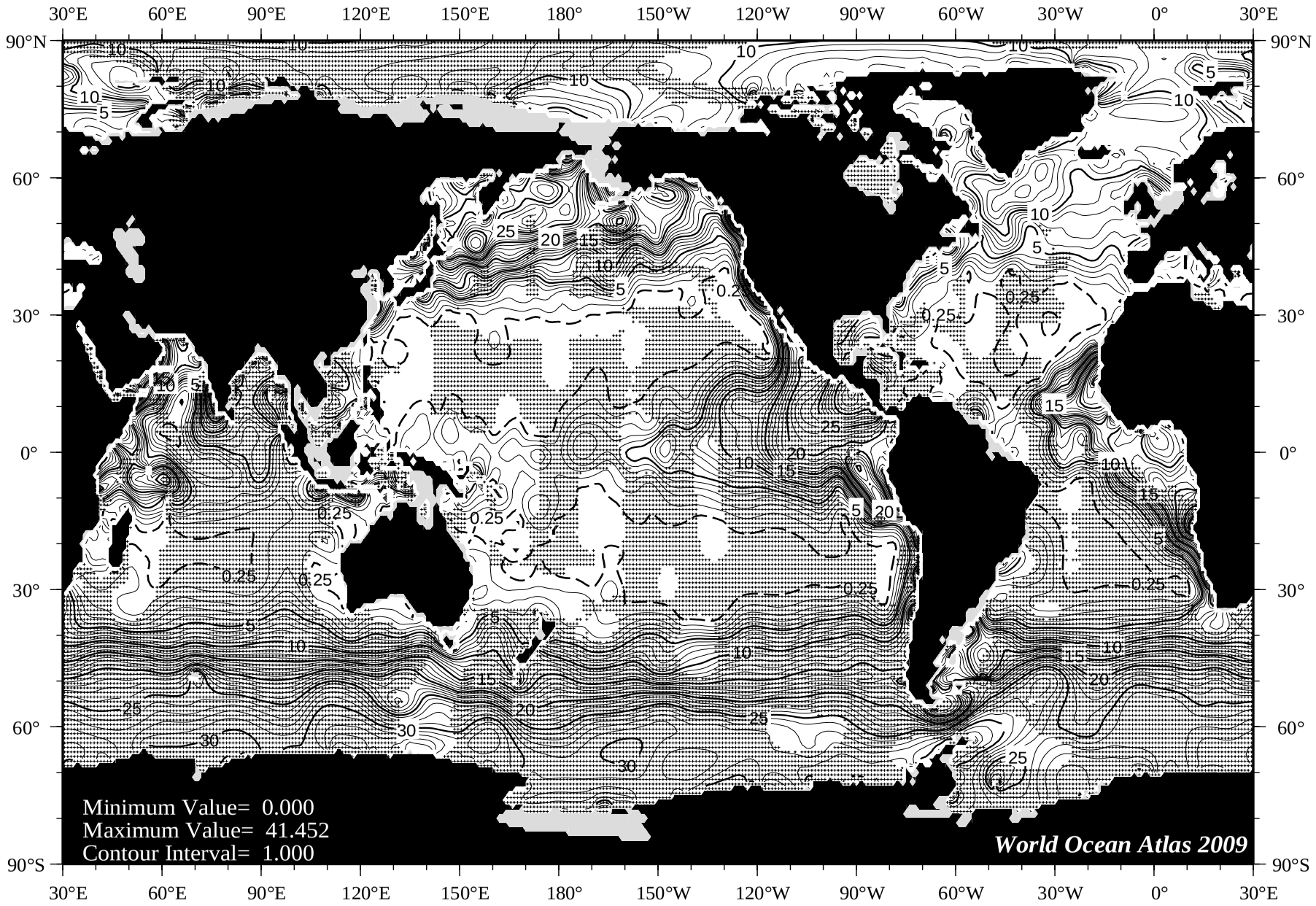

Fig F51 July mean nitrate [umol/l] at 75 m. depth.

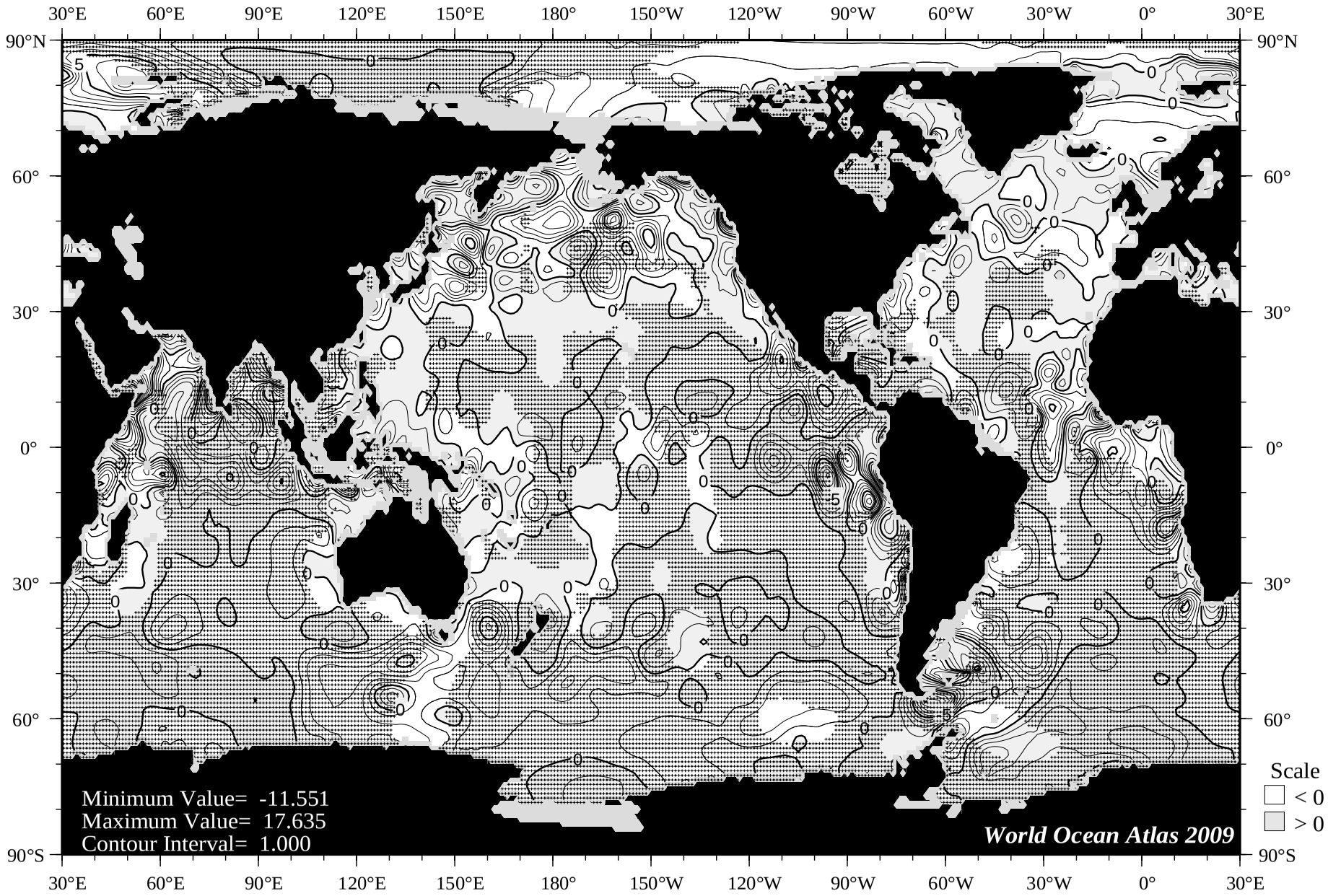

Fig F52 July minus annual nitrate [umol/l] at 75 m. depth.

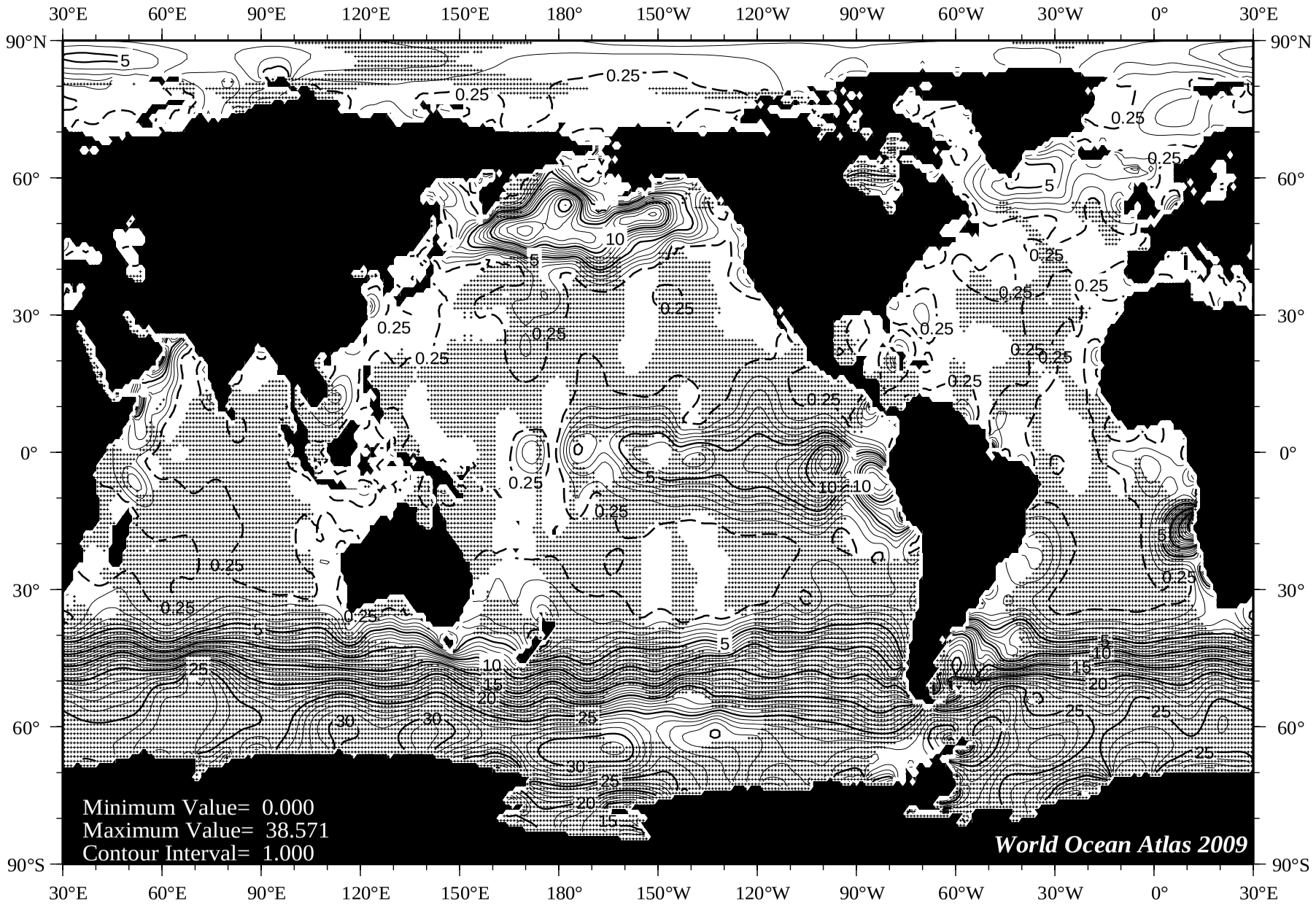

Fig F53 August mean nitrate [umol/l] at the surface.

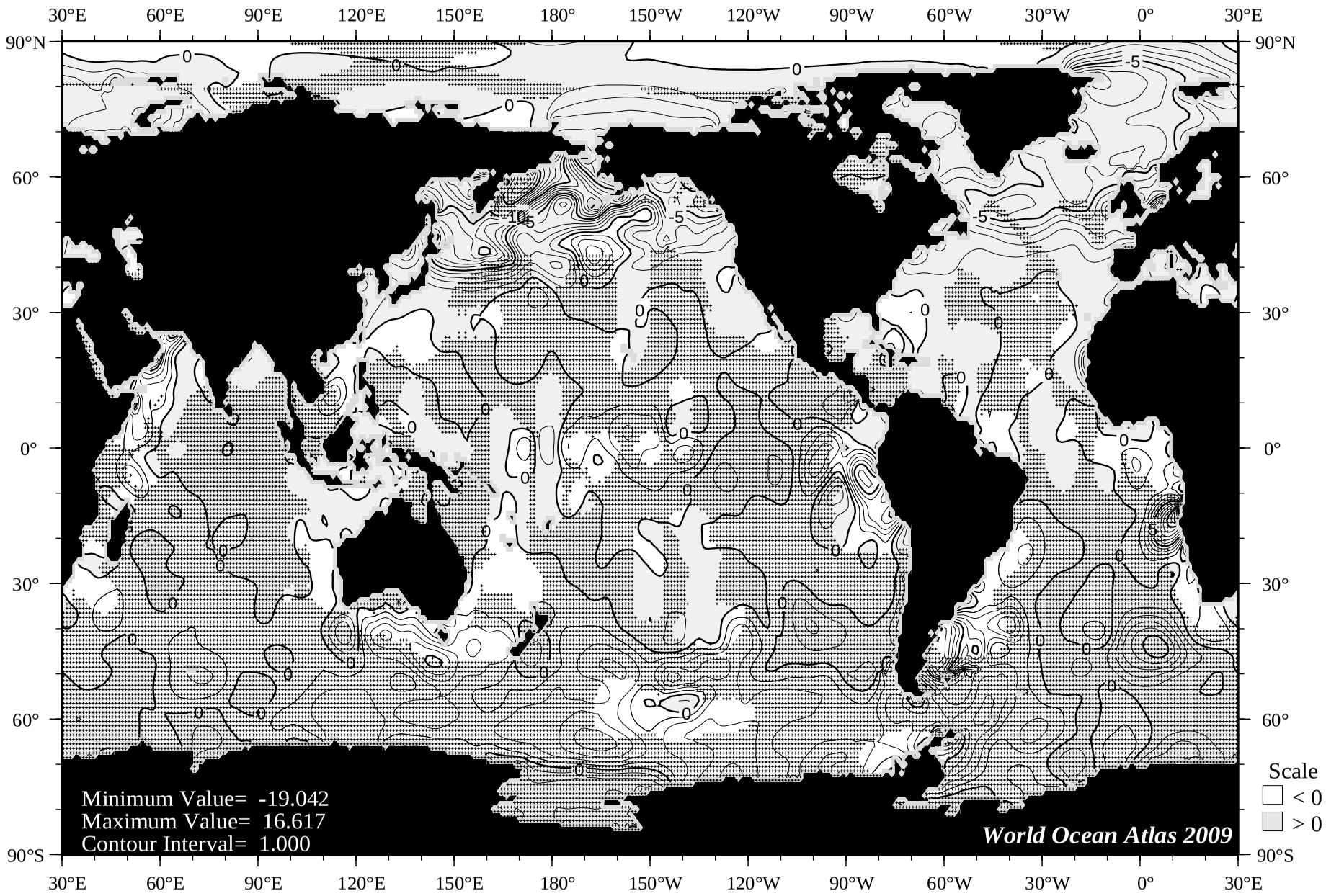

Fig F54 August minus annual nitrate [umol/l] at the surface.

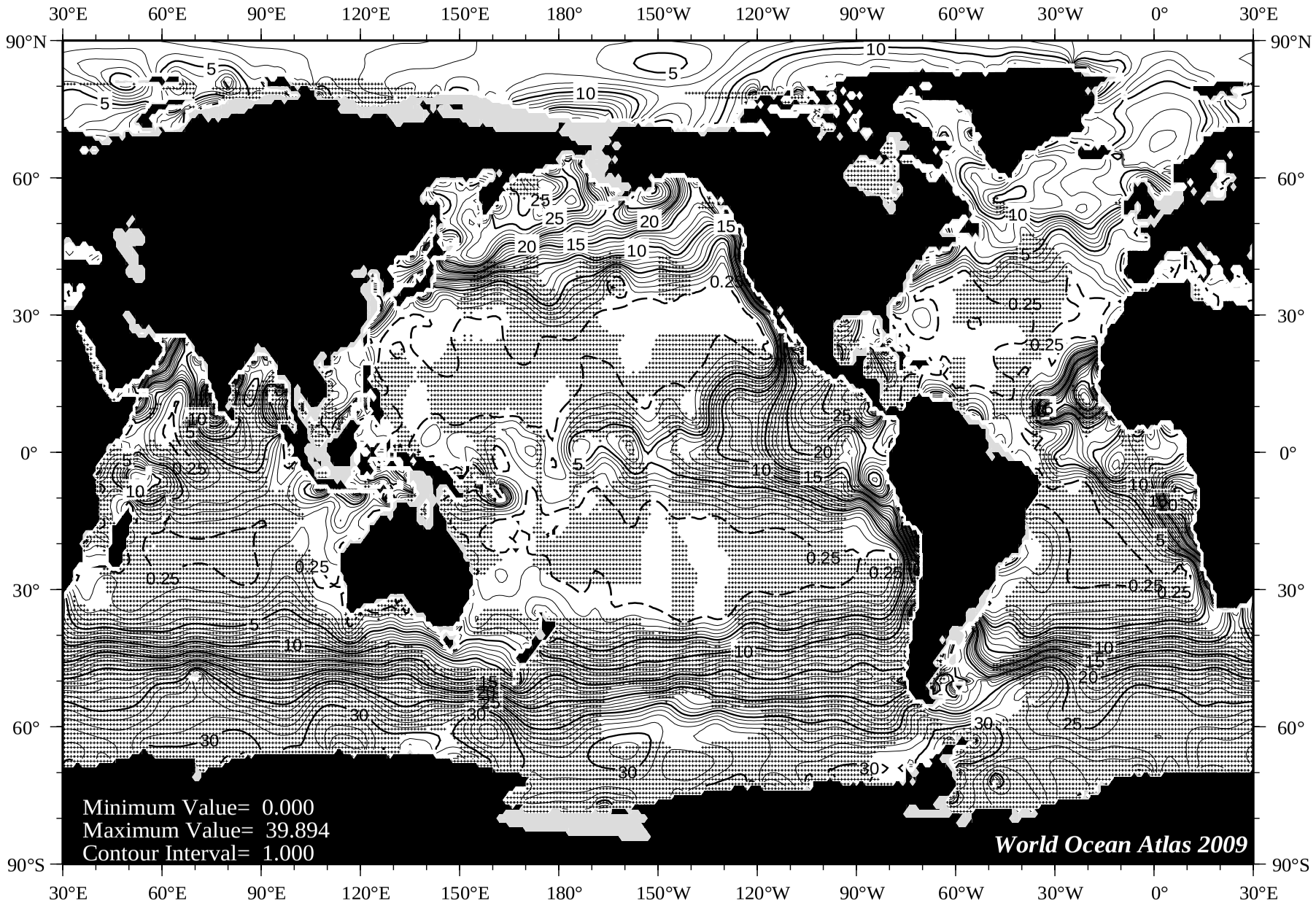

Fig F55 August mean nitrate [umol/l] at 75 m. depth.

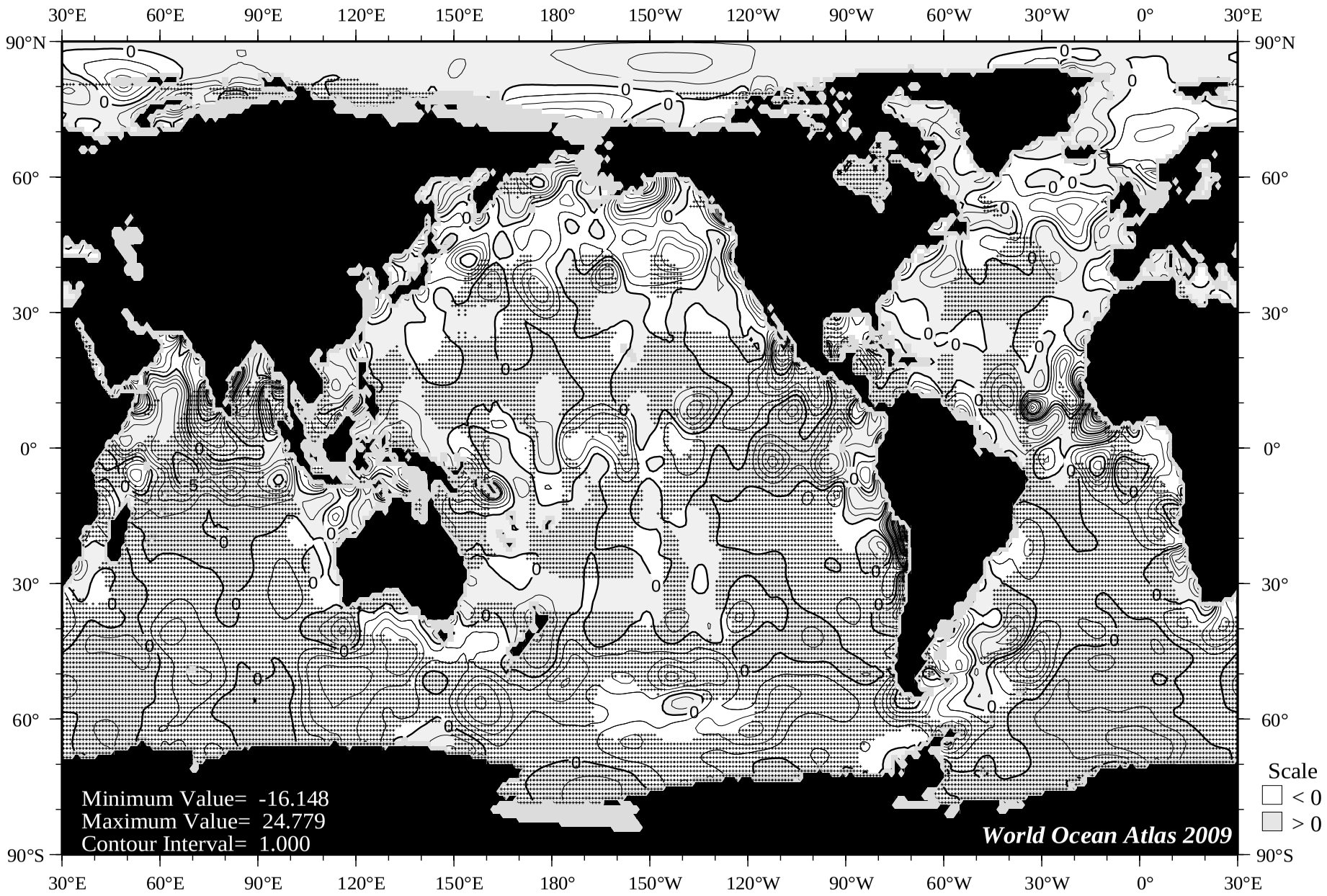

Fig F56 August minus annual nitrate [umol/l] at 75 m. depth.

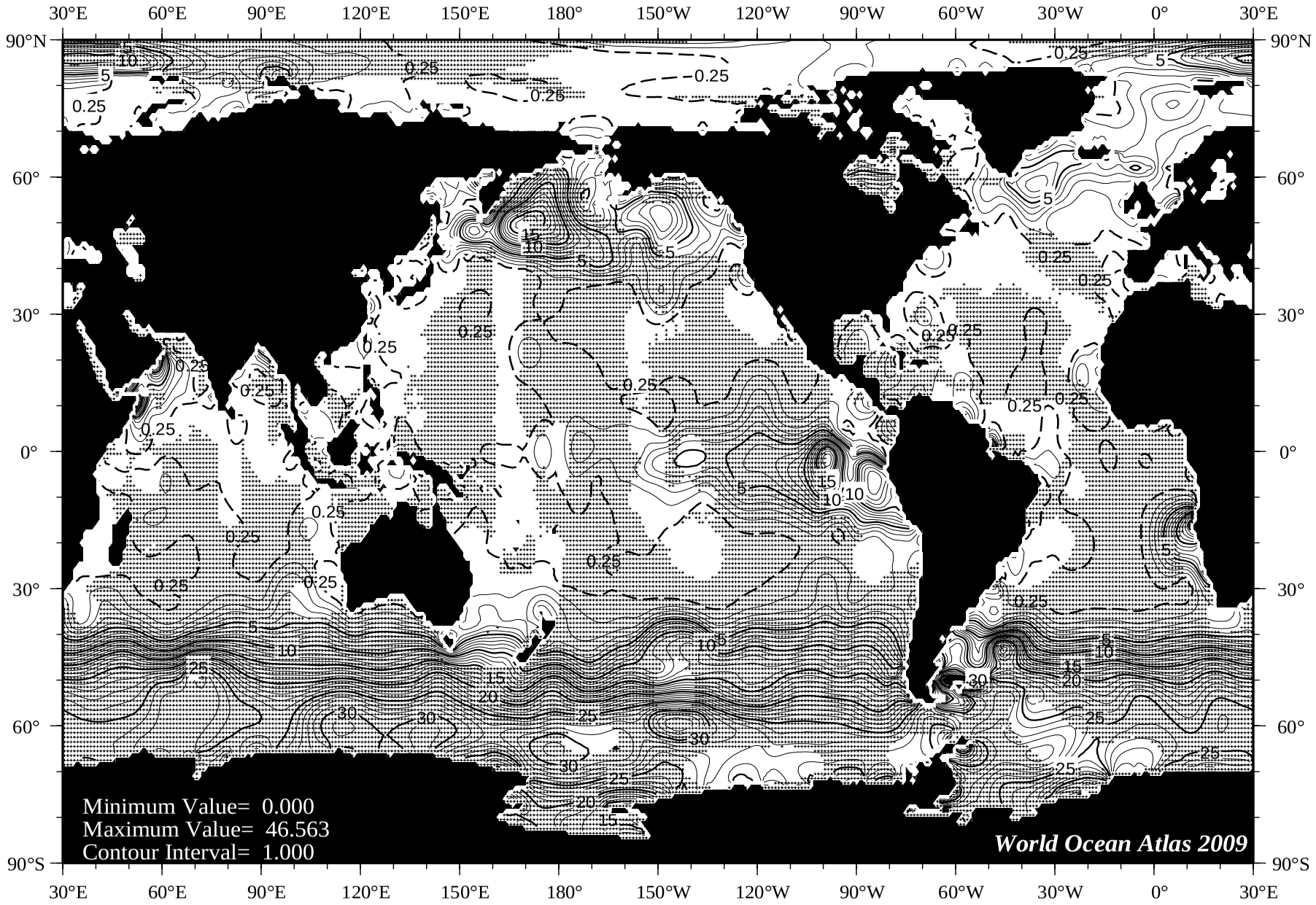

Fig F57 September mean nitrate [umol/l] at the surface.

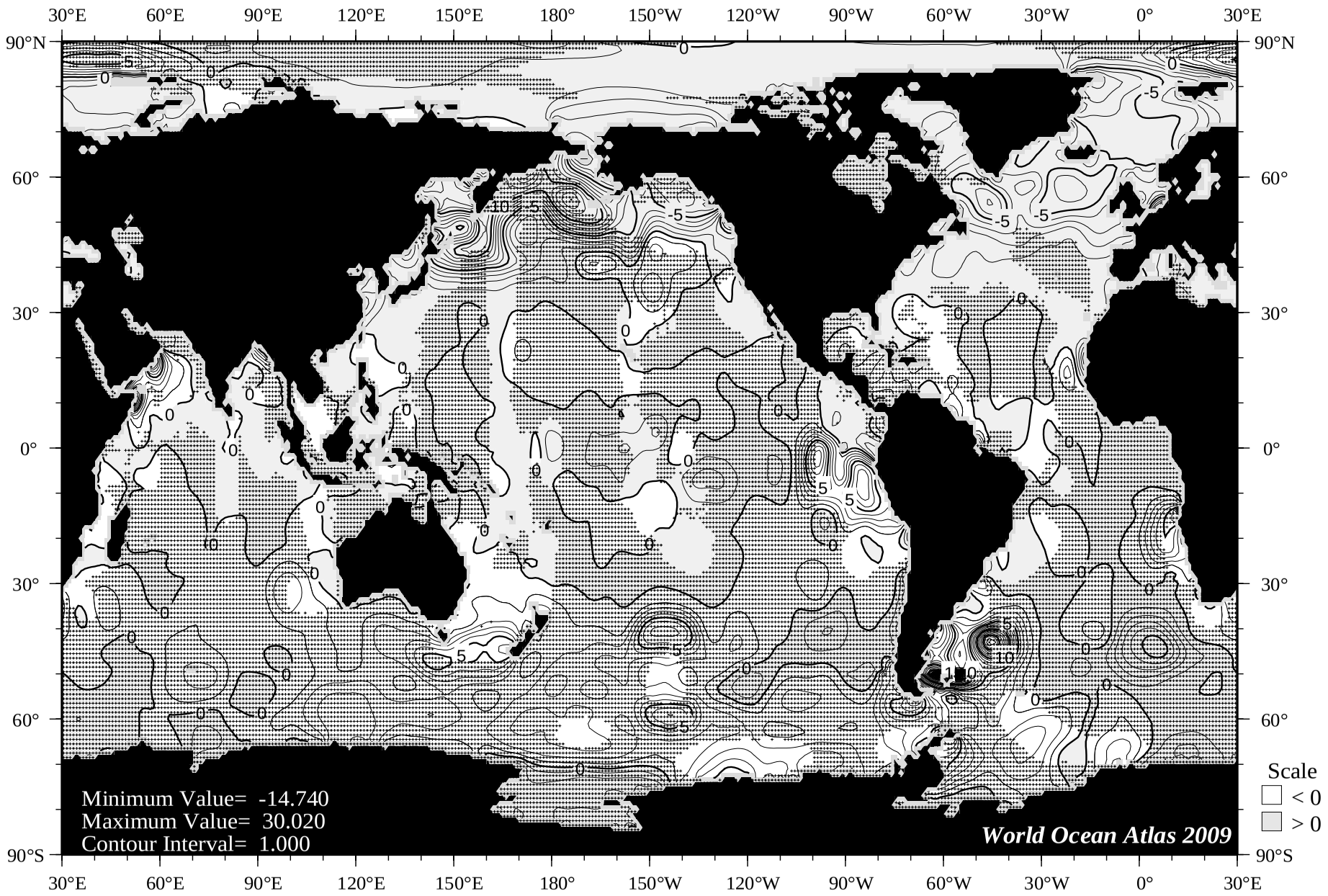

Fig F58 September minus annual nitrate [umol/l] at the surface.

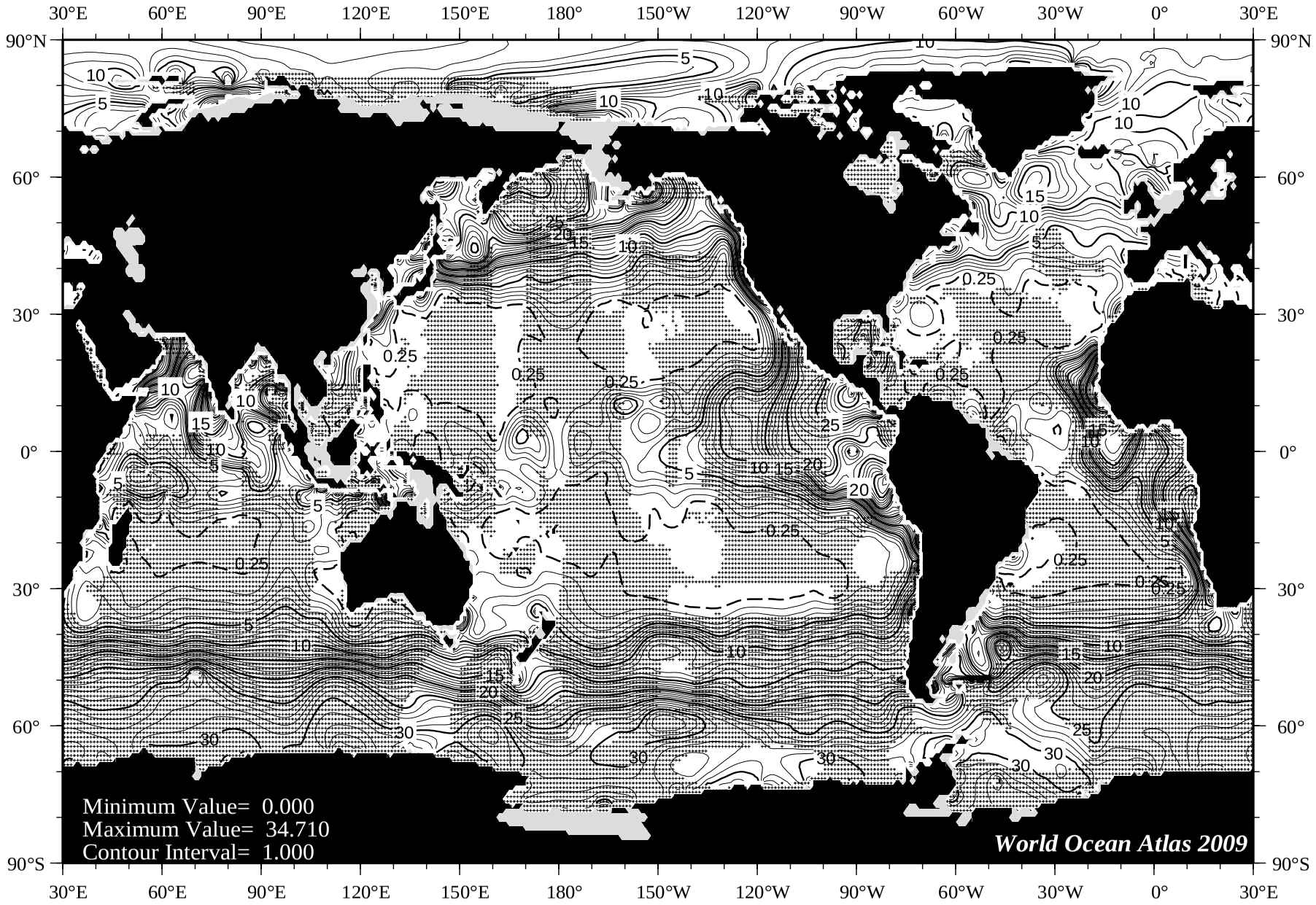

Fig F59 September mean nitrate [umol/l] at 75 m. depth.

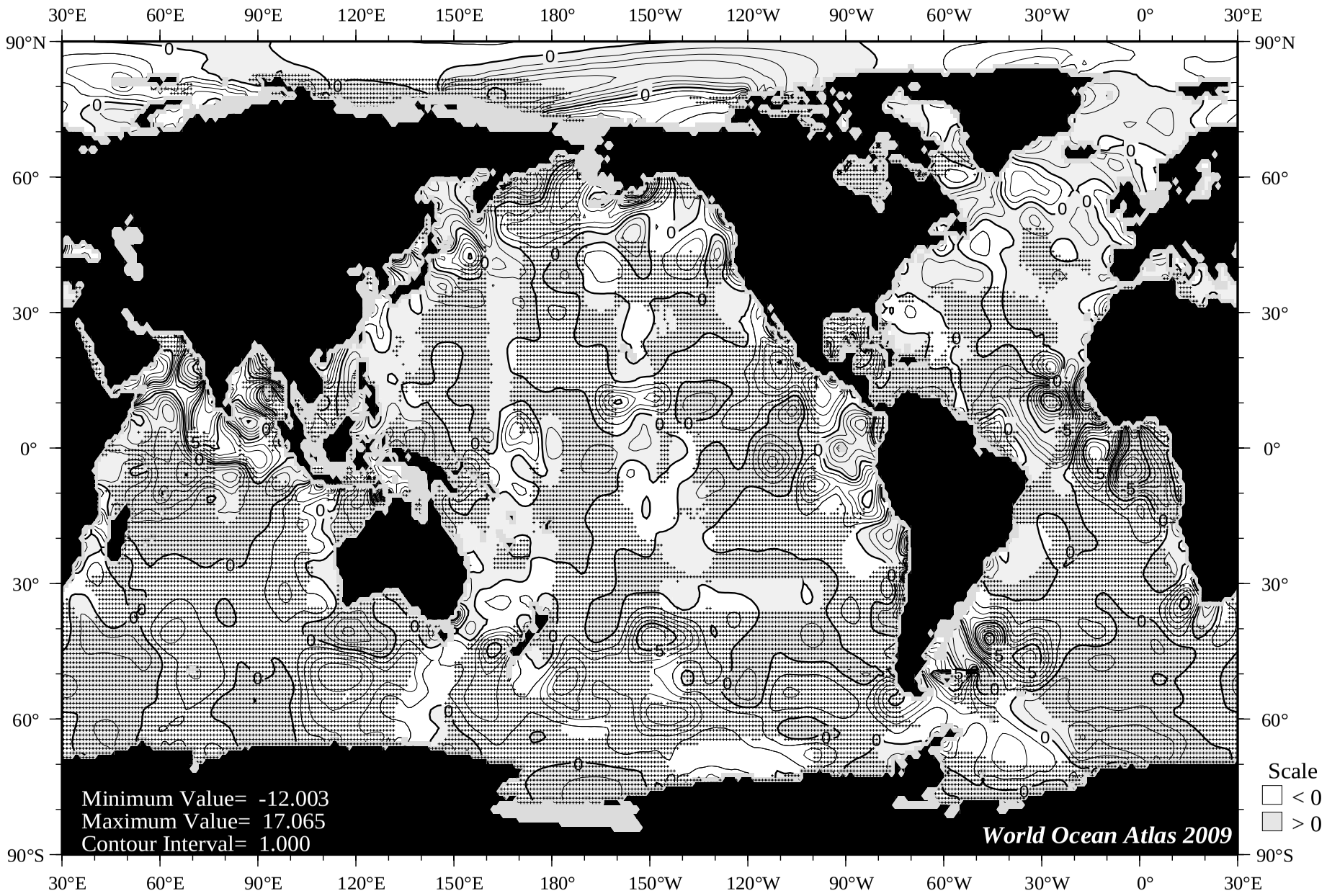

Fig F60 September minus annual nitrate [umol/l] at 75 m. depth.

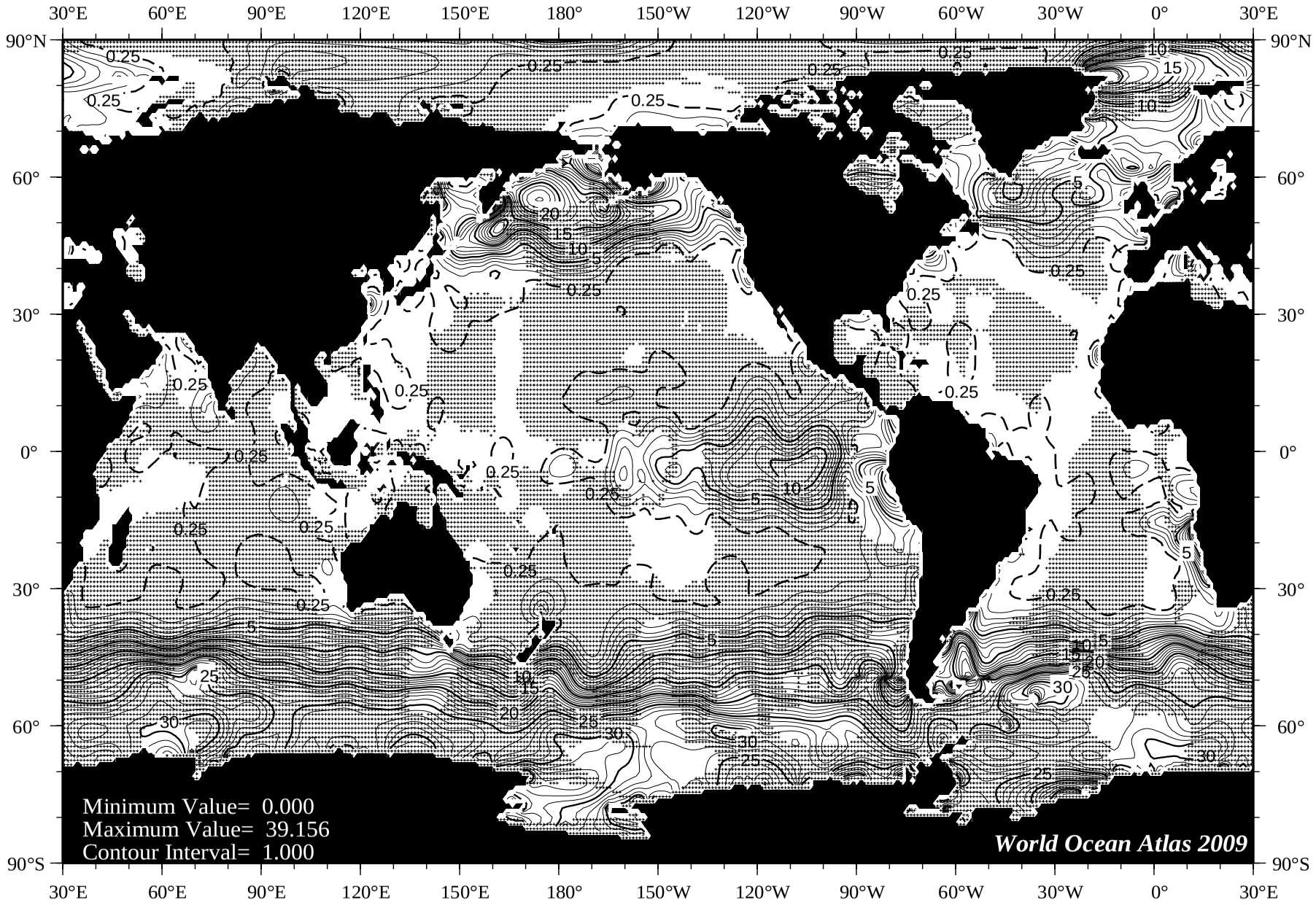

Fig F61 October mean nitrate [umol/l] at the surface.

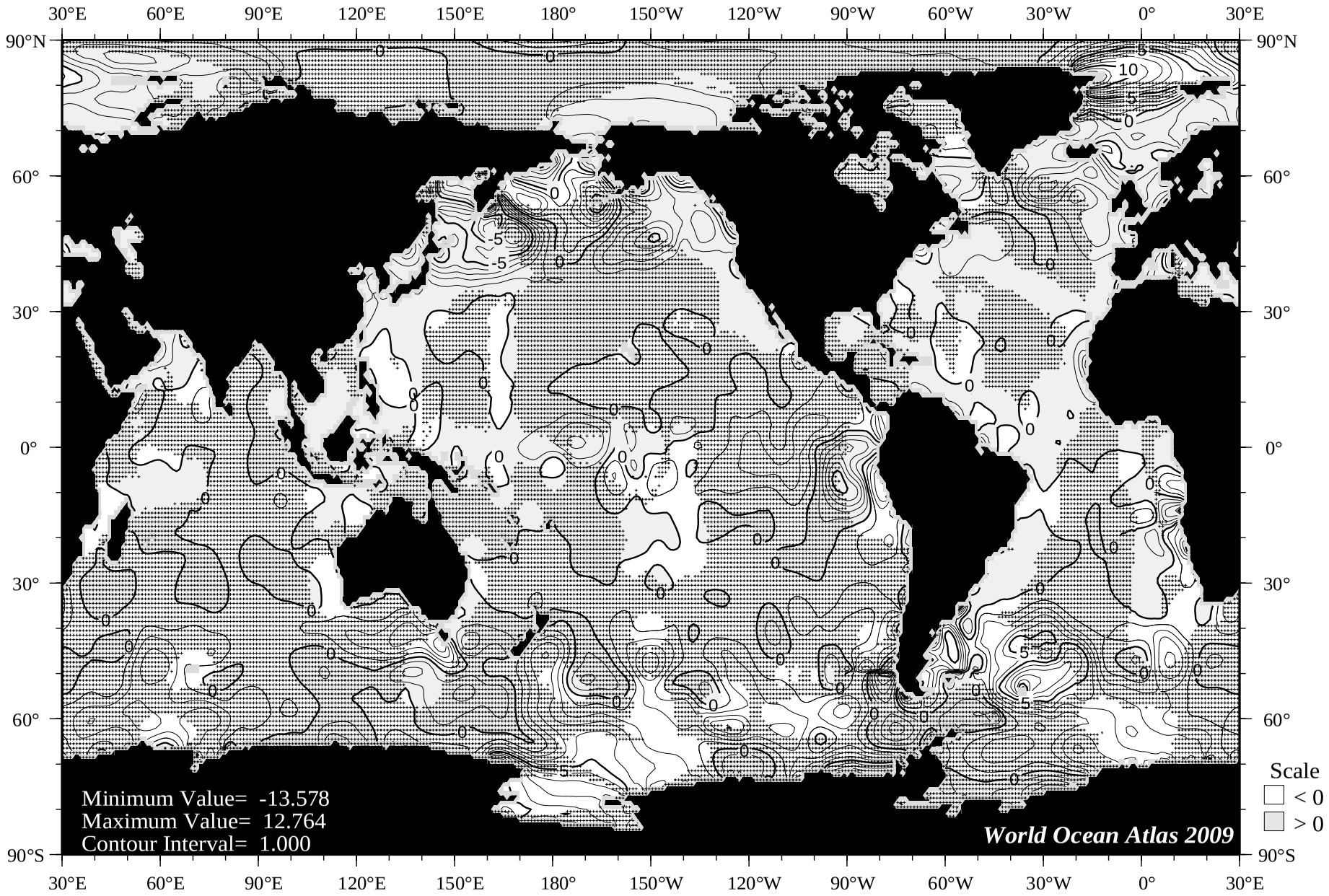

Fig F62 October minus annual nitrate [umol/l] at the surface.

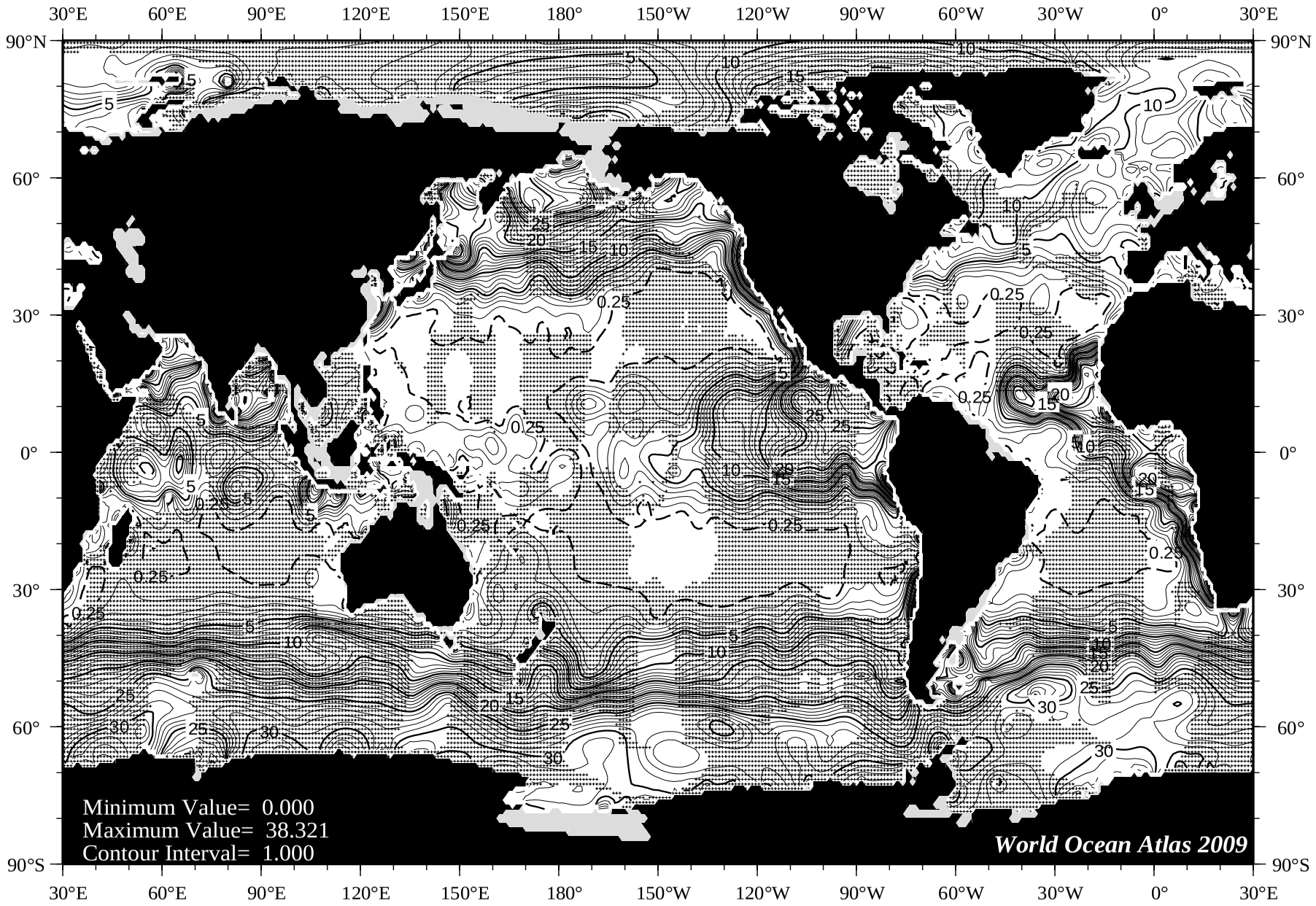

Fig F63 October mean nitrate [umol/l] at 75 m. depth.

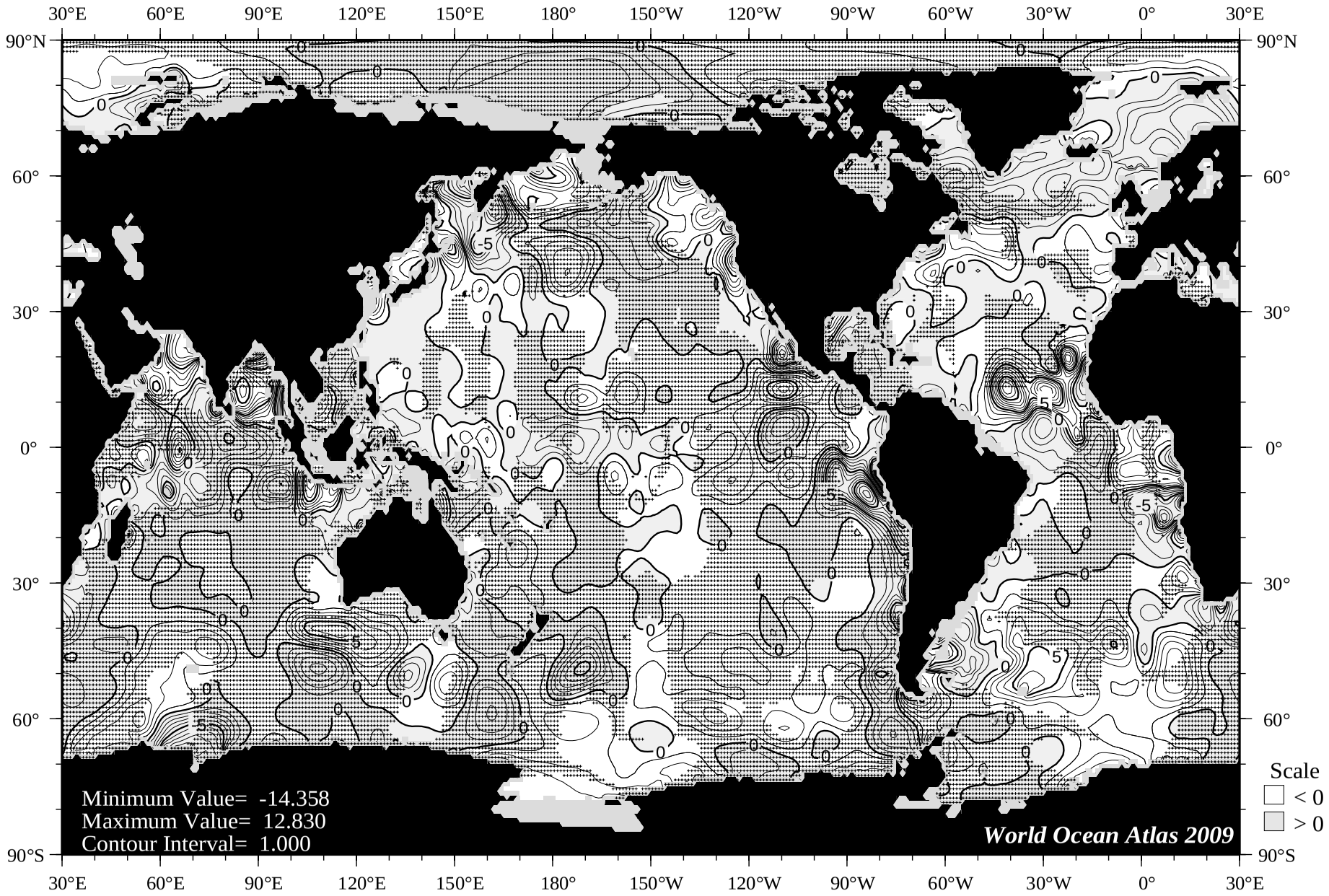

Fig F64 October minus annual nitrate [umol/l] at 75 m. depth.

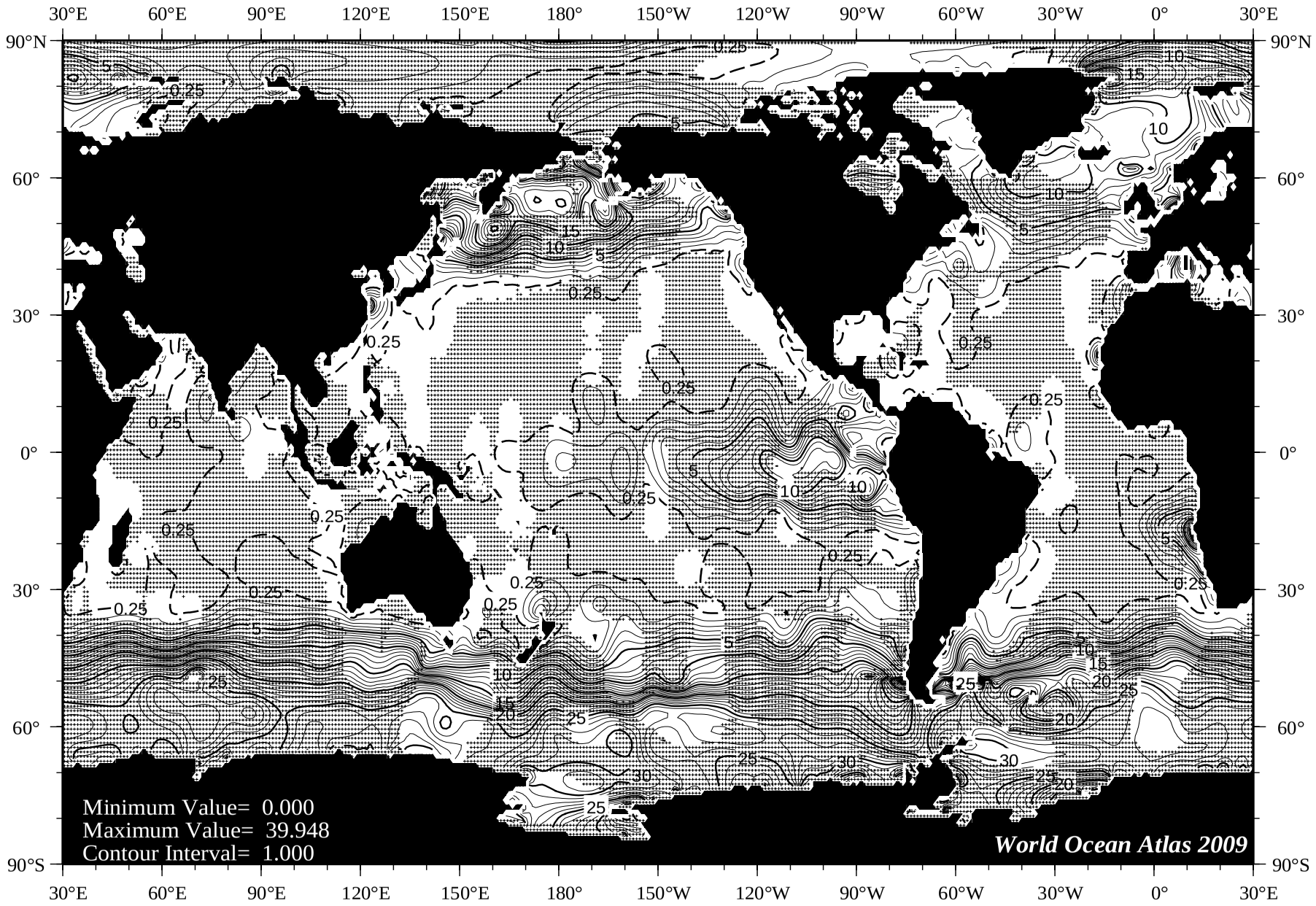

Fig F65 November mean nitrate [umol/l] at the surface.

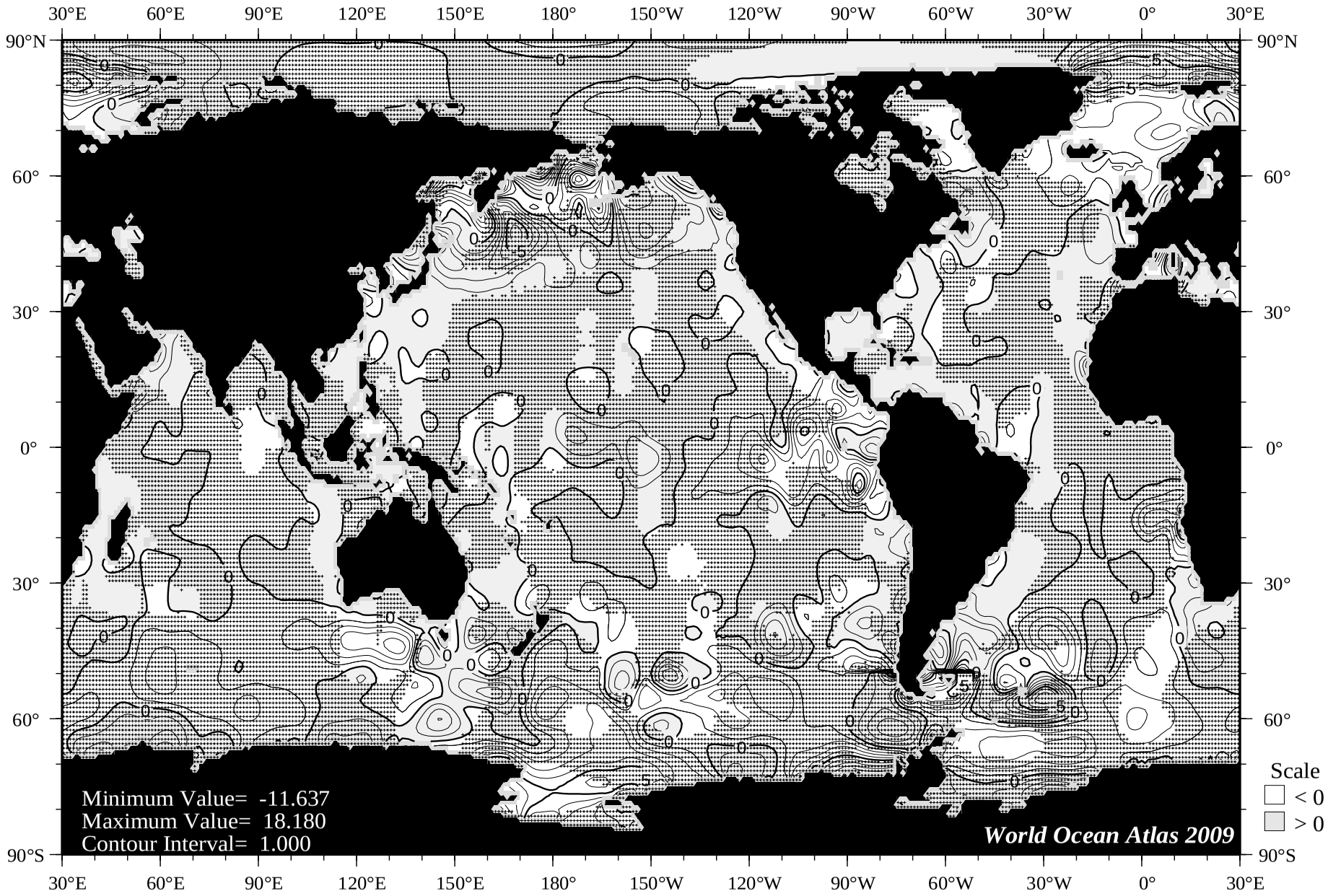

Fig F66 November minus annual nitrate [umol/l] at the surface.

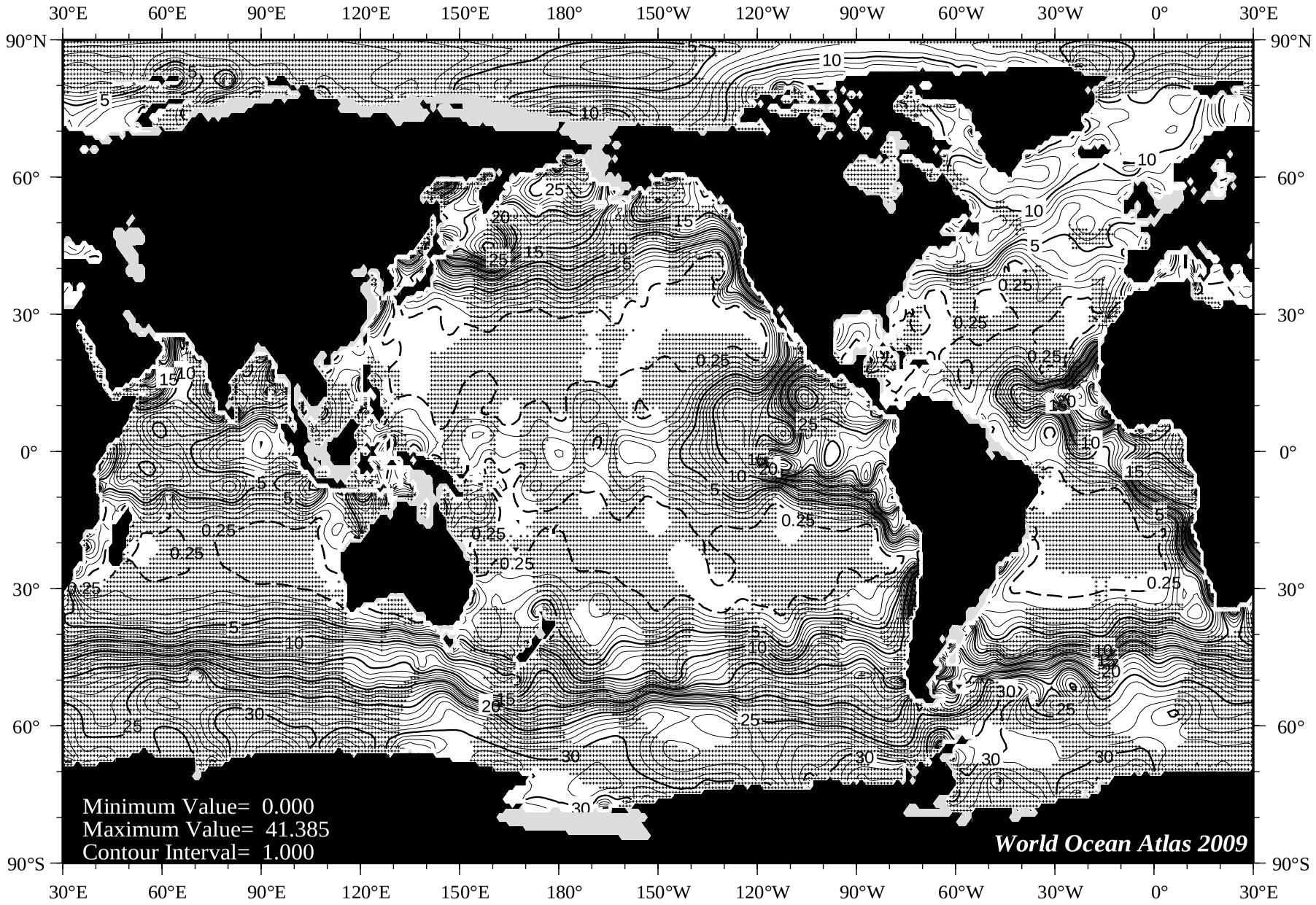

Fig F67 November mean nitrate [umol/l] at 75 m. depth.

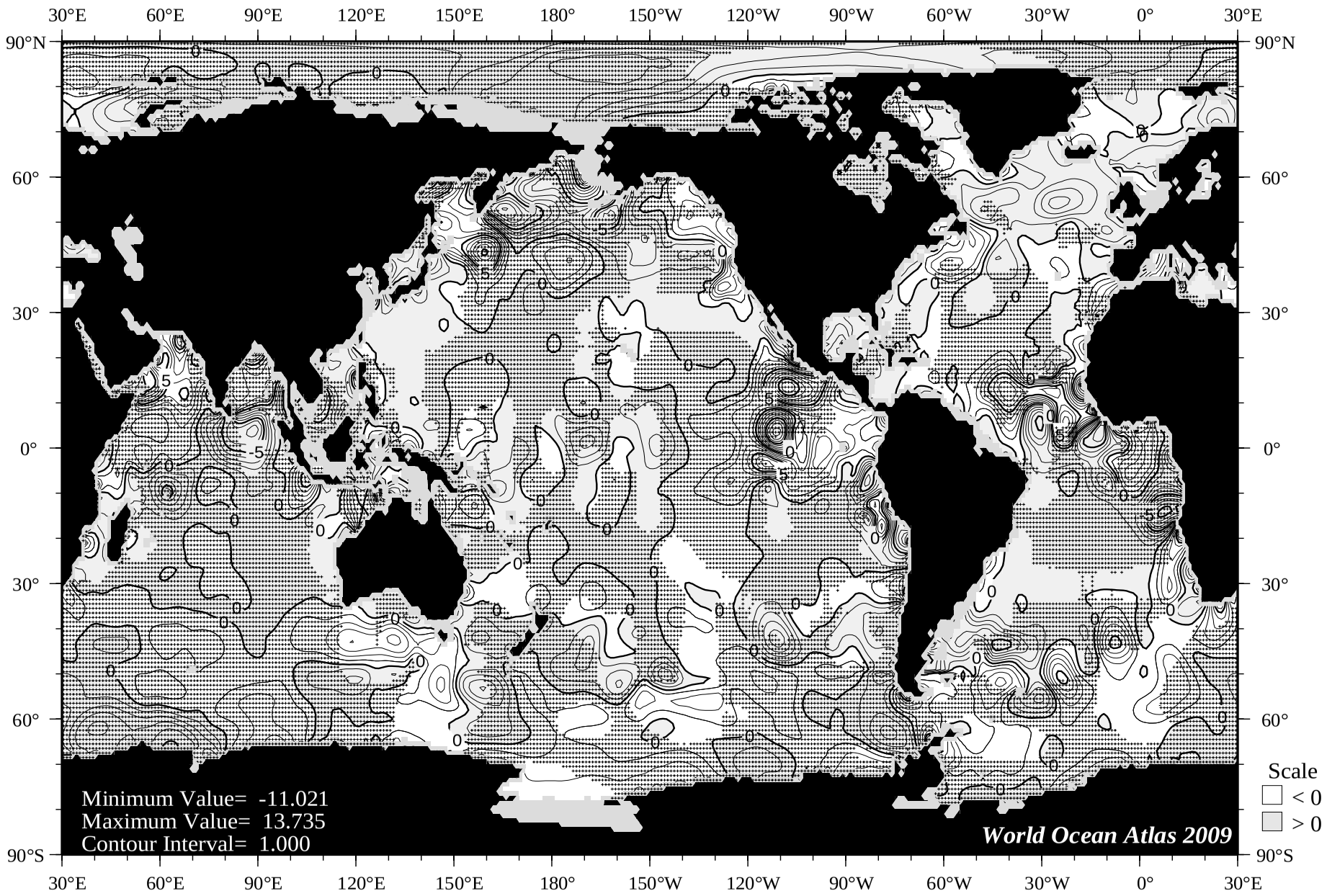

Fig F68 November minus annual nitrate [umol/l] at 75 m. depth.

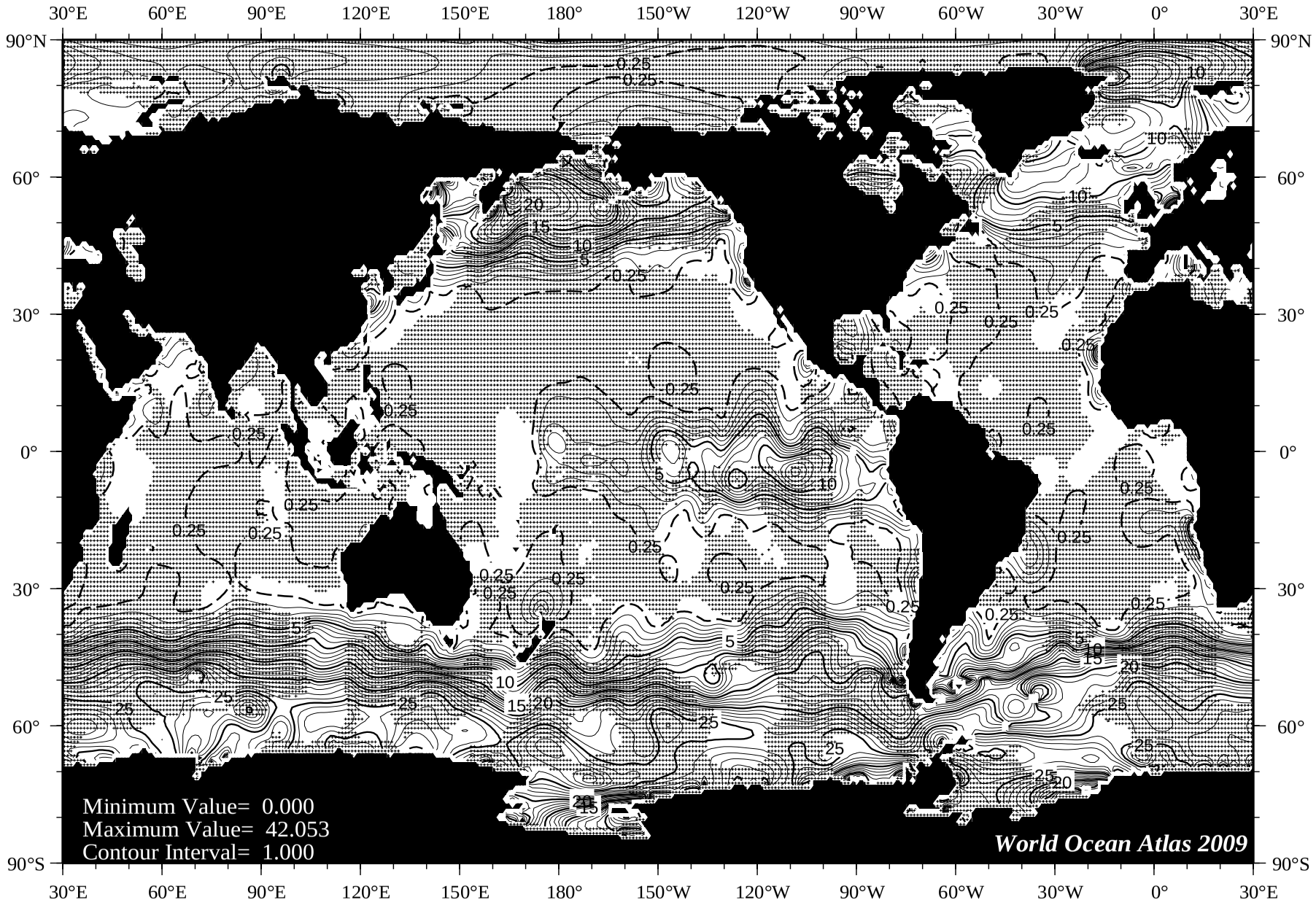

Fig F69 December mean nitrate [umol/l] at the surface.

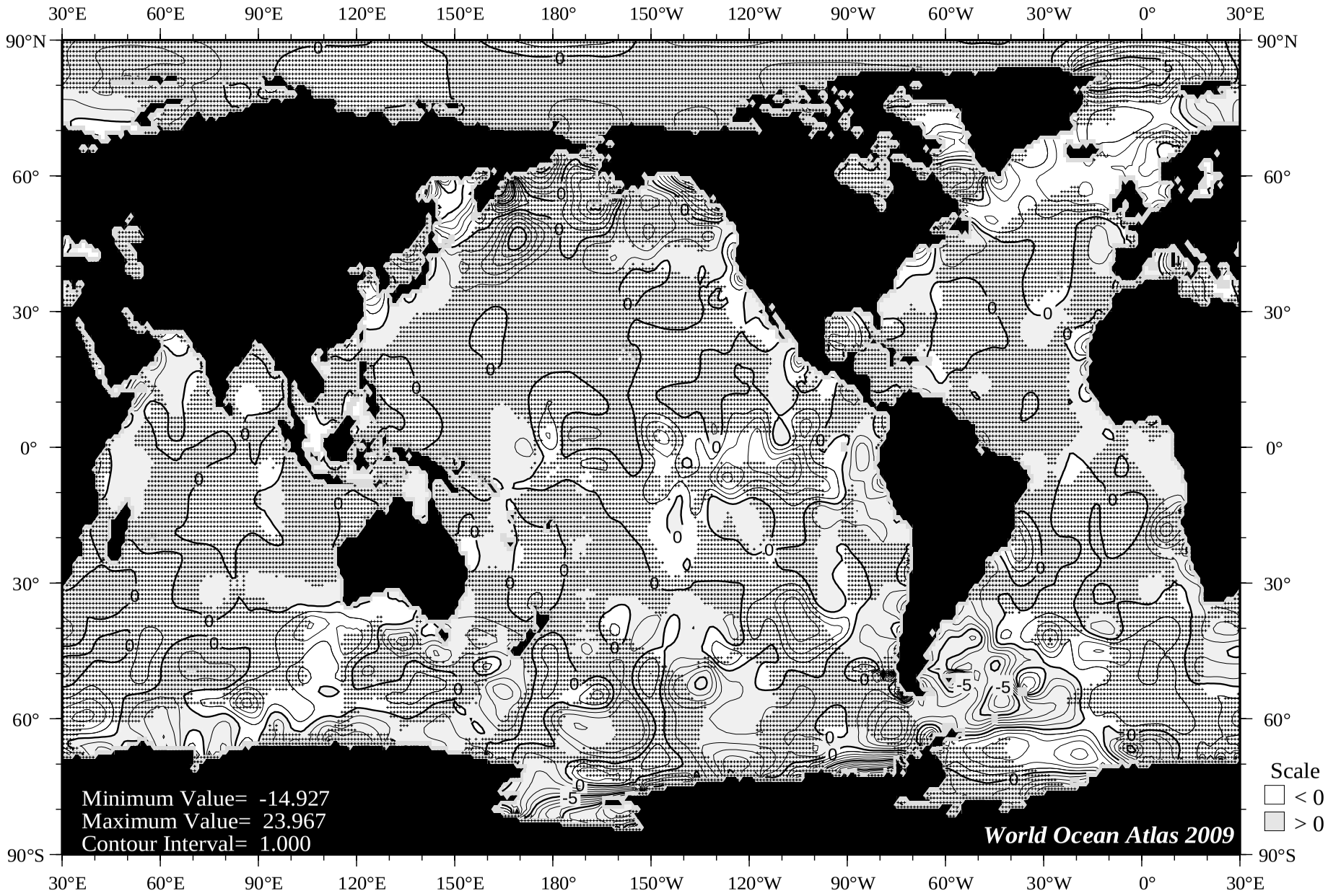

Fig F70 December minus annual nitrate [umol/l] at the surface.

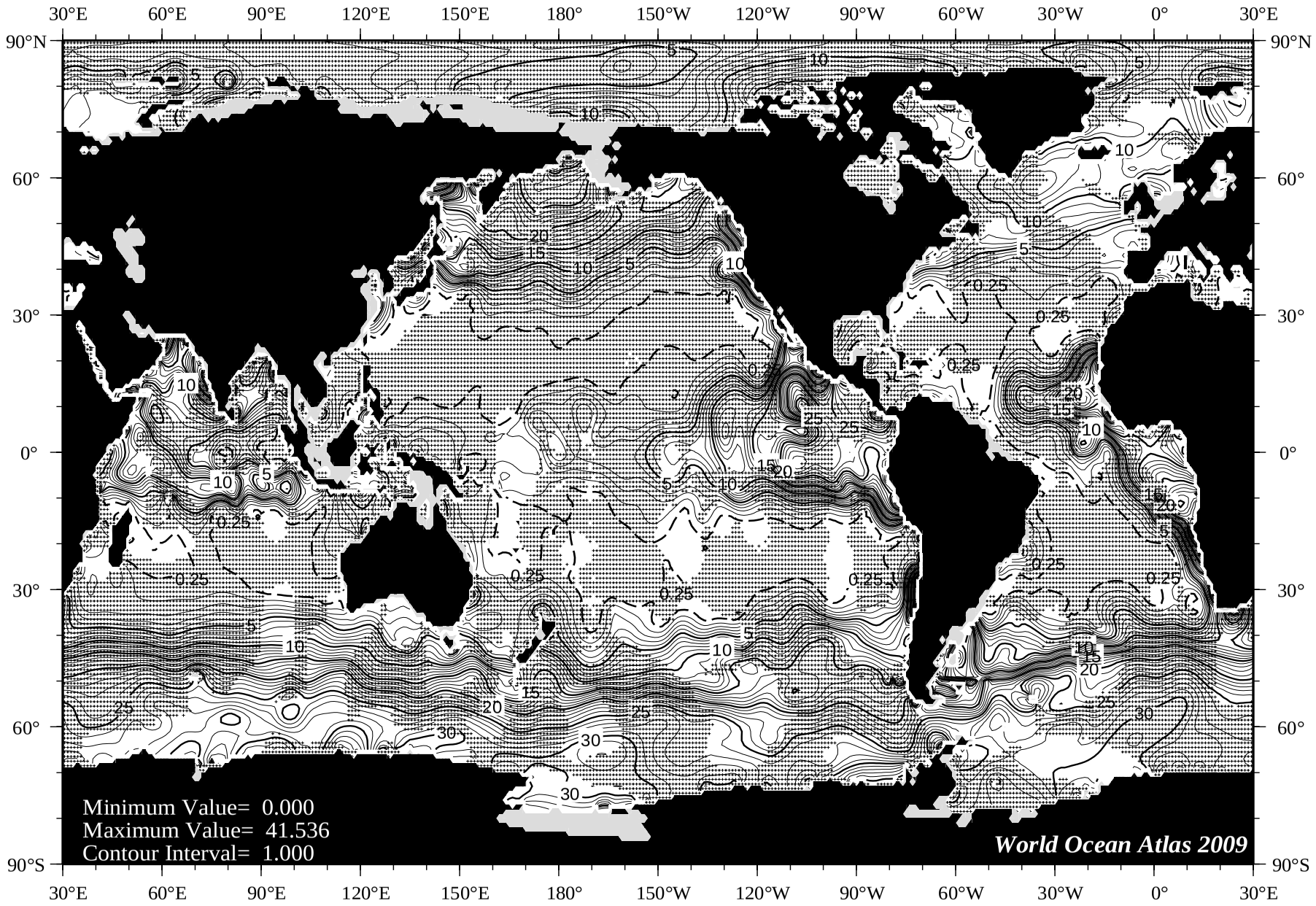

Fig F71 December mean nitrate [umol/l] at 75 m. depth.

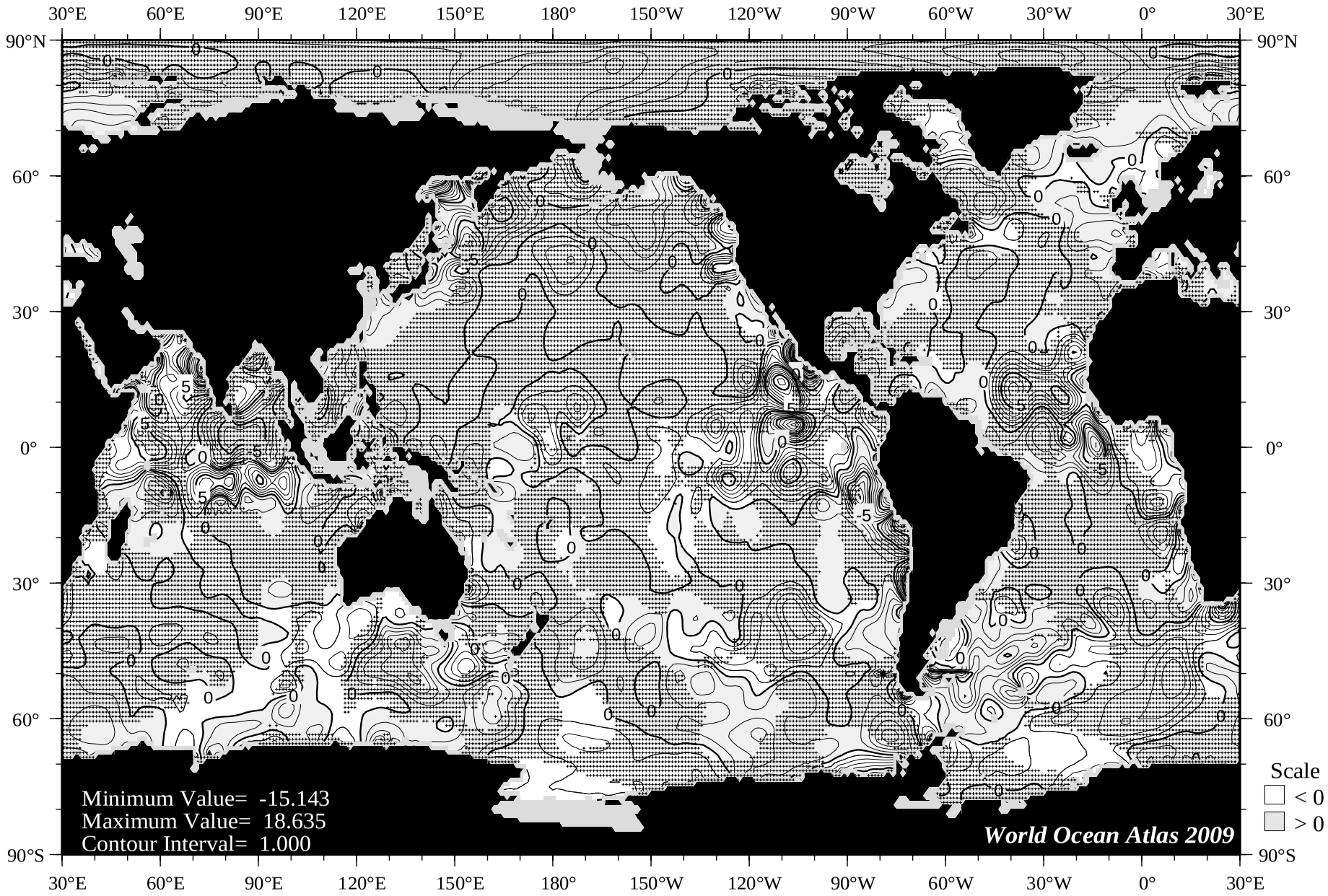

Fig F72 December minus annual nitrate [umol/l] at 75 m. depth.

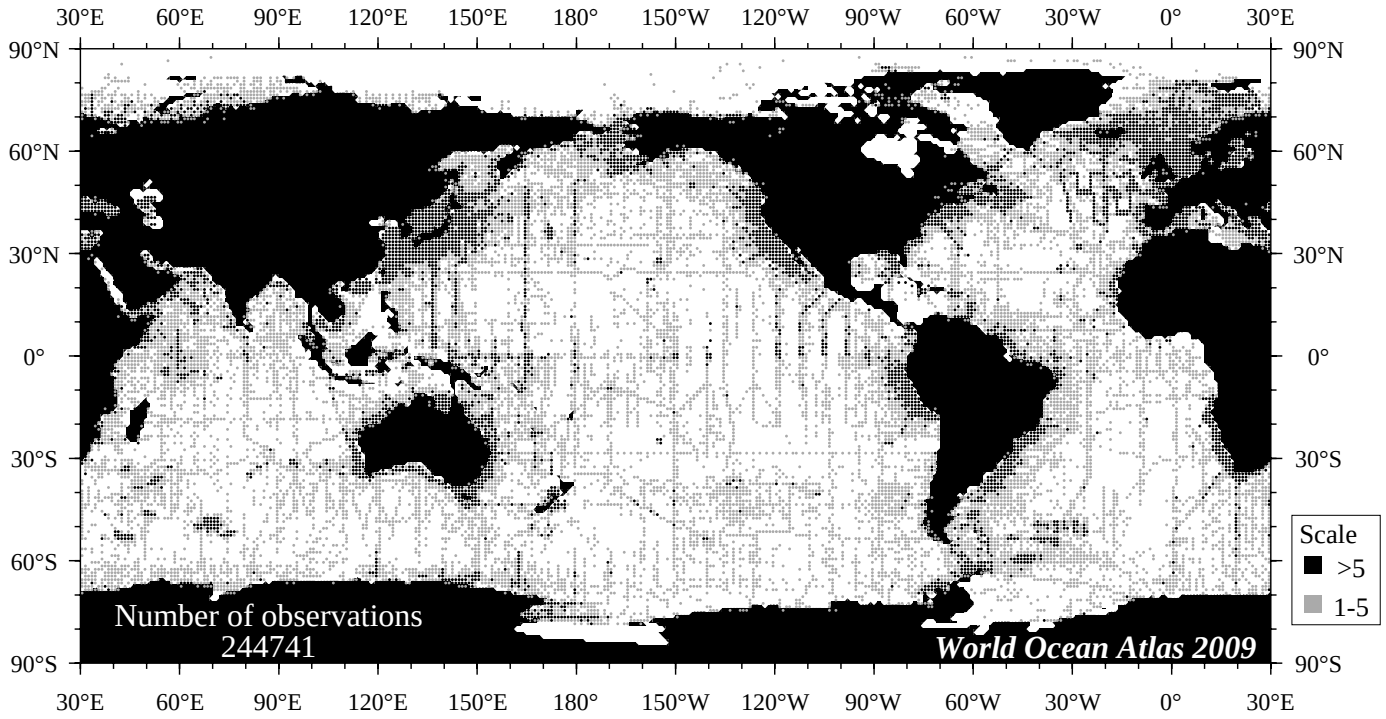

Fig G1 Annual silicate observations at the surface.

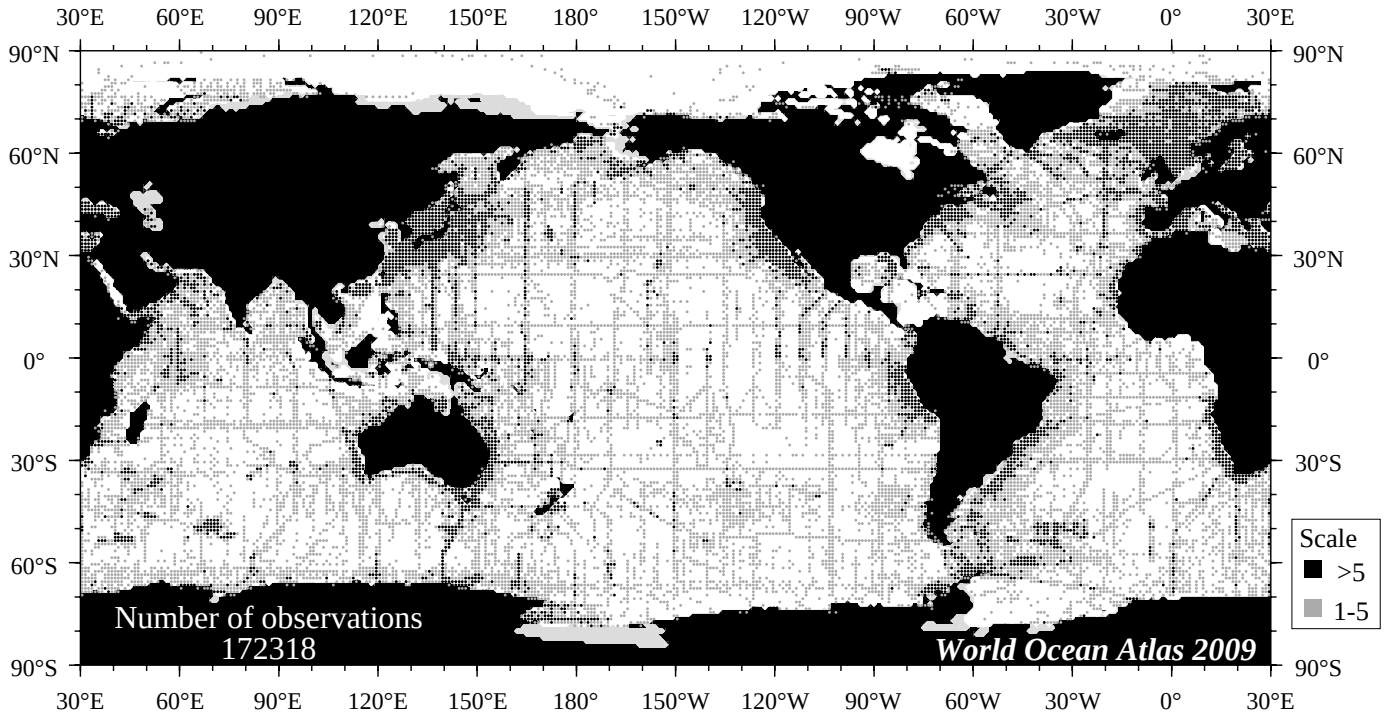

Fig G2 Annual silicate observations at 50 m. depth.

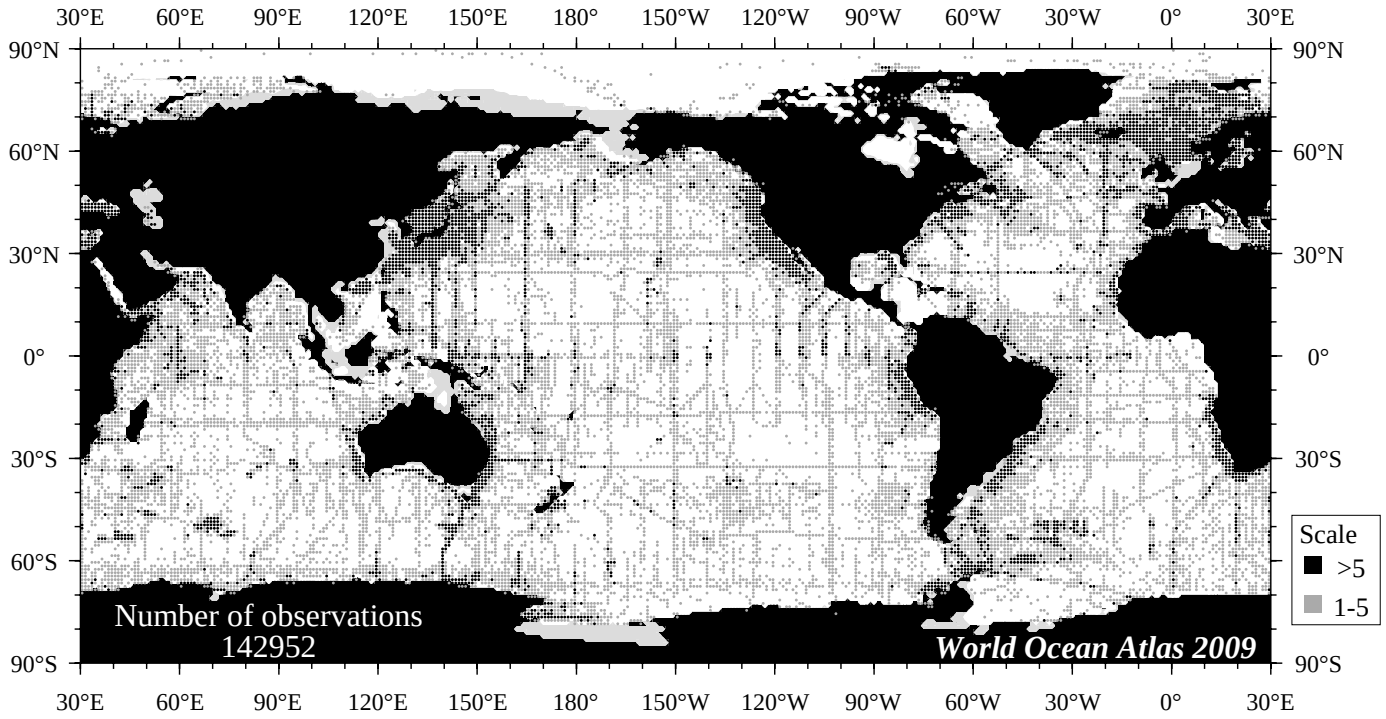

Fig G3 Annual silicate observations at 75 m. depth.

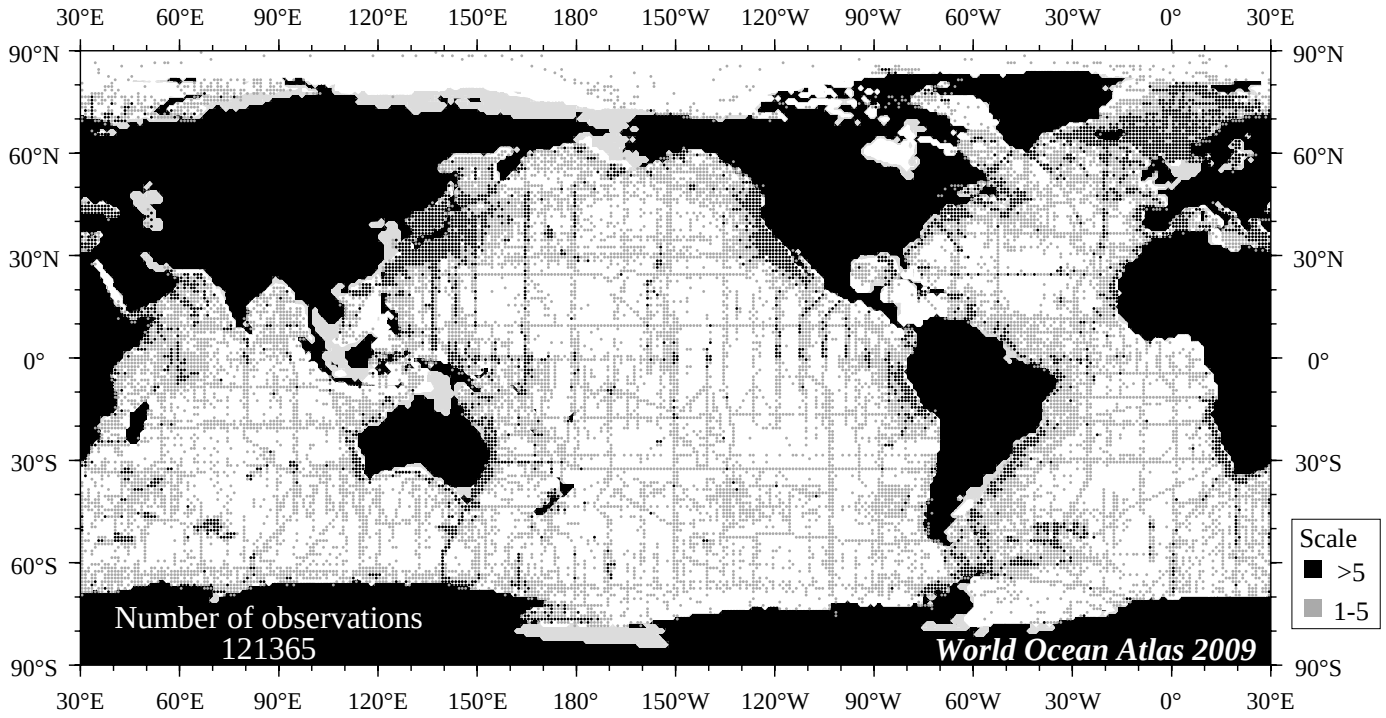

Fig G4 Annual silicate observations at 100 m. depth.

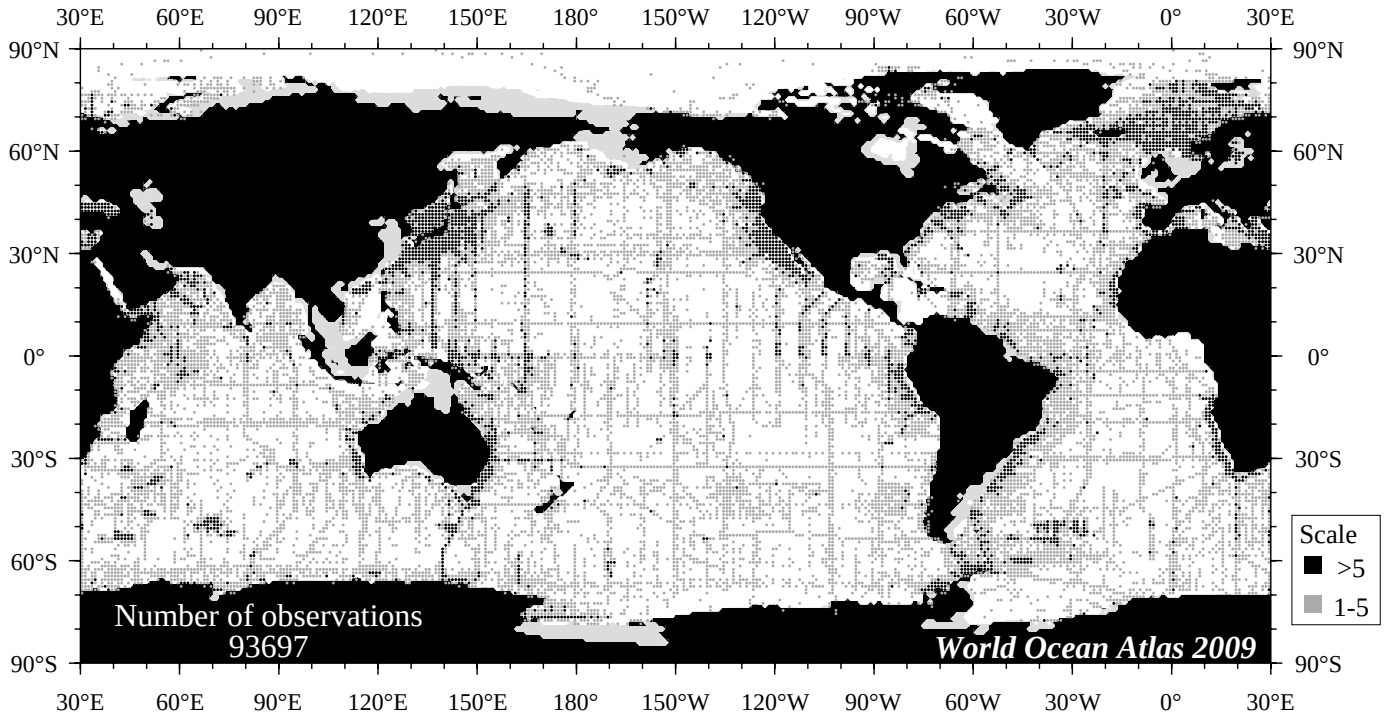

Fig G5 Annual silicate observations at 150 m. depth.

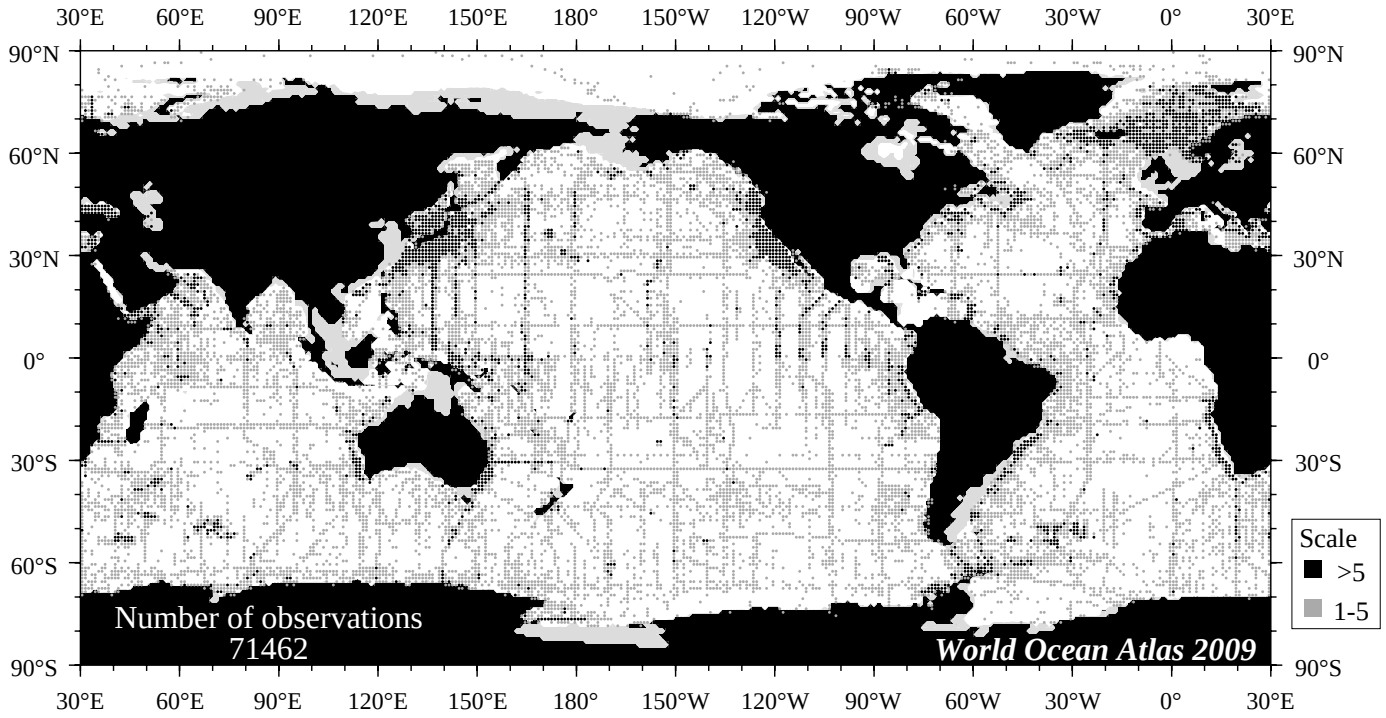

Fig G6 Annual silicate observations at 200 m. depth.

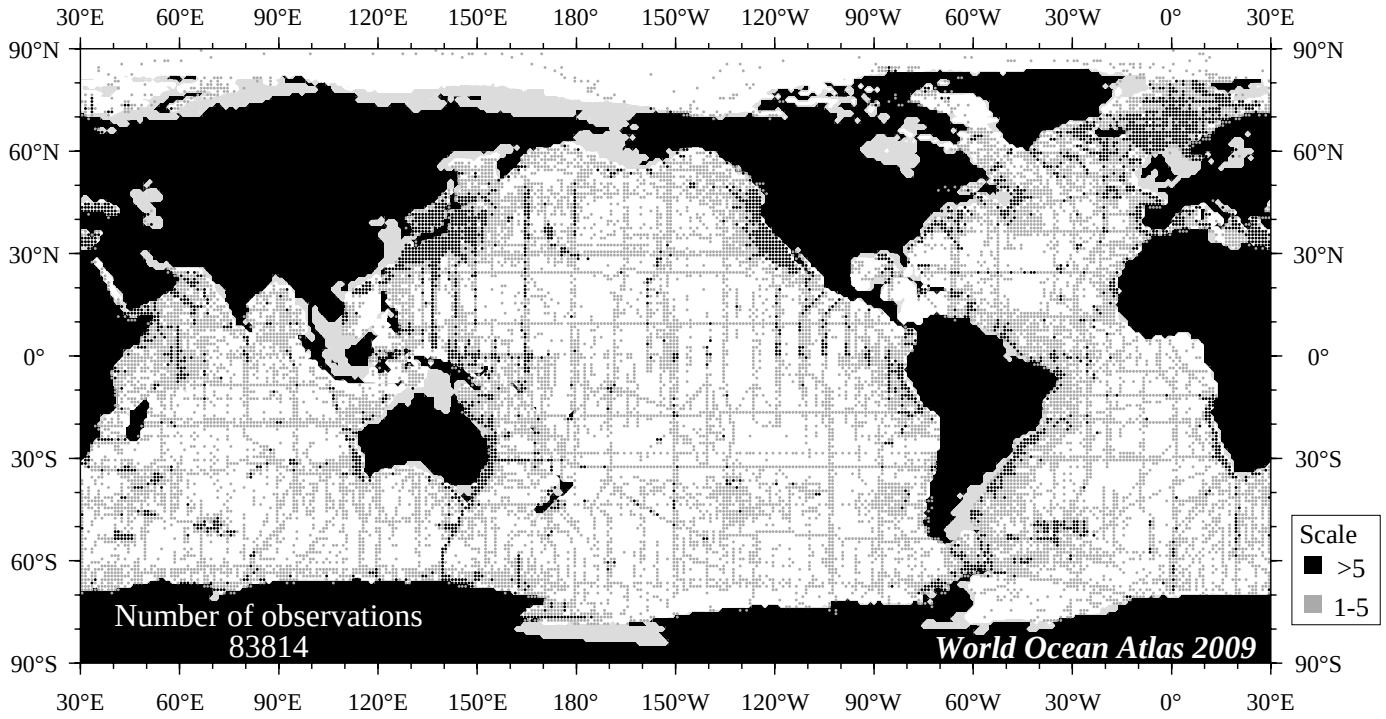

Fig G7 Annual silicate observations at 250 m. depth.

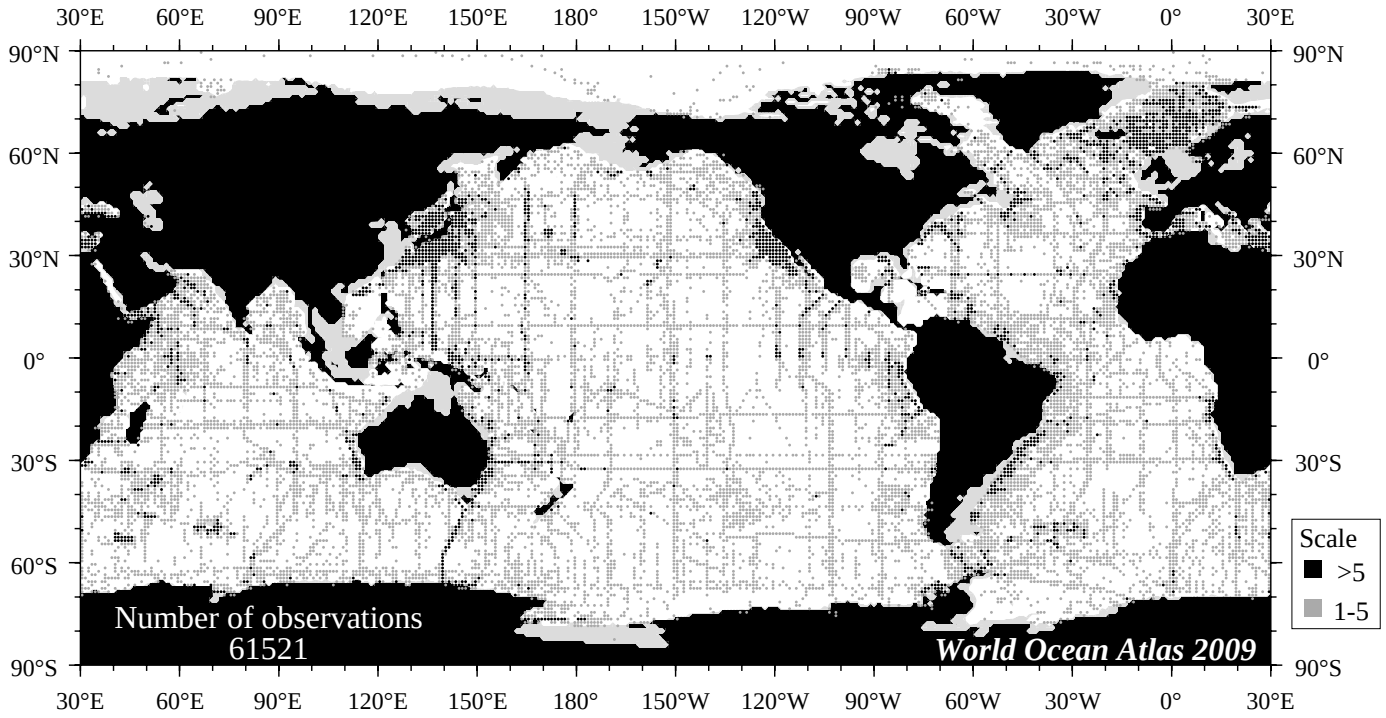

Fig G8 Annual silicate observations at 400 m. depth.

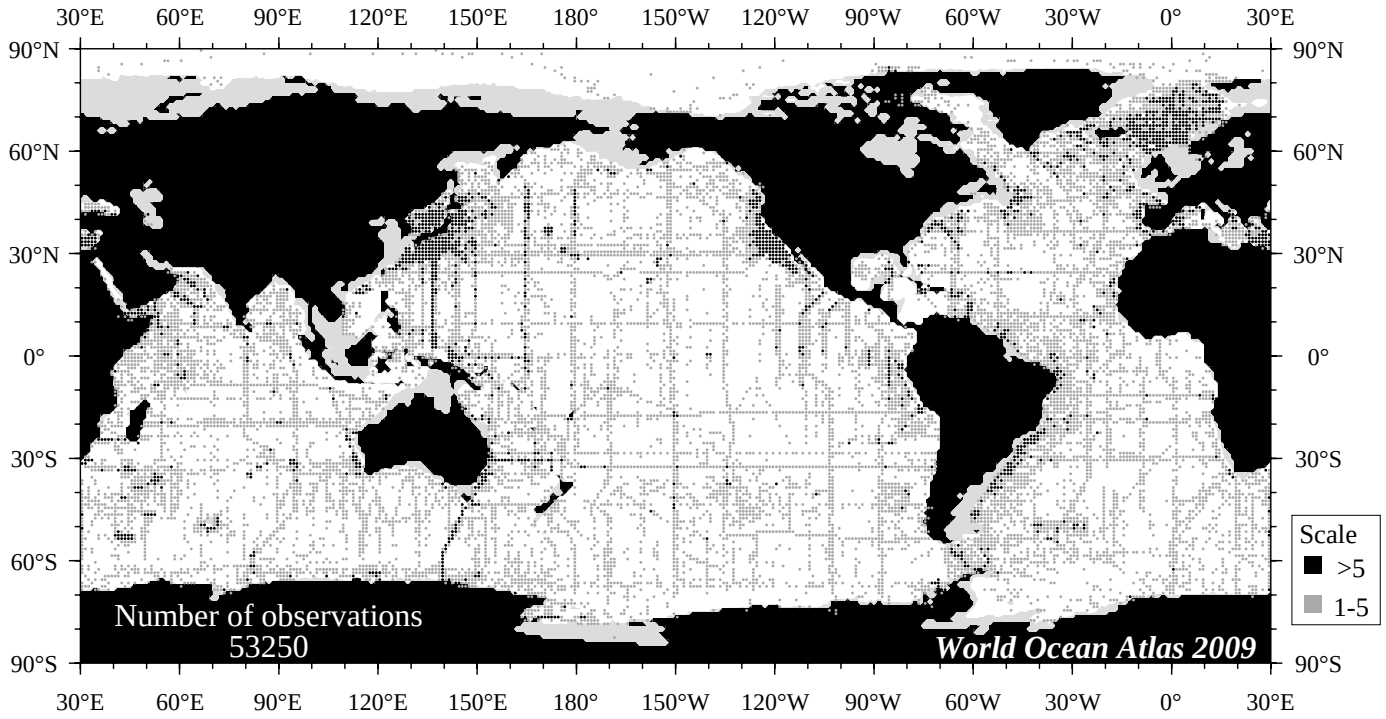

Fig G9 Annual silicate observations at 500 m. depth.

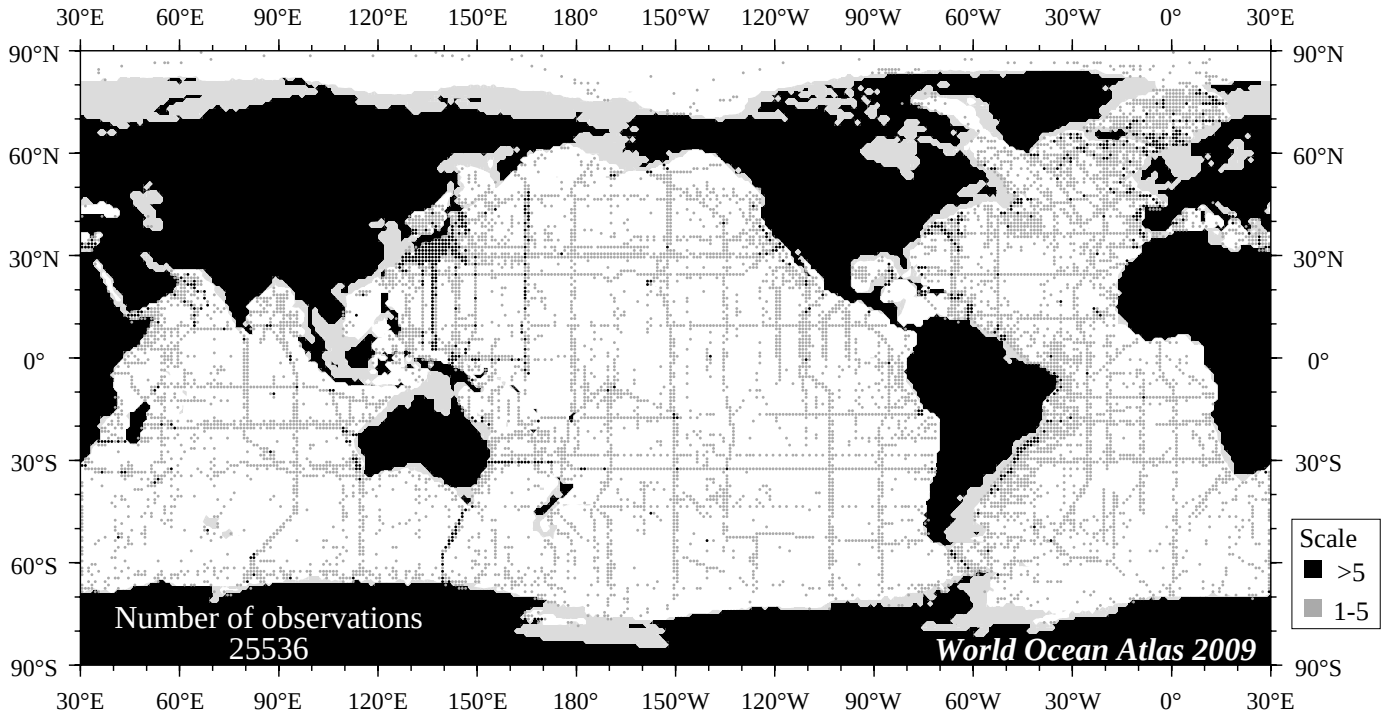

Fig G10 Annual silicate observations at 700 m. depth.

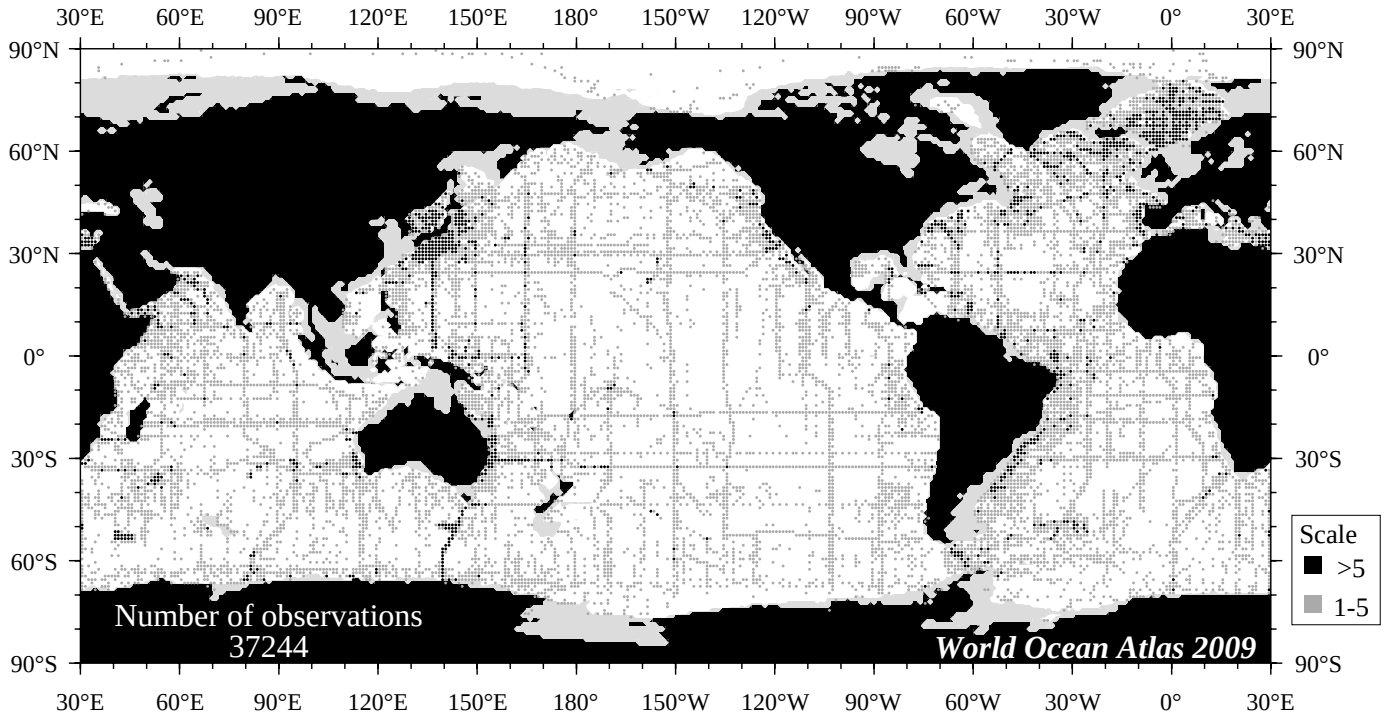

Fig G11 Annual silicate observations at 1000 m. depth.

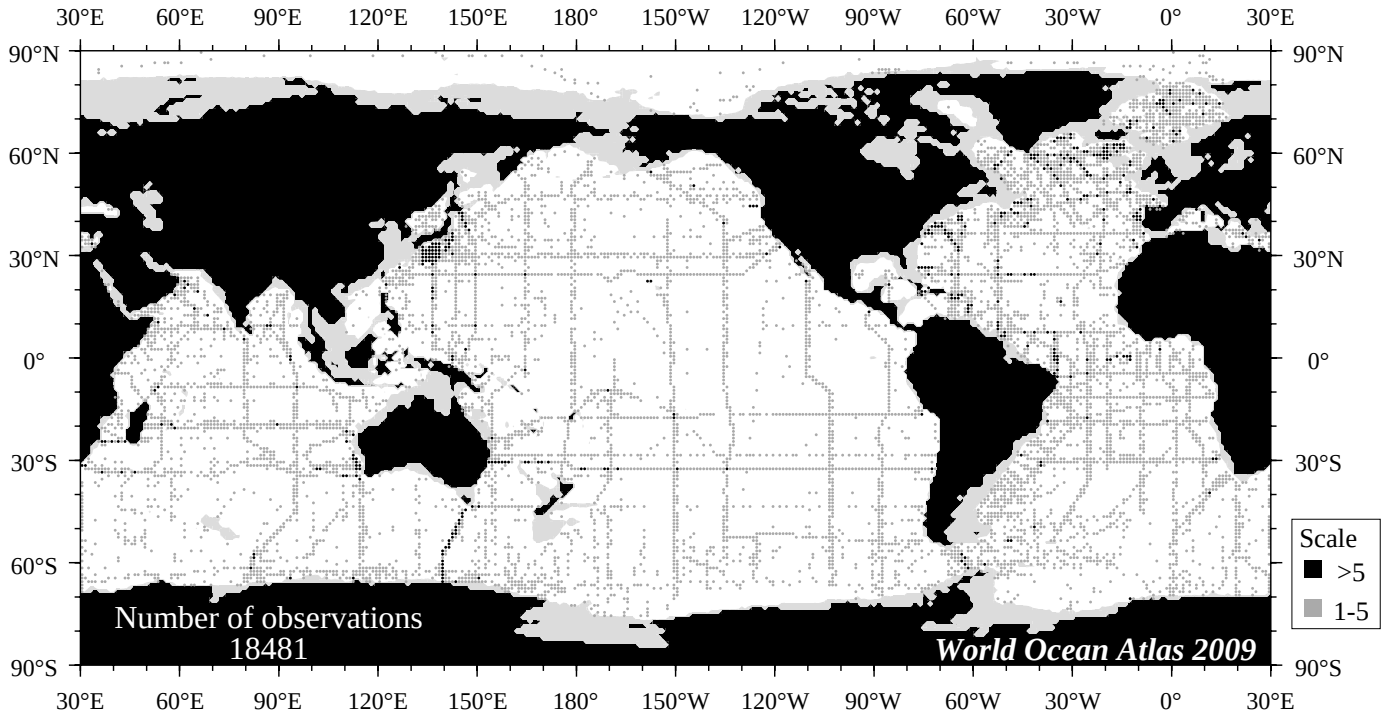

Fig G12 Annual silicate observations at 1500 m. depth.

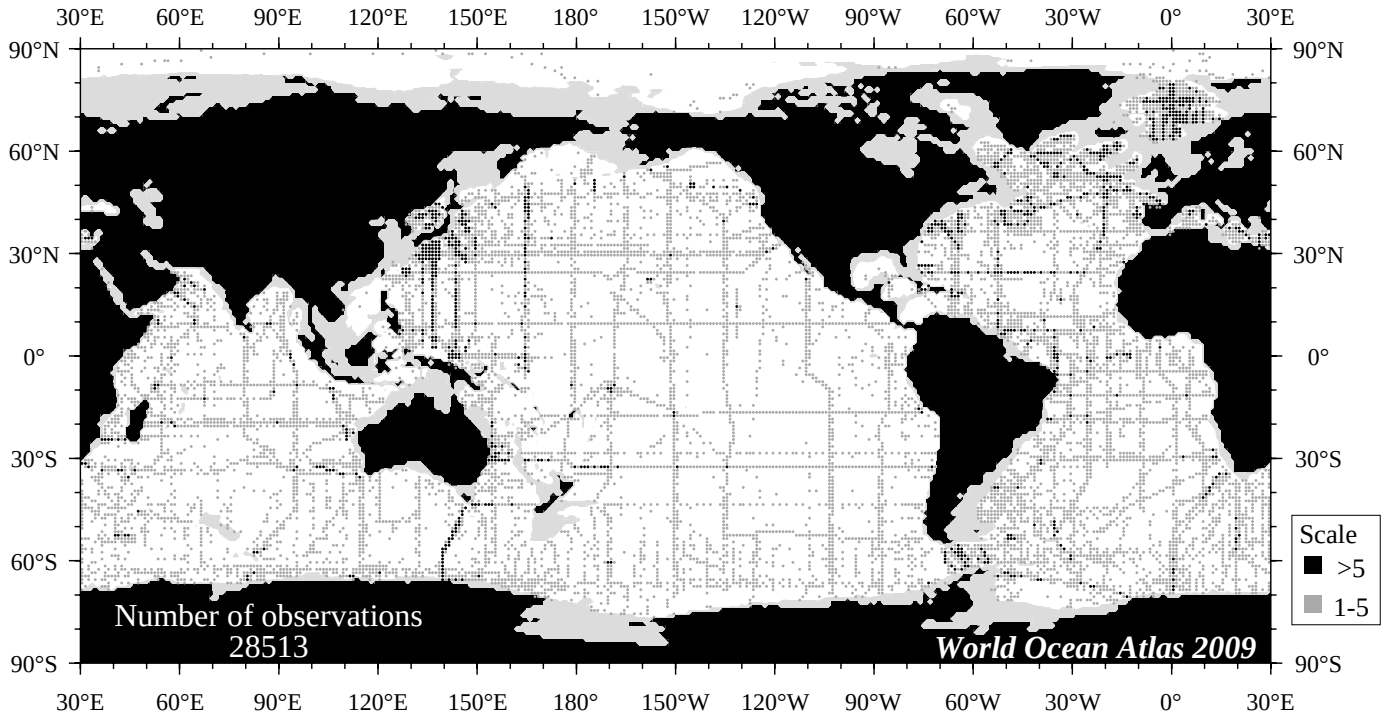

Fig G13 Annual silicate observations at 2000 m. depth.

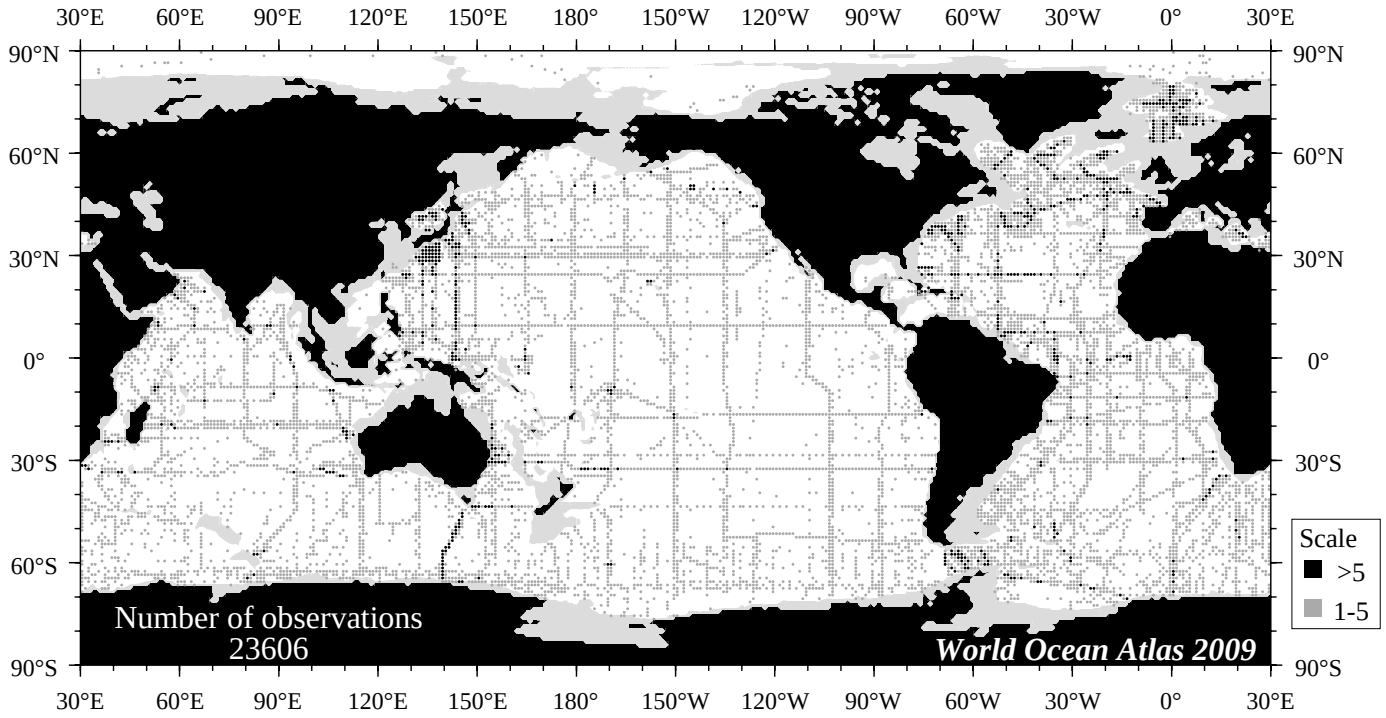

Fig G14 Annual silicate observations at 2500 m. depth.

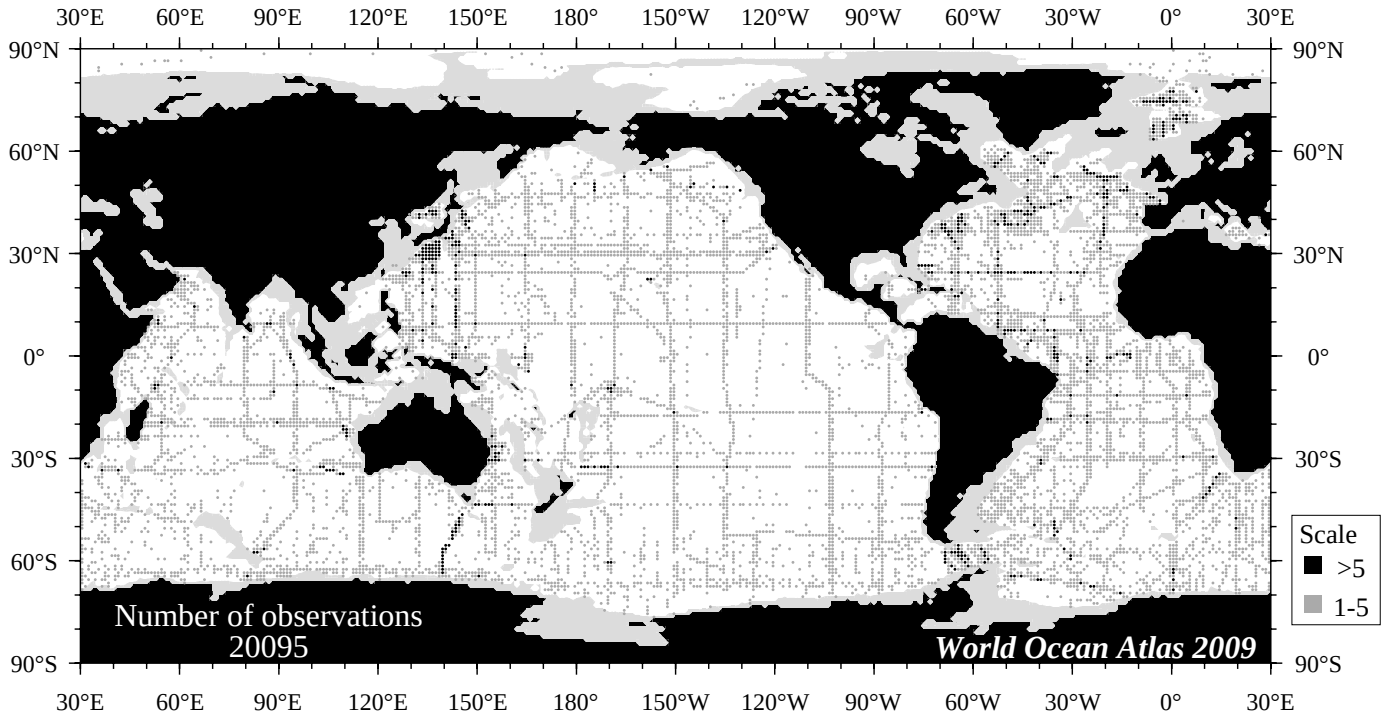

Fig G15 Annual silicate observations at 3000 m. depth.

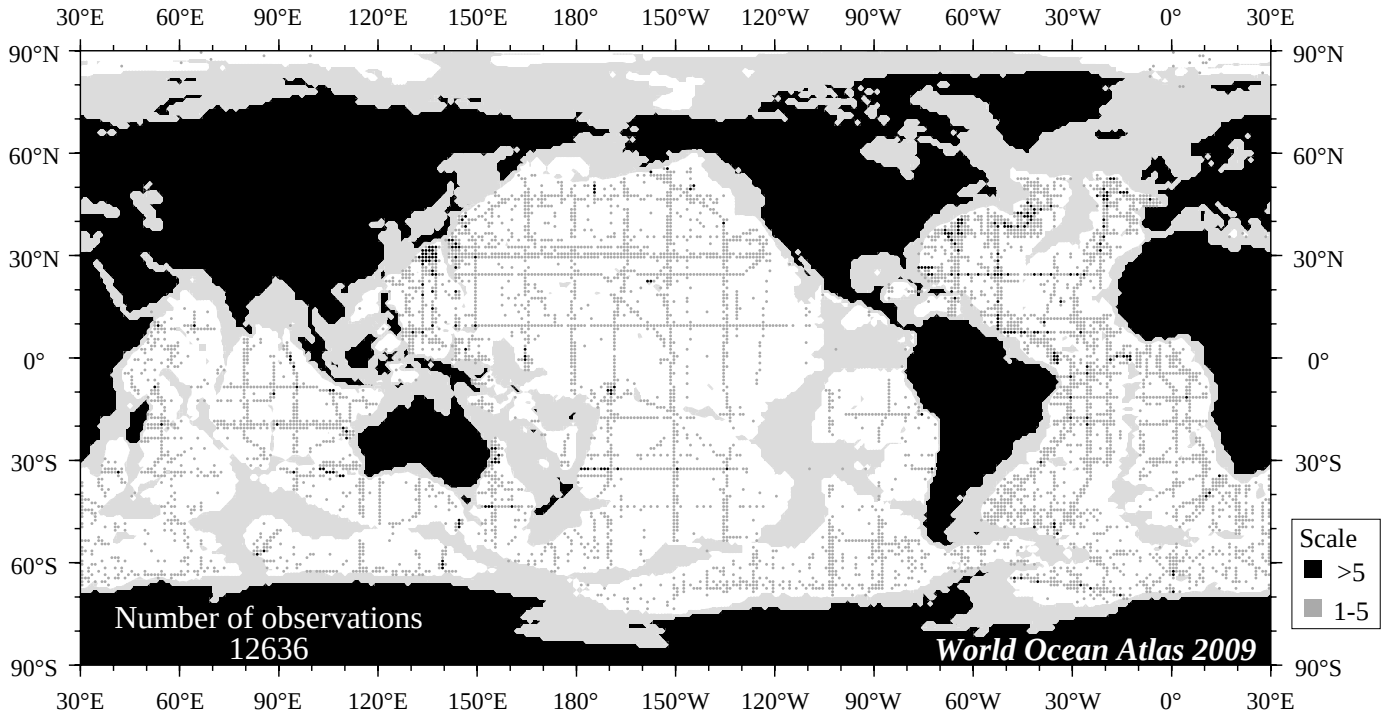

Fig G16 Annual silicate observations at 4000 m. depth.

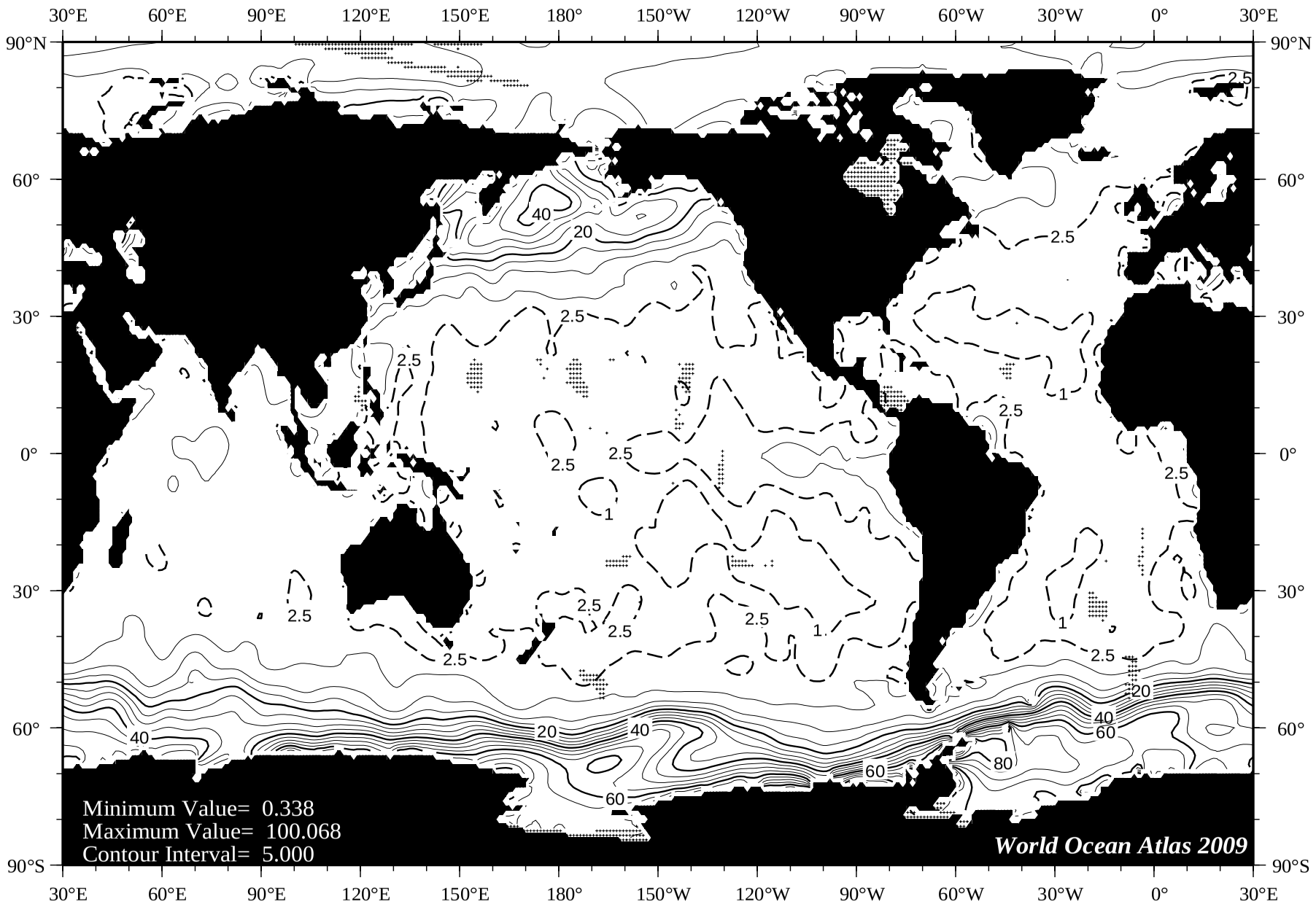

Fig G17 Annual silicate [umol/l] at the surface.

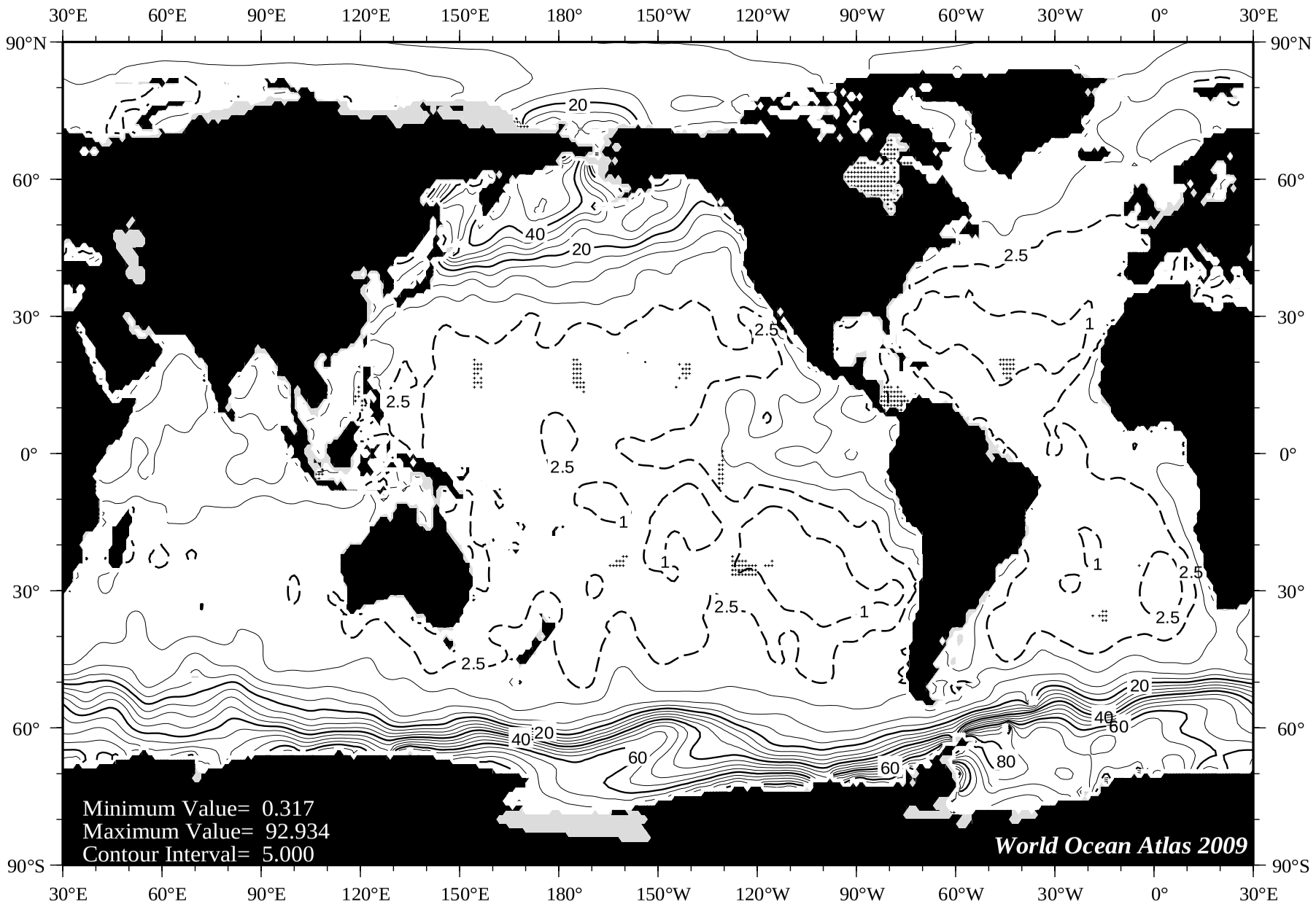

Fig G18 Annual silicate [umol/l] at 50 m. depth.

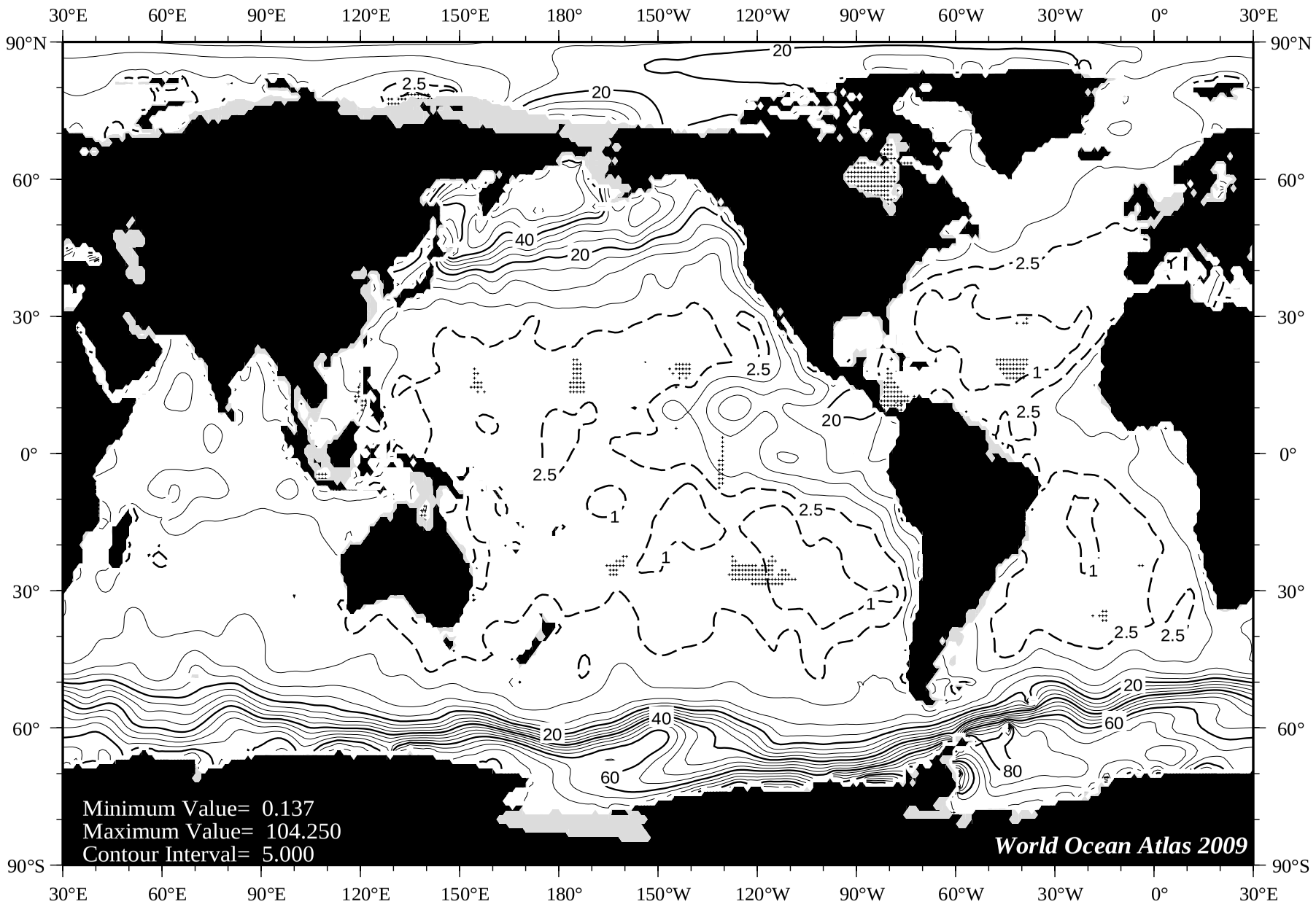

Fig G19 Annual silicate [umol/l] at 75 m. depth.

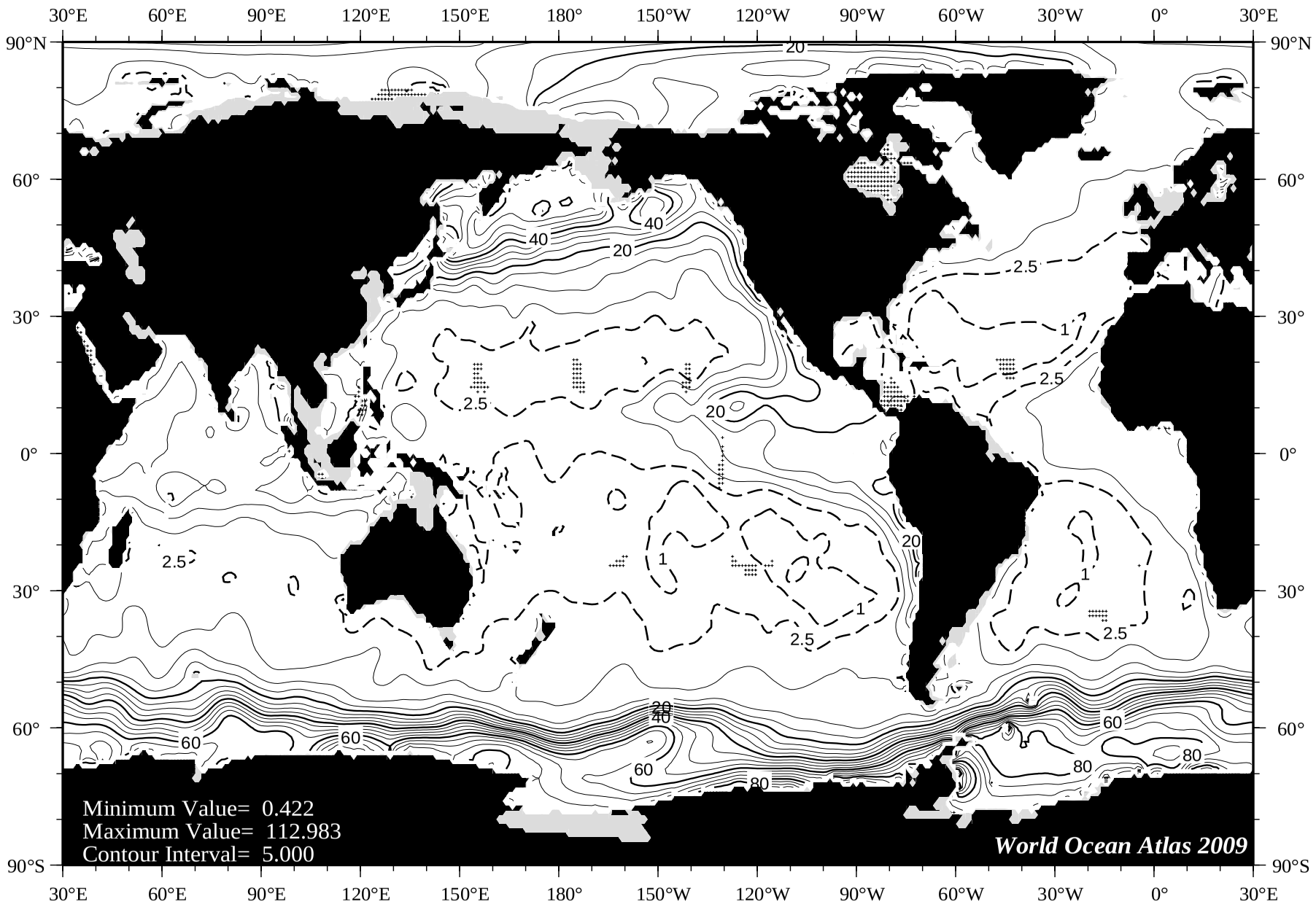

Fig G20 Annual silicate [umol/l] at 100 m. depth.

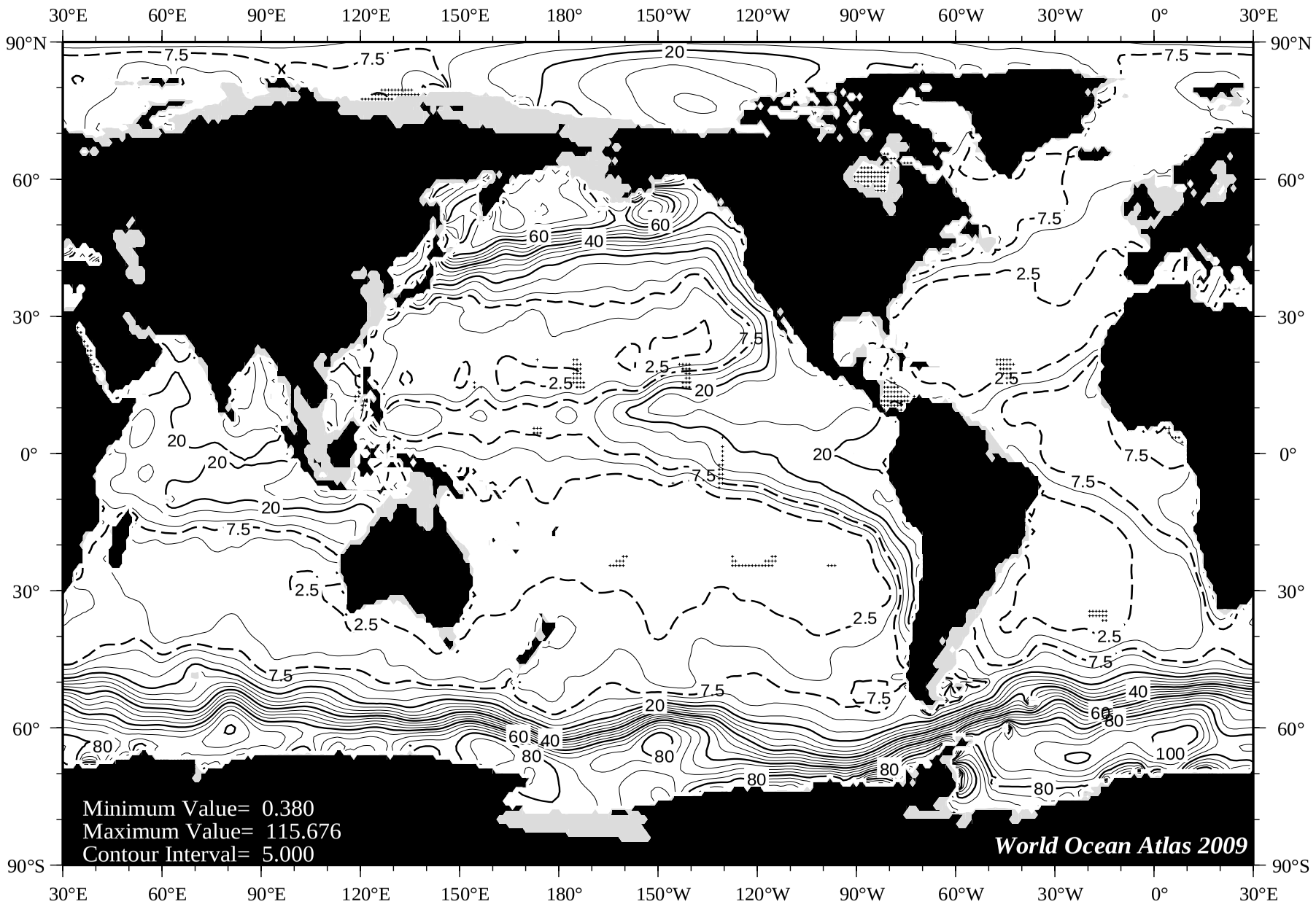

Fig G21 Annual silicate [umol/l] at 150 m. depth.

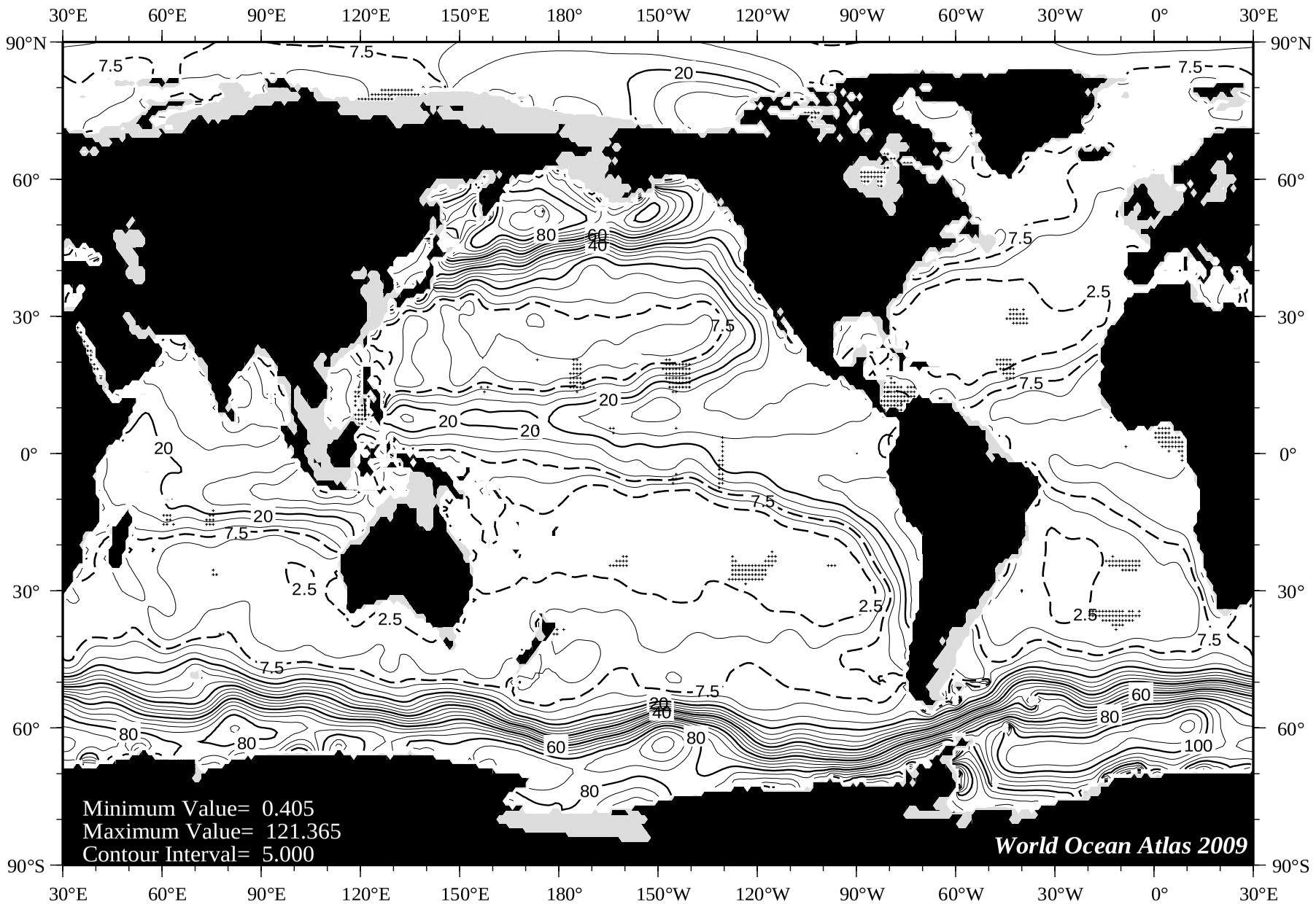

Fig G22 Annual silicate [umol/l] at 200 m. depth.

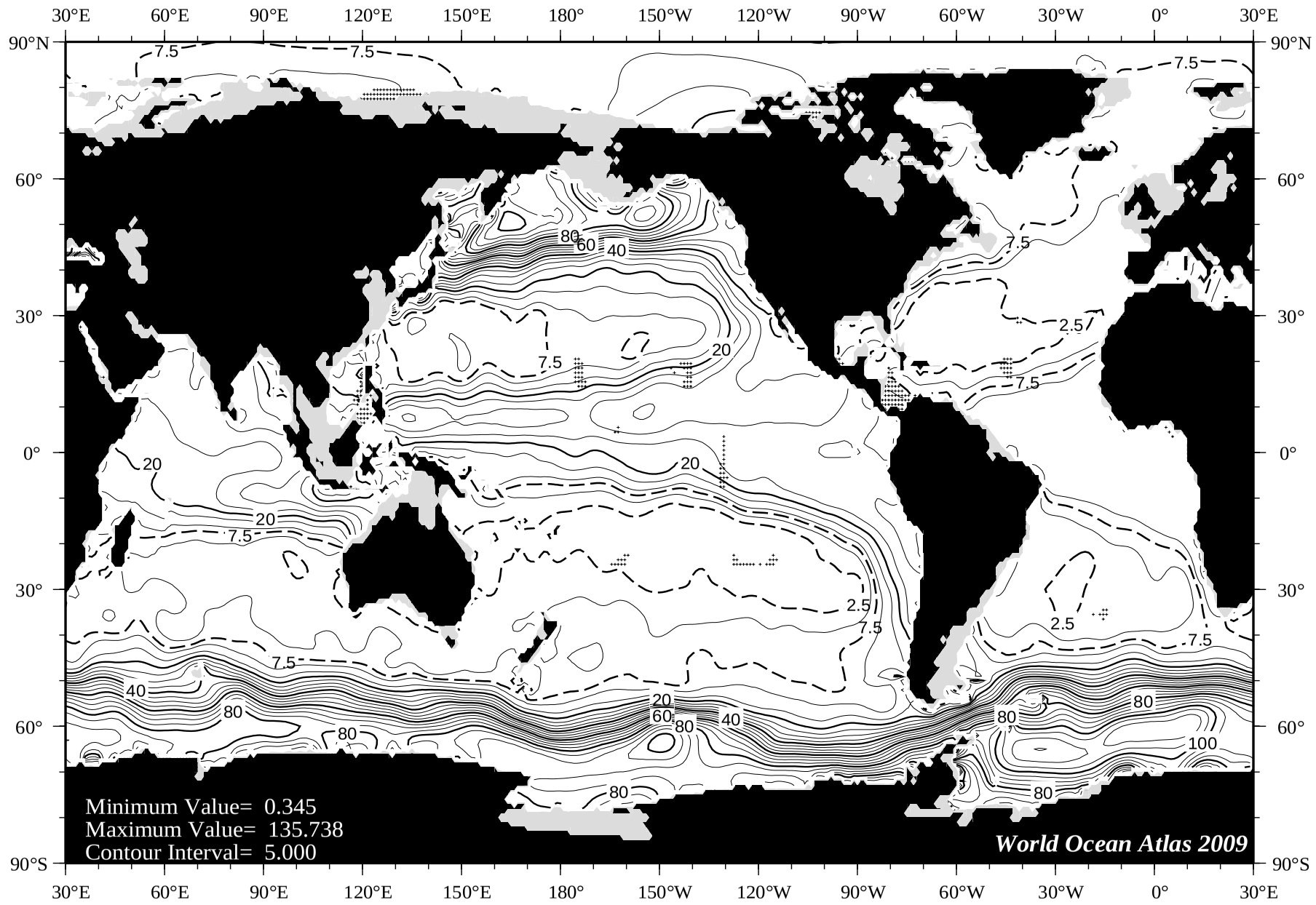

Fig G23 Annual silicate [umol/l] at 250 m. depth.

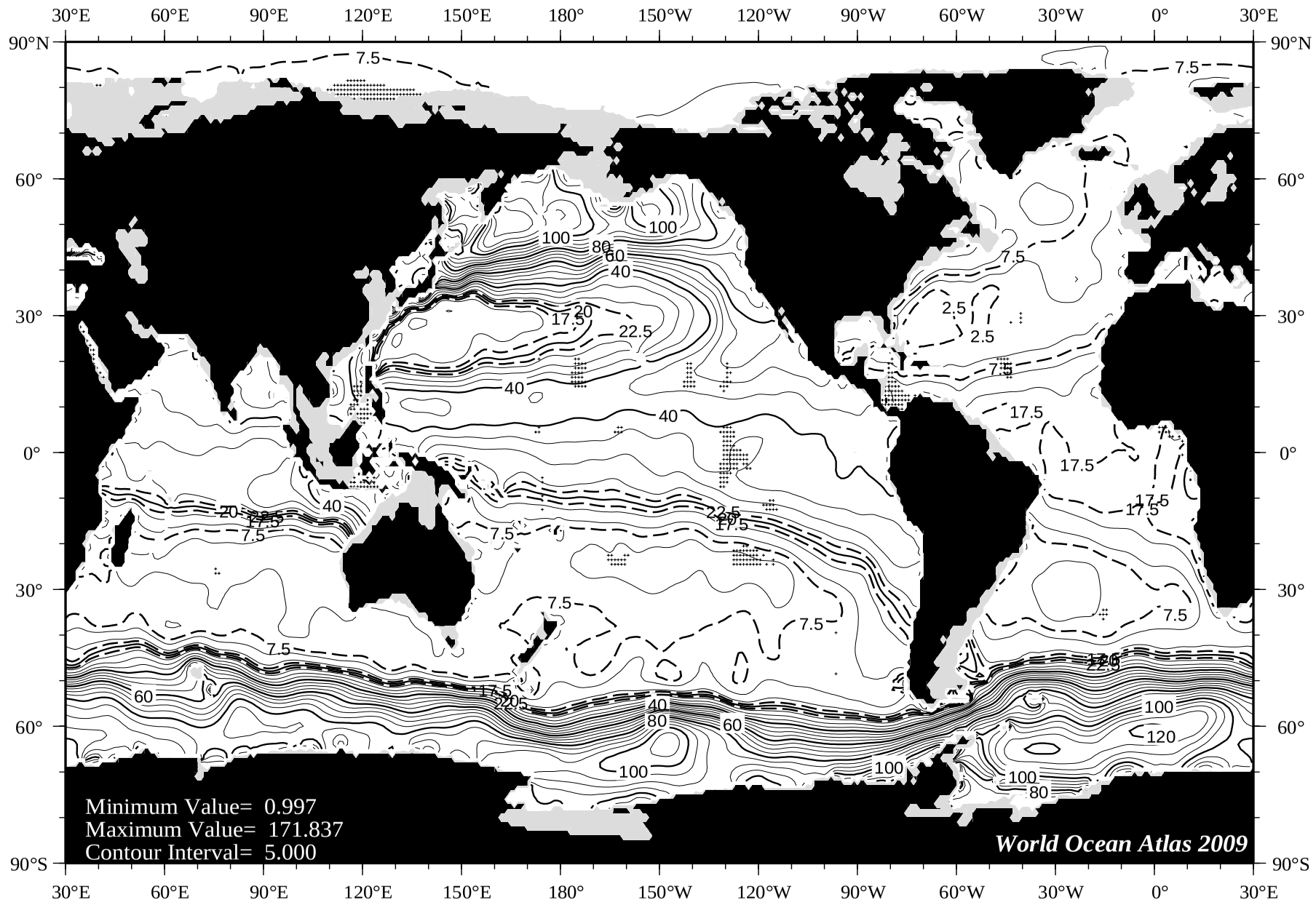

Fig G24 Annual silicate [umol/l] at 400 m. depth.

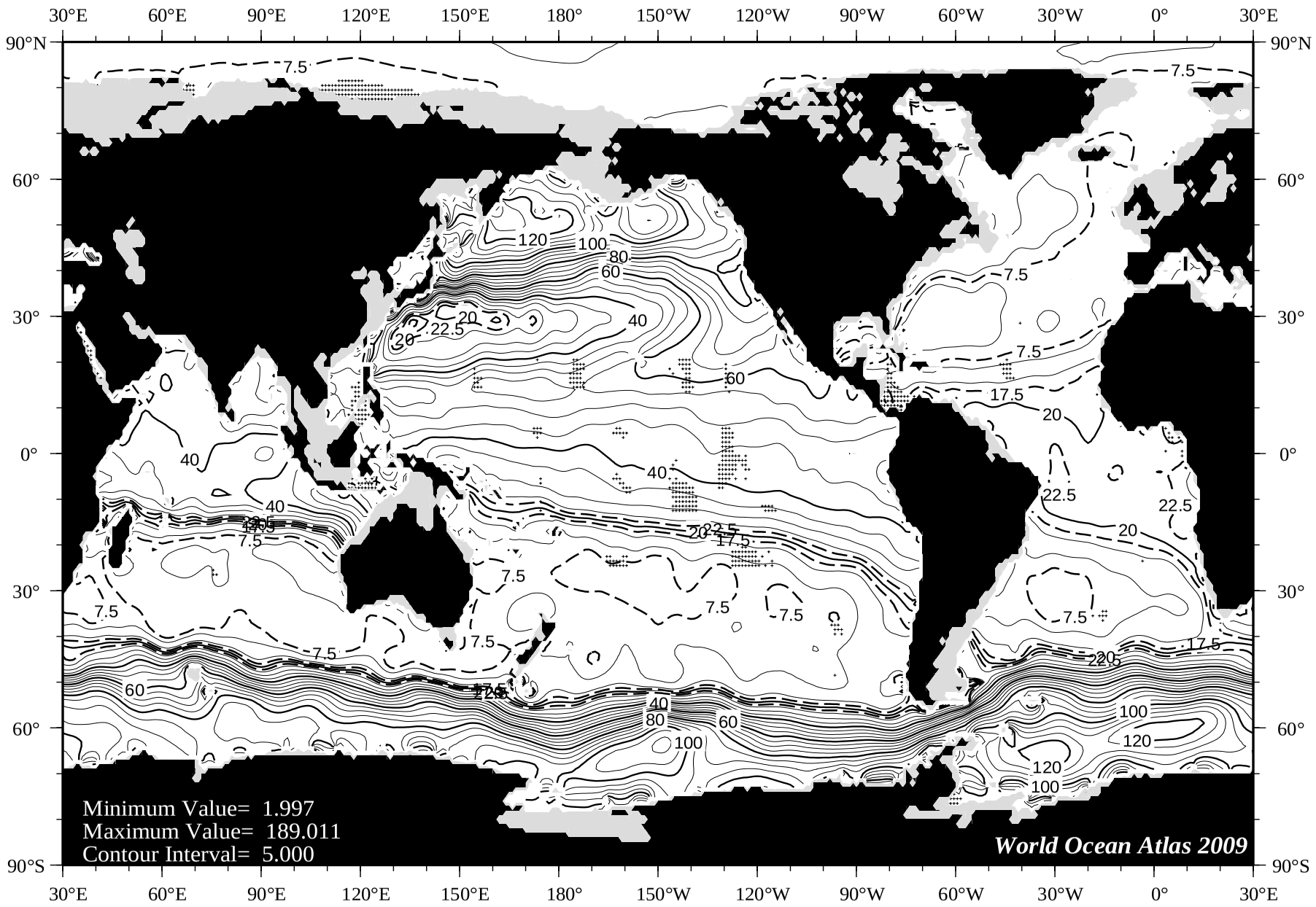

Fig G25 Annual silicate [umol/l] at 500 m. depth.

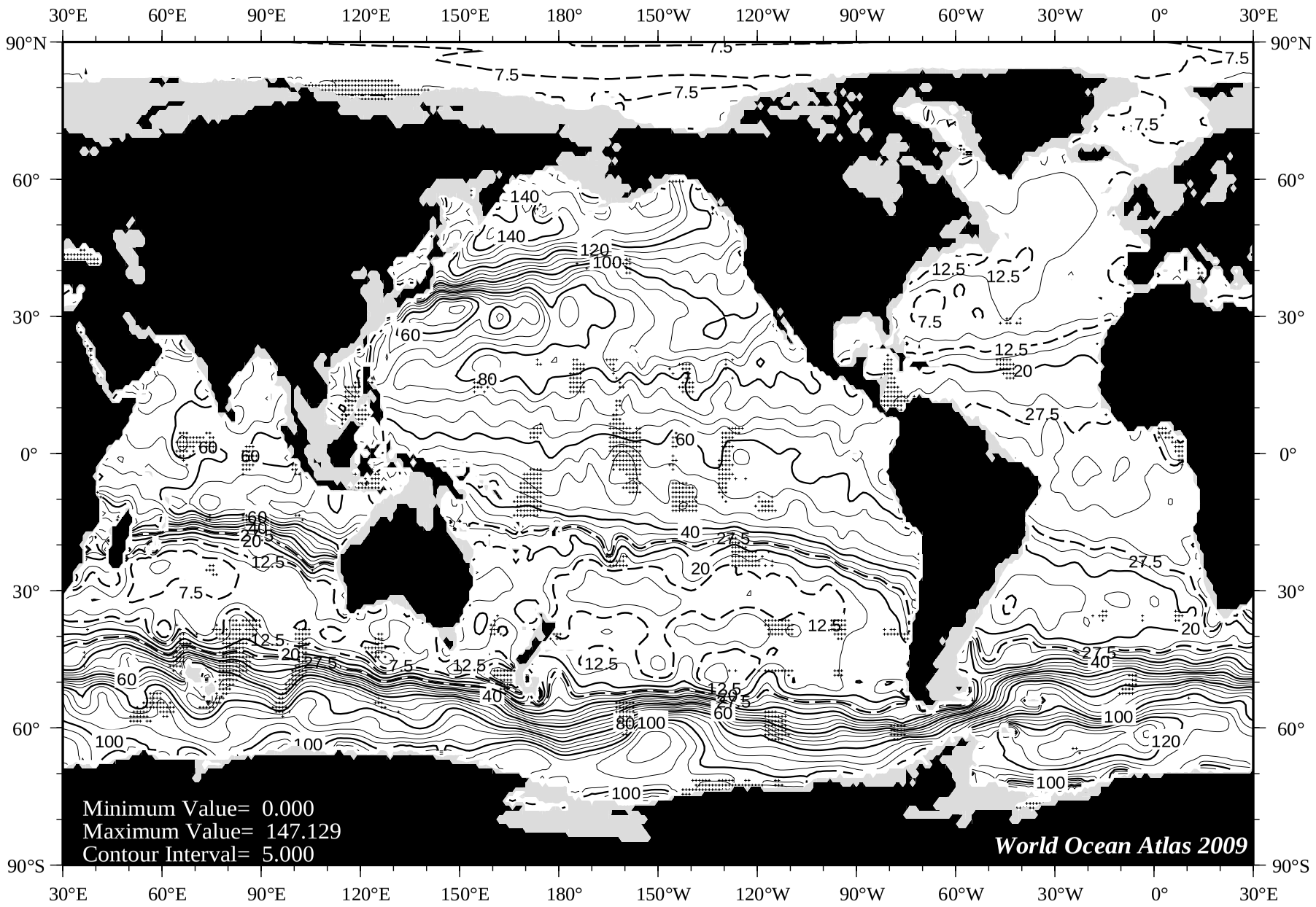

Fig G26 Annual silicate [umol/l] at 700 m. depth.

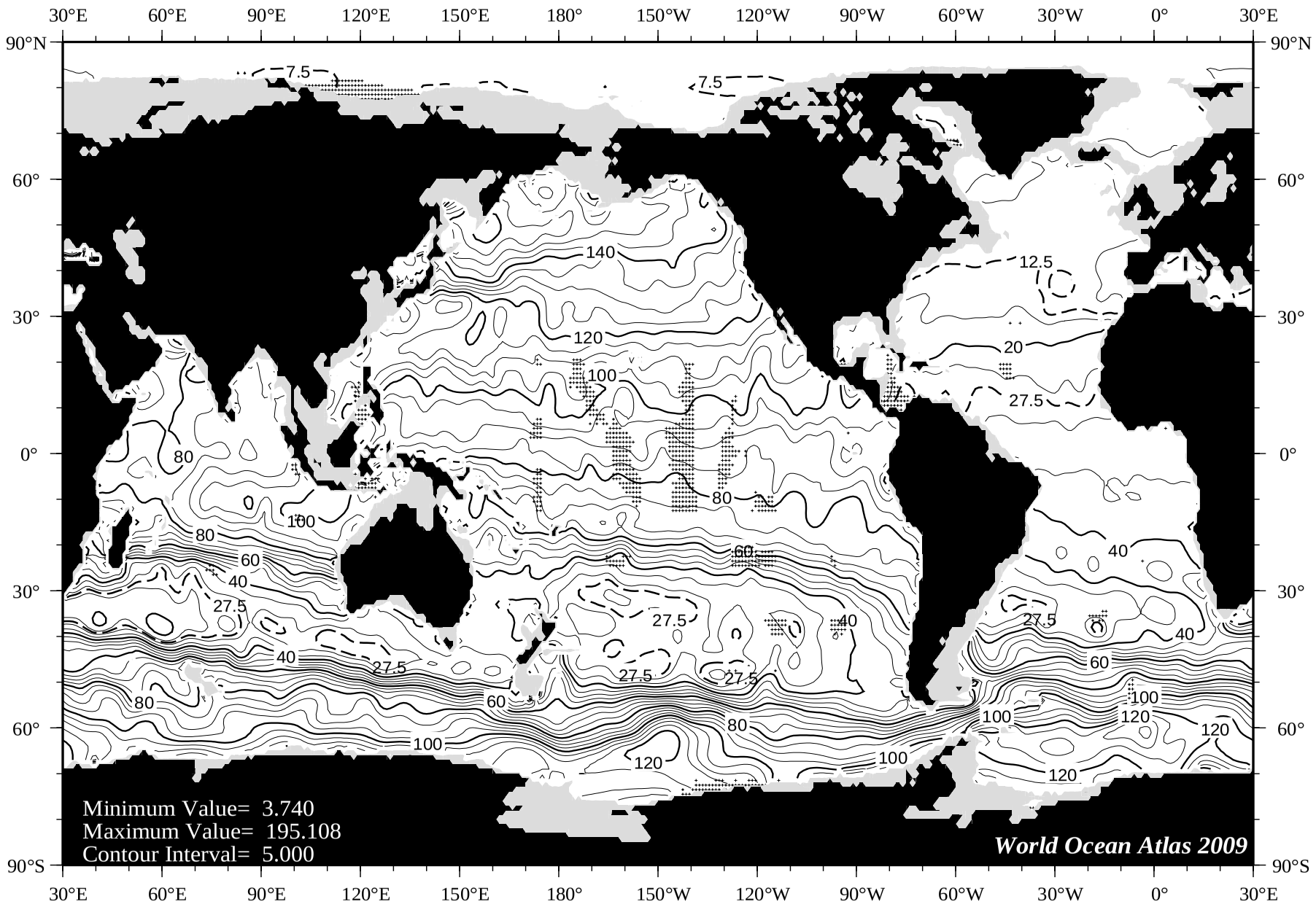

Fig G27 Annual silicate [umol/l] at 1000 m. depth.

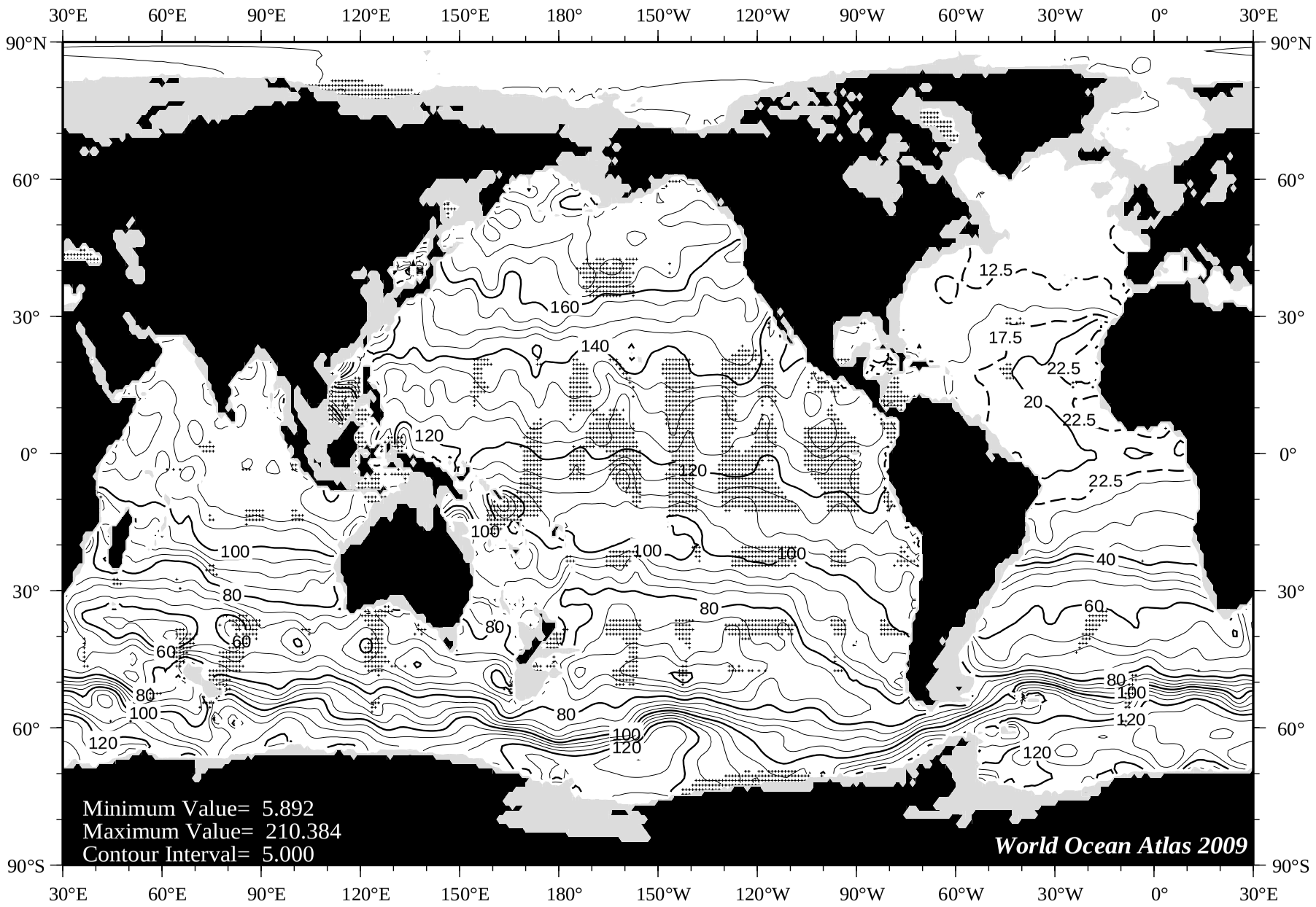

Fig G28 Annual silicate [umol/l] at 1500 m. depth.

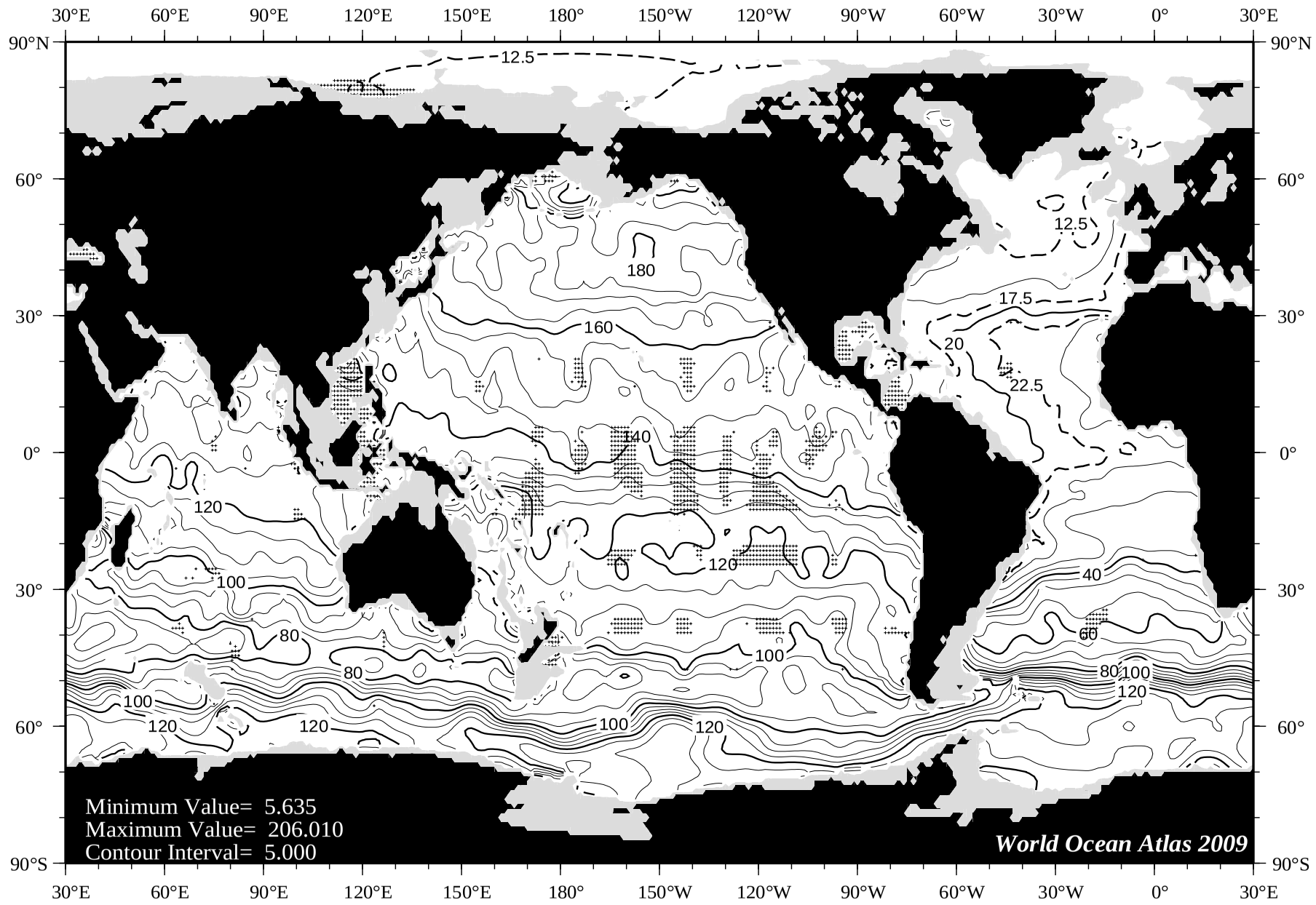

Fig G29 Annual silicate [umol/l] at 2000 m. depth.

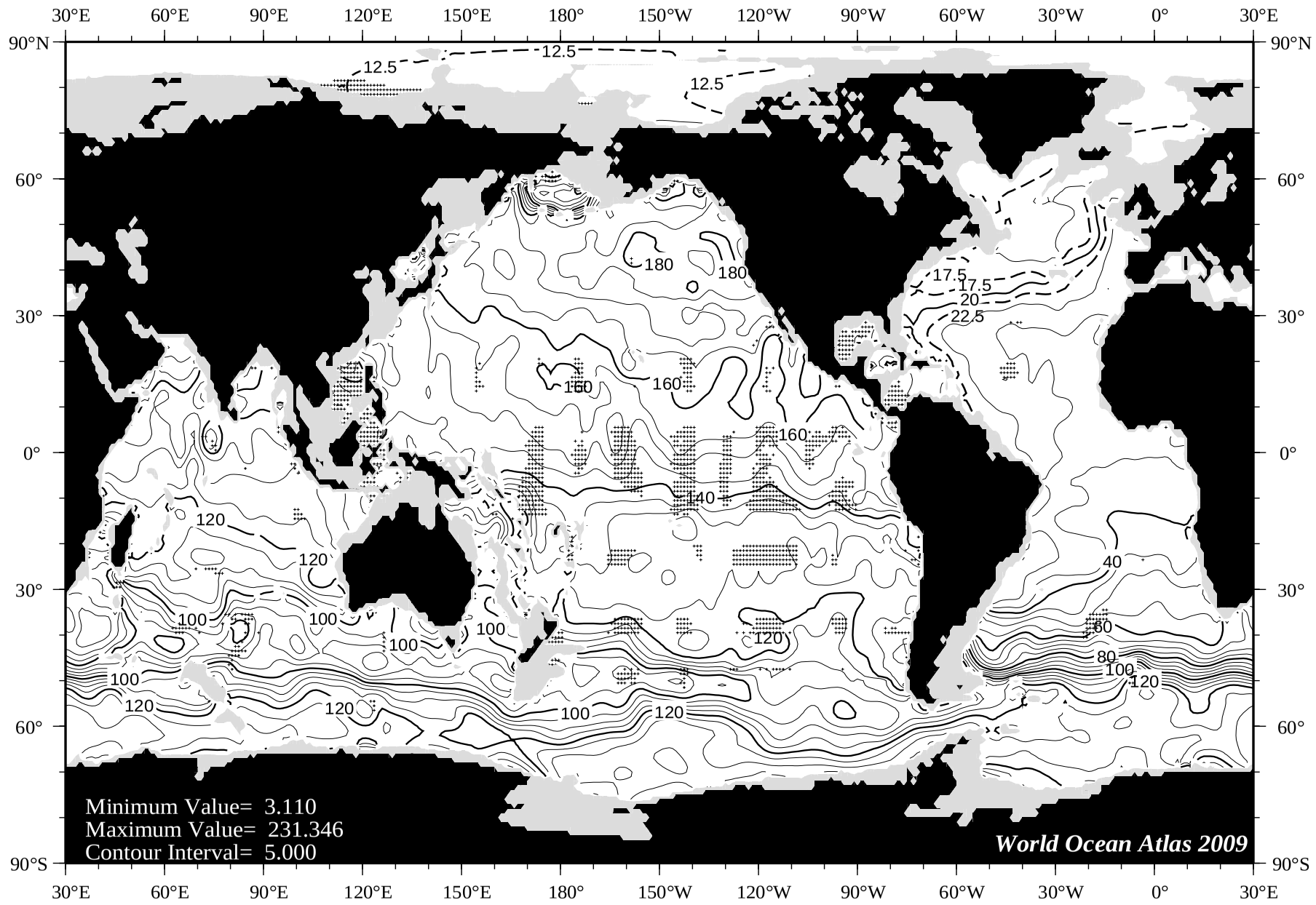

Fig G30 Annual silicate [umol/l] at 2500 m. depth.

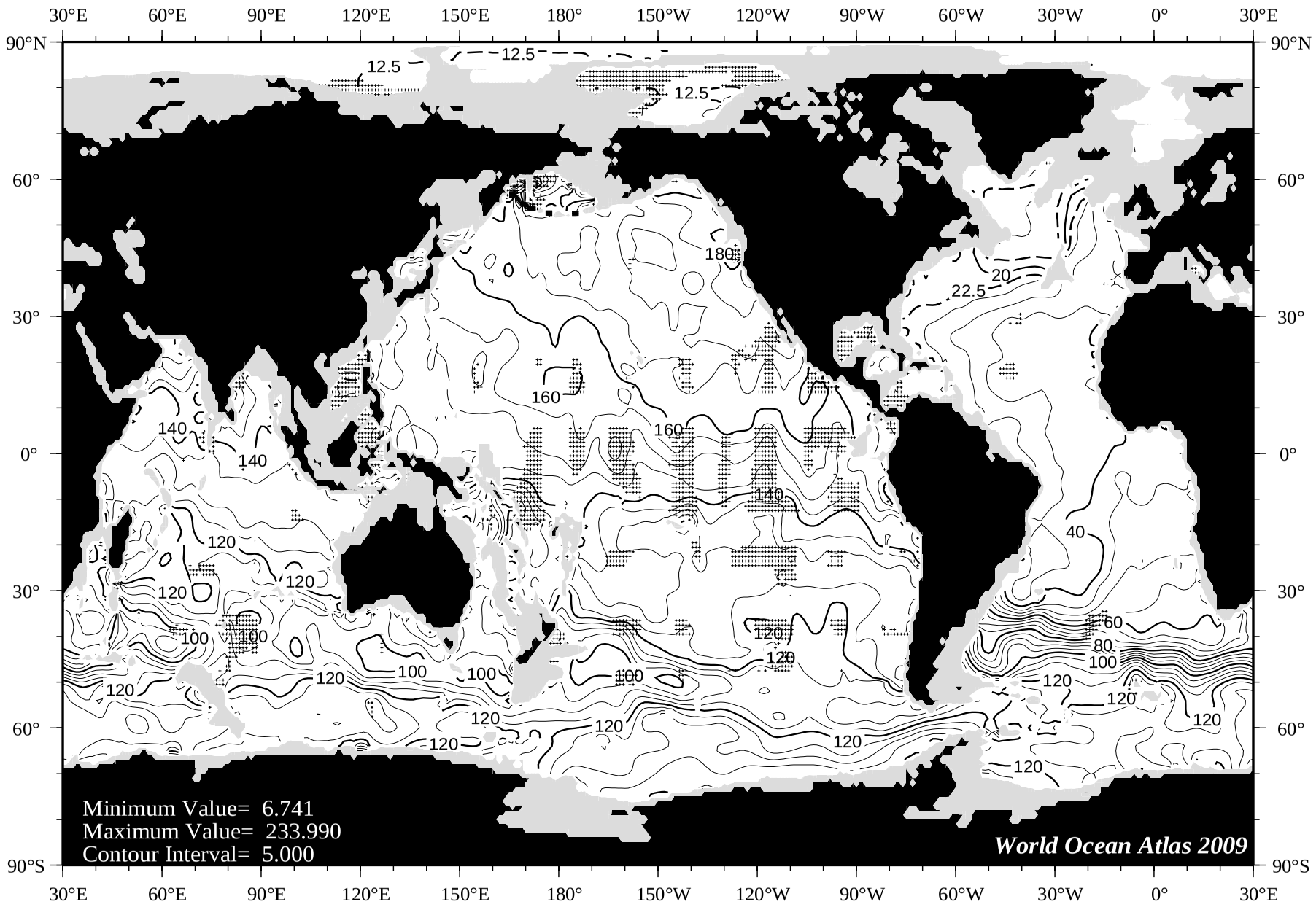

Fig G31 Annual silicate [umol/l] at 3000 m. depth.

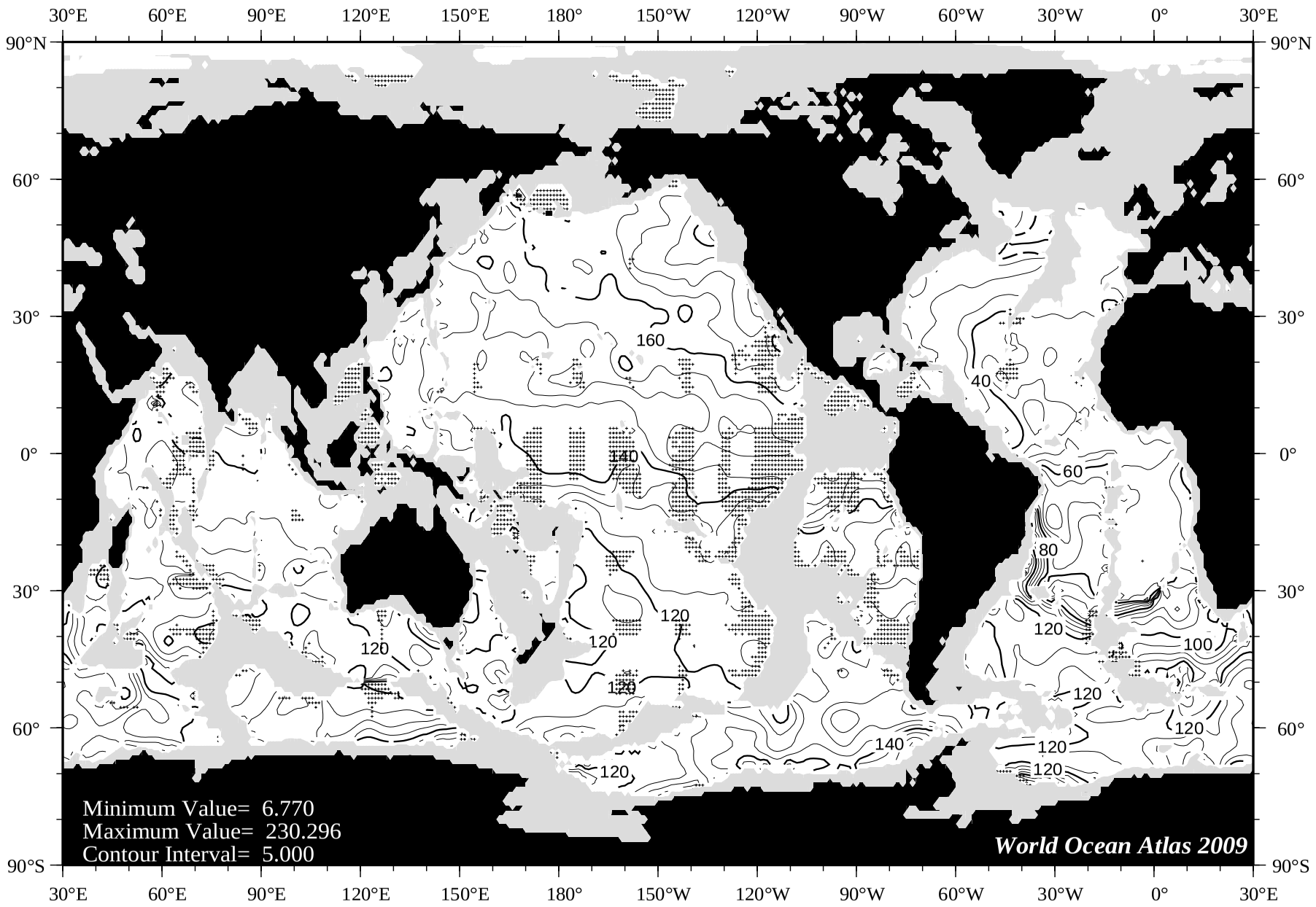

Fig G32 Annual silicate [umol/l] at 4000 m. depth.

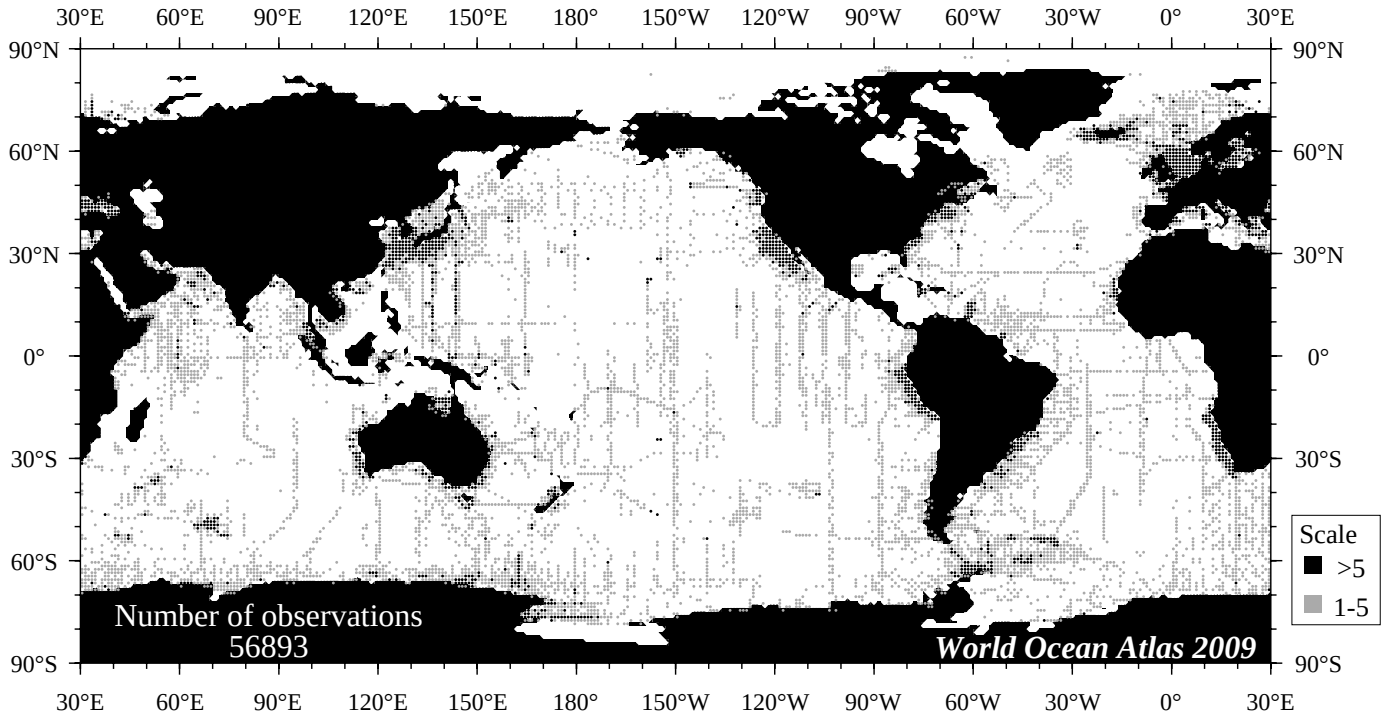

Fig H1 Winter (Jan.-Mar.) silicate observations at the surface.

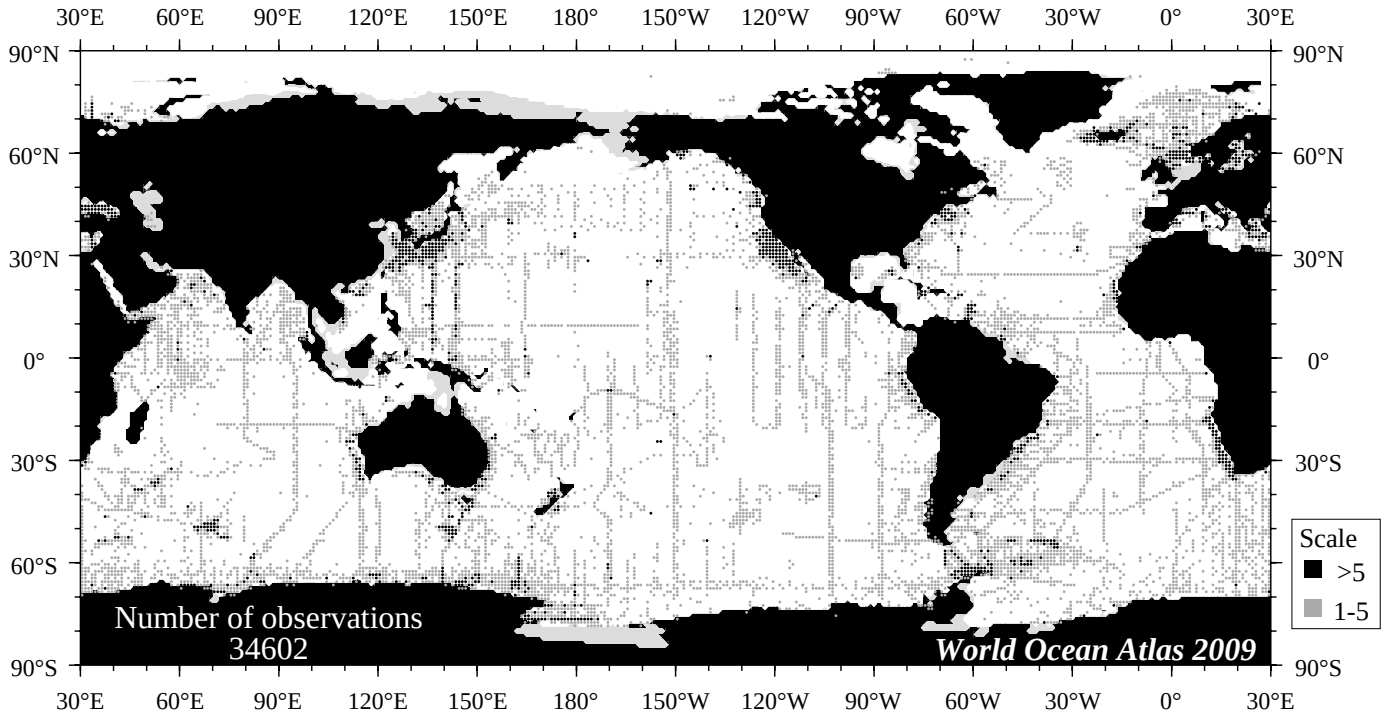

Fig H2 Winter (Jan.-Mar.) silicate observations at 75 m. depth.

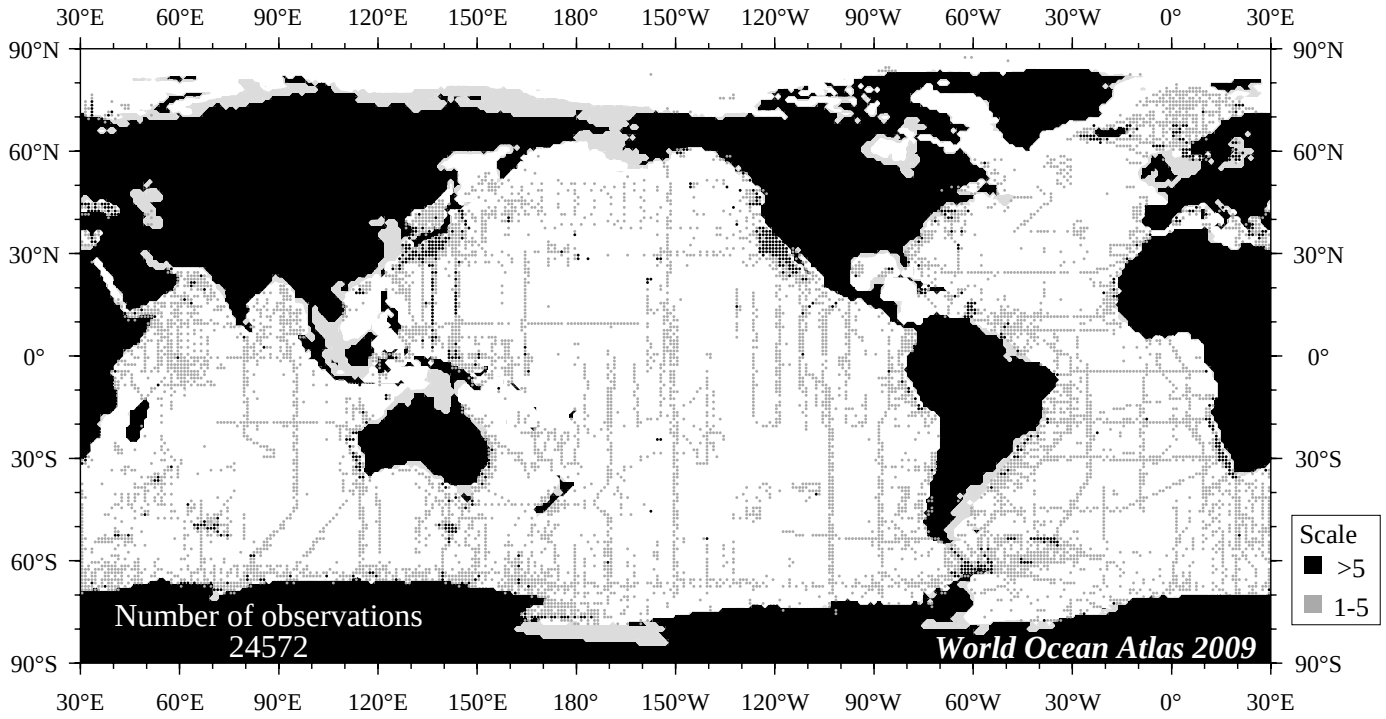

Fig H3 Winter (Jan.-Mar.) silicate observations at 150 m. depth.

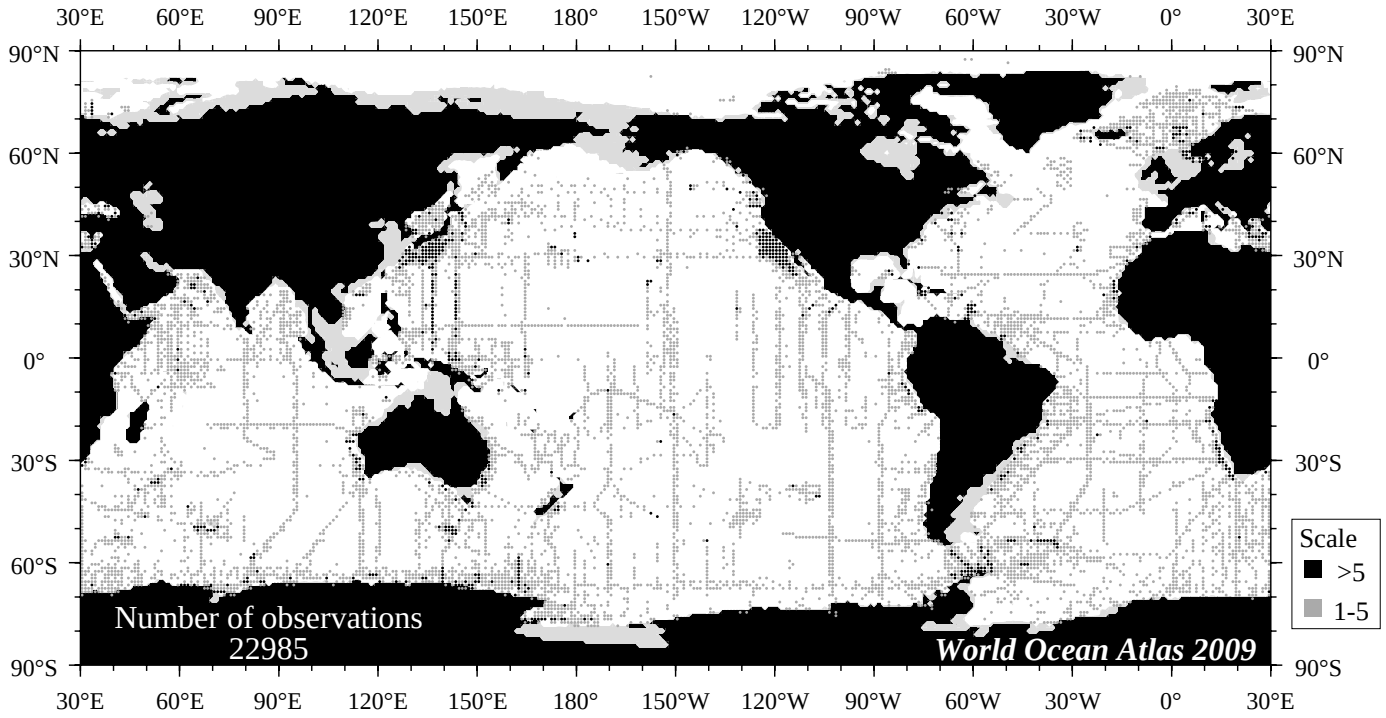

Fig H4 Winter (Jan.-Mar.) silicate observations at 250 m. depth.

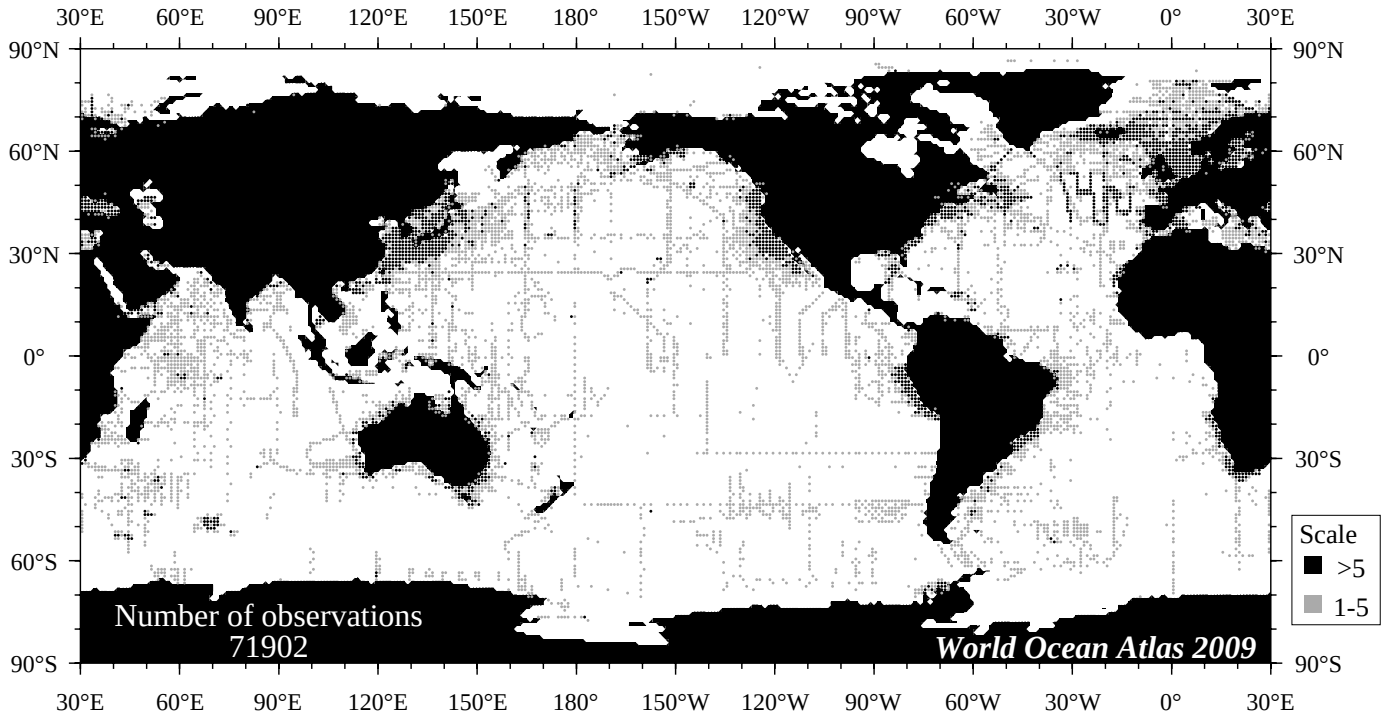

Fig H5 Spring (Apr.-Jun.) silicate observations at the surface.

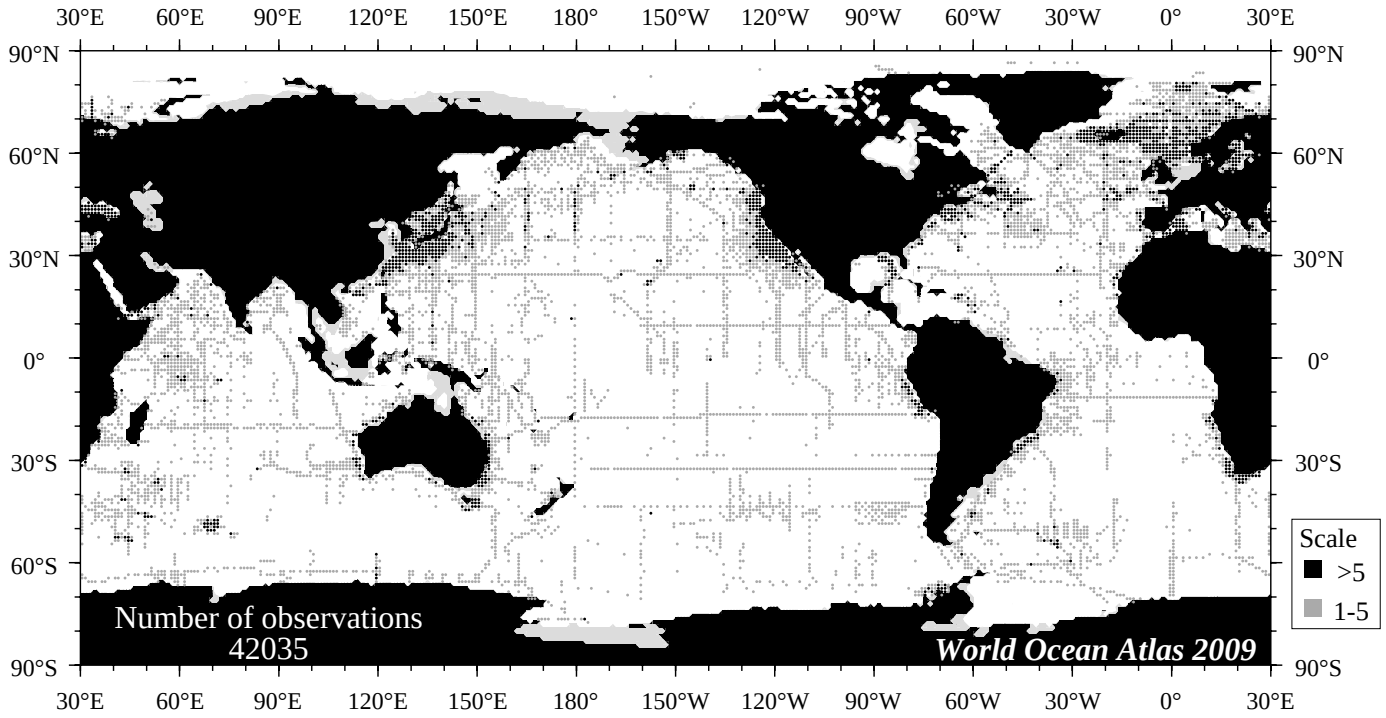

Fig H6 Spring (Apr.-Jun.) silicate observations at 75 m. depth.

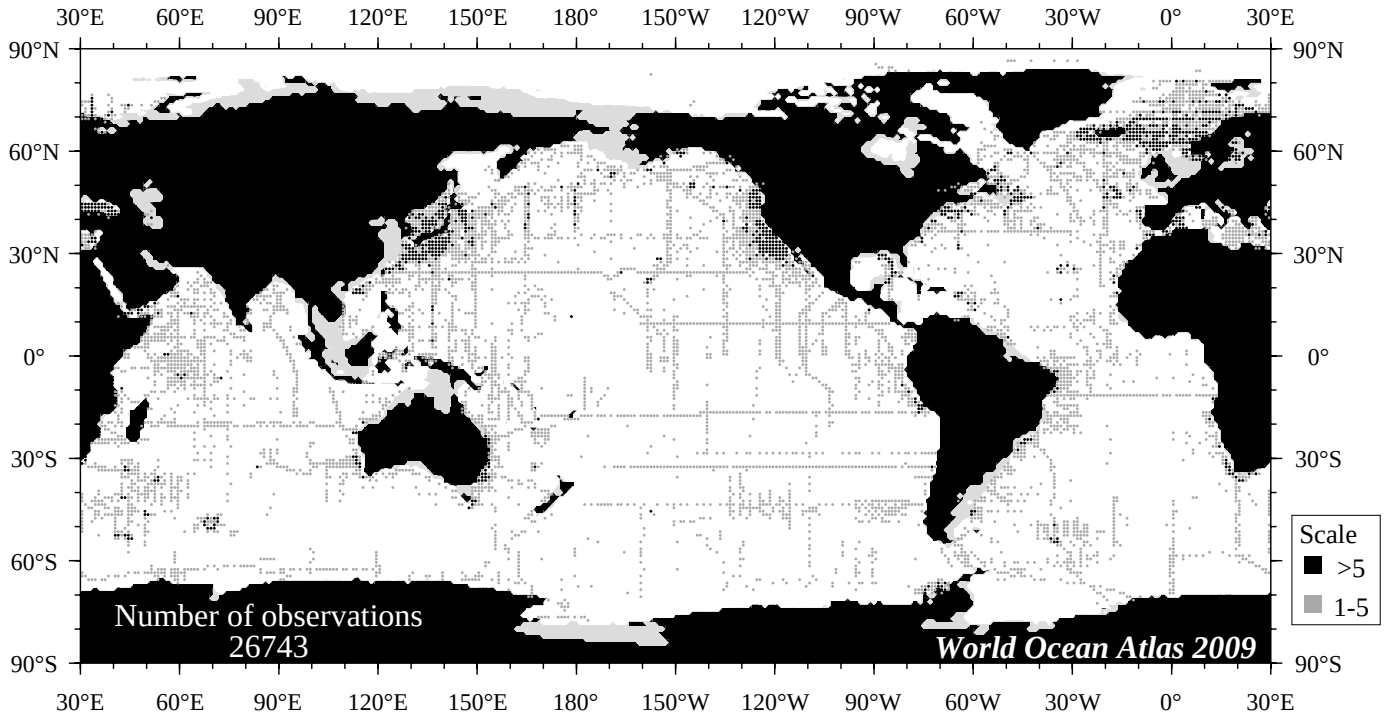

Fig H7 Spring (Apr.-Jun.) silicate observations at 150 m. depth.

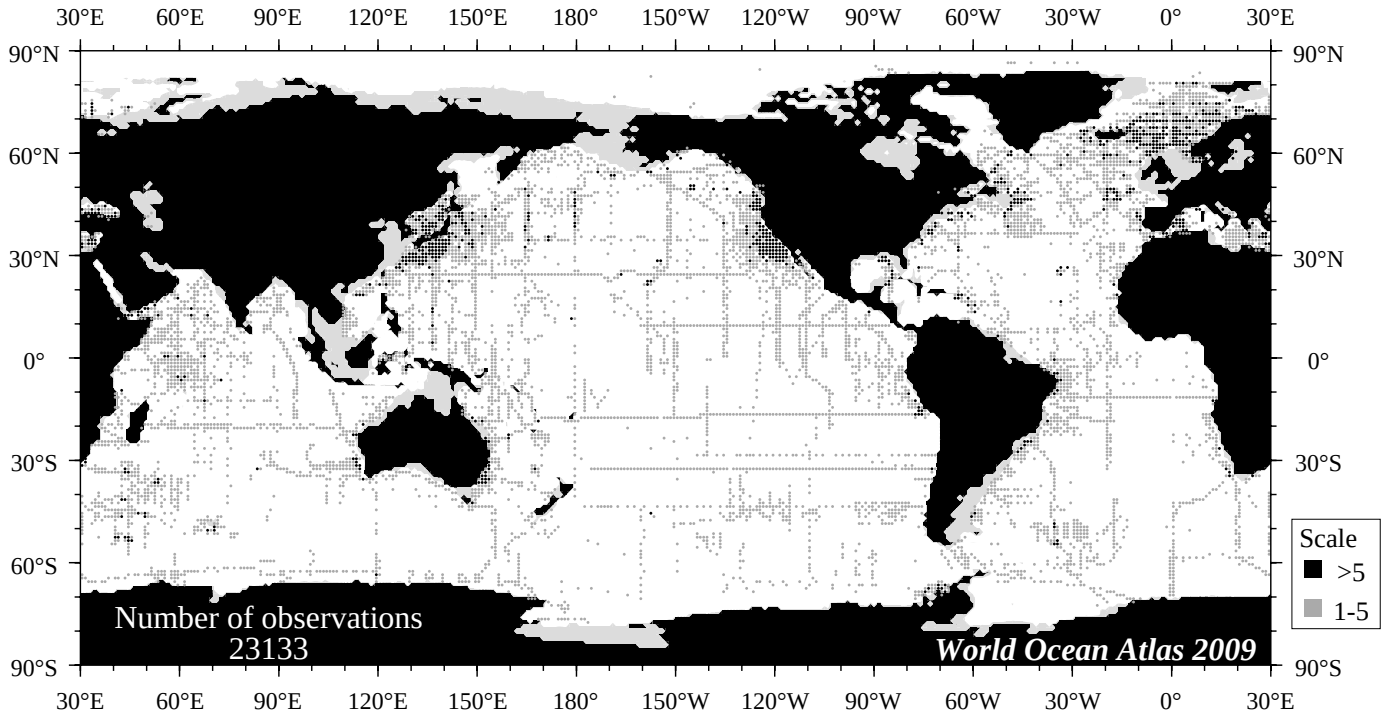

Fig H8 Spring (Apr.-Jun.) silicate observations at 250 m. depth.

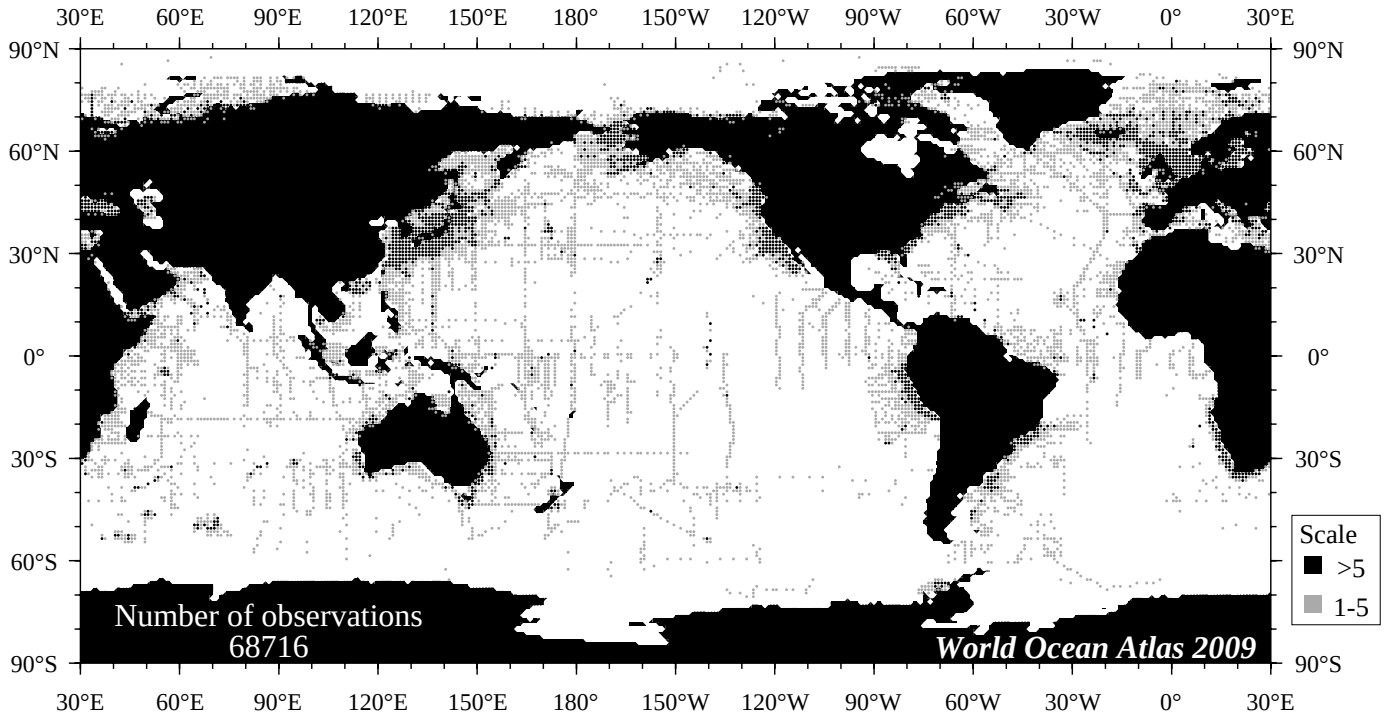

Fig H9 Summer (Jul.-Sep.) silicate observations at the surface.

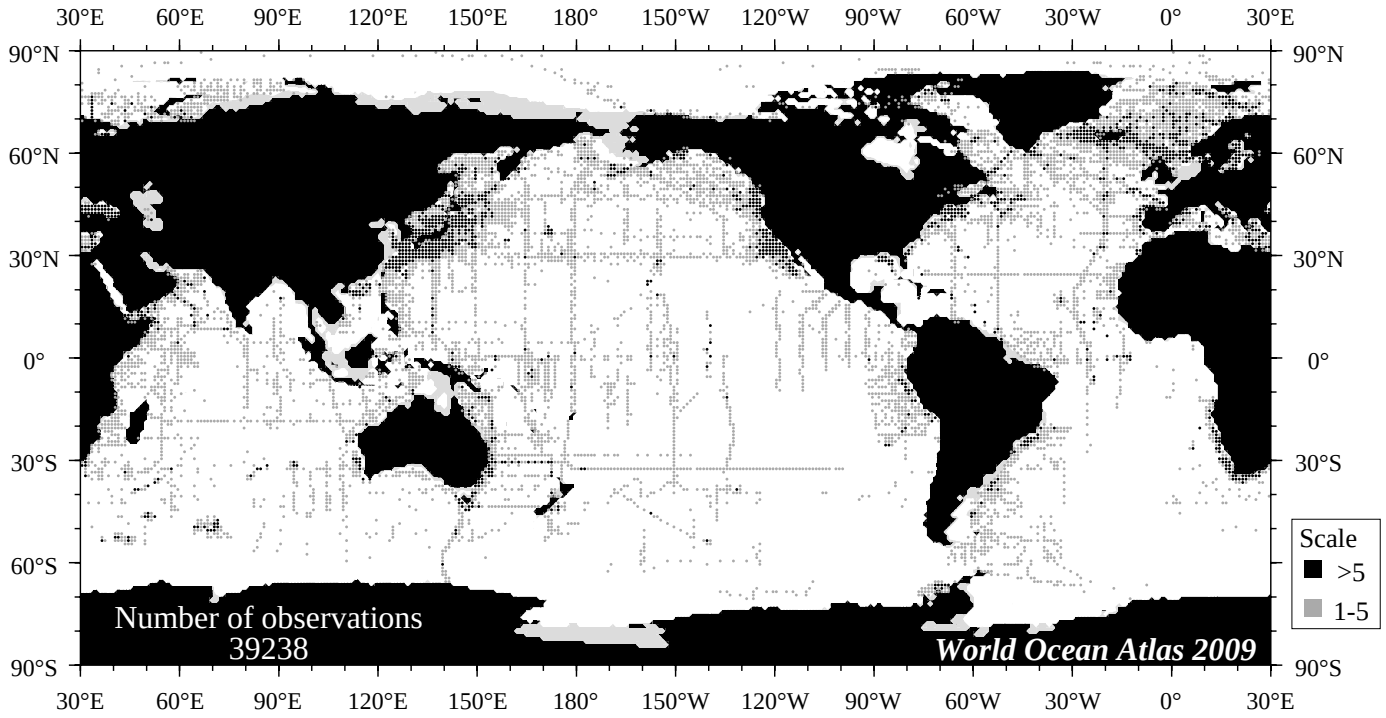

Fig H10 Summer (Jul.-Sep.) silicate observations at 75 m. depth.

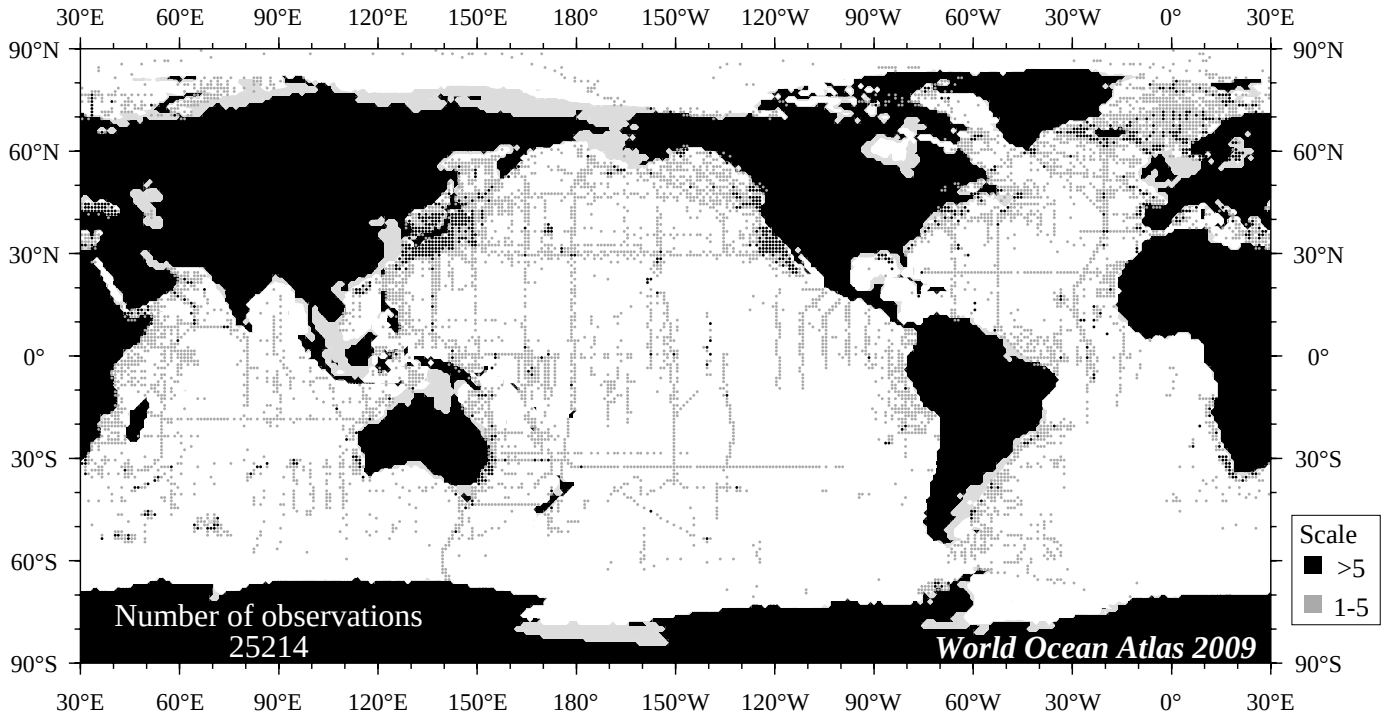

Fig H11 Summer (Jul.-Sep.) silicate observations at 150 m. depth.

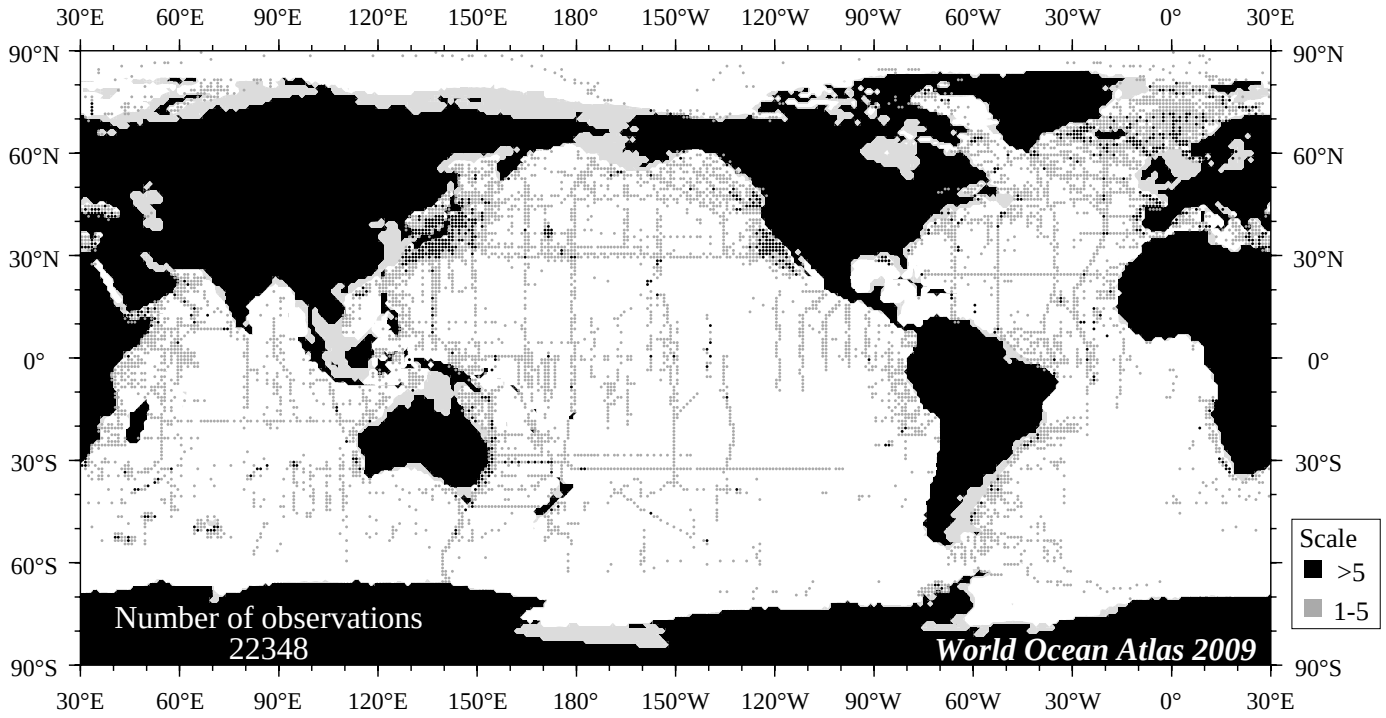

Fig H12 Summer (Jul.-Sep.) silicate observations at 250 m. depth.

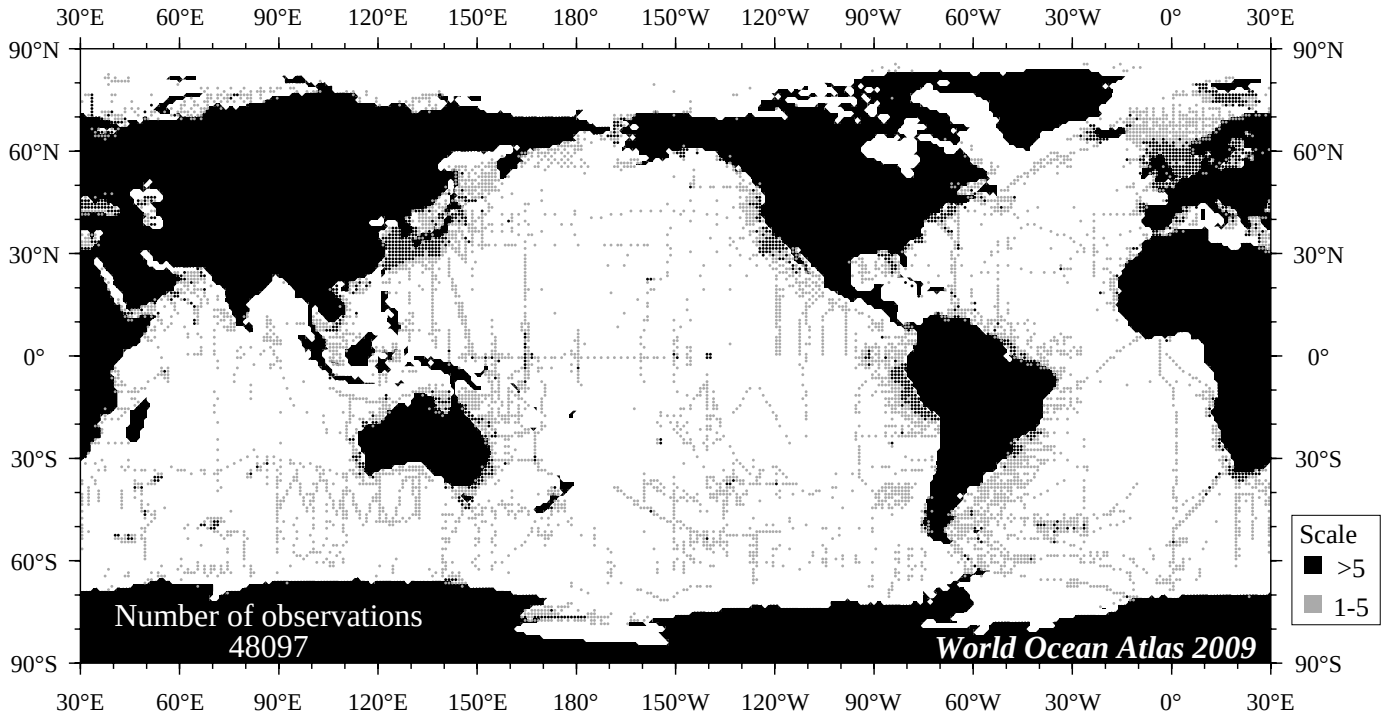

Fig H13 Fall (Oct.-Dec.) silicate observations at the surface.

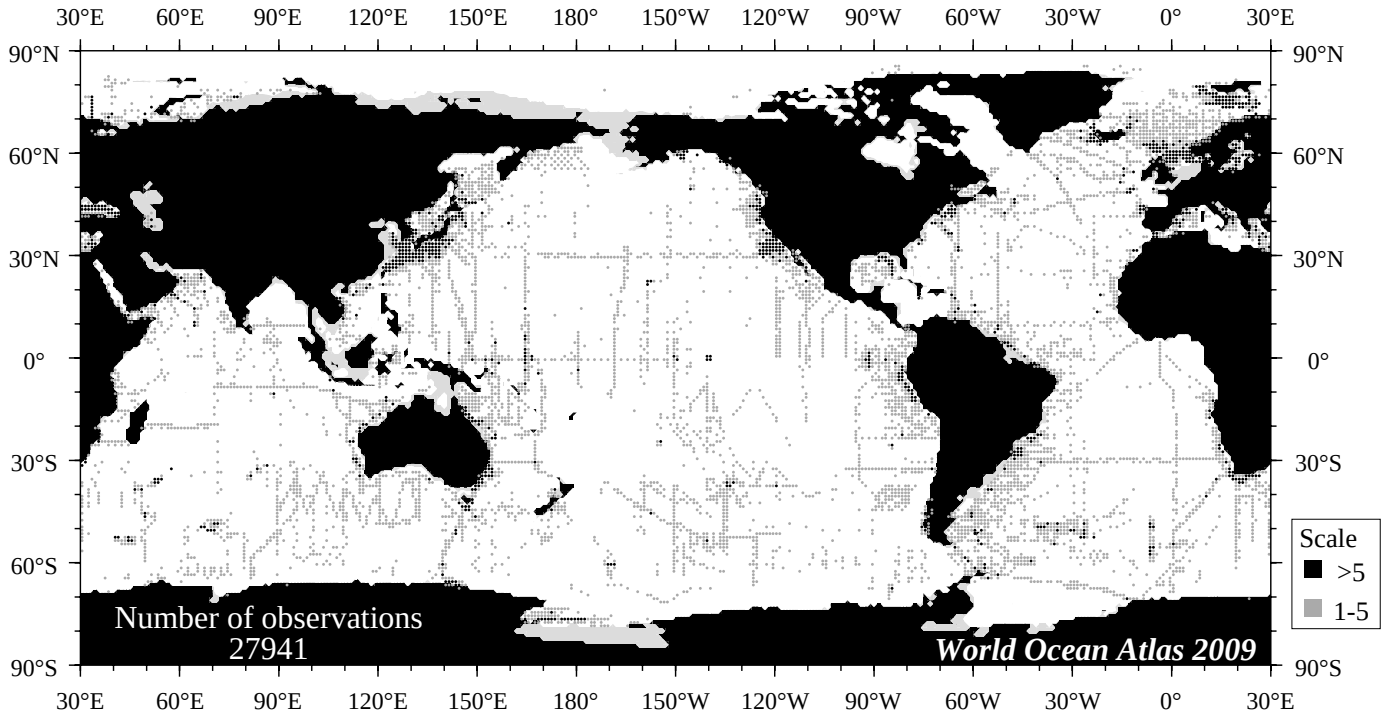

Fig H14 Fall (Oct.-Dec.) silicate observations at 75 m. depth.

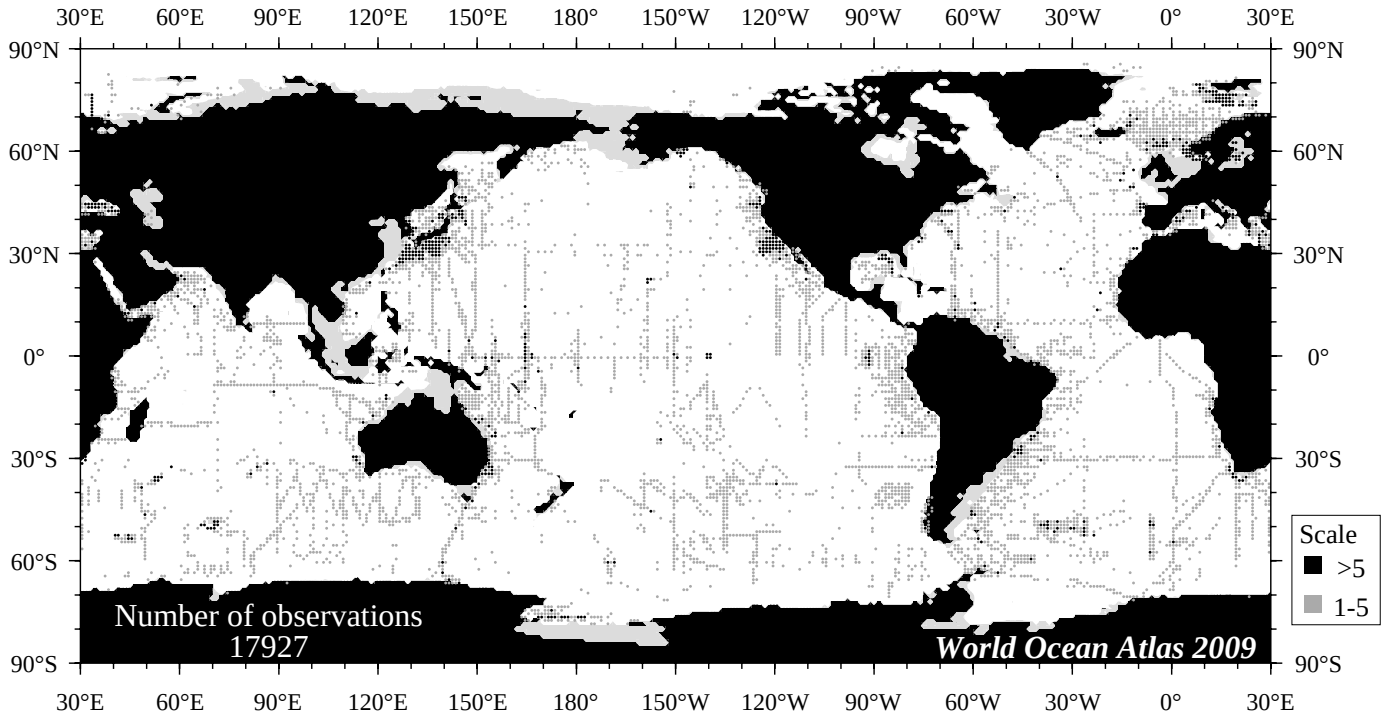

Fig H15 Fall (Oct.-Dec.) silicate observations at 150 m. depth.

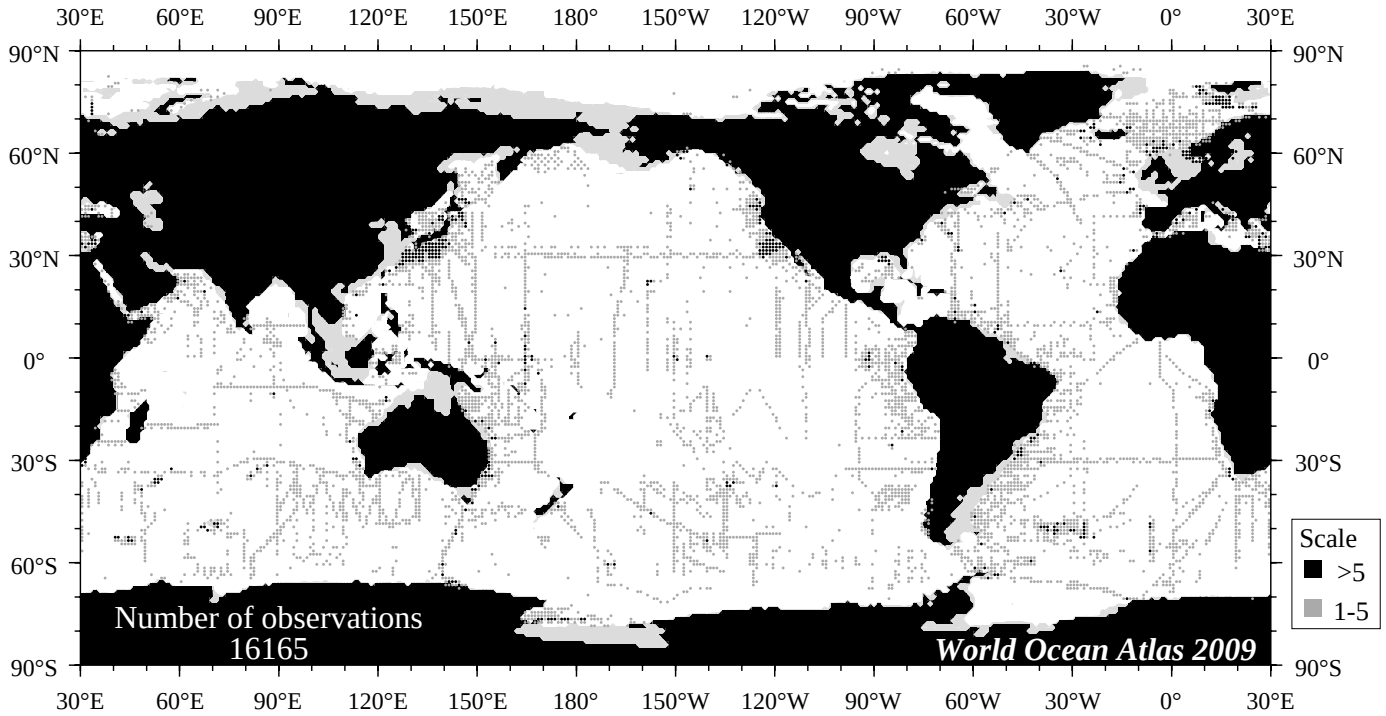

Fig H16 Fall (Oct.-Dec.) silicate observations at 250 m. depth.

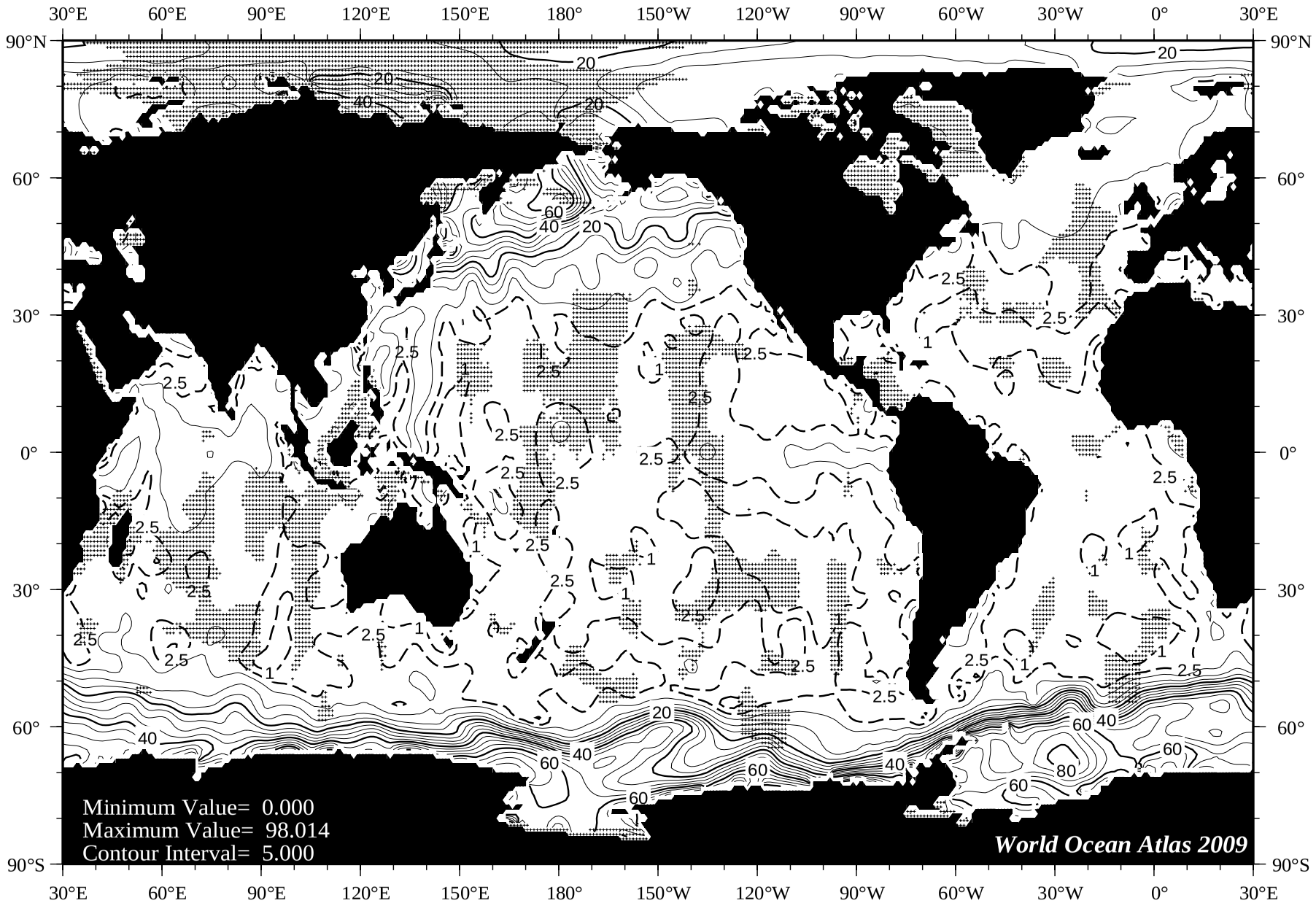

Fig H17 Winter (Jan.-Mar.) silicate [umol/l] at the surface.

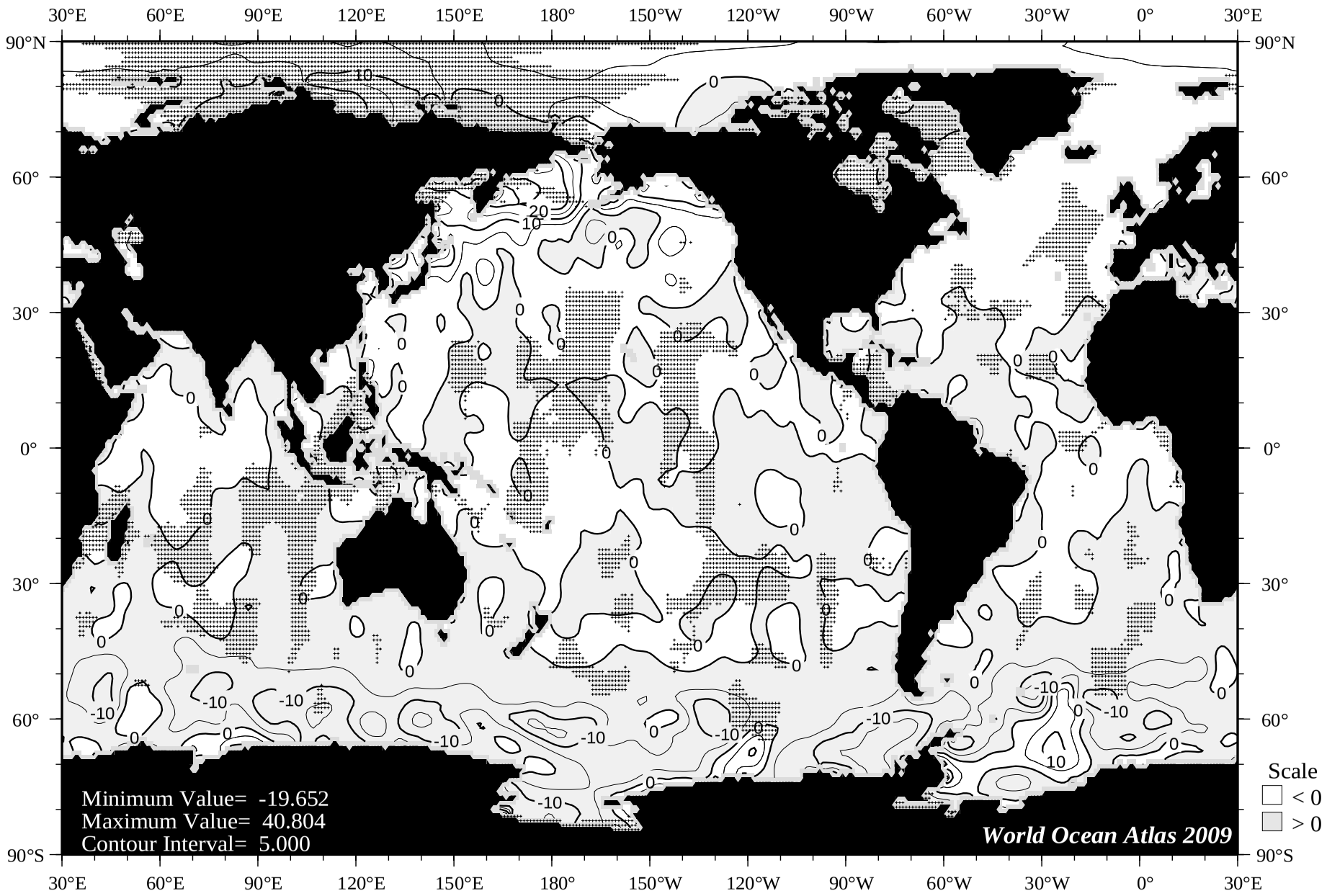

Fig H18 Winter (Jan.-Mar.) minus annual silicate [umol/l] at the surface.

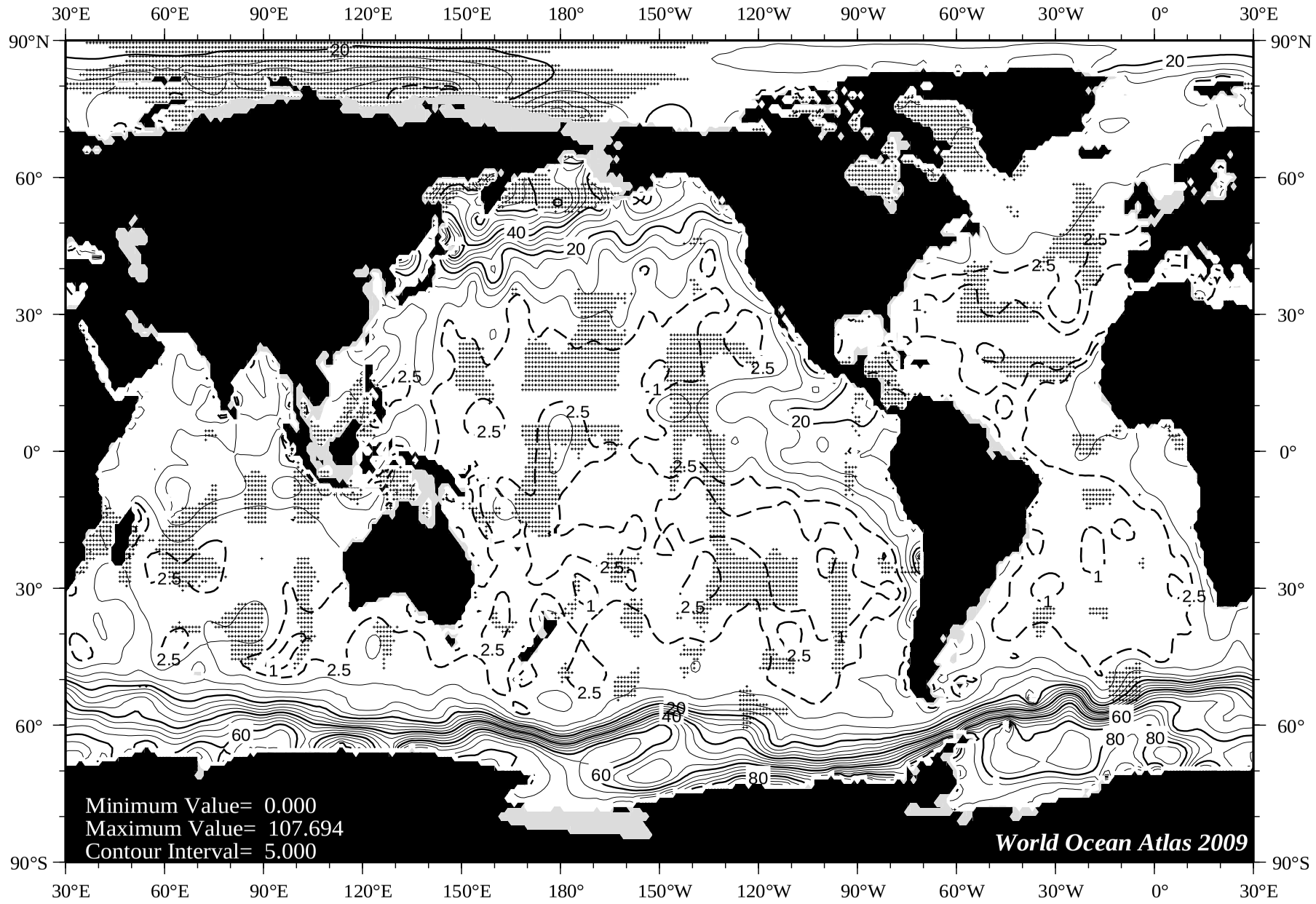

Fig H19 Winter (Jan.-Mar.) silicate [umol/l] at 75 m. depth.

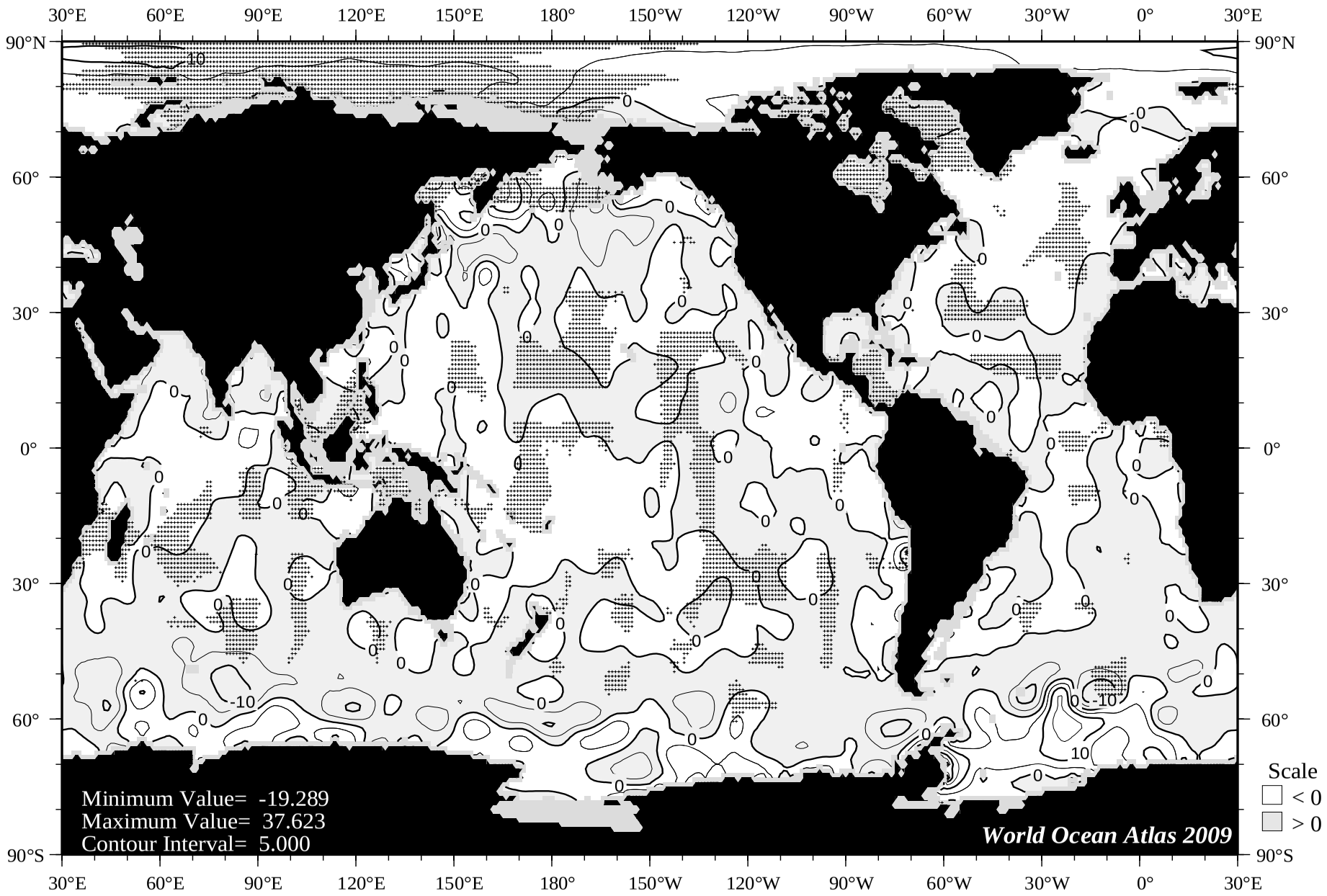

Fig H20 Winter (Jan.-Mar.) minus annual silicate [umol/l] at 75 m. depth.

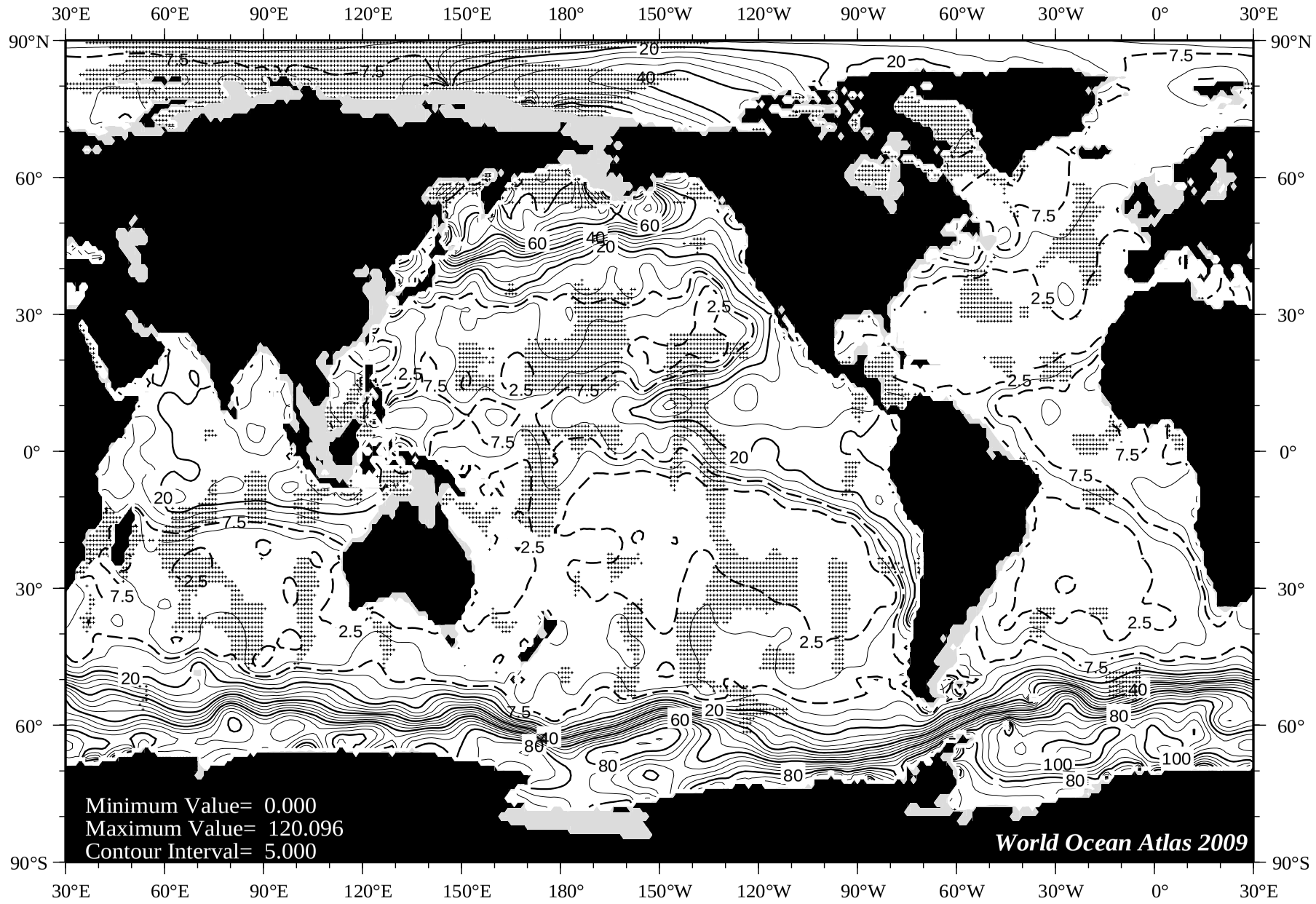

Fig H21 Winter (Jan.-Mar.) silicate [umol/l] at 150 m. depth.

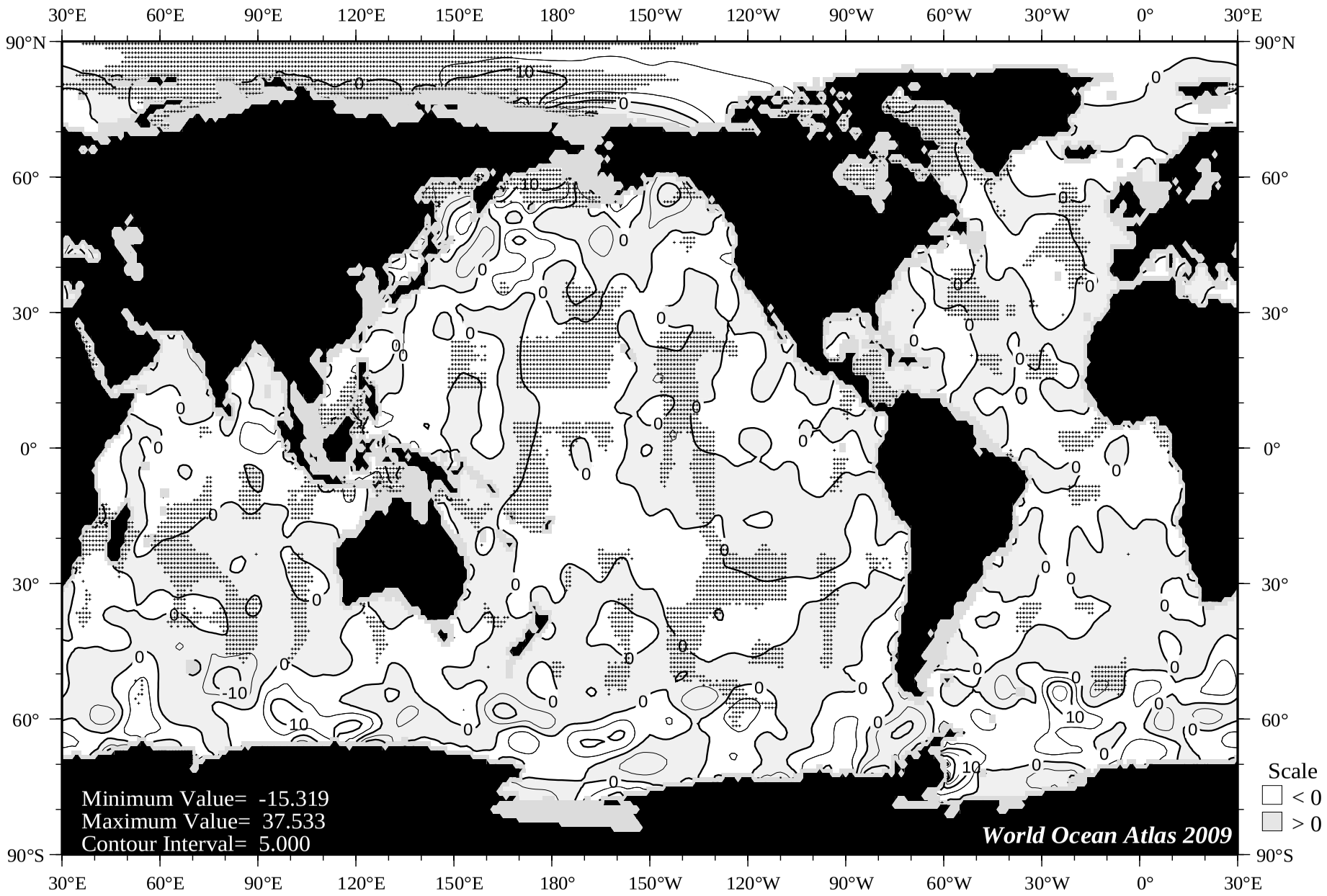

Fig H22 Winter (Jan.-Mar.) minus annual silicate [umol/l] at 150 m. depth.

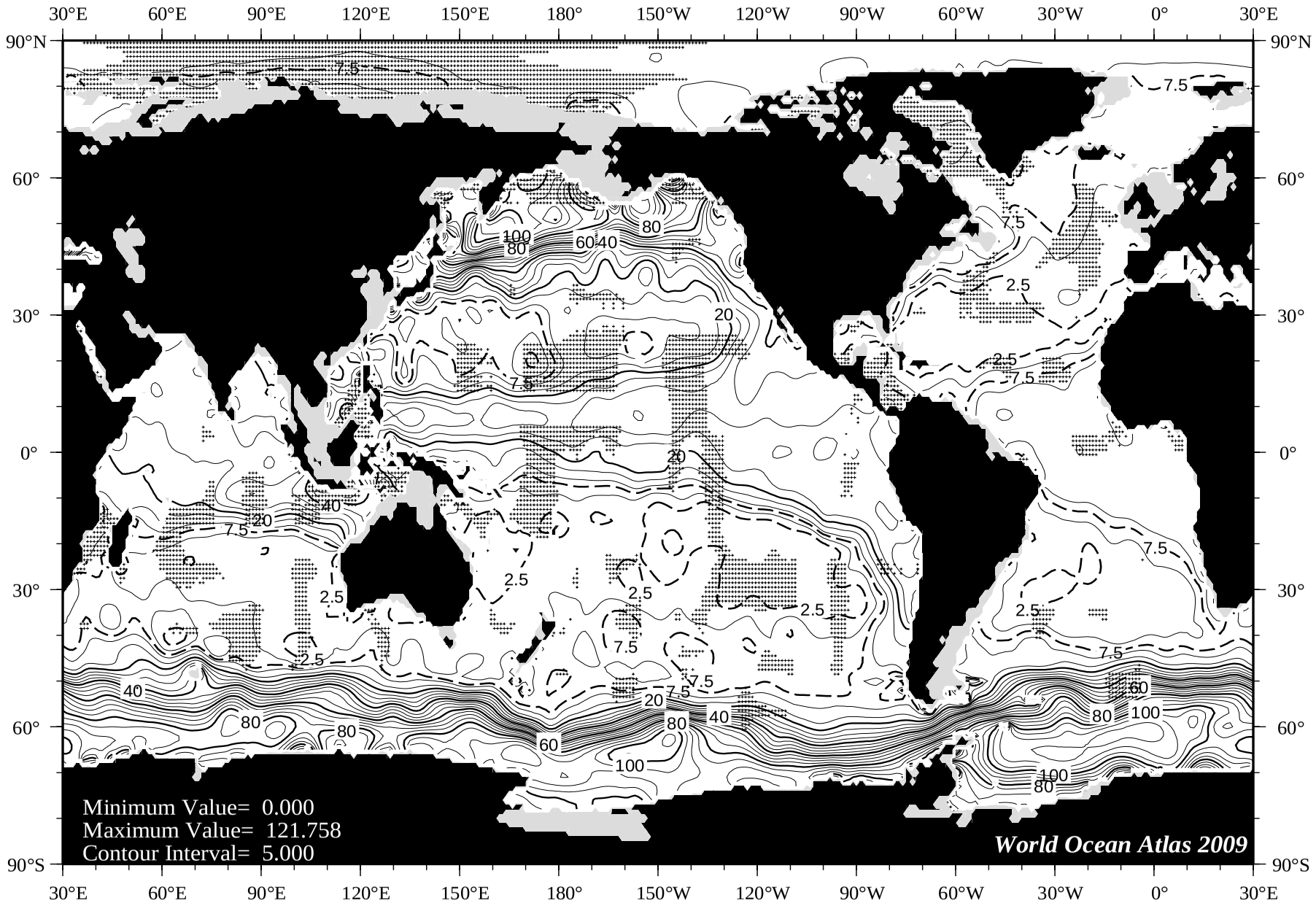

Fig H23 Winter (Jan.-Mar.) silicate [umol/l] at 250 m. depth.

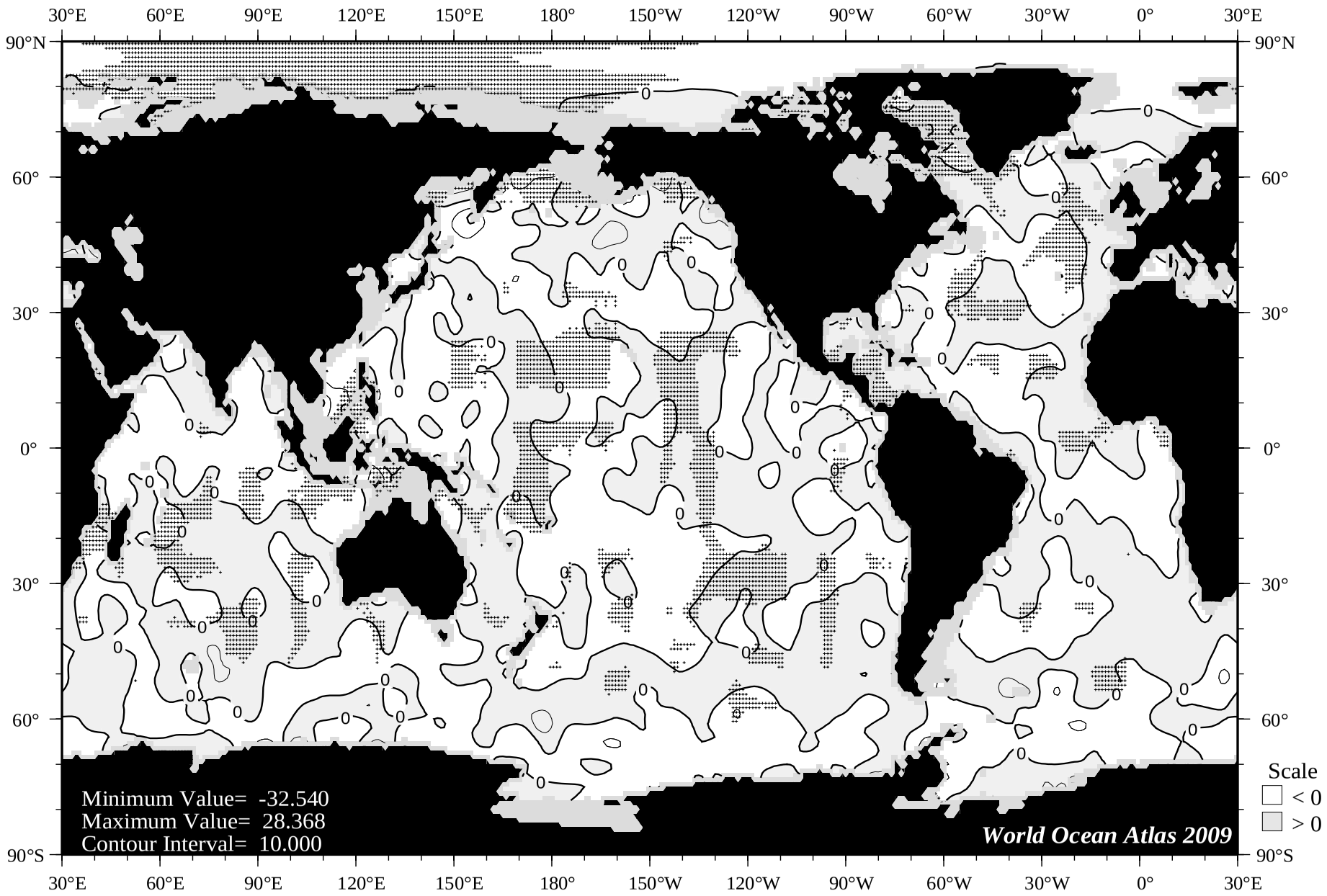

Fig H24 Winter (Jan.-Mar.) minus annual silicate [umol/l] at 250 m. depth.

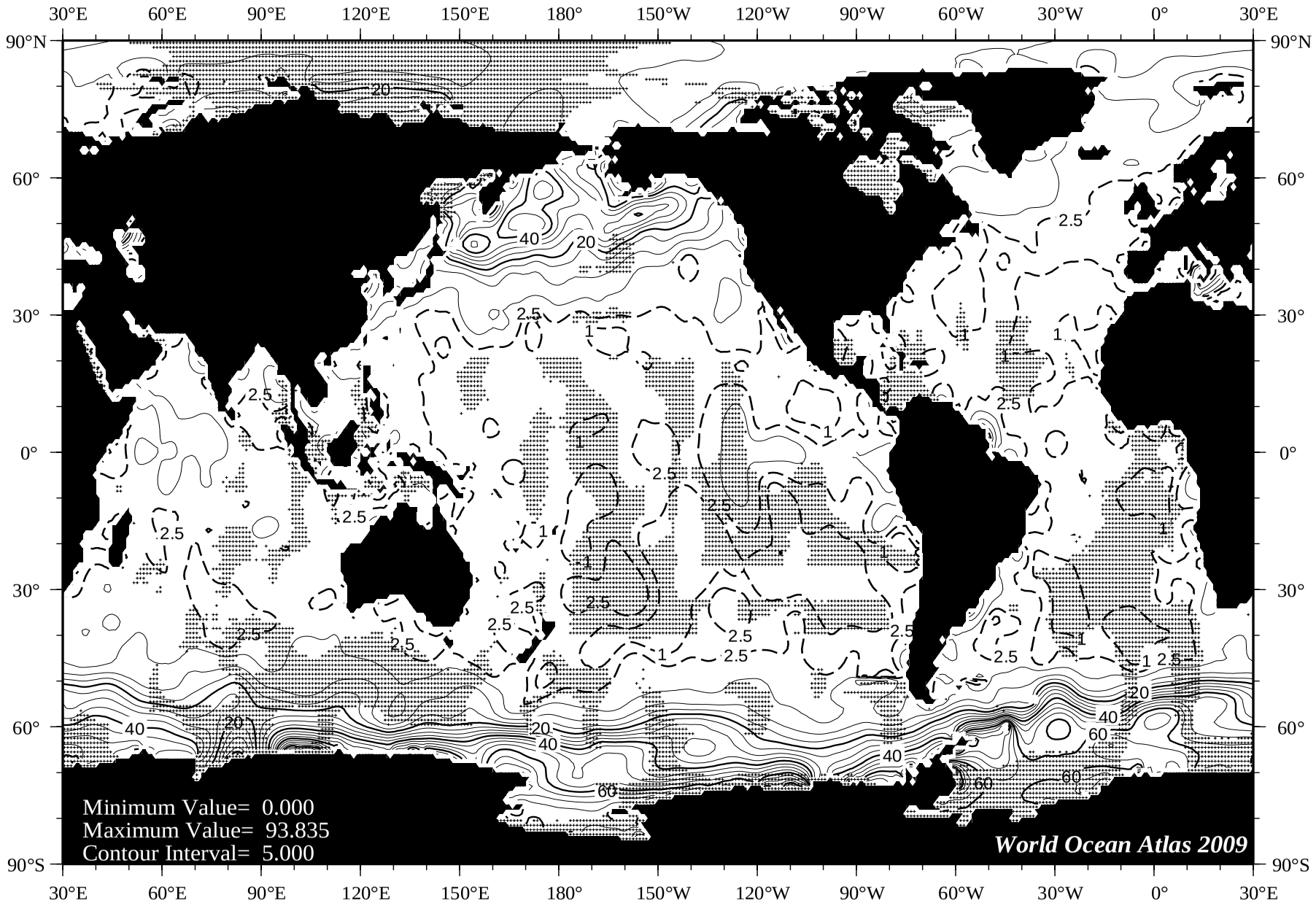

Fig H25 Spring (Apr.-Jun.) silicate [umol/l] at the surface.

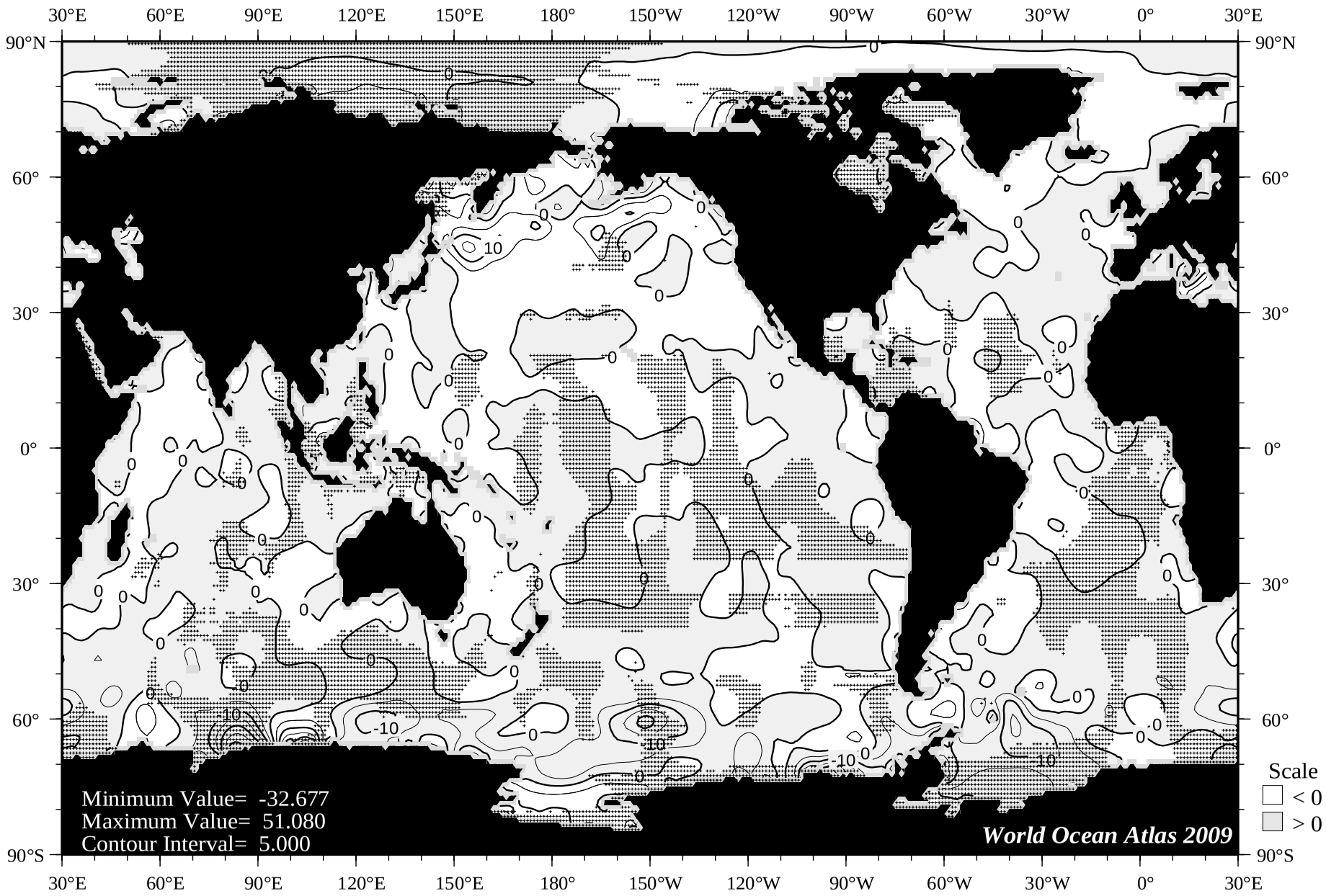

Fig H26 Spring (Apr.-Jun.) minus annual silicate [umol/l] at the surface.

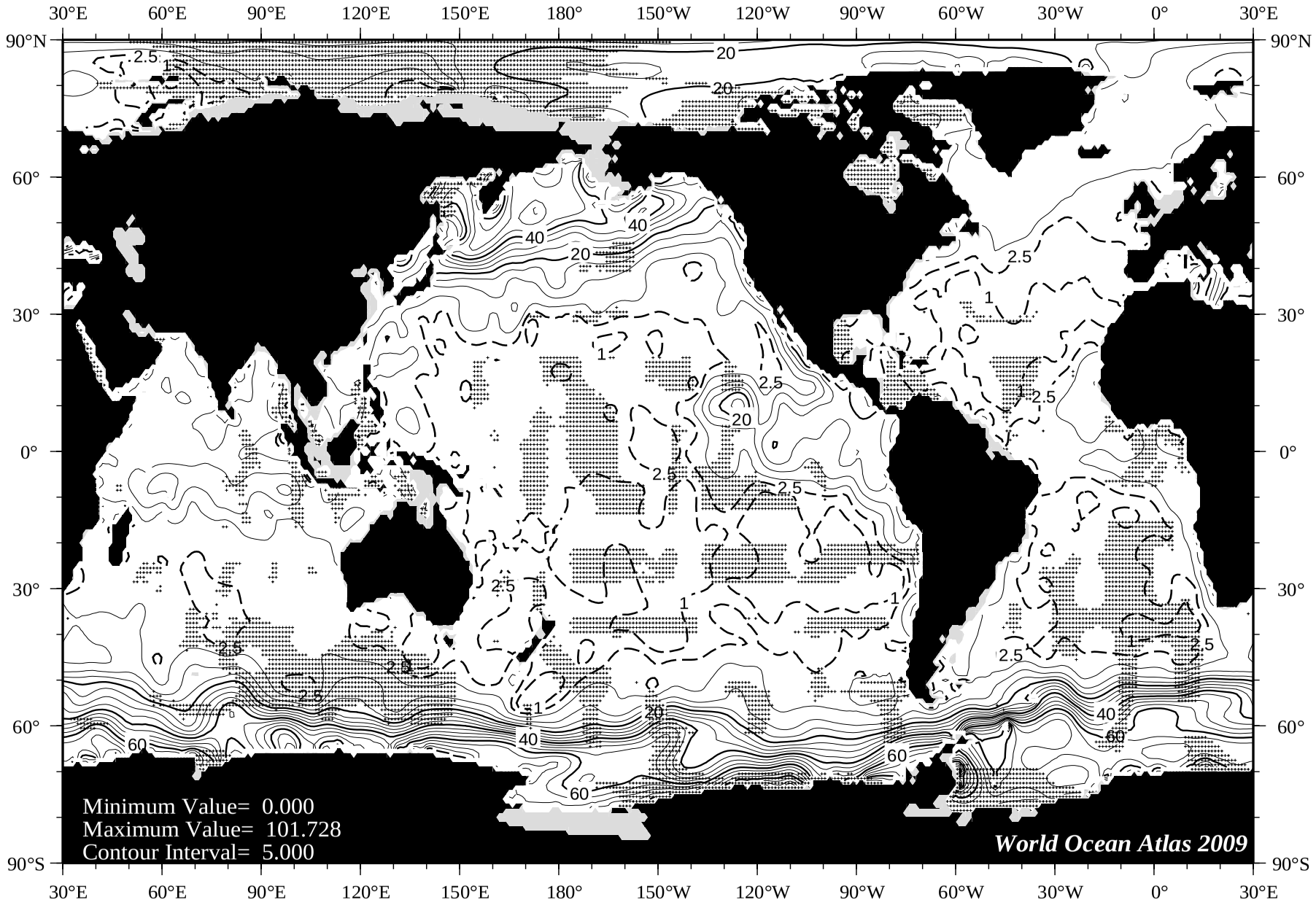

Fig H27 Spring (Apr.-Jun.) silicate [umol/l] at 75 m. depth.

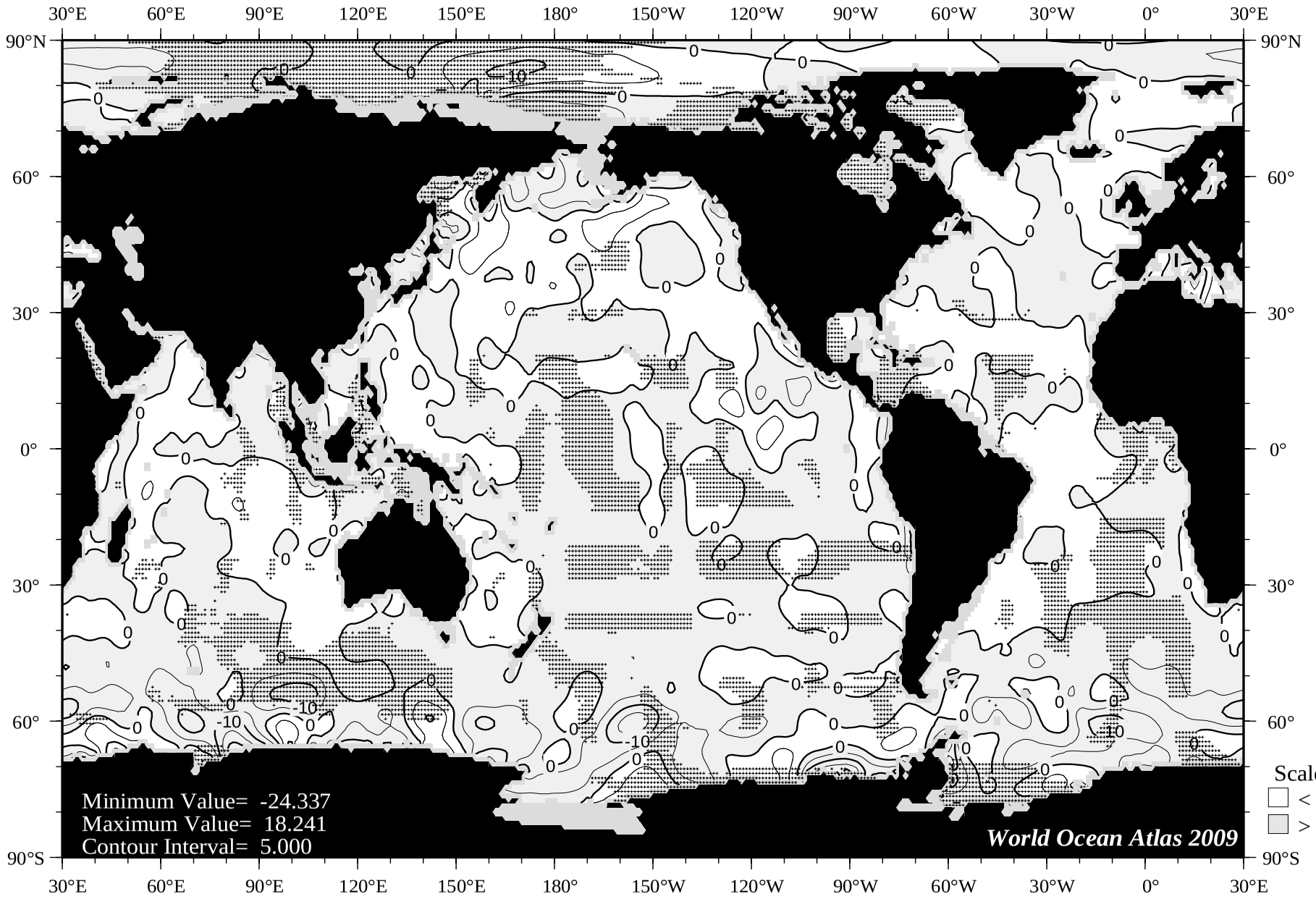

Fig H28 Spring (Apr.-Jun.) minus annual silicate [umol/l] at 75 m. depth.

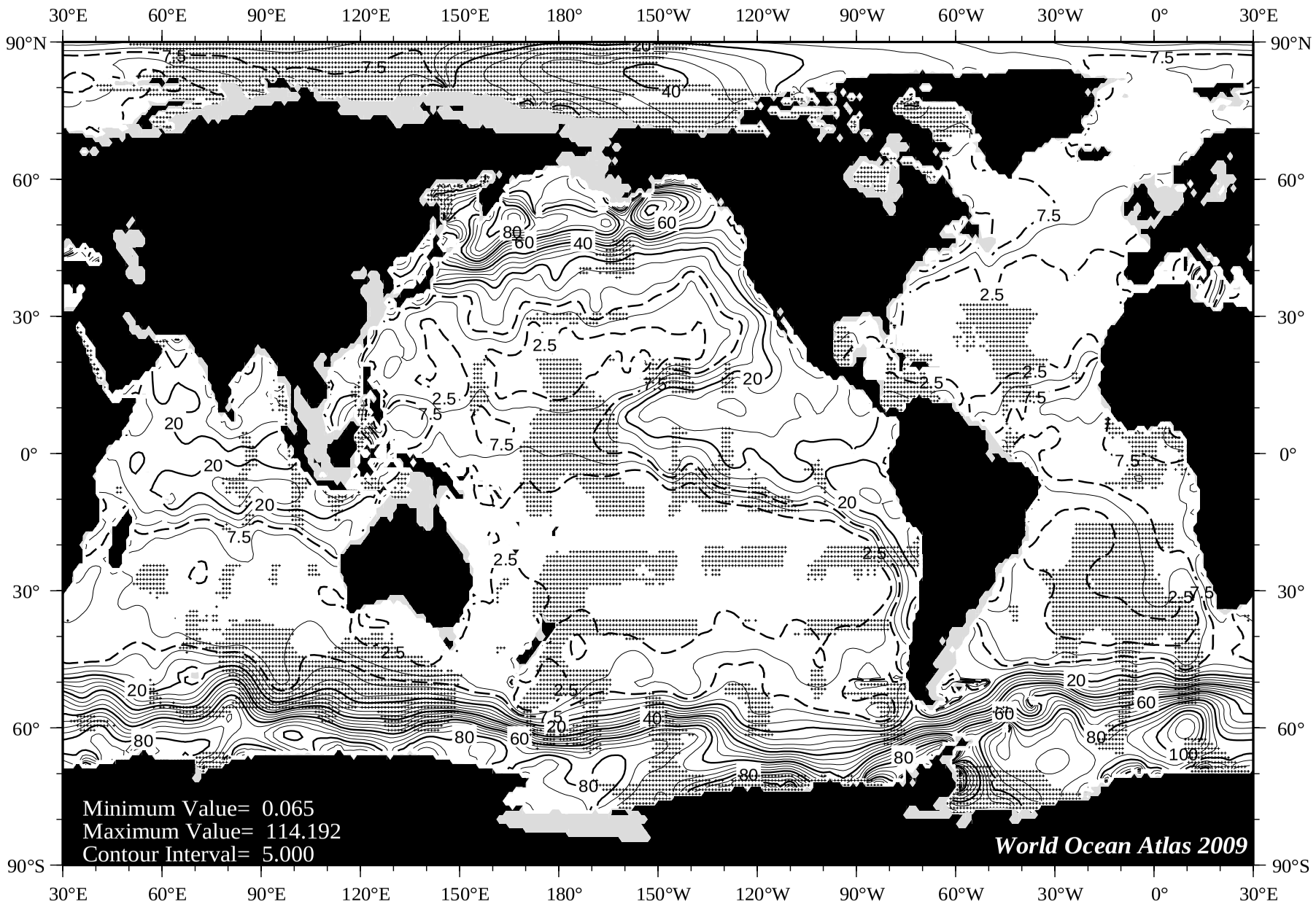

Fig H29 Spring (Apr.-Jun.) silicate [umol/l] at 150 m. depth.

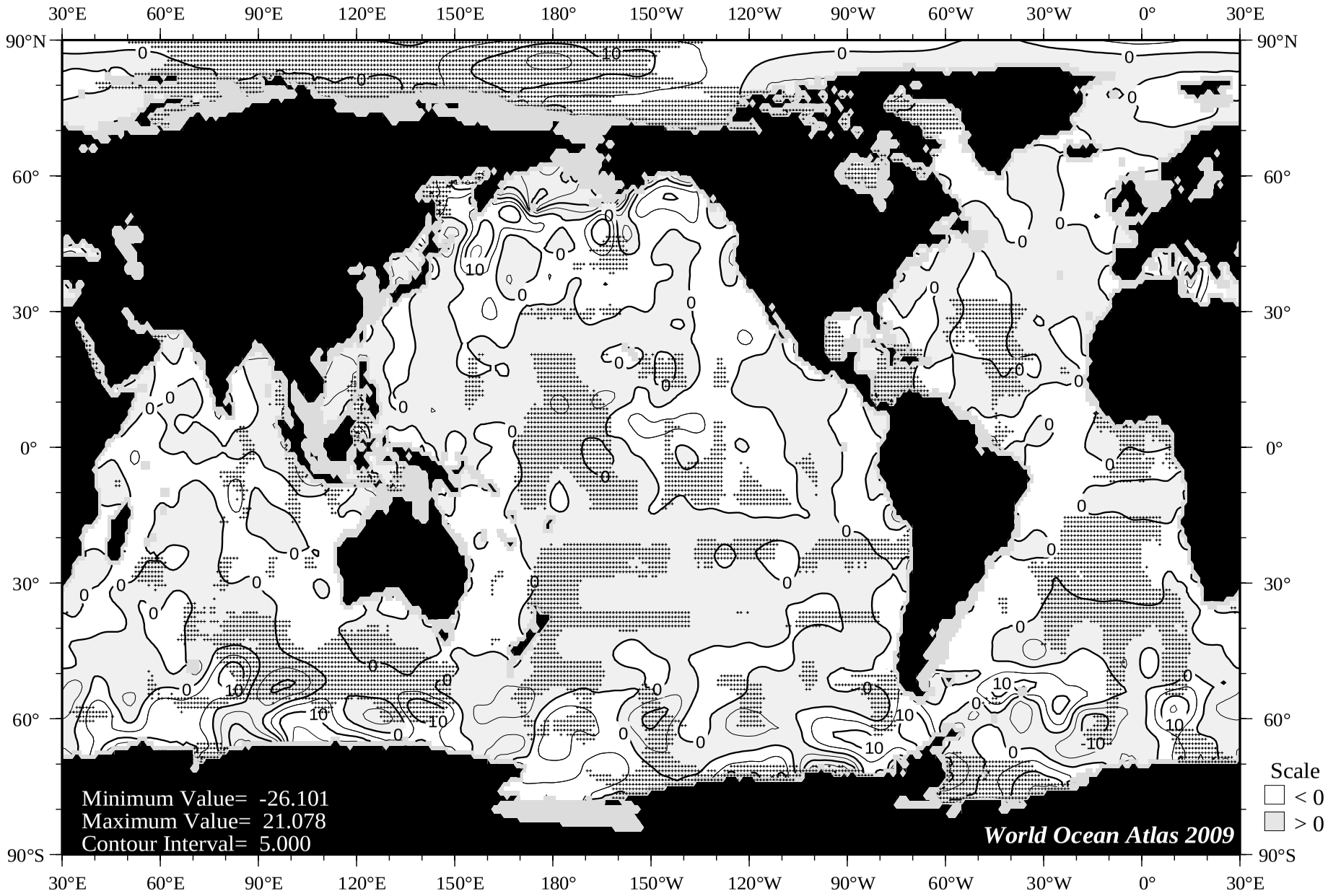

Fig H30 Spring (Apr.-Jun.) minus annual silicate [umol/l] at 150 m. depth.

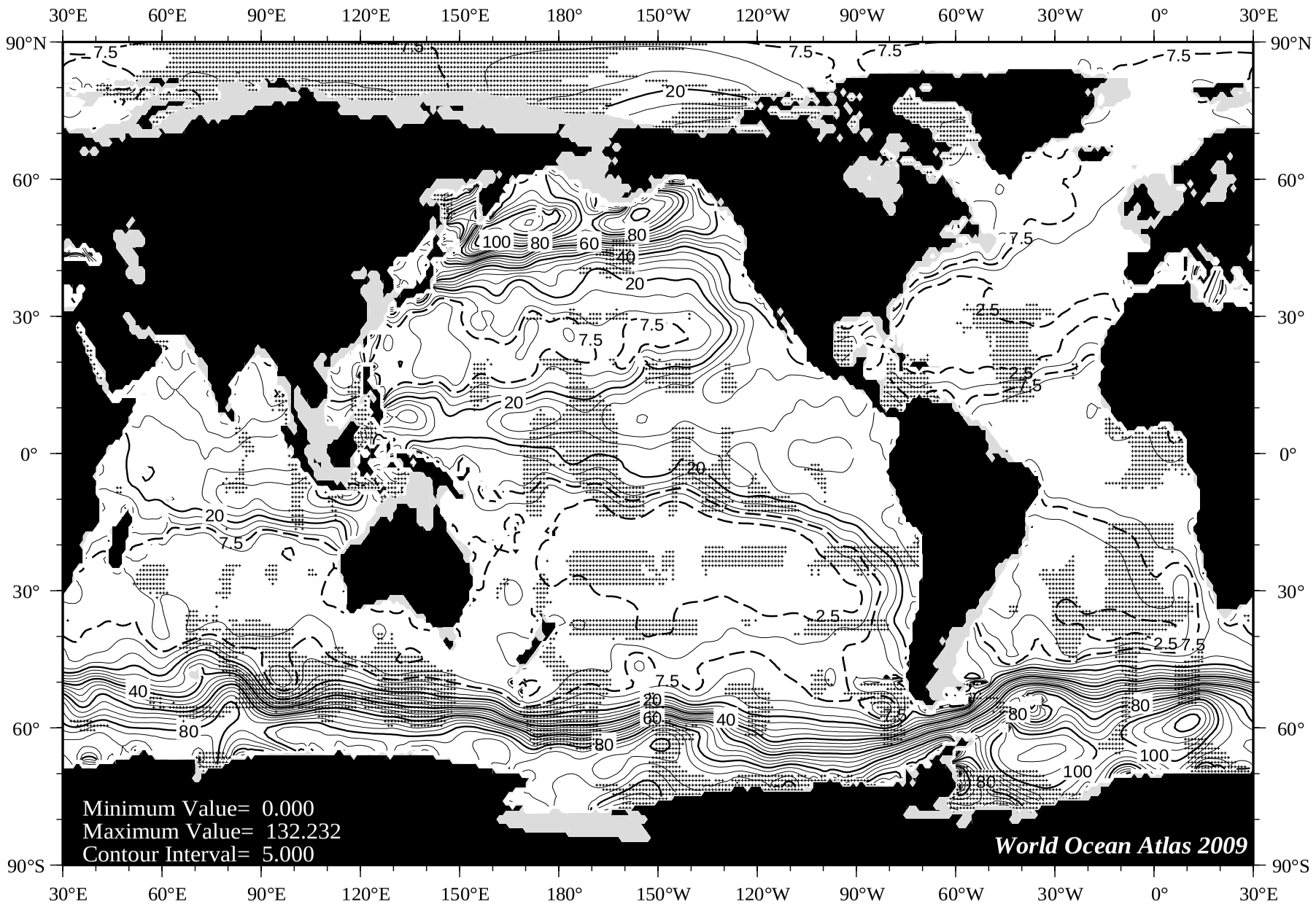

Fig H31 Spring (Apr.-Jun.) silicate [umol/l] at 250 m. depth.

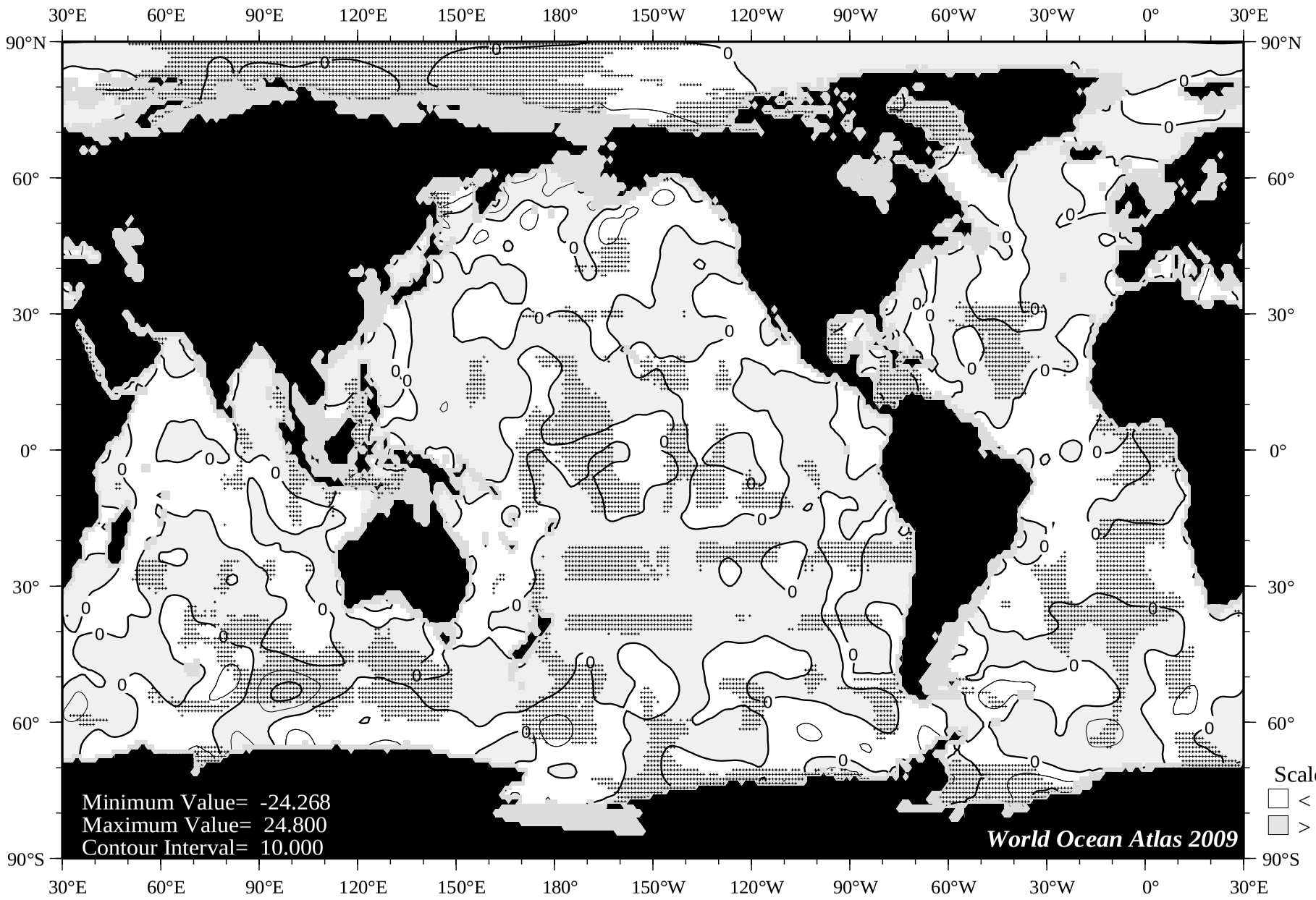

Fig H32 Spring (Apr.-Jun.) minus annual silicate [umol/l] at 250 m. depth.

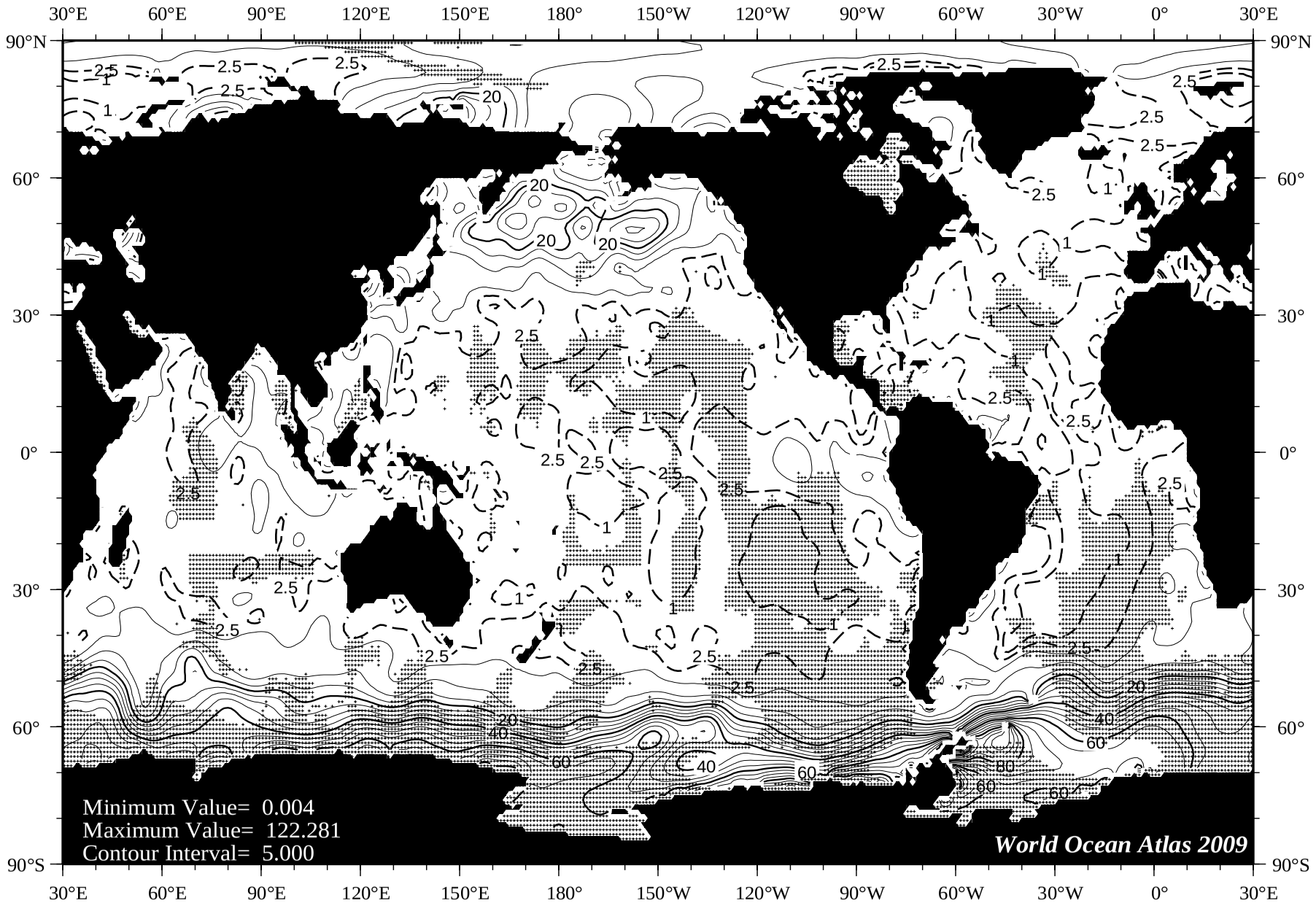

Fig H33 Summer (Jul.-Sep.) silicate [umol/l] at the surface.

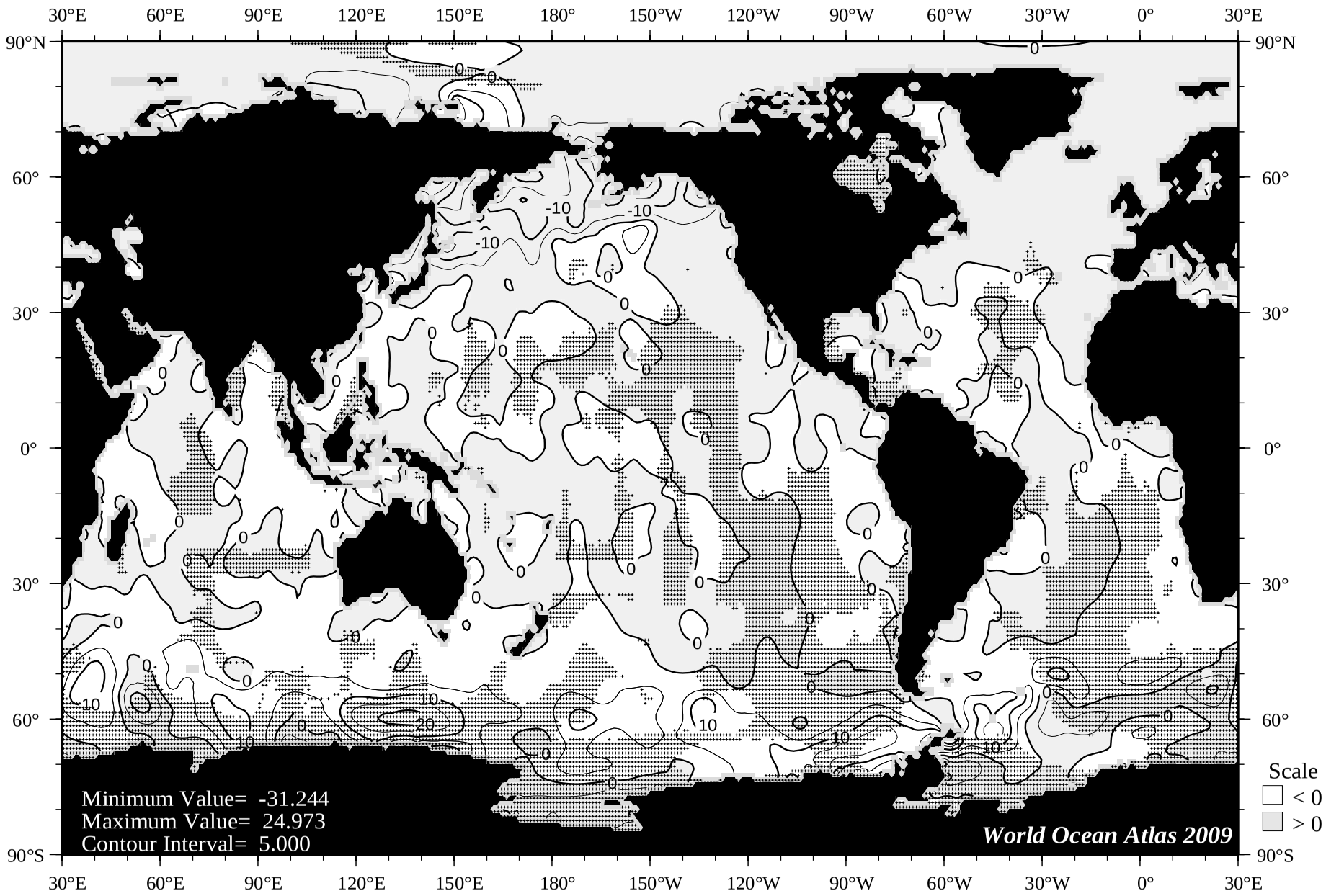

Fig H34 Summer (Jul.-Sep.) minus annual silicate [umol/l] at the surface.

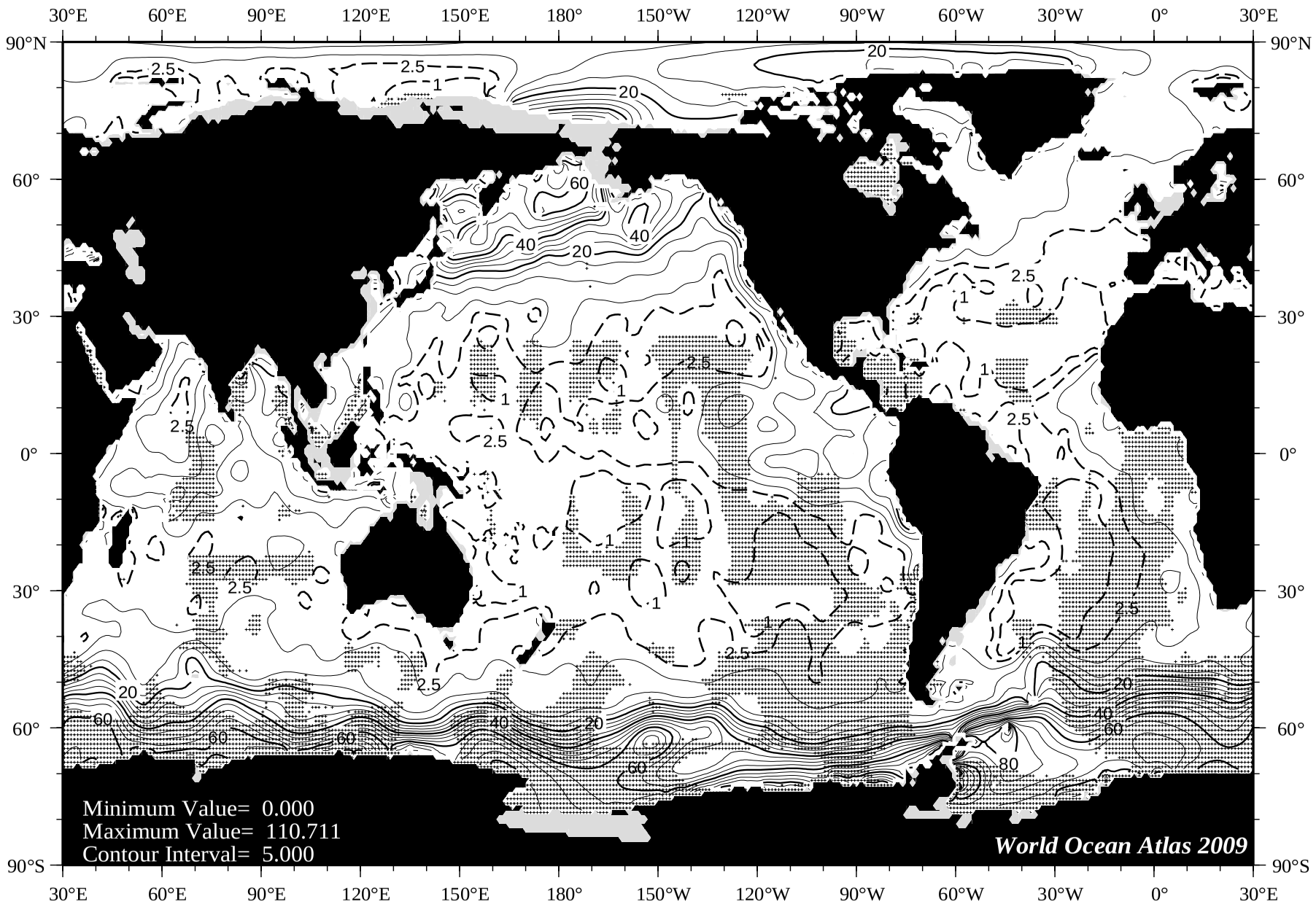

Fig H35 Summer (Jul.-Sep.) silicate [umol/l] at 75 m. depth.

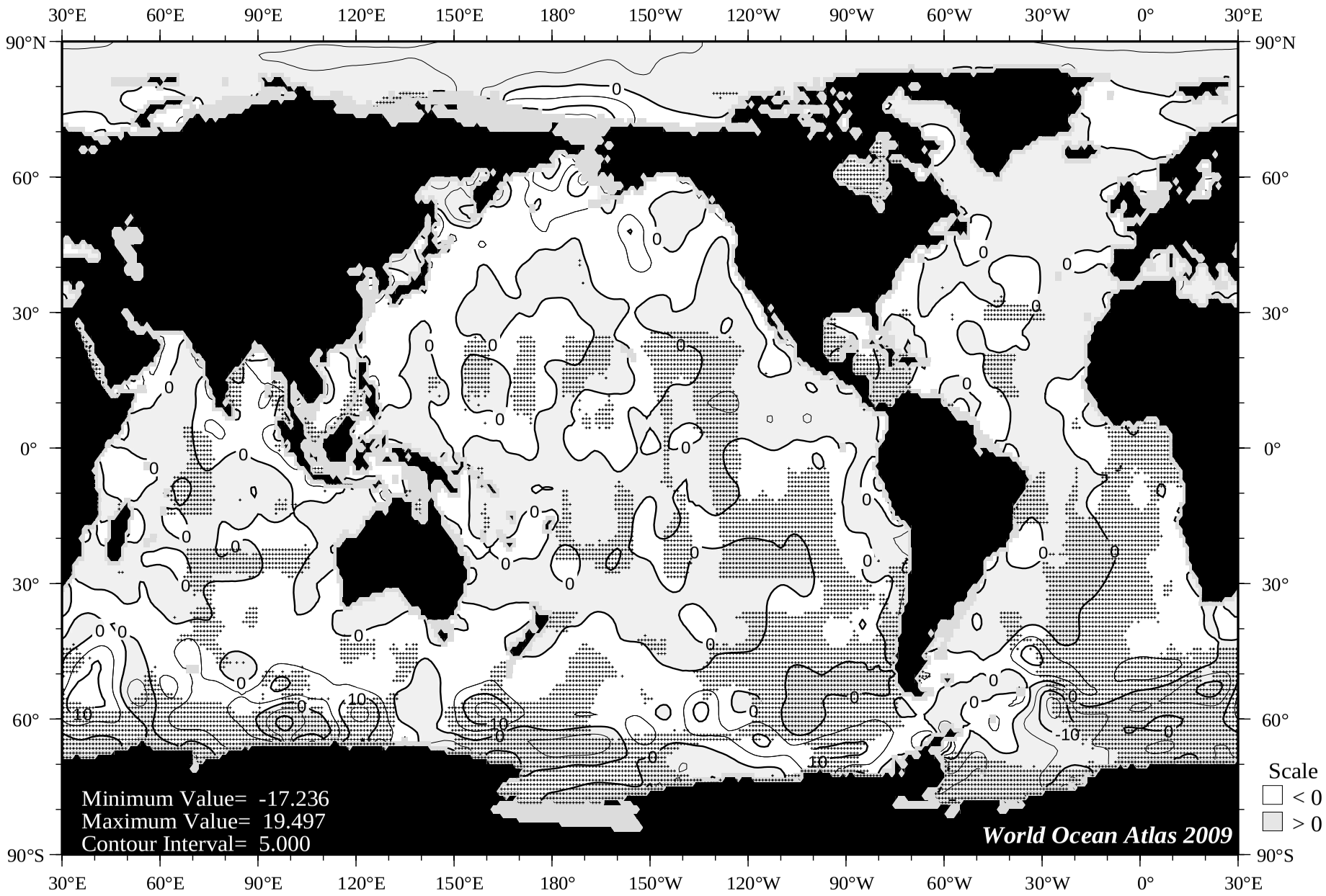

Fig H36 Summer (Jul.-Sep.) minus annual silicate [umol/l] at 75 m. depth.

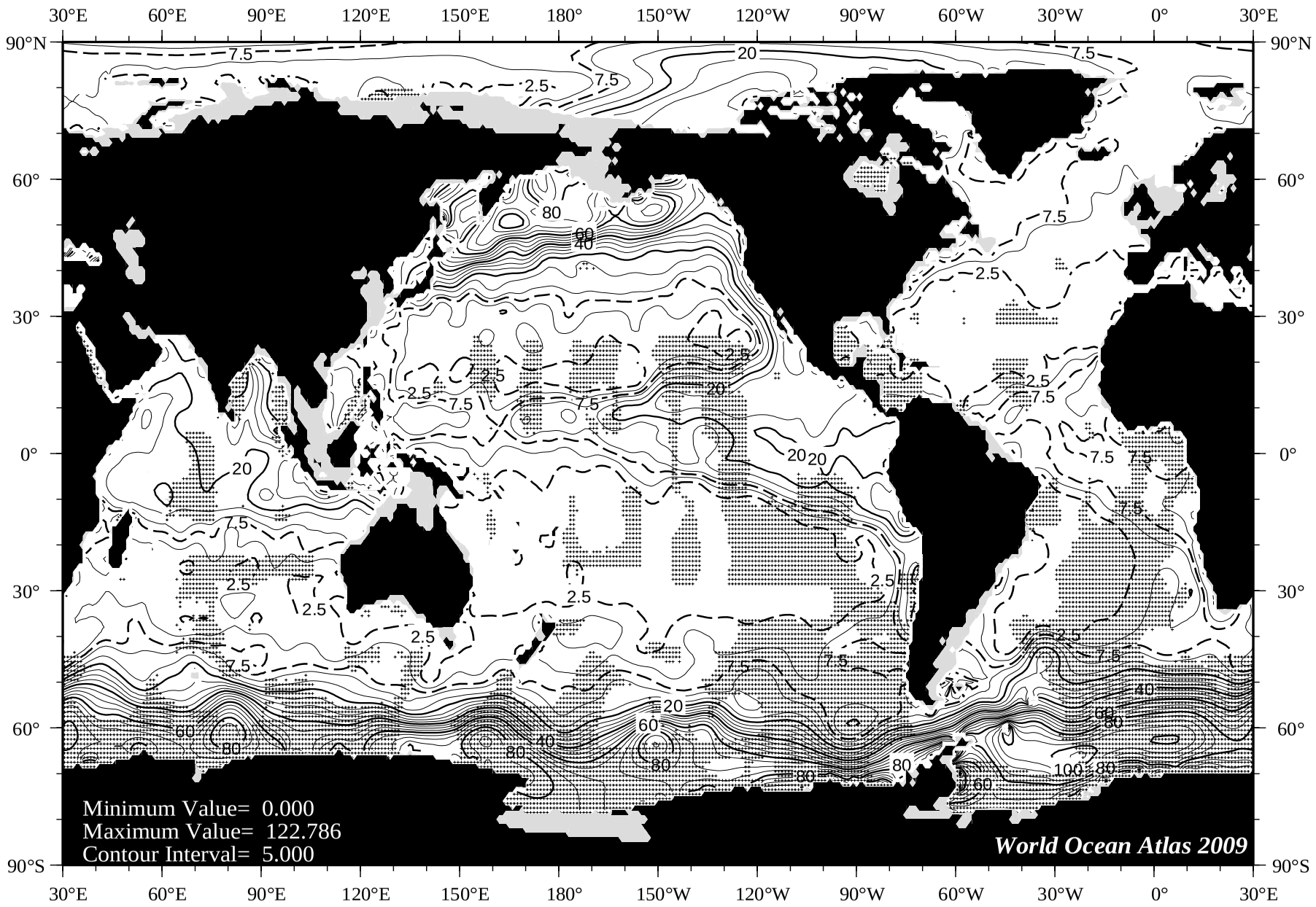

Fig H37 Summer (Jul.-Sep.) silicate [umol/l] at 150 m. depth.

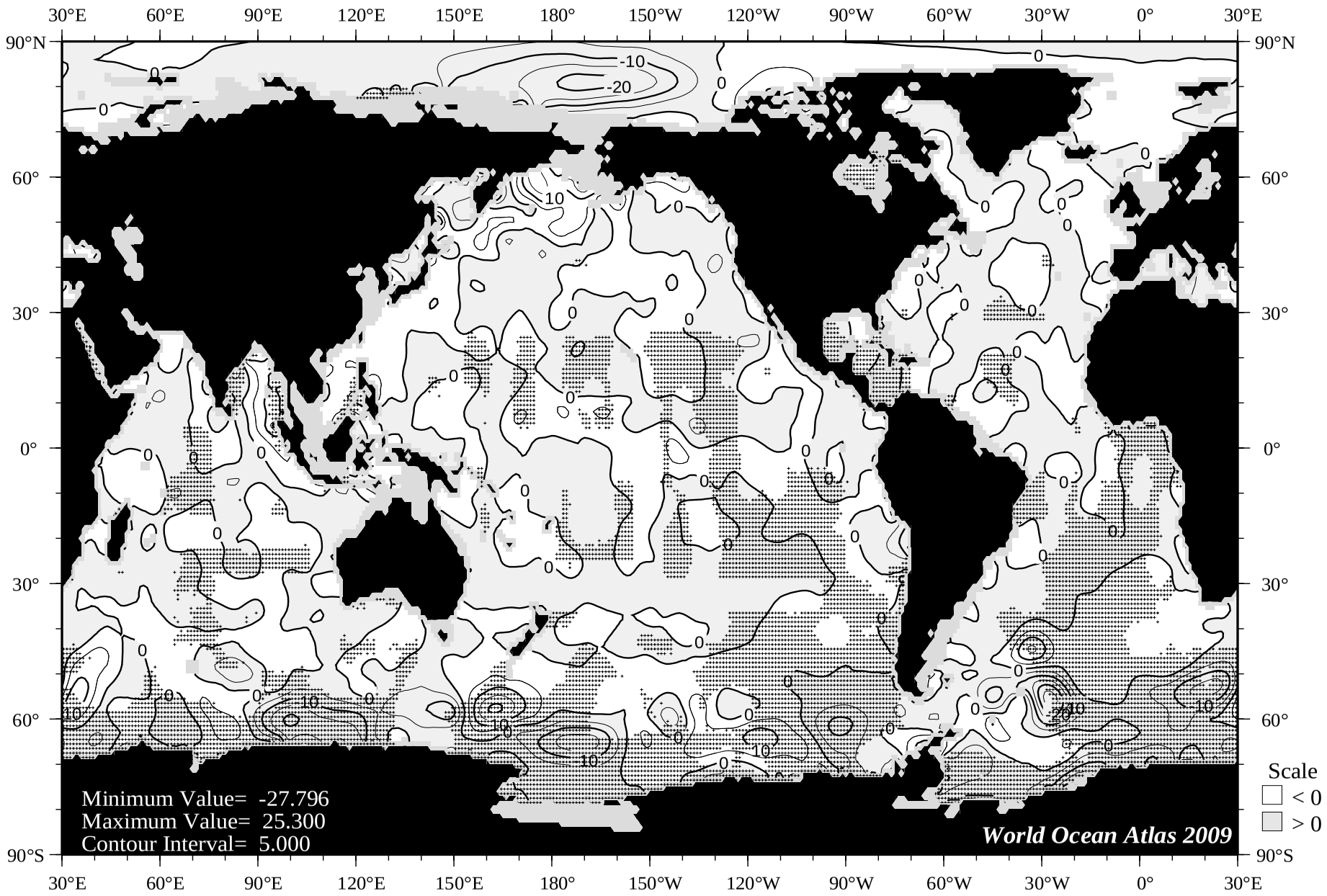

Fig H38 Summer (Jul.-Sep.) minus annual silicate [umol/l] at 150 m. depth.

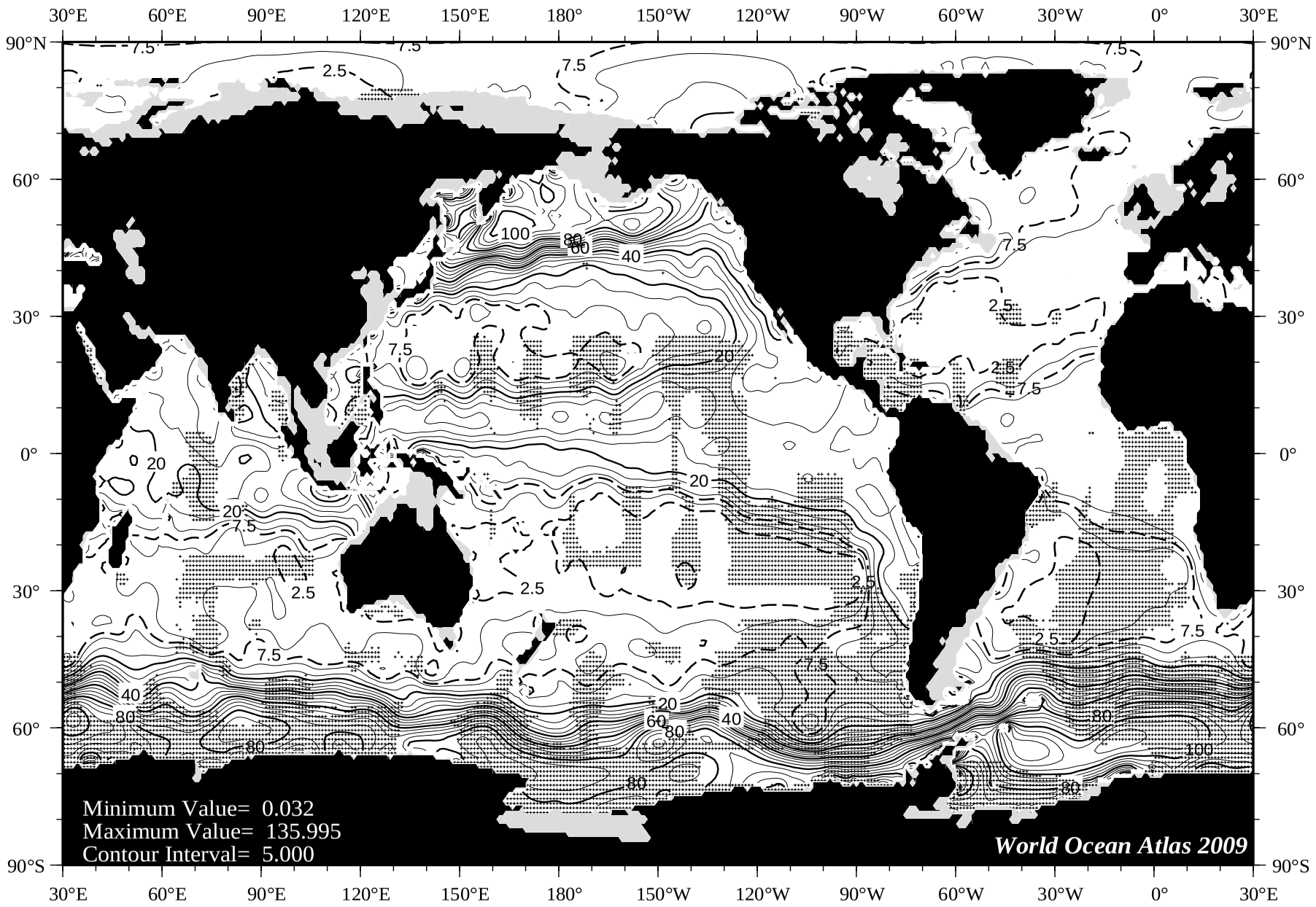

Fig H39 Summer (Jul.-Sep.) silicate [umol/l] at 250 m. depth.

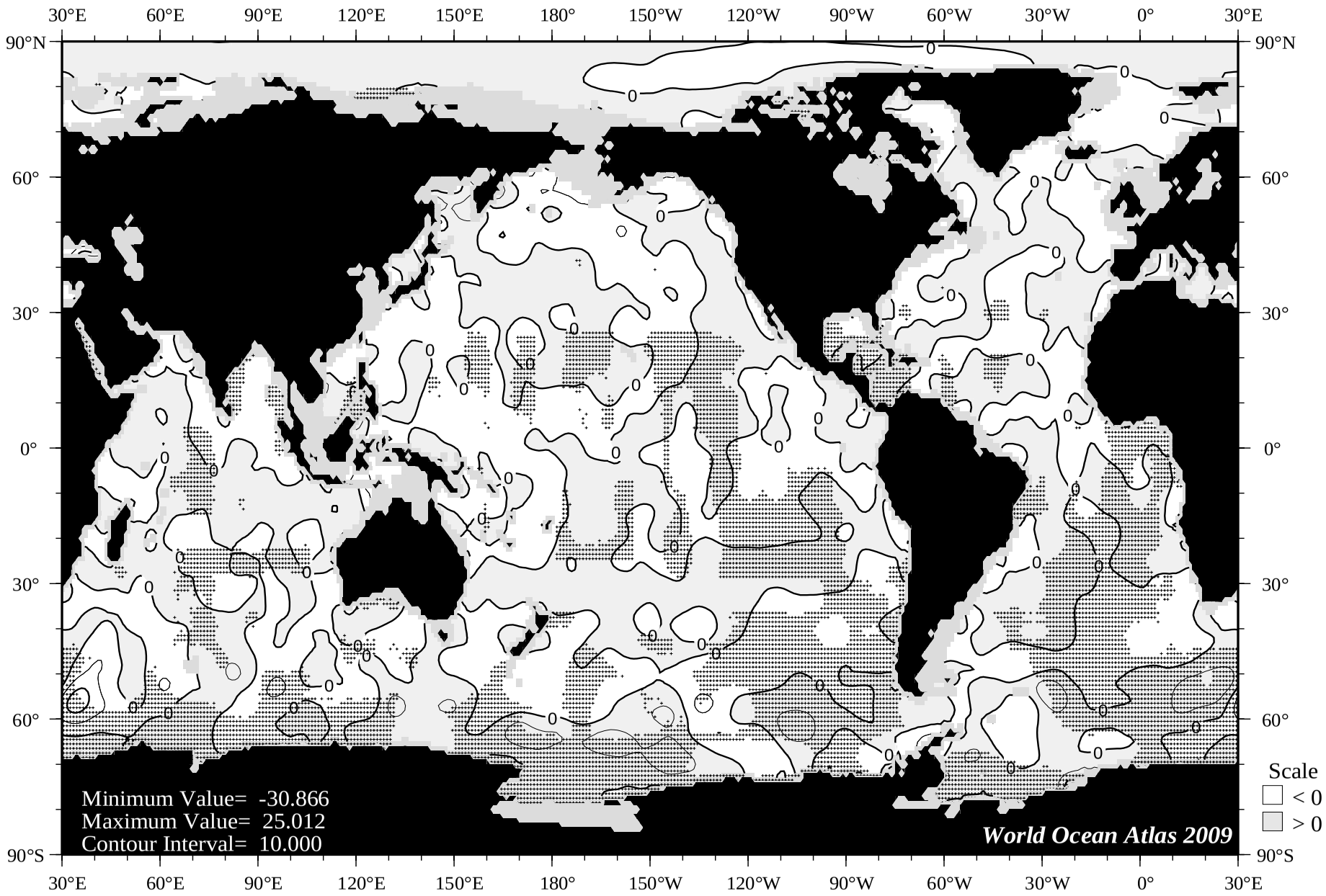

Fig H40 Summer (Jul.-Sep.) minus annual silicate [umol/l] at 250 m. depth.

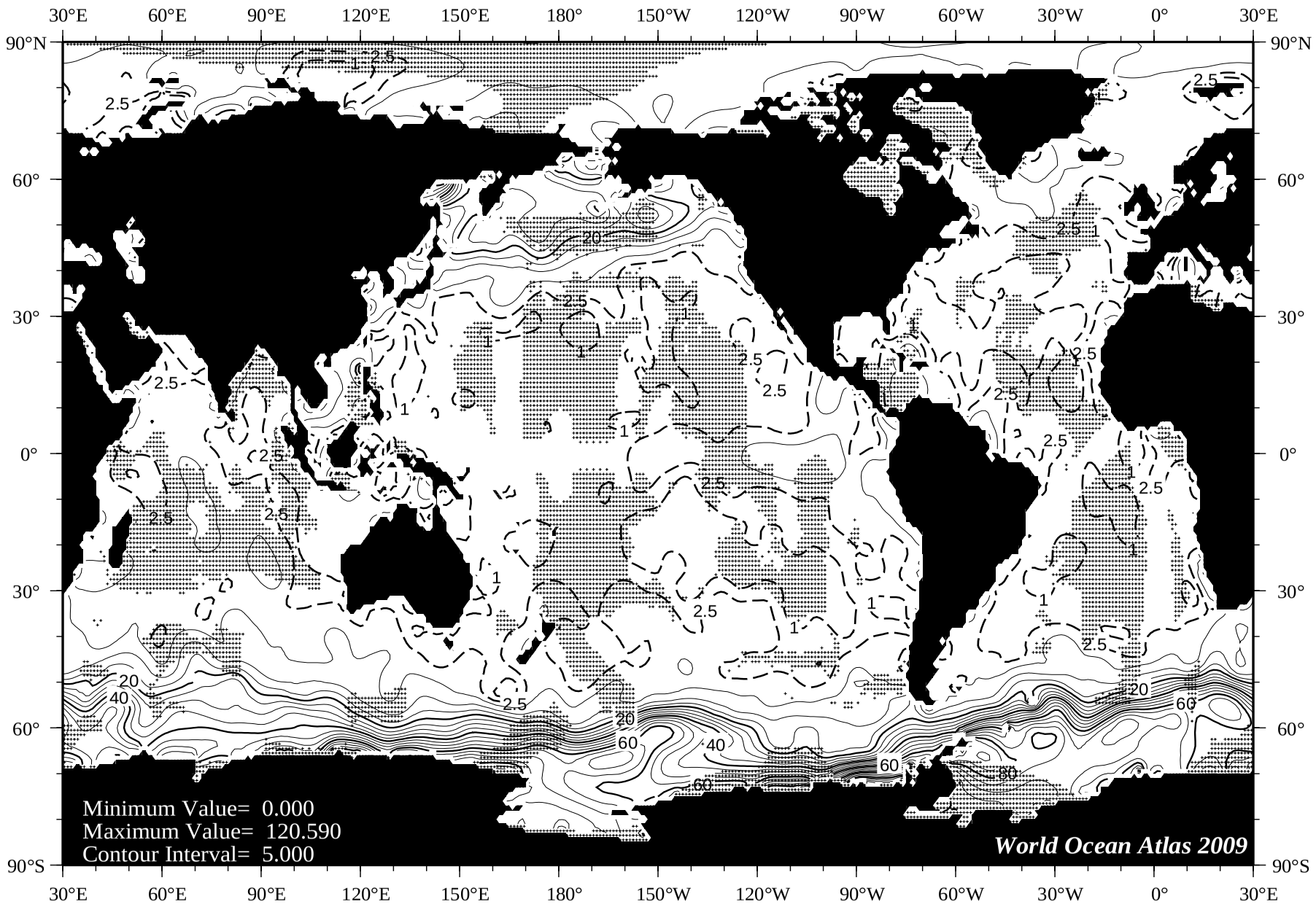

Fig H41 Fall (Oct.-Dec.) silicate [umol/l] at the surface.

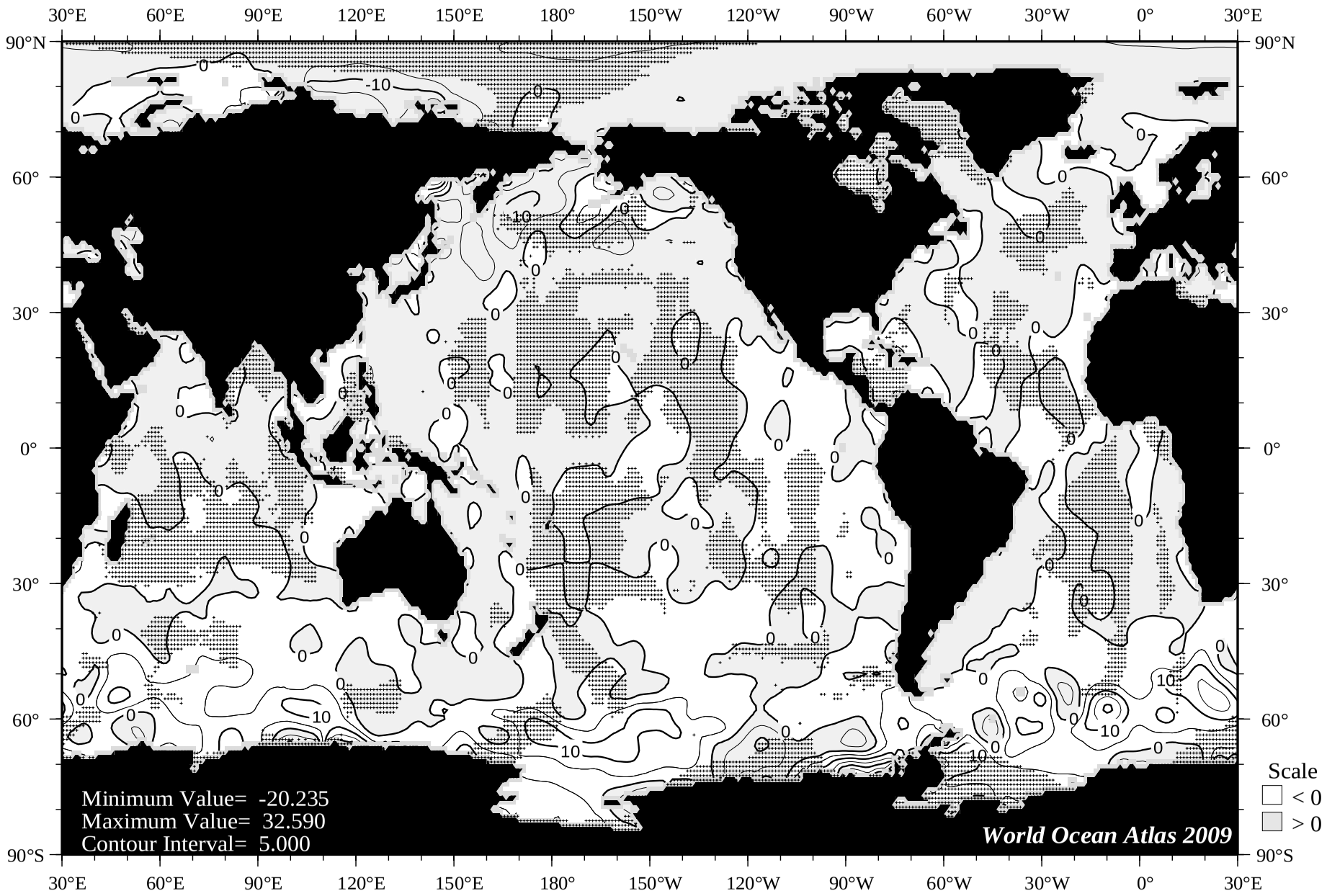

Fig H42 Fall (Oct.-Dec.) minus annual silicate [umol/l] at the surface.

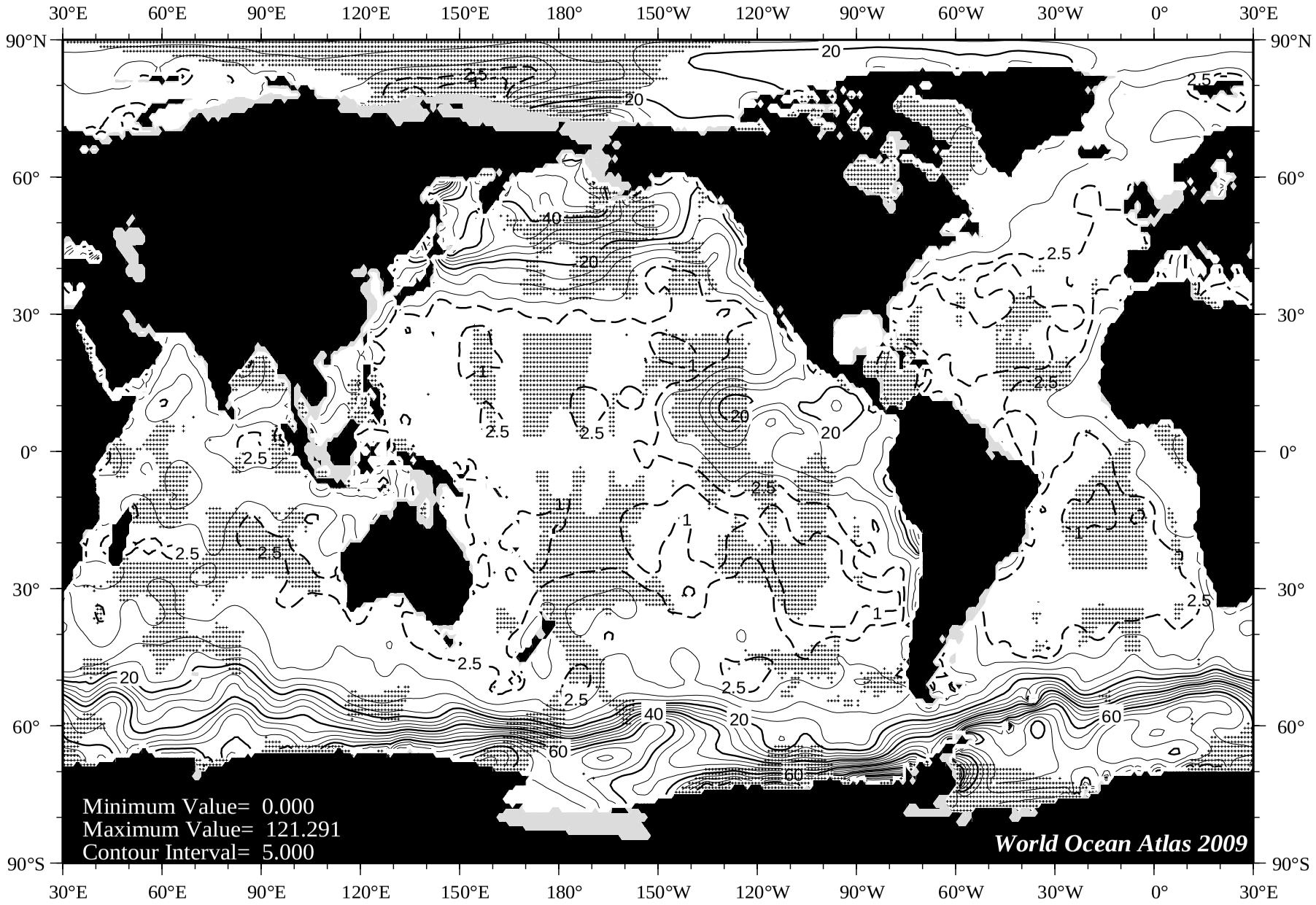

Fig H43 Fall (Oct.-Dec.) silicate [umol/l] at 75 m. depth.

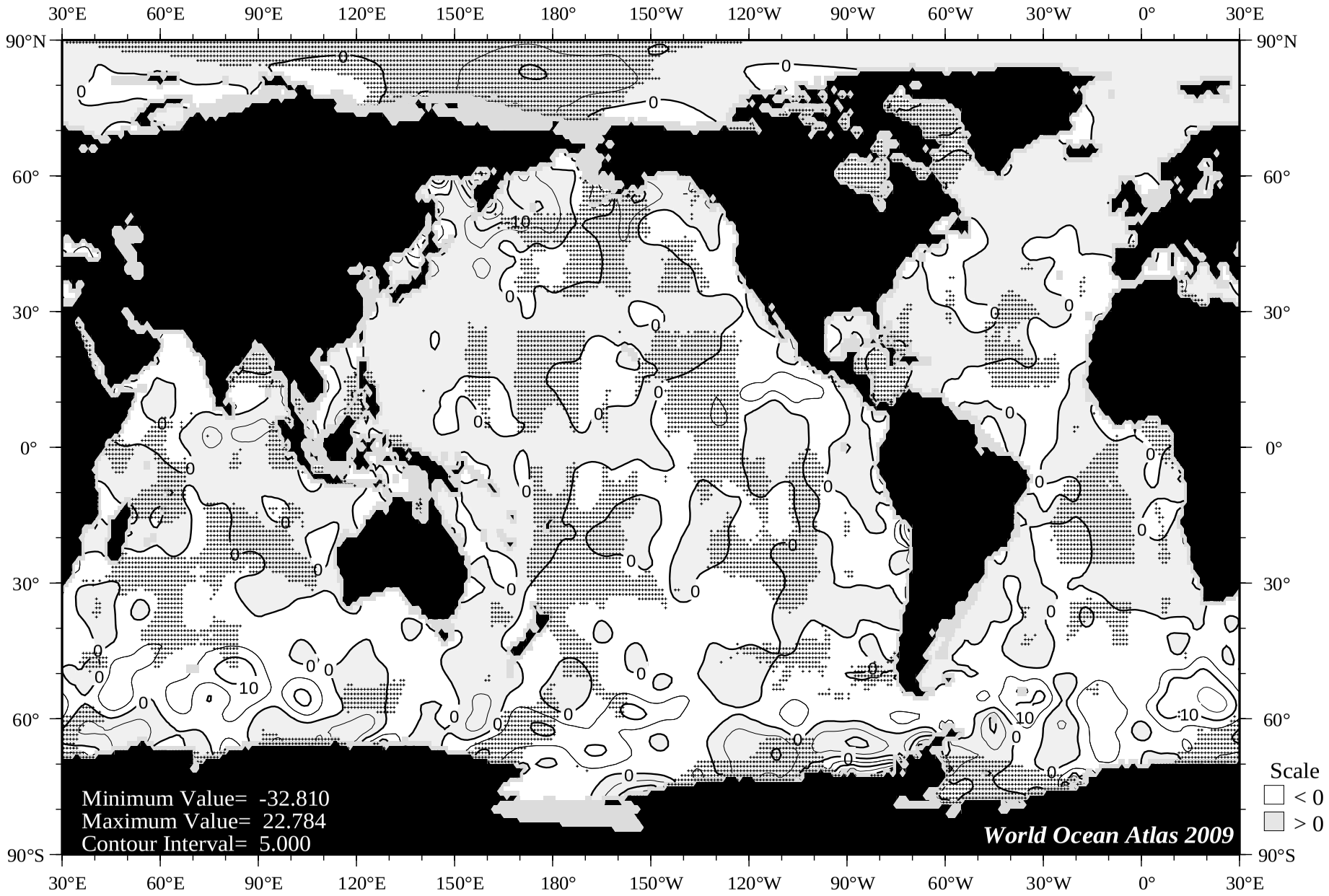

Fig H44 Fall (Oct.-Dec.) minus annual silicate [umol/l] at 75 m. depth.

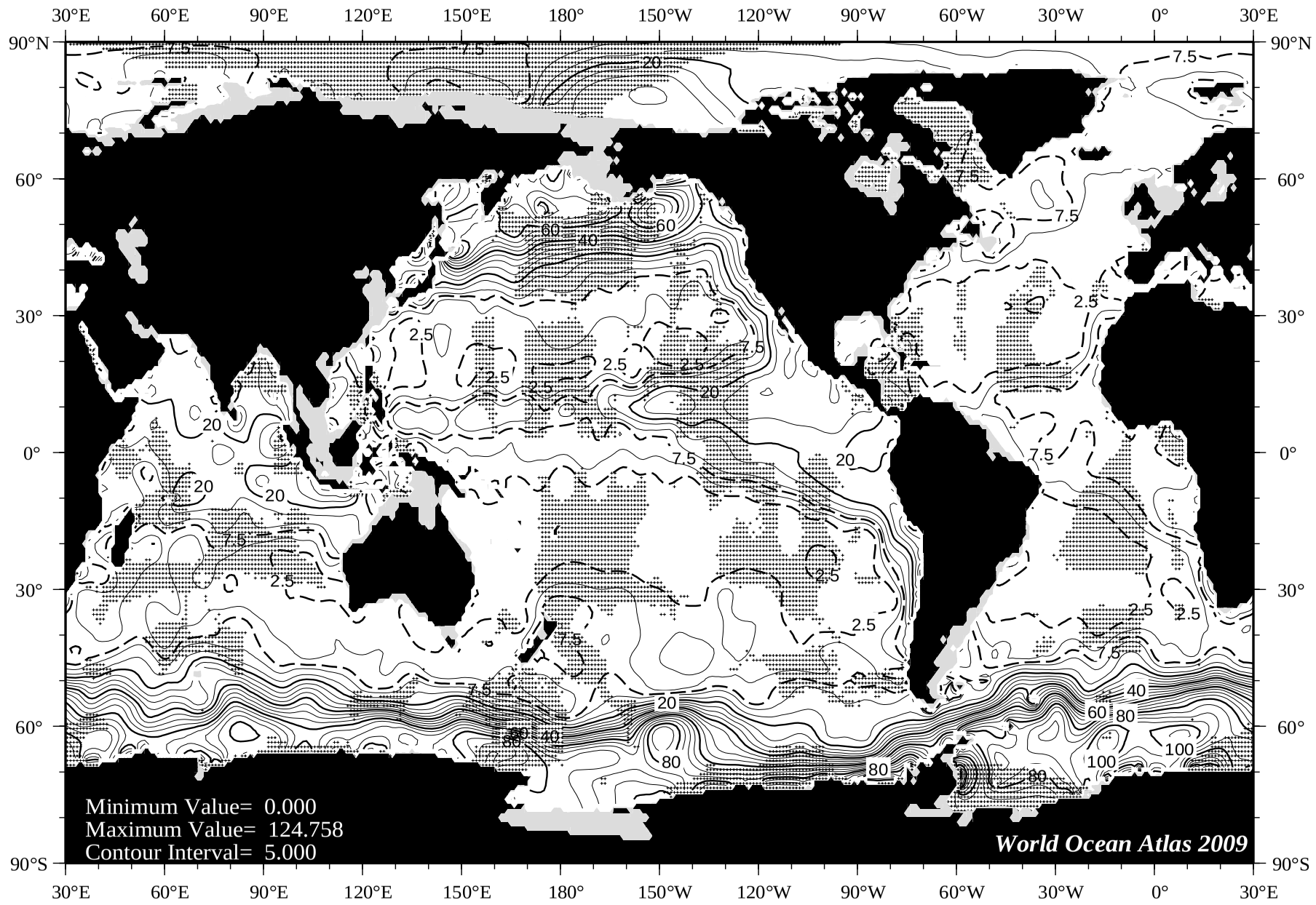

Fig H45 Fall (Oct.-Dec.) silicate [umol/l] at 150 m. depth.

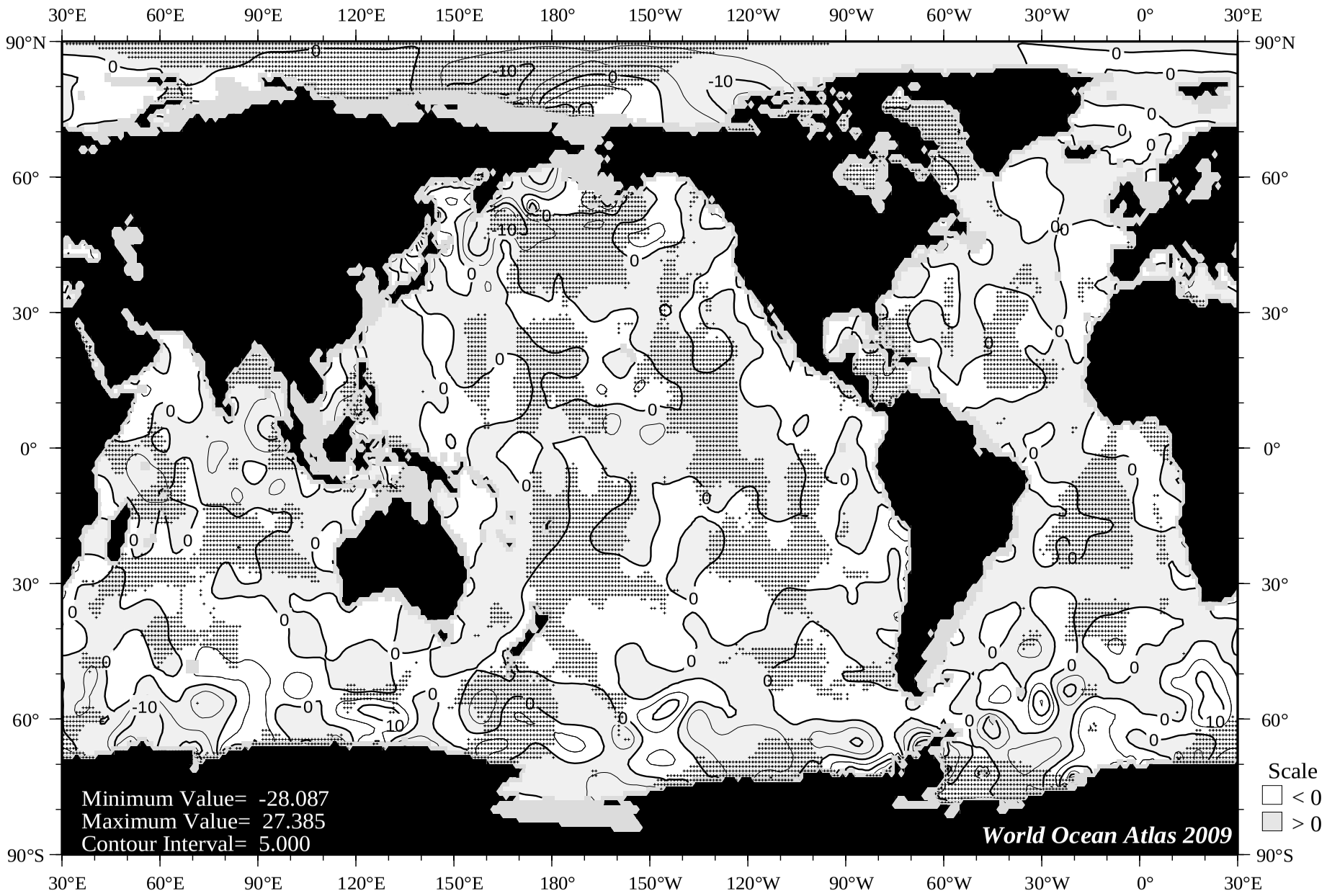

Fig H46 Fall (Oct.-Dec.) minus annual silicate [umol/l] at 150 m. depth.

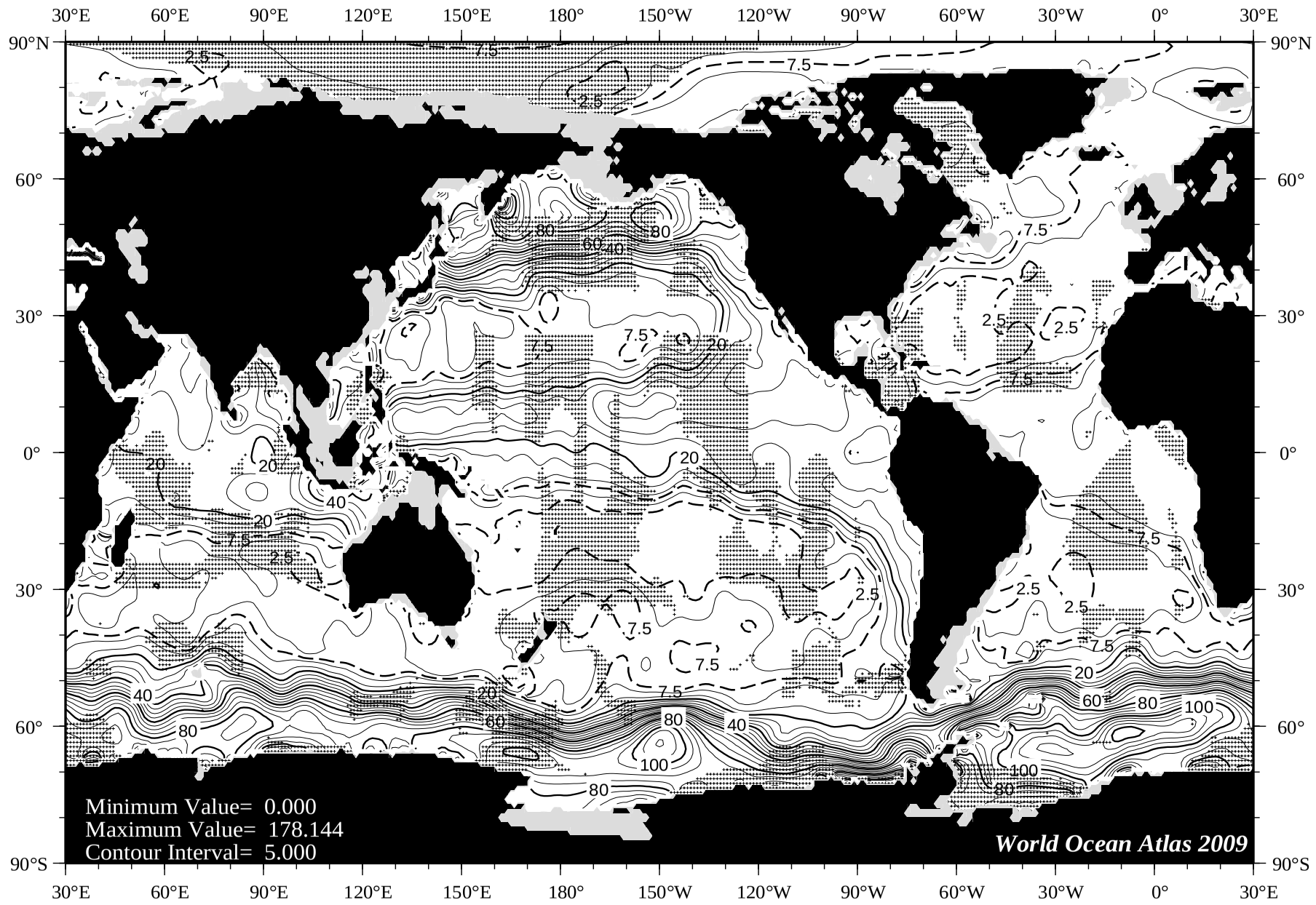

Fig H47 Fall (Oct.-Dec.) silicate [umol/l] at 250 m. depth.

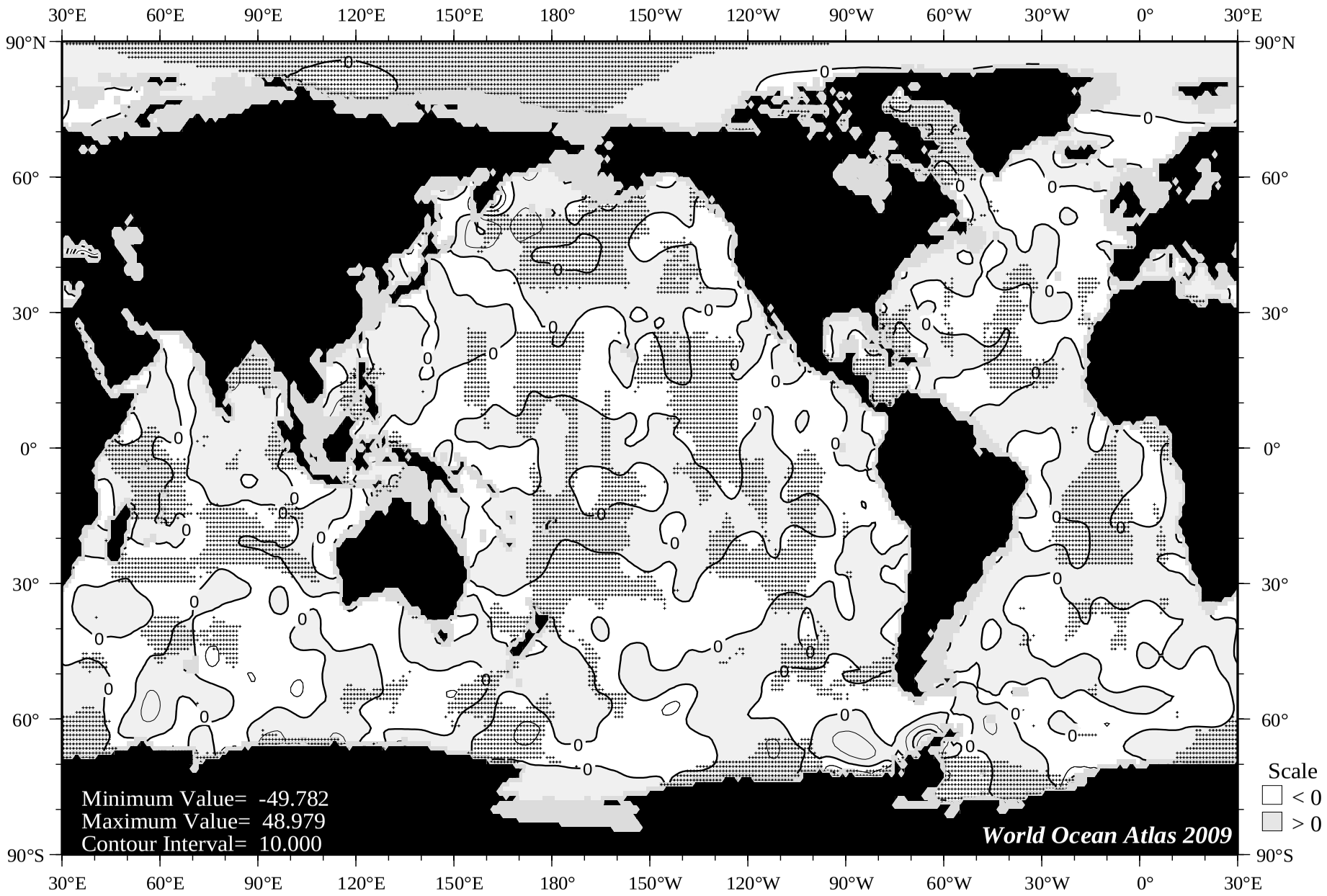

Fig H48 Fall (Oct.-Dec.) minus annual silicate [umol/l] at 250 m. depth.

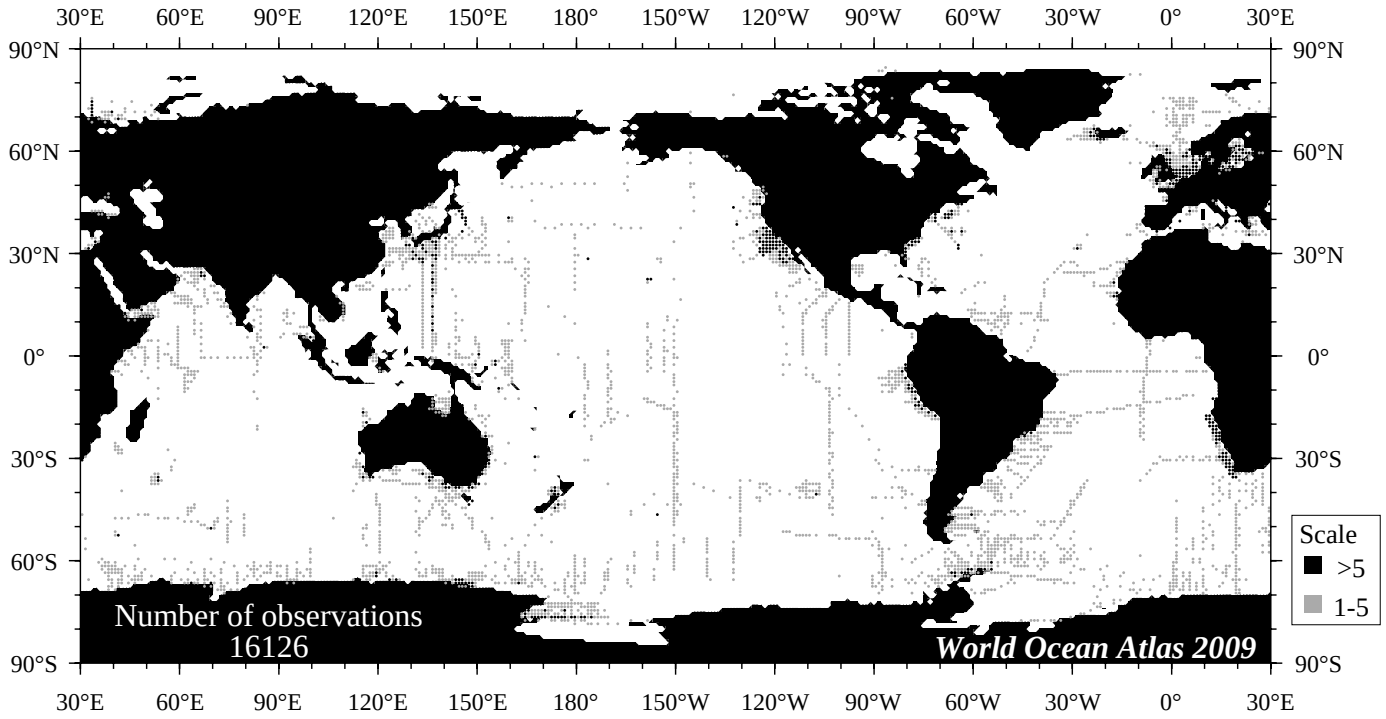

Fig I1 January silicate observations at the surface.

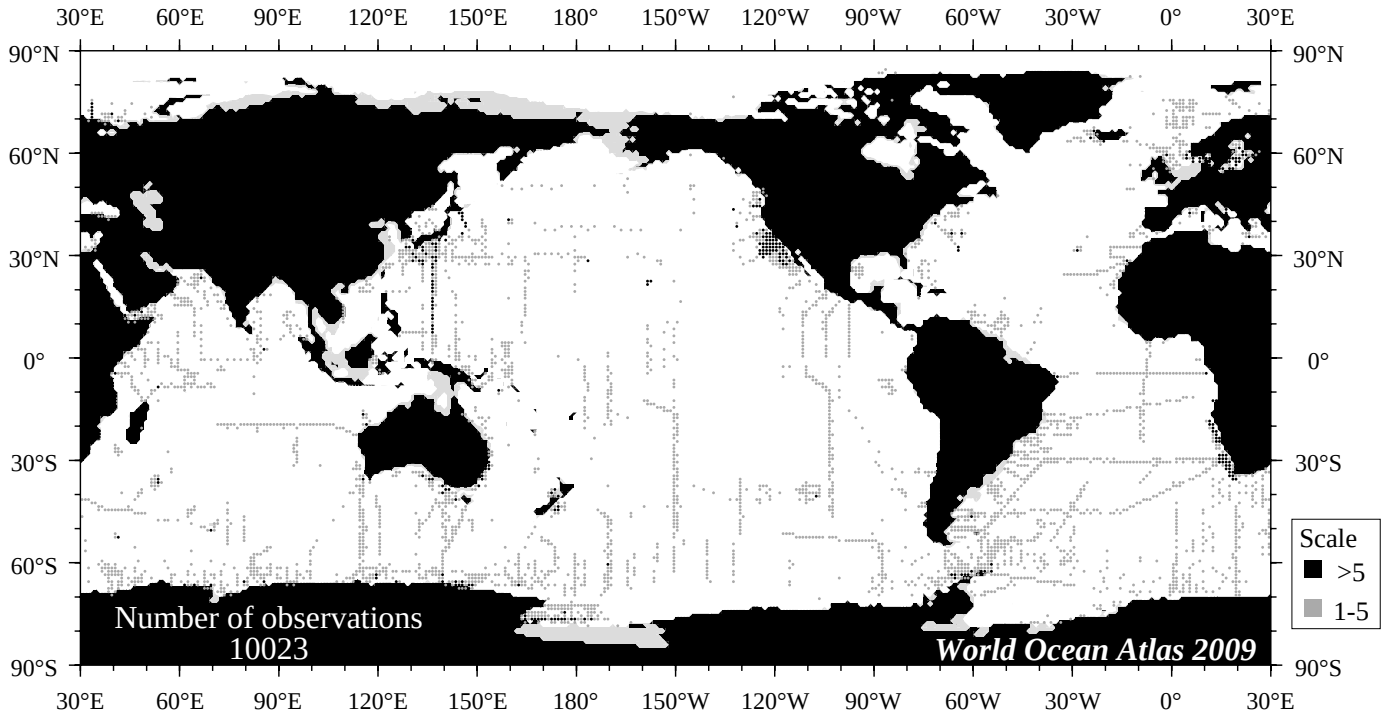

Fig I2 January silicate observations at 75 m. depth.

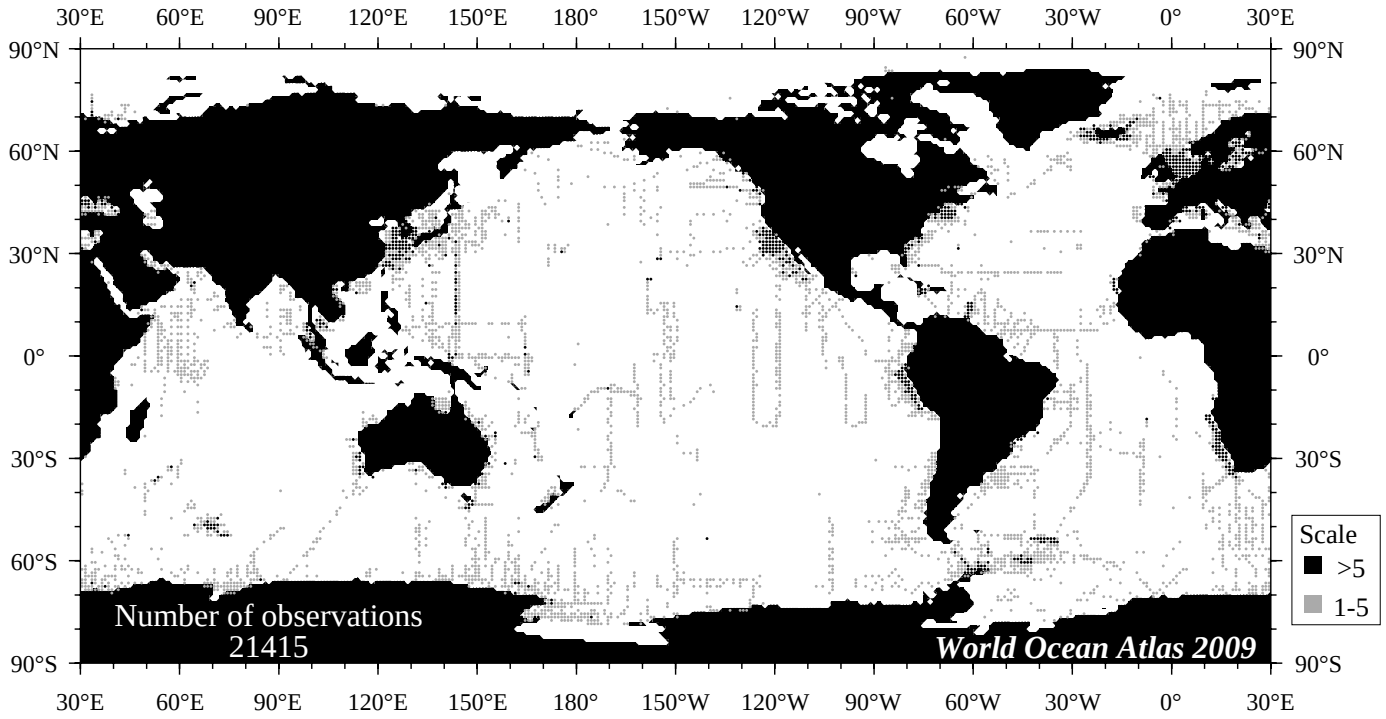

Fig I3 February silicate observations at the surface.

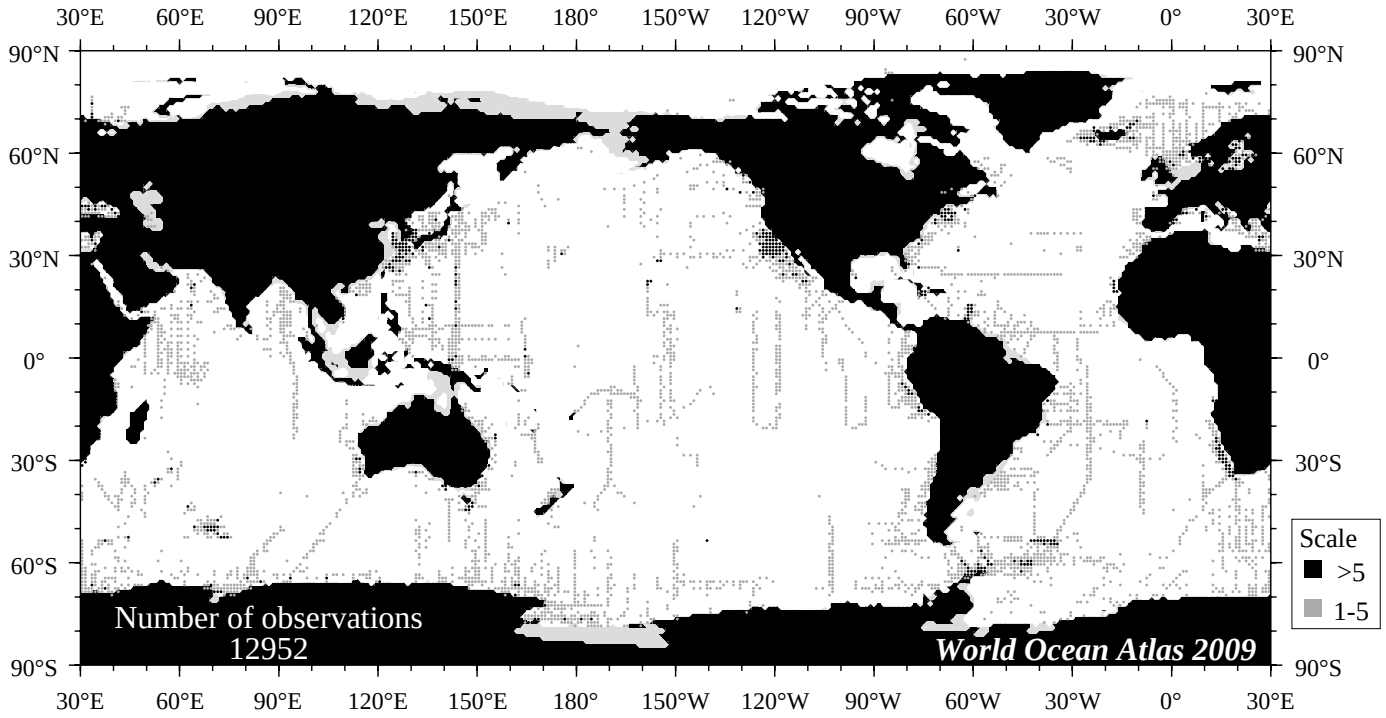

Fig I4 February silicate observations at 75 m. depth.

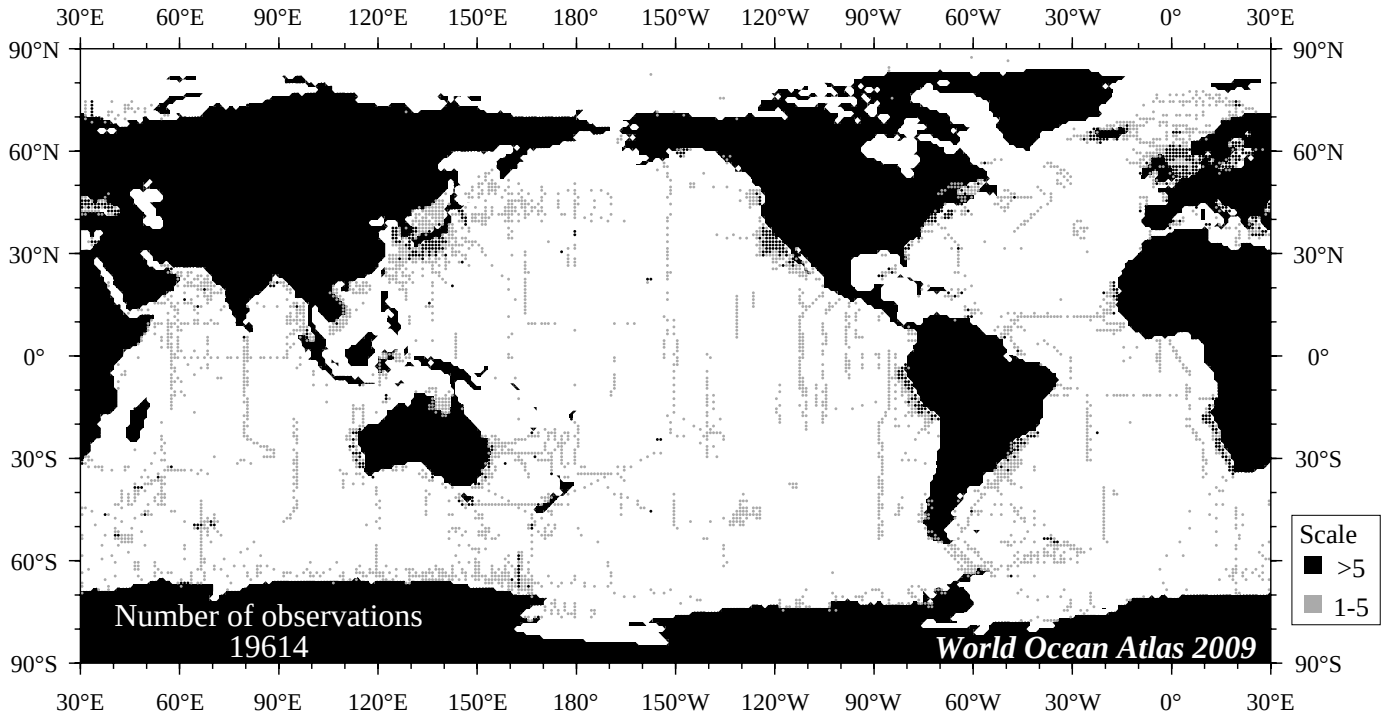

Fig I5 March silicate observations at the surface.

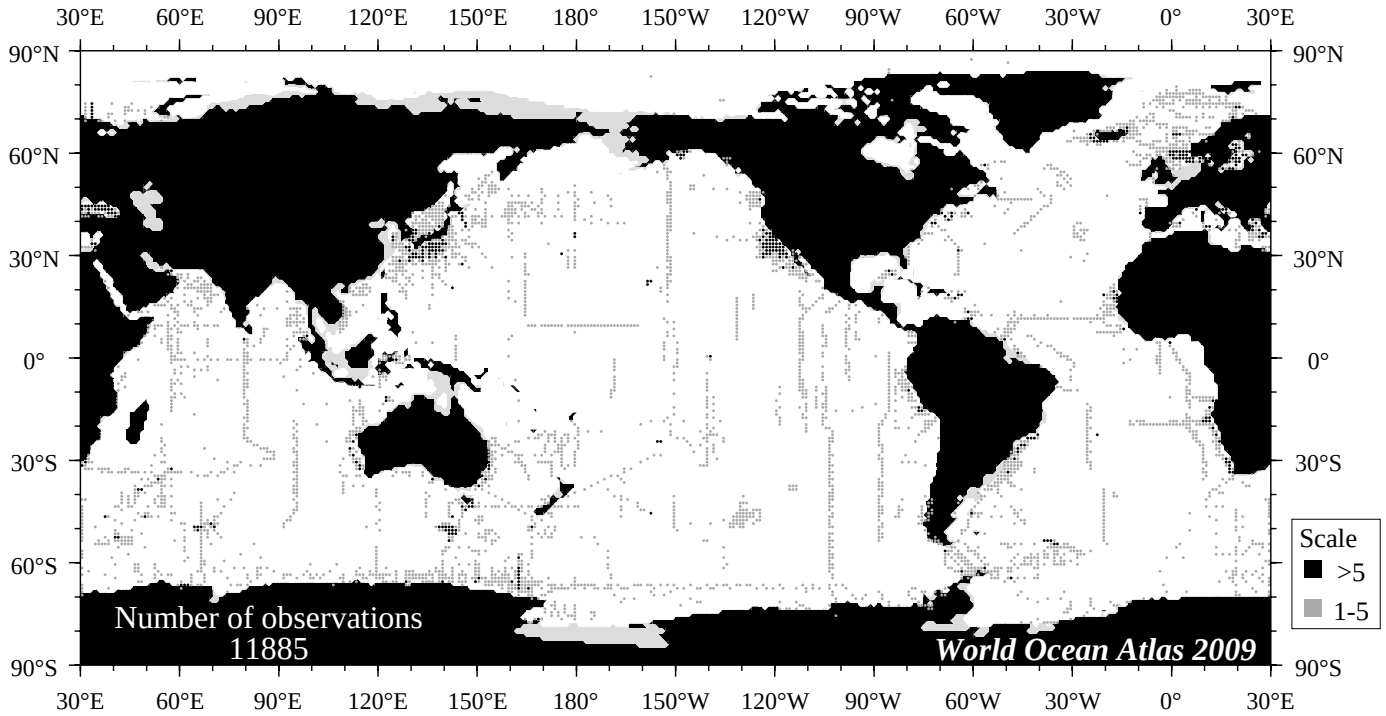

Fig I6 March silicate observations at 75 m. depth.

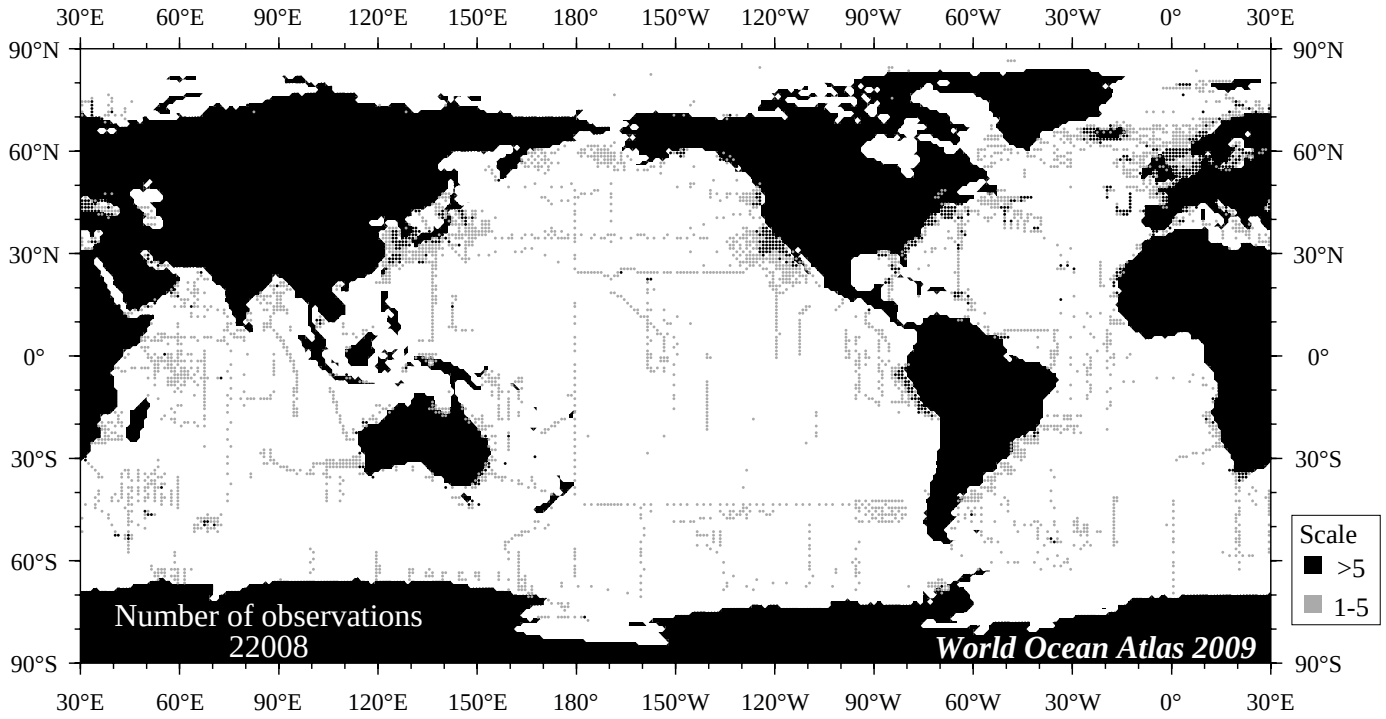

Fig I7 April silicate observations at the surface.

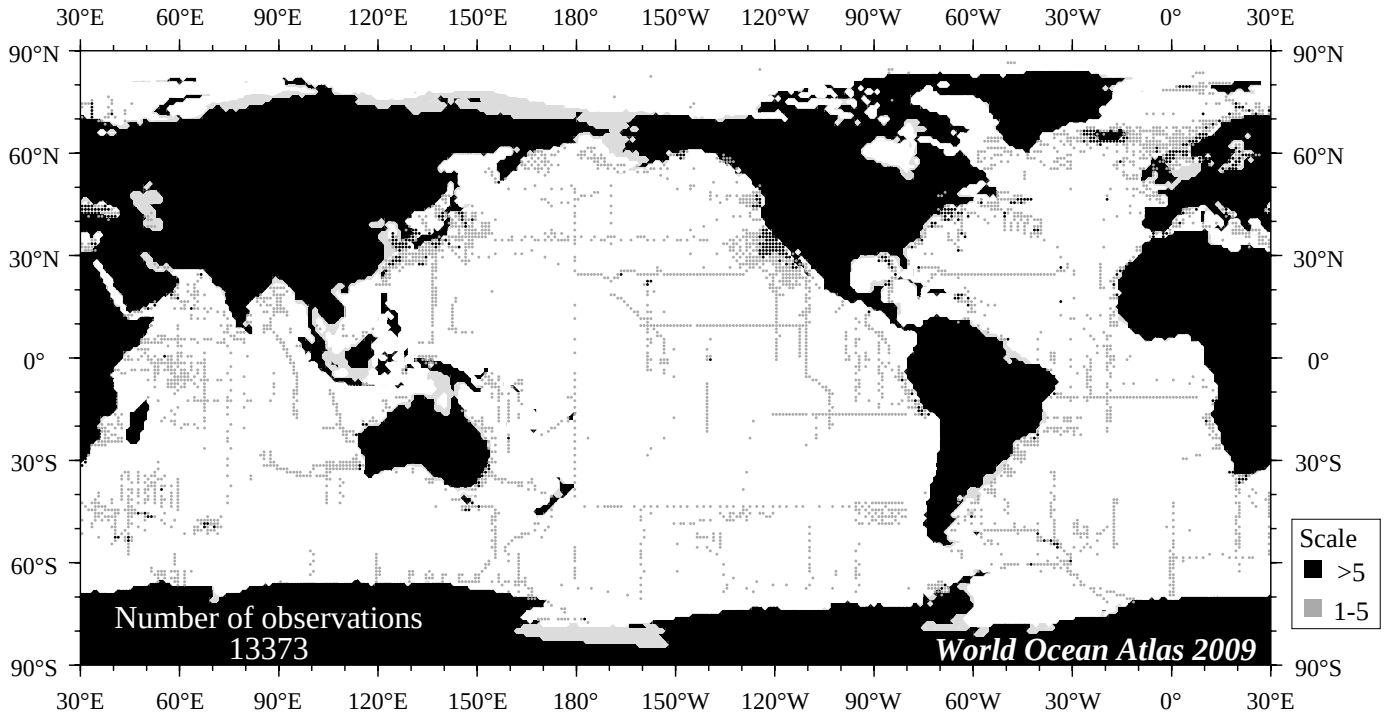

Fig I8 April silicate observations at 75 m. depth.

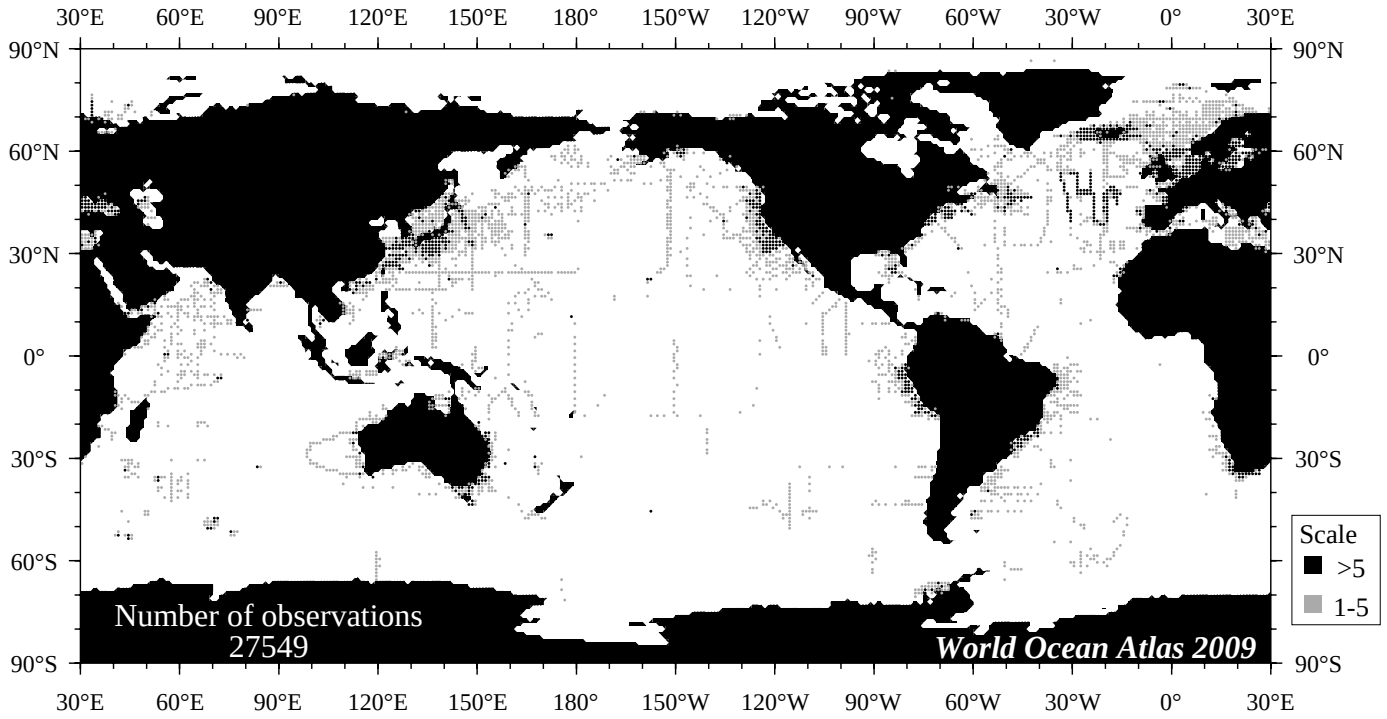

Fig I9 May silicate observations at the surface.

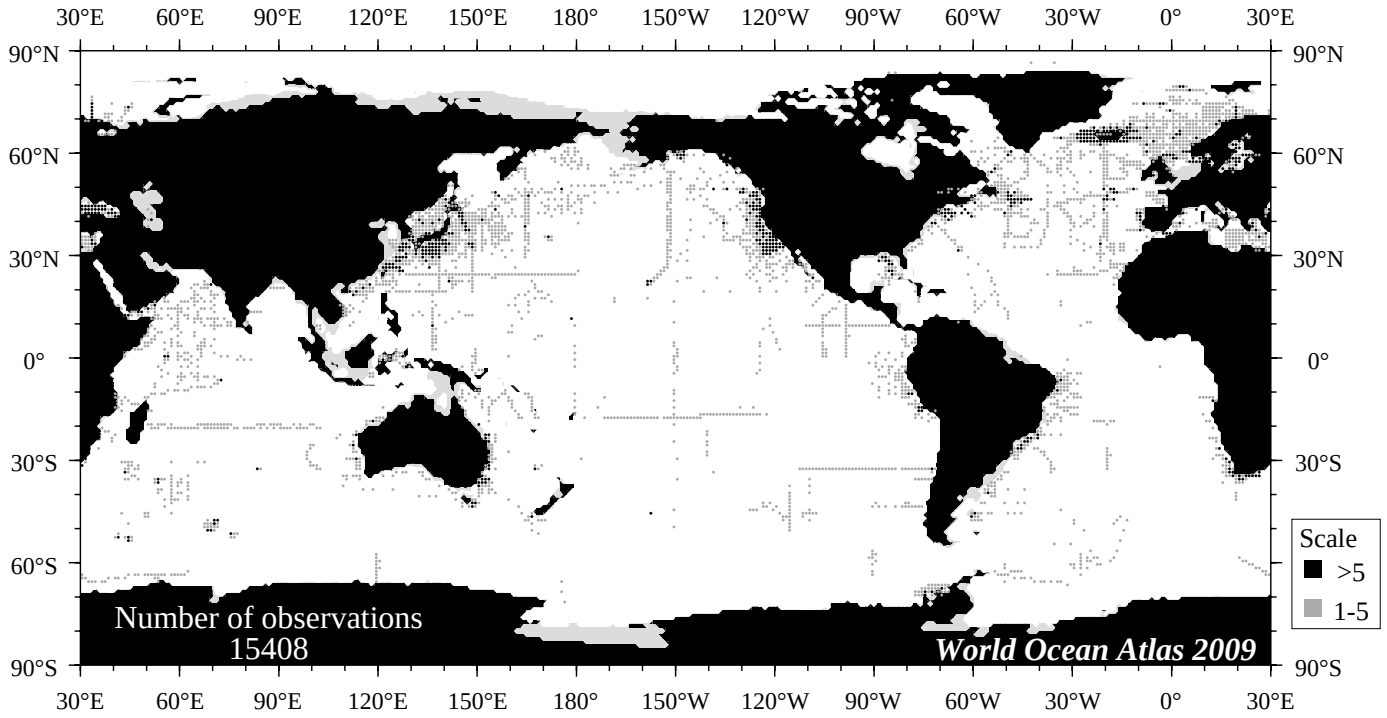

Fig I10 May silicate observations at 75 m. depth.

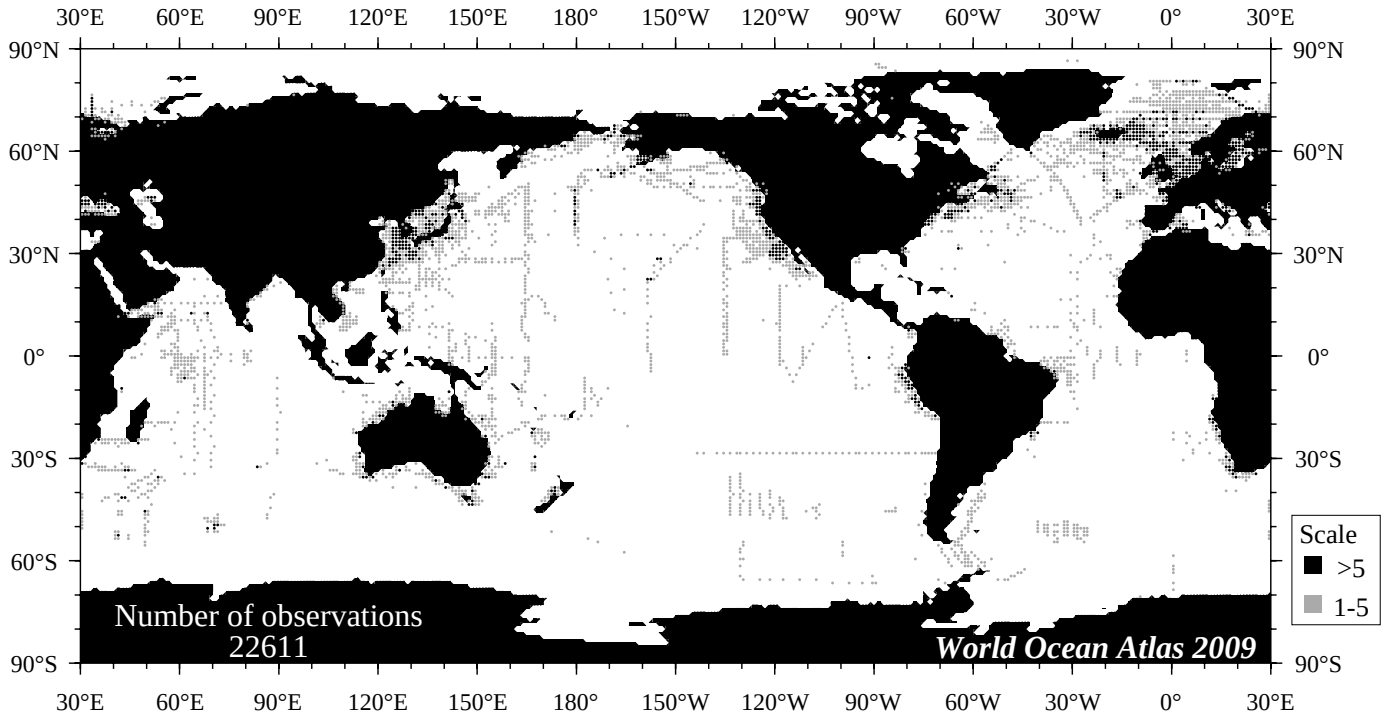

Fig I11 June silicate observations at the surface.

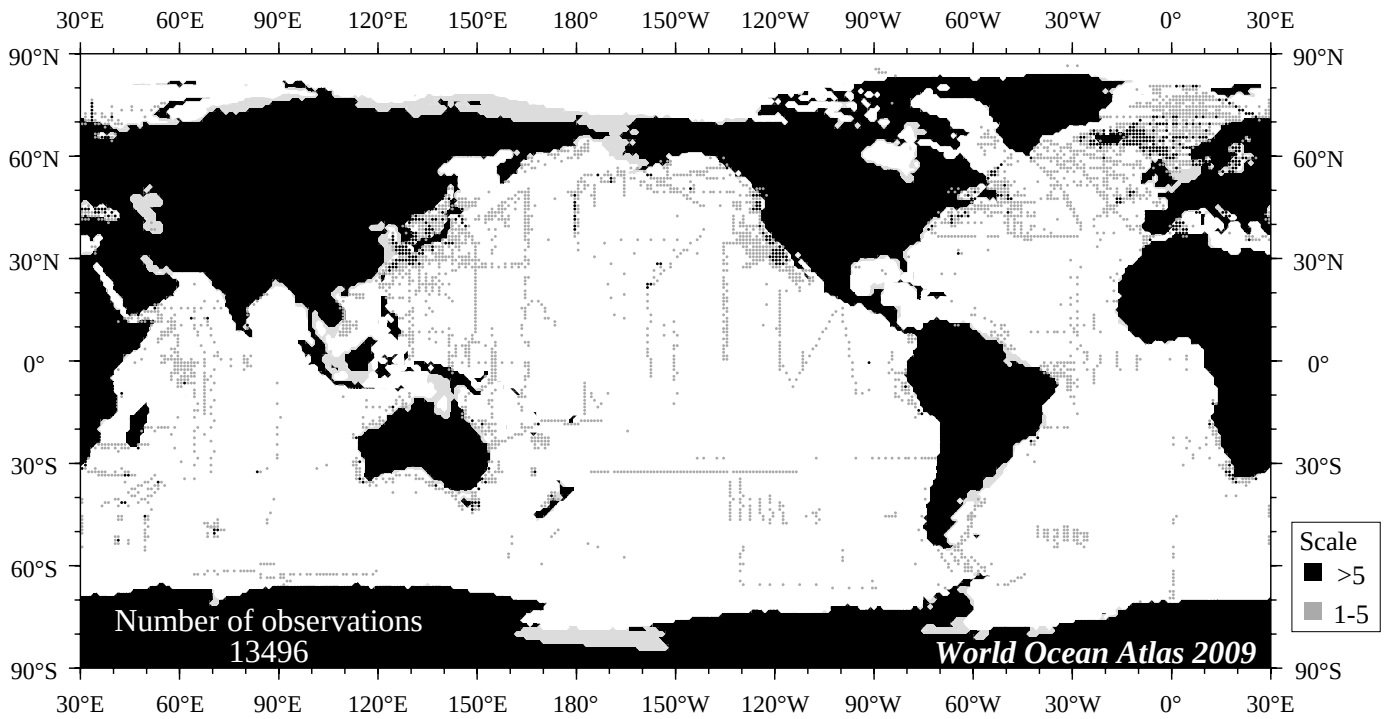

Fig I12 June silicate observations at 75 m. depth.

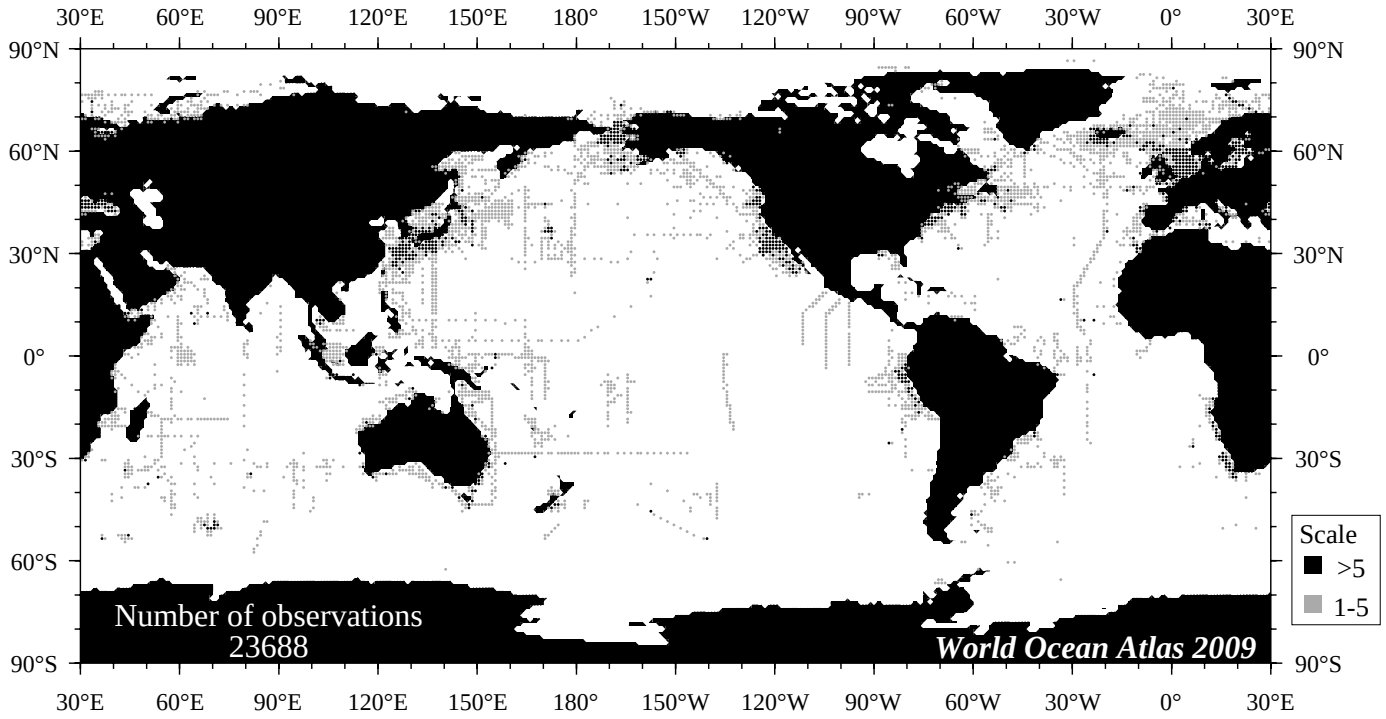

Fig I13 July silicate observations at the surface.

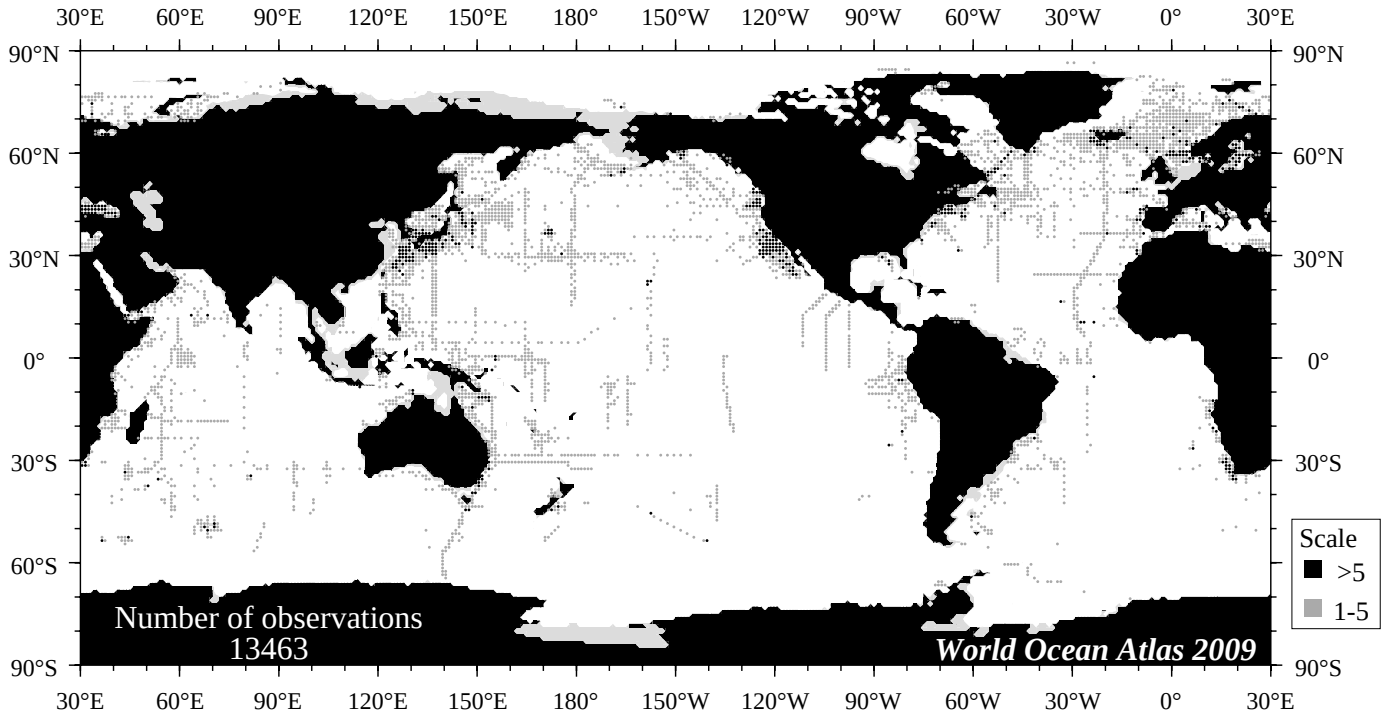

Fig I14 July silicate observations at 75 m. depth.

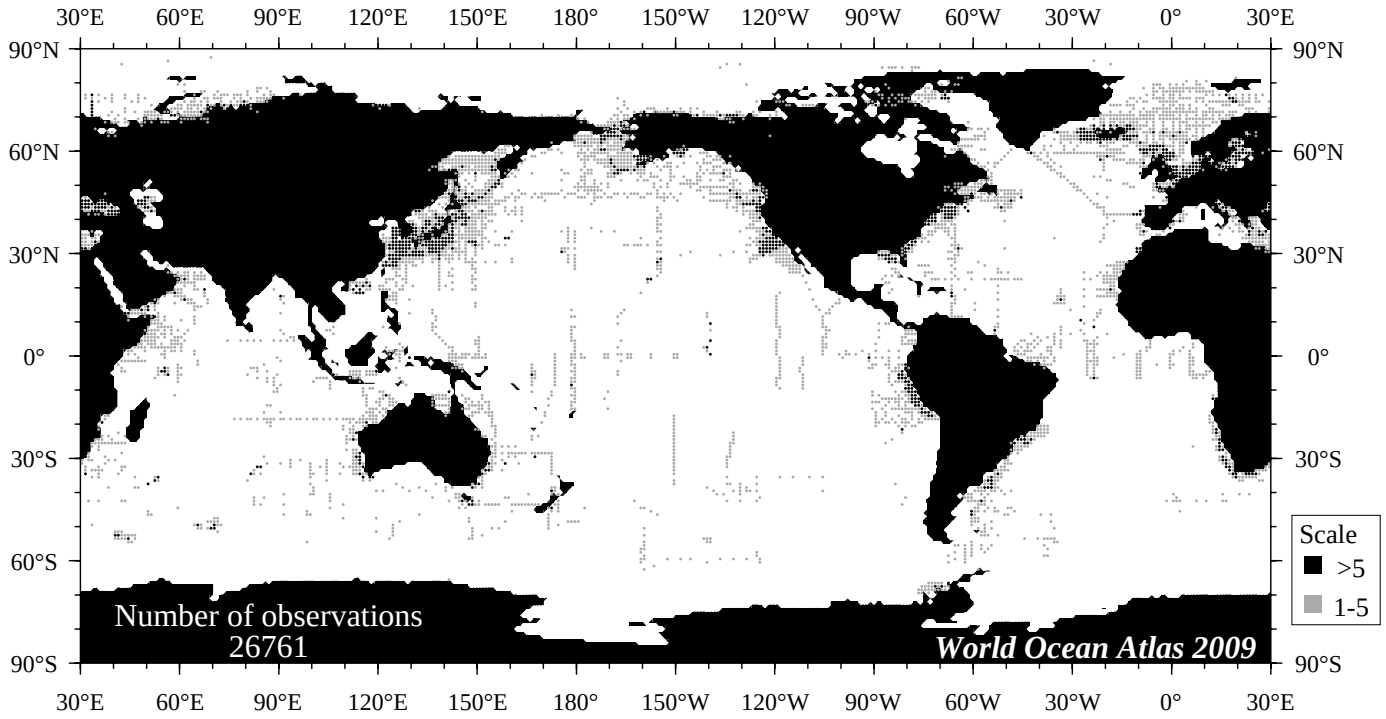

Fig I15 August silicate observations at the surface.

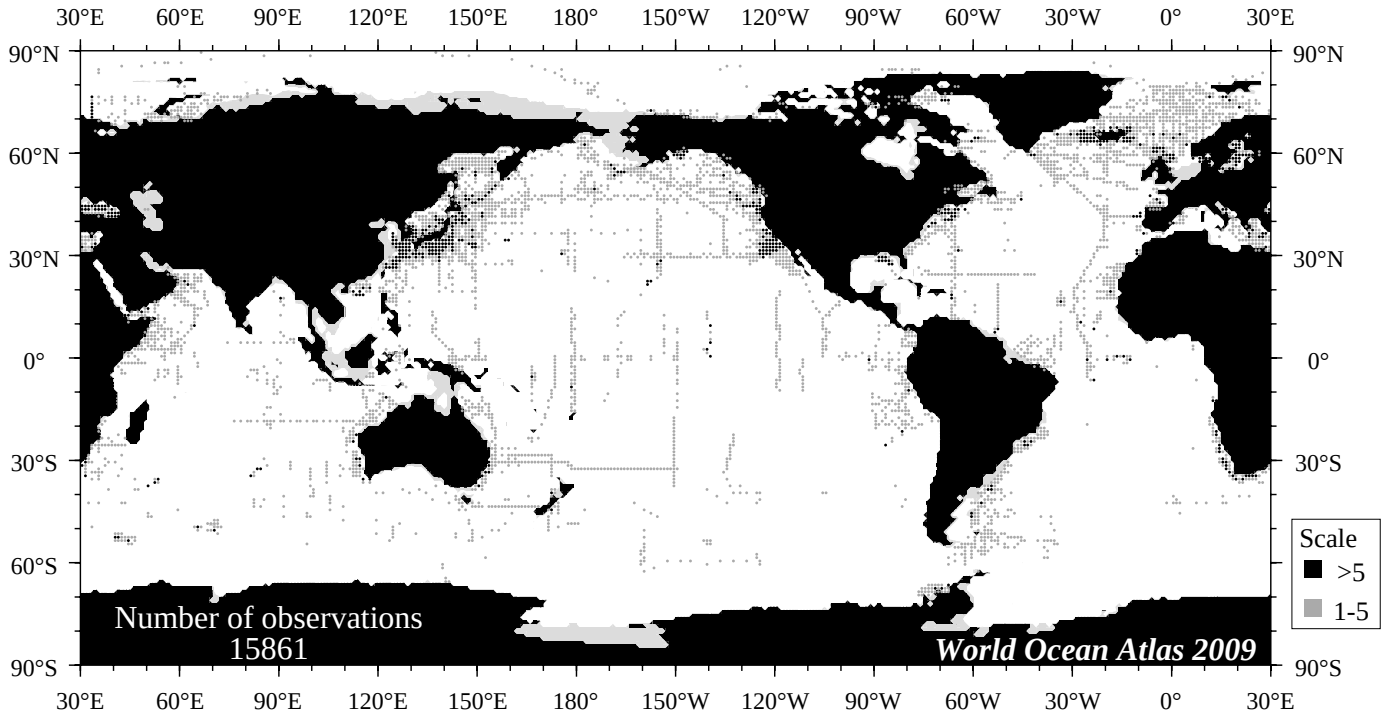

Fig I16 August silicate observations at 75 m. depth.

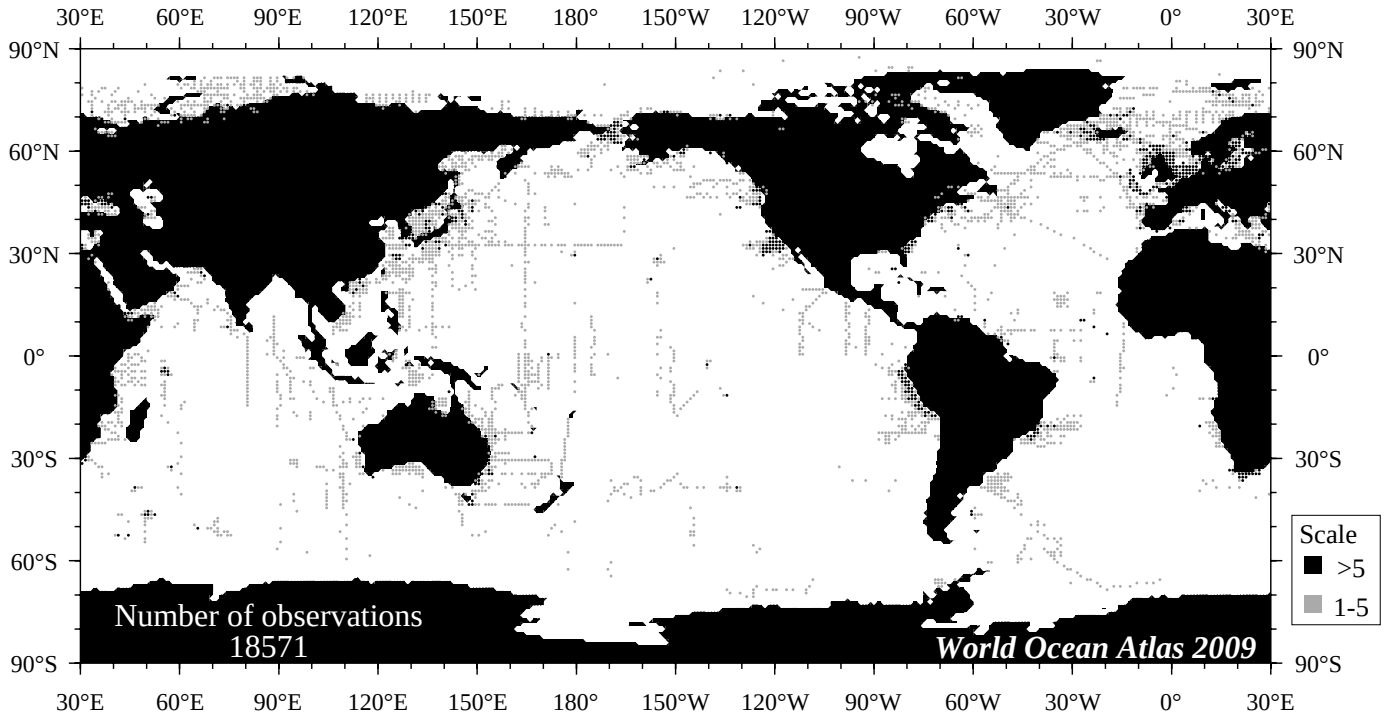

Fig I17 September silicate observations at the surface.

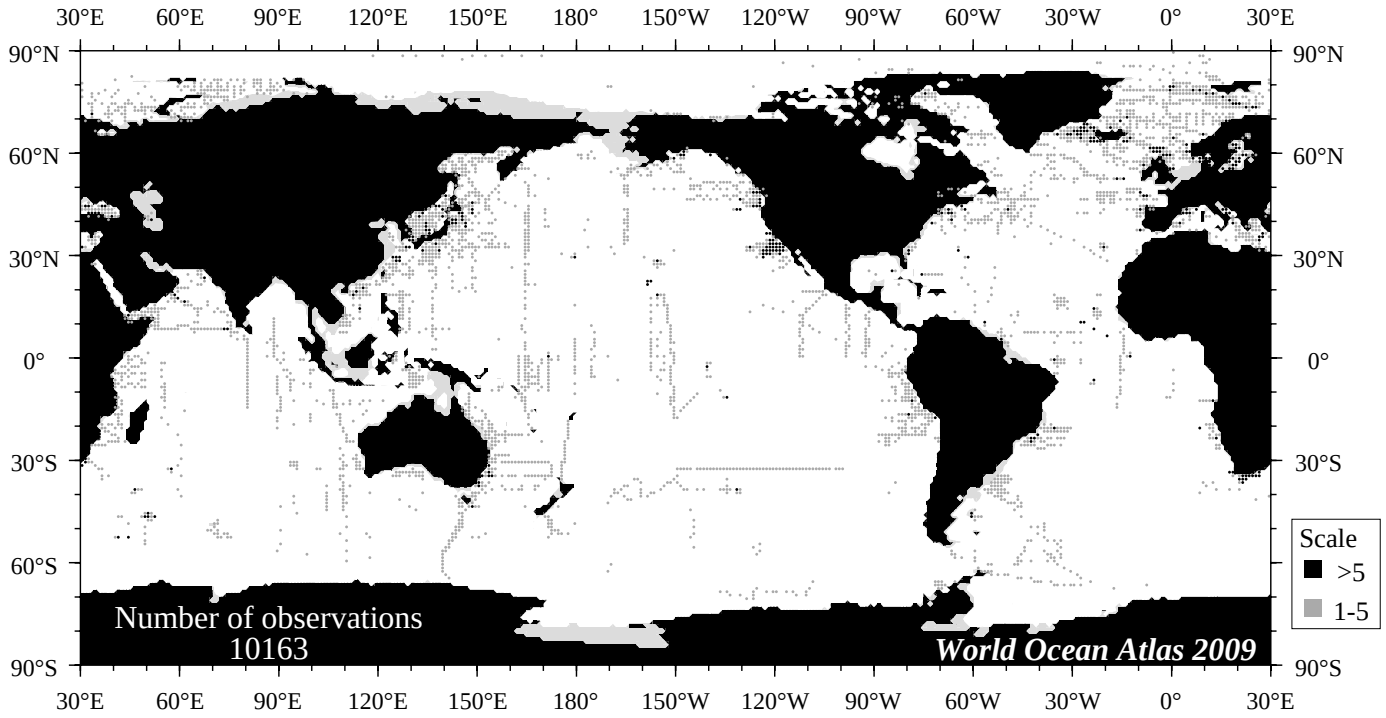

Fig I18 September silicate observations at 75 m. depth.

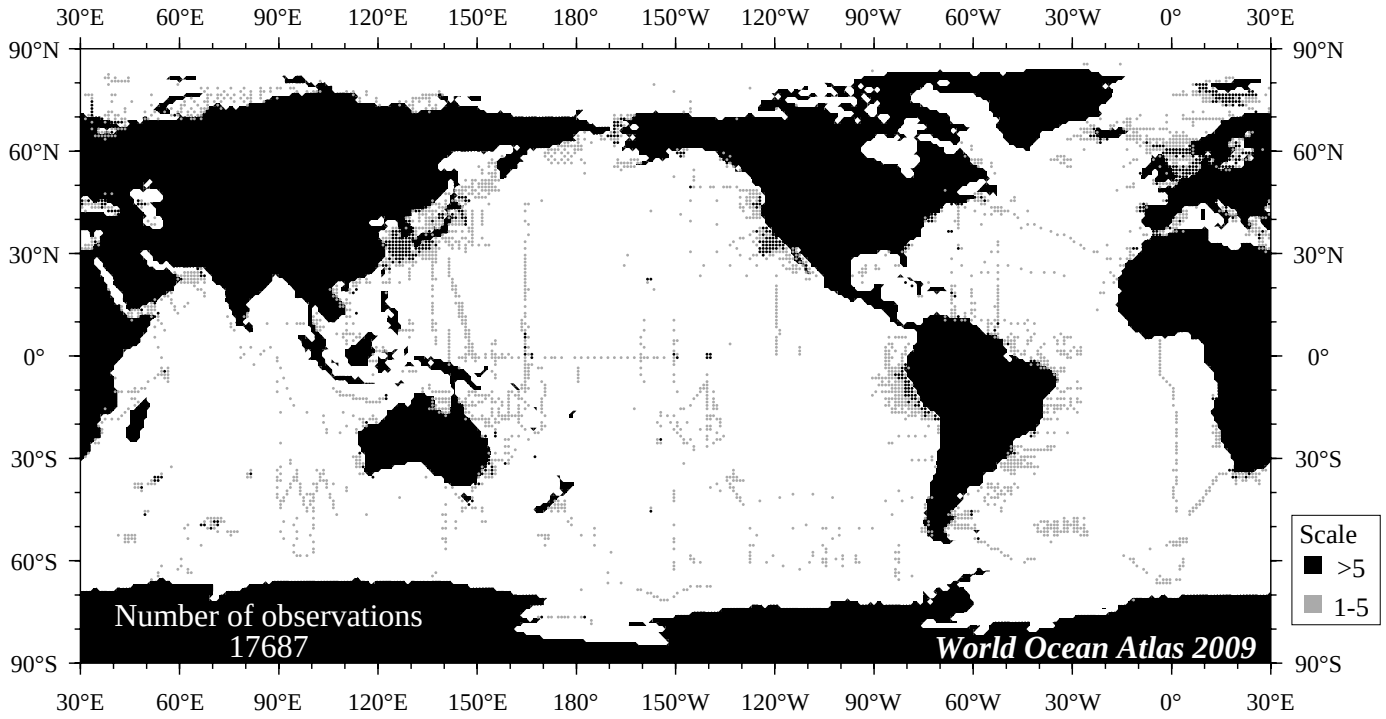

Fig I19 October silicate observations at the surface.

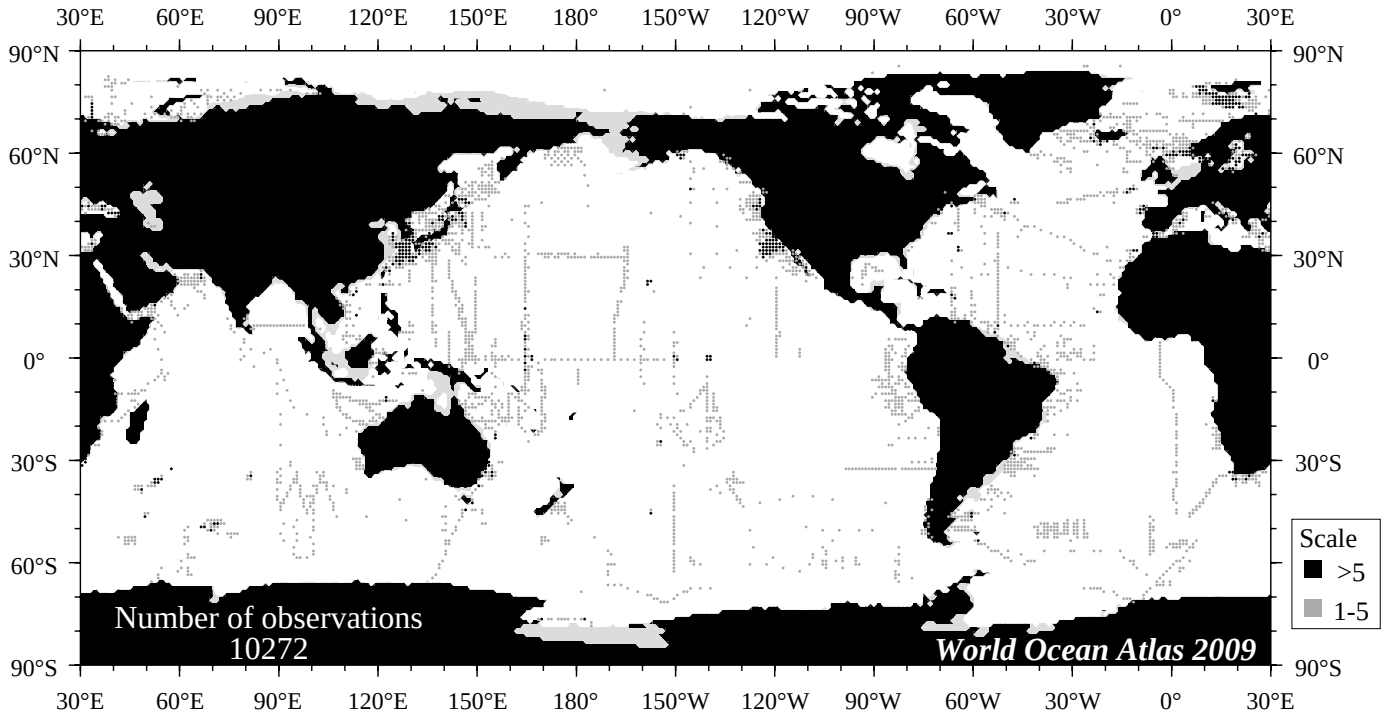

Fig I20 October silicate observations at 75 m. depth.

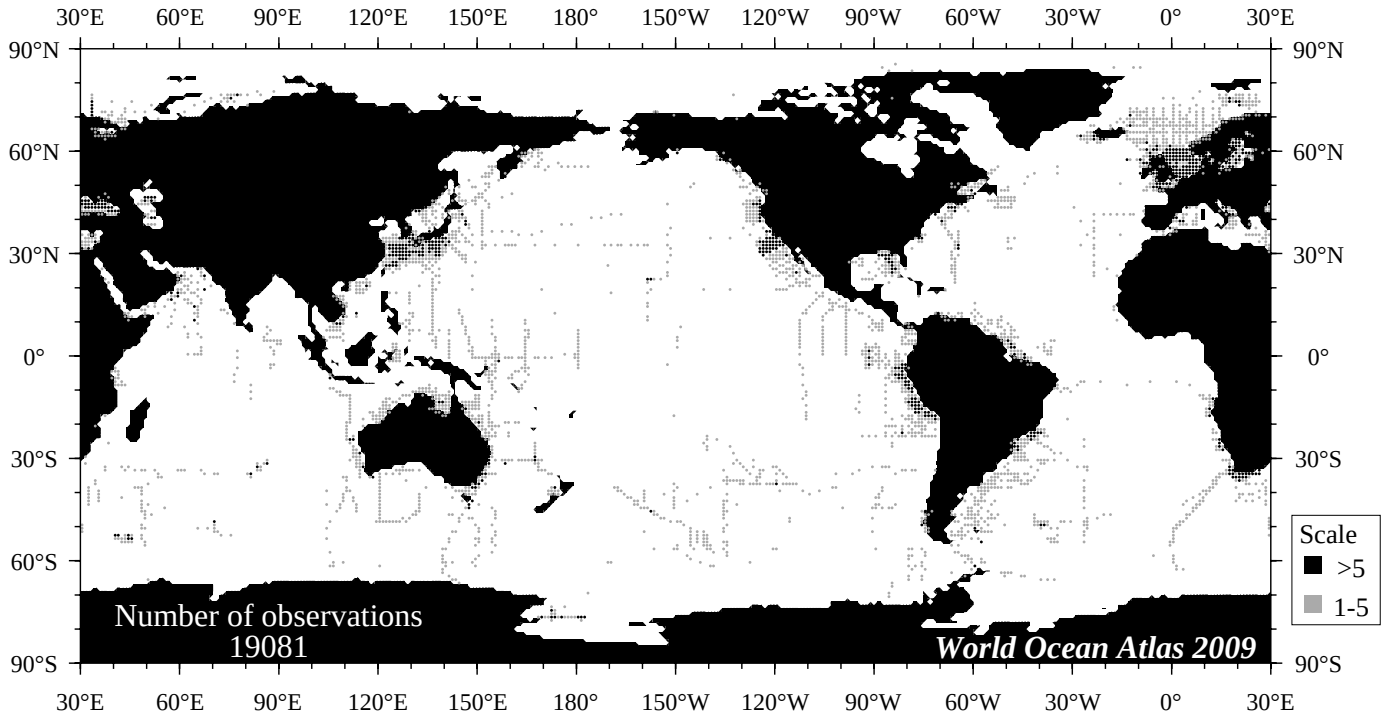

Fig I21 November silicate observations at the surface.

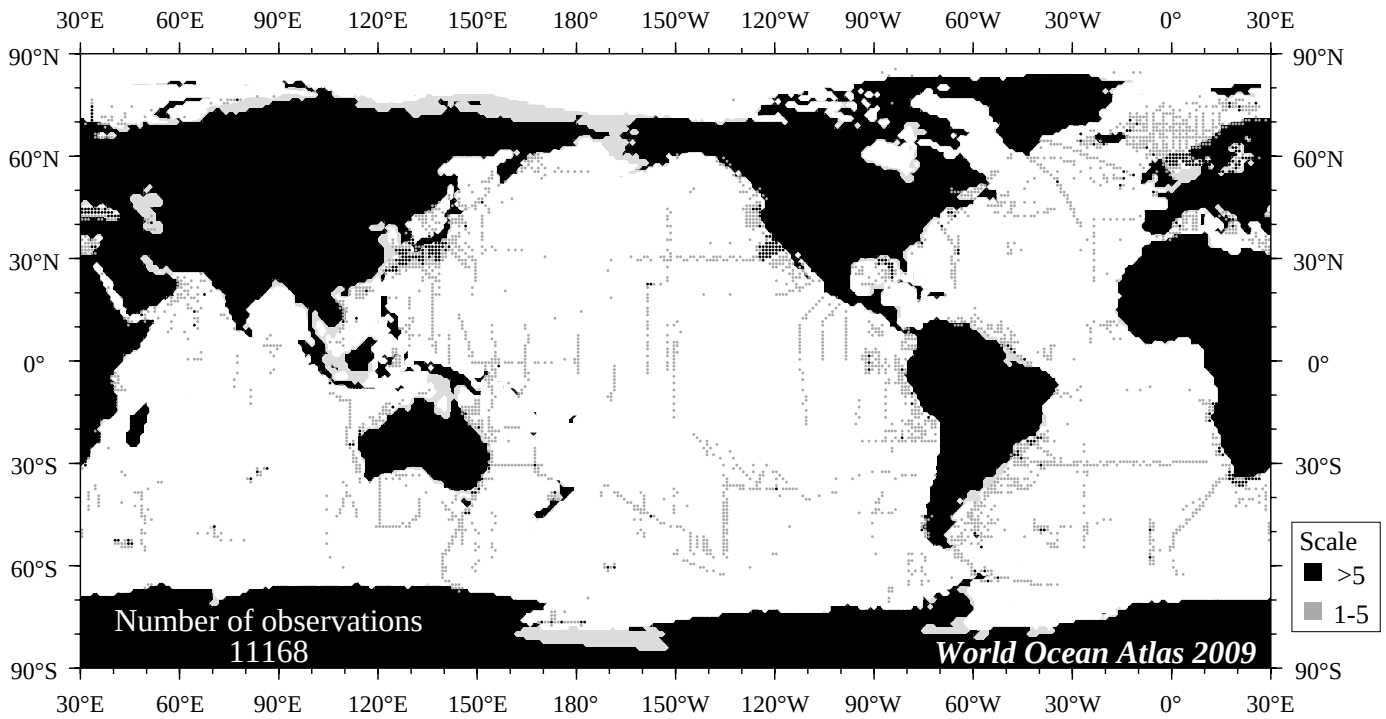

Fig I22 November silicate observations at 75 m. depth.

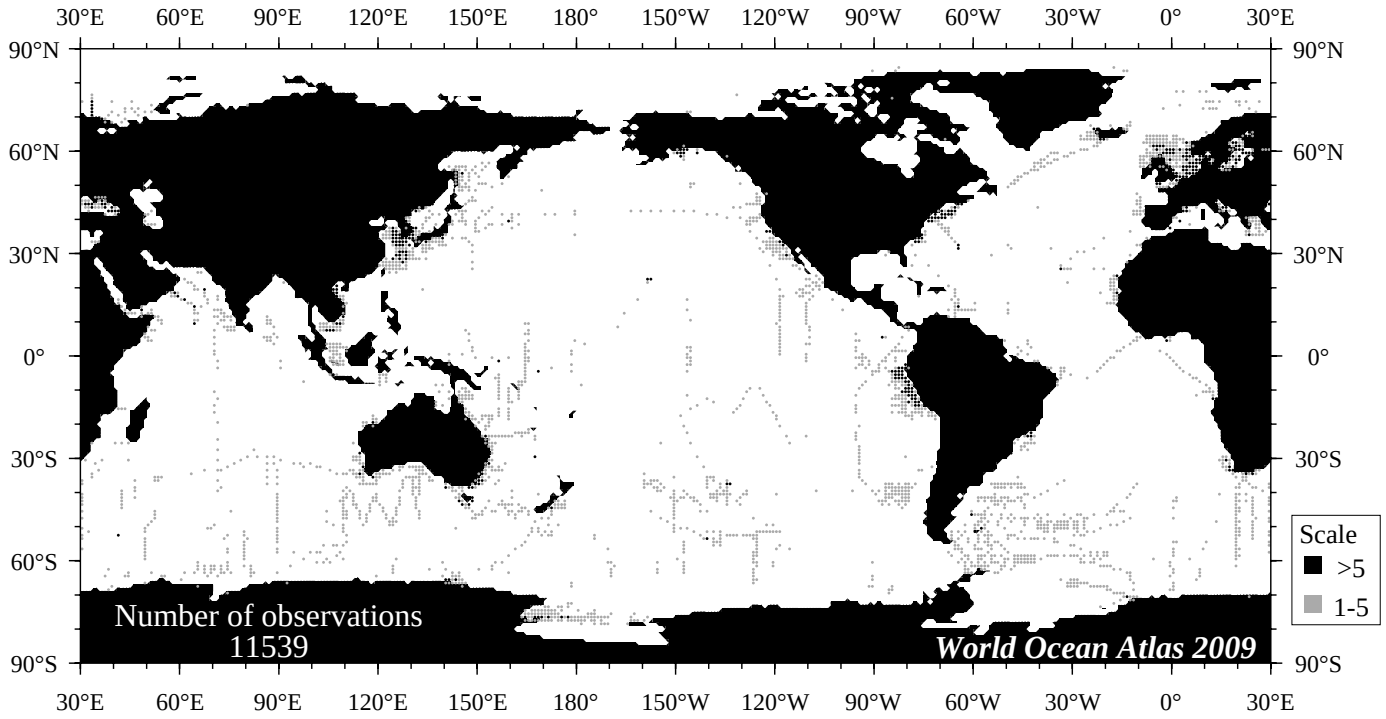

Fig I23 December silicate observations at the surface.

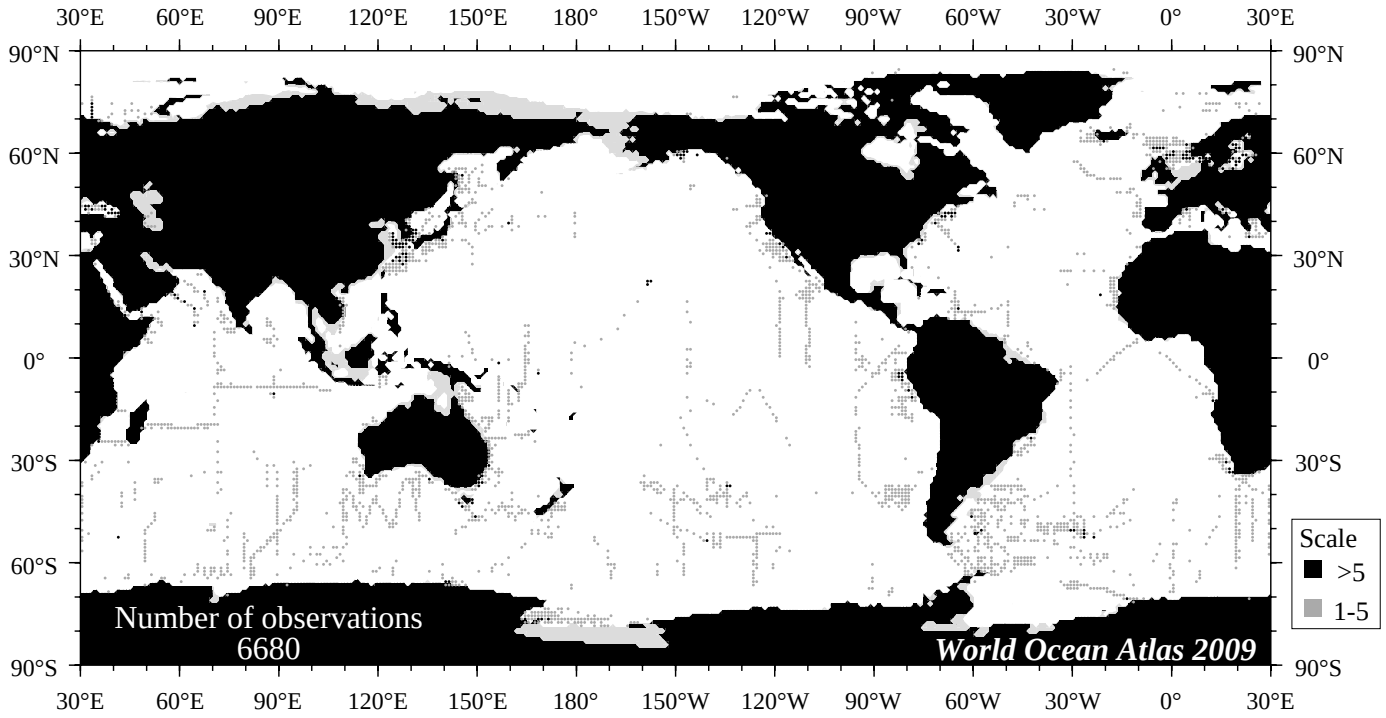

Fig I24 December silicate observations at 75 m. depth.

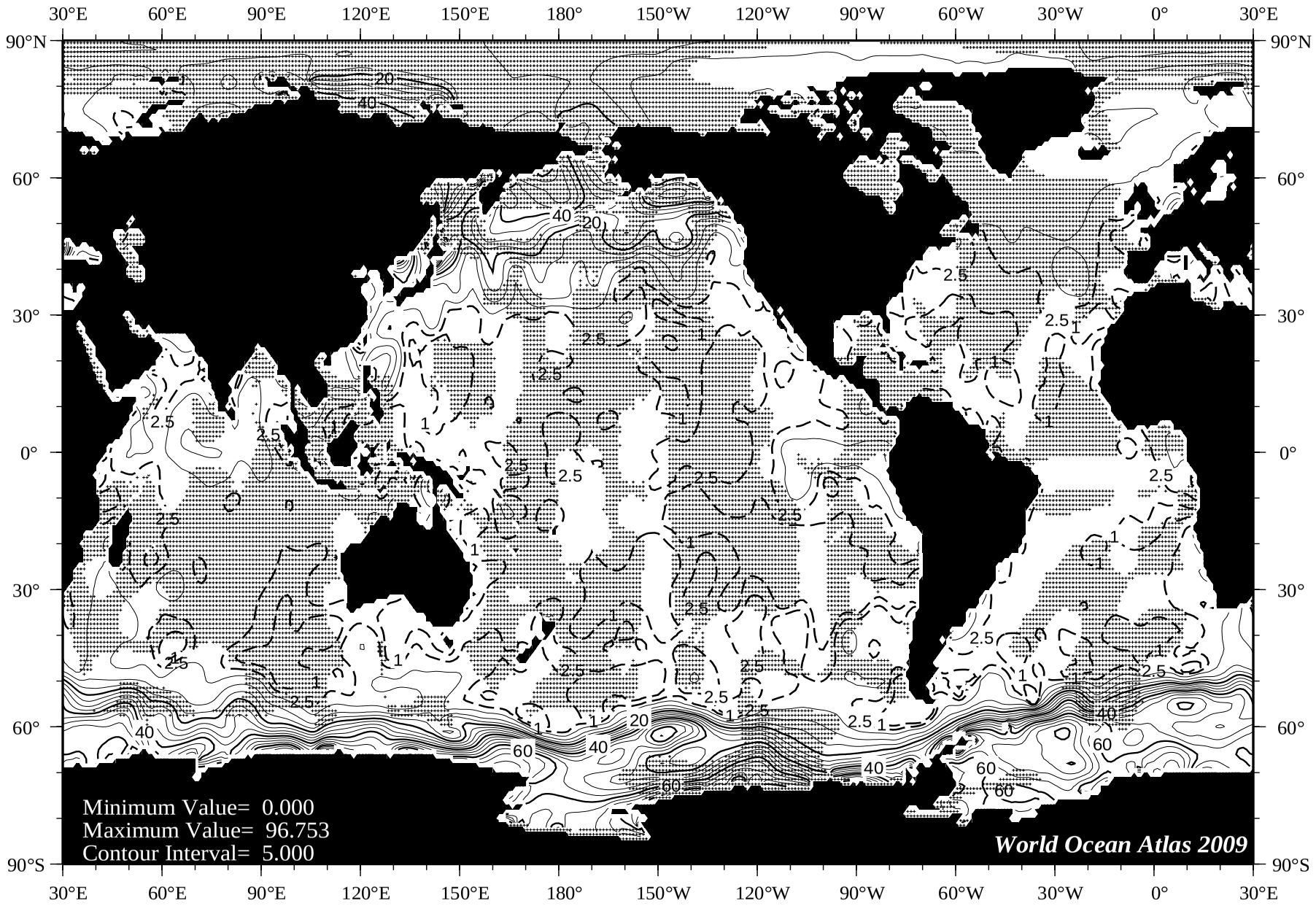

Fig I25 January mean silicate [umol/l] at the surface.

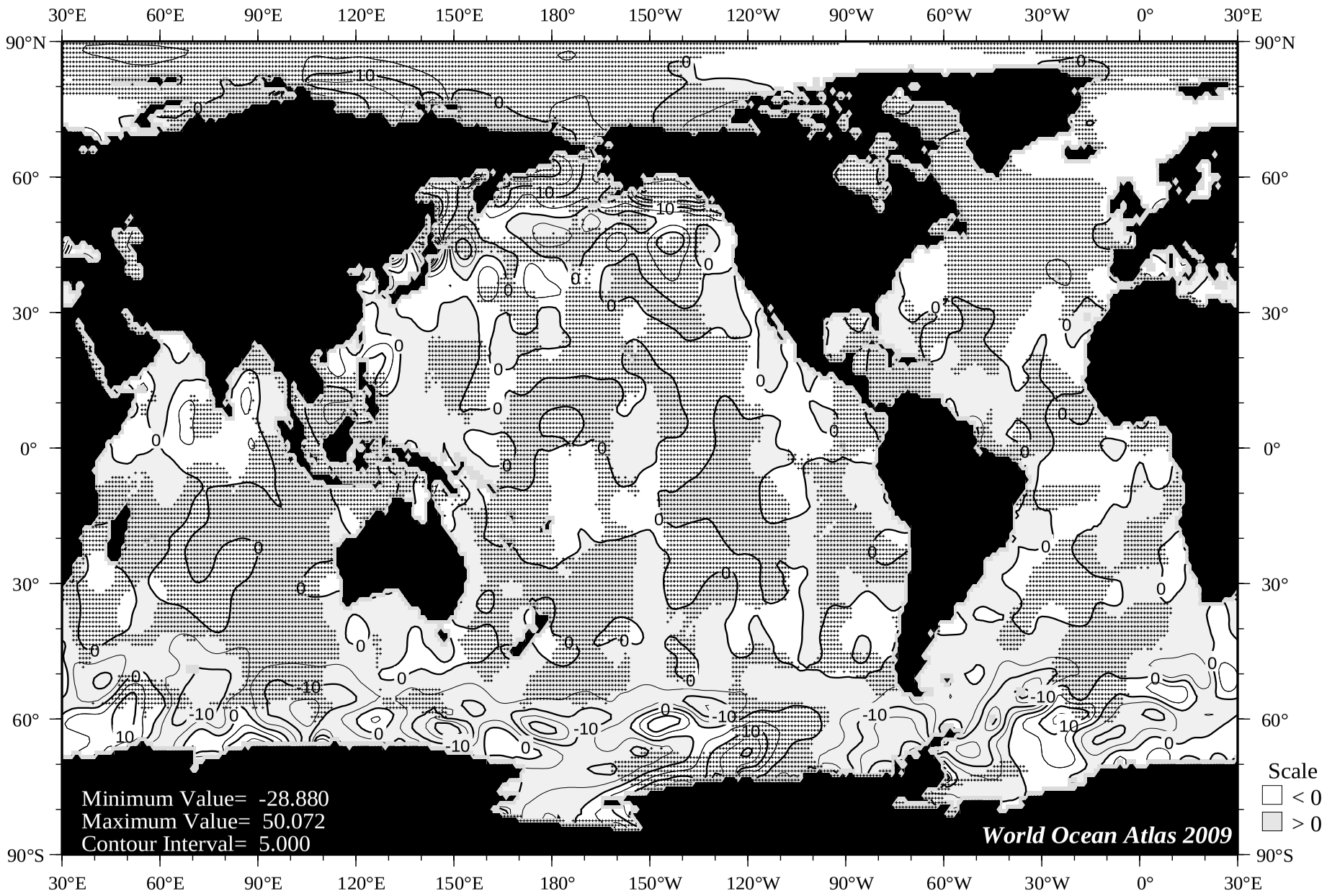

Fig I26 January minus annual silicate [umol/l] at the surface.

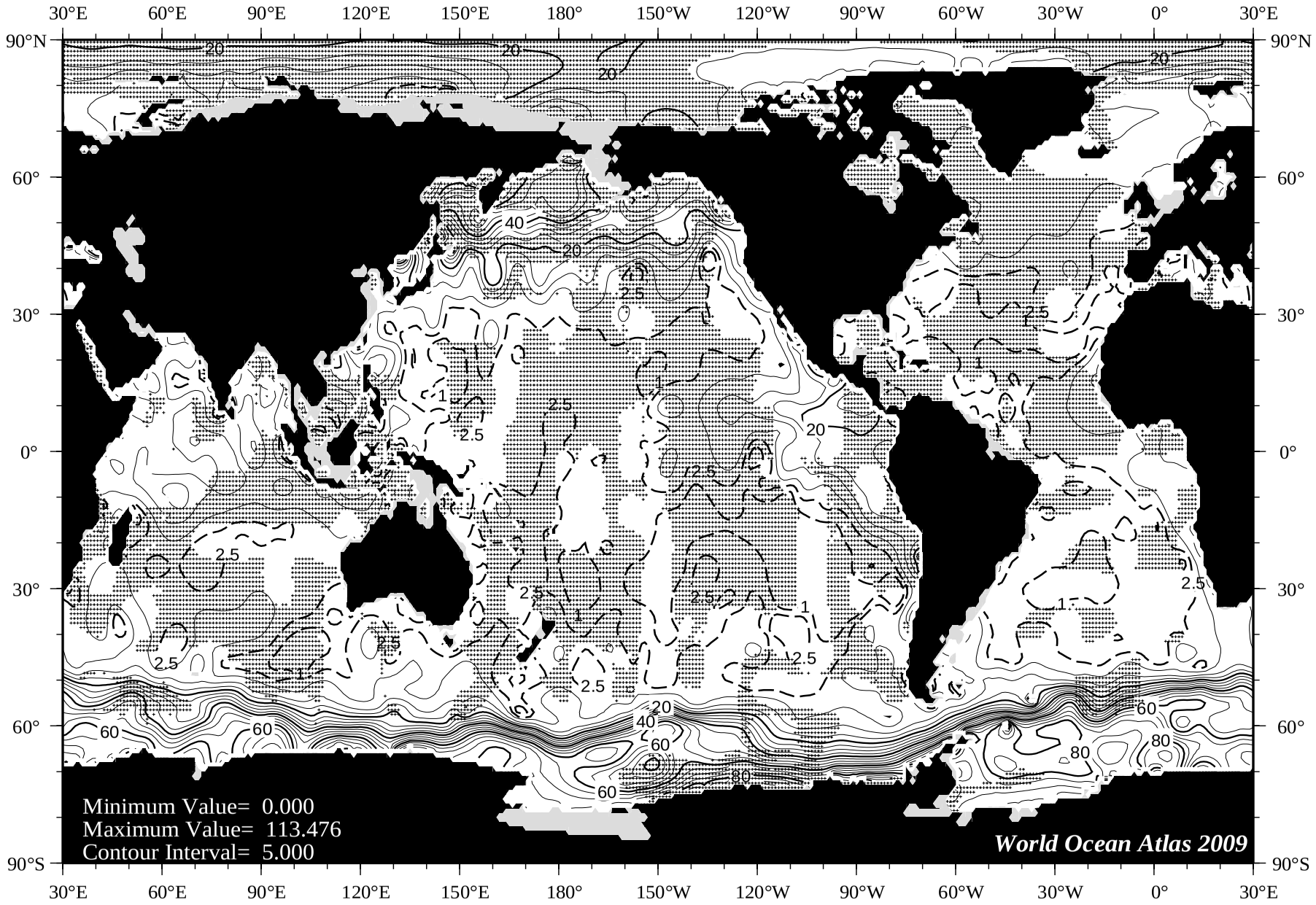

Fig I27 January mean silicate [umol/l] at 75 m. depth.

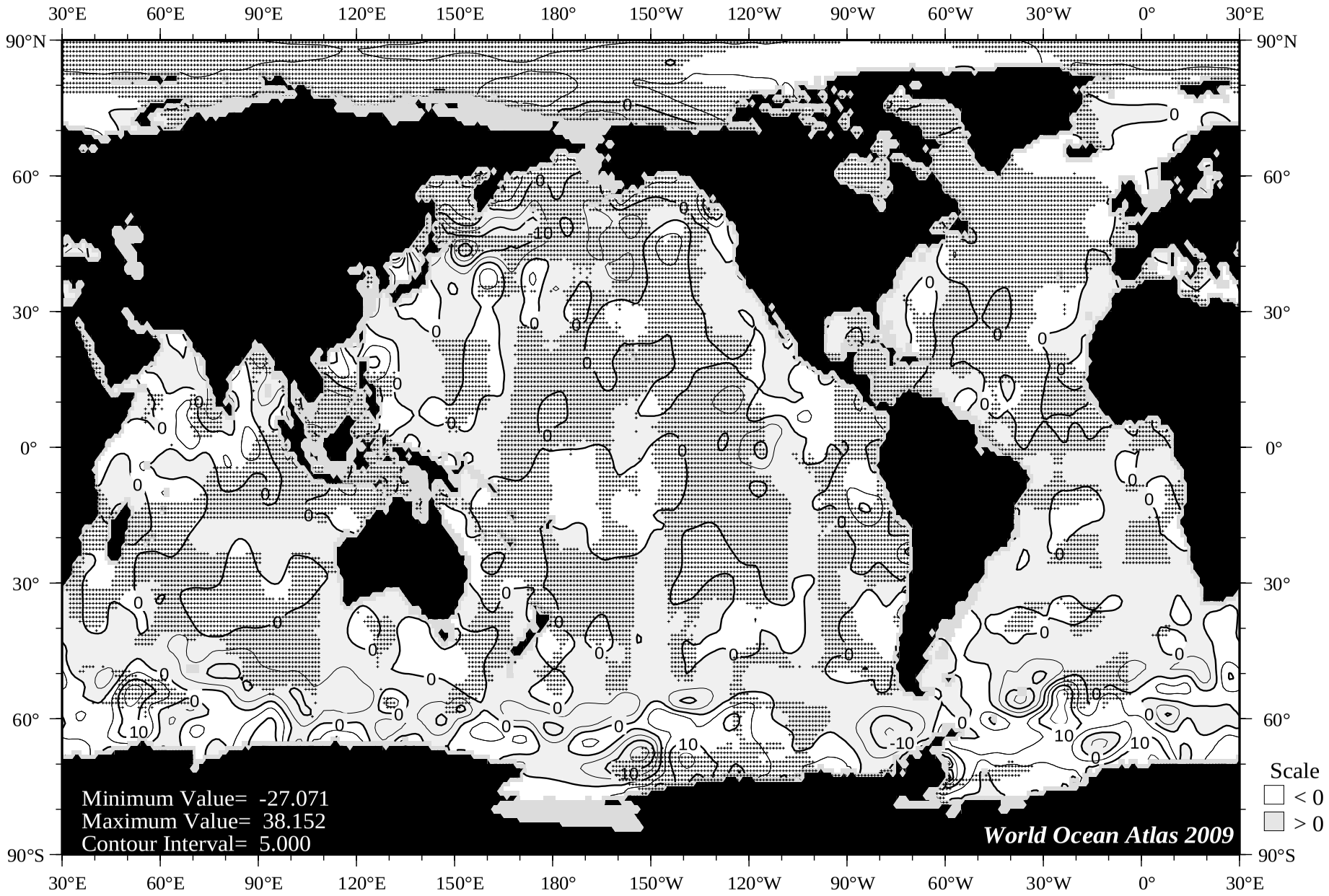

Fig I28 January minus annual silicate [umol/l] at 75 m. depth.

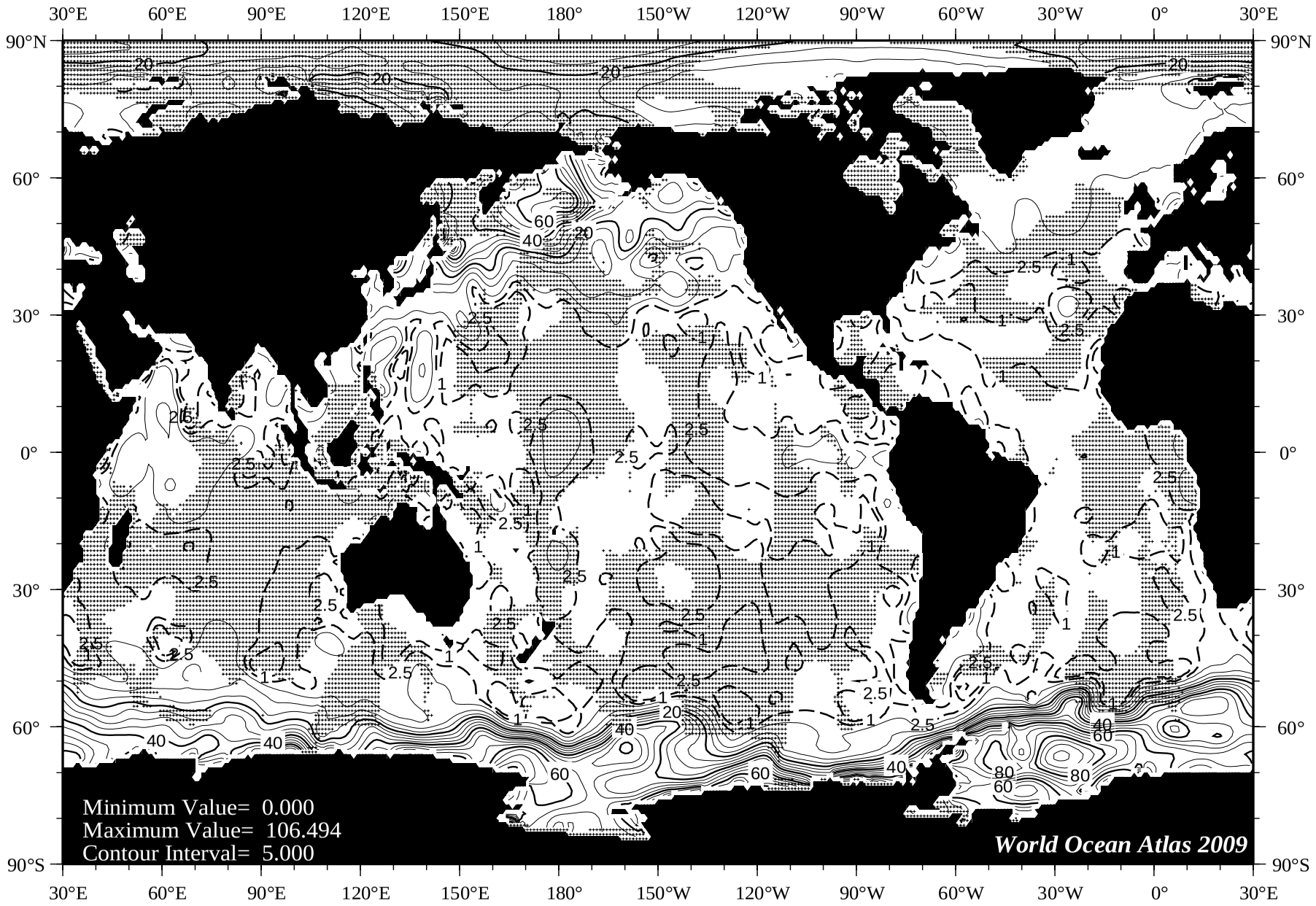

Fig I29 February mean silicate [umol/l] at the surface.

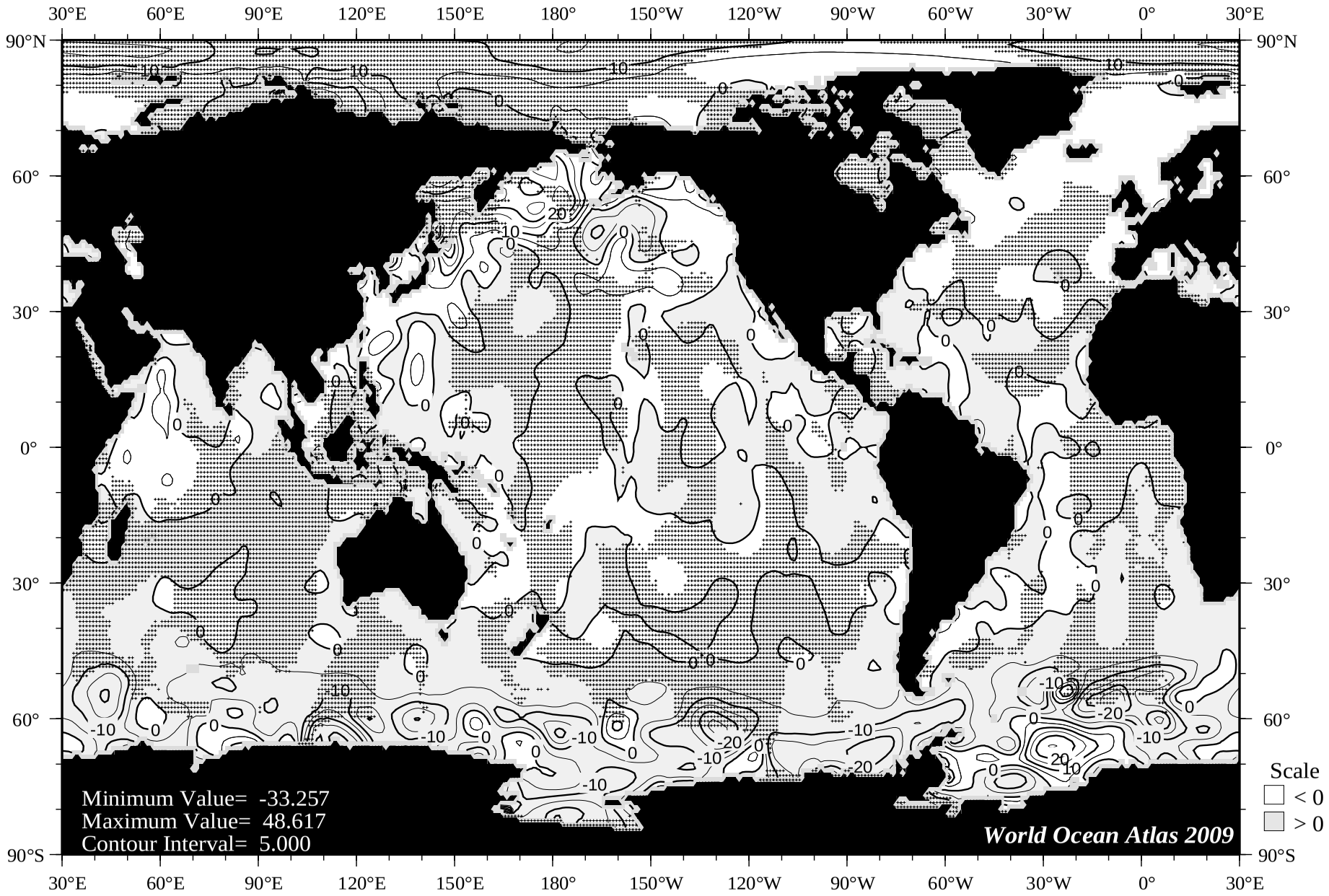

Fig I30 February minus annual silicate [umol/l] at the surface.

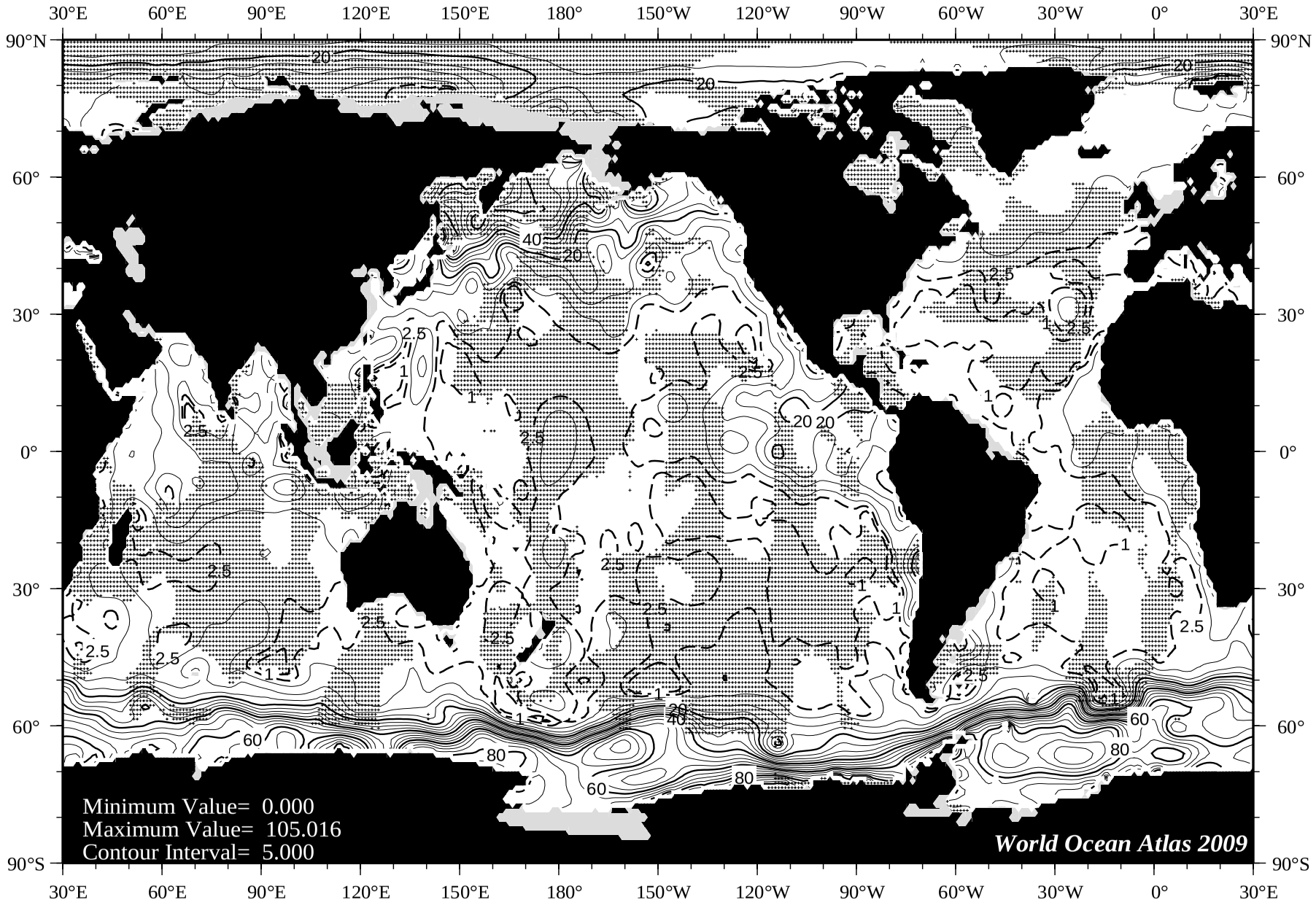

Fig I31 February mean silicate [umol/l] at 75 m. depth.

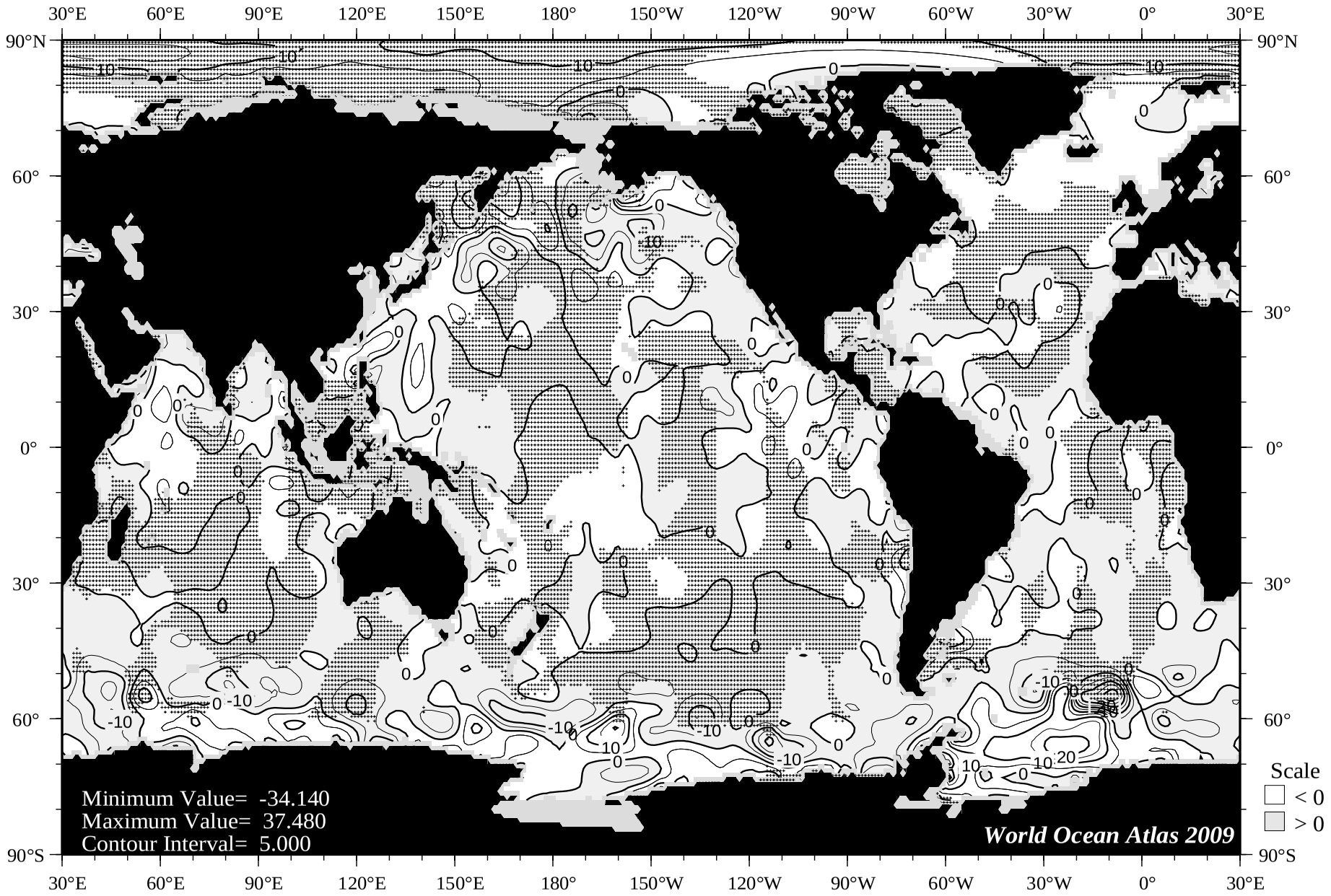

Fig I32 February minus annual silicate [umol/l] at 75 m. depth.

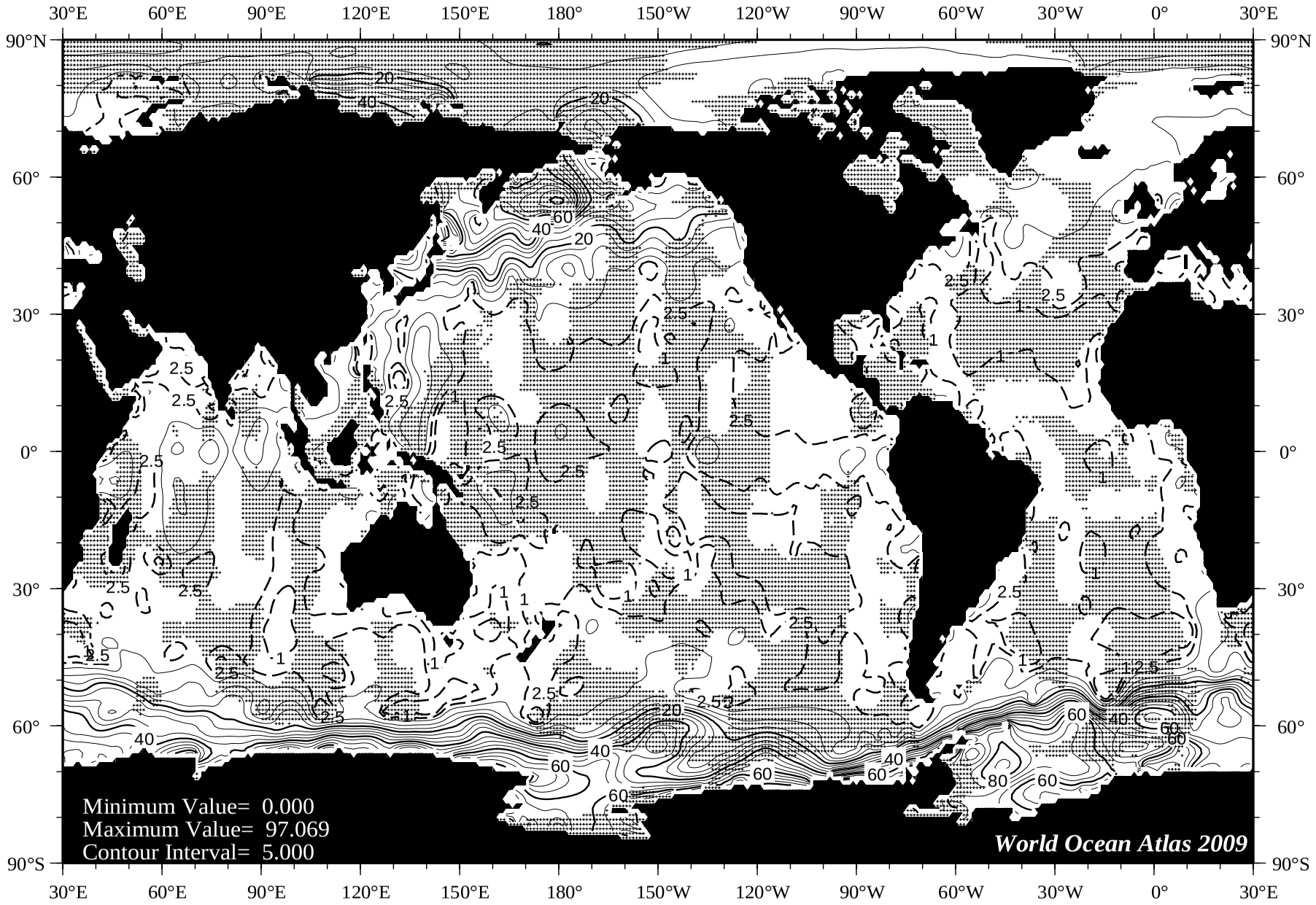

Fig I33 March mean silicate [umol/l] at the surface.

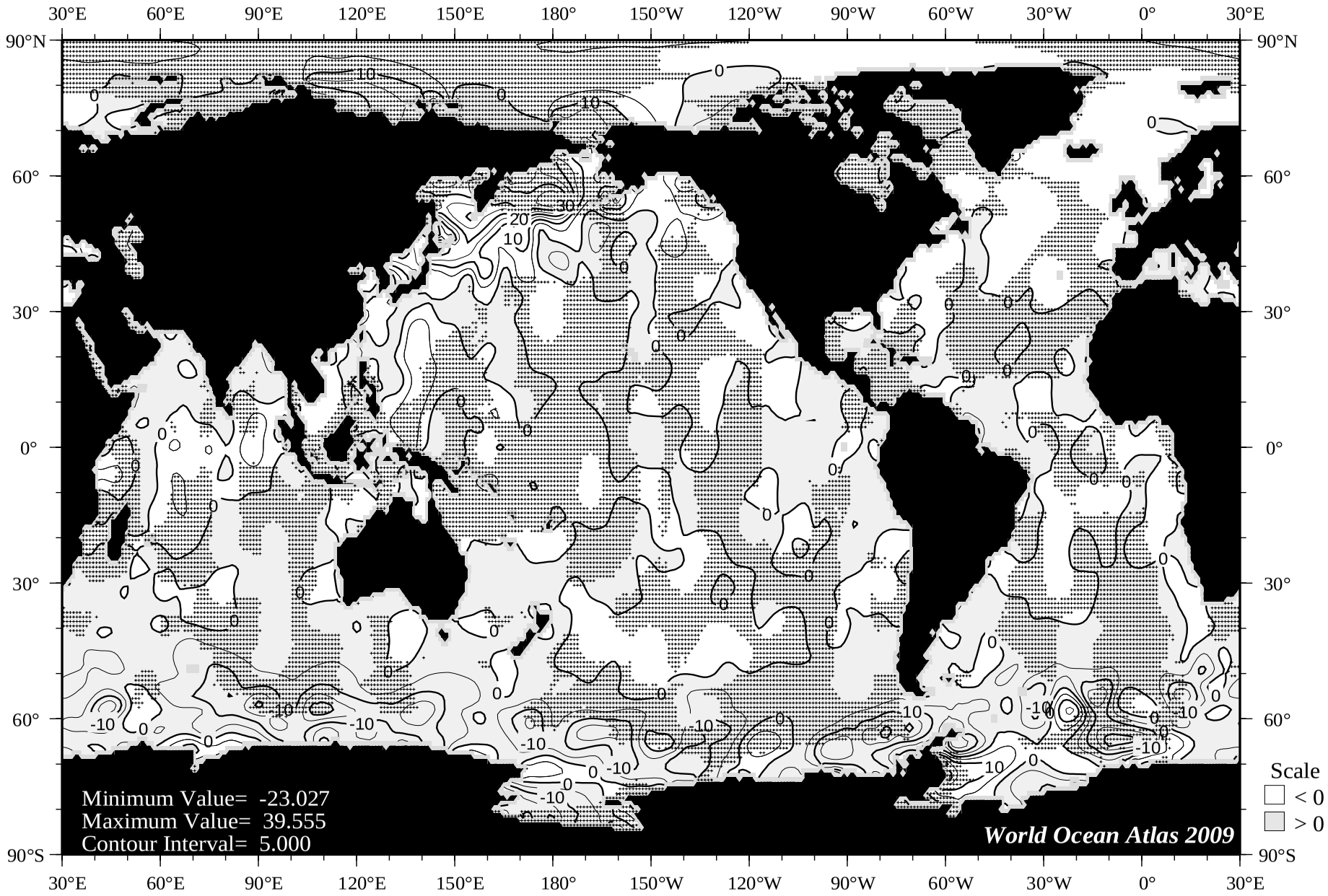

Fig I34 March minus annual silicate [umol/l] at the surface.

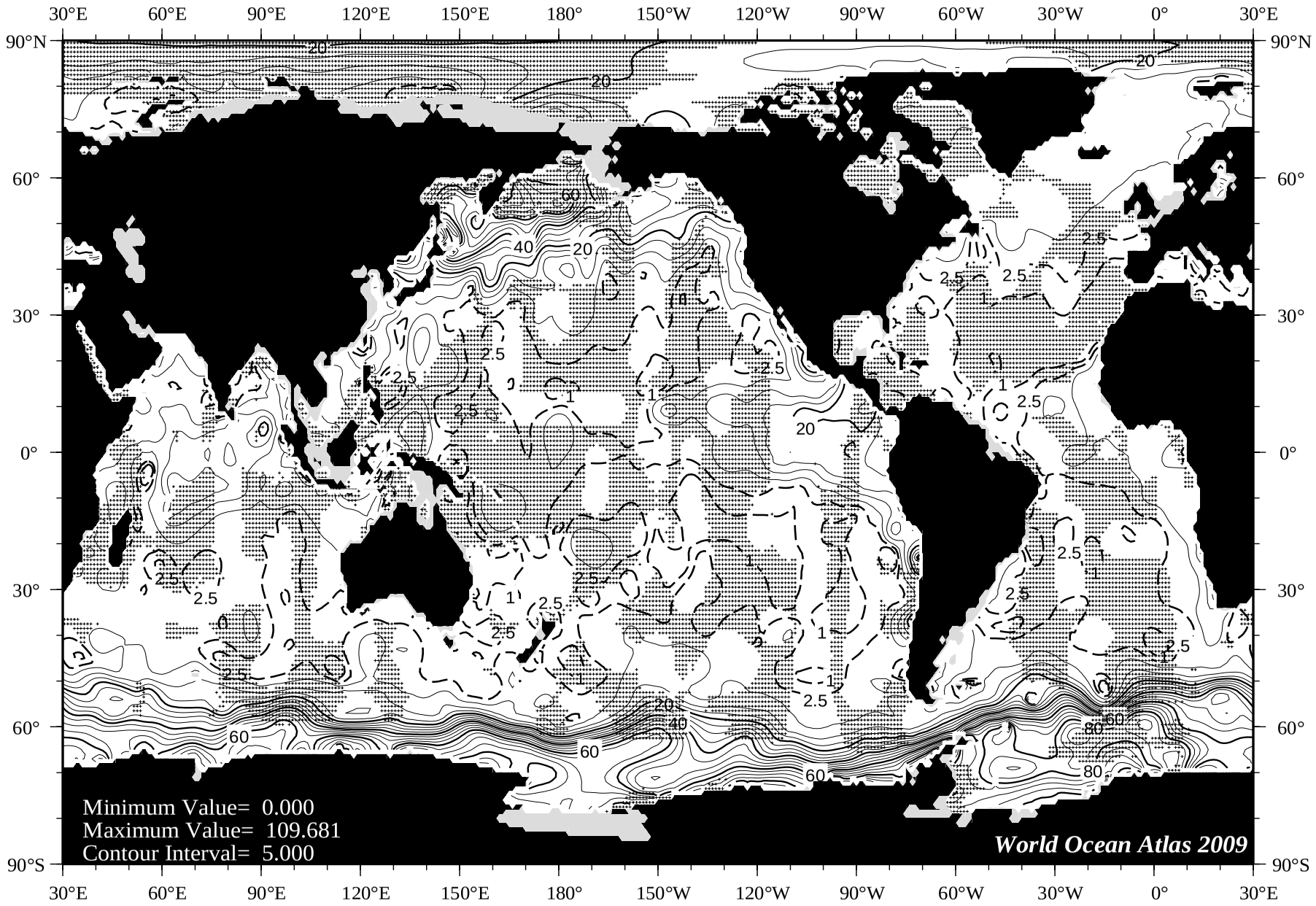

Fig I35 March mean silicate [umol/l] at 75 m. depth.

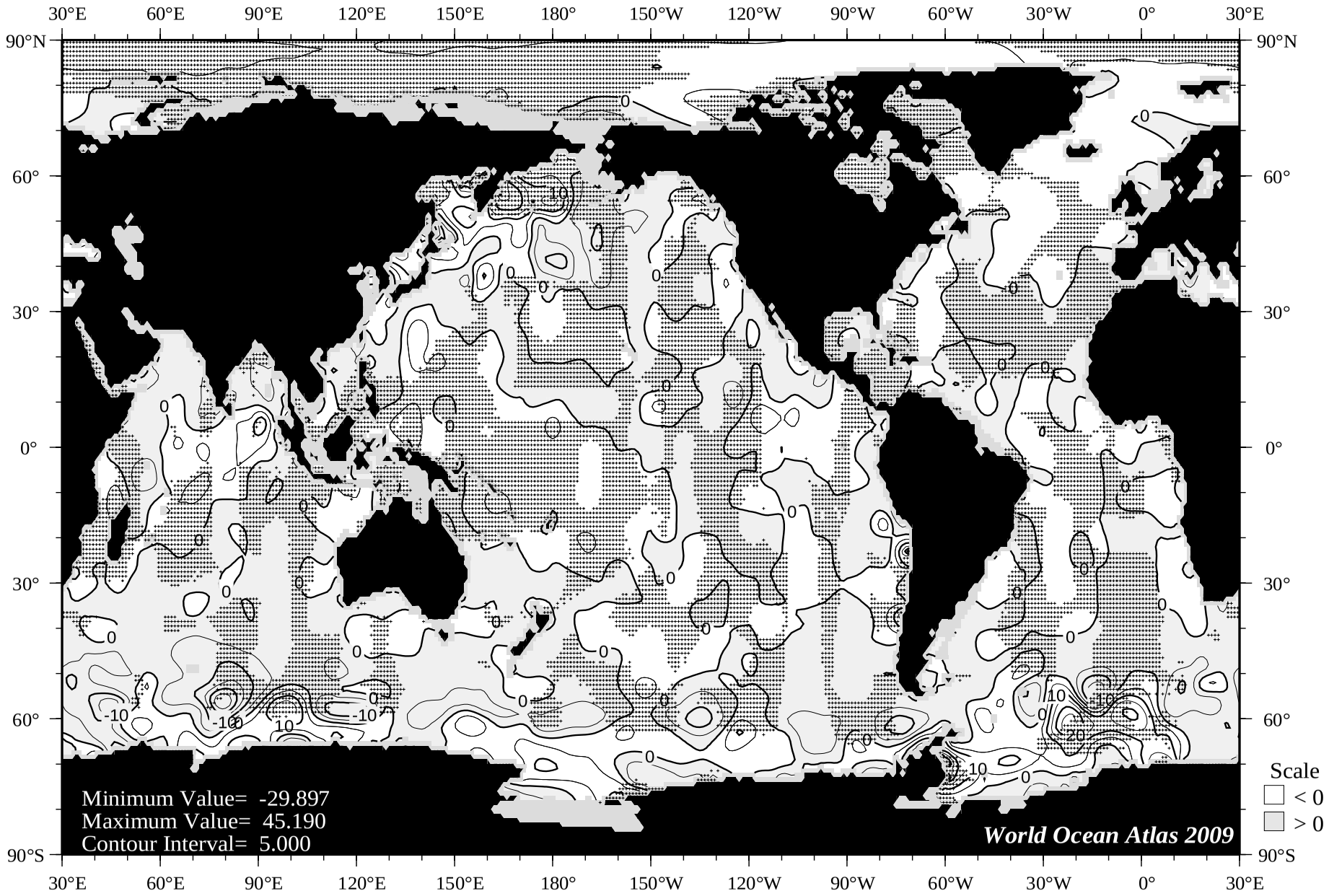

Fig I36 March minus annual silicate [umol/l] at 75 m. depth.

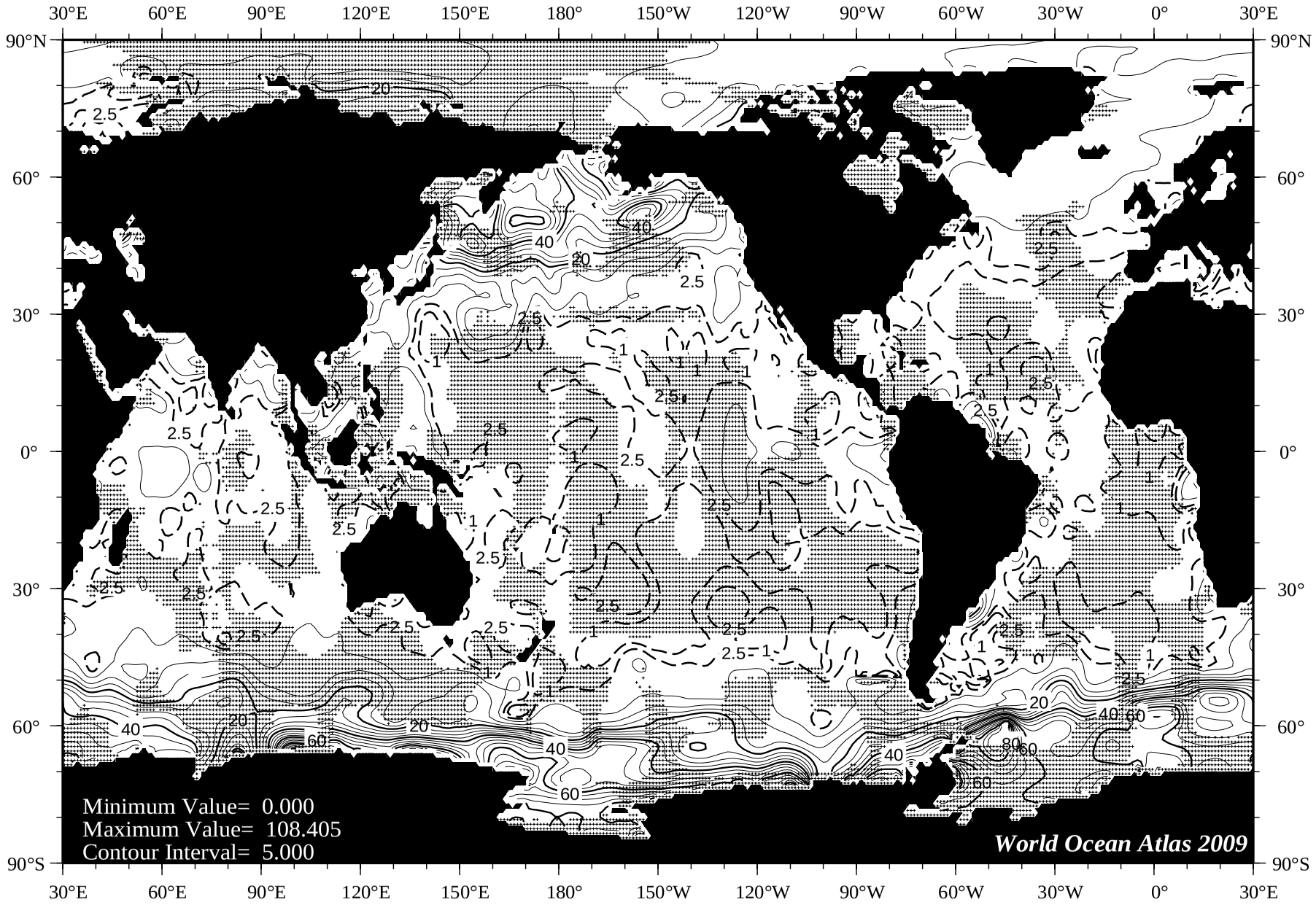

Fig I37 April mean silicate [umol/l] at the surface.

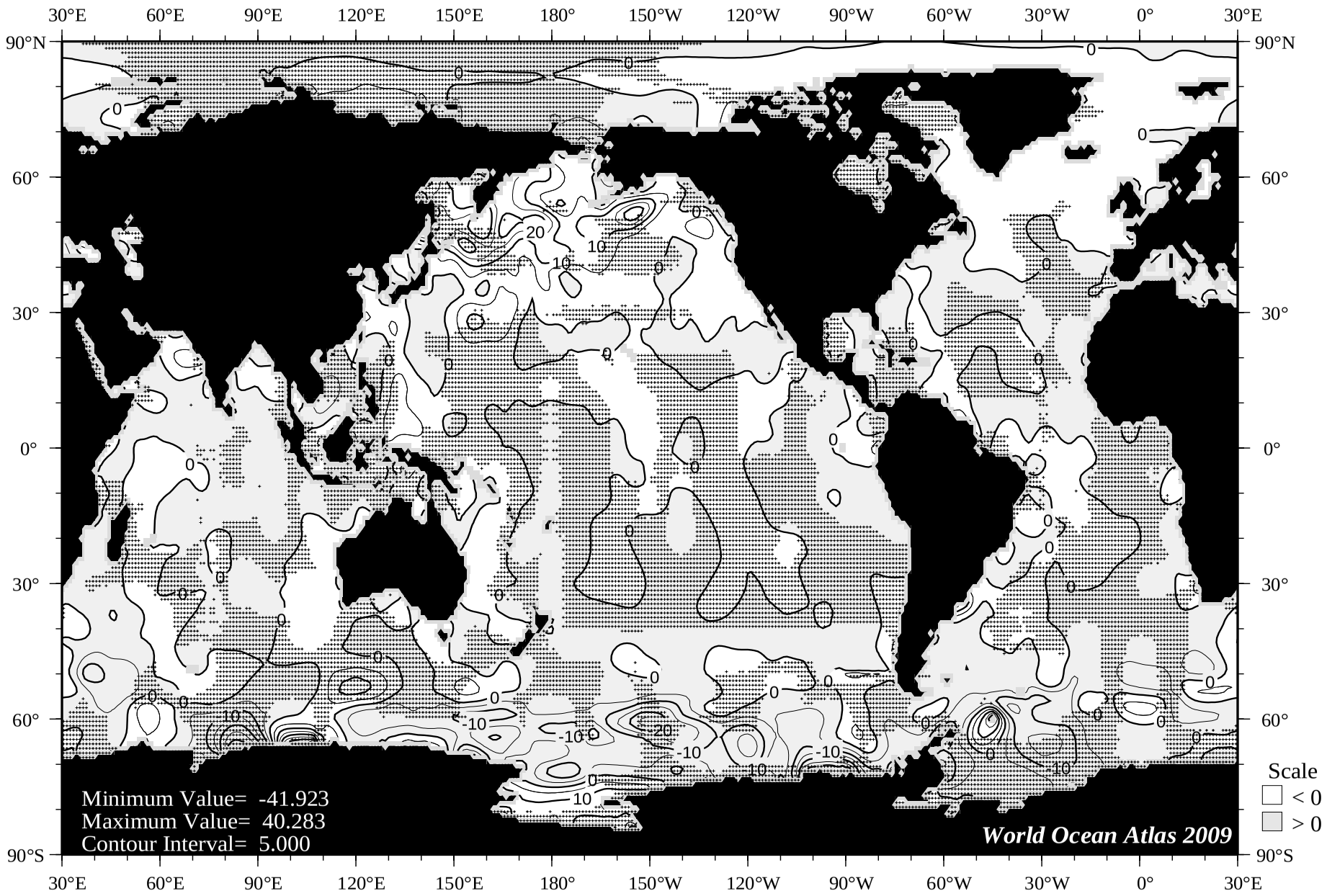

Fig I38 April minus annual silicate [umol/l] at the surface.

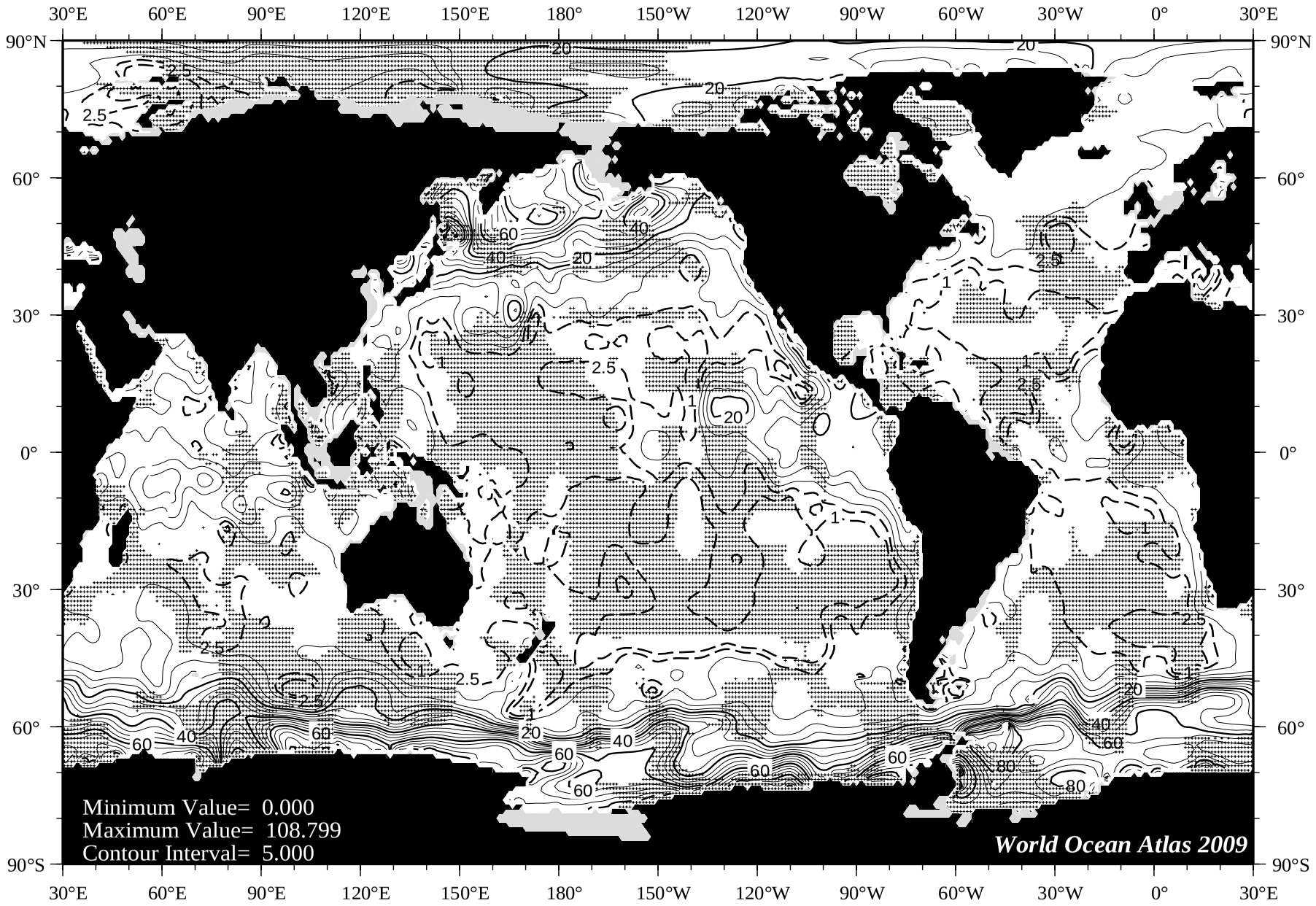

Fig I39 April mean silicate [umol/l] at 75 m. depth.

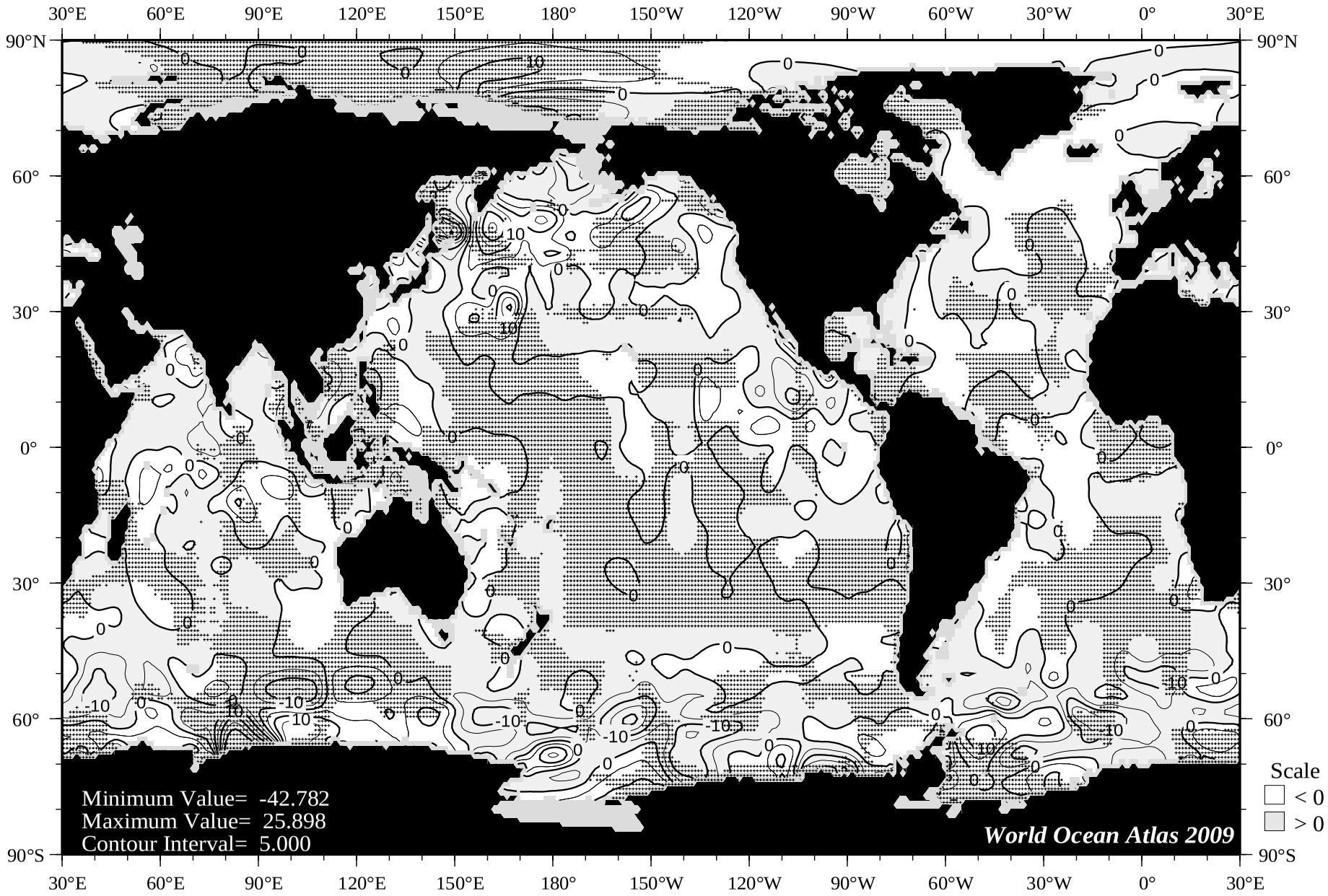

Fig I40 April minus annual silicate [umol/l] at 75 m. depth.

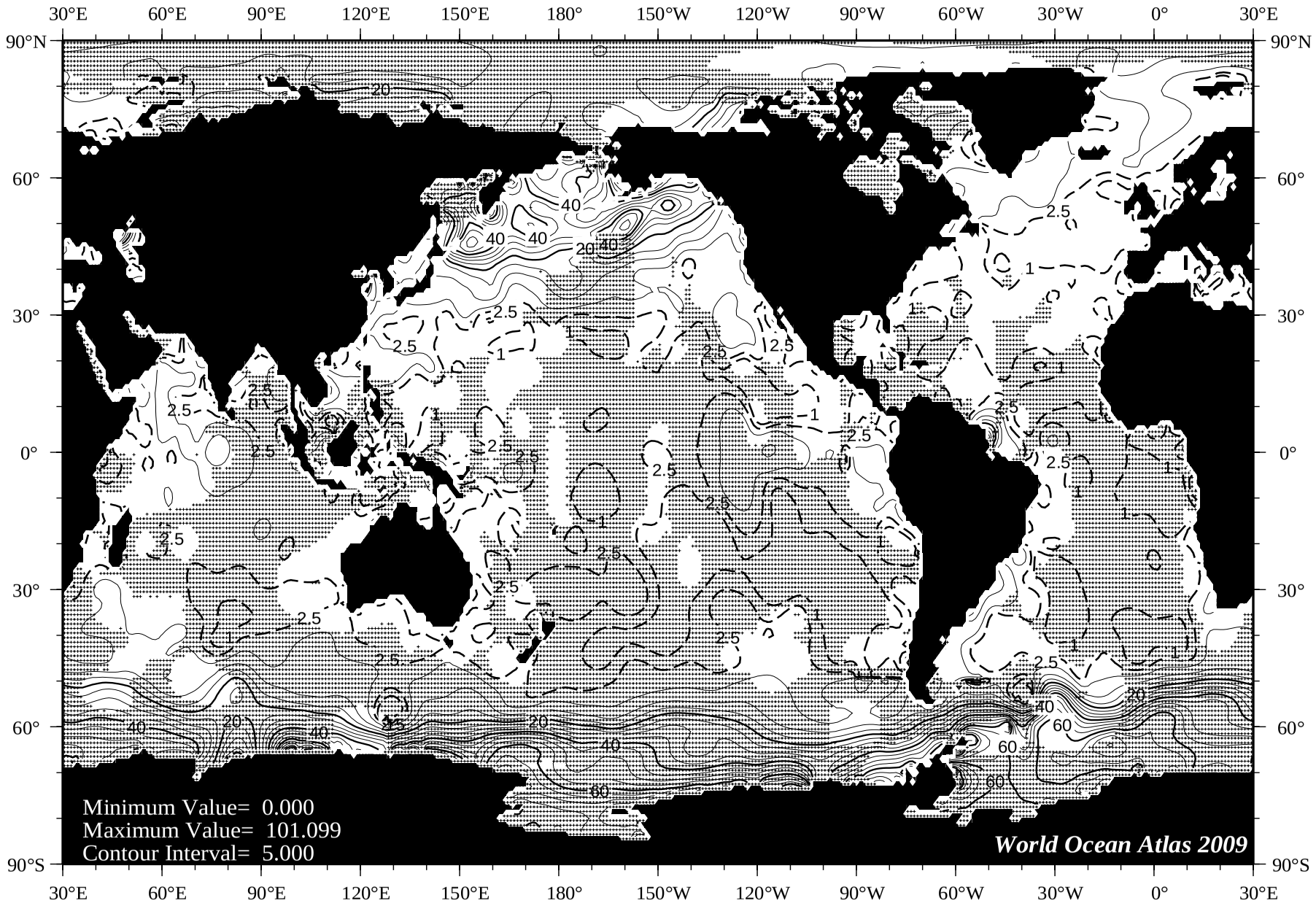

Fig I41 May mean silicate [umol/l] at the surface.

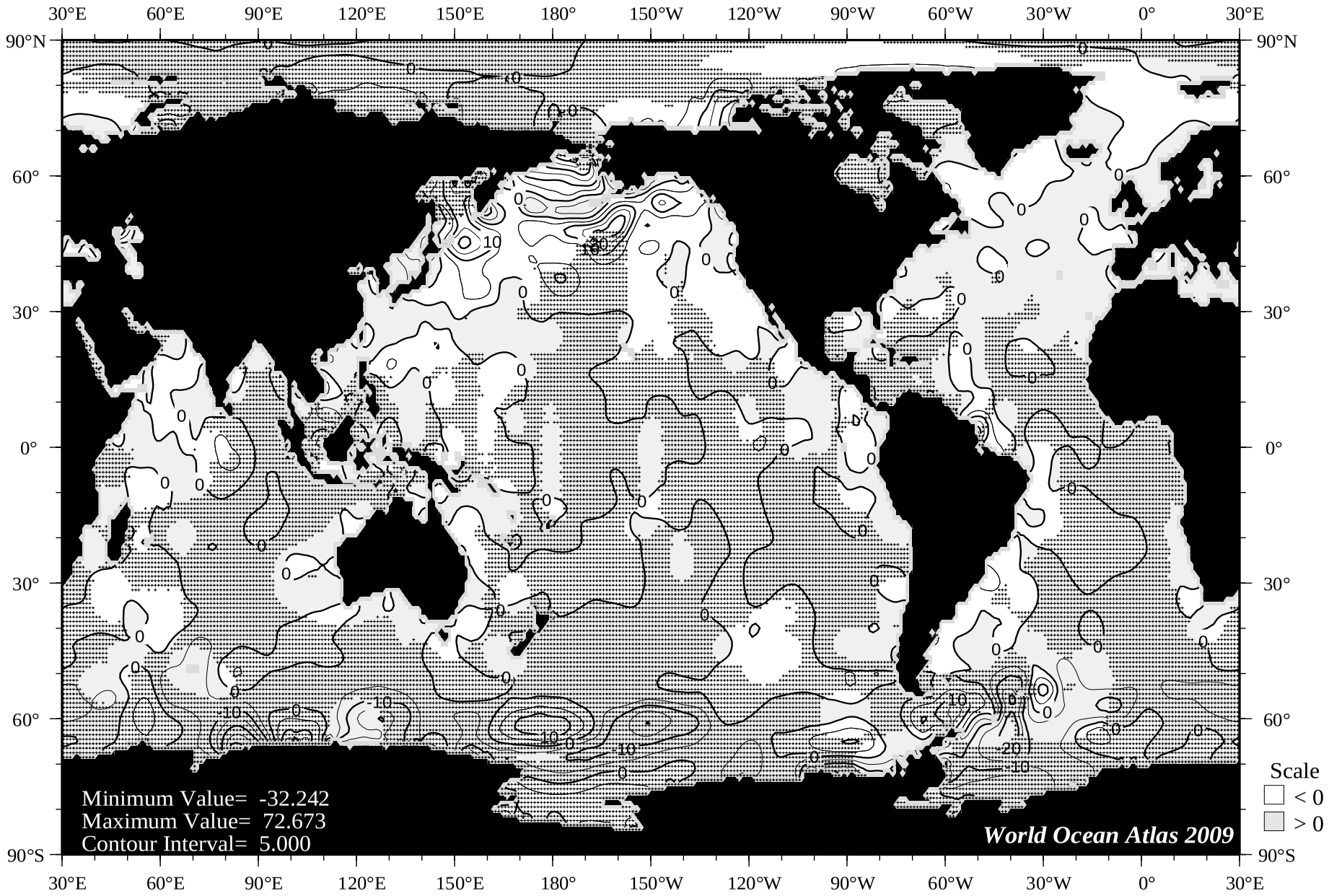

Fig I42 May minus annual silicate [umol/l] at the surface.

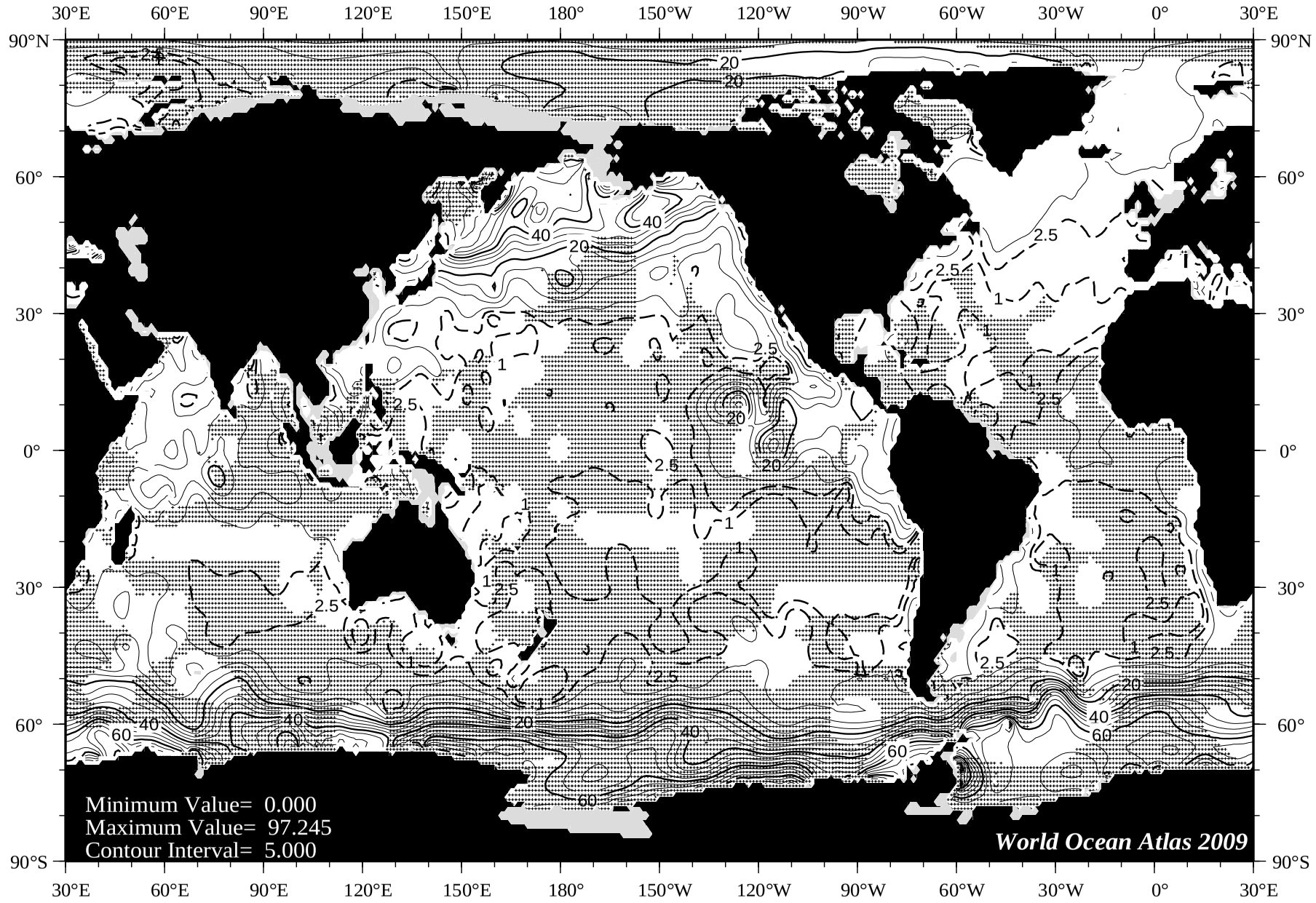

Fig I43 May mean silicate [umol/l] at 75 m. depth.

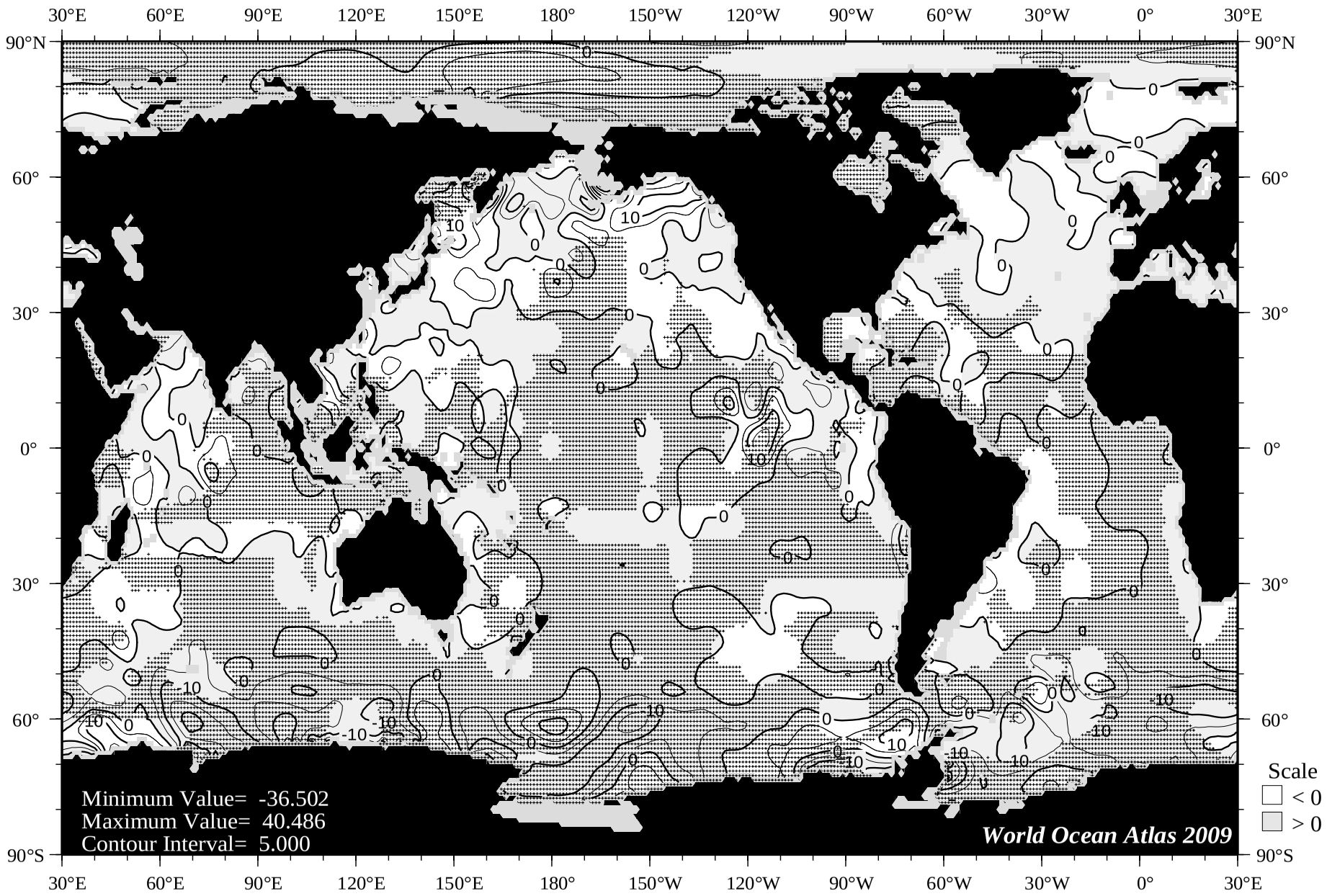

Fig I44 May minus annual silicate [umol/l] at 75 m. depth.

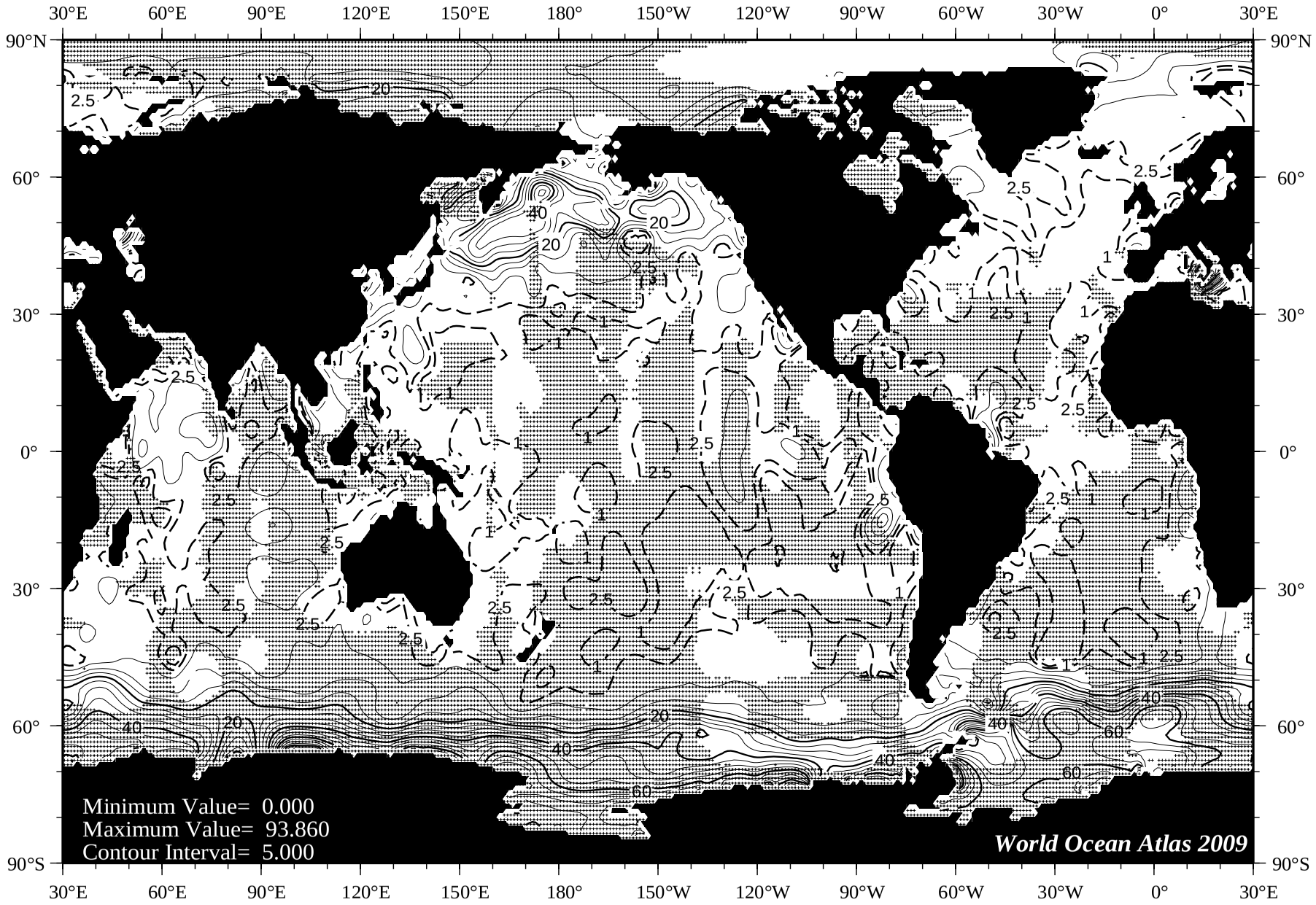

Fig I45 June mean silicate [umol/l] at the surface.

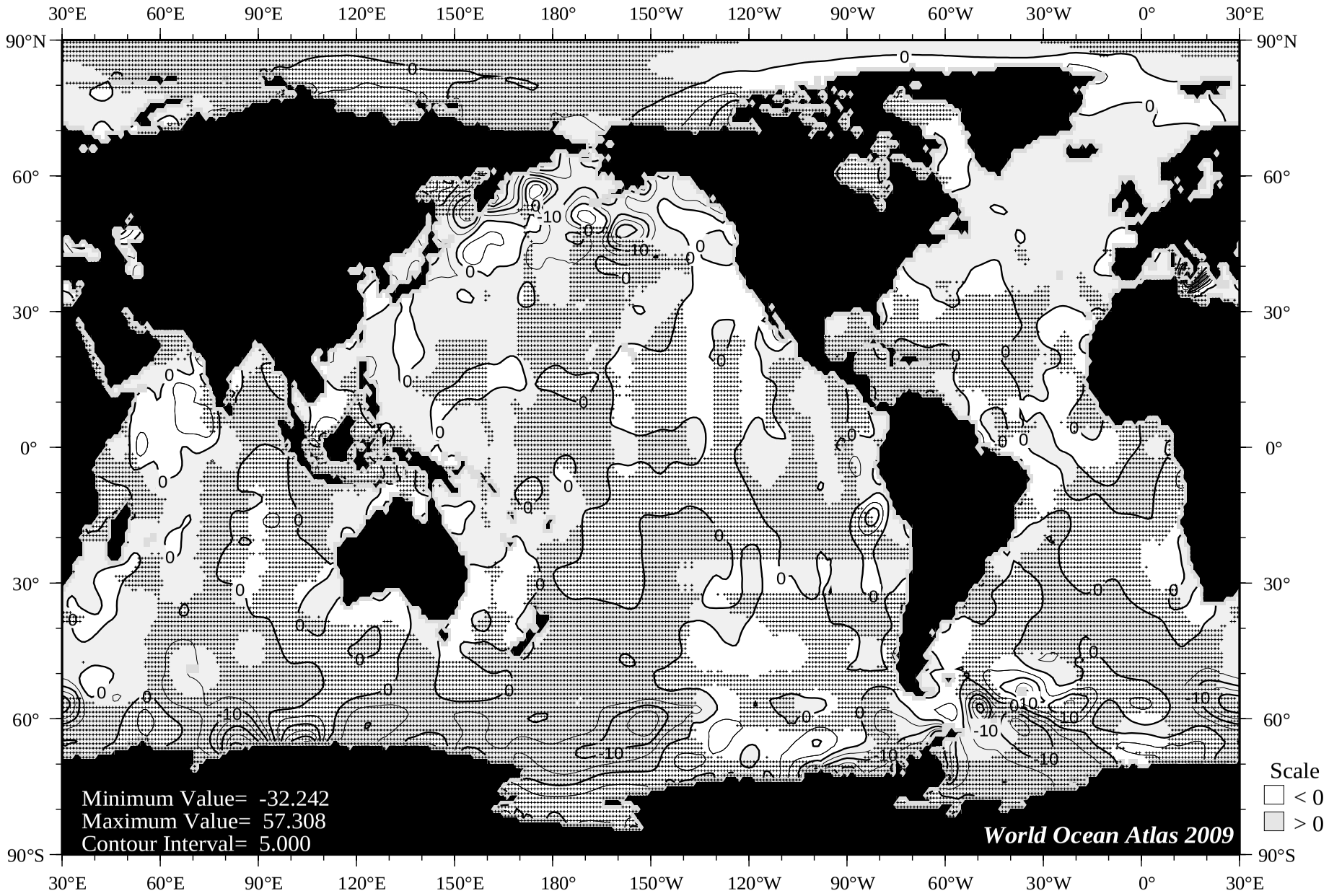

Fig I46 June minus annual silicate [umol/l] at the surface.

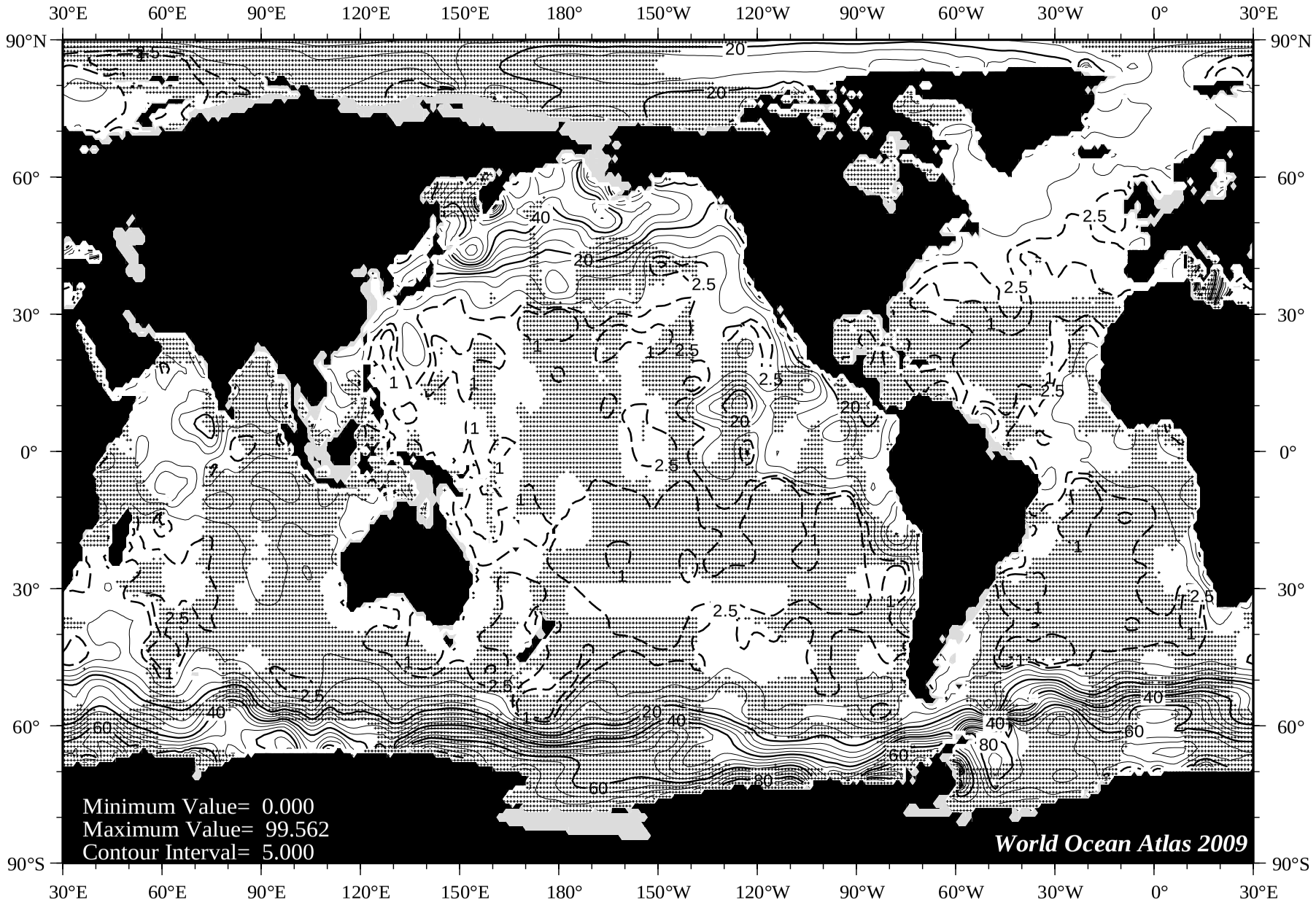

Fig I47 June mean silicate [umol/l] at 75 m. depth.

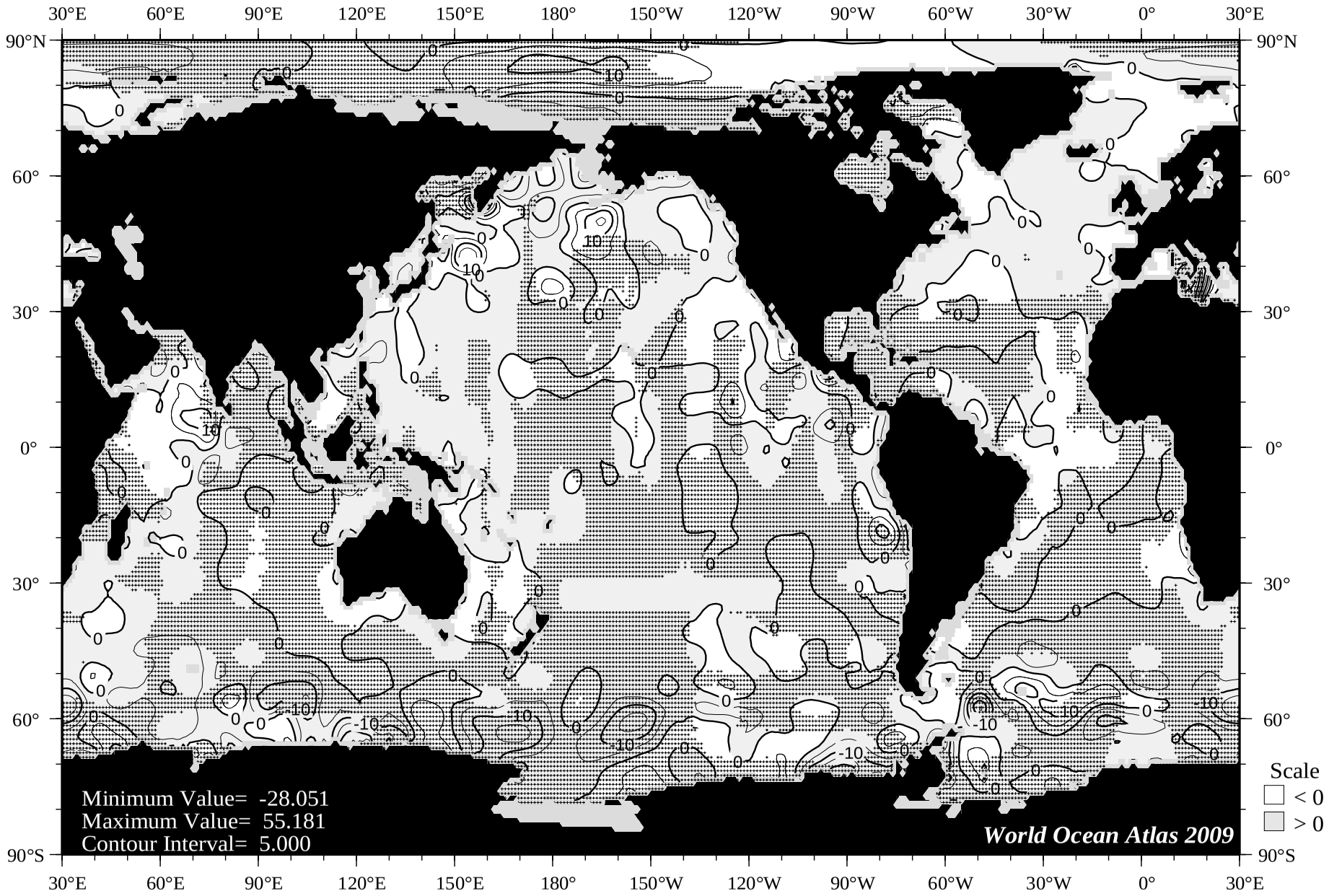

Fig I48 June minus annual silicate [umol/l] at 75 m. depth.

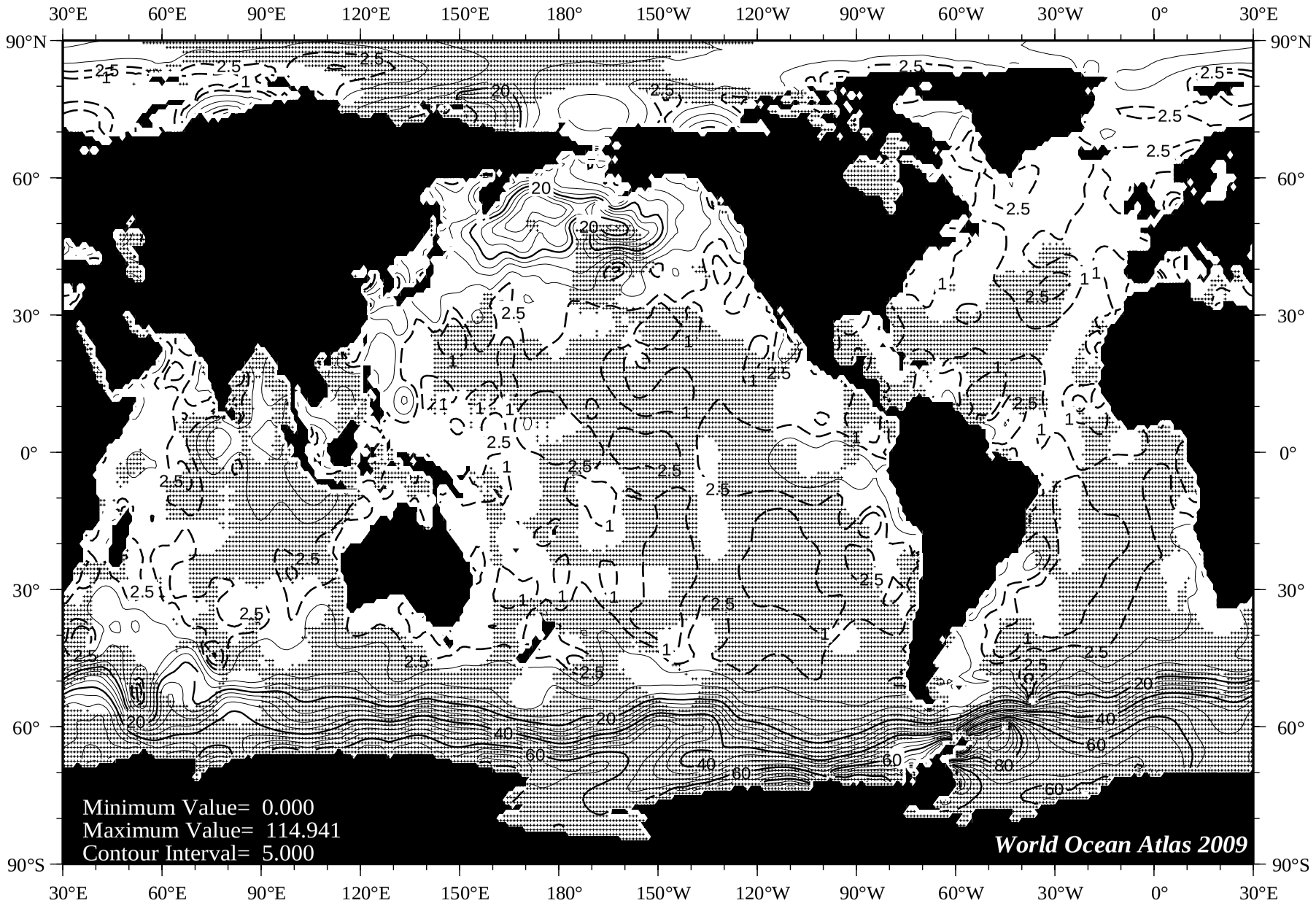

Fig I49 July mean silicate [umol/l] at the surface.

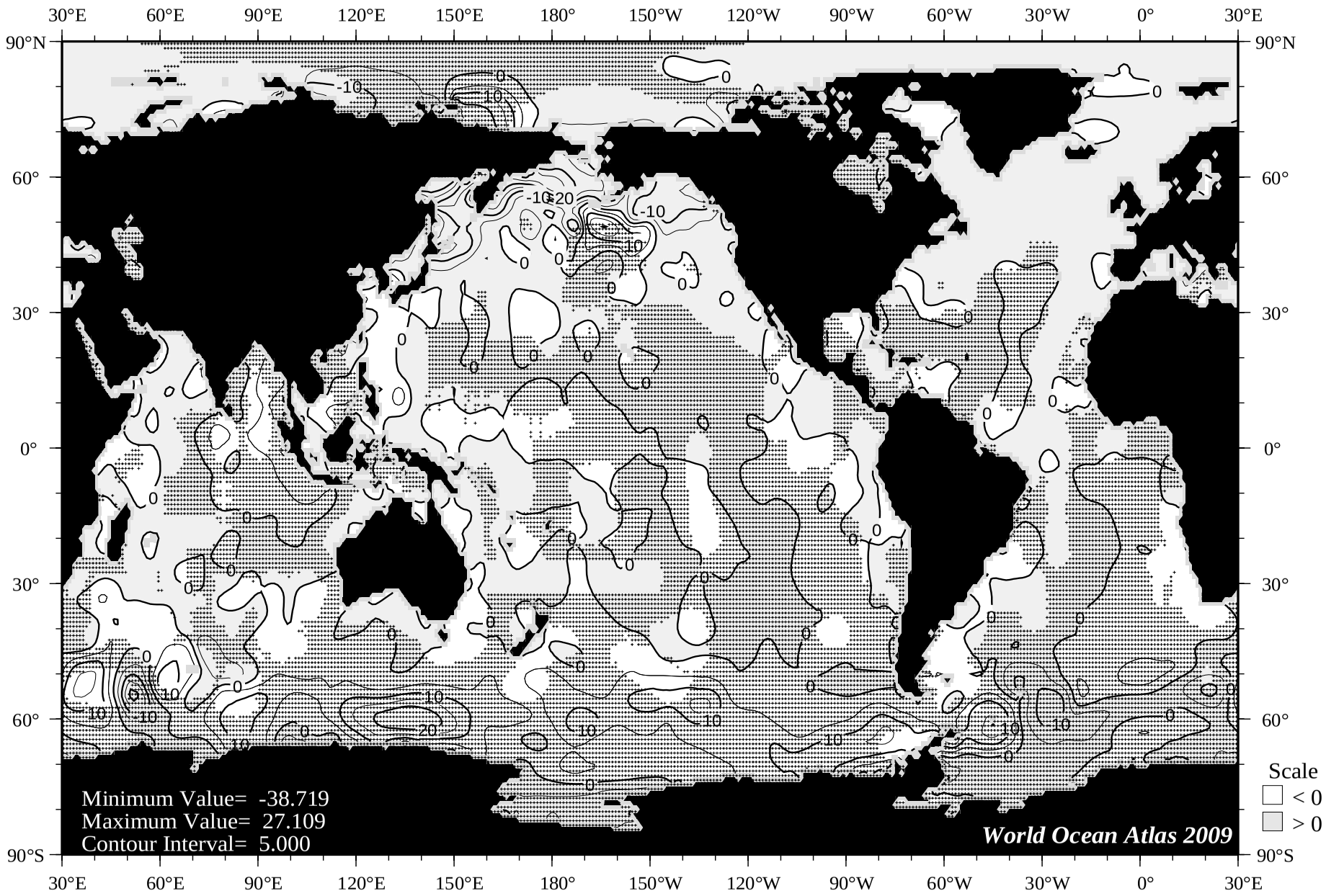

Fig I50 July minus annual silicate [umol/l] at the surface.

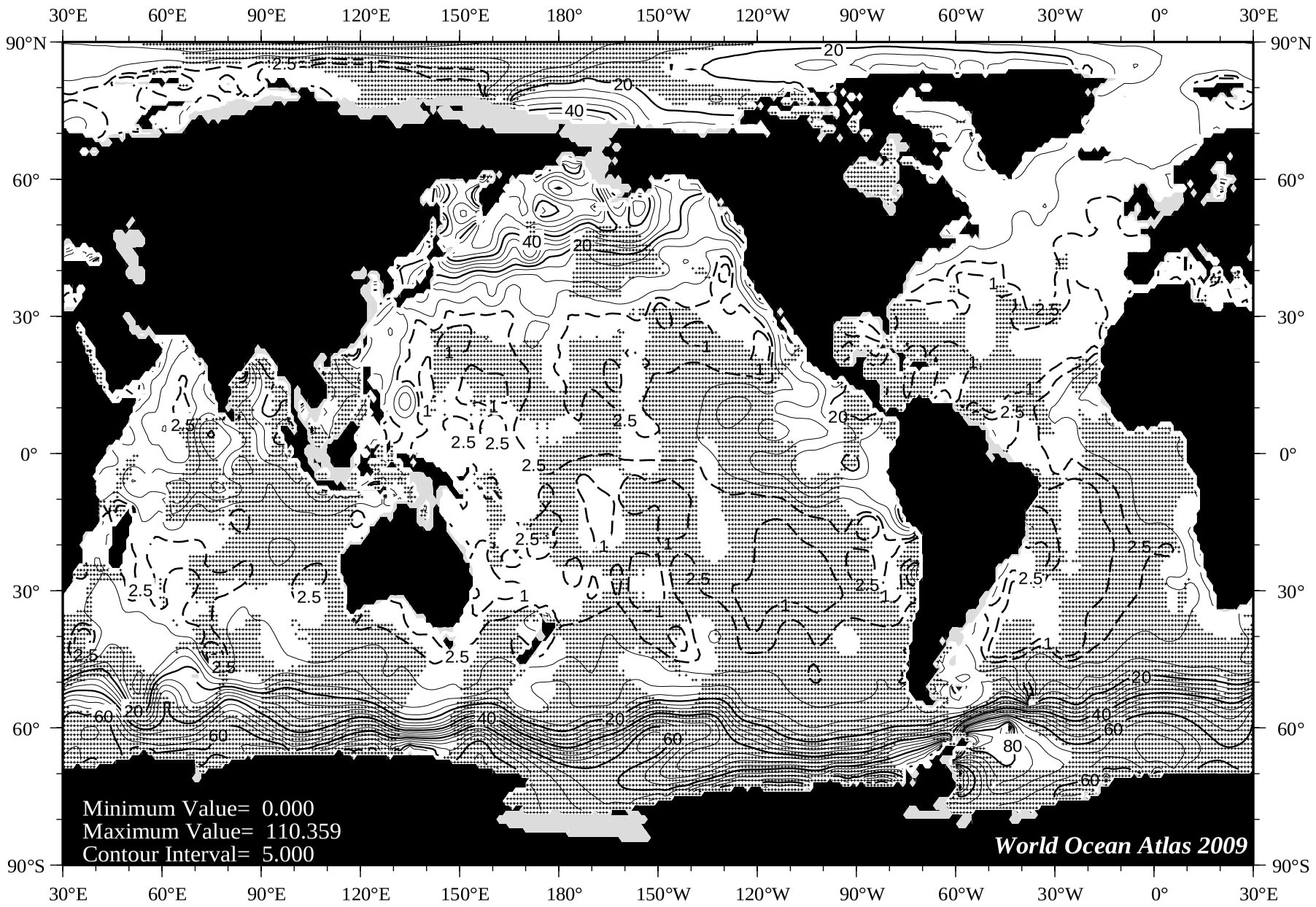

Fig I51 July mean silicate [umol/l] at 75 m. depth.

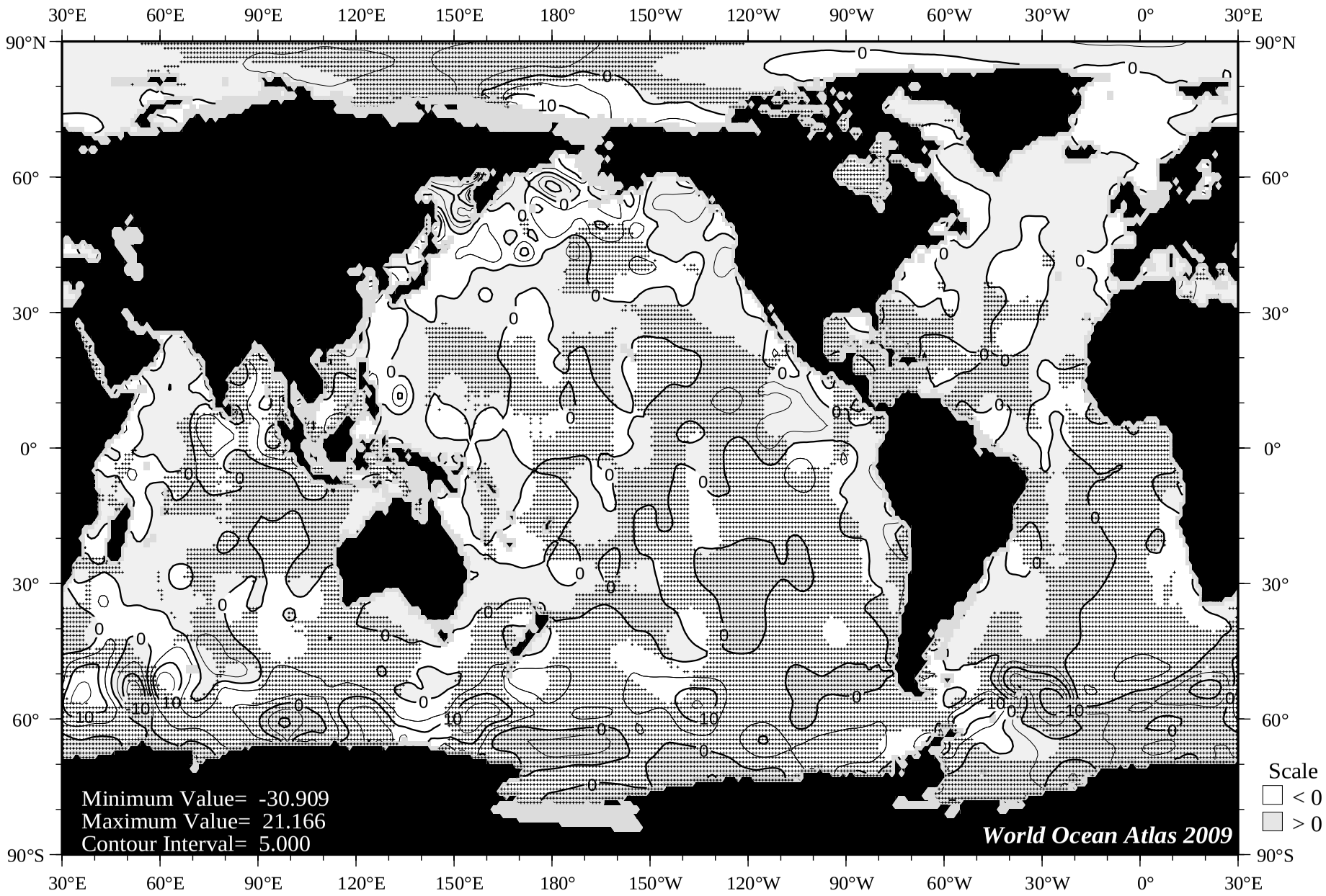

Fig I52 July minus annual silicate [umol/l] at 75 m. depth.

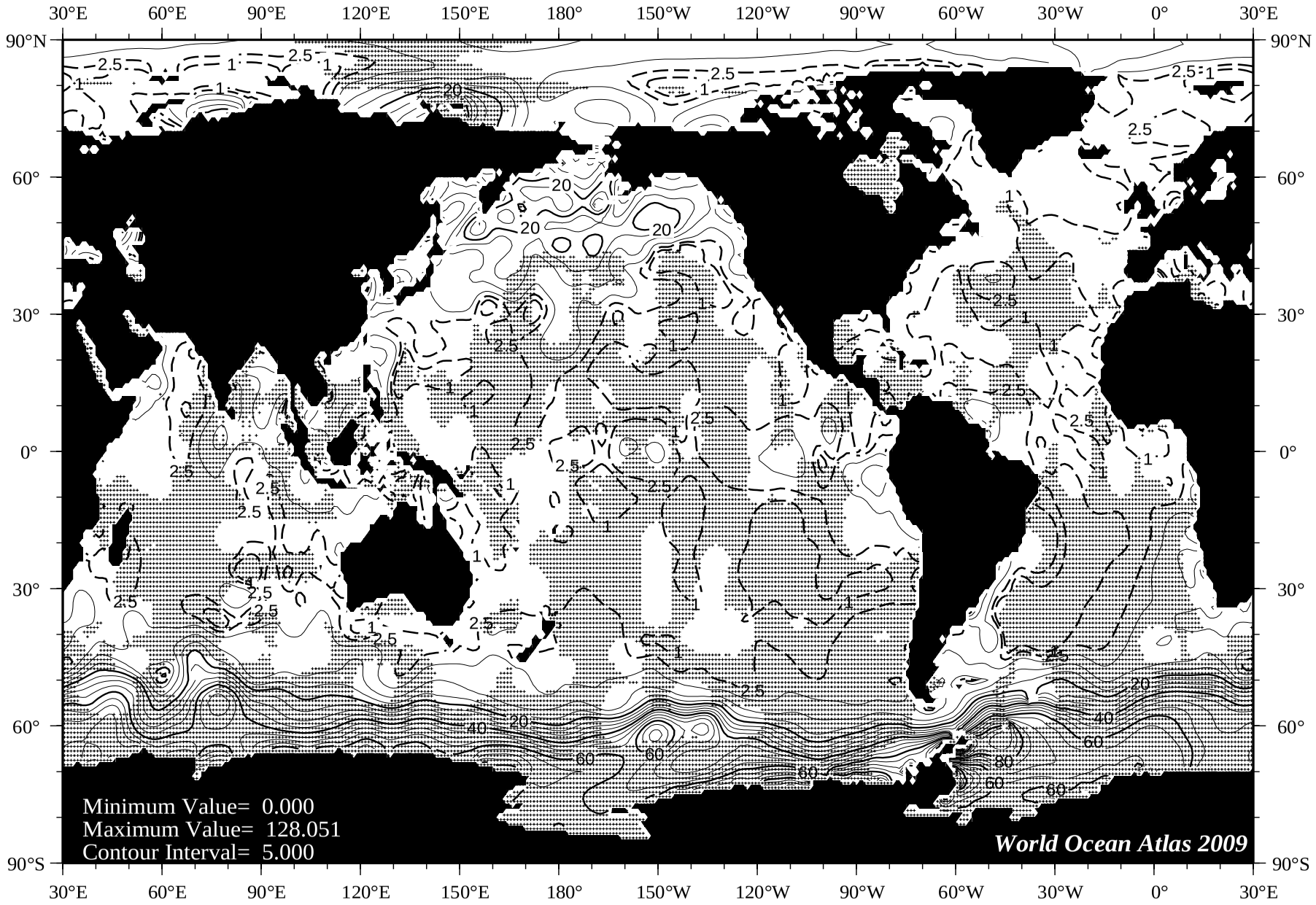

Fig I53 August mean silicate [umol/l] at the surface.

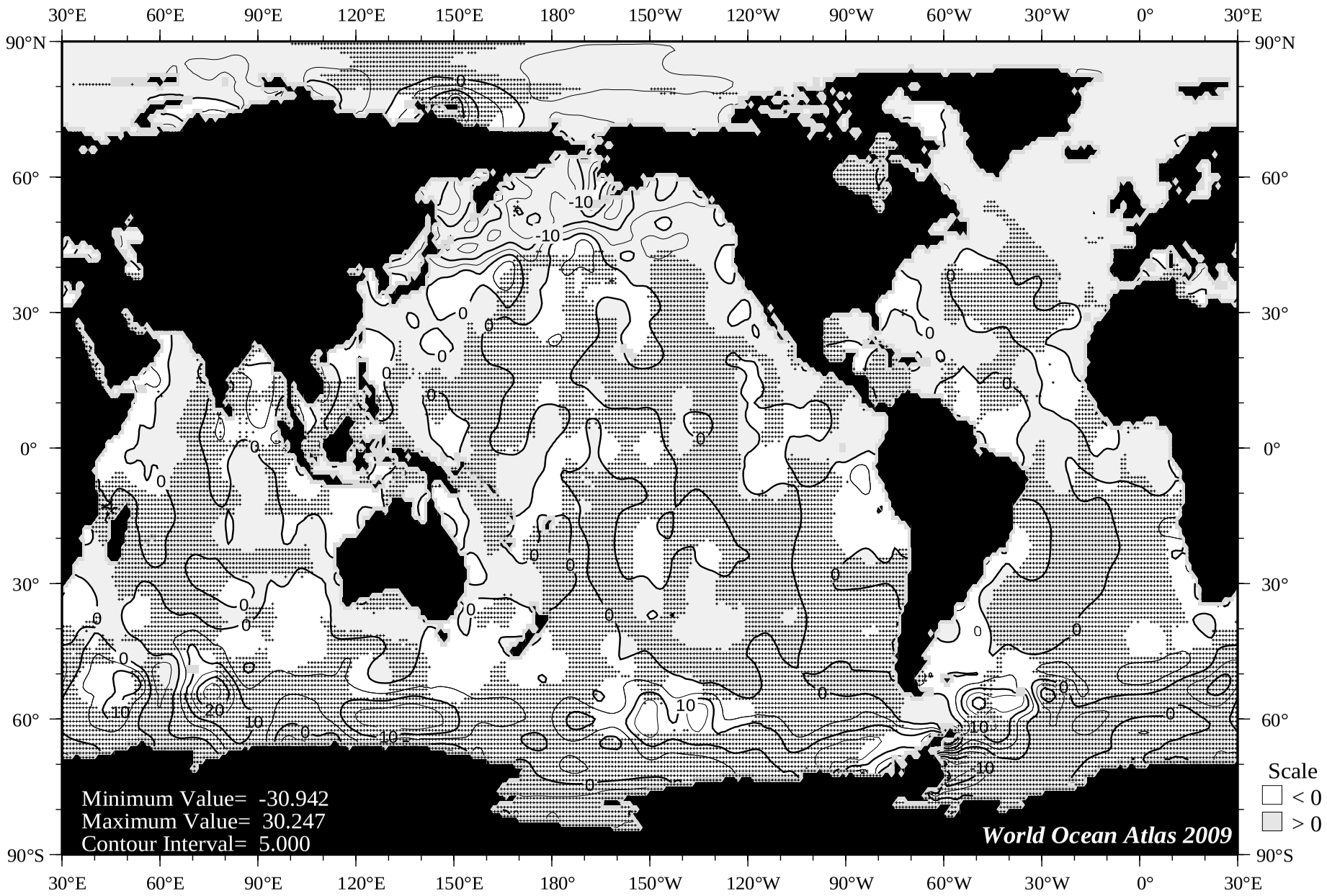

Fig I54 August minus annual silicate [umol/l] at the surface.

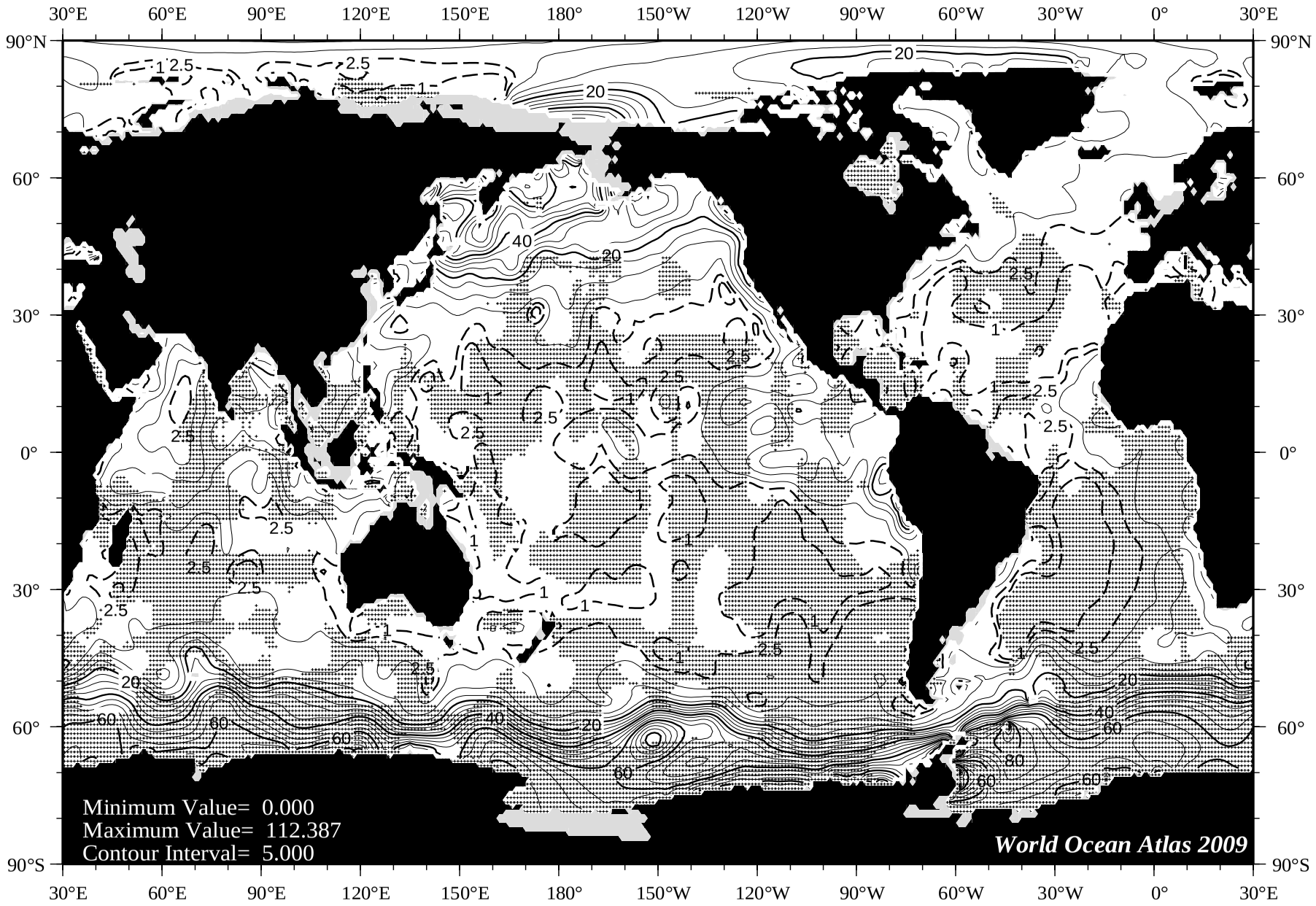

Fig I55 August mean silicate [umol/l] at 75 m. depth.

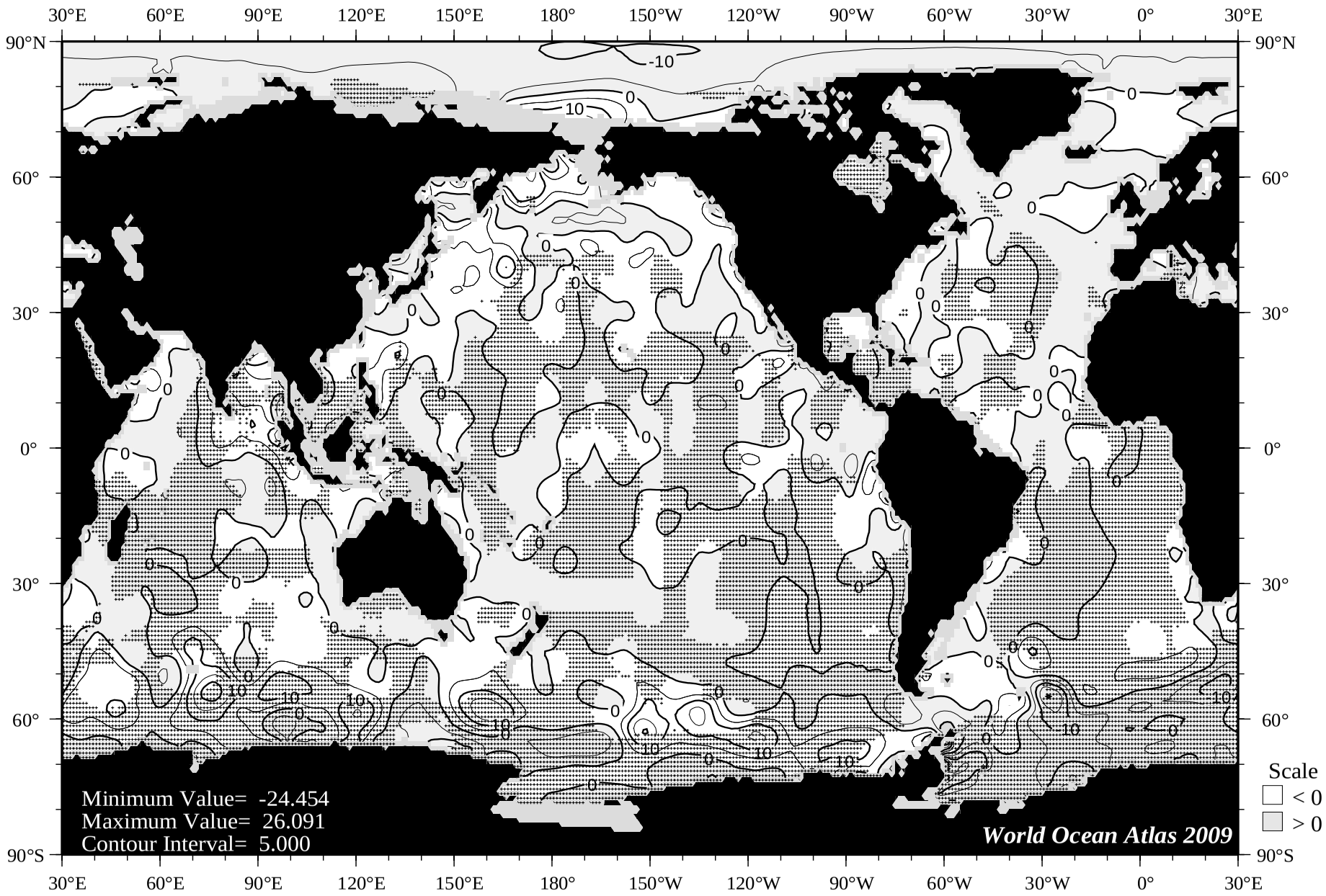

Fig I56 August minus annual silicate [umol/l] at 75 m. depth.

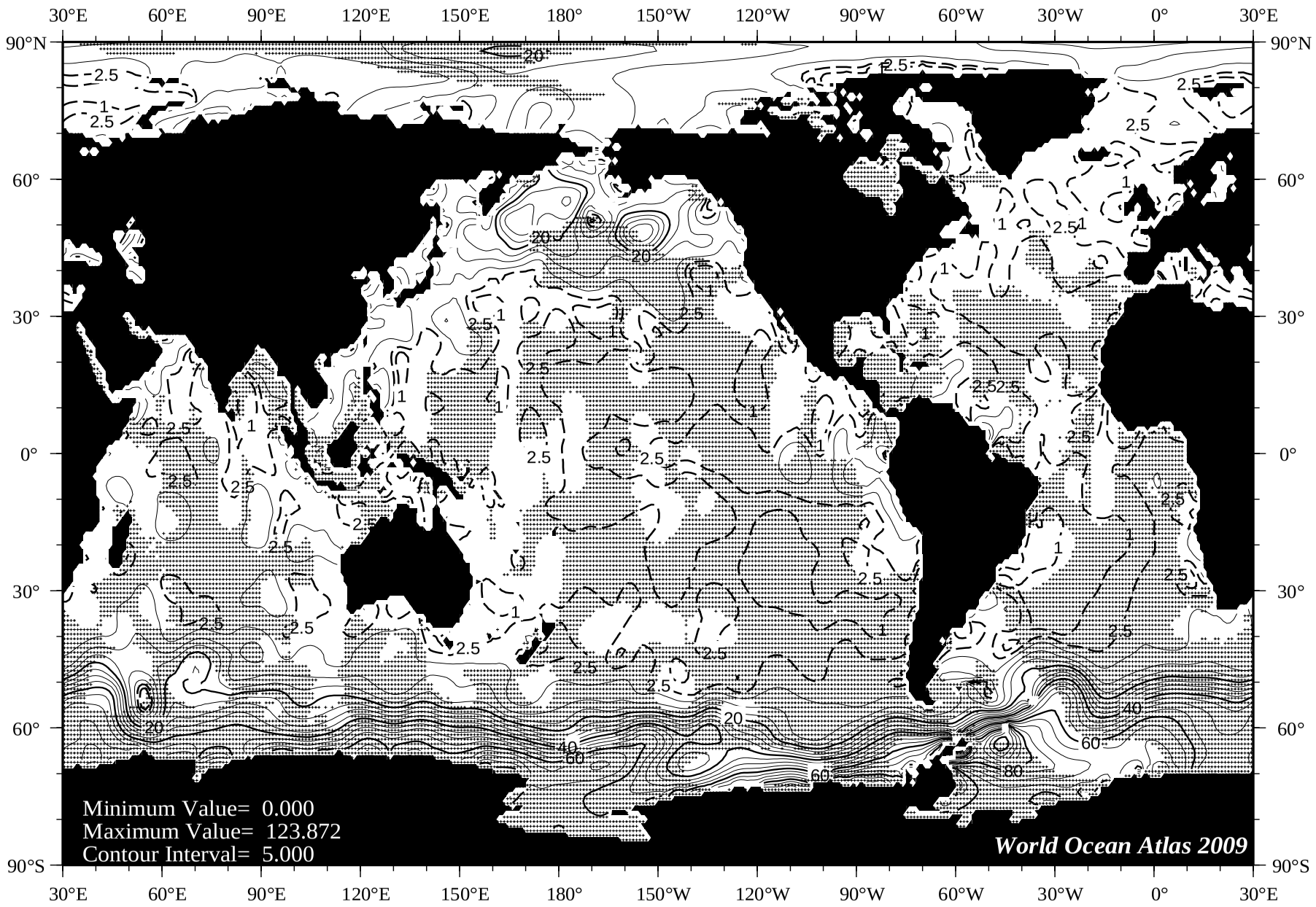

Fig I57 September mean silicate [umol/l] at the surface.

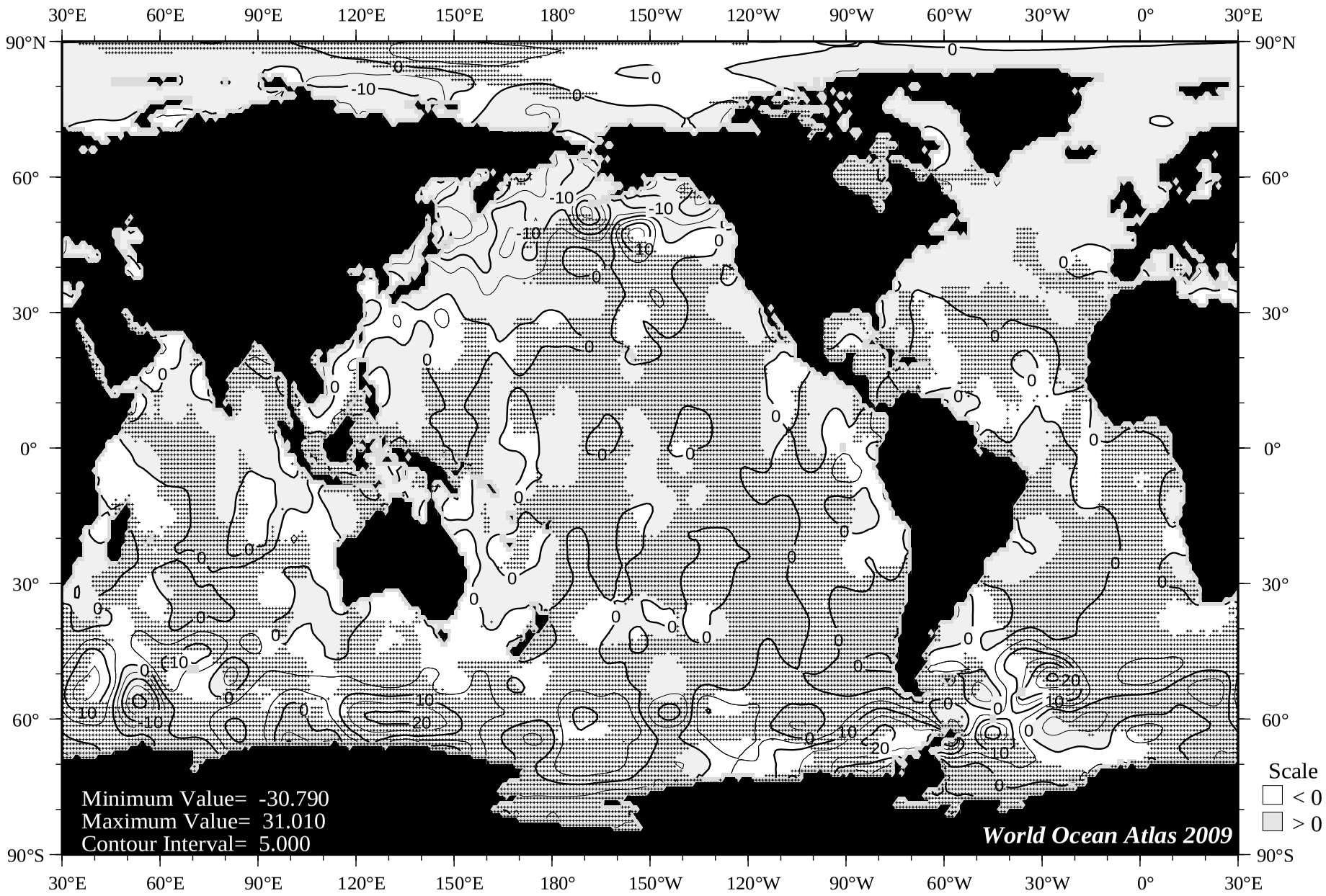

Fig I58 September minus annual silicate [umol/l] at the surface.

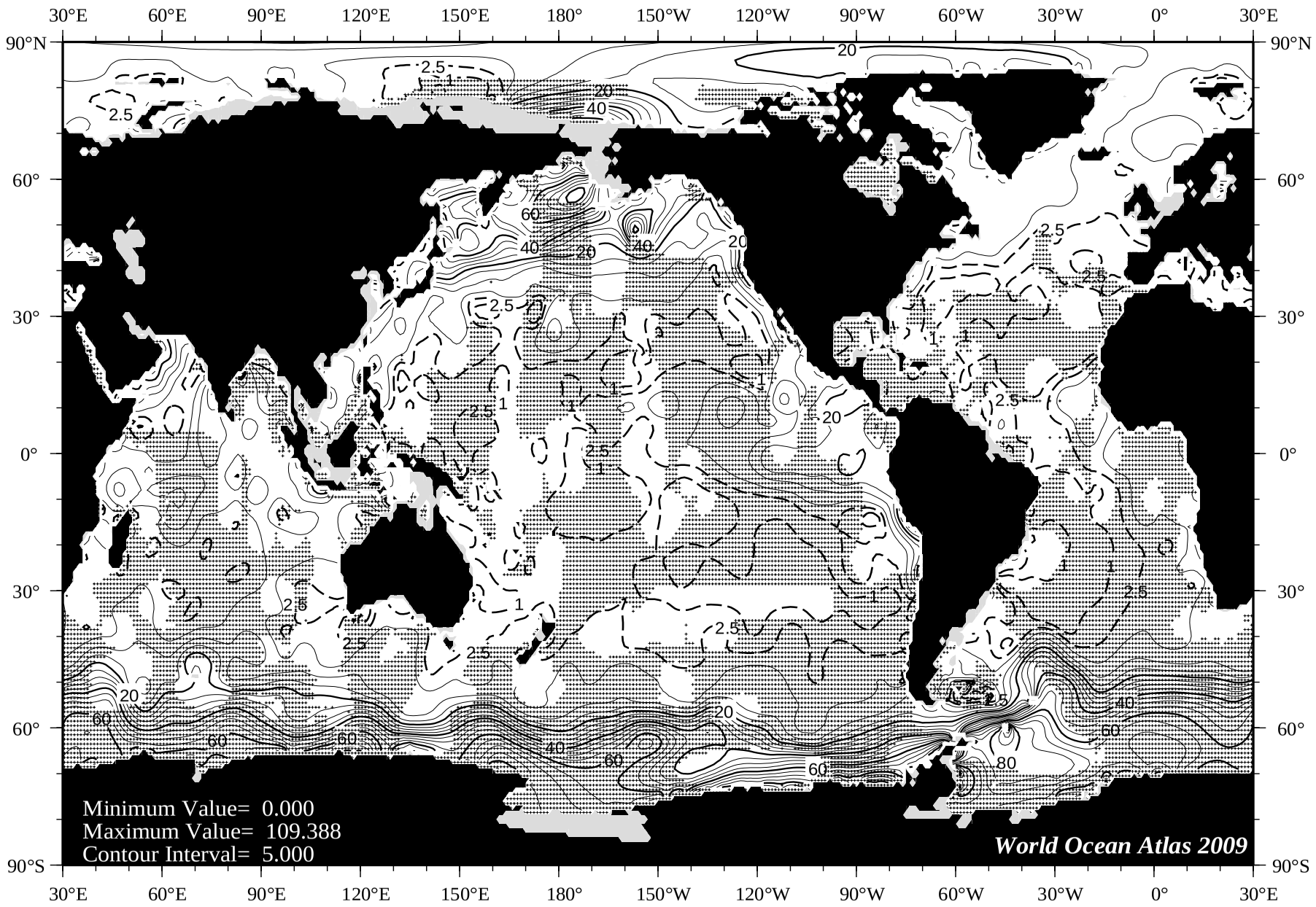

Fig I59 September mean silicate [umol/l] at 75 m. depth.

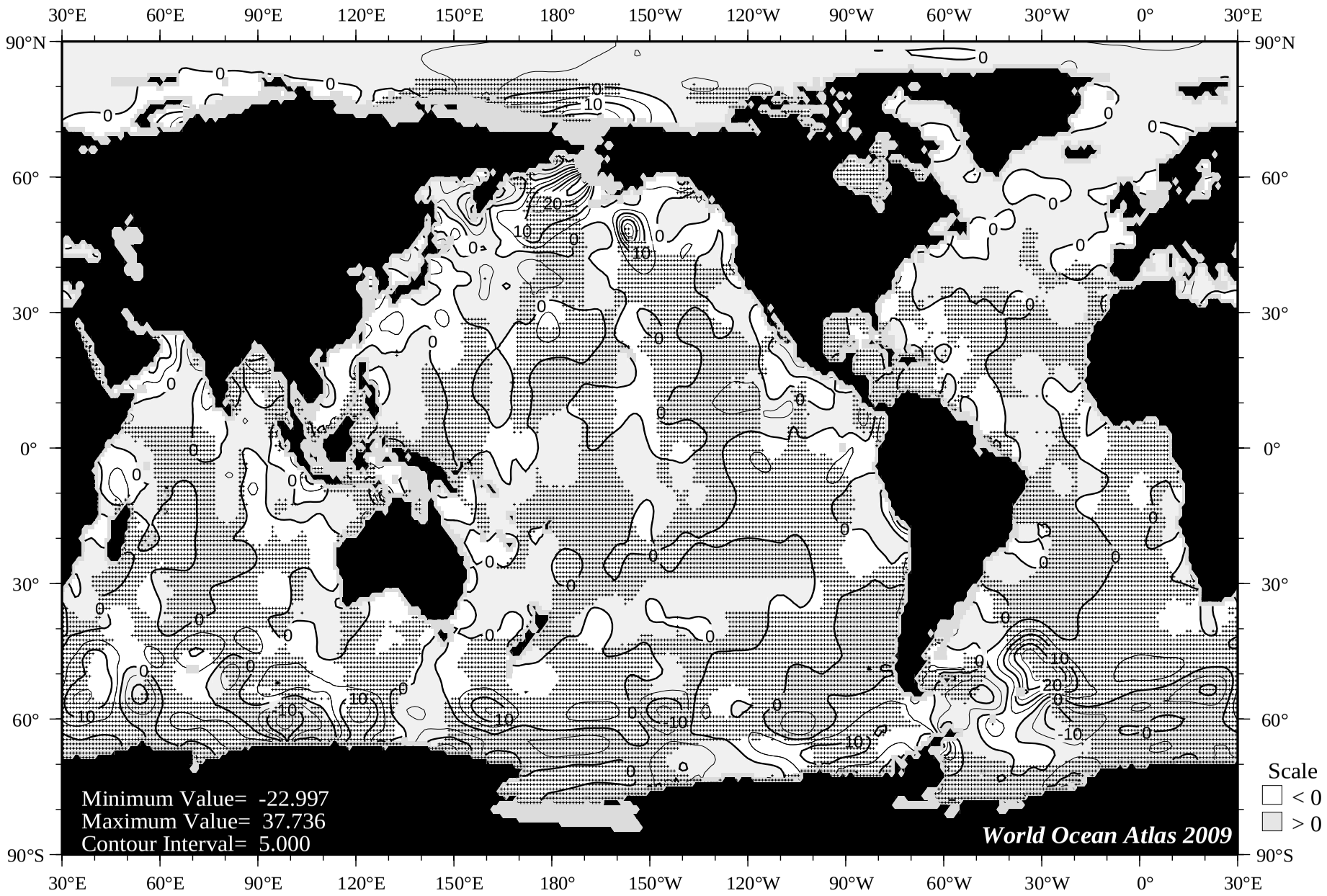

Fig I60 September minus annual silicate [umol/l] at 75 m. depth.

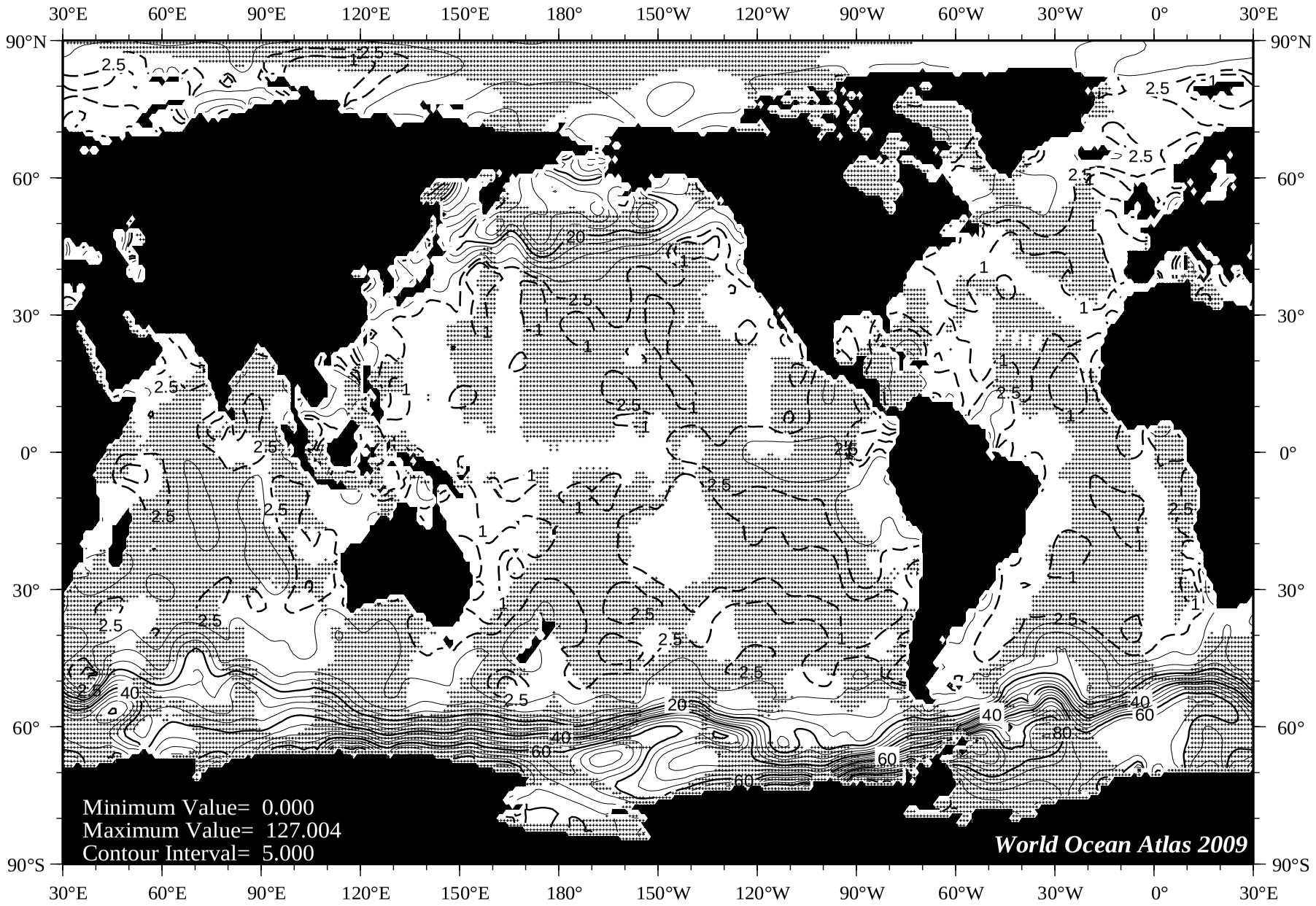

Fig I61 October mean silicate [umol/l] at the surface.

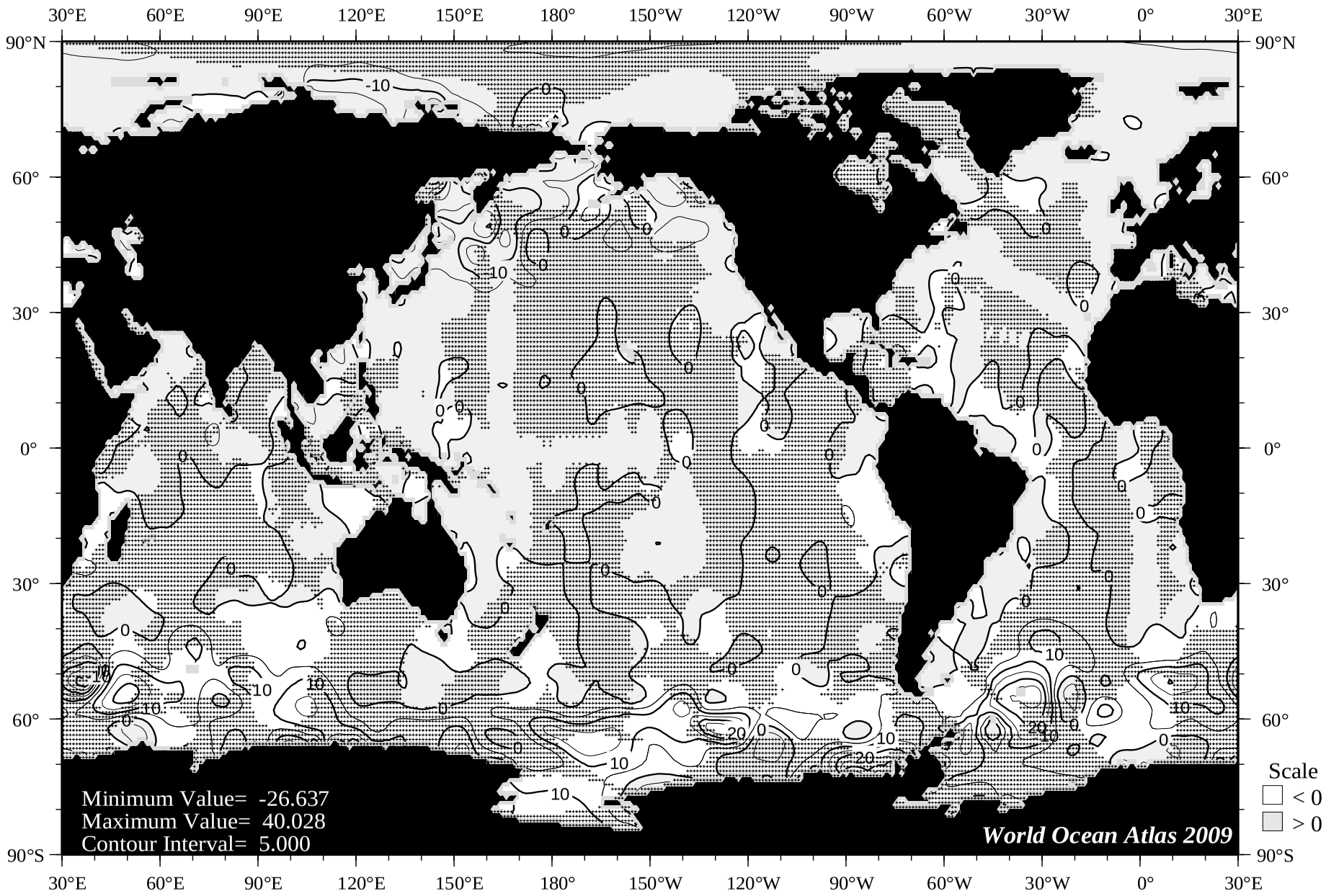

Fig I62 October minus annual silicate [umol/l] at the surface.

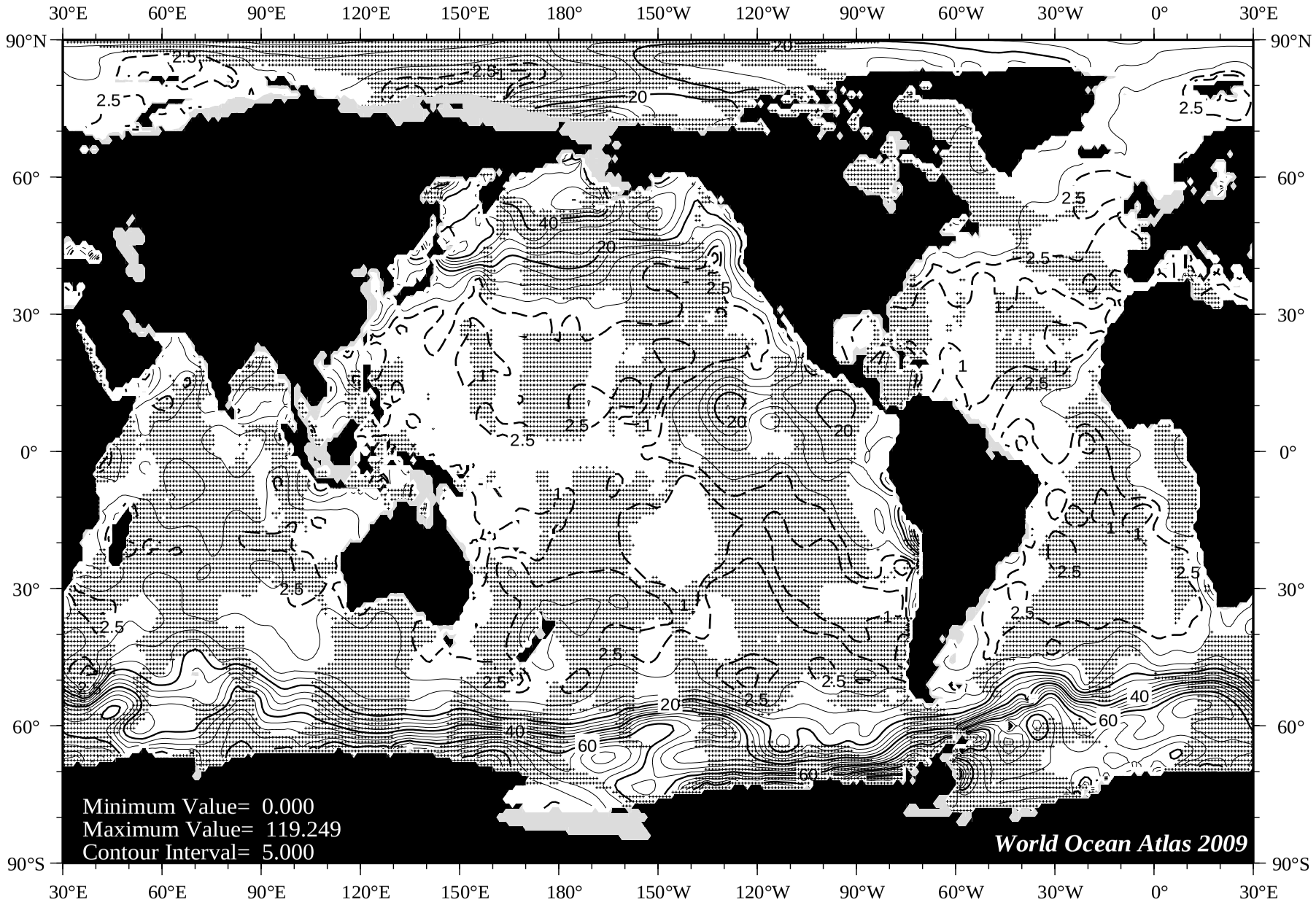

Fig I63 October mean silicate [umol/l] at 75 m. depth.

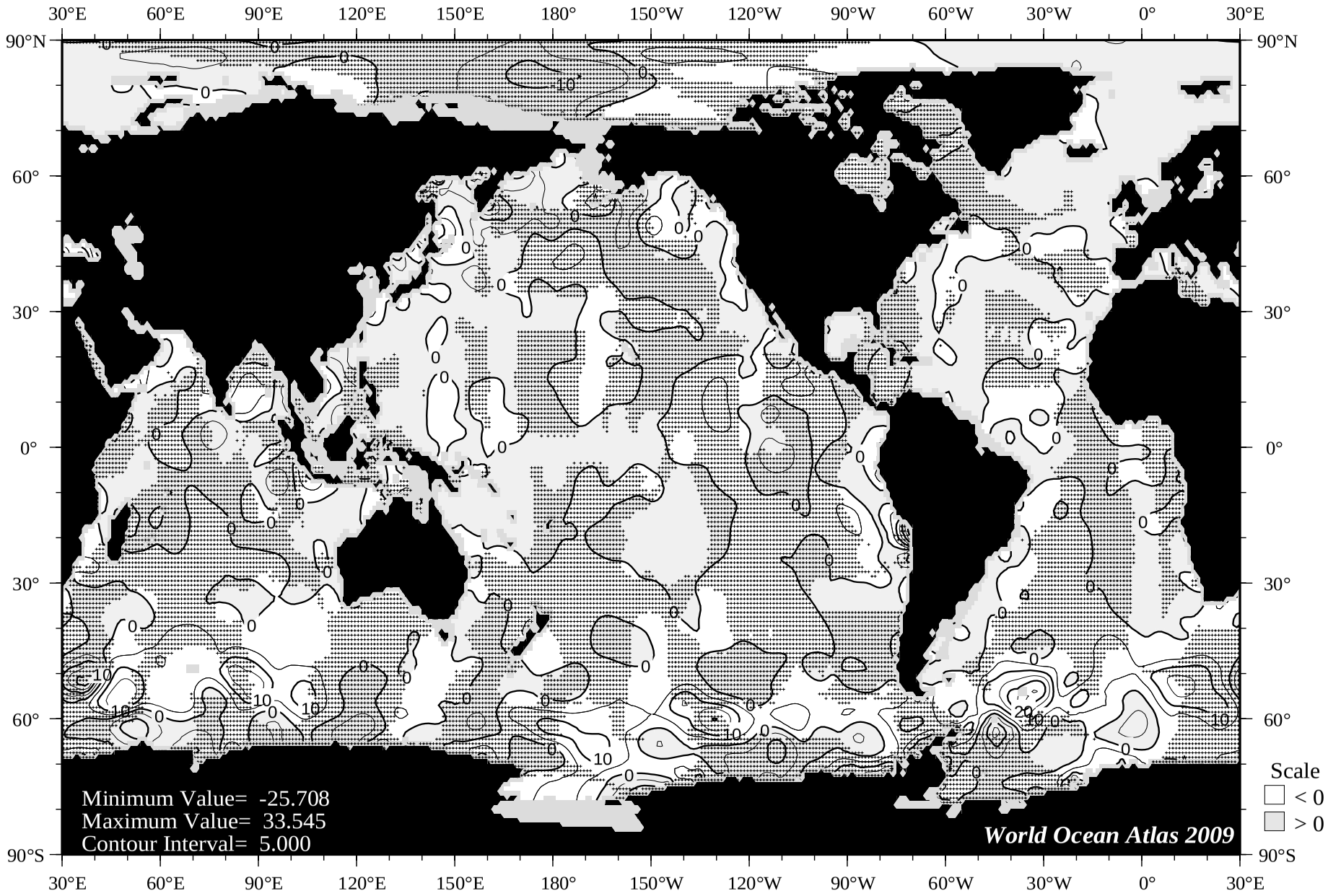

Fig I64 October minus annual silicate [umol/l] at 75 m. depth.

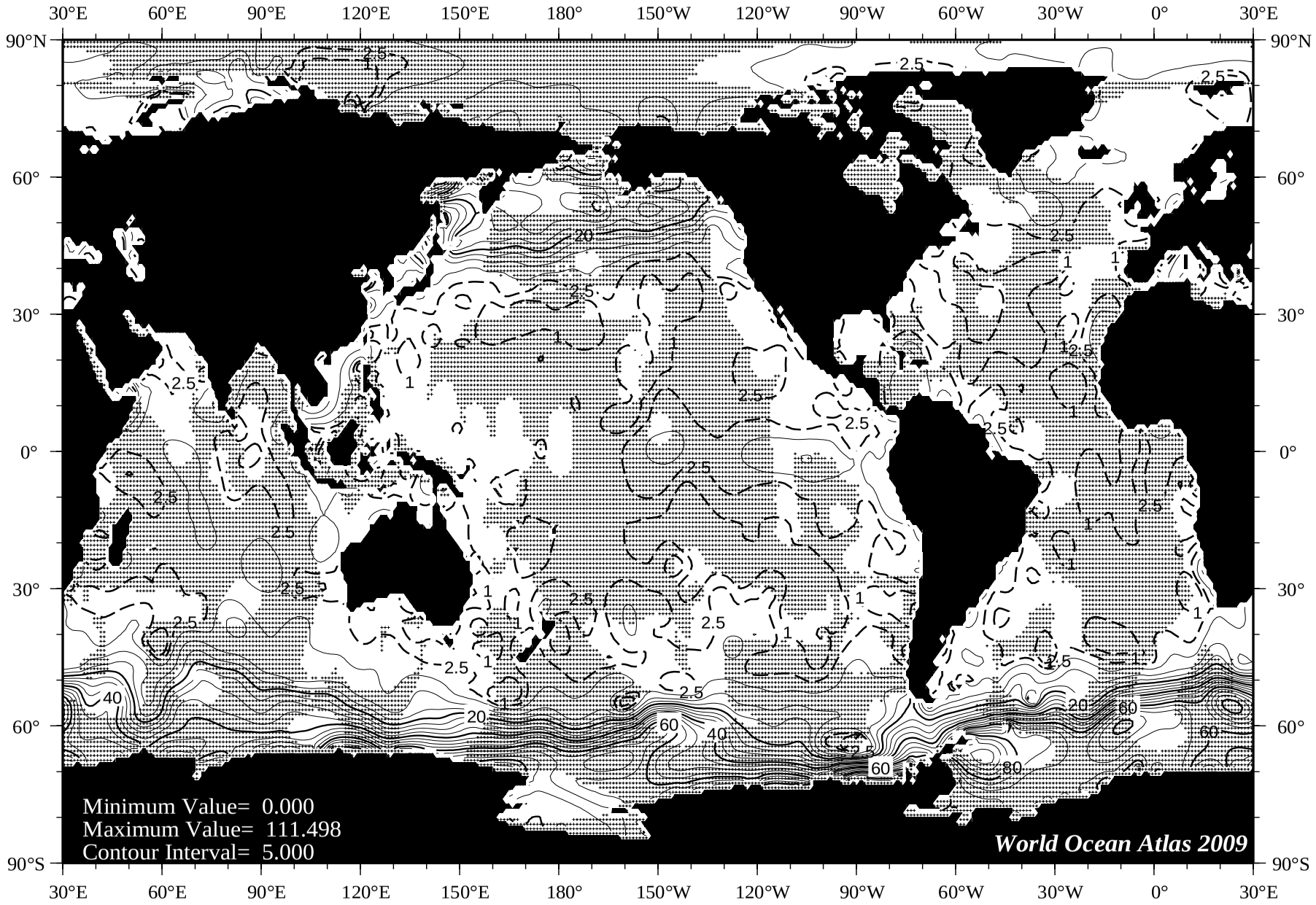

Fig I65 November mean silicate [umol/l] at the surface.

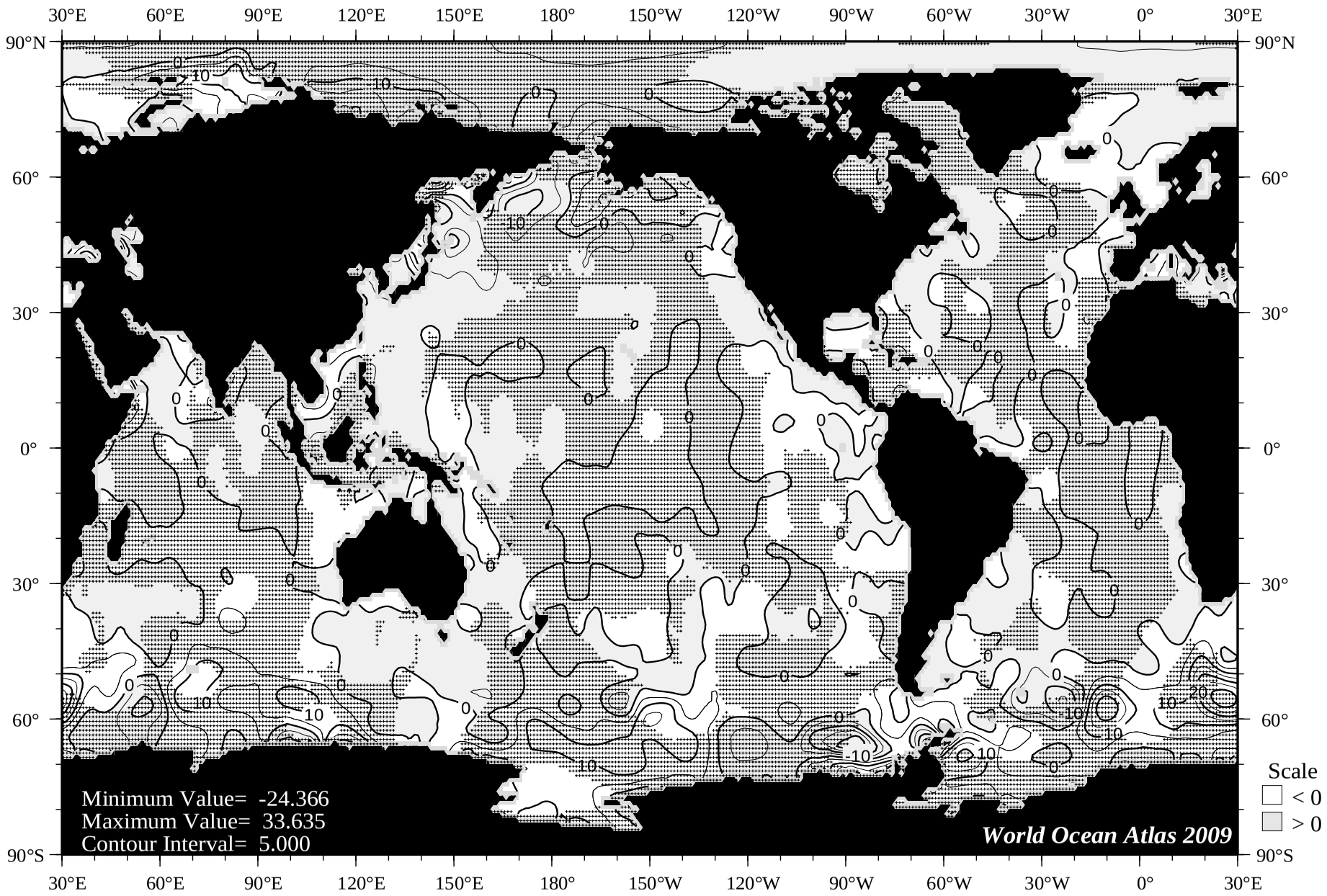

Fig I66 November minus annual silicate [umol/l] at the surface.

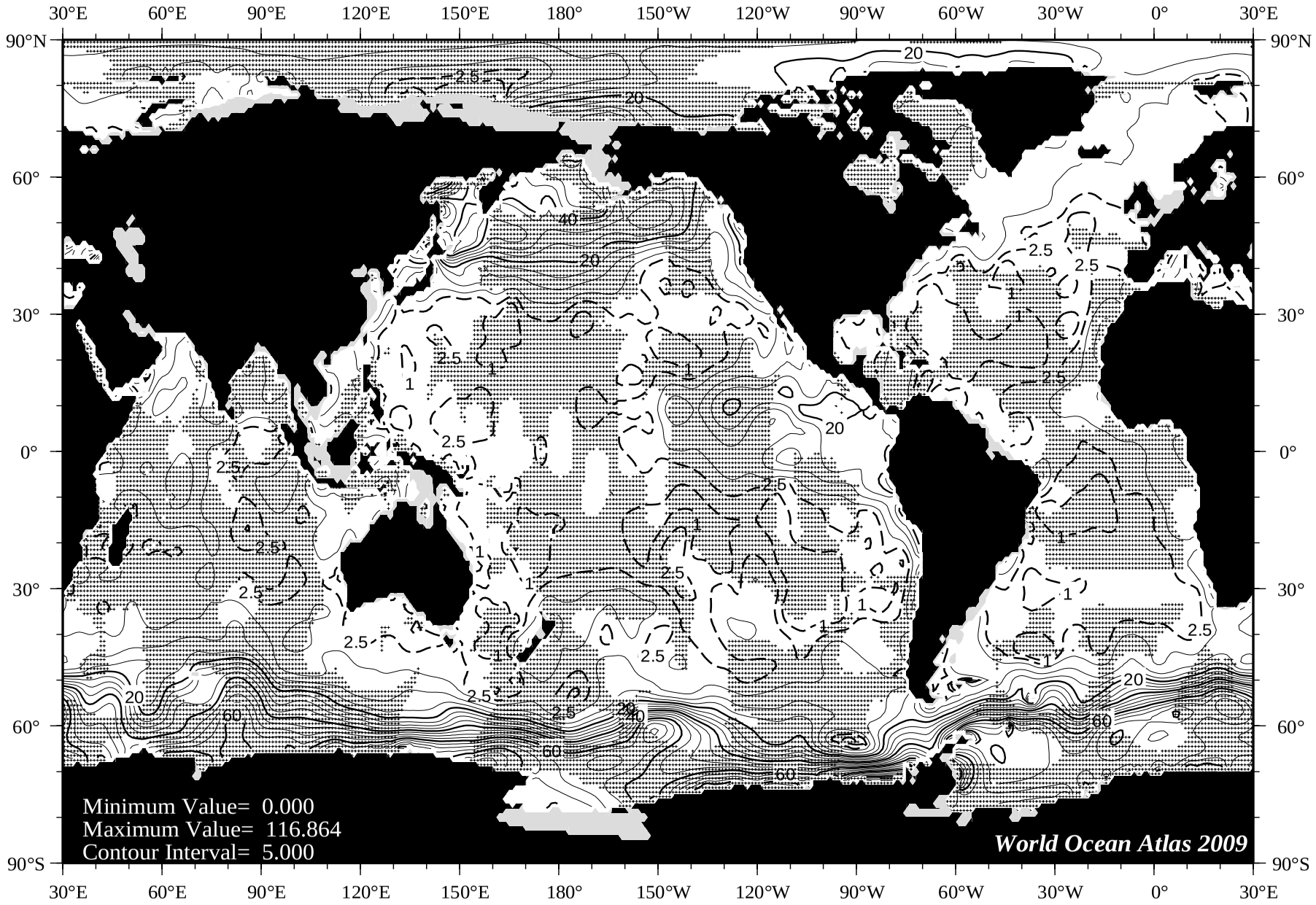

Fig I67 November mean silicate [umol/l] at 75 m. depth.

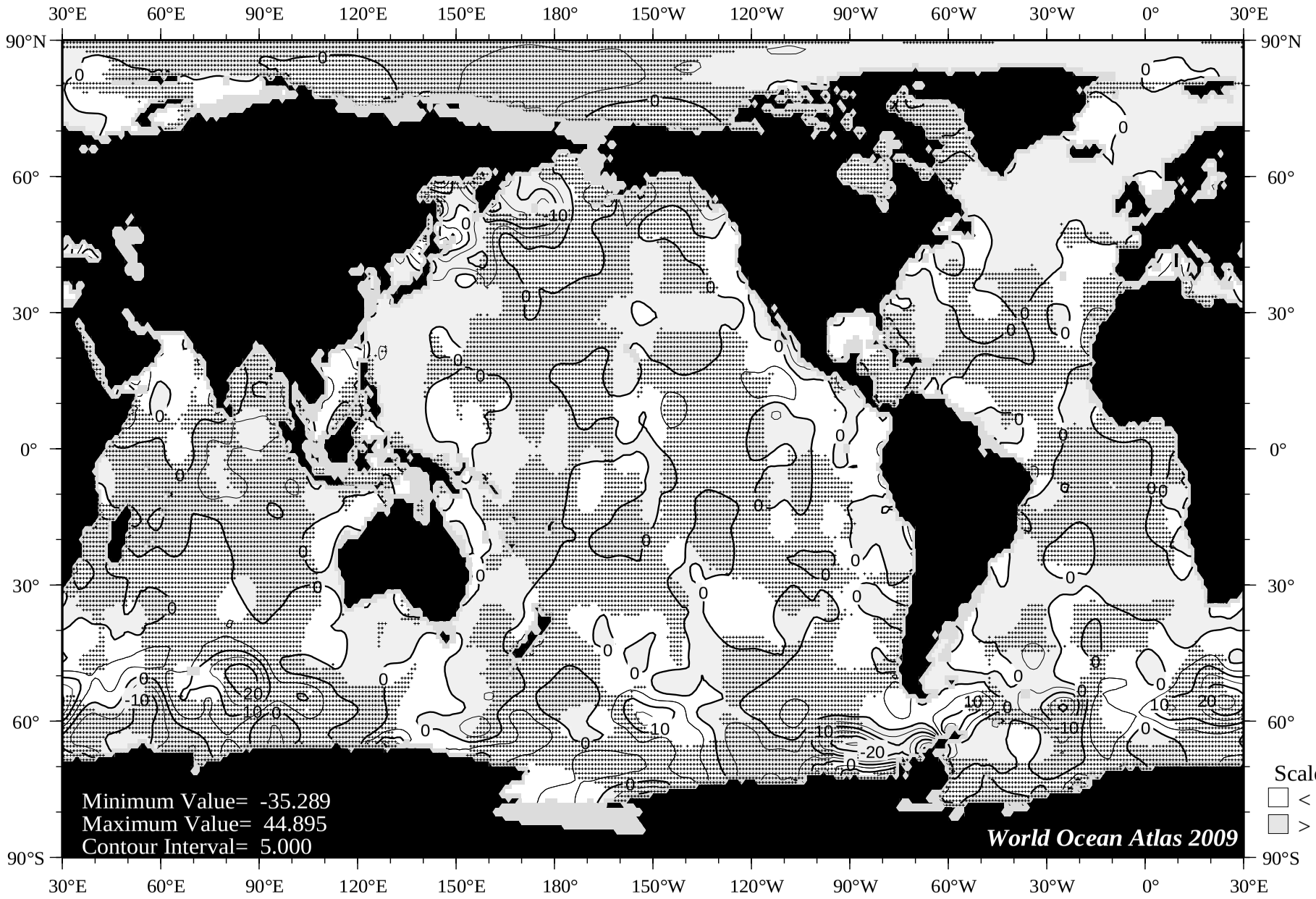

Fig I68 November minus annual silicate [umol/l] at 75 m. depth.

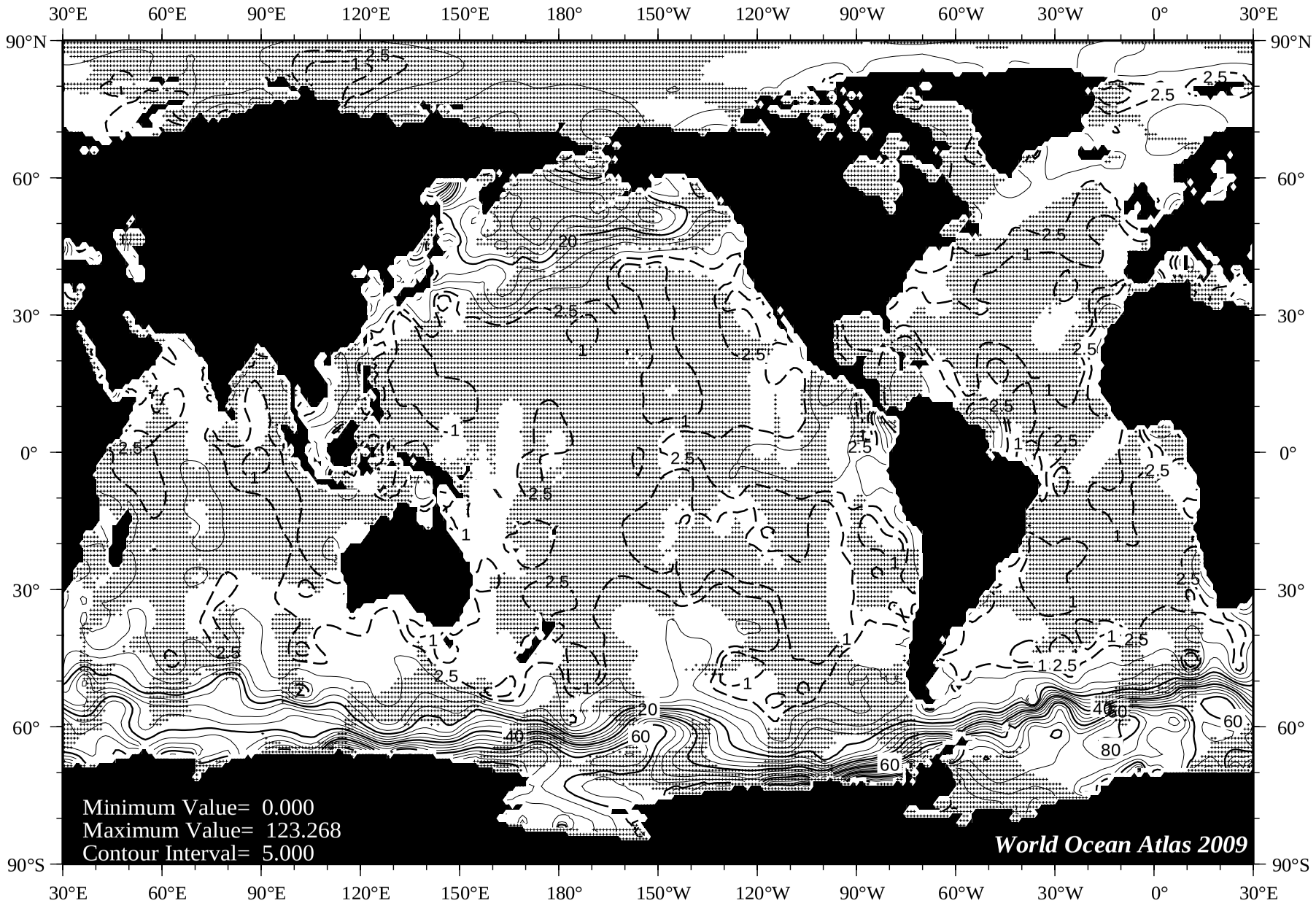

Fig I69 December mean silicate [umol/l] at the surface.

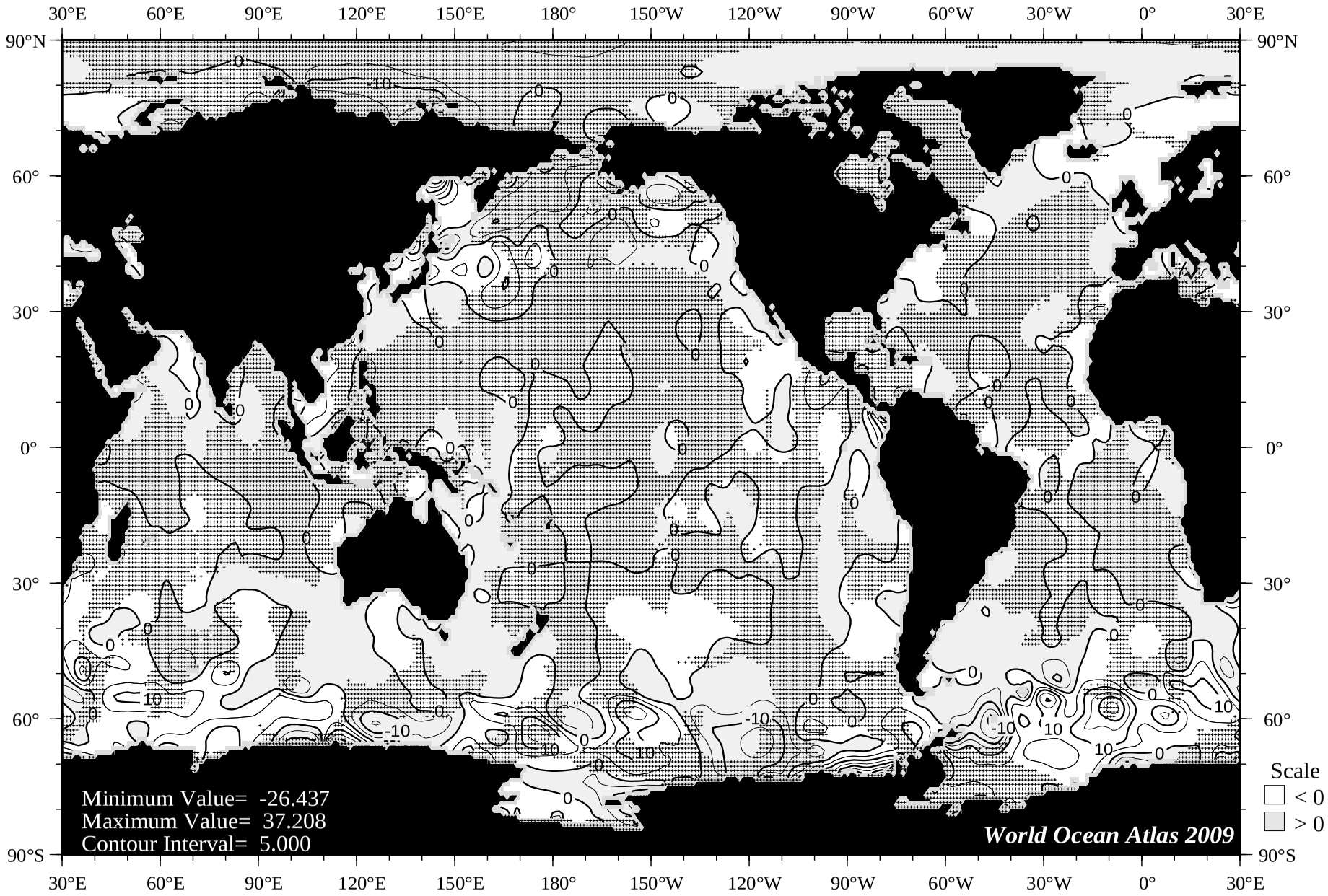

Fig I70 December minus annual silicate [umol/l] at the surface.

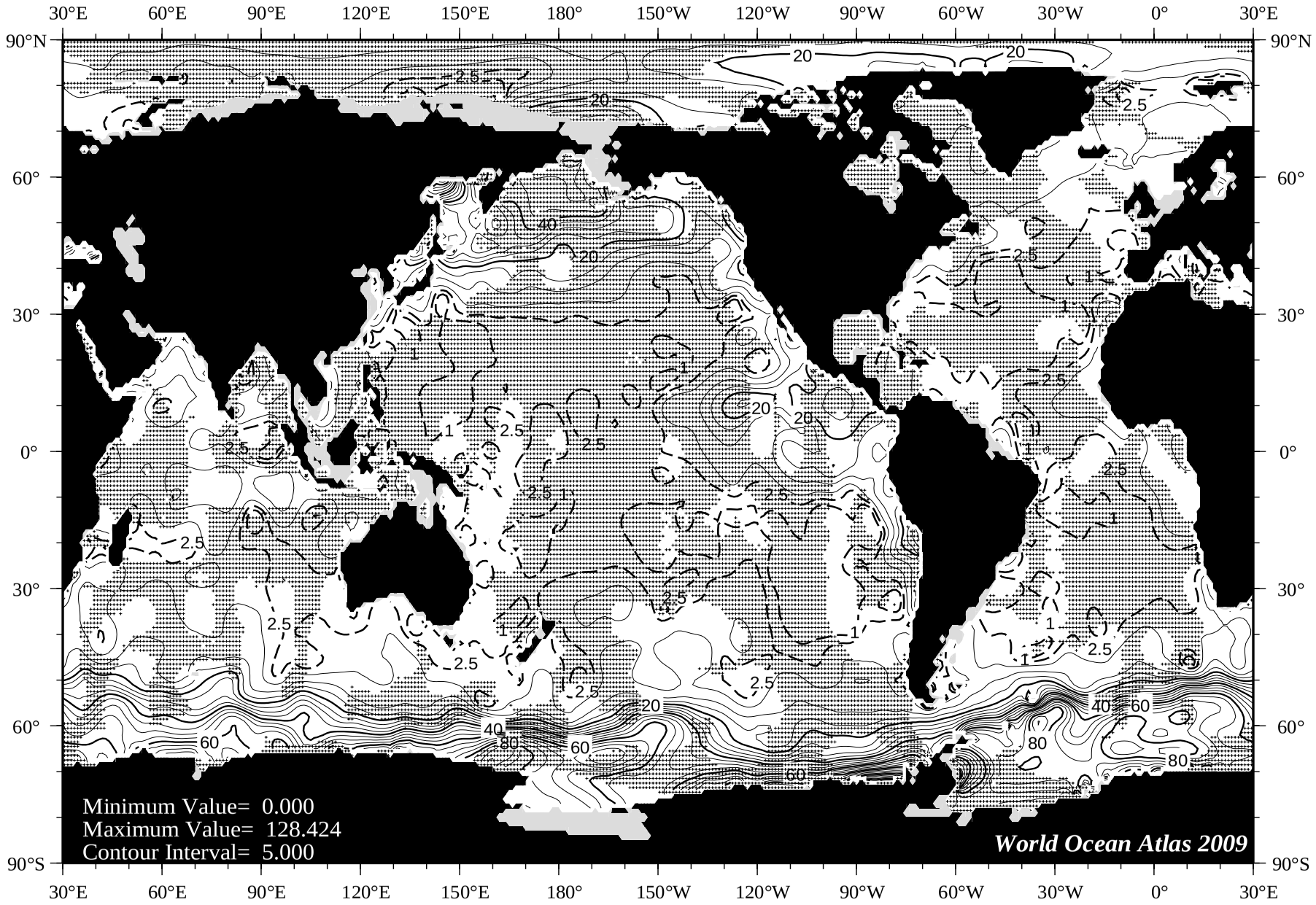

Fig I71 December mean silicate [umol/l] at 75 m. depth.

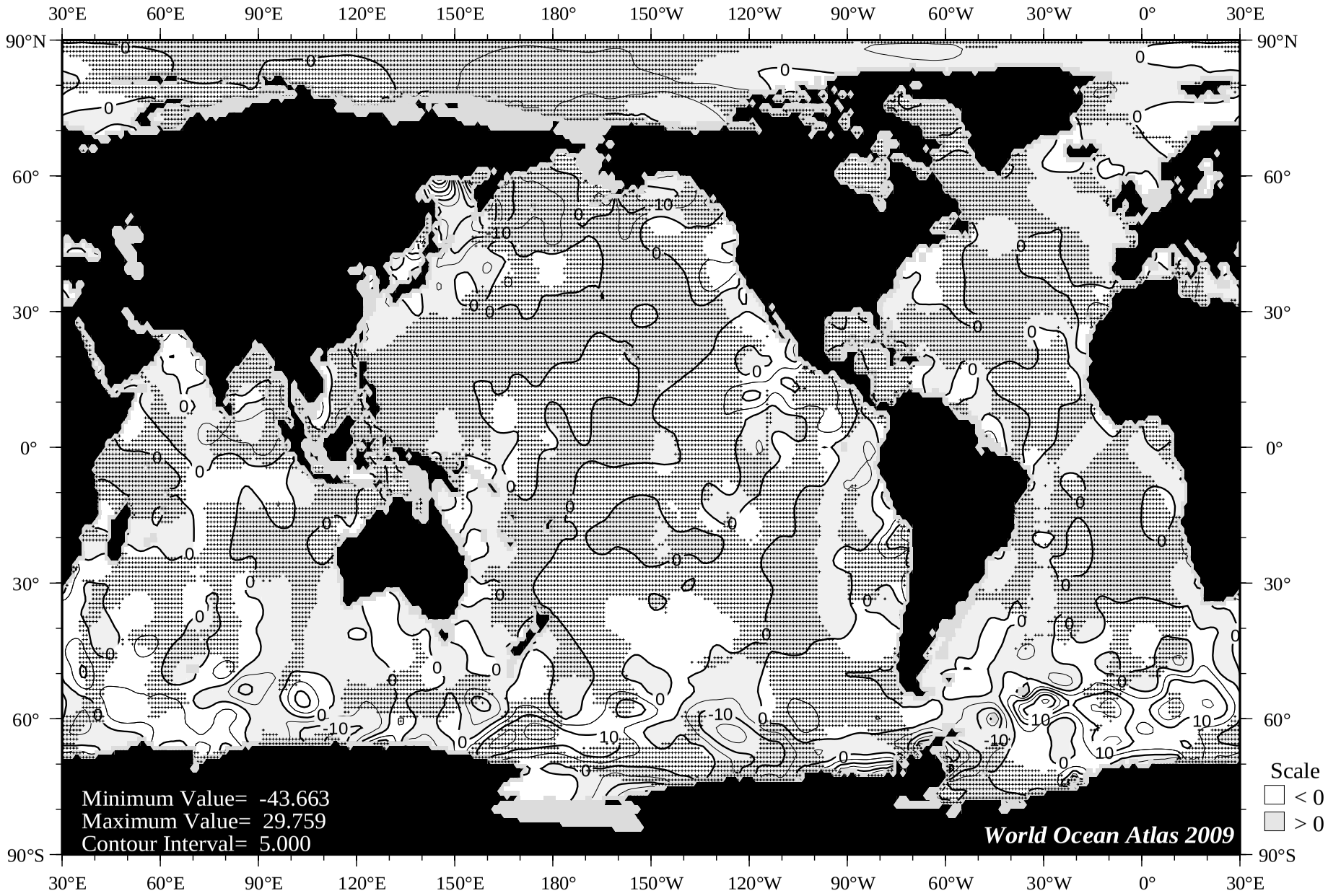

Fig I72 December minus annual silicate [umol/l] at 75 m. depth.